International Association for the promotion of co-operation with scientists from the New Independent States of the former Soviet Union

INTAS Project – 0511 REBASOWS

Final report

"The rehabilitation of the ecosystem and bioproductivity of the Aral Sea under conditions of water scarcity"

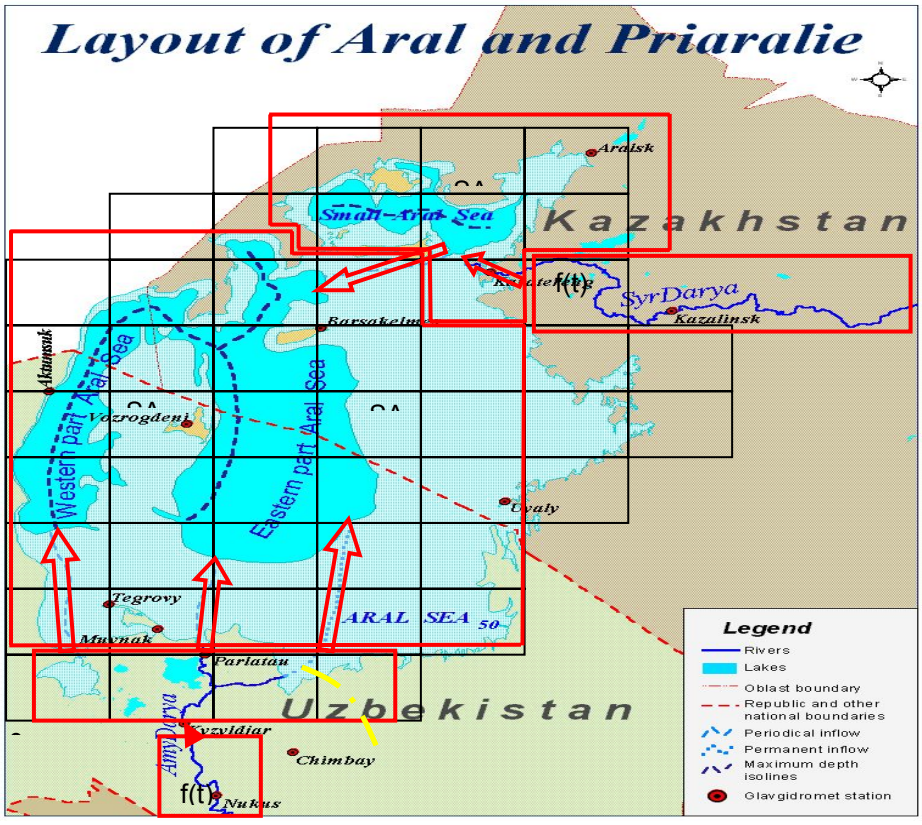

Coordinator: H.P. Nachtnebel
IWHW-BOKU

Vienna - Tashkent
December 2006

Executors:

C0
University of Natural Resources and Applied Life Sciences, Dept. of Water Management, Hydrology and Hydraulic Engineering
o.Univ.Prof. DI.Dr. Dr.h.c.Hans Peter Nachtnebel
a.o.Univ.Prof.DI.Dr. Hubert Holzmann

CR-2
SIC ICWC:
Prof. Dir. Victor Dukhovny
Dr. Anatoly Sorokin
Yelena Roschenko
Raisa Kadirova

CR-3
The Center of Intergrated Water Systems Research
Dir. Dr. Alexander Tuchin
Dr. P.D. Umarov
Dr. U. Uhalin
A. Beloglazov
E. Korshak
Elena Temlyanceva

CR-4
Institute of Physiology and Biophysics & Institute of Zoology at the Academy of Sciences, the Republic of Uzbekistan
Prof. Dr. Bek Tashmukhamedov
Dr. Iskandar Mirabdullayev
Dr. A. Lola

CR-5
Institute for Water and Environmental Problems of the Russian Academy of Sciences
Prof. Oleg Vasilyev
Dr. Vissarion I. Kvon
Prof. Dr. Victor I. Kuzin
Aleksander N. Semchukov
Victor V. Martyanov

General edition and writing of the main part of report is undertaken by Prof. V.Dukhovny and final editing was done by Prof. H.P. Nachtnebel.

C O N T E N T

Report of CR2 and CR3

TABLES

FIGURES

INTRODUCTION

The general water development in the Central Asian region was the reason behind the impossibility to restore the Aral Sea in its biologically active form and to initial volumes. At the earliest stage of independence, the Central Asian states recognized this fact in “The Concept for Socio-Economic and Environmental Development in the Aral Sea and its Coastal Zone (Priaralie)”, which was adopted by the Heads of State in January 11, 1994. Moreover, they considered that it was appropriate to focus on protection of Priaralie in social and natural directions. The Governments of Kazakhstan and Uzbekistan took respective measures and decisions that largely contributed to stabilization of situation in Priaralie and to development of its living and environmental capacities. Meanwhile, the future of the Aral Sea itself remains problematic and is still in the regional agenda, but the both countries use their own scenarios for problem solution. The nature itself, which has a certain defense reaction for self-preservation and adaptation to new conditions of still shrinking sea, corrected the previous awesome forecasts of million tons of salt- and dust-transfer by forming zones of self-planting and expanding naturally watered deltas in some places because of intensive natural surface water inflow. For instance, whereas the NATO Project “Southern Priaralie” ("Resource Analyses" and SIC ICWC) planned to expand wetland area to 230 … 250 thousand ha from previous 80 … 127 thousand ha, in June 2005, according to satellite observations, wetlands increased to 329,6 thousand ha in Amudarya delta. Intensive natural growing of saxaul, tamarisk, various solonchaks was detected by field expedition organized by SIC on GTZ’s demand to the former Akpetkin Archipelago in eastern part of dried sea.
Nevertheless, a problem related to the sea itself and its future should be thoroughly analyzed: what would happen under business as usual; what kind of hazard is posed to the nature and population; and, what should be done in the first place by Kazakhstan and Uzbekistan under suggested socio-economic development and water use in the region in order to achieve ecological sustainability and bioproductivity in the Aral Sea and the surroundings.
It is very important that this assessment can be made within the framework of the present project INTAS 01-0511, which is virtually a pioneer in making a scientific prediction and developing a set of models that form a basis for solution.

1. Main project tasks and responsibilities among executors

The INTAS 01-0511 Project’s tasks are as follows:

- predict salt and water balances of the Aral Sea under various scenarios of inflow to the coastal zone (Priaralie);
- identify sustainable ecological profile of the remained water body in different options;
- outline a strategy for rehabilitation of ecosystems and bioproductivity of the Aral Sea.

Practically, the first task was given to executors of CR2, CR3, CR5; the second task – CR4; and, the final one –CR2, CR3 and CR4. In this context, the work program was divided into the following sub-tasks:

1. Develop a set of mathematical models and software for comprehensive research on forming and development of the Aral Sea –CR3, CR5;
2. Predict hydrological inflow to the Aral Sea under various scenarios of delta watering and of development in Central Asian countries – CR2;
3. Study allocation of resources between water bodies to identify water-salt dynamics in Eastern and Westerns parts on annual and long-term basis under various scenarios of delta watering –CR3;
4. Analyze current environmental conditions in different areas of the sea and identify sustainable ecological profile requirements and restorable biological parameters for the remained sea. Identify the basic options of bioproductivity development in Western sea under probable inflow variations – CR4;
5. Select an optimal strategic management for rehabilitation of bioproductivity in Western sea, based on p.4 – CR2, CR4, CR4, CR5.

Besides, database was established on the Aral Sea and the basin in general, as well as research was conducted on the basis of remote sensed observations of the sea’s dynamics and comparison with bathymetric maps of the sea as a whole and of its parts, including Small (Northern) Sea, Eastern Sea and Western Sea (CR2 and CR3).
Moreover, regarding modeling, it was agreed that the CR2 team would compute water-salt regime of Northern Sea in non-dimensional model; the same, non-dimensional water-salt models of Large Sea

would be made by CR3 team; while CR5 team would develop a three-dimensional model of hydrodynamic, hydrophysical, and hydrochemical processes taken place in the Aral Sea.
According to above agreements, the work components are interlinked as shown in Fig. 1.1.
Given report describes results achieved by teams CR2 and CR3, including:

- database on the Aral Sea (A.I.Tuchin, D.A.Sorokin);
- description of sea transformation dynamics and mapping of bathymetric curves (Ye.M.Roschenko);
- Aral Sea basin development scenarios (V.A.Dukhovny);
- basic model ASBMM (A.G.Sorokin);
- Amudarya and Syrdarya deltas and their development options (V.A.Dukhovny);
- design inflows to deltas (A.G.Sorokin);
- delta development model (A.I.Tuchin);
- N/D Aral Sea model (A.I.Tuchin);
- calibration of the N/D Large Sea model (A.I.Tuchin);
- sea's bodies development options (A.I.Tuchin);
- proposals on future development and scenarios (V.A.Dukhovny, A.I.Tuchin, A.G.Sorokin).

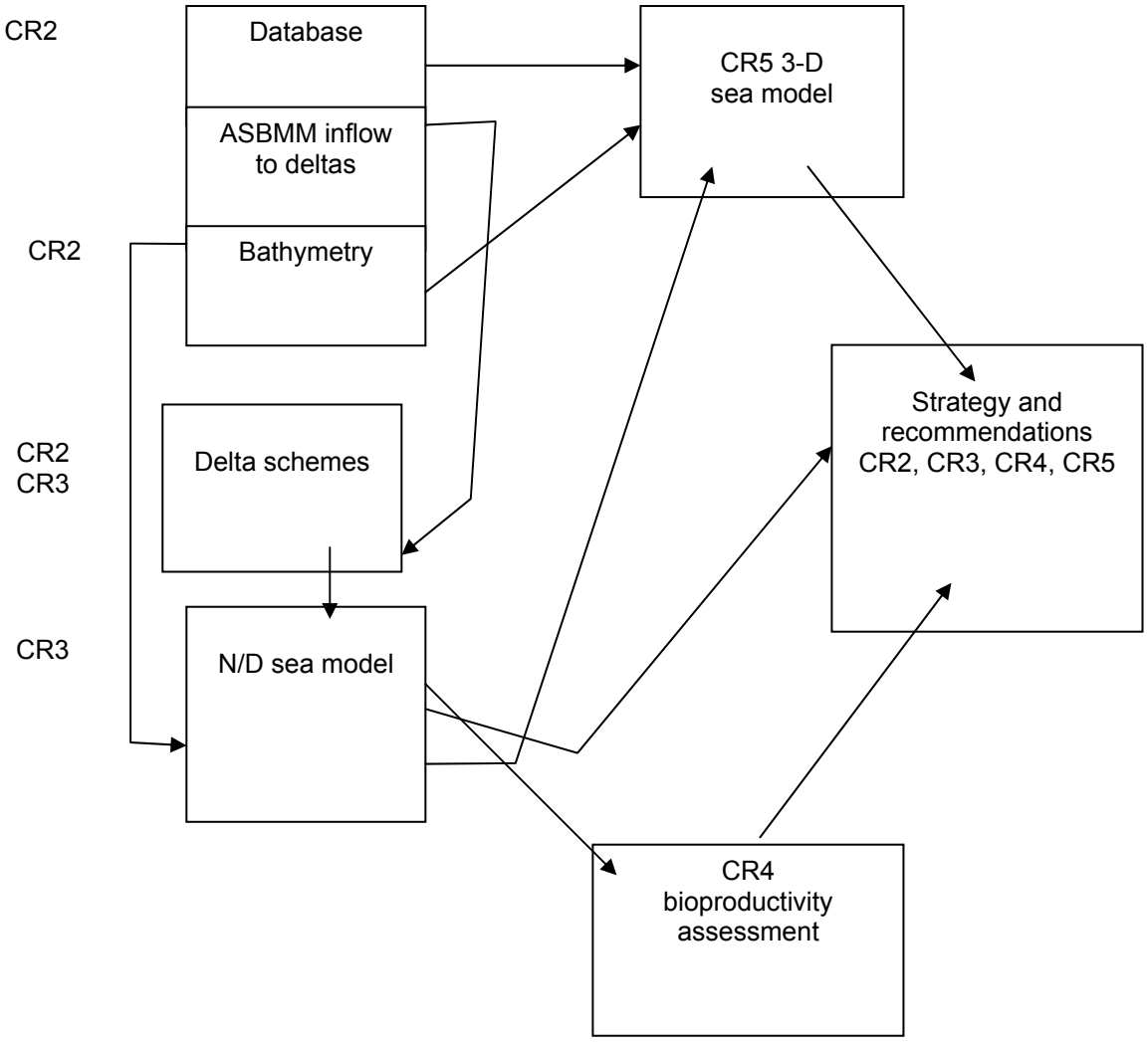

Fig. 1.1 Diagram of interlinking and sequence of tasks within the INTAS Project

2. The Aral Sea and its basin

Probably, most in the world and the former Soviet scientific literature sources and research are dedicated to history and phenomenon of the Aral Sea. Though references to the Aral Sea were not found in the Greek and Roman sources, the Arabian literature, records of scientists from ancient Khorezm and the Holy Book of Avesta have mentioned the Aral Sea (Varakhsha in Avesta and Dengiz as attested by Al Beruni) when telling about Oksa (Amudarya) and Aksarta (Syrdarya). Rene Letal and Monica Mainglo have given detailed description of Aral bibliography in their monograph "Aral"[*]. In 1995, L.A. Trouw by his book "The Interrelationship between Irrigation, Drainage and Environment in the Aral Sea Basin" contributed to synthesis of various sources on the Aral Sea and its basin. Finally, SIC ICWC published in 1999 the detailed bibliography «Problems of the Aral Sea Basin" (UNDP), which contained titles and abstracts of more than 2000 literature sources.

Based on all available materials, in our work "South Prearalie – New Perspectives" (ICWC, Tashkent, 2003) we have summarized modern views of Aral dynamics – prehistoric, historic, and present – that is briefly described below. The hypothesis regarding the prehistoric period is based on geological surveys of Russian researchers carried out at the end of the nineteenth century and the beginning of the twentieth century and it proved that in the *post-Pliocene epoch* the part of the Karakum Desert between cliffs of the Usturt Plateau in the north and the mouths of the Murgab and Tedjen rivers in the south, and the Kopetdag Mountain foot in the west had been flooded by the Big Aral Sea. The eastern half of the united Caspian-Aral Sea had, in their opinion, a cliff of the Unguz shoreline as the border of the former Karakum Bay. This united sea had covered a wide strip of the present pre-Caspian area right up to a foot of the western Kopetdag ridges, and linked with Karakum and Chilmetkum bays by two straits - the Bolshoy Balkhskiy and Maliy Balkhskiy. At that time the Aral part of the united sea flooded entirely the Sarykamysh depression and formed the bay stretched out to the Pitnyak, which is now occupied by the present-day delta of the Amudarya and the Khiva oasis (as well, this explains the presence of salts deposit at the Pitnyak). The Uzboy Strait had linked both water areas, but it is obvious that its form with steep slopes arose due to separation of the Caspian Sea from the Aral Sea and increase in their water surface elevations. During the subsequent geological epoch and to our time, division of the united Aral-Caspian into its component parts and its gradual reduction up to the current boundaries took place. At first, the watershed between the Aral-Sarykamysh and the Caspian Sea at Balla Ishem on the Usturt Plateau formed, and then the Uzboy river channel gradually developed. The sequence of desiccation is confirmed by layers of transition deposits from the latest Caspian mollusks burials (along the former Uzboy river, in the sands of the Chilmetkul, and along the south-eastern shoreline of the Caspian Sea) covered by incoherent sands with sparse and young vegetation to ancient formations in the Central Karakum Desert, which have transformed into sors (deposits of super-salty water bodies under drying up), takyrs, compacted sand hills overgrown with woody vegetation. Sors, being the lowest places of the sea bottom and fed by saltish artesian water, kept the pattern of ancient coastal lakes.

Since the ancient times, all the researchers and historians were describing transformations of the Aral and Caspian seas depending on water availability and irrigation development in their united drainage basin. They have confirmed the fact of complete desiccation of the Sarykamysh Lake by the end of the sixteenth century, when inflow of the Amudarya River into the Sarykamysh Lake via the Kunya-Darya, Daudan and Uzboy rivers had stopped. At the section from the Caspian Sea to the Bally Item watershed, the Uzboy channel is lifting by 40 m at a distance of more than 200 km. According to V. Obruchev, the existence of the Sarykamysh Lake took place during the period since the VII century B.C. until the XVI century A.D. On the way to Khiva, in 1559, Jenkinson has observed the presence of the Sarykamysh Lake, which he recognized as the inflow of the Oksus into the Caspian Sea. He also relied on the similar evidences of Abdulghazi-Khan, Ghamdudla and other chroniclers of Khorezm.

Based on geological and historical investigations, most researchers (B.V. Andrianov, A.S.Kes, P.V. Fedorov, V.A. Fedorovich, Y.G. Maev, I.V. Rubanov, A.L. Yanshin and others) have came to the almost unanimous conclusion, which was well formulated by N.V. Aladin: "in prehistoric times, changes in the Aral Sea level and salinity took place due to natural climatic changes". During the humid climatic phase, the Syrdarya and Amudarya rivers were abounding in water, and the lake reached the maximum level of 72 to 73 m +BSL.

In contrast to that, in arid climatic phases both rivers became containing little water, the Aral Sea level also dropped, and the salinity level increased. In historical times, during the existence of the ancient Khorezm, the changes in the water level depended to some extent on climate change, but mainly on irrigation activity in the basins of two rivers. In the periods of intensive development of the countries adjacent to the Aral Sea, the increase in irrigated areas resulted in withdrawal of most of water for this

[*] Springer – Verlag France, Paris, 1993

purpose, and the sea level had immediately dropped. Unfavorable periods (wars, revolutions, etc.) in the region were followed by reduction in irrigated areas, and the rivers filled up again.
The Amudarya and Syrdarya rivers changing regularly their flow direction and migrating throughout Central Asian in the historic period have not often reached the Aral Sea, and as a result the sea has dried up and a desert zone has formed on its territory. At the same time, as the sea was drying up, water salinity was considerably increasing and promoting precipitation of salts, which were found by the geologists at the bottom of the Aral Sea. Thick layers of mirabilite precipitations are especially impressive. The migration of both the Amudarya and Syrdarya deltas has established a very peculiar downstream area, where the depressions filled with boggy deposits alternating with deserted, fine-silty, and sandy deposits that formed the delta and the most part of the Amudarya River bed itself and its branches.
Table 2.1 prepared by us on the basis of extracts made from numerous historical sources and the latest research, shows the interaction between the rivers, the Aral Sea and the Uzboy Channel, through which a share of waters from the Amudarya flowed into the Caspian Sea. The occurrence, in the late Stone Age, of cross-flow from the Amudarya River (about 20 percent of river flow) via two united lakes Sarykamysh and Assana-Audan and through the Uzboy channel to the Caspian Sea has formed the unique and periodical linkage between the Aral Sea and the Caspian Sea (Table 2.1).

Table 2.1 Historical sources regarding water systems in Central Asian

Dates	Source	Conditions of the Aral Sea	Conditions of the Uzboy channel	Level of the Caspian Sea with respect to that of 1990, m + BSL	Note
5th century B.C.	Herodotus	the sea exists	Uzboy = Amu Darya		
3rd century B.C.	Patrocle	filled up with water	dry		The Amu Darya and Syr Darya flow into the Aral Sea
1st century B.C.	Strabon	the Amu Darya and Syr Darya rivers flow in, but the latter not to full extent	Amu Darya	+ 25	
891 A.D.	Al Balkhi	the sea exists	along the Uzboy Channel to the Caspian Sea	+ 9.8	
10th century	Idrisi	the sea exists		- 4.2	
1211	Jiveni Murkhand	almost dry	with flow		Descendants of Genhgis Khan diverted the Amu Darya from Khiva
1320	Marino Sanuto	mean level	Flow through the Uzboy channel from the Sarykamysh Lake into which the Amu Darya empties		The Small Aral is identical to a small lake (Sarykamysh)
1375	Catalonia	the sea exists	with flow	+ 5.64	The Syr Darya flows into the Aral Sea and Amu Darya flows into the Sarykamysh Lake
	Sanuto	the sea exists	with flow		
1400	Merashi	low level			
1575	Abul Ghazi	high level	dry		
1638	Olirey	low level	with flow	+ 5.34	The Amu Darya and Syr Darya flow into the Aral Sea
1680	Abdul Ghazi Baghadur	the sea exists			The Amu Darya empties into the Caspian Sea, since 1220 and finally they were separated in 1575
1734	Kirilov	not mentioned	alternates	+ 4.03	
1826	Kolodkin	high level	not shown	+ 3.12	
1858	Ivanichev	high level	dried	+ 0.99	

At present, it is clear to a certain extent that (according to the recent radiocarbon measurements of bottom sediments) the Aral Sea has undergone five or seven transgressions, out of which the strongest ones formed the highest terraces (elevations of 72 to 73 m + BSL), pertaining obviously to the early Pliocene (A.V. Shitikov) or to the Akchagyl period (Fig. 2.1).

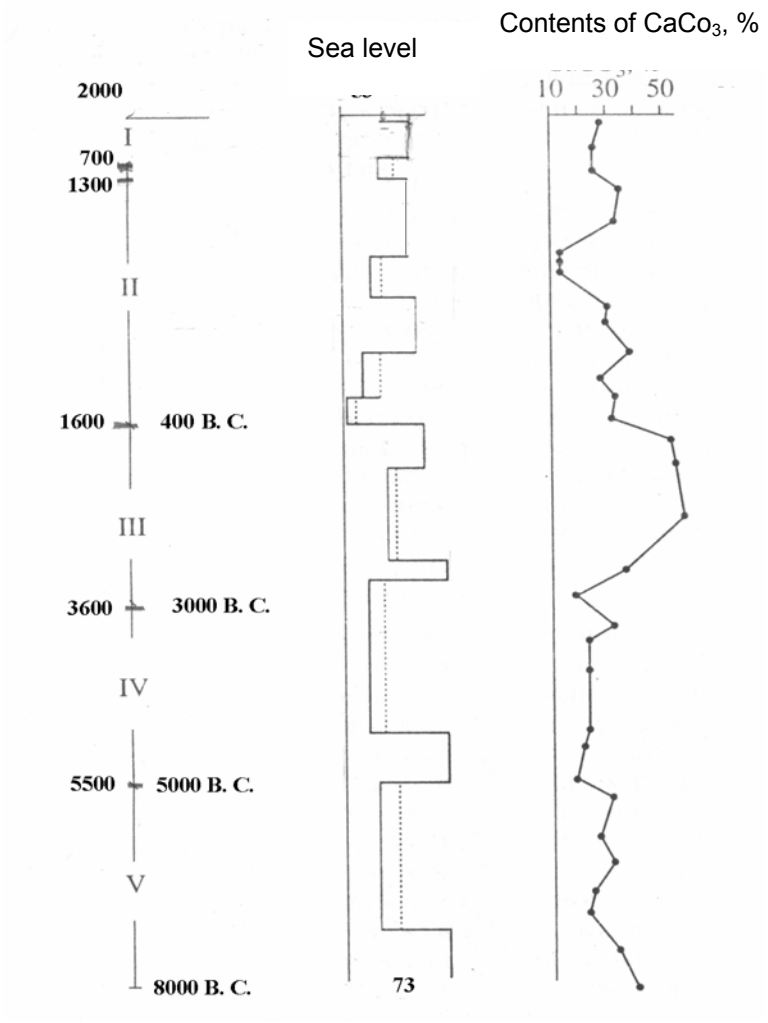

Fig. 2.1 Historic Development of Sea Level and $CaCO_3$ Concentration

The source of such high flooding is not clear. This might be either consequences of melting of northern ice masses, as V.A. Kovda and V.V. Yegorov have supposed in their work “Behavior of salt accumulation in the Aral-Caspian lowland” (the Academy of Sciences of the USSR, 1956), or water inflow of the Great Amudarya, which was mentioned in the Avesta (supposedly, this river has united not only waters of all the Great Amudarya tributaries including the Zeravshan, Tedjen, Murghab but also the Syrdarya and Chu prior to damming the Buam isthmus).

In this context, the results of revising the investigations of P.I. Chalov and others (1966) carried out by A.S. Kes are of interest. The first stage of the Aral depression flooding began in the late Pliocene. At that time, western plains in Central Asia were flooded at first by water of the large Akchagyl Sea, and then by the Apsheron Sea. Their eastern border was not determined, but fauna, terraces and beach ridges dated by this age are found in the Sarykamysh and Assaka-Audan, Aral Sea depressions, and in some depressions of the Kyzylkum desert.

The modern period of the Aral depression flooding began in the 1st millennium B.C., when the Amudarya having formed the pre-Sarykamysh and Akchadarya deltas moved towards the Aral depression and together with the Syrdarya, which flowed through the Janadarya and Kuvandarya channels, started filling it up and formed the modern sea.

At the beginning of the 19th century, the Aral Sea level was low. In 1845 and after the 1860s some increases in the level were observed. At the early 1880s, the level became unusually low; the researchers of that time came to the conclusion that progressive reduction of water resources in Central Asia was taking place.

However, in the 1880s the Aral Sea level began rising, at first rather slowly, then more quickly. That continued till 1906. The level stopped changing in 1907, and then it increased again in 1908 and lowered in 1909. The rise was registered once again in the period since 1910 until 1912, and then the level slowly changed till 1917. The decrease began after the year 1917, which is known by the high level of aridity in

Central Asia. By 1921, the level of the sea had reduced by 1.3 m in comparing with 1915. However, the observations in 1924 showed new increase (a little less than by 0.5 m).
Since late XIX century, tsarist government and then the Soviet government had intensively used the Aral Sea basin for irrigation development. However, by 1960, increased water withdrawals for irrigation had been compensated by increased return flows due to construction of collector-drainage networks in old and new irrigation areas. Interaction between the rivers and the sea is shown in Table 2.2.

Table 2.2 Mean annual water balance values of the Aral Sea for different periods

Periods (years)	Inflow				Outflow (evaporation)		Water balance		Actual increment		Odds	
	River runoff		Precipitation						In volume	In level		
	km^3	cm	km^3	cm	km^3	cm	km^3	cm	km^3	cm	km^3	cm
1911-1960	56.0	84.,7	9.1	13.8	66.1	100.0	-1.0	-1.5	0.1	0.1	-1.1	-1.6
1961-1980	30.0	48.9	7.1	11.8	59.7	99.4	-22.6	-38.7	-22.8	-39.1	0.2	0.4
1971-1980	16.7	29.3	6.2	11.0	53.7	95.4	-30.8	55.1	-32.3	-57.1	1.5	2.2
1981-1990	3.45	8.04	7.1	16.5	40.4	94.1	-29.8	-69.5	-30.4	-73.2	1.6	3.7
1991-1999	7.55	26.5	5.8	20.4	28.1	98.6	-14.8	-51.9	-17.5	-41.8	2.2	10.1

The modern period of the Aral Sea, since 1961, may be described as the period of active anthropogenic impacts on its regime. Drastic increase of irretrievable river water withdrawal (which amounts to 70-75 km3/year in recent years), exhaustion of compensating abilities of the rivers, and natural aridity in 1960 to 1980 (92 percent) resulted in disequilibrium of water and salt balances. The considerable exceeding of evaporation over the sum of all inflow constituents1 was typical for the period of 1961 to 2002. The river water inflow into the sea has decreased in 1965 up to 30.0 km3/year; in 1971-1980, it amounted to 16.7 km3/year, on average, or 30 percent of mean annual runoff, and over the period since 1980 till 1999 it made up 3.5 to 7.6 km3/year or 6 to 13 percent of the mean annual runoff. During some dry years, runoff of the Amu Darya and Syr Darya rivers has not actually reached the sea.
River water quality has also changed owing to increase of share of highly saline waste and drainage water that resulted in a significant increase of salinity and deterioration of river sanitary conditions. During dry years, the mean annual salinity of the Amu Darya water entering into the sea reaches 0.8-1.6 g/l, and salinity in the Syr Darya amounts to 1.5-2.0 g/l. In some seasons, higher salinity levels are observed. As a result, in spite of decrease of annual river runoff by 46 percent over the period of 1961 to 1980, the annual salts entry has decreased only by 4 million metric tons or by 18 percent for the same period. Other constituents of the salt balance have also substantially changed. Due to decrease of carbonates content in the river inflow, sedimentation of salts under mixing of river and marine waters was reduced by two times.
As a result, since 1961 the sea water level has steadily dropped. The total sea level drop, in comparison with the average annual value (prior to 1961) has reached 12.5 m by the beginning of 1985. The average annual rate of the sea level dropping was about 0.5 m, reaching 0.6-0.8 m/year in dry years. The annual sea level fluctuations were also changed. At present, the annual sea level rise is practically not observed, at best, it does not change in winter, and in summer an abrupt drop takes place.
The gradual drop in the sea water level has considerably exceeded predicted rates. Modeling carried out by the State Institute of oceanology (Dr. V.N. Bortnik) in 1983 has predicted that by 1990 the sea water level would reach 41 to 42.5 m + BSL at probability of 90 percent, and by 2000 - 35.5 to 38.5 m + BSL. In fact, as Table 1-2 shows, by 1990 the sea water surface elevation was 38.24 m +BSL, and by 2000 – about 34 m +BSL. Similarly, seawater salinity has increased at higher rates - by 1990, it was 32 percent instead of predicted 26 percent, and by 2000 it was 40 percent instead of predicted 38 percent: by 2000 the sea water surface decreased by 34 m +BSL against the expected 38, 5 m +BSL.
The sea level drop and water salinization have resulted in an increase in the amplitude of annual temperature over an all water column and in some shift in phases of the temperature regime. Modification of winter thermal conditions is the most important factor for the biological regime of the sea. Further lowering of a freezing point and modification of the autumn-winter convection mixing process under transition from brackish to high saline waters cause intensive cooling of all sea water mass to very low temperatures (-1.5 to - 2.0o C). This is one of the main factors restricting implementation of

[1] It was only in 1998 when the inflow of 29.8 km^3 exceeded evaporation of 27.49 km^3

acclimatization measures and hindering rehabilitation of fishery in the sea in the nearest future. Lowering the sea level may result in rather noticeable modification of ice conditions, and even in moderate cold winters, ice cover of the entire sea water area with a maximum thickness of 0.8 to 0.9 m may be expected. Cooling and freezing of the sea will occur approximately during the same periods of time; however, reduction of its total heat storage will cause more rapid ice spreading. Increase in a mass of ice per unit area will lead to a more prolonged period of ice melting.

Extremely low specific values of biogenic substances inflow into the sea predetermine their low concentrations in seawater, further constraint for development of photosynthetic processes in the sea, and its low biological productivity. Deteriorating of the oxygen regime of the sea in summer owing to decrease in photosynthetic production and intensive oxygen consumption for oxidation of an organic substance causes formation of oxygen deficit zones and kill phenomena.

Further salinity increase causes both reduction of species of phyto- and zooplankton, phyto- and zoo benthos, and appropriate reduction of their biomass resulting in further degradation of food resources for aquatic life. The existence of endemic fauna is impossible owing to increase in the Aral Sea water salinity.

Quantitative assessment of anthropogenic factors affecting the current water regime of the Aral Sea was carried out by means of calculation of reconstructed values of sea levels and salinity for the period of 1961 to 1980 using the values of reconstructed conditional-natural inflow into the sea. According to these calculations, more than 70 percent of current sea level lowering and of salinity increase are caused by the anthropogenic impact, the rest of these changes are implication of climatic factors (natural aridity).

Major consequences of the Aral Sea shrinkage, apart from the decrease of its water volume and area, increase in water salinity and modification of salinity pattern is the formation of a vast saline desert with the area of almost 3.6 million ha on the exposed seabed. As a result, a huge bitter-saline lake and a vast saline desert located at the interfaces between three sand deserts have replaced the unique freshwater water body.

After separation of the Small Aral Sea from the Large Aral Sea, their regimes started developing according to different scenarios. Since the Syr Darya River inflow has been higher than the Amu Darya river inflow, the Small Aral Sea level started rising and water salinity decreasing. A break in the Small Aral Sea temporary dam caused the water level to lower; however, previous filling has proved the correctness of the decision to create the separate Small Aral Sea at the elevations of 41 to 42.5 m + BSL. The developed project of an engineered dam, with a regulated spillway in the Berg's Strait, will provide the possibility of establishing a sustainable ecological profile of this water body and its environment.

Thus, the Aral Sea has transformed from being an integral water body in the past into a series of separated water bodies each with its own water-salt balance and own future depending on what policy will be selected by five countries that are economic entities of these river basins.

3. Socio-economic and Environmental Consequences of Water Sector Development "vis a vis" the Aral Sea Drying Up

The Aral Sea is an inland catchment basin, which is not linked with the open sea, and therefore ant changes in its natural inflows and increase in water use in the basin and adjacent area should lead to decreased inflow to the Sea and, consecuently, to its degradation. Pioneer ideologists of irrigation development in Russia clearly understood this in the beginning of 20 century. This idea was ventilated as early as in 1908 by A.I. Voyejkov and then in 1913 by the head of the water sector in the former tsarist Russia V.I. Masalsky. He considered that a final goal was "use of all water resources of the region and creation of new Turkestan…, developing million hectares of new lands and providing cotton demanded for Russian industry… ".

This strategy followed in former tsarist Russia and then in Soviet Unions was also practiced by the U.S. Government in developing all water resources in the rivers such as Colorado, San Joakin, by African countries in Chad and Victoria lake basins and in many other places of the world.

Since 1960, intensive development of irrigated agriculture and water sector provoked by rapid population growth and, at the same time, by industrial development undoubtedly has had positive impact on social development in the Aral Sea region, despite the resulted great increase in withdrawals from the rivers and, respectively, decrease in inflow to Aral. Table 3.1[2] shows basic parameters of water use in the Aral Sea basin. These parameters indicate that since the moment the Aral Sea level started to drop, water withdrawal increased 18 times, but at the same time population grew 2,7 times, irrigated areas - 1,7 times, agricultural production - 3 times, and gross domestic product almost 5 times by 1990!

[2] «Irrigation management for combating desertification in the Aral Sea basin. Assessment and tools» edited by L.S.Pereira, V.A.Dukhovny, M.G.Horst, Tashkent, Vita Color, 2005 – 422 p.

Table 3.1 Water use dynamics since 1960

Parameter	Unit	1940	1960	1970	1980	1990	2000	2003
Population	10^6	10.6	14.1	20.0	26.8	33.6	41.5	43.78
Irrigated area	10^3 ha	3.8	4510	5150	6920	7600	7890	7900
Total withdrawal,	km^3/yr	52.3	60.61	94.56	120.69	116.27	100.87	118
of which , irrigation	km^3/yr	48.6	56.15	86.84	106.79	106.4	90.3	109.56
	m^3/ha	12800	12450	16860	15430	14000	11445	13868
Water use	m^3/person /yr	5000	4270	4730	4500	3460	2530	2695
GDP	10^6 $US	12.2	16.1	32.4	48.1	74.0	54.0	34.4

During last three decades of the Soviet era (1960 … 90), irrigated agriculture and associated sectors, including industrial production for irrigated agriculture, agricultural product processing, hydrpower, construction and operation acconted for more than 50 % of the total gross product in the region[3] and provided most job places for rural people, which averaged 60 % of the total population. GNP growth for these thirty years in water-using sectors was almost 30 billion US$ under economic system of the former USSR. However, even now given the sharp landslide of agricultural production prices, this increase, in absolute values of 1960, is more than 10 billion US$/year despite the fact that production share of water sector, including agriculture, hydropower, and associated sectors has fallen to 18 … 24 % in different countries in the region by 2000.[4] Undoubtedly, sharp setback in regional production as a whole, increased share of mineral, particularly fuel extraction and processing, decreased attention to water sector have affected water use efficiency. And it was significant that observed decrease in water use regarding the environmental indicators was found to be much less than decline rates of many industrial production sectors.

It should be fairly noted that volumes of GNP and agricultural production could be much higher on the basis of water sector development if two probable ways for improving efficiency of multipurpose water use were taken into account in Soviet time:

- intensive application of water conservation technologies as was practiced in old irrigation systems in Hunger, Karshi, Kzylkum steppes, where the system efficiency reached 0,75 instead of 0,56 … 0,60 on average and the water productivity was 0,2 … 0,3 $/m^3$ against the average one of 0,11 … 0,13 $/m^3$[5] in the basin;
- elimination of low processing level of irrigated agriculture's output in the region rather than aiming at meeting demand of the center of empire for raw materials and improvement of employment through wider involvement of population in production of final output. Currently Kazakhstan, Turkmenistan, and Uzbekistan have taken this path but time was lost.

Calculations show that if the above positions were taken into account during the Soviet period, the total water withdrawal could be limited at a level of 86 – 95 km^3/year so that the Aral Sea surface would be at 35 m +BSL.

Nevertheless, one cannot but admit as economically sound for that period of time – to ensure substantial growth of national income in the region through development of water sector that yielded billion dollars annually under the total environmental and social losses from the sea level dropping and from all associated costs within 200 million dollars a year. These figures were obtained by researchers from a number of European and Russian institution together with SIC ICWC when evaluating socio-economic and environmental damage at the level of 2002[6] (it was comprised of the following components) (Table 3.2):

[3] Dukhovny V.A., Water management system in irrigation zone, 1984, publishing house Kolos, Moscow, 1984, 255 p.
[4] Dukhovny V.A., Sokolov V.I., Lessons on cooperation building to manage water conflict in Aral Sea Basin, Paris, UNESCO, PCCP, 2003
[5] Dukhovny V.A. et al. Scientific and technological process and land reclamation in Central Asia, Tashkent, «Mehnat», 1985, 141 p.
[6] INTAS – Арал – 2000-1059 Economical assessment of joint and local measures for the reduction of socio-economical damage in the coastal zone of Aral Sea, Vienna-Amsterdam-Moscow-Almaty-Tashkent, 2004, 156 p.

Table 3.2 Elements of damage from ecologic disaster – Aral Sea shrinking in Kazakh and Uzbek Prearalie, million USD/yr

Damage elements	Kazakh Prearalie	Uzbek Prearalie
1.Losses in agriculture, total	25,8	38,31
2. Losses in recreation and tourism	4,3	11,16
3. Indirect losses in industry	5	52,42
4. Maritime transport decline	0,3	1
5. Social losses	14,1	8,24
TOTAL	49,5	111,13

Thus, total direct and indirect social-economic losses from ecologic catastrophe in Prearalie amounted to 160,63 million USD/yr.

4. Dynamics of Aral Sea Transformation and Bathymetric Curves

4.1 General description of the Aral Sea

The Aral Sea is situated in the Northern desert part of Central Asia, within the territories of riparian states of Uzbekistan and Kazakhstan. The place near the Amudarya mouth was called as Aral, and later this name was given to the whole lake. Geologically, the Aral Sea is young; its age is 139±12 thousand years. During the Elephantine epoch, three deep depressions such as Aral, Khorezm, and Sarykamysh were formed due to intensive tectonic activities in the center of Turan plain in Central Asia. At the same time, the predecessor of the Amudarya – PraAmudarya flew through the center of Karakum desert westward to the Caspian (Khvalynskoye) Sea. About 70 thousand years ago, the river turned to the north and by cutting deep canyon near Tuyamuyun it reached the Khorezm depression, where a vast lake was formed. In the late pleistocene (10-12 thousand years ago) the Amudarya (Dzheikhun) turned to the west and reached the Sarykamysh depression while changing the latter into a lake. About 4 thousand years ago, the Amudarya turned to the north and flew into the large Aral depression, into which the Syrdary already flew. That time, a vast plain, with dissected relief, was bordered by the Ustyurt chinks in the west, Priaralsk Hills in the north, Betpak-Dala desert and Karatou mountain range in the east, and Karakum and Kyzylkum deserts in the south.

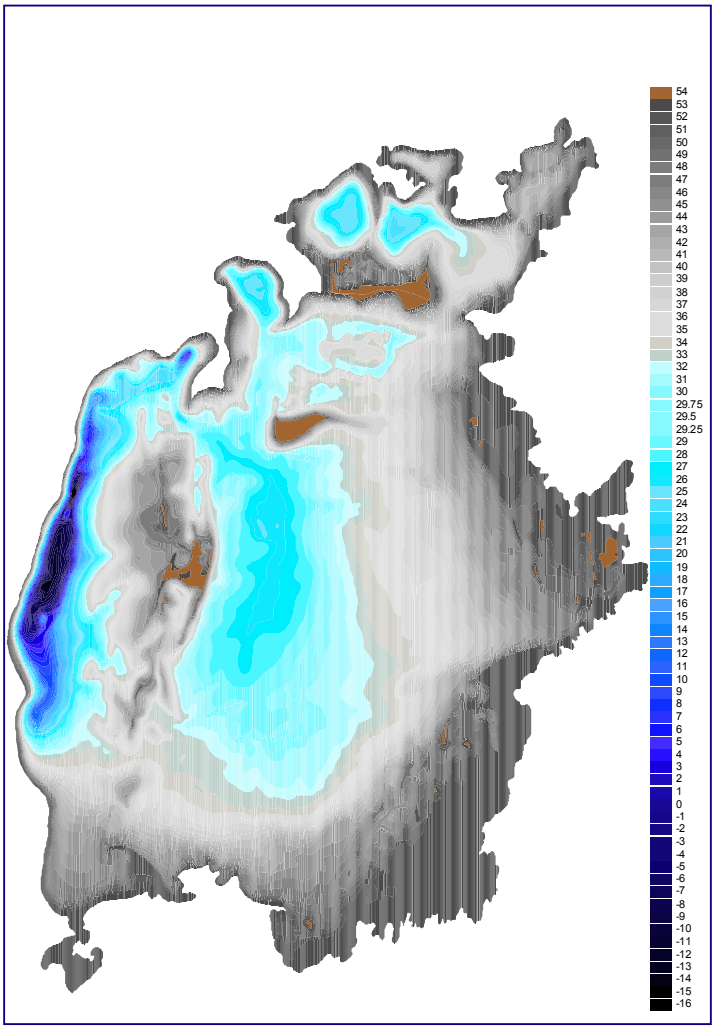

Fig. 4.1 Bathymetry of the Aral Sea Area

Sink of the Aral Sea (Fig. 4.1) has complex structure. Eastern and Western parts of the Large Sea and three less deep depressions in the Small Sea have formed the asymmetric sink of the Aral Sea, which under the sea level dropping, since 1960, was gradually divided into Small and Large Seas at the altitude of

39 m, with the Large Sea divided into Eastern and Western parts at the altitude of 29 m. Western sink is deepest and stretches north southward along the Ustyurt chink.
Between 1900 until 1960, during the period of sustainable ecosystem of the Aral Sea at an altitude of 53 m, which is almost 80 m higher of the altitude in the Caspian Sea, the sea width was 265 km in parallel 45°, while the shoreline length was more than 4430 km. Water surface area of the sea until level lowering in the 1960s of XX century was 69,79 thousand sq.km, and the maximum depth was 69 m, while the water-mass volume was about 1056 cubic km.
During that period of time, about 1100 islands (area more than 0,01 km^2) totaling 2235 km^2 were present in waters of the Aral Sea. All the islands are of land origin and the largest of them are (Fig. 4.2):

- Kokaral, area - 311 km^2
- Barsa-Kelmes, area - 170 km^2
- Vozrozhdeniye, area - 169 km^2
- Small offshore islands (periodically flooded), area - 1585 km^2.

Peculiar Akpetkin (Karabaily) Archipelago was situated in the south. More than 50 islands of the Archipelago constituted sand belts of Kyzylkum underflooded by sea waters. Small offshore islands together with bays, capes, separating reservoirs and larger islands had formed specific type of coasts that played important role in stabilization of sea's chemical regime.

Hydrological regime of the Aral Sea, as of most inland reservoirs in arid zone, is subject to large fluctuations under influence of natural and anthropogenic factors. Geological, geo-morphological, and archeological research in the Aral Sea area showed that in recent 4-5 thousand years the amplitude of level fluctuations has been about 20 m, and the lowest regression has been observed 2 thousand years ago (Fig. 4.3).

The level regime over 1700-1990 was reconstructed by L.S.Bergh and V.P.Lievov, and they estimated fluctuation amplitude at 3 m during this period. Level fluctuations in Aral have been observed recently as well, but their amplitude did not exceed 4 m in recent 200 years and was within 1 m in the first half of previous century. In the 1950s of XX century, ecological situation in the region was quite stable.

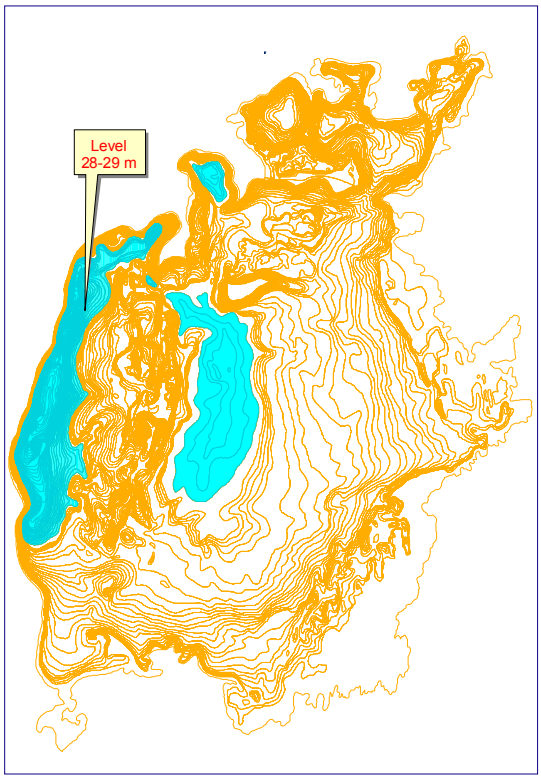

Since the beginning of systematic observations of the level, 2 periods have been identified [1]:

1. Conditionally natural - 1911-1960 – with relatively stable hydrological regime, fluctuations in the level approximately at the altitude of 53 m, and the amplitude of inter-annual fluctuations at not more than 1 m.
2. Intensive anthropogenic impact - since 1960 until now.

Starting from 1960, the sea level has been lowering. This has led to reduction of the water surface area, decrease in water volume and depths, and great change in shoreline configuration (Fig. 4.4).
The Table 4.1. gives the morphometry of the Aral Sea for 1960-1985, when the sea was an integral water reservoir. The below table indicates to slight water level lowering until the 1970s. For example, for the period of 1960-1970 the sea level decreased by 2 m, i.e. the mean water level lowering was 1 m in 5 years. The sea level lowering has visibly intensified since the mid-seventies due to irrigation withdrawals of natural river flow. In the period of 1975-1980, the sea level decreased by as much as 3,26 m, i.e. 0,65 m a year on the average. The most intensive sea level lowering took place when flow of the Amudarya did not reach the Aral Sea.

Fig. 4.2 Lowest Water Level of Aral Sea about 2000 Years ago

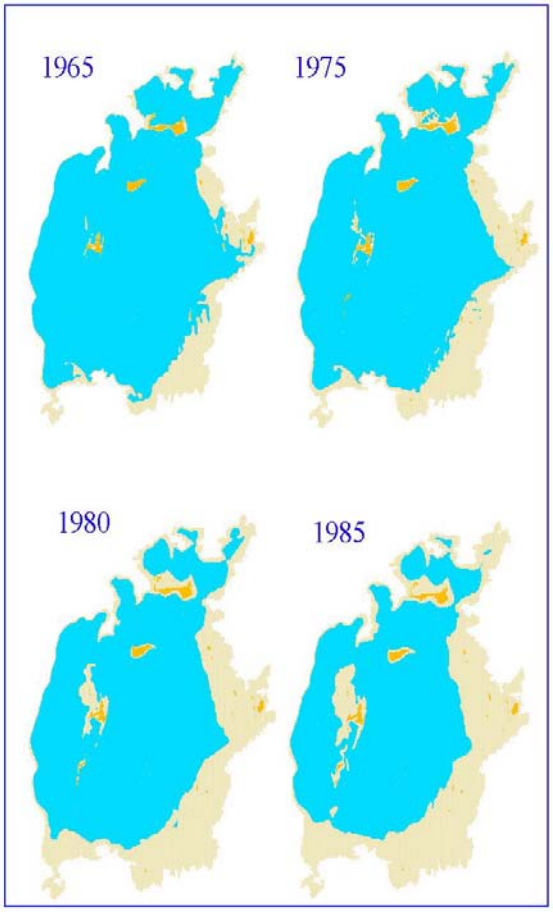

Fig. 4.3 Aral Sea Level Changes

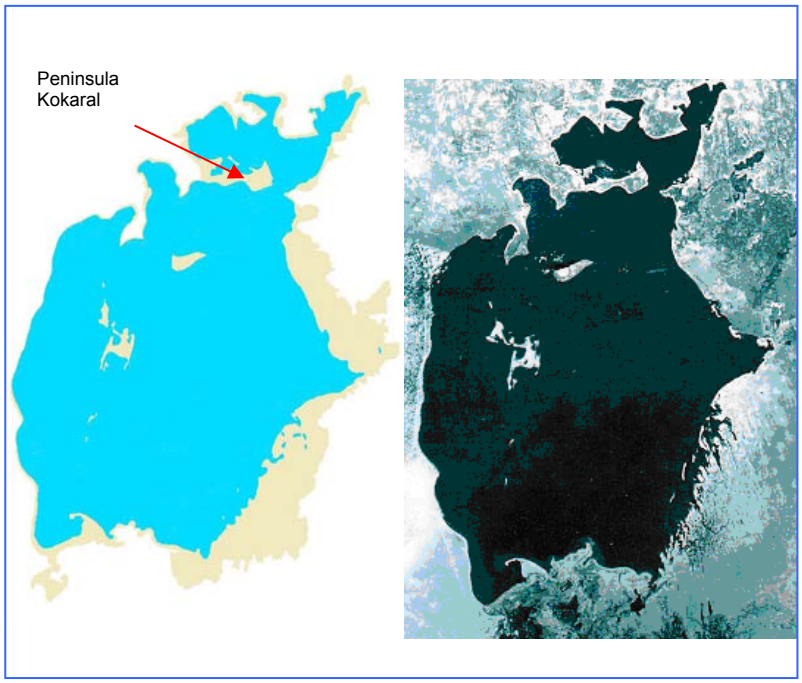

Fig. 4.4 Aral Sea as of 1975 (above)

Kokaral was the first of large islands which joined the shoreline in the west and became a peninsula, thus separating the Small Sea (Fig. 4.5). By 1986 the peninsula practically had got detached from the Large Sea while leaving only narrow flow passage. Starting from that period of time, hydrological regimes of Small and Large Seas has become distinctly different (Table 4.2). Construction of Kokaral dam, 12 km long and 8 m high, which separated Small Sea from Large Sea has contributed to changes in the hydrological regimes. Despite numerous dam breaks, the level in the Small Sea was slightly higher than in the Large Sea during the period of 1990 – 1998. The Small Sea's area varied within 2900-3200 km^2.

Table 4.1 Dynamics of key morphometric characteristics of the Aral Sea, 1960-1985

Characteristics / **Year**	Water level, m	Water-surface area, thousand km^2	Volume, km^3
1960	53,40	69,79	1056,12
1965	52,30	62,38	972,47
1970	51,43	58,92	941,23
1971	51,06	57,73	902,43
1972	50,54	56,85	875,12
1973	50,22	56,17	845,47
1974	49,85	56,01	844,46
1975	49,01	54,67	802,74
1980	45,75	49,21	631,81
1981	45,18	48,63	625,78
1982	44,39	47,13	578,65
1983	43,55	46,07	532,58
1984	42,75	44,92	487,66
1985	41,94	43,08	444,58

Table 4.2 Dynamics of main morphometric characteristics of Small and Large Seas, 1986 – 2000

Characteristic / Year	Large Sea			Small Sea		
	Water level, m	Water surface area, thousand km^2	Volume, km^3	Water level, m	Water surface area, thousand km^2	Volume, km^3
1986	41,02	38,56	380,63	40,90	2,83	22,47
1987	40,19	37,13	343,17	40,80	2,81	22,39
1988	39,67	36,18	312,65	40,50	2,75	21,84
1989	39,10	35,30	306,92	40,20	2,71	20,28
1990	38,24	33,67	280,44	40,50	2,75	21,84
1991	37,66	32,02	257,16	40,40	2,73	20,92
1992	37,20	31,83	240,17	40,20	2,71	20,28
1993	36,95	31,42	231,70	39,37	2,57	18,43
1994	36,90	31,31	229,87	40,10	2,69	20,01
1995	36,50	30,04	217,25	40,50	2,75	21,84
1996	35,48	28,54	195,63	40,50	2,75	21,84
1997	34,80	26,91	173,44	41,20	2,91	22,67
1998	34,21	25,75	168,43	42,50	3,24	27,03
1999	33,98	24,12	147,62	36,80	2,09	12,03
2000	33,50	22,93	139,53	39,80	2,62	19,26

In autumn 1989, a waterway constructed with dredger for navigation between Small Sea and Large Sea became completely silted and looked like a chain of lakes. By spring 1990, level in the Small Sea has started rising and the waterway deepened. In spring 1992, the depth of waterway connecting Small Sea with Large Sea achieved 2 m, with a length of 5 km and width of 100 m. According to Glavgidromet's measurements, overflow was 100 m^3/s in that period. In late July-early August, a dam, 1 m high, was constructed in Bergh Strait. When in April 1993 water level in the Small Sea raised to additional 1 m, the dam was broken. Break occurred in three points. Flow was restored in the old waterway where the depth of closure channel was about one meter; however, flow from the Small Sea did not exceed 100 m^3/s [2].
Next dam in the Small Sea existed from August 1996 till late April 1999. The second structure represented a blind fill dam, 12,7 km long. The crest width was 4 m, while the crest elevation was +44 m. Volume of the dam body was estimated at 980 Mm^3. Before dam break, water level in the Small Sea was 42,8 m. The outburst flood amounted to 300-500 m^3/s. The flood subsided throughout the exposed seabed, and flood-water filled local depressions and through a few small ditches reached the Large Sea. Break of Kokaral dam in April 1990 led to water level lowering by 2,5 m in the Small Sea.
Technical parameters of Kokaral dam in Bergh Strait in the Small Sea (Northern Aral Sea - NAS) are as follows: length - 13 km; crest width - 10 m; maximum height in Bergh Strait – about 3 m, with respective spillway for maintaining water level at a maximum elevation of 42,0 m. Considering process engineering and cost estimations of alternative options, preference was given to dam with beach profile: dam crest elevation is 44.5 m BS, with upstream slope of 1V:45H and downstream slope of 1V:5H (the latter is protected with gravel). Spillway structure dedicated to pass flood-water and flush reservoir from excessive salinity has a dock design, with 5,5 m high and 3,9 m wide eight openings. For passing of waste water from spillway point to natural channel connecting two (northern and southern) reservoirs, tailrace canal is planned and has the following parameters: bed width - 150 m; slope - 0,0001; depth - 2,8-3,4 m. Maximum spillway discharge will amount to 367 m^3/s. Construction of new dam in Bergh Strait and development of NAS having capacity of 27,07 km^3 and maximum water-surface area of 3290 km^2 would enable stabilization of water level in Northern Aral Sea and prevention of ecosystem degradation in the Syrdarya delta and neighboring areas.

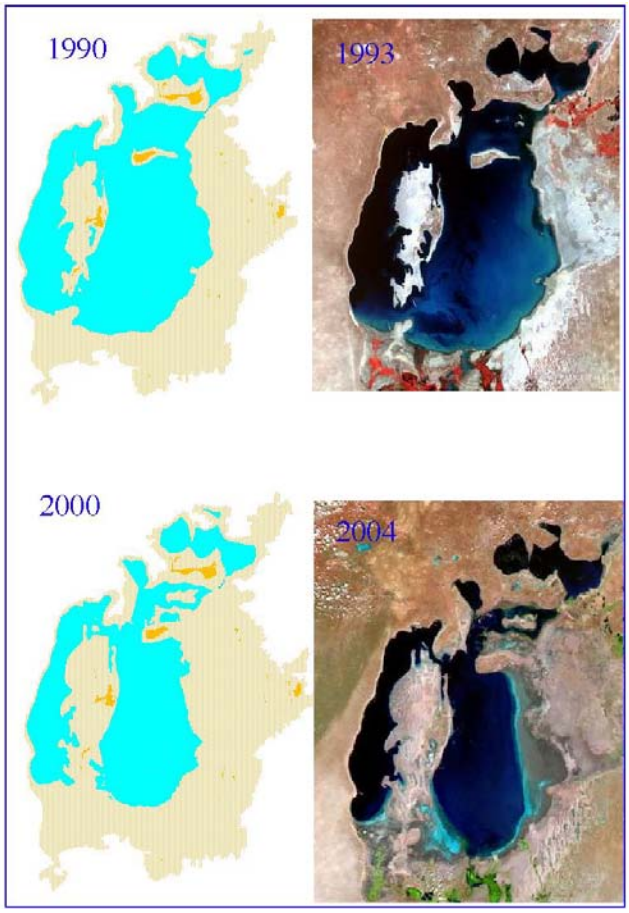

Fig. 4.5 Aral Sea Dynamics between 1990 and 2004

The ridge stretched from Myinak Peninsula to Kulunda Peninsula is a characteristic of the Large Sea's sink. While studying the Large Sea, one should note that western and northern slopes of the sink are steeper, and eastern and southern slopes are very gentle. Eastern coast, where more gentle spots of apron observed, is greatly subjected to drying off (Fig. 4.5).
Intensive reformation of coasts, generation of beach ridges, eolomotion of sand deposits from the exposed bed leads to gradual smoothing of eastern coast. Since the Barsakelmes Island joined the eastern coast, poor-indented coastal strip has been formed. This strip receded from the sea boundaries by 60-100 km in 1960. Islands of the Akpetkin Archipelago have joined to mainland and a unique Aral type of coasts has disappeared. Configuration of shoreline has greatly changed in southern coast, where Adzhibay Bay and Tigroviy Khvost Peninsula have disappeared, while Dzhiltyrbas Bay has changed into lake. More detailed description of geomorphological processes taking place on the exposed seabed is given below.

In case of business as usual, i.e. continued level lowering in the Large Sea, the sea will be divided into two individual reservoirs at the altitude of 29 m (Fig. 4.6):

1. Eastern shallow part of Large Sea;
2. Western deep part of Large Sea.

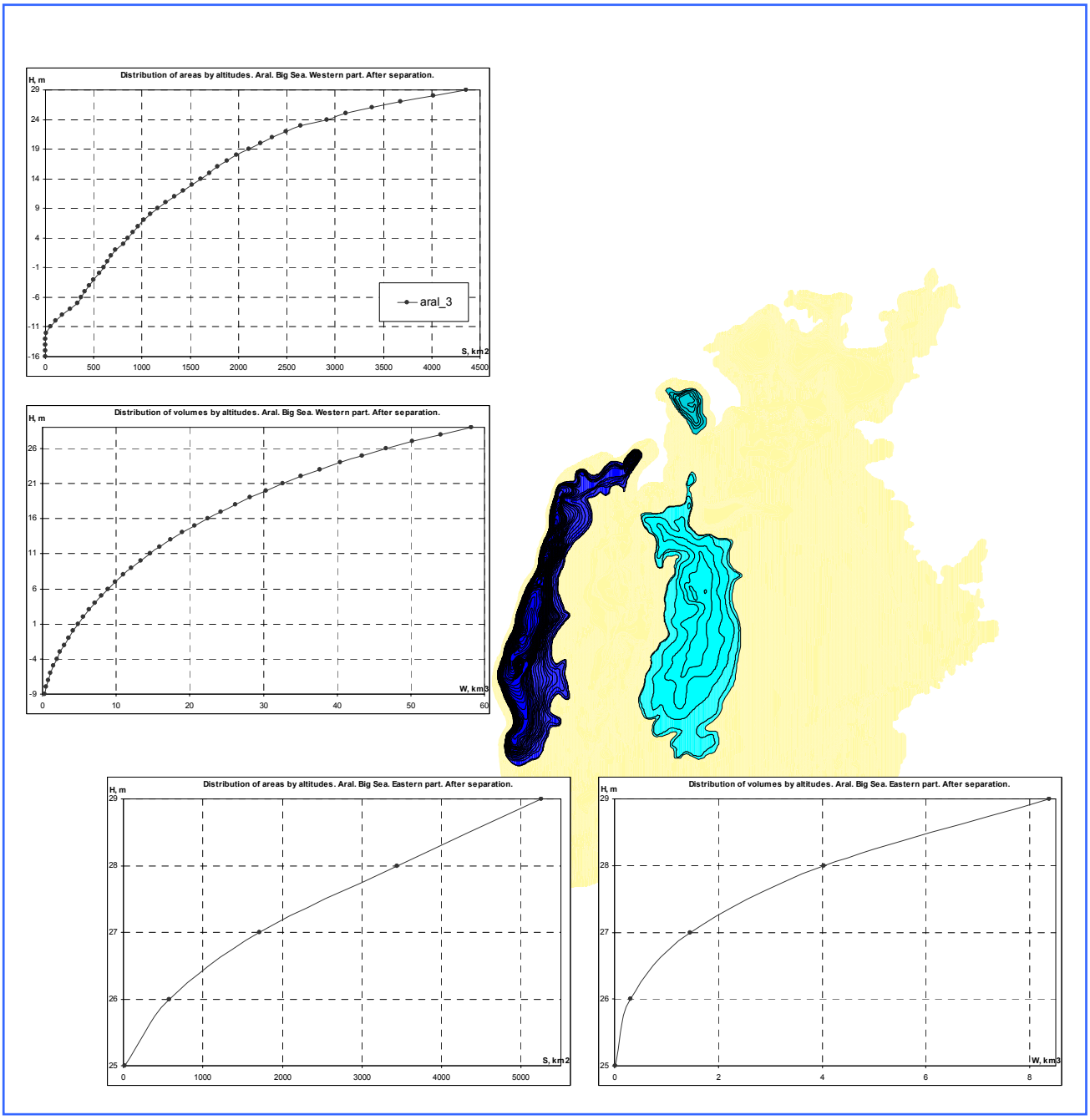

Fig. 4.6 Separation of Large Aral Sea into Eastern and Western Parts

Geomorphological processes taking place on the exposed seabed are not similar in different coasts (Fig. 4.7). This is explained first of all by type of exposed coast depending closely on its width, slope, lithology, micro-relief, salinity, etc.
Structure of the exposed bed is defined by the following:

1. Before the water level lowering in the sea, its coast had complex structure and strongly indented shoreline in all parts, besides western one due to structural and geomorphological specificities of Priaralie. The dried areas inherit basic characteristics of adjacent mainland.
2. Currently exposed area was subjected to long-term exposure of coast-based processes under level fluctuations at the altitude of +53m abs. In addition, over the last one and a half century, the sea level dropped twice to the altitude of +50m (in the 1820s and 1880s). This contributed to a vide variety of coastal forms [5].
3. According to existing coastal-marine sedimentation patterns, the dried area mostly is comprised of sands interchanged with siltstone and silt in mezzo- and micro-depressions. Lithology of zones formed under prevalent effect of original coast is defined by structural characteristics of the latter.

The dried area represents an inclined coastal strip bordered by marine terrace referred to as the terrace of the 1960s in all parts, except for live deltas [6].

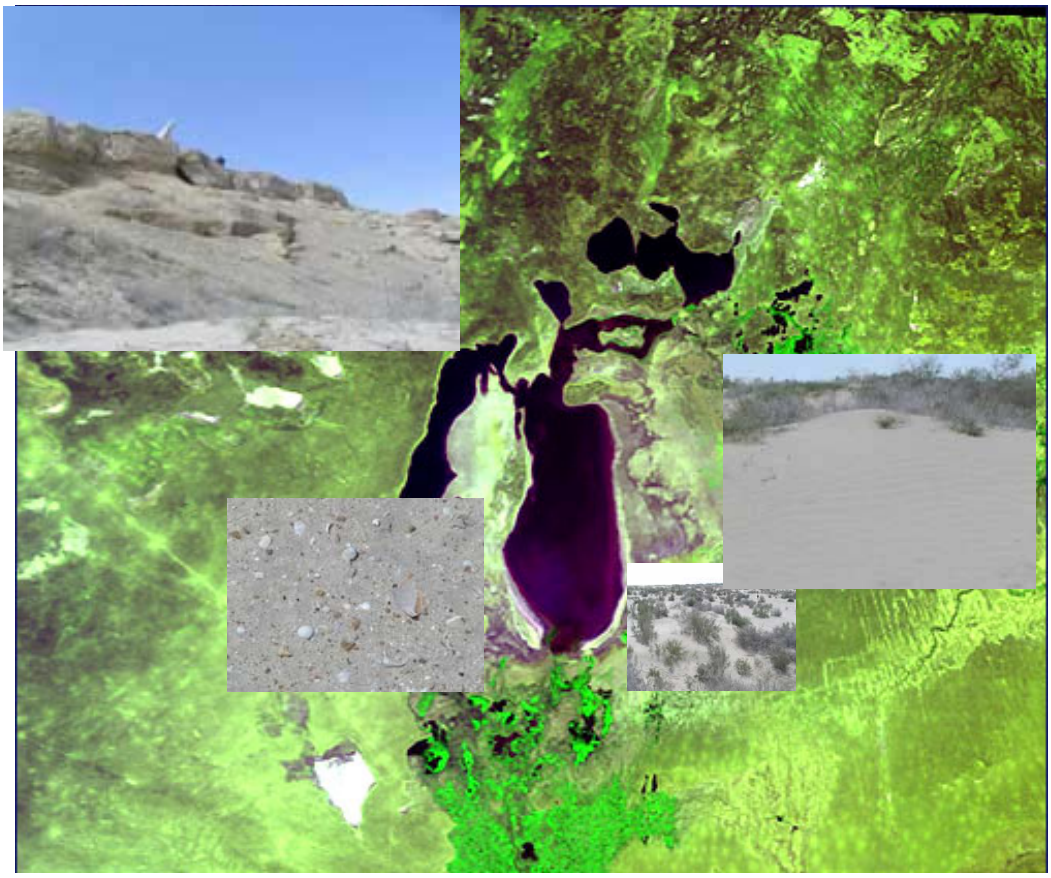

Fig. 4.7 Relief Types of Dried Coast

4.2 Relief Types of the New Coast Lines

Depending on structural and geomorphological conditions, coastal process nature and lithological characteristics, the following main relief types are outstanding (Fig. 4.8):

I. Plain of abrasion (fossil bench) develops in former cliffed parts of the coast and stretches along western and, in places, northern coast under cliffs of Plato of Ustyurt and upland outliers. The dried surface is a wave-cut terrace or platform developed on marl, sandstone, clay of Paleogene and Neogene and covered by thin (about several tens of centimeters) accumulative stratum.

II. Accumulative plain widely developed in Aral coast. The most typical is poor-inclined sandy coast strip. One characteristic of such coasts before sea level lowering was widespread development of accumulative sandy coastal strips – spits, bay bars and separated lagoons. At present, former lagoons completely separated from the sea, dried off and changed into solonchaks, while bordering them accumulative forms became a part of dried strip.

II a. Quite specific relief type is represented by the exposed bed in south-eastern coast within the former Akpetkin archipelago. Here the relief is more indented and diverse.

Two types are outstanding among the dried territories: former shelves and shallows occupying vast areas in western part of archipelago; bottoms of former channels with complex micro-relief. Major salt precipitation occurs just here after drying of highly saline residual lakes. Larger areas are taken by accumulative coasts comprised of sandy loam - loam and clay sediments.

III. Delta plain (Holocene, modern) of the Syrdarya and the Amudarya comes out to the sea in eastern and southern coasts. The ancient delta plain of the Syrdarya (Kazalinsk, Holocene) is particularly large and reaches 40-50 km in width. The plain character is broken by former sand-bar islands joined to the mainland.

IV. Delta front plain covers the youngest delta plain areas of the Amudarya and the Syrdarya.

In eastern part of Akpetkin archipelago, which dried off first of all, bottoms of all channels, lagoons and piezometric lakes are represented by solonchaks being mostly free of vegetation. Thickness of salt deposits is 1-2 m in some places, For example, sectors comprised mainly of salts were detected in coastal area of dried Toguzarkan Strait.

Fig. 4.8 Major Relief Types

Comparison of soil-formation and vegetation conditions in various areas of dried Akpetkin archipelago shows that salinity of channels, lagoons and piezometric lakes has decreased in eastern margin areas. Populations of salt-tolerant halophytes (*Halocnemum strobilaceum*, *Karelinia*) and single specimen of reed and rare bushes of black saxaul are evidence of this fact. One needs to note that tops of sand ridges are less saline here than in central part. These indicate that salt accumulation intensity has become lower than salt transfer intensity in eastern margin of the archipelago.

It is questionable that so small precipitation (80-100 mm) could leach so thick salt strata over a short period of time (7-15 years). Therefore, it may be naturally assumed that in this case the key relief-forming factor is wind, which is very intensive and strong here. Wind transfer of salts is promoted by a number of circumstances: increasing aridity and air temperature; and, groundwater lowering.

Due to high concentration of sulphates, salt horizons are regularly made light and became subjected to wind erosion promoted by precipitation as well. Therefore, dried bays, channels, lagoons and piezometric lakes are viewed as the main sources of wind transfer of salts over adjacent areas.

4.3 Salt accumulation processes in the Aral Sea.

The salt accumulation processes in the Aral Sea were studied by I.V.Rubanov, N.M.Bogdanova, O.Ye.Semenov, T.E.Mavlyanov, B.I.Pinkhasov and other researchers. As earlier mentioned, the Aral Sea is the main water and salt accumulator for the whole Syrdarya-Amudarya catchment. A share of salts returns back through wind to Priaralie [10,15,17,22]. The primeval inland outwash-deflation Aral depression originated approximately 2 million years ago at the end of Pliocene. In late Akchagyl period, the depression was flooded for the first time. Industrial salt fields of Kushkanatou and Akkala were formed in this the most ancient reservoir (its southern coastal zone) [12,18,20].

Kushkanatou salt field occupies 67 km^2 (11 km long and 6 km wide). Thickness of halogenic strata is 0,6 – 15,5 m. Salts are mainly represented by bloedite ($Na_2SO_4 \cdot H_2O$ – 60%) and halite (NaCl – 20%), less by mirabilite ($Na_2SO_4 \cdot 10H_2O$ – 10%), thenardite and glauberite (Na_2SO_4 и $Na_2SO_4 \cdot CaSO_4$ – total 10%). The total salt reserve is 600 Mt, of which bloedite is 360 Mt. Akkala field takes an area of 288 km^2, and projected area is 400 km^2. Thickness of halogenic strata is 47,5 m. Salts are comprised of prevailing mirabilite (2,3 billion t), less bloedite and epsomite (39 and 46 Mt, respectively). The total salt reserve is about 5 billion t [19].

The above-mentioned data indicate that an intensive salt accumulation took place in the Aral depression far back in the past.

In early and mid Pleistocene, the Aral depression developed under sub-aral conditions and was re-deepened by deflation. In late Pleistocene, the Amudarya moved towards the north and filled up again the Aral-Sarykamysh depression that formed the present Aral Sea. During the period of late Pleistocene, when the Amudarya flew through Sarykamysh both into Caspian Sea and Aral Sea, water level of the latter did not rise higher than +35 - +40 m. But in Holocene, the Aral level experienced repeated drops and rises [7].
The sea level of the earliest (drevnearal) transgression reached the elevation of +60 - +73 m, and the following (1500 years ago) late Oxiyan regression (when the sea level lowered to +25 - +27 m) led to formation of “Oxiyan swamp” on an area of 5 000 km^2 in the center of Aral. At the same time, mirabilite was accumulated in Pre-chink trench [14,19].
At present, mirabilite is deposited under 48-265 cm layer of bottom silt (limestone clay) in an area of 1425 km^2 in trench; 100 km^2, in Tshe-Bas Bay; 200-225 km^2, in the Small Sea. The total area of salt distribution is 1950 km^2. Their exposed thickness is less than 80 cm, while the projected one is first meters. Salt reserves are approximately 3 billion t under salt thickness of 1 m [13]. Share of dry mirabilite is 24 to 96 percent by weight, gypsum – 0,49% , other water-soluble salts – up to 6%, silica skeleton - up to 26%. Ion composition is as follows: sodium - 2,83 to 13,73%; sulphate - 7,5 – 30,14%; calcium - to 1,08%; magnesium – 3,03%; potassium – 0,93%; carbonate – 0,18%; chlorine – 2,09%; water – to 55,23%.
Later, during the period of novoaral transgression (until the early 1960s), terrigenous-carbonate sediment accumulation – carbonate stage (Fig. 4.9A) - took place in the Aral Sea and gypsum was deposited in shallow Akpetkin archipelago and eastern-aral bays [16]. The Novoaral deposits are represented by terri-, chemo- and organogenic formations. Terrigene (detrital) sediments account for more than 50-60% of their total mass. Among them are sand, siltstone and clays (Fig. 4.9A). Chemogenic sediments are comprised of carbonates, sulphates (gypsum), and water-soluble salts. Carbonates were accumulated all over the Aral Sea, except for Akpetkin archipelago, where their precipitation was suppressed by gypsum deposition. Gypsum having formed directly from the sea water salinized to 35-45 g/l deposited on the seabed in form of individual crystals with a size of 1 mm fractions (0,1 – 0,01 mm) and then (in time) either enlarged to 0,5 – 1 mm or changed into coral-like aggregates (5 – 10 mm). Thus, accumulated gypsum strata, from 0,2 to 0,5 m thick, covers mainly central parts of bays.
Since 1961, the Aral has started shrinking catastrophically. By 1997, the water level had dropped more than 1 m and lowered to the elevation 35,7 m. The exposed bed, area of which exceeded 34 thousand km^2, has changed into the youngest sandy-solonchak desert of Aralkum (Fig. 4.9B). The latter is a great source of salt and dust transfer and thus affects the environment of Priaralie. Aeoline transformations of original exposed seabed relief and salt accumulation processes in Aralkum desert are very intensive [11]. Two zones, such as Akpetkin archipelago and the remained dried area slightly differ in salt accumulation patterns. In the archipelago, portion of salts was formed through seawater evaporation, while the other portion – through groundwater flowing from the mainland. At present, salt accumulation processes still continue through both in-soil evaporation and seasonal discharge of high-saline groundwater in many small brine lakes. Salts are represented by thenardite-mirabilite deposits (up to 1 m thick), central depressed parts of which are confined by stratal halite with bloedite or halite-brine lakes. Thenardite-mirabilite and bloedite-halite deposits gravitate towards the deepest parts of dried bays and occur both inside fields of earlier accumulated gypsum or separately. The most developed are thenardite puffed solonchaks formed under mirabilite dewatering. Puffed solonchaks occupy about 250 km^2 of dried area. Thenardite-mirabilite salt reserves are 80 Mt. Stratal halite, 0,3 – 0,5 m thick, covers bottoms of numerous dry and brine lakes, with salinity of 240 – 350 g/l. Halite reserves are approximately 22 Mt. Thenardite puffed solonchaks are the main sources of salt transfers to atmosphere. The observations showed that 1,5 – 2 cm of puffed solonchaks are deflated per year, totaling approximately 3,6 Mt/year from the whole archipelago. Moreover, the puffed layer is rehabilitation and again blown into the atmosphere.

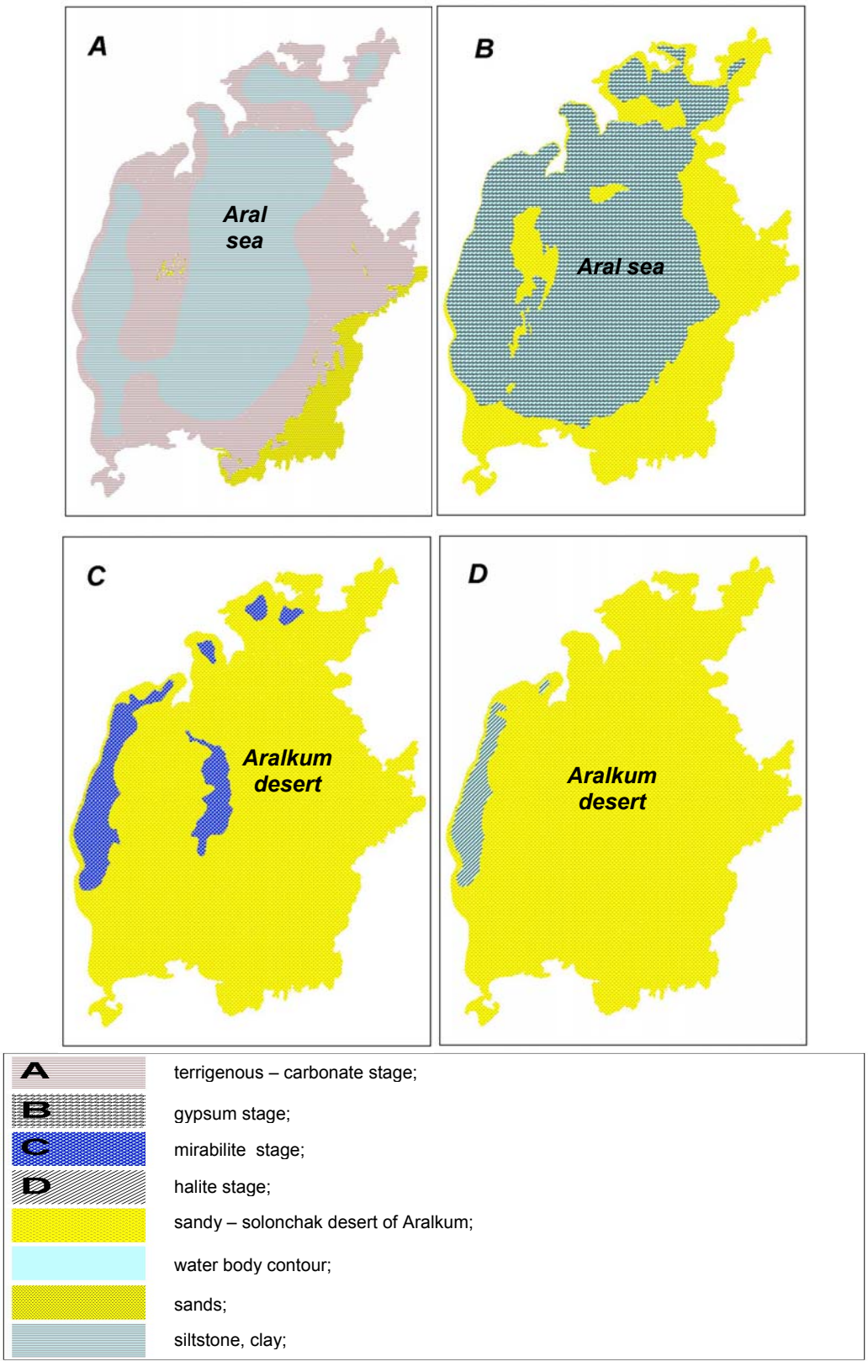

Fig. 4.9 Stages of Sediment Deposition in the Aral Sea and Shrinked Water Body

Let's consider the state of the shrinking Aral reservoir. Since sea water salinity increased from 10 to 30-45 g/l (by 1990), the terrigenic-carbonate sediment accumulation has been replaced by gypsum one – gypsum stage (Fig. 4.9B). This is proved also by many experimental research efforts. Thus, gypsum starts precipitating from salinized sea water, according to experiments on water evaporation at the temperatures of +35 and 40°C [8-9], when salinity reaches 2,55% and 2,98% or 29,33 g/l and 34,27 g/l, respectively. Then the authors of experiment indicate that halite precipitates under salinity of 31% (about 350 g/l). Later, bloedite, hexahydrite and epsomite precipitate. In case of density equaling 1,180 – 1,266,

that corresponds to 200 – 300 g/l salinity, glauberite is formed and halite occurs under higher values. We have also conducted experiments with the Aral Sea's water [21] by using freezing-out. In reducing volume of "rapa" by 12,5 times (up to salinity 154,05 g/kg, that is 15,31% or 184,92 g/l), first crystals of mirabilite occurred. Further condensation of "rapa" by 13 – 15 times (to 15,99% or 195 g/l) did not lead to formation of other minerals.

4.4 Generation of the Aral Sea isobaths map

In order to provide the modeling groups within the framework of the INTAS – 01 – 0501 Project with source information, the bathymetric map of the Aral Sea was generated. The bowl of the Aral Sea is limited by the true altitude of 50 m. Increment is 1 m. Areas and volumes of water mass were computed for each elevation.

Various thematic and topographic maps and actual data on the state of the Aral Sea were used to generate the electronic map of the Aral Sea isobaths. Thematic maps, such as the Aral Sea isobaths map, the Aral Sea sounding map, and topographic maps at different scales were produced in the period from 1940 to 1980.

The following work stages were completed:

1. Generation of the electronic map of Aral Sea isobaths on the basis of source map 1:500 000 - Fig. 4.10.
2. Generation of the electronic map of the Aral Sea sounding on the basis of source map 1:500 000.
3. Processing of satellite information.
4. Evaluation of topology adequacy for the electronic map of the Aral Sea isobaths.
5. Evaluation of the adequacy of obtained Aral Sea morphometry data.
6. Correction of Aral Sea topology (using output from stage 5).
7. Electronic mapping of the Aral Sea isobaths every 1 m.
8. Evaluation of the adequacy of obtained Aral Sea morphometry data.

Fig. 4.10 Bathymetric Map of the Aral Sea (increment 1 m)

9. Correction of Aral Sea topology using outputs from stage 9. Final computation of the areas and volumes of water mass on the basis of produced map of the Aral Sea isobaths.
10. Input of additional contour lines between 30 and 29 altitudes of the Aral Sea.

Thus, at the first work stages the basic thematic layers of information were obtained and areas and volumes of the Aral Sea were computed. At this stage, the Aral Sea is considered as a whole water body, without its division into the Small Sea and the Large Sea, with elevation increment of 1 m (Table 4.3.).
Fig. 4.11 and Fig. 4.12 show the morphometric characteristics of the Aral Sea. Fig. 4.11 shows distribution of areas by elevation, while Fig. 4.12 shows distribution of volumes by elevation. The obtained data were used for computation of actual areas and volumes of the Aral Sea till 1986 as by that period of time the sea was a single water body.

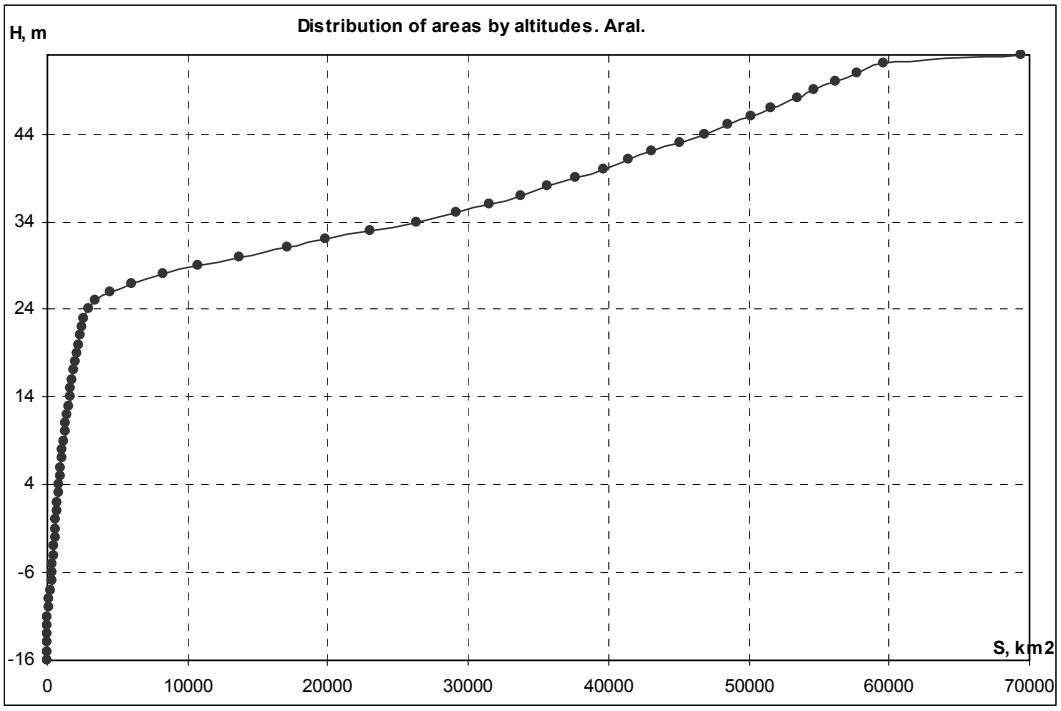

Fig. 4.11 Water Surface Versus Sea Level

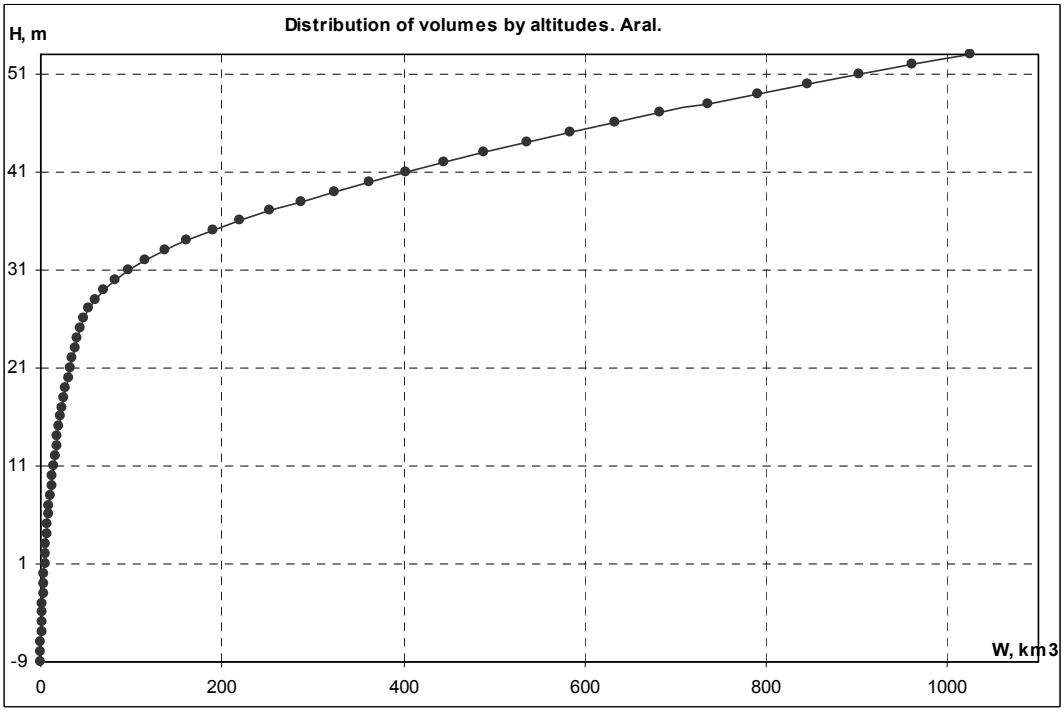

Fig. 4.12 Water Volume Versus Sea Level

Since the beginning of shrinkage, hydrothermal, hydrological, and biogenic regimes of the Aral Sea have been changing. This in turn leads to the change in natural processes related to formation of macro- and micro-relief of the seabed. The exposed seabed is subject to denudation processes caused mainly by wind erosion - this leads to changes in macro- and micro-relief in some parts of the seabed. Available satellite information was used to assess such changes in macro- and micro- relief of the seabed.
As an example, Fig. 4.13 shows changes in the seabed relief within Tshe-Bas Bay (the left side of the Figure represents relief derived from the Aral Sea isobaths map, while the right side shows the status of site by April 2001).

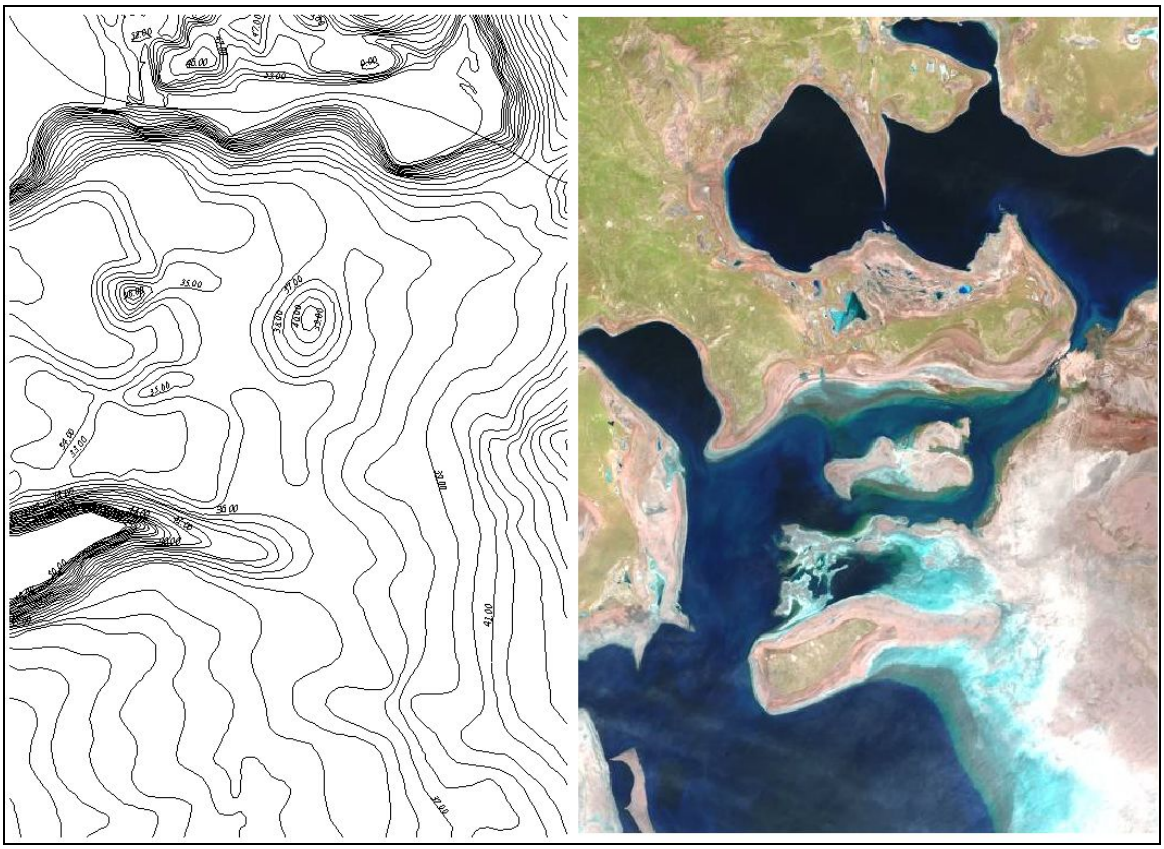

Fig. 4.13 Relief transformation in Tshe-Bas Bay

Evaluation of the adequacy of data produced during processing of thematic maps and images has shown that there exist some changes in the Aral Sea microrelief. The executor made correction of the base cover for electronic map representing the Aral Sea isobaths, produced final thematic cover and performed final computation of areas and volumes of the water mass. For modeling, the space between 30 and 29 height marks of the Aral Sea was detailed (additional work was done on input of contour lines every 25 cm) since the flow between the eastern and western parts of the Large Sea is formed just in this zone.
Based on the obtained data (areas and volumes of the Aral Sea), graphs showing relationships between areas and volumes of water mass at different elevations were plotted. Besides, the bathymetric curves derived from processing of thematic maps and actual data on both the Aral Sea as a whole and its conditional components – Small Sea (Fig. 4.14 - Fig. 4.15), Large Sea (Fig. 4.16 - Fig. 4.17) were analyzed.

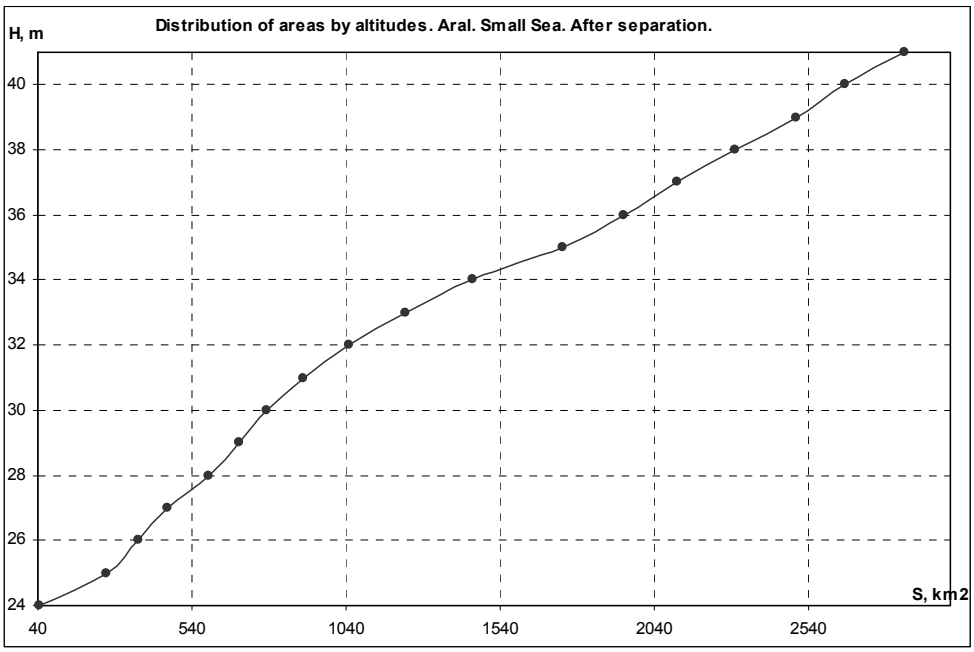

Fig. 4.14 Sea Surface Versus Water Level in the Small Sea (after Separation)

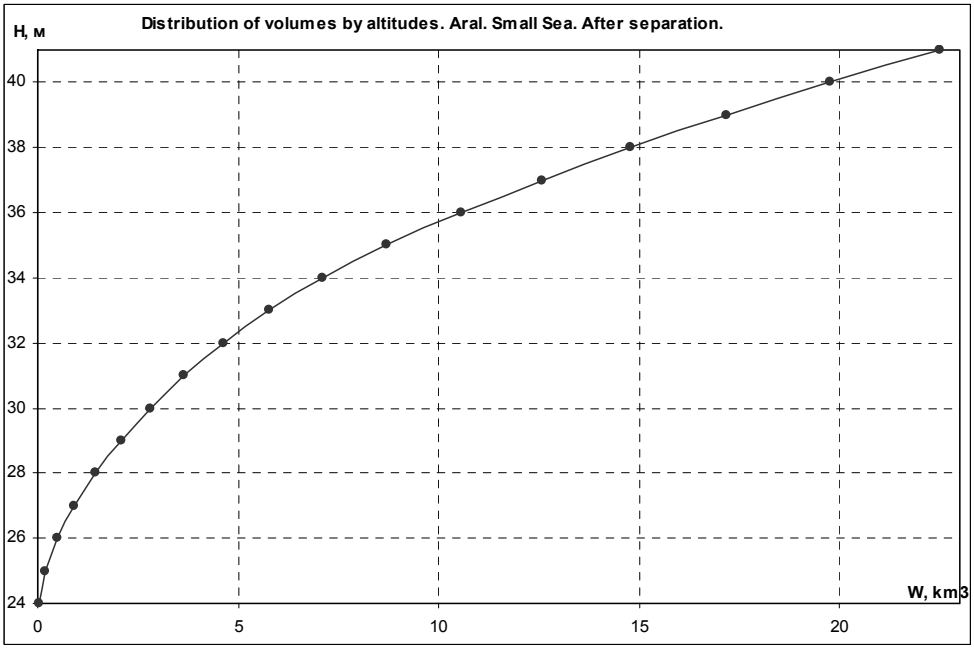

Fig. 4.15 Sea Volume Versus Water Level in the Small Sea (after Separation)

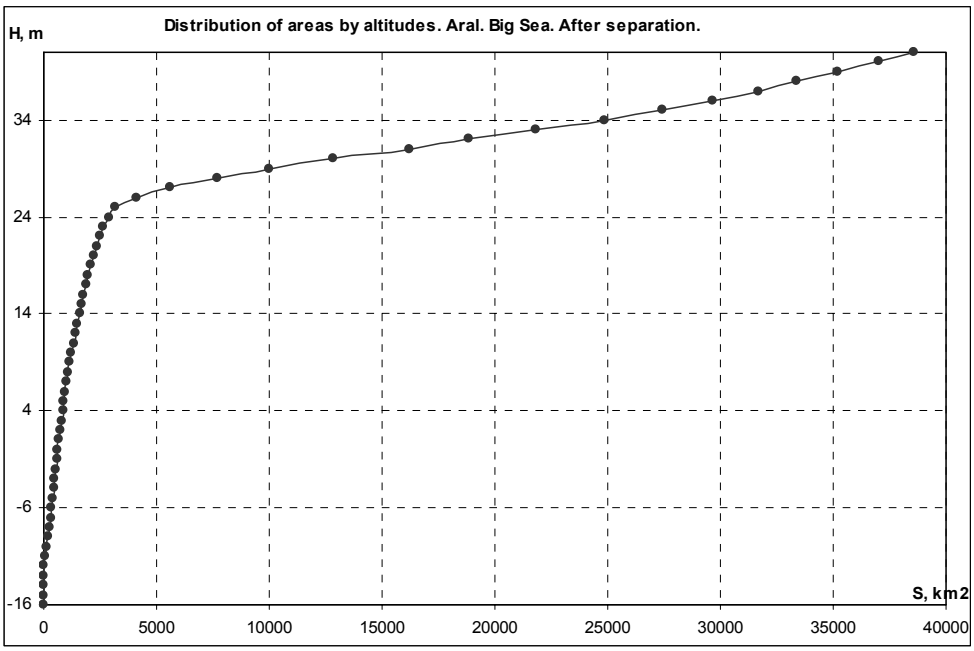

Fig. 4.16 Water Surface Versus Water Level in the Big Sea (after Separation)

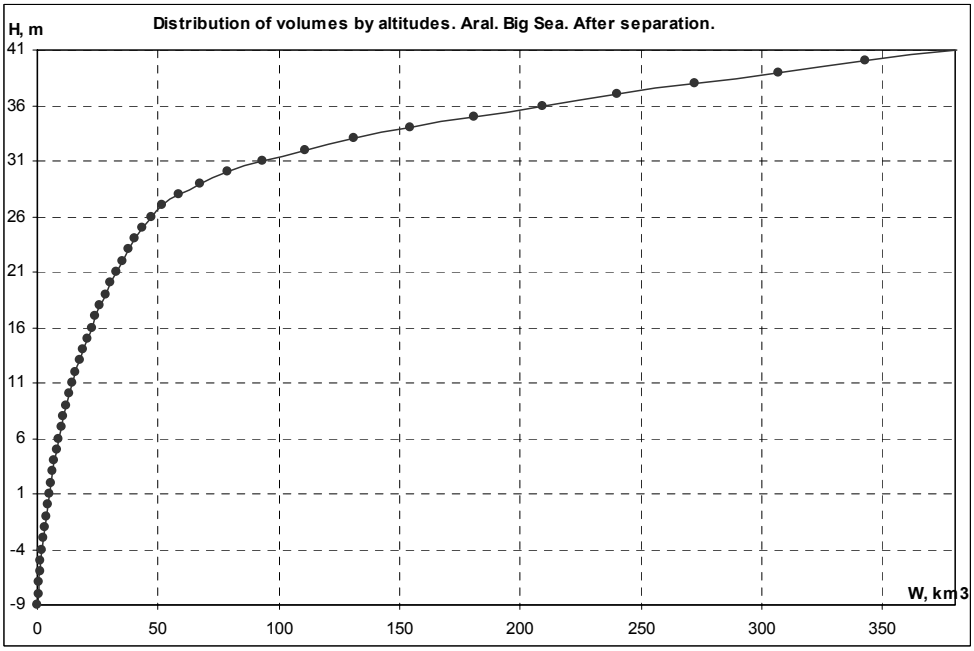

Fig. 4.17 Water Volume Versus Sea Water Level in the Big Sea (after Separation)

Then, areas and volumes of water mass at different sea parts are presented in Table 4.4.

5. Description of the long-term ASB development scenarios

SIC ICWC suggested 7 future development scenarios:

- Optimistic option under close cooperation (chapter 5.1).
- Optimistic option without cooperation.
- Pessimistic option with intensified cooperation.
- Pessimistic option without cooperation
- “Medium” option between 1 and 6 (chapter 5.2).

- Business as usual (chapter 5.3).
- "Realistic" option – based on trends derived from analysis of last 10 - 15 years and with account of outlined socio-economic tendencies and improvement of integration processes.

The following basic scenarios are considered in the model ASB-MM:

5.1 Optimistic Option (Close Cooperation)

It is assumed that the regional integrated development is supported by all the states, including:

- mutually beneficial use of transboundary water resources on the basis of water conservation and common environmental approaches;
- mutually beneficial agricultural development with maximum focus on regional specialization in agricultural production;
- maximum approaching to potential water and land productivities
- economic growth, mainly, through industrial and services development.

By 2020, population growth rates will decrease to 0,98 % per year, the regional population being about 54 million; the mean annual GNP growth will be 4-6 % per year in 2000-2010, approximately 6 % per year in 2010-2015 and more than 5 % per year in 2015-2020. Moreover, GNP is expected to be about 86 billion $ or more than 1600 $ per capita a year. Thus, in this scenario, given indicator will increase almost 2,5 times as compared to 2000.

Power sector will be developed mainly on the basis of hydropower stations and their joint construction so that to establish sustainable priority of clean energy production.

It is assumed that by implementing water conservation policy at national level the following water use efficiency figures will be achieved: unit irrigation water use - 9,4 thousand m3/ha; unit water consumption by population - 0,08 m3/capita/year.

A set of measures for reduction of irrigation water use will contribute to expansion of irrigated areas to 8,5 Mha against 7,85 Mha (current level). Irrigated area increase is mainly expected since 2010 through improvement of general economic situation in the region by that time and availability of adequate funds for implementation of large-scale water conservation measures. In addition, measures for increase of agricultural production productivity up to 80% will enable improvement of food provision. Mean food production is expected to be 3500 Kcal/capita/day, with prevailing vegetables and fruits in a diet. The optimal combination of food and non-food crops under extensive regional cooperation and integration will allow us to reduce import of grain and meat-milk products and increase export of vegetables and fruits and their processing products. There will be no food deficit if planned land and water productivities are achieved.

Substantial GNP growth will be ensured through outstripping industrial growth rates. Taking into account industrial development, on the one hand, and introduction of water recycling in industrial plants, on the other hand, it is assumed that industrial water use will reach 3,3 billion m^3/year against 1,9 billion m^3/year in 2000.

Under planned figures of water use efficiency in various economic sectors, the total water use will be 91,1 km^3/year. At the same time, 80,1 km^3/year will be used for irrigation and 11 km^3/year for industry and household and drinking water supply.

5.2 Medium Option

This scenario includes:

Integration processes in transboundary water resources management will be developed more slowly than in optimistic option. Besides, no regional crop specialization and the coordinated processing in agriculture are assumed.

The population growth rates will decrease slightly to 1,44 % a year by 2010 and 1,23 % a year by 2020. In 2020, the population will be 55 million. GNP growth rates will be 2-4 % per year. It is expected that GNP will be about 62 billion $ or 1133 $ per capita/year in 2020.

Development of new land is limited by both water availability and quality and lack of investments. Taking into account that this scenario assumes minor economic development and limited financial resources for introduction of water conservation in all economic sectors, the water use efficiency figures will be as

follows: unit water use for irrigation - 11 thousand m^3/ha; unit water consumption by population - 0,09 m^3/capita/year. Irrigated areas will increase approximately by 500 thousand ha and expand to 8,4 Mha in 2020.

Given the planned water use efficiency, the total water consumption will equal 101,8 km^3/year. Irrigation water demand will be 91 km^3/year, while industry and household and drinking water supply will need 2,5 km^3 and 4,9 km^3, respectively.

5.3 Business as Usual

It is assumed that:

- The region will be developed in a way of business as usual in joint transboundary water management, each country being tending to food self-provision.
- Integration processes in transboundary water resources management will be developed slowly.
- Regional integration in agricultural production progresses poorly.
- Major national efforts are aimed at maintaining current infrastructure while paying little attention to water conservation.

Population growth rates are constant at a level of 1,9 % per year, and the population is about 61 million. The mean annual GNP growth is not more than 4 % per year. The regional GNP is expected to be 44,7 billion $ or about 800 $ per capita/year.

According to current tendencies, water use efficiency figures will be as follows: irrigation - 12 thousand m^3/ha; population - 0,1 m^3/capita/year.

The irrigated area will remain practically unchanged until 2020.

The total water use will be 108,4 km^3/year, of which: irrigation - 96 km^3/year; industry - 3,05 km^3/year; and, household and drinking water supply – 6 km^3/year.

5.4 Scenario Based on National Future Development Strategies/Plans in ASB

The GEF Project, sub-component A-1 has suggested various development scenarios, from worsening situation to strengthening and rehabilitation. The main positions of these scenarios[*] for a period of 2000-2020 are given below. Those were served as input information for calculating variables of scenarios and measures used in the model when testing national future development plans/strategies. Here one should note that the considered plans/strategies did not give the full volume of input information (scenarios and measures' variables) used for model simulations and therefore in case of non-available information we used indicators of the optimistic scenario.

Kazakhstan

Long-term priorities and aims of strategic development in Kazakhstan were presented in the message of the President of Kazakhstan to nation "Kazakhstan - 2030. Prosperity, security, and improvement of the well-being for all people of Kazakhstan". The following seven long-term priorities are emphasized in development prospects:

National security.
Domestic stability and society consolidation.
Economic growth based on open market economy, with high level of foreign investments and domestic savings.
Health, education and prosperity of people in Kazakhstan.
Energy resources.
Infrastructure, particularly transport and communication.
Professional government.

[*] National visions discussed here do not represent their final versions. The GEF Project, sub-component A-1 suggested new «Draft national policies, strategies and action programs for water and salt management». At present, we are working on application of the ASB-mm model for the visions.

Kyrgyzstan
The determinants of needed prospective economic development rates were: prevalent socio-economic conditions of population; population size; projected population growth rates; people's demand for farm commodities and raw materials for given outlook; and, necessary volumes of water resources.
During the period from 2001 to 2020, uniform population growth (mean annual rate - 1,5 %) is expected, and population will increase from 2,3 to 3,5 million. Unit water consumption will increase from 100-120 to 200-250 l/day in urban areas and from 50-70 to 150-200 l/day in rural areas in 2020.
However, agriculture will be still the largest water consumer. Future increase in agricultural water use will depend on irrigated agriculture development, which, in turn, is in direct relationship with domestic population growth, respective growth in demand for farm products and raw materials. In order to ensure food provision according to standards, it is planned to develop additional land and water resources by 2010 –2020. In this context, irrigated areas will expand by 20 –22 thousand ha by 2010 and 56-58 thousand ha by 2020.
According to optimistic estimations, the annual GDP growth will be 5%, of which private sector share will increase from 65 to 80% by 2010.

Tajikistan
For nearest 5-10 years, prospective water and land use in the Republic will be mainly governed by intensive population growth (2,3-3% per year). According to forecasts, by 2010, the population will be 8,9 million. Food provision challenge requires that additional irrigated land be developed and current agricultural land productivity be improved.
According to National Water Strategy of the Republic of Tajikistan (Dushanbe, 1995), irrigated area will amount to 753,0 thousand ha and 822,0 thousand ha by 2005 and 2010 respectively.
Household and drinking water use is predicted to be 0,83 km^3/year, while withdrawals for agricultural needs are estimated at 1,2 km^3/year by 2010.
In 2000, water withdrawal totaled 11.2 km^3 in Tajikistan. Given the population growth, inclusion in agricultural production of non-used lands, and industrial enhancement, water withdrawal was planned at a level of 11,1 km^3 by 2005, while water-resources output in economy as a whole would not exceed a level of the year 1990, i.e. 12.8 km^3 by 2010.
It was assumed that in the period of 2001-2005, actual volume of GDP would increase by 34,7 %, and the mean annual growth rate would be 6,1 %. In 1996-2000, agricultural share in GDP averaged 21,6 %, industrial share was 19,6 %, while share of services increased from 33,9 % in 1996 to 39-40 % in 2000. For the next 5 years, it was expected that the ratio of these economic sectors would be kept constant, with slight increase in industrial and agricultural shares as conditions for sustainable development of these sections would be created.
Share of domestic investments to national economy was planned to account for 3,9 % in 2001 and 5% in 2005.

Turkmenistan
According to forecast published in the National economic development program for 2010, the mean annual population should be 6,9 million in 2005 and 8,6 million in 2010 that is, as compared to 1999, the population should increase by 36,5 % and 70 %, respectively.
Economic reform strategy in Turkmenistan assumes that the mean annual economic growth rates should not be less than 18 % until 2010. National industrial structure will be developed gradually and its share will account for 32 % in GDP.
The mean annual growth of agricultural production should be 14,3 % in 2000-2005 and 10,1% in 2005-2010. The irrigated area should be increased to 2000 thousand ha by 2005 and to 2240,7 thousand ha by 2010.

Uzbekistan
According to Concept of Economic Structural Reforms in the Republic of Uzbekistan until 2010, it was assumed that annual GDP growth would be 7,6 % in 2001-2005 and 8 % in 2006-2010.
Industrial share in GDP should amount to 18% by 2005 and 25% by 2010, whereas agricultural share should be 27 and 24 %, respectively.
Based on State Statistical Agency's (Goskomprognozstat) data, the population would be 30,0 million by 2010 and 36,4 million by 2020.
The irrigated area would expand to 4915,0 thousand ha by 2010. Moreover, irrigated area per capita should decrease from 0,21 ha in 1990 to 0,17 ha in 2000 and to 0,16 ha in 2010-2015.
Aggregated information on the main indicators from the national long-term development strategies, visions, and plans that are used in model simulations is given in the Table 5.1.

Table 5.1 Main indicators of the national long-term development strategies, visions, and plans

Indicator	Year	Unit	South. Kazakhstan	Kyrgyzstan	Tajikistan	Turkmenistan	Uzbekistan
Population growth rate	2010	%	1.30	1.50	4.20	3.20	1.95
	2020	%	1.30	1.50	3.00	3.20	1.95
Population	2010	*million*	2.77	2.72	8.84	8.52	30.08
	2020	*million*	3.16	3.15	12.15	11.68	36.48
GNP	2010	*billion* $	6.5	2.4	2.9	12.2	33.8
	2020	*billion* $	11.3	4.2	5.5	64.1	65.2
GNP growth rate	2010	%	6.0	6.0	6.1	18.0	8.0
	2020	%	5.0	5.0	6.0	18.0	6.5
Agricultural share in GNP	2010	%	34	50	30	15	24
	2020	%	32	50	30	15	24
Industrial share in GNP	2010	%	24	20	26	32	25
	2020	%	26	22	26	32	25
Irrigated land	2010	1000 *ha*	809.5	447.5	822.6	1897.5	4712.9
	2020	1000 *ha*	881.8	479.7	959.7	2343.9	4915.0
Irrigated land per capita	2010	ha/capita	0.29	0.16	0.09	0.22	0.16
	2020	ha/capita	0.28	0.15	0.08	0.20	0.13
Unit water use for household and drinking water supply	2010	*1000m3/ man./year*	0.06	0.04	0.08	0.07	0.09
	2020	*1000m3/ man./year*	0.07	0.06	0.08	0.08	0.09

Subsequently, proceeding from minutes of report revision of 2004 and inclusion of additional calculations on maximal and minimal hydrological series, quantity of scenarios was reduced to three.
On base of numerical experiments three scenarios of water resources management were selected by water consumption volume, flow losses and reservoir cascade operation regime as well as sanitary-ecologic releases limitations.

The selected scenarios have following characteristics:

- Business as usual scenario – scenario of water requirements from transboundary rivers and productivity stabilization, on base of local sources potential. According to scenario, deficit in irrigation agriculture of Syrdarya basin (average for 50 years) is estimated as 6 % of the limit with maximum depth up to 20 %. Releases to Arnasai are 0.8 with maximum of 12 km^3/yr. Scenario is characterized by Toktogul reservoir operation in power regime when power deficit in Kyrgyzstan is absent. In Amudarya basin water deficit in irrigated agriculture averages 3.6 % of the limit with maximum up to 20 % over states and 28% (sometimes 37%) over planning zones. Ecologic requirements for Amudarya are met in humid years.
- Optimistic scenario – scenario of 80% potential land productivity, water conservation, significant reduction of water diversion from transbounary rivers, Torkotogul reservoir irrigation-power operation regime, stable water supply to Priaralie, minimization of unproductive flow losses. According to this scenario, water deficit in irrigated agriculture is absent, power deficit in Kyrgyzstan is 1.9 billion kWh. Releases to Aranasai are estimated at 0.25km^3/yr that is necessary for lake system maintenance. In Amudarya basin deficit in irrigated agriculture is practically absent, ecologic requirements for Amudarya (sanitary flow, water supply to irrigation systems and deltaic lakes) are met.
- National vision scenario – scenario based on analysis of national visions for perspective development (GEF project, sub-component A-1), option of operating Toktogul reservoir in power generation regime. This regime leads to releases to Arnasai in an amount of 0,7 km3/yr with maximum 9,9 km^3/yr, deficit in irrigated agriculture is 18 % of water requirements with maximum 28 % over states and 35 % over planning zones. For the entire basin it is 9% with maximum 34 % over states and 40 % over planning zones. Ecologic requirements for Amudarya are met only in some humid years.

As to water sources, actual flows observed during the period 1952/1953 – 2001/2002 on inflows to upper reservoirs (Nurek, Toktogul, Charvak) and side inflow to rivers transformed for perspective since 2005 were taken. Prospective water consumption was defined on base of coefficients (relation between water diversion and its limits) changing present water diversion (limits).

Return flow is defined by transition coefficients changing (proportionally to change of diversion) volume of present collector-drainage outflow to the river and having temporal lag (shift) in separate planning zones regarding water intake that leads to even more flow transformation increasing it during non-growing period and impact power releases from Toktogul.
For optimistic scenario coefficients were defined on base of analysis of social-economic modeling on ASBMM model, for national vision scenario on base of GEF project analysis (level of 2010-2015, 2025-2030).
Afghanistan requirements for all scenarios were accepted as annual growth of water diversion since 2010 from 2,1 to 6,0 km^3/yr.

Table 5.2 Water diversion (limits) from transboundary rivers (km^3/yr)

	Country	Syrdarya	Amudarya	Total
1	Kazakhstan	8.2	-	8.2
2	Kyrgyzstan	0.22	0.15	0.37
3	Tajikistan	2.0	8.3	10.3
4	Turkmenistan	-	22.15	22.15
5	Uzbekistan	11.15	22.65	33.8
	Total	21.57	53.25	74.82

Table 5.3 Coefficients of water diversion limit change by 2030 over scenarios

Country	National vision		Optimistic
	Syrdarya	Amudarya	Syrdarya and Amudarya
Kazakhstan	1.00	-	0.74
Kyrgyzstan	1.56	1.00	0.31
Tajikistan	2.73	1.44	0.56
Turkmenistan	-	1.00	0.82
Uzbekistan	1.29	1.56	0.70

Table 5.4 Syrdarya's design flow (km^3) and water salinity (g/l), average for 50 years, by major alignments over scenarios, seasons (X-III, IV-IX) and for year (X-IX)

Alignments and scenarios	Indicator	X-III	IV-IX	X-IX
Kal				
1. Business as usual	River flow	8,04	5,73	13.77
	Water salinity	0.40	0.46	0.42
2. Optimistic	River flow	6.59	7.61	14.20
	Water salinity	0.39	0.40	0.39
3. National vision	River flow	8.17	5.32	13.49
	Water salinity	0,39	0.45	0.41
Inflow to Chardara				
1. Business as usual	River flow	9.60	5.41	15.01
	Water salinity	1,0	0.85	0.94
2. Optimistic	River flow	8.51	7.18	15.69
	Water salinity	0.85	0.79	0.82
3. National vision	River flow	9.51	4.95	14.46
	Water salinity	1,02	0.90	1,08

Table 5.5 Amudarya river flow (km^3) and water salinity (g/l), average for 50 years, in main alignments over scenarios, seasons (X-III, IV-IX) and for year (X-IX)

Alignments and scenarios	Indicator	X-III	IV-IX	X-IX
Kelif				
1. Business as usual	River flow	16,77	38,53	55.30
	Water salinity	0.52	0.38	0.42
2. Optimistic	River flow	16.74	40,76	57.50
	Water salinity	0.47	0.35	0.38
3. National vision	River flow	16.85	37.54	54.39
	Water salinity	0.58	0.42	0.46
Darganata				
1. Business as usual	River flow	10.01	19,90	29,91
	Water salinity	1.45	0.89	1.08
2. Optimistic	River flow	9.45	24.63	34.08
	Water salinity	1.25	0.70	0.85
3. National vision	River flow	9,94	19.39	29,33
	Water salinity	1.63	1.03	1.24

6. Basic ASBMM Model and its Modification

The ASB-MM model was developed by SIC ICWC and Resource Analysis (Delft, The Netherlands) within the framework of the UNDP Project “Capacity Building in the Aral Sea Basin” and the IFAS WEMP Program.
The Aral Sea basin management model is a decision support tool, which helps:

- to promote understanding of the general public (students, scientists, etc.) about the Aral Sea basin problems and probable solutions;
- decision makers to assess adequacy and timeliness of taken decision and to show possible consequences.

This is achieved by playing various scenarios of future development for both a riparian country and the region as a whole in order to identify potential of future economic and social development linked to use of available water resources and meeting of Aral and Priaralie’s environmental requirements.
The ASB-MM model is comprized of a set of models, including the socio-economic model, the hydrological model, and the Aral Sea model.
Recently, an additional block “Planning zone” has been included into the model. This block describes in details water use, agricultural and associated sectors development in every of 42 planning zones in the Aral Sea basin (Fig. 6.1 and Fig. 6.2). The ASBMM is described below[*].
Socio-economic model (Fig. 6.3) tries to predict what will happen in social and economic system. The model is based on the following parameters:

- population (rural and urban)
- economy (GNP, GNP per capita, contribution of economic sectors to GNP)
- water (demand of economic sectors; availability is calculated in the hydrological model)
- agriculture (irrigated land productivity by crops, including technical and food crops)
- investments (investments in agriculture, direct foreign investments)
- energy (production and consumption)
- food (calories production and consumption, with regard to food basket)

Hydrological model reflects formation, regulation and use of water resources in transboundary rivers of the Syrdarya and the Amudarya basins, and in simulation and optimization regimes for 20 years ahead allows a user the following:

(1) check national development scenarios for harmonized relationship “water demands – available water”;

(2) play alternatives of storage reservoir operation based on selected criteria and restrictions;

(3) compute river, storage reservoir, and lake water balances.

In order to apply the ASB-MM model for given task – consider climate change effects in estimating various future development scenarios – the basic model needed to be changed in algorithms and database. In this context, in the socio-economic model the block “Water” was changed in order to

[*] "ASBMM" – report "Resource Analyze", Netherlands and SIC ICWC, Tashkent, 2002, UNDP Project.

consider climate change effects on local water resources and the block “Agriculture” was modified to consider climate change effects on unit water use and crop yields. The hydrological model was modified to include estimation of climate and related hydrological change effects on flow, regime and management of the Amudarya and the Syrdarya in the long-term (20-year series), as well as on Priaralie and the Aral Sea in each regional development alternative.

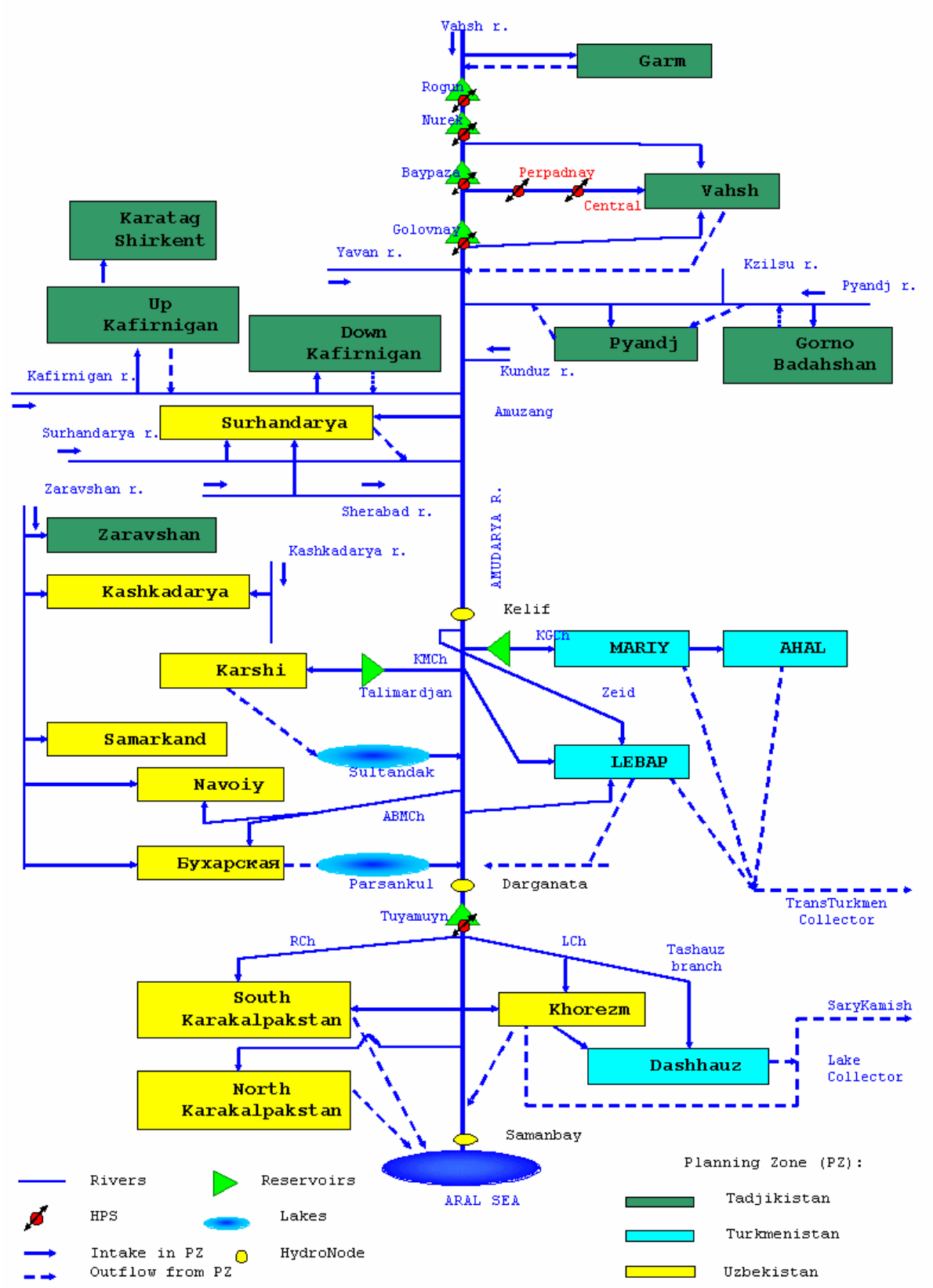

Fig. 6.1 Schematic Representation of the Major Flow Paths and Consumers of Water

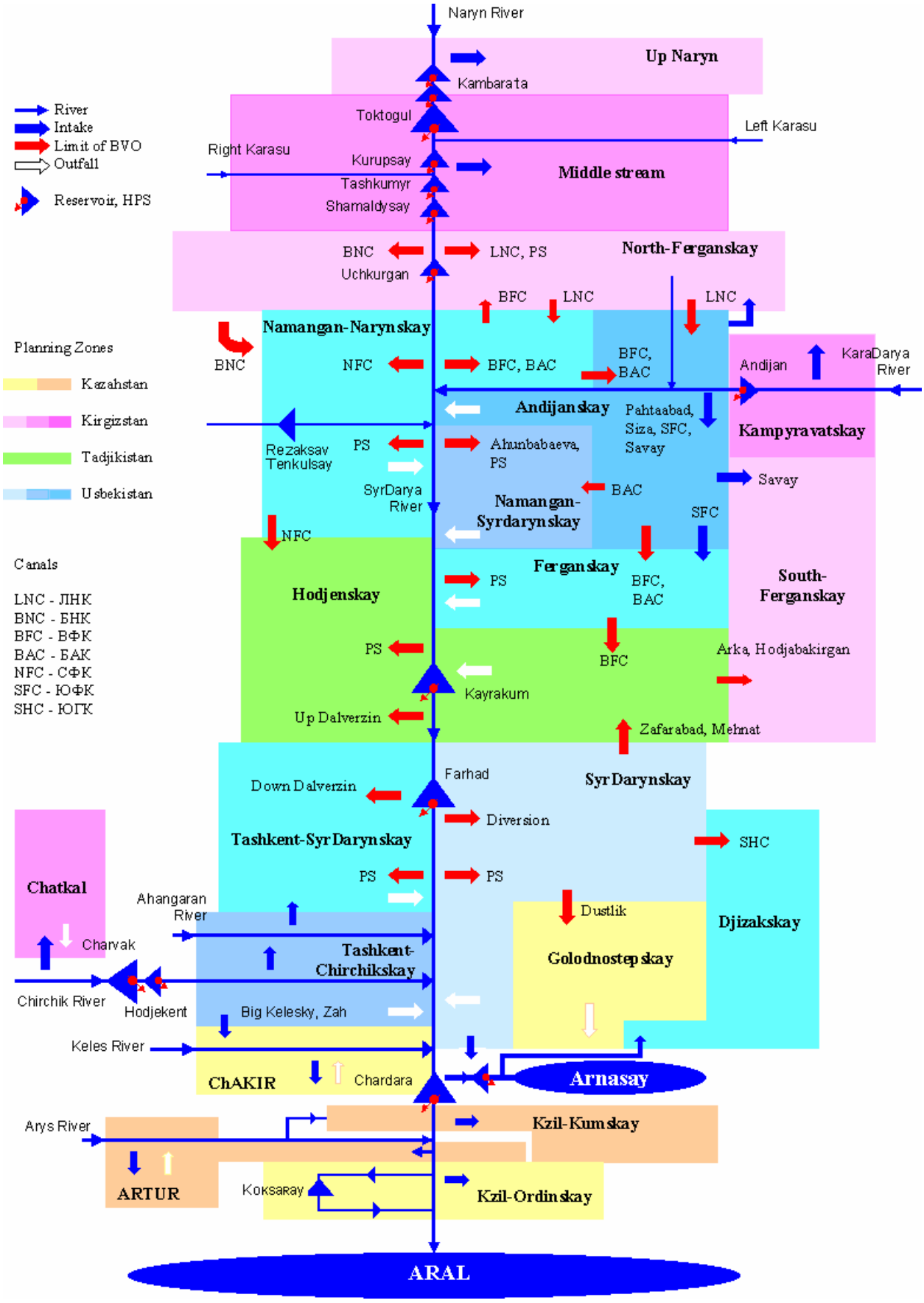

Fig. 6.2 Flow Paths of Water and Reservoirs

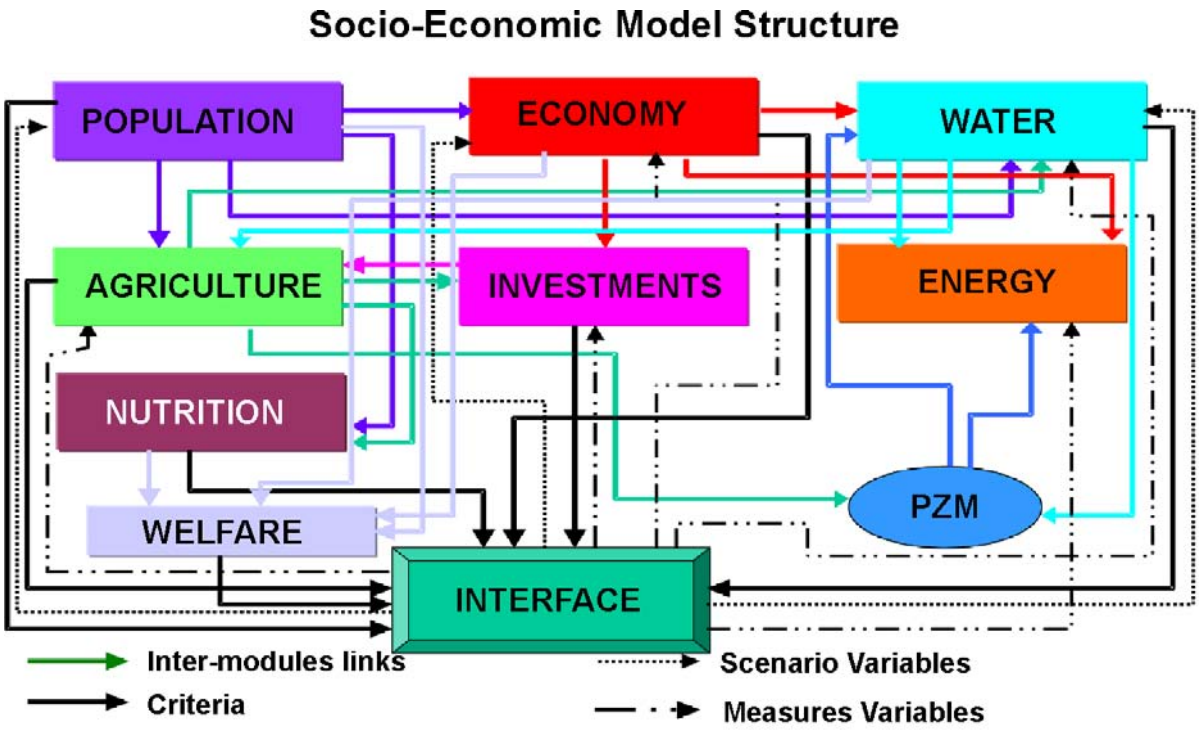

Fig. 6.3 Structure of Socio-economic Model

In given work, some changes and additions were made as applied to the project tasks. These changes mainly concerned the hydrological model and the Northern Sea model.
The hydrological model (HM) is a part of the model for the Aral sea basin management (ASB-MM). It has been developed in GAMS system and has information link with social-economic model (SEM) through interface (in Access system) and set of program-translators.
Brief description:

- Time step – season (growing season – April…September, non-growing season - October…March), period - 20 years.
- Modules: Amudarya and Syrdarya river basins.
- States: Kazakhstan, Kyrgyzstan, Tajikistan, Afghanistan, Turkmenistan, Uzbekistan.
- Objects: rivers (Naryn, Karadarya, Ahangaran, Chirchik, Aris, Syrdarya, Vahsh, Pyanj, Kafirnigan, Surhandarya, Amudarya), storage reservoirs (Toktogul, Kairakkum, Andijzhan, Charvak, Chardara, Nurek, Tuyamuyun), power plants (Naryn-Syrdarya, Chirchik, Vahsh cascade, Andijan, Tuyamuyun), lakes (Arnasai), water-related regions (Ferghana valley, Syrdarya middle reaches, Syrdarya lower reaches + Chirchik-Ahangaran region, Syrdarya lower reaches, Amudarya upper reaches, Amudarya middle reaches, Amudarya lower reaches).
- Reservoir management criteria: (1) maximum energy generation, (2) maximum net income in irrigated farming under obligatory damage compensation in power engineering, (3) maximum total net income in power engineering and irrigated farming.
- Main input information: hydrological time series on transboundary rivers in upper reaches (volume, salinity), required water diversion from transboundary rivers (information from SEM), return flow from water-related regions to transboundary rivers (volume, salinity), water amount and salinity in reservoirs and lakes by the date of calculation, economic information (value of $1m^3$ water use in irrigated farming, 1kWh energy generated, etc.), reservoir operation mode (used under simulation experiment).
- Main output information: design water diversion from transboundary rivers (revised water requirements), water-salt balance constituents and parameters of rivers, reservoirs and lakes regime, indicators of agricultural production and power engineering, economic indicators of water-power resources use (effects, damages).

Method of river system presentation is a graphs method. River system is partitioned into design sites and transects, reservoirs, lakes with aggregated water intakes to canals and collectors, which are simulated in algorithm by grid of arch-nodes. Graph **G(J,I)** is determined by two sets: **J ={1, . .,j}** - nodes and

l ={1, . . i} - arch. Each arch **i** is characterized by two nodes **(j,k)**: starting **j** and end **k**, where **j∈J, k ∈J, i ∈I**

Model is based on equations of water and salt conservation. Salt is considered as conservative admixture. Equations are solved for each node.

$$\frac{dW_j}{dt} = \sum_{(k,j)\in l_j^+} Q_{k,j} - \sum_{(j,k)\in l_j^-} Q_{j,k} \quad \ldots\ldots \quad (6\text{-}1)$$

$$\frac{d(S_j * W_j)}{dt} = \sum_{(k,j)\in l_j^+} (S * Q_{k,j}) - \sum_{(j,k)\in l_j^-} (S * Q_{j,k}) \quad \ldots\ldots \quad (6\text{-}2)$$

The task is to find management $\mathbf{W_u (t)^*}$ **, t∈{0:T},** which satisfies criterion of management quality and restrictions. Different conditions (on user's choice) can be taken as a criterion, in particular, maximum annual net income from water resources use in water-related regions

$$\sum_{1}^{z} \left[P_z * \int_{0}^{T} \sum_{(j,z)\in lz^+} Q_{j,z}\, dt \right] \rightarrow max \quad \ldots\ldots \quad (6\text{-}3)$$

Main restrictions

$$Q_{j,k}^{min} \le Q_{j,k} \le Q_{j,k}^{max} \quad \ldots\ldots \quad (6\text{-}4)$$

$$W_u^{min} \le W(t)_u \le W_u^{max} \quad \ldots\ldots \quad (6\text{-}5)$$

where: $\mathbf{W_j}$ – water volume in ***j*** -node (m^3), $\mathbf{S_j}$ – water salinity (kg/m^3); $\mathbf{Q_{j,k}}$ - discharge between ***j*** and ***k*** (m^3/s); $\mathbf{Q_{k,j}}$ – discharge between ***k*** and ***j*** (m^3/s); $\mathbf{Q_{j,z}}$ – discharge between ***j*** and **z** (m^3/s); $\mathbf{Q_z}$ – required inflow to **z-**node (m^3/s); **z∈J -** node of consumption (water-related region), **z∈Z; Z –** number of water-related regions; $\mathbf{W_u}$ – water volume in **u** node (m^3), **u∈J** - node of management (reservoir), **u∈U; U –** number of management nodes, $\mathbf{- l_j^+, l_j^-}$ - sets of archs coming into the node ***j*** and coming out of the node ***j***, respectively; $\mathbf{P_z}$ – irrigation water productivity ($/$m^3$), ***t*** – current time coordinate; ***0*** and ***T*** – beginning and end of calculation.

One of the requirements to hydrological model (according to ToR) – is to transform design river flow hydrographs (period – 20 years, step – season) into average monthly values over typical water distributions.

In order to calculate river water inflow to Priaralie with step of one month for final river transects (Amudarya – Samanbai, Syrdarya – Kazalinsk) according to actual data for recent 10 years typical hydrographs of in-season water distribution over months were obtained (percent of total seasonal runoff) for typical humidity years (dry, medium, wet) separately for growing and non-growing seasons. Hydrographs are included in calculation algorithm where used depending on period (season) and year humidity for transformation of seasonal values into monthly ones.

For re-calculation of seasonal average salinity values (growing and non-growing seasons) into average monthly ones, transient empiric coefficients are included into algorithm (for Samanbai and Kazalinsk) presenting ratio between average monthly and average seasonal values. Coefficients are obtained based on actual data of recent years and differentiated depending on season (growing and non-growing) and diapason of salinity changes (C < 1 g/l, 2 g/l > C > 1 g/l , C > 2 g/l).

Model foresees possibility to take into account requirements of Kazakh Priaralie on water diversion from Syrdarya downstream Kazalinsk. This variable is manageable, has range of allowable values (minimum, maximum) and is presented by temporal function, which can be set within given diapason. It is supposed that optimal value of this function will be obtained during numerical calculations over versions depending on both taken strategy of states development and considered versions of the Northern Sea level stabilization (altitudes 42, 47m, etc.).

For model calibration, numerical experiment has been made, which permitted "tune up" the model on real phenomena. Main difficulty was in definition of runoff losses taking into account that they take significant place in basin's water balance. Hydrological model for each site allows inserting channel losses function in tabular form which do not depend on time and have no link with parameters of channel flow.

Our task was to revise given functions for each season. For correction SIC ICWC data were used obtained from: (i) calculations on detailed channel models of in-year water resources use (step – month,

decade), (ii) from reports on structure of channel losses. Numerical calculations were performed in simulation mode, e.g. under design (actual) reservoir operation mode. Calculation period – 10 years or 20 seasons, starting since growing season 1990 up to non-growing period 1999-2000 inclusively.
Comparison of design and actual (measured) river regimes allowed evaluating flow discrepancies including both modeling and flow accounting errors. Flow discrepancies were determined by difference between design and actual values. Negative discrepancy characterizes availability of unaccounted inflow, positive – unaccounted losses and diversion.

№	Gauging station on river	Flow Discrepancy km^3/yr		
		Max	Min	Average for 1990-2000
1	Amudarya - Samanbai	- 1.51	0.03	- 0.69
2	Syrdarya - Kazalinsk	- 1.78	- 0.22	- 0.55

In river tail transects flow discrepancy was as follows: (i) Amudarya (Samanbai) - 0.69 km^3 /yr or 0.9 % of available water resources, (ii) Syrdarya (Kazalinsk) - 0.55 km^3 /yr or 1.2 % of available water resources. Discrepancies are negative and within permitted error. Highest discrepancies were observed at the boundaries between middle and lower reaches: (i) Amudarya (Darganata) – 4.3 km^3 /yr or 5.5 % of available water resources, (ii) Syrdarya (inflow to Chardara reservoir) – 1.2 km^3 /yr or 2.5 % of available water resources. Main reason for this is low reliability of flow monitoring at gauging stations.
The obtained results indicate that the hydrological model should be used in computing prospective aggregated water balances of the main rivers in the Amudarya and the Syrdarya basins, particularly for estimation of inflow to Priaralie.

6.1 Balance models for Amudarya and Syrdarya river basins

Testing results on the basin models that computed water inflows from the Syrdarya river and the Amudarya river to the deltas are shown in Table 6.1 - Table 6.2 and in graphs in the Annex.
Testing was made in simulation regime under specified (actual) reservoir operation regimes over 1990-2000. Comparison of simulation and actual (measured) river regimes in control stations allowed estimation of flow mis-tie, including both errors of model simulations and inaccuracies of flow measurement at gauging stations and intake points (negative mis-tie indicates to presence of unaccounted inflow, while positive one – to unaccounted losses and withdrawals).

Table 6.1 Flow mis-tie (actual - simulation) under basin model testing for 1990-2000

№		Mis-tie, km^3/year		
	Gauging station	Max	Min	Mean
1	Amudarya - Samanbai	- 1.51	0.03	- 0.69
2	Syrdarya - Kazalinsk	- 1.78	- 0.22	- 0.55

In tail river stations, the mean flow mis-tie was: (i) 0.69 km^3/year or 1 % of available water for Amudarya (Samanbai); (ii) 0.55 km^3/year or 1.2 % of available water for Syrdarya (Kazalinsk). Mis-ties are negative and within the permissible error.

Table 6.2 Distribution of flow mis-ties among river sections of Amudarya and Syrdarya (actual - simulation) under basin model testing, mean values for 1990 - 2000

Station	River section	Mis-tie (actual – sim.)		Unaccounted losses	Unaccounted inflow
		km^3/year	%	km^3/year	km^3/year
Kelif	Upstream	0.34	0.5	-	0.5
Darganata	Upstream and midstream	4.3	6.5	-	6.5
Samanbai	Whole river	0.69	1.0	0.69	-
Inflow to Chardara	Upstream and midstream	1.2	2.6	1.2	-
Kazalinsk	Whole river	0.55	1.2	0.55	-

6.2 Northern Aral balance model

A numerical experiment was performed for model calibration in order to "adjust" the model to actual developments in Northern Sea.
The model was calibrated for the following indicators:

- water level in Northern Sea,
- water salinity in Northern Sea.

The data from the Geographical Institute of Kazakhstan were used for comparison of simulation results with actual (measured) values [1].
The comparison series length was 11 years, since 1988 to 1998. An objective of comparison was to validate the calculation algorithm and its transformation into the code, as well as to check accuracy of the bathymetric table used in the model for the Northern Sea.
Comparative graphs of simulated and measured data on water level and salinity in the Northern Sea are presented in the Annex.
Accuracy of simulated water balance would depend on balance element measurement error. It is calculated by formula:

$$\sigma_0=\sqrt{\sigma_п+\sigma_c+\sigma_y+\sigma_o+\sigma_и+\sigma_ф}, \quad (6.6)$$

where σ_0 – balance error,
$\sigma_п$ – inflow estimation error,
σ_c – collector-drainage flow estimation error,
σ_y – volume estimation error,
σ_o – precipitation estimation error,
$\sigma_и$ - evaporation estimation error,
$\sigma_ф$ – groundwater exchange estimation error.

If estimation error of the mean monthly river discharge (acc. to Yu.N.Ivanov) is 5%, collector flow - 10%, and volume estimation from level - 5%, then water balance error will be 7,4%.

The mean deviation of simulated values from observed ones was derived from the following equation

$$S_{yx} = \sigma_y \sqrt{1-r^2}, \quad (6.7)$$

where σ_y - standard deviation of time series data,
r - correlation coefficient of simulated and observed time series.

In our case, the value S_{yx} is 3,3% (correlation coefficient – 0,98; standard deviation – 23,37). At 95% of the confidence interval (degree of correctness - 95%), the permissible error will be within $\pm 2S_{yx}$, i.e. 6,6% which is less than balance element measurement errors (7,4%).
By using the same methodology, let us compare simulated water salinity. The mean deviation of simulated values from observed ones is S_{yx} = 2% at correlation coefficient r = 0,99 and standard deviation of time series data σ_y - 13,6. The instrumental error of water salinity measurement is 5%. Thus, we can say about 95% probability in water salinity simulation.
The obtained results allow us to conclude that the model is suitable for production of future water and salt balances of the Northern Sea (temporal resolution is not less than one month), in particular for both estimation of its state (level, volume, area, salinity) and balance elements, including precipitation, evaporation losses and releases to Large Aral Sea (under set limitations on inflow to Northern Sea, stabilization level in Northern Sea and capacity for release to Large Aral sea).

Flow accounting within Kazalinsk-Aral river reach

Investigations in this area are fragmentary and do not permit to build reliable water balance structure downstream of Kazalinsk. The issue requires detailed modeling including calculation of losses, assessment of ecosystems functioning and their water requirements. Within the framework of given project flow inputs will be defined by inclusion of two types functions in hydrological model's algorithm: (1) flow losses, (2) ecological releases to Priaralie. To evaluate flow inputs and build functions the following

research will be performed: (1) analysis of design developments on Syrdarya and the Northern Aral Sea regulation (Kazgiprovodhoz, Kazakhstan), (2) analysis of data on water consumption in delta (SIC ICWC Kazakh Branch), etc.
According to N.Kipshakbayev (SIC ICWC Kazakh Branch), before intensive development of irrigation Syrdarya delta received 4-5 km3/yr. Natural-economic complex consisting of lakes, hayfields, tugai forests and wetlands has been developed in normal way. Then delta watering was sharply reduced. In 80-es water inputs in Syrdarya delta were evaluated as follows (D.Ratkovich, Water Resources, № 2, 1992):

Year	Inflow to delta, (km^3)	Inflow to sea, (km^3)	Losses in delta, (km^3)	Year	Inflow to delta, (km^3)	Inflow to sea, (km^3)	Losses in delta, (km^3)
1981	2.4	1.1	1.3	1986	0.5	0.0	0.5
1982	1.7	0.0	1.7	1987	1.6	0.0	1.6
1983	0.9	0.0	0.9	1988	6.9	5.1	1.8
1984	0.6	0.0	0.6	1989	4.3	2.9	1.4
1985	0.7	0.0	0.7	1990	3.4	2.0	1.4

In 90-es flow inputs in Kazalinsk-Karatereng reach were evaluated by Karlihanov A.K., Almaty, 2002):

Gauging stations		1993	1994	1995	1996	1997	1998	1999	2000	2001
Kazalinsk	(km^3)	9.01	9.90	5.50	6.72	5.68	9.23	7.24	4.83	4.32
Karatereng	(km^3)	-	8.99	4.53	5.60	4.78	7.72	6.03	3.87	3.56
Flow inputs	(km^3)	-	0.91	0.97	1.12	0.90	1.51	1.21	0.96	0.76

Thus, during recent 20 years flow inputs in delta (watering, losses) varied within 0.6... 1.8 km^3/yr. According to Kazgiprovodhoz - from 0.42 to 1.5 km^3/yr. Present design inputs are as follows: for dry year - 0.46 km^3/yr, normal year - 1.05 km^3/yr, wet year - 1.5 km^3/yr.
According to prospective water balance for Syrdarya lower reaches (Kazgiprovodhoz, 1999) design water consumption in delta varies depending on year water availability (probability P, %) and Naryn-Syrdarya cascade operation regime (irrigation, power, inflow to Chardara reservoir), km^3/yr:

	Average	P = 20 %	P = 50%	P = 70%	P = 90%
Under irrigation releases	1.310	1.652	1.357	1.080	0.865
Under power releases	1.267	1.566	1.331	1.199	0.810

Our computations of delta's water demand in years of various water availability are 1,4 to 2,4 km^3/year and shown in Section 2.
Enlarged balance model for the Northern Aral Sea allows calculate its water balance including evaporation from aquatic surface, water overflow from the Northern Sea to Large Aral Sea (Eastern part). Input information is as follows: inflow to Syrdarya river (can be computed from Syrdarya basin's hydrological model), drainage outflow, ground inflow (outflow), precipitation and evaporation from aquatic surface.
Typical Northern Aral sea levels create restrictions: (1) maximum, (2) optimum (over versions of level stabilization), (3) dike outlet's threshold separating Northern sea from Large sea as well as outlet capacity. Period is 20 years, step – month. Water balance equation for the Northern Sea is described as follow:

$$dV/dt = (Q_{пр} - Q_{от}) - (E-O) * dV(z)/dZ + Q_{ф} \quad \ldots\ldots\ldots \quad (6\text{-}8)$$

where: **V** - reservoir volume (m3); $\mathbf{Q_{пр}}$ - constituents of surface inflow – river runoff and drainage outflow (m3/s); $\mathbf{Q_{от}}$ - surface outflow – release to the Large Aral Sea (m3/s); **dV(Z)/dZ** - derivative on depth from volume curve – aquatic surface area (m2); **O, E** - precipitation and evaporation from aquatic surface for 1 m^2 area (m/s); $\mathbf{Q_{ф}}$ - water exchange with ground water (m3/s), if < 0 - outflow, if > 0 - inflow.
Model allows calculation og salt balance based on water balance using surface and ground water salinity (average monthly) as initial information. Salt is presented as conservative admixture. At the same time,

possibility to take into account water salinity transformation under partial salt sediment (under high salinity) is foreseen.
Empiric sediment coefficient $\mathbf{K_s}$ is used, which can be obtained from relation $\mathbf{K_s=f(S)}$ while comparing computed salinity values with measured ones. Water salinity **S** is corrected by formula:

$$S^* = S * (1 - K_s) \quad . . . \qquad (6\text{-}9)$$

But this correction can be used for the Northern Sea only in case of theoretically possible (unreal) version modeling supposing refusal from sea stabilization at certain level and its further degradation.
After database development, Northern sea model will be integrated with it. Initial information input, data exchange between models and information output for users will be performed though database and interface. Sub-base for the Northern Sea includes (at current stage): bathymetric curves for the sea (relation between water surface area and volume and water level), meteorological data (evaporation from aquatic surface, precipitation), retrospective hydrological data (inflow, water level, water salinity, aquatic surface area).

7. The Amudarya and Syrdarya Deltas – Development Alternatives

Taking into account that actual conditions are fit for development of new sustainable profiles of the both rivers in terms of water supply volume and capital investments, Kazakhstan in the Syrdarya delta and Uzbekistan in the Amudarya delta initiated design works and implementation of plans for improvement of the both deltas. However, morphological structure of the deltas and terrain specificities, as well as economic conditions dictated quite different approaches to rehabilitation of the natural and economic values of the deltas.
The Amudarya delta is described in details in the NATO Project SFP 974357 "Southern Priaralie"[7]. According to the project, the delta is formed of three parts:
Corresponding to water interchange pattern, all water bodies of the South Prearalie are divided into: flow-through water bodies – Mezhdurechie water reservoir and Makpalkol lake; those with weak (periodical) flow-through – lakes Karateren, Large Sudochie, Begdulla-Aidyn, Mashankol, Hojakol and Ilmenkol, bays Ribachy, Muinak, Jiltyrbas; and with no outflow collector waters accumulators – lakes Akushpa and Tayli.
At present, the first zone, where the lakes are fed with drainage water (Main Drains KKS and Ustyurt) is regarded to be unfavorable in terms of further water availability development. In future, transportation of water to this zone through the Raushan canal will be practically impossible due to the reduction of water availability in the Amudarya river downstream of the Takhiatash hydroscheme. The key issue in this zone is conservation of Sudochie lake as a natural water body, as well as the chain of lakes in the Kyvsyr system[8].
The Amudarya river adjacent zone is the most promising for further development. Provided there is a guaranteed outflow from the Takhiatash hydroscheme, the more or less favorable ecological and hydrological situation will be created along the whole length of the river channel from the Takhiatash hydroscheme down to the Sea. A large regulating water body is needed here that will allow recovering productive fish-farming, muskrat breeding and distant-pasturing. This will be determined by the way the water is transported through the Takhiatash hydroscheme to the delta.
The situation in the third zone depends on water supply through the Kyzketken canal. There are numerous lakes of the local significance in this zone fed by both fresh and drainage waters (lakes Jiltyrbas, Kokchiel, Karateren, Dautkul, Atakul, Mautkul and others) (Fig. 7.1).
Our design proposal stipulated that unstable landscapes and more socially tense zones would be watered through reconstruction and construction of sustainable hydraulic structures in the delta. This hydraulic complex along with afforestation of riparian areas should promote stabilization of landscapes and their enough high productivity in terms of fish, reed, muskrat and, simultaneously, establish areas for nesting of migratory birds. The suggested scheme (Fig. 7.2) was comprised of two lines of reservoirs: the first line from the west to the east – Sudochie, Mezhdurechie, and Jiltirbas 1, each of reservoirs having its own source from the Amudarya and recharge from collectors; the second line – Muinak, Ribachy, Dumalak fed from Mezhdurechie storage reservoir and Jiltirbas 2 fed from Jiltirbas 1. Further, as flow is regulated between these two lines, excess water should be directed to wetlands Jiltirbas 1 and Jiltirbas 2.
Unfortunately, the special engineering scheme in the NATO Project was not taken as a single set according to our proposals and implemented by breaking down to a number of sub-engineering projects. As a result, in 2004, there was break of spillway dam at Mezhdurechie storage reservoir, and, in 2005,

[7] Joop de Schutter, Victor A. Dukhovny "South Priaralie – New Perspectives", Tashkent, 2004
[8] The Sudoche Lake Improvement Project, implemented within the framework of the GEF WEMP project, Component E, is described in Section VIII.

much simplified, as compared to our proposal, spillway structure from this storage reservoir experienced failure due to not well-considered engineering decisions. Consequently, four low-water years (2002 … 2005) formed such situation in the delta that was greatly different from the design one (Fig. 7.3, Table 7.1) due to more intensive watering of a zone to the north of Jiltirbas and under-watering of Mezhdurechie storage reservoir zone and under-inflow to Sudochie. But through uncontrolled releases, quite a new scheme of water distribution took place in the delta. This is shown in the Table comparing situation before the dry period of 2000 … 2001, during the dry period, as well as design and current conditions.

Table 7.1 Water surface areas in the Amudarya river delta, ha

№	Reservoir	Date and data type					
		Design** water surface	8.04.2000 Wetlands	14.06.2001 wetlands	4.08.2002 wetlands	June 2005 water surface	June 2005 wetlands
1.	Sudochie	43,200	41897,73	9570,04	6497,2	11607,93	62146,73
2.	Mezhdurechie	39850,00	10050,42	592,79*	18375,21	15191,43	19738,06
3.	Ribachy	6240,00	5317,64	2019,68	5513,1	3809,86	5631,72
4.	Muinak	9740,00	8623,34	1292,23	5163,2	2101,77	9514,86
5.	Jiltirbas	35300,00	29357,73	5277,33	27620,5	6720,21	125938,9
6.	Former Adzhibay bay	28,130	10980,9	656,53	6784,7	321,37	39887,68
7.	Dumalak	-	4576,89	927,23	6784,9	108,46	19608,71
8.	Mashan Karajar	-	16835,18	726,27	2813,9	-	-
9.	Adzhibay 2	17,440	-	-	-	-	6025,87
10.	Makpalkol	2500,00	-	-	-	2315,62	4028,73
11.	Others	-	-	-	-	4537,95	36764,43
	Total	93718,77	127639,83	21062,1	79552,71	46714,60	329285,69

*)In the period from 2000 to 2002, water surface is negligible and overgrown with vegetation. Vegetation is concentrated along the Amudarya river and Shegekol lake.
**) Water surface as estimated in the Project SFP NATO 974357

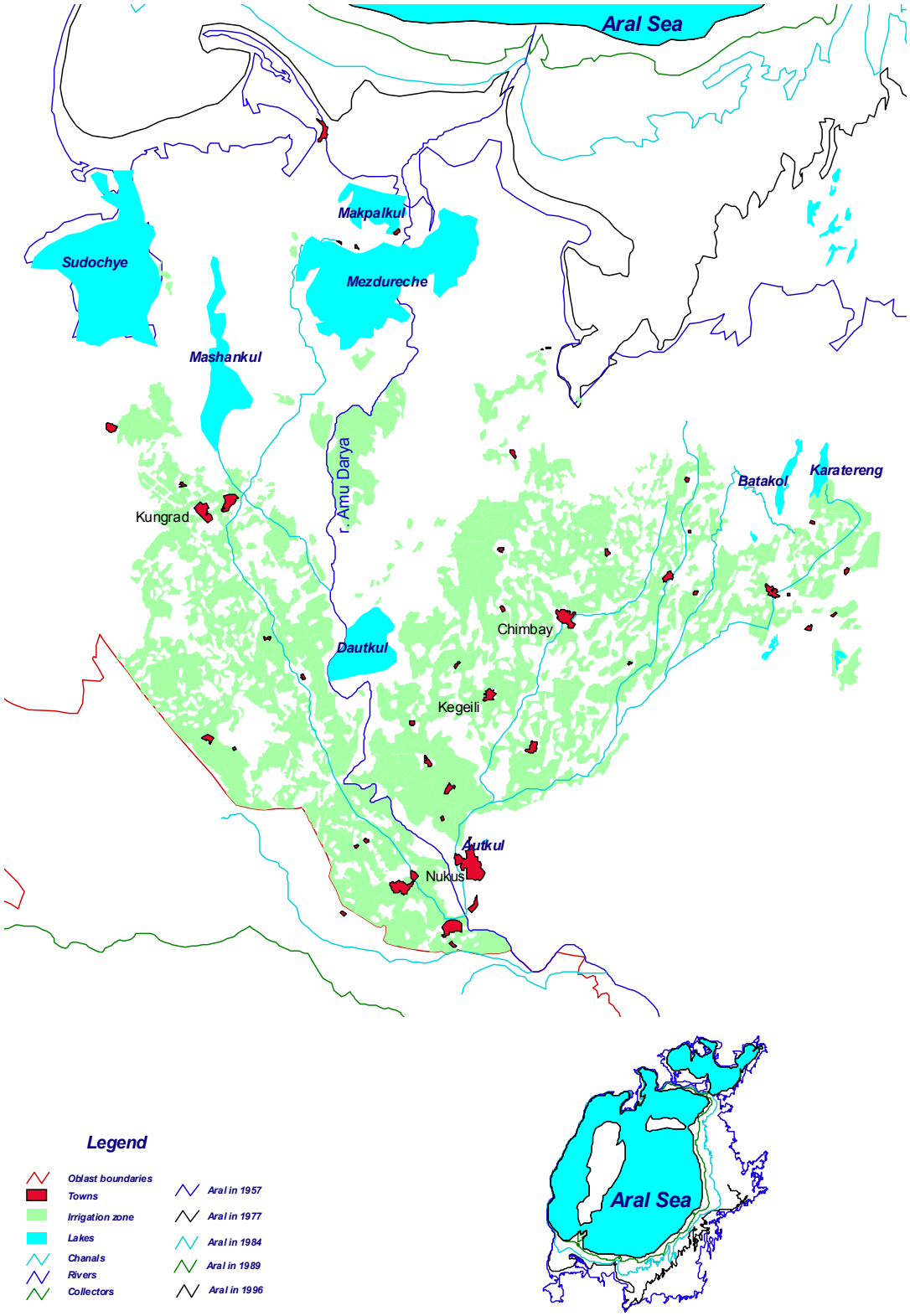

Fig. 7.1 Layout of Amudarya delta, current conditions

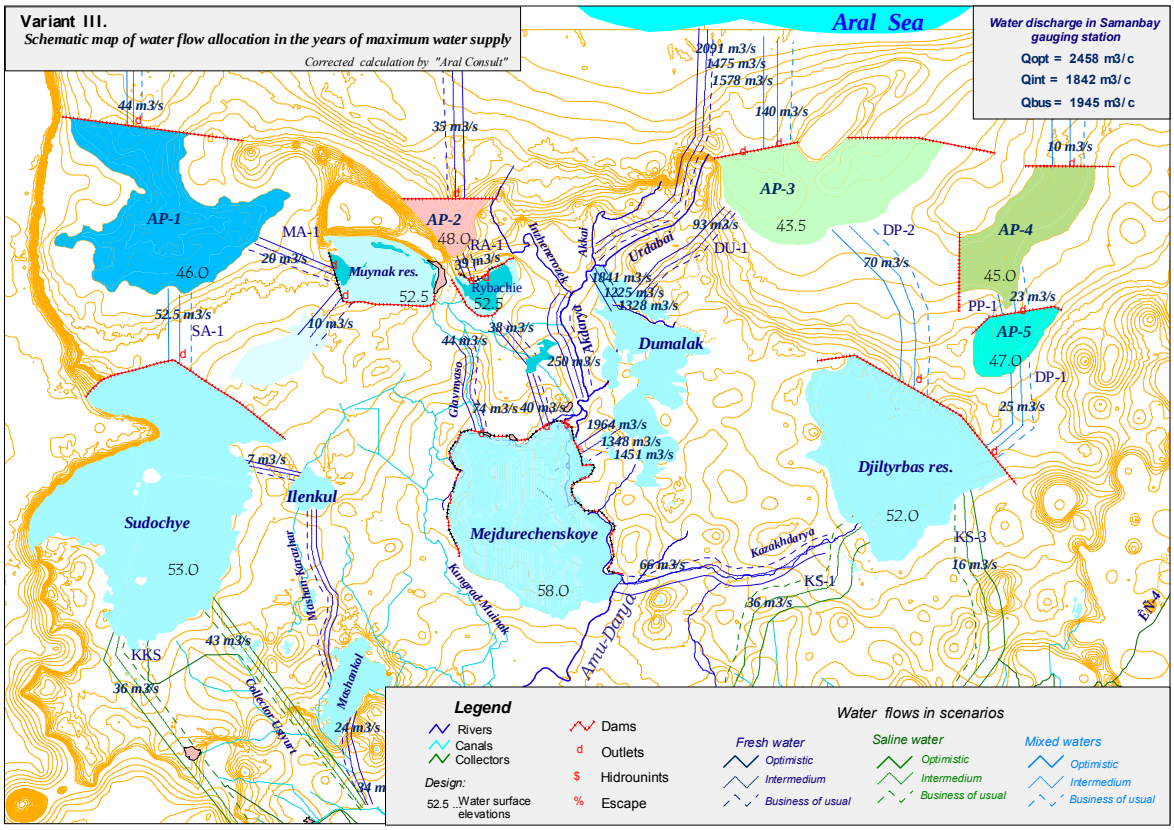

Fig. 7.2 Water Bodies, Reservoirs and channel System in the Amudarya Delta Region

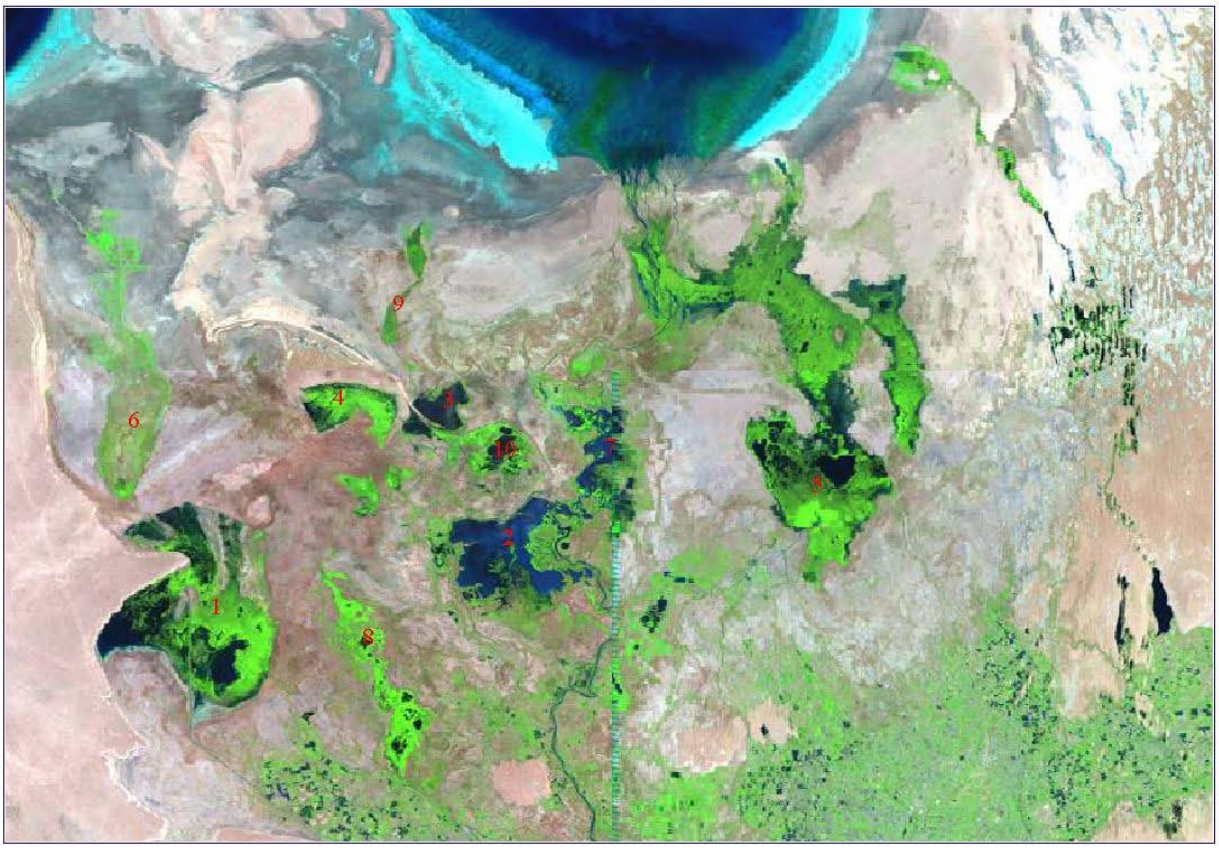

Fig. 7.3 Satellite Photo from the Amudarya Delta Region

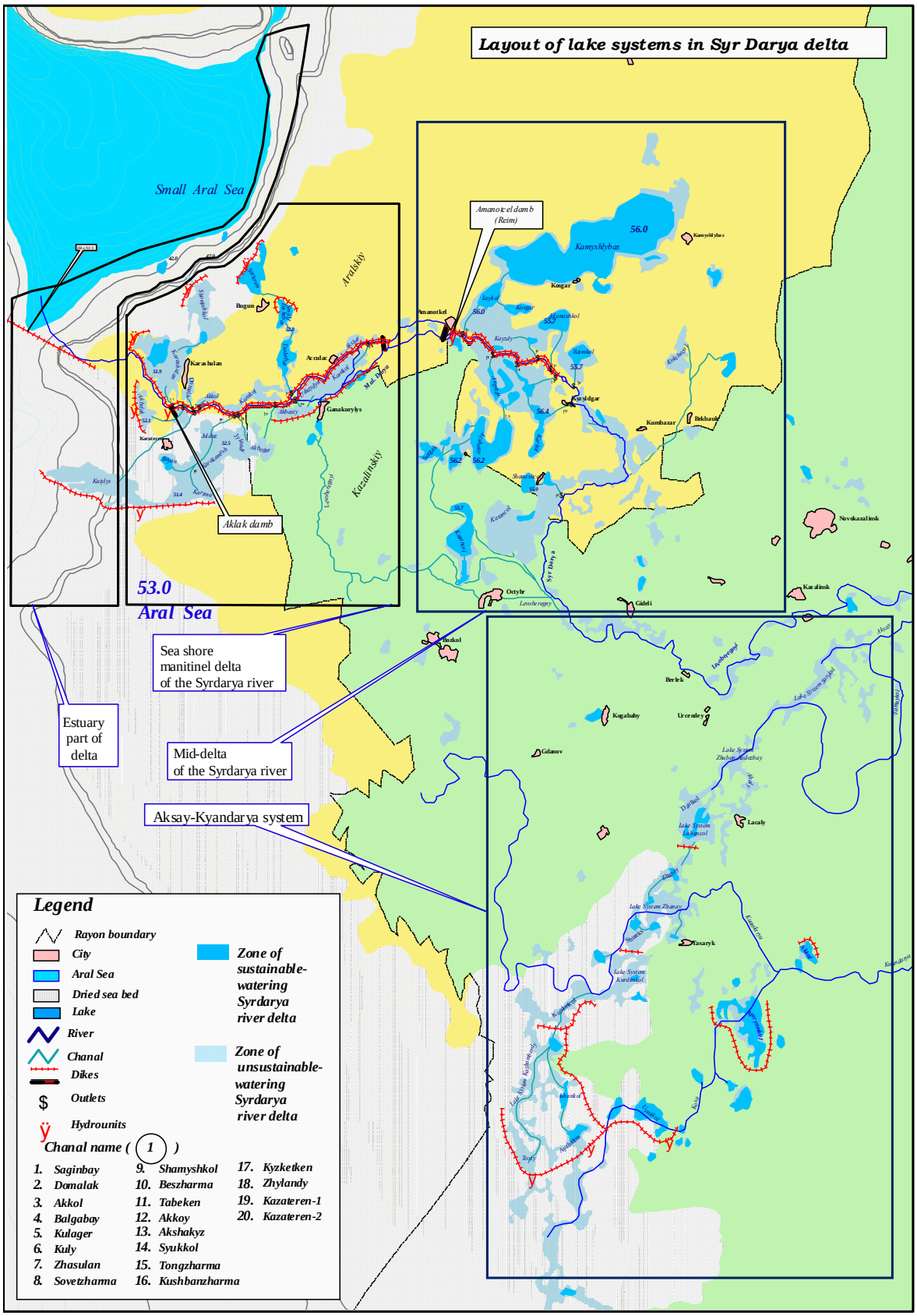

Fig. 7.4 Syrdaria Delta Region

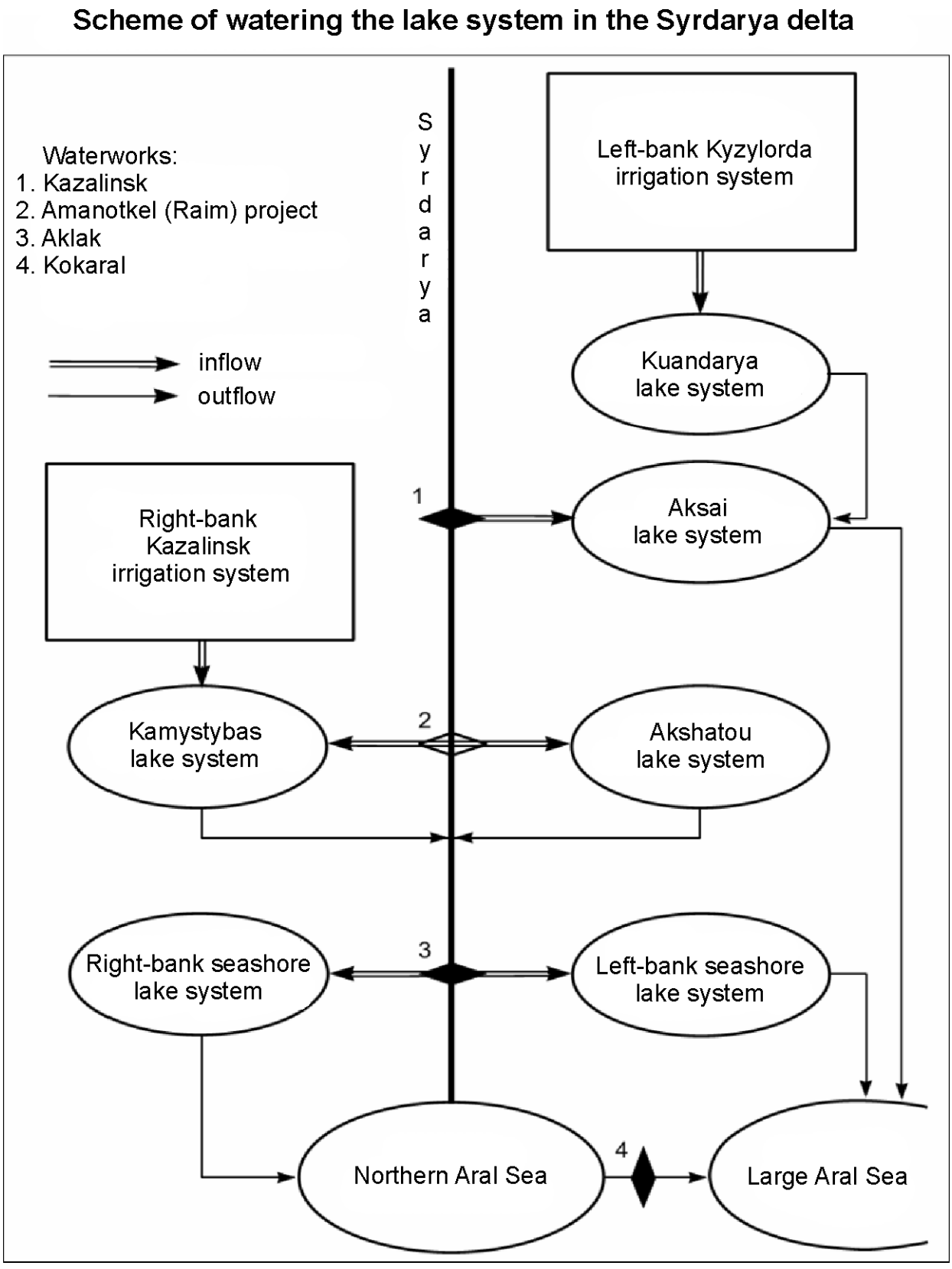

Fig. 7.5 Water Distribution in the Sydaria Delta Region

As the table shows, the total wetland area has not increased at expense of high-water years but the water surface area was even smaller than that it 2002 (the first humid year since the drought) since the delta was practically uncontrollable. As a result, flow inputs to the delta were slightly higher than those planned in the project, though the delta project has been far from completion.
In general, irrevocable water inputs into the delta approximated 6 km^3 in 2003 … 2005, i.e. the level of design inputs under much lower efficiency.

The Syrdarya delta has quite different morphological and hydrological structure. The detailed research was conducted by Ph.D. T.I. Budnikova, SIC ICWC's researcher I.B. Ruziev, engineer V.A. Bensman, and economics V.G.Prikhodko and published in the report of the Prohect INTAS-ARAL – 2000 – 1059 and relevan brochure*.
The Syrdarya river delta downstream of Kazalinsk (Fig. 7.4) represents few independent lake systems that are separated from the Syrdarya river and fed from the river, mainly, during floods that recently shifted to winter period.
The six lake systems are emphasized within the four zones described in mentioned report.
Zone "a" – Coastal part including Syrdarya mouth (25 km) and dried bed zone from the dam in Bergh Strait around Northern Sea.

Zone "b" – Seashore lake system of lower delta being under impact of Aklak waterworks destroyed later and to be rehabilitated. The seashore system covers Syrdarya river reach 44 km long with provisional artificially created left-bank lake system, including Zhilandi, Zhulduz, Bayan, Kartma, Akboget,Karakol, Uchaidin, Akbasti and canal network: Tangzharma, Kushbanzharma, Kizketken, Zhilandi, Karatereng-1, Karatereng-2; and right-bank lake system, including lakes Karashlan, Shoshka-Aral, Domalak, Akkol, Tusebas, Sarteren and canal network: Saginbai, Domolak, Akkol, Balgabai.
Zone "c" – Middle delta with river reach 145 km long, with two lake systems: right-bank Kamislibas including lakes Kamislibas, Laikol, Kayazdi, Zhalanashkol, Raimkol and canals: Kulager, Kul, Zhaslan, Sovietzharma; left-bank Akshatau lake system: Shomishkol, Karakol, Akshatau, Sorgak and canals: Shomishkol, Beszharma, Tabeken, Akkoi, Akshakiz, Siukkol. This part of delta is situated in backwater zone of Kazalinsk and Amanotkel (later Aklak) waterworks.
Zone "d" – Aksai-Kuvandarya lake and wetland system consisting of two chains of lake in delta of former Aksai and its channel Tamaikol and along Kuvandarya. First chain consists of lakes Sarikol, Zhubai-Sadirbai, Lahankol, Zhanai; second - Akkol, Maryamkol, Ubakkol, Ishankol, Kurdimkol, Kojamberdi, Tosti, Shurke. This territory is supplied from two sources: Aksai water intake takes water from Kazalinsk waterworks and Kuvandarya takes water from Kyzyl-Orda irrigation massif.
Current water-related situation in Syrdarya delta is determined by changes of inflow to upper delta – Kazalinsk gauging station and flow use dynamics and state of hydraulic structures.
According to I.N.Malkovsky's report (Project NATO SFP 980986, 2004 … 2007), the Kazakh branch of SIC ICWC estimated the delta flooding area to be 697,6 thousand ha in 2005 against current design estimation of 105,7 thousand ha and actual water inputs for flooding of 1120 Mm^3 against, in their opinion, the design net requirements of 1,2 km^3/year or gross requirements of about 1,8 km^3. Linear scheme of design systems is shown in Figure 7.5.
Thus, data from the both projects similarly estimate delta's water requirements.
In these research efforts, the total water demand of the delta is estimated to be 1697 Mm^3/year, including 1300 Mm^3 for dry year and 2700 Mm^3 for humid year.

8. Design Inflows to River Deltas

Design inflows to river deltas – Samanbai section on the Amudarya and Kazalinsk section on the Syrdarya – were calculated several times during the project, according to tasks and inflow parameters. The general scheme of calculations is shown in Fig. 8.1.

* Veidel G., Dukhovny V.A. et al.. "Economic evaluation of the local and joint measures to mitigate damage to Priaralie", Ташкент, 2004

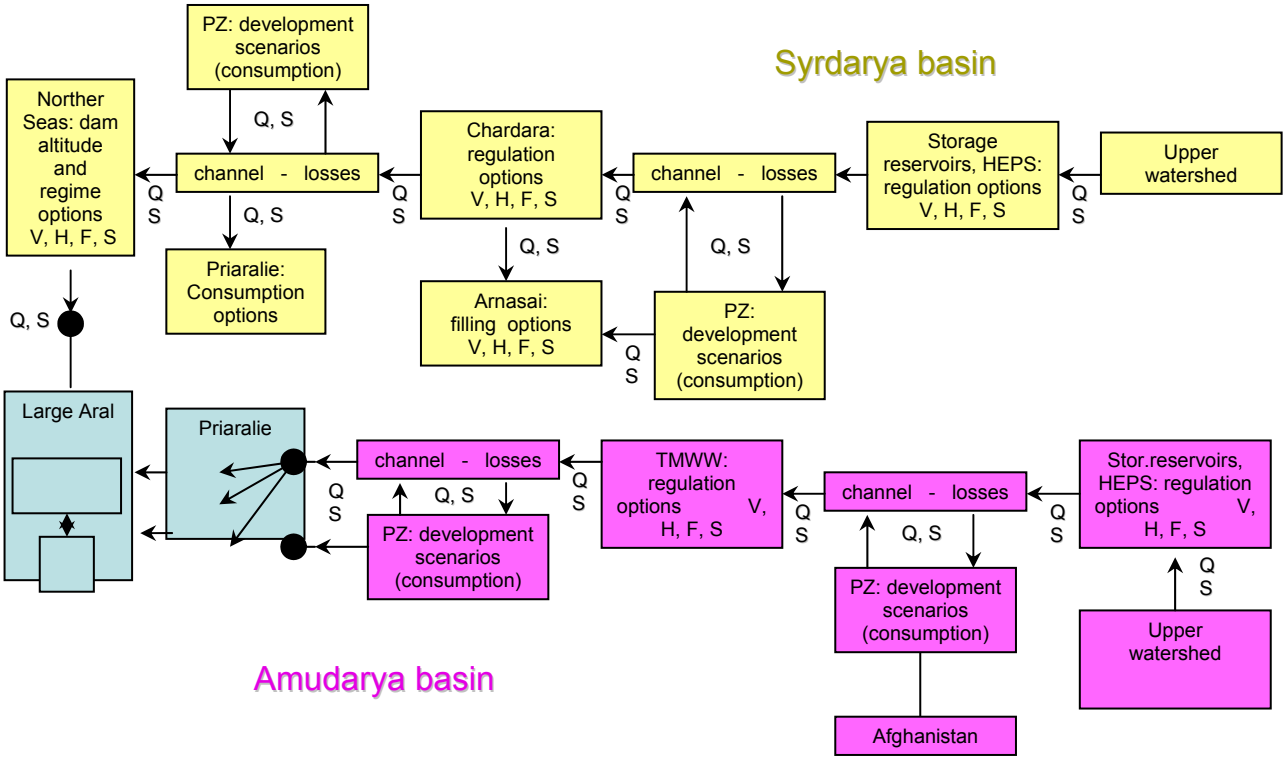

Fig. 8.1 General Modelling Scheme for the Arial Sea Basin

Initially, future inflow to Priaralie was estimated over fifty-year period for two seasons: non-growing – October-March, and growing – April-September. The estimation was made by simulation and optimization modeling of river regimes. Here it was more difficult to model regimes of the Syrdarya river since the main long-term regulation reservoir Toktogul in the Naryn-Syrdarya cascade could have many filling and release regimes, two of which such as irrigation and power generation regimes would be determinants.
Flow losses, both natural and artificial (discharge into Arnasai), will depend on these regimes.
During optimization management criteria were used: maximum power generation by power plants of Kyrgyzstan, maximum net profit in power engineering, maximum net profit in irrigated agriculture, with and without compensation of damage to power engineering, maximum total net profit both in power engineering and irrigated agriculture meeting ecologic requirements (sanitary flows, releases to Priaralie, etc.).
Presently, regulation degree in Syrdarya basin is 0,94 (natural flow is almost fully regulated), in Amudarya basin - 0,78 (there are some reserves of further regulation). This led to situation when flow use in Syrdarya basin more depends on reservoir operation mode than in Amudarya basin.
Naryn river irrigation regime change downstream of Toktogul reservoir for power one after 1992 led to significant reduction of guaranteed available water supply in irrigated agriculture in Syrdarya middle and lower reaches (deficit occurred during growing season) and river flow losses in winter time. During this period only in 1994 (6.72 km^3) and 2000 (6.48 km^3) releases from reservoir in summer were close to regular (norm – 9.26 km^3) meeting ecologic and irrigation requirements.
Water reservoir ceased to work for irrigated agriculture when releases during growing season became less than regular flow. Toktogul reservoir filling in long-term aspect is made in power engineering interest and only for very dry years additional water for irrigation is available from long-term component of reservoir volume.

Table 8.1 Toktogul reservoir – inflows and releases (km^3)

Indicators	Average annual	1985…1991		1992…1999	
		winter	summer	winter	summer
Inflow to reservoir	12.06	2.77	9.29	2.98	10.18
Releases from reservoir	11.46	3.53	7.93	7.59	5.73

Toktogul operation mode change led to ecologic damages to natural ecosystems due to peak flow shift from summer to winter and artificial dry season in summer.

As a result of river channel drying up in summer it looses its function of natural drain that leads to epidemiologic crisis. Lack of sanitary flow and unproductive flow losses are negative consequences of poor basin management.
Below are some results of numerical experiments to assess various reservoir management criteria impact on economic situation in Syrdarya basin over following target functions:

- Criterion 1 - maximum net profit in irrigated agriculture under limitations at upper boundary of water diversion (limits) and lower one (limits cut by 20%),
- Criterion 2 - maximum net profit in power engineering;
- Criterion 3 – maximum total net profit in irrigated agriculture and power engineering.

Calculations show that highest water consumption from transboundary rivers for long-term period (20, 50 years) were received by the first criterion (sum of annual net profit was maximized for long-term period), the same criterion permits receiving the best indicators of net profit for dry years, power generation deficit is observed.
Under optimization by the second criterion best indicators on net profit were observed in power sector but significant losses in irrigated agriculture. Best result in total net profit in irrigated agriculture and power engineering was received in transboundary flow distribution modeling by the third criterion revised for prospective basin model by summing given indicators over years and introducing discount factor.
Irrigation-power regime supposes compensation of power damage (in case of its availability) by irrigation consumers as well as ecologic restrictions. Nevertheless, it is worthy to note that compensation is possible only in case when additional irrigation releases are really needed by downstream countries. Releases from Toktogul reservoir should ensure ecologic requirements to flow providing minimum water supply during dry years. On the other hand, releases in autumn-winter period should not exceed design values established to avoid excessive releases to Arnasai and land inundation downstream of Chardara reservoir.
Possible water and power deficit under optimal “power” and “irrigation” regime of Toktogul reservoir operation has been found. At the same time, optimal irrigation-power regime is found, which differs from fixed releases determined by Agreement (it shows possibility of its improvement).
Calculations show that irrigation regime of Toktogul reservoir operation mostly meets “business as usual” and “national vision” scenarios (optimization by criterion 1), and irrigation-power regime – “optimistic” scenario (optimization by criterion 3).
Study demonstrated that rational reservoir management can both satisfy economic sectors needs and smooth maximum river flow peaks (additional losses and releases) increasing minimum flows up to sanitary ones. But for this it is necessary to work in irrigation-power regime established by ICWC for Toktogul reservoir.

Table 8.2 Net profit in irrigated agriculture and power engineering from transboundary flow use in Syrdarya basin based on modeling results (M$/yr).

	Criterion 1	Criterion 2	Criterion 3
Irrigated agriculture	455	370	440
Power engineering	115	155	140
Total	570	525	580

Theses actions will decrease water deficit over water intakes (irrigation, delta ecologic needs, etc.). In case of situation change from “business as usual” scenario to irrigation-power regime, irrigation water deficit can be practically eliminated (0.5% from limit for the period with maximum depth less than 5%). Compensation to Kyrgyzstan from Uzbekistan and Kazakhstan is estimated as 2.0 billion kWh and releases to Arnasai can be reduced by 3 times.
In case of optimistic scenario, irrigation-power regime guarantees river flow discharge (in middle and lower reaches) under water salinity reduction (compared with business as usual scenario) that happens due to water diversion and collector outflow reduction as well as more effective (regarding environment) Toktogul reservoir operation regulating Naryn and Syrdarya flow and reducing unproductive losses.

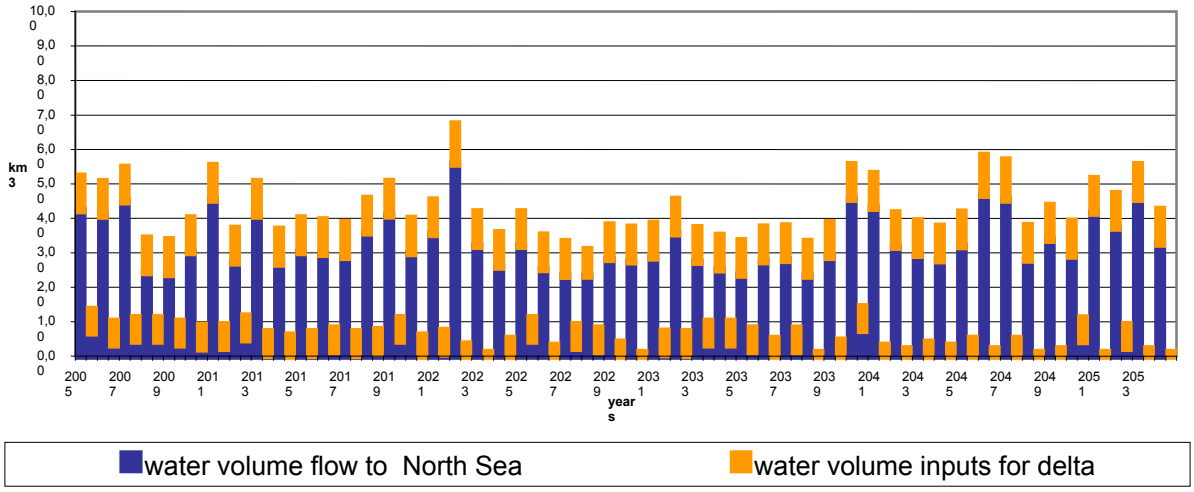

Fig. 8.2 Forecast of inflow on Syr Darya (Kazalinsk) under business as usual scenario for 50 years over season (non-growing season)

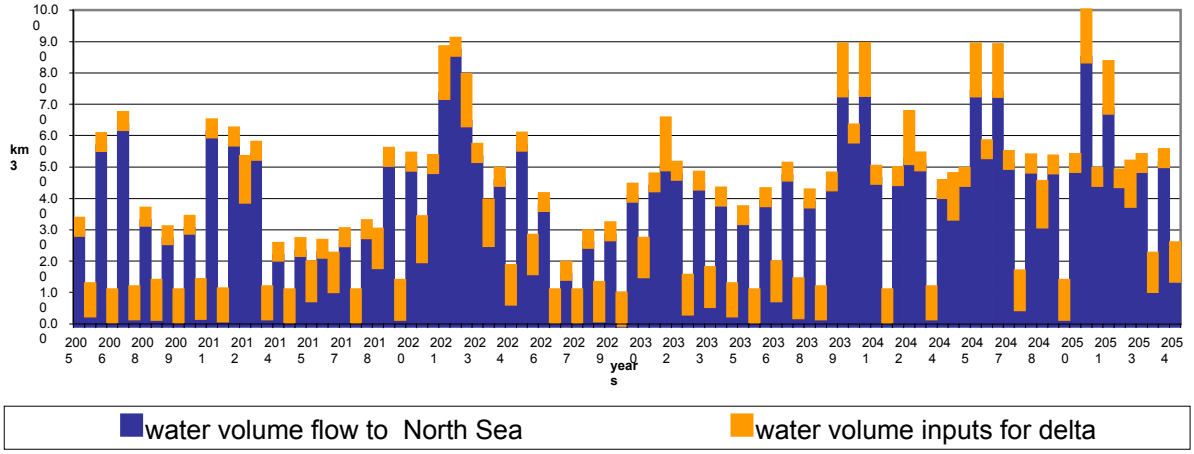

Fig. 8.3 Forecast of inflow on Syr Darya (Kazalinsk) under optimistic scenario for 50 years over season (non-growing and growing season)

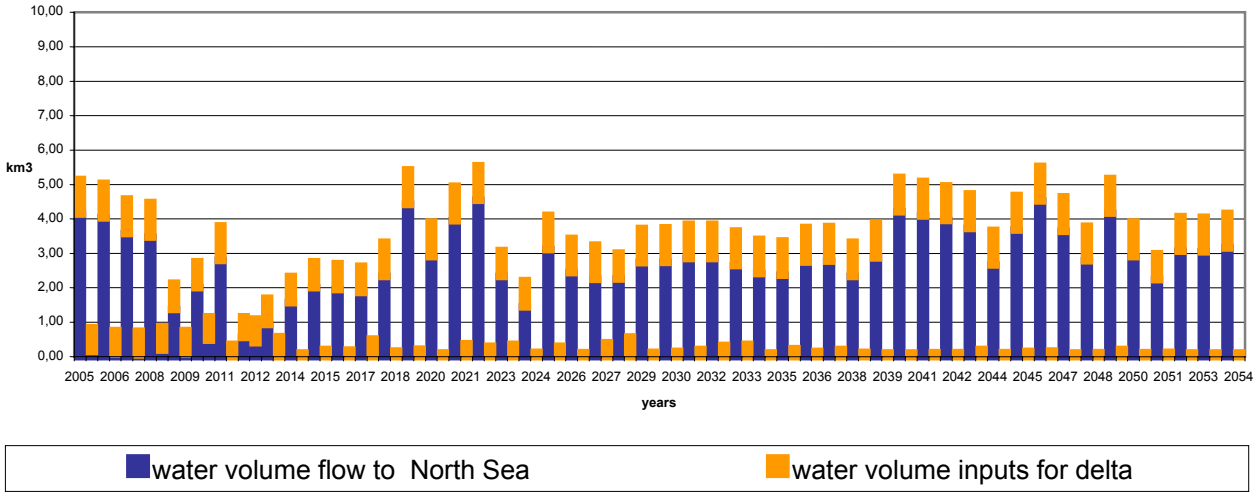

Fig. 8.4 Forecast of inflow on Syr Darya (Kazalinsk) under national vision scenario for 50 years over season (non-growing and growing season)

In case of Toktogul reservoir operation shift to irrigation-power regime under "national vision" scenario (GEF project, sub-component A-1), water deficit in irrigated agriculture can be reduced by 3 - 4 % from limit for calculating period with maximum depth less than 10 % and to reduce releases to Arnasai down to 0.1 – 0.2 km^3/yr changing river regime and shifting part of flow from winter to summer.
Design water inflow to Prriaralie is presented over scenarios in graphic (Fig. 8.2, Fig. 8.3, Fig. 8.4). Data characterize inflow dynamics along Syrdarya (Kazalinsk) and Amudarya (Samanbai) rivers with one month step and 20 years duration. Inflow along Syrdarya over seasons for 50 years with separation on components: inflow to Kazalinsk, water diversion and losses between Kazalinsk and Northern Sea, inflow to Northern Sea.
Calculations show that under business as usual scenario average release to Syrdarya delta is 4.96km^3/yr with average annual salinity 1.37 g/l. Average release to Amudarya delta is 6.6km^3/yr with average annual salinity 1.32 g/l. Inflow to Amudarya delta varies within 16 - 16.2 km^3 during growing season and 0.8 - 7 km^3 during non-growing season. Average salinity by Samanbai varies within 0.8 – 2g/l.
According to optimistic scenario, inflow to Syrdarya delta (Kazalinsk) is estimated as 7.9 km^3/yr with average annual salinity 1.0 g/l. Average annual Amudarya (Samanbai) runoff is 12.65 km^3 that is 6.0km^3 more compared with business as usual scenario and 8.8 km^3 more compared with national vision scenario. Average annual salinity by Samanbai is 0.95 g/l.
According to national vision scenario, at expense of winter releases to Syrdarya delta (Kazalinsk) inflow to delta is maintained at the level of 4.0 km^3/yr with sharp fluctuations: during non-growing season - 5.5 km^3, during growing season - 0.1 km^3 and salinity varying within 1.2 - 2.2g/l. Average annual Amudarya (Samanbai) runoff is – 3.9 km^3, average salinity - 1.55 g/l. Inflow to delta varied within 0.2 - 8.6 km^3 during season) because its smoothing depends on controllability of reservoirs working like seasonal regulators: Nurek in power regime, Tuyamuyun and in-system reservoirs – in irrigation mode.
Maximum seasonal salinity by Samanbai reaches 3.0 - 5 g/l, minimum – 1.0 g/l.

Table 8.3 Average for 50 years Syrdarya and Amudarya design flow (km^3) and water salinity (g/l) over scenarios, seasons (X-III, IV-IX) and for year (X-IX)

Alignments and scenarios	Indicator	X-III	IV-IX	X-IX
Syrdarya - Kazalinsk				
1. Business as usual	River flow	4.30	0,66	4,96
	Water salinity	1.38	1.33	1.37
2. Optimistic	River flow	4.71	3.21	7,92
	Water salinity	1.06	1,00	1.03
3. National vision	River flow	3,81	0.31	4.12
	Water salinity	1.45	1.36	1.44
Amudarya - Samanbai				
1. Business as usual	River flow	2,74	3,84	6,58
	Water salinity	1.52	1.19	1.32
2. Optimistic	River flow	3.75	8,90	12.65
	Water salinity	1.22	0.90	0.95
3. National vision	River flow	2.39	1.52	3,91
	Water salinity	1.64	1.40	1.55

Calculation shows that water level stabilization in Northern Sea at the altitude of 41.5 - 42.0m is possible under all scenarios during nearest 3-5 years (Fig. 8.5). But for national vision scenario level can fall down to 40m. Level stabilization at the altitude of 47m is observed only for two scenarios: business as usual scenario after 2040 and for optimistic scenario after 2020 (Fig. 8.6).
Maximum releases are observed according to optimistic scenario under altitude 42m, minimum – optimistic scenario (only under level 41.5 - 2.0m).

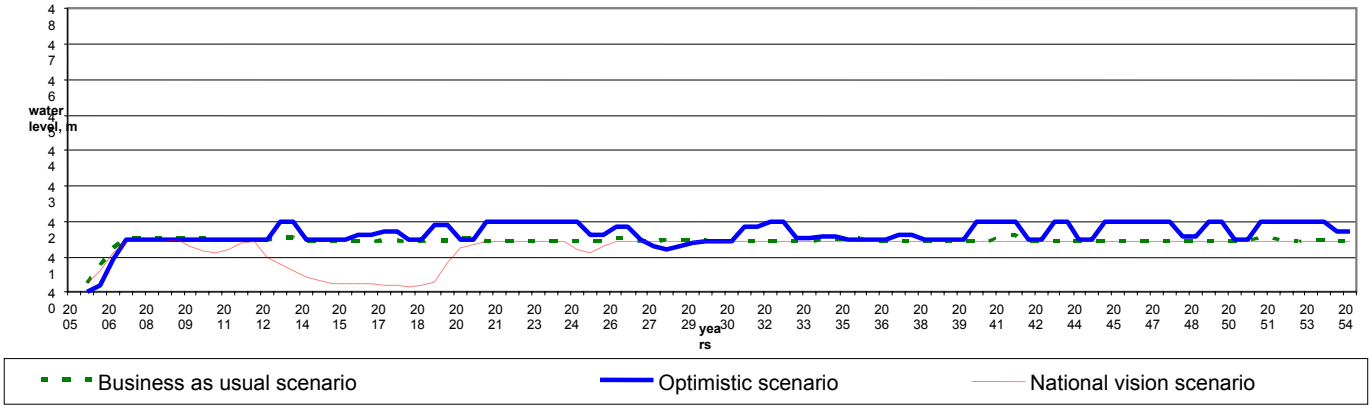

Fig. 8.5 Dynamics of water level in Northern sea with overflow threshold 42 m – forecast for 50 years

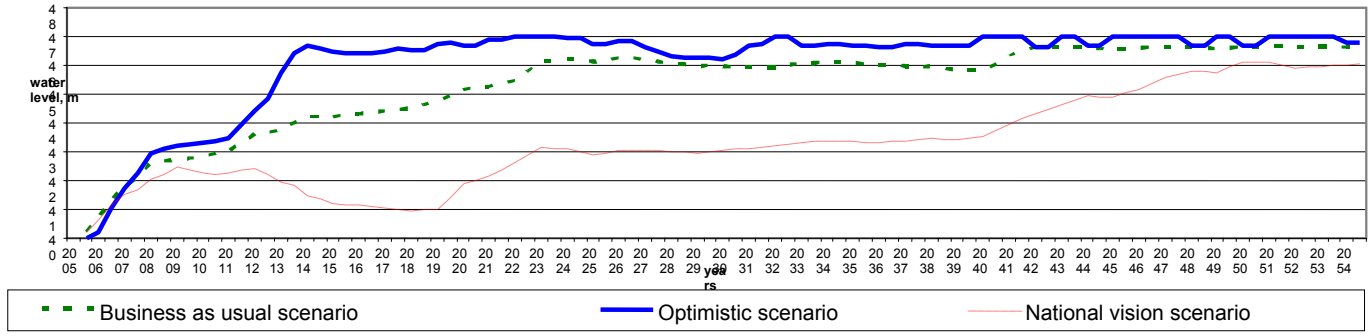

Fig. 8.6 Dynamics of water level in Northern sea with overflow threshold 47 m – forecast for 50 years

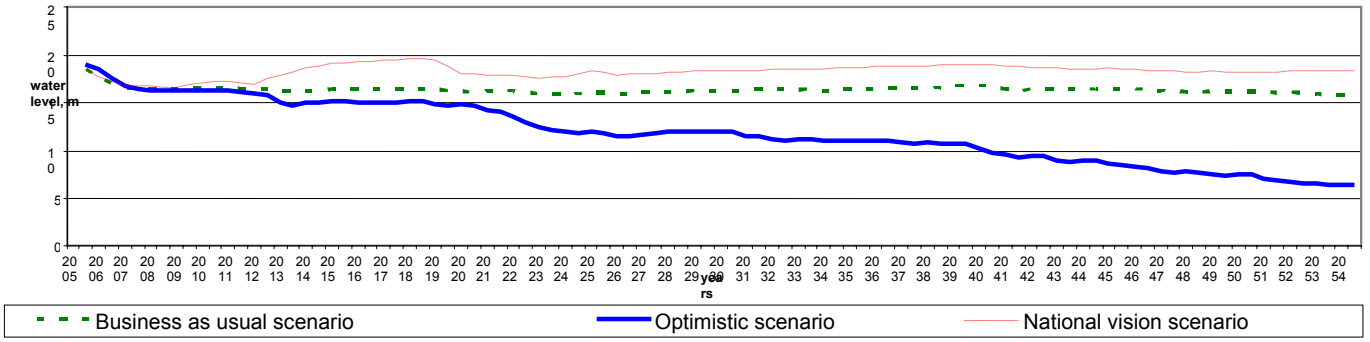

Fig. 8.7 Dynamics of water salinity in Northern sea with overflow threshold 42 m – forecast for 50 years

Options differ by water salinity dynamics in Northern Sea (Fig. 8.7). Under level stabilization at 42m salinity in first 5 years (2010) decreases under all scenarios to 16 - 17 g/l and then: under business as usual scenario increases to 18 g/l, under national vision scenario – decreased to 15 g/l, under optimistic scenario – decreases to 12 g/l by 2025 and to 6 g/l by 2050.

Table 8.4 Average for 50 years Syrdarya flow by Kazalinsk for the period since 2005 till 2055 over options for non-growing season (X-III) and growing season (IV-IX), km^3.

Year	X-III			IV-IX		
	Business as usual	Optimistic	National vision	Business as usual	Optimistic	National vision
2005-2009	4.52	4.52	4.27	1.12	1.13	0.79
2010-2014	4.40	4.84	2.35	0.86	1.95	0.66
2015-2019	4.30	3.39	3.37	0.82	1.87	0.26
2020-2024	4.61	6.05	3.94	0.46	5.13	0.26
Average for 20 years	4.46	4.70	3.48	0.82	2.52	0.49
2025-2029	3.59	3.60	3.50	0.71	1.39	0.31
2030-2034	3.88	4.64	3.70	0.70	2.71	0.23
2035-2039	3.62	4.38	3.62	0.54	2.84	0.17
2040-2044	4.54	5.20	4.74	0.53	4.48	0.14
2045-2049	4.77	5.33	4.76	0.31	5.01	0.15
2050-2054	4.72	5.18	3.84	0.49	5.61	0.12
Average for 50 years	4.30	4.71	3.81	0.66	3.21	0.31

Henceforth, it was suggested to estimate various important series in low-water and high-water periods.
Several water availability phases (of low- and high-water periods) with duration of a few years can be emphasized in natural flow regimes of the Amudarya and Syrdarya. There both large phases and shorter phases.
Based on irregular flow pattern, one can assume occurrence of a particular combination of low-, medium- and high-water years in the future.
The extreme scenarios in terms of water availability ("low-water N-year period", "high-water N-year period", etc.) can be developed and estimated in terms of flow probability for the period under review.
Such analysis made for 20-year periods from the natural water resources series since 1914 to 2001 (Fig. 8.8, Fig. 8.9), indicates to great variability of water availability both of the Amudarya and the Syrdarya basins as a whole and of rivers in given periods. The total water availability of 20-year periods varies from 87.2 km^3/year (mean for 1972-1991) to 96.1 km^3/year (mean for 1952-1971) in the river basins as a whole. This corresponds to 94% probability of low-water period and 3% probability of high-water period. River flow variability by 20-year periods is shown in the Table 8.5.

Table 8.5 River flow volume by 20-year periods (sampling from series 1914…2001)

River	Years	Probability, %	Mean flow for the period, km3/year
Amudarya	1970-1989	99	63.56
	1951-1970	2	69.53
Syrdarya	1925-1944	99	22.09
	1952-1971	2	26.78

The periods 1972-1991 (dry) and 1952-1971 (humid) were selected as design ones transferred to the future (2006-2025).

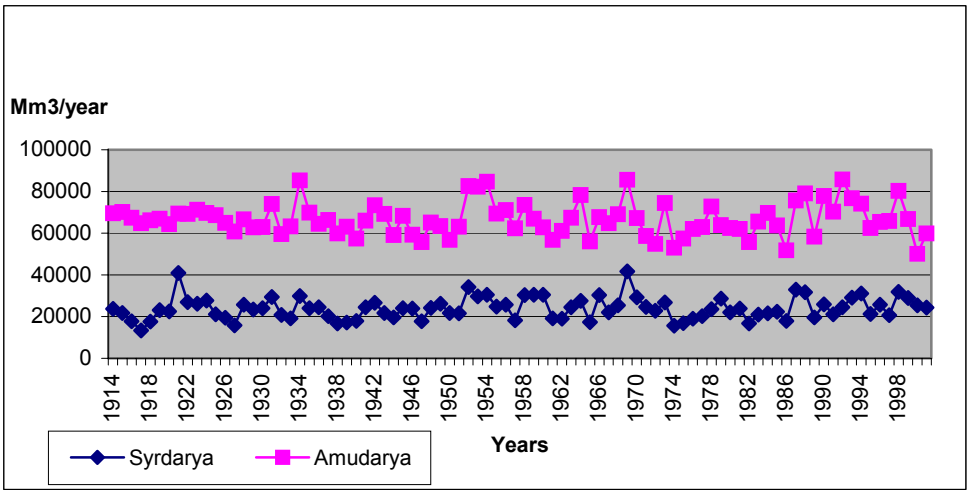

Fig. 8.8 Natural Resources of the Amudarya and the Syrdarya (sample 1914-2001)

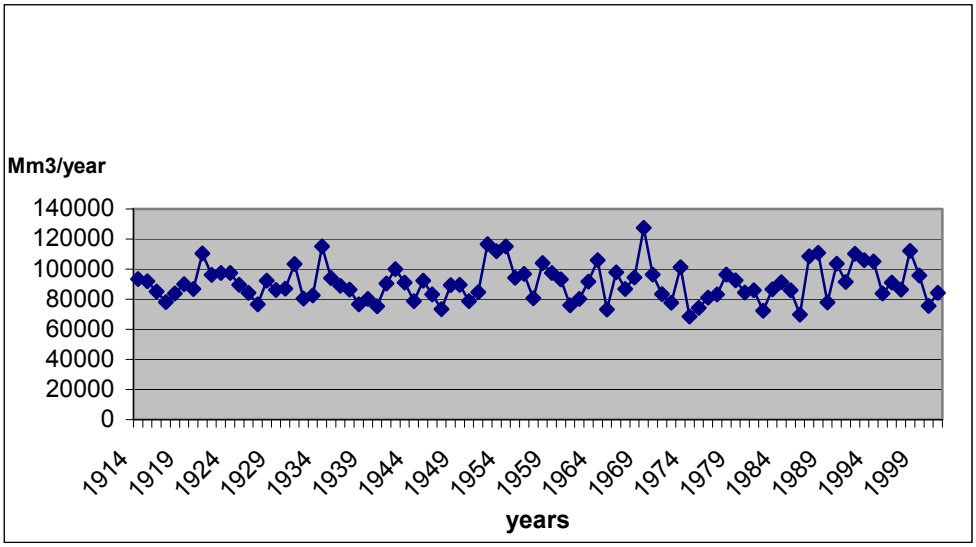

Fig. 8.9 Total Resources of the Amudarya and the Syrdarya (sample 1914-2001)

Table 8.6 shows natural flows of the Amudarya and the Syrdarya, i.e. mean flows for dry period of 1972-1991 (MIN) and humid period of 1952-1971(MAX) that are considered as hydrological series of extreme water availability for future scenarios (dry and humid 20-year periods).

Table 8.6 Flows of the Amudarya and the Syrdarya (km^3/year) averaged for a period of 20 years corresponding to water availability scenarios (MAX, MIN).

River basin	MAX	MIN	Difference
Amudarya	69.30	64.68	4.62
Syrdarya	26.80	22.52	4.28
Total	96.10	87.20	8.90

8.1 Results of Numerical Experiment on Estimation of Probable Water and Salt Inflow to Priaralie

The numerical experiment was performed in the ASBMM model, the experiment's results were analyzed and design river flow and salt hydrographs were developed at the border of Priaralie based on water availability scenarios (dry and humid 20-year periods) and national development scenarios (national vision, business as usual, optimistic).

8.1.1 Amudarya basin

The Table 8.7 gives inflow to Priaralie from the Amudarya as computed by ASBMM for two water availability scenarios – dry (MIN) and humid (MAX) – for 20-year period and three national development scenarios (national vision, business as usual, optimistic). It was assumed that dry and humid 20-year periods would occur in the future (over the period 2005/2006 – 2025) (Table 8.7, point A). Computation was corrected based on inflow for 2005/2006 (Table 8.7, point B) for all scenarios. To this end, actual flow data for October 2005 – May 2006 and flow forecast for June-September 2006 (derived from expected trend) were used.

Table 8.7 Design flow of the Amudarya (Samanbai gauging station), mean for 2005/2006-2025 (km^3/year).

Development scenarios	MAX	MIN	Difference
A. Computation by series	1952-1971	1972-1991	
1. National vision	7.51	6.04	1.47
2. Business as usual	8.24	6.96	1.28
3. Optimistic	11.47	9.08	2.39
B. Adjustment to 2005/2006			
1. National vision	7.04	5.5	1.54
2. Business as usual	7.77	6.48	1.29
3. Optimistic	11.16	8.9	2.26

Comparison of Table 8.6 and Table 8.7 shows that the difference (4.6 km^3/year) in mean natural flow volumes for dry (MIN) and humid (MAX) 20-year periods at the border of Priaralie (Samanbai gauging station) decreases to 1.3…2.3 km^3/year, depending on basin development scenario.
Distribution of inflow to Priaralie among the seasons and river water salinity are given in the Table 8.8 for the scenarios.

Table 8.8 Flow (km^3/season) / salinity (g/l) of the Amudarya (Samanbai g/s), mean for 2005/2006-2025, growing (April-September) and non-growing (October-March) seasons, adjusted to 2005/2006

Development scenario	Season	MAX	MIN
National vision	non-growing	3.98 / 1.40	2.29 / 1.77
	growing	3.06 / 1.34	3.21 / 1.36
Business as usual	non-growing	3.00 / 1.45	1.46 / 1.80
	growing	4.77 / 1.28	5.02 / 1.27
Optimistic	non-growing	3.61 / 1.25	2.32 / 1.35
	growing	7.55 / 0.90	6.58 / 0.95

8.1.2 Syrdarya basin

The Table 8.9 gives inflow to Priaralie from the Syrdarya as computed by ASBMM for two water availability scenarios – dry (MIN) and humid (MAX) – for 20-year period and three national development scenarios (national vision, business as usual, optimistic). It was assumed that dry and humid 20-year periods would occur in the future (over the period 2005/2006 – 2025) (Table 8.9, point A). Computation was corrected based on inflow for 2005/2006 (Table 8.9, point B) for all scenarios. To this end, actual flow data for October 2005 – May 2006 and flow forecast for June-September 2006 were used.

Table 8.9 Flow of the Syrdarya (Kazalinsk g/s), mean for 2005/2006-2025 (km^3/year).

Development scenarios	MAX	MIN	Difference
A. Computation by series	1952-1971	1972-1991	
1. National vision	3.98	2.91	1.07
2. Business as usual	5.27	4.02	1.25
3. Optimistic	7.22	4.96	2.26
B. Adjustment to 2005/2006			
1. National vision	3.95	3.04	0.91
2. Business as usual	5.22	4.12	1.10
3. Optimistic	7.27	5.03	2.24

Comparison of Table 8.5 and Table 8.9 shows the same behavior in the Syrdarya basin as in the Amudarya basin: natural flow variability is “smoothed” down the stream through withdrawal fluctuations and flow losses.
Fig. 8.10 – Fig. 8.15 show the flow hydrographs of the Syrdarya in Kazalinsk g/s for various scenarios of water availability and basin development and the integral curves, and the Table 8.10 gives inflow distribution among the seasons and salinity.

Table 8.10 Flow (km^3/season) / salinity (g/l) of the Syrdarya, mean for 2006-2025, growing (April-September) and non-growing (October-March) seasons.

Development scenario	Season	MAX	MIN
National vision	non-growing	3.46 / 1.47	2.61 / 1.61
	growing	0.49 / 1.35	0.43 / 1.51
Business as usual	non-growing	4.43 / 1.36	3.50 / 1.50
	growing	0.79 / 1.30	0.62 / 1.46
Optimistic	non-growing	4.76 / 1.05	3.17 / 1.12
	growing	2.51 / 1.00	1.86 / 1.10

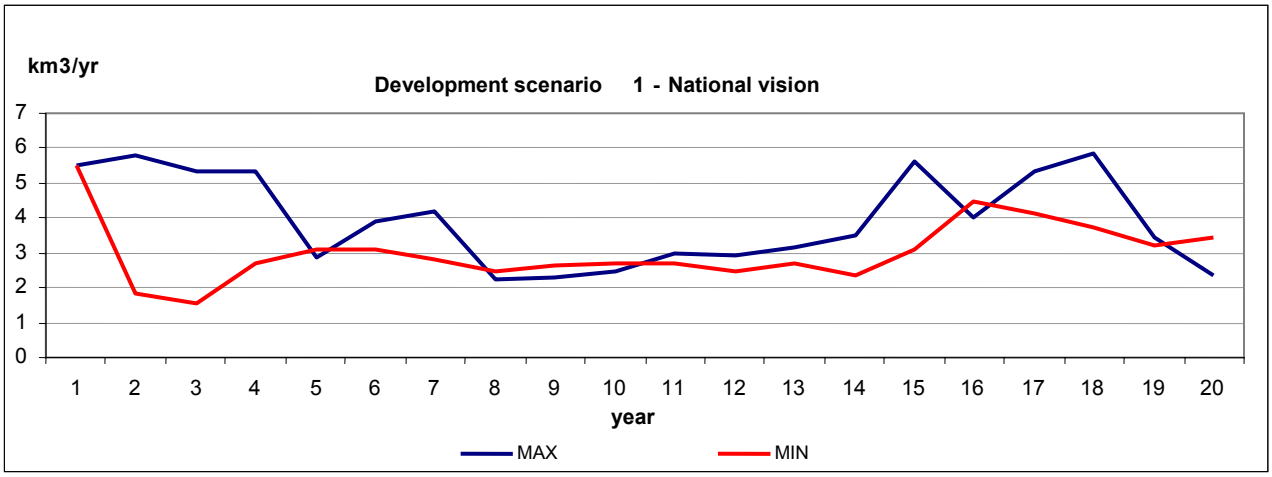

Fig. 8.10 MIN and MAX flow hydrographs of Syr Darya at Kazalinsk (ASBMM simulations for period 2005/06-2025) – Scenario 1

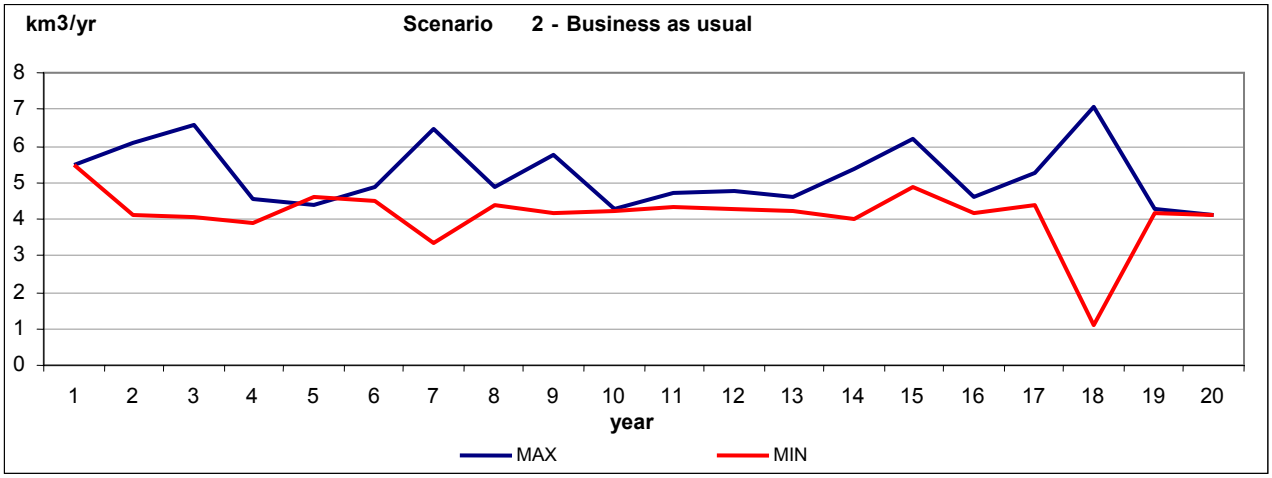

Fig. 8.11 MIN and MAX flow hydrographs of Syr Darya at Kazalinsk (ASBMM simulations for period 2005/06-2025) – Scenario 2

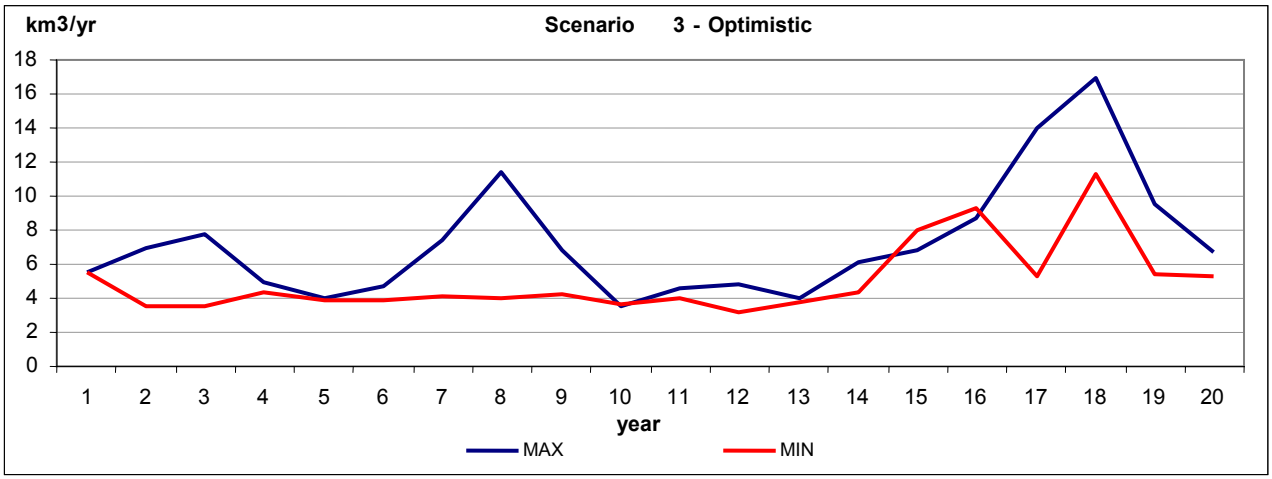

Fig. 8.12 MIN and MAX flow hydrographs of Syr Darya at Kazalinsk (ASBMM simulations for period 2005/06-2025) – Scenario 2

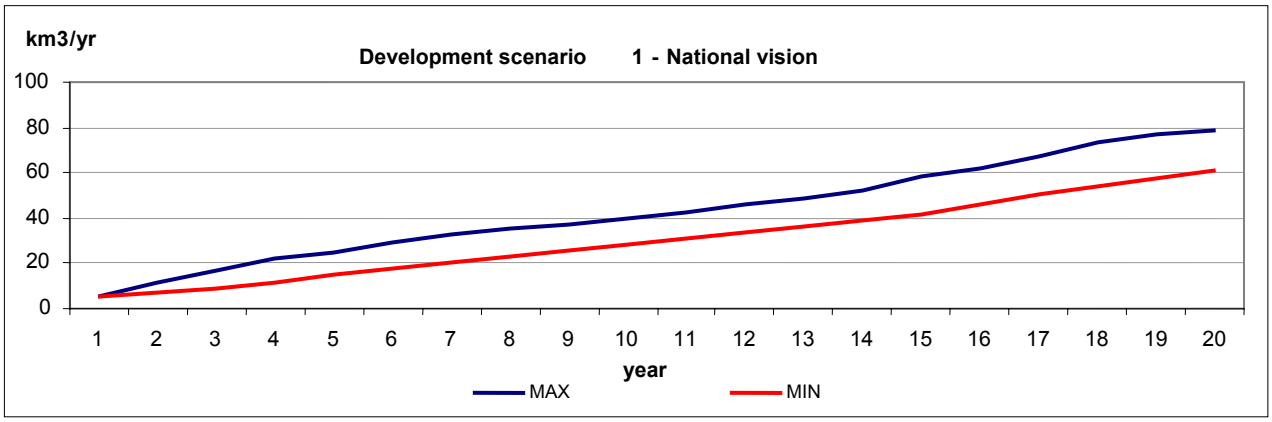

Fig. 8.13 Cumulative MIN and MAX Flow Hydrographs of Syrdarya at Kazalinsk (ASBBM simulations for the Period 2005/06-2025) – Scenario 1

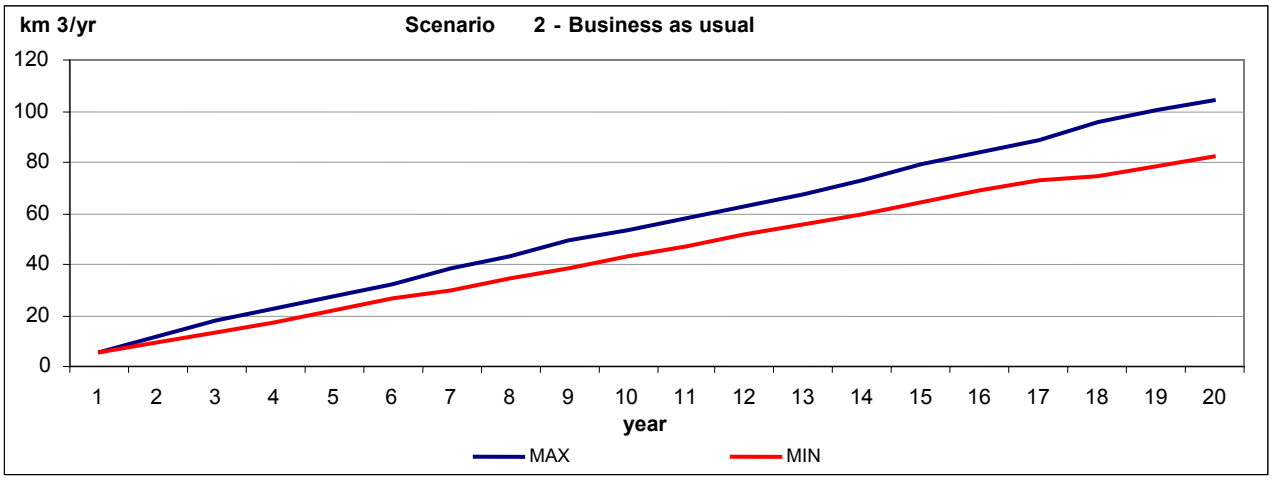

Fig. 8.14 Cumulative MIN and MAX Flow Hydrographs of Syrdarya at Kazalinsk (ASBBM simulations for the Period 2005/06-2025) – Scenario 2

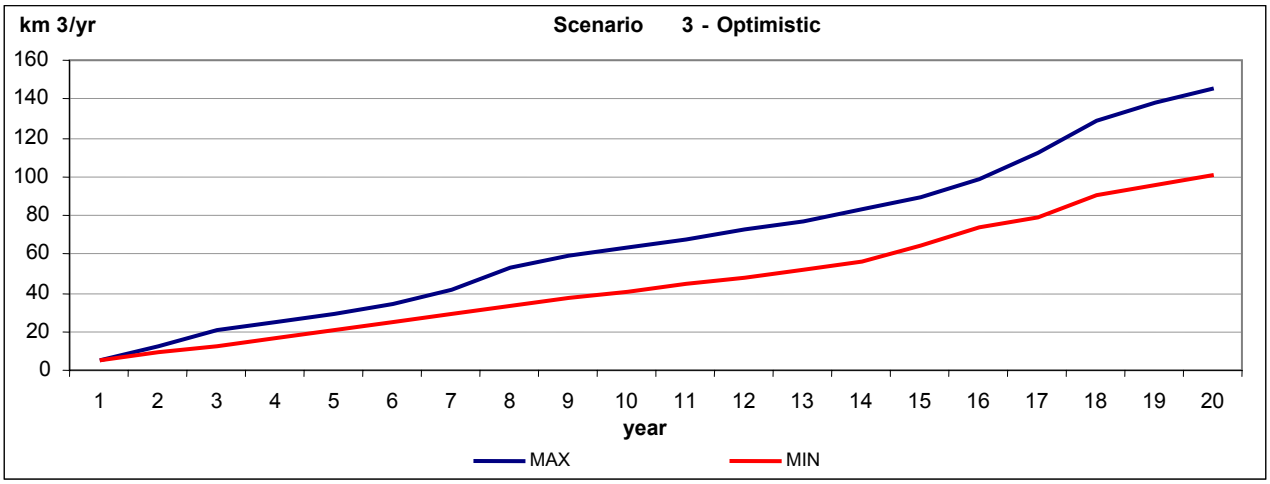

Fig. 8.15 Cumulative MIN and MAX Flow Hydrographs of Syrdarya at Kazalinsk (ASBBM simulations for the Period 2005/06-2025) – Scenario 3

The expected inflows were inputted into the database.
If inflows to Amudarya delta are input data for non-dimensional Aral Sea model, inflow to Syrdarya delta should be adjusted in a part of filling regime of the Small Sea, from which releases are formed to the Large Sea. To this end, at first, the Small Sea model was calibrated on field data.

8.1.3 Model calibration

For model calibration numerical experiment has been organized, which permitted “tune” the model on real events occurring in Northern Sea. Calibration was performed by following indicators:

- Water level in Northern Sea,
- Water salinity in Northern Sea.

To compare modeling results with actual (measured) data, Geography Institute’s of Kazakhstan data were used.
Length of comparative series was 11 years since 1988 till 1998. Goal of comparison was verification of calculation algorithm and its transformation into computer code as well as verification of used bathymetric table for Northern Sea.
Water balance accuracy will depend on error of balance elements measurement. It can be calculated by formula:

$$\sigma_0 = \sqrt{\sigma_п + \sigma_c + \sigma_y + \sigma_o + \sigma_и + \sigma_ф}, \qquad (8.1)$$

where σ_0 – balance error,
$\sigma_п$ – inflow definition error,
σ_c – collector-drainage flow definition error,
σ_y – volume definition error,
σ_o – precipitation definition error,
$\sigma_и$ - evaporation definition error,
$\sigma_ф$ – ground water exchange definition error.

If error in average monthly river discharge (acc. to Yu.N.Ivanov) equals 5%, collector flow - 10%, and volume definition by level - 5%, water balance error will be 7,4%.

$$S_{yx} = \sigma_y \sqrt{1 - r^2}\ , \qquad (8.2)$$

where σ_y -standard deviation of time series,

r - correlation coefficient of calculated and observed time series.

Value S_{yx} in our case is 3,3%. (correlation coefficient – 0,98; standard deviation – 23,37). Under 95% confidence interval (defencibility - 95%) error will be within $\pm 2S_{yx}$, e.g. 6,6%, that is less than water balance measurement error (7,4%).
On base of the same methodology let us compare design water body salinity. Average deviation between calculated and observed values S_{yx} – 2% under correlation coefficient r - 0,99, standard deviation of time series is σ_y - 13,6. Instrumental error of water salinity definition is 5%. Thus, we can say about 95% probability in water salinity calculation.
Obtained results allow us to consider as expedient model use for preparation of prospective water and salt balance of the Northern sea (with step more than one month), in particular, for both definition of its state (level, volume, area, salinity) and balance elements including precipitation, evaporation and releases to Large Aral sea (under set limitations on inflow to Northern sea, stabilization level and capacity for release to Large Aral sea).

Based on approbation results, 6 options were computed for three scenarios for two possible sea levels – 42 (options 1, 3 and 5) and orientation to 47 (options 2, 4, 6). The modeling results are shown in the Table below and in Fig. 8.14.

Table 8.11 Dynamics of water level (m) and salinity (g/l) in Northern sea (by the beginning of year) over options *)

Year	Option 1	Option 2	Option 3	Option 4	Option 5	Option 6
2010	42 / 16,2	43,32 / 14,3	42 / 15,8	43,75 / 13,7	41,60 / 16,7	42,47 / 15,7
2015	42 / 15,8	44,65 / 13,0	42 / 14,7	46,69 / 10,9	40,61 / 18,5	41,66 / 17,5
2020	42 / 15,7	45,63 / 12,4	42 / 14,1	47 / 10,8	42 / 17,2	42,49 / 16,7
2025	42 / 15,4	46,55 / 11,9	42 / 11,4	47 / 9,8	42 / 17,2	43,35 / 15,6
2030	42 / 15,6	46,29 / 12,6	42 / 11,4	46,84 / 10,2	42 / 17,7	43,43 / 16,1
2035	42 / 15,9	46,34 / 13,0	42 / 10,6	47 / 9,9	42 / 18,1	43,63 / 16,3
2040	42 / 16,0	46,61 / 13,2	42 / 9,6	47 / 9,6	42 / 18,2	44,27 / 15,8
2045	42 / 15,9	4,97 / 13,2	42 / 8,4	47 / 9,1	42 / 17,8	45,50 / 14,6
2050	42 / 15,6	46,68 / 13,5	42 / 7,2	47 / 8,4	42 / 17,5	46,44 / 13,9
2055	42 / 15,2	47 / 13,5	42 / 6,3	47 / 7,8	42 / 17,6	46,41 / 14,3

Thus, these computations show that the level 42 is guaranteed in all development options for the Syrdarya river, though salinity in options 1, 2, 5, 6 will be favorable for fish growing but unfavorable for spawning which, evidently, will take place at the point of Syrdarya inflow into the Small Sea. Obviously, it makes sense to increase the level of the reservoir to 47 only in the optimistic option.
Computations of Small Sea regime were adjusted on hydrographs of dry and humid 20-year periods. 6 options of Amudarya river flow in Samanbai g/s and of Syrdarya river flow in Kazalinsk g/s are shown in Fig. 8.16, Fig. 8.17, and the results and schemes of basic indicators in 6 options are shown in Fig. 8.18 - Fig. 8.23.
These results prove that the level of 47 in the Northern Sea can be ensured at the mean inflow to the Large Aral of 1,6 km^3/year only in humid five-year period of the optimistic option. The level of 43 … 46 is preferable in other options.

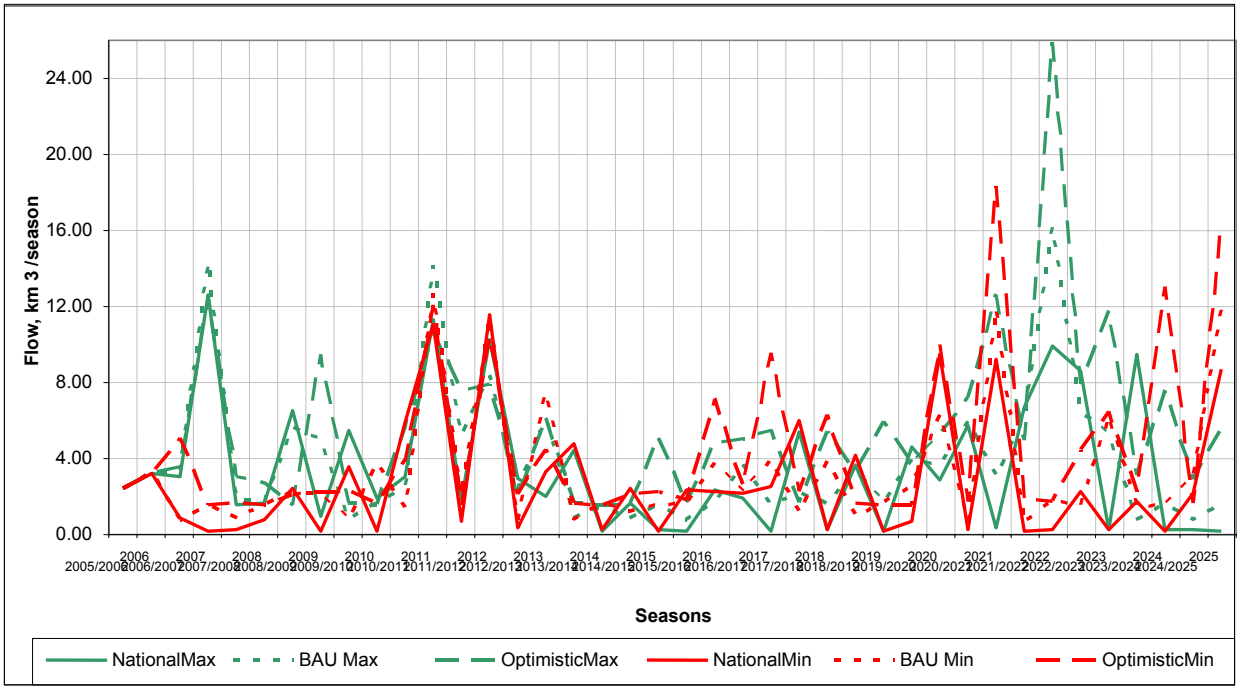

Fig. 8.16 Amudarya river flow in Samanbai, scenarios for 2005/06 – 2025 by season (non-growing, growing)

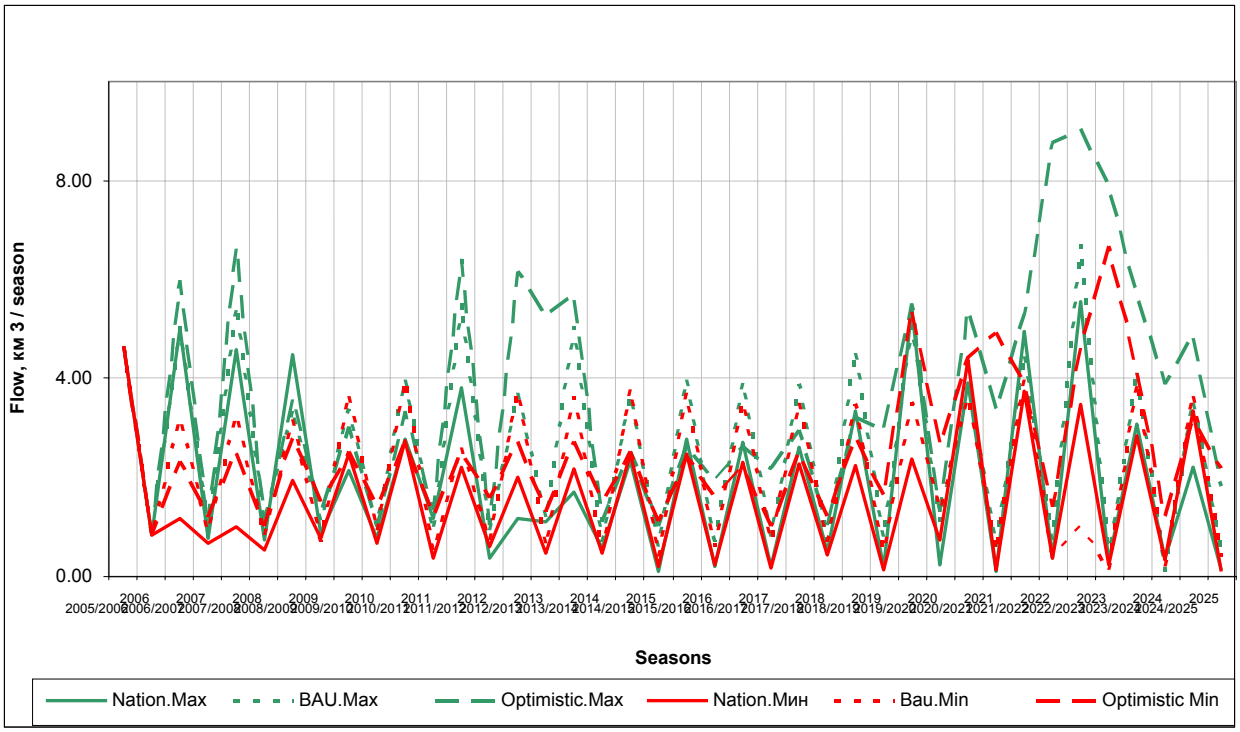

Fig. 8.17 Syrdarya river flow in Kazalinsk, scenarios for 2005/06 – 2025 by seasons (non-growing, growing)

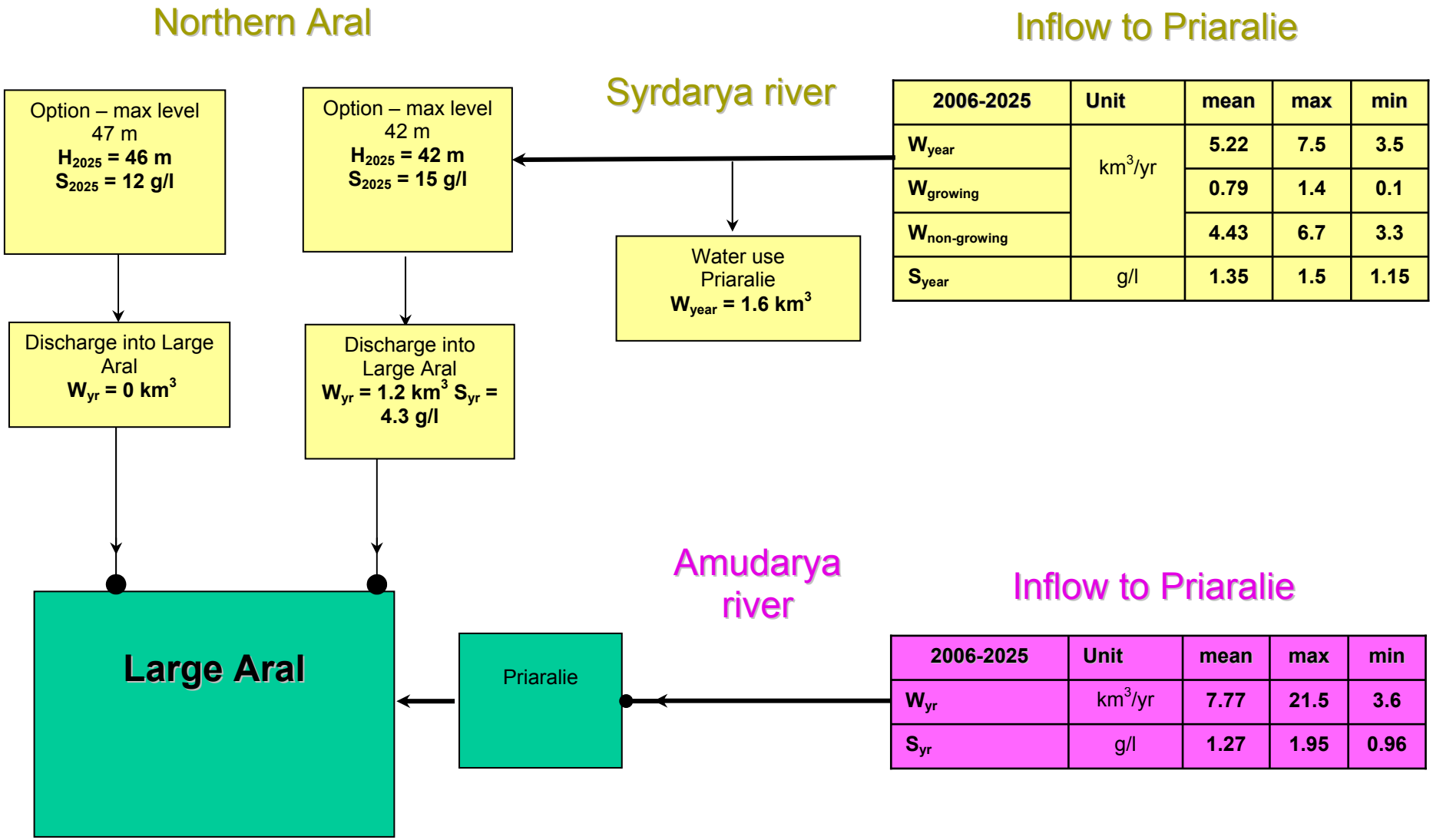

2006-2025	Unit	mean	max	min
W_{year}	km^3/yr	5.22	7.5	3.5
$W_{growing}$		0.79	1.4	0.1
$W_{non-growing}$		4.43	6.7	3.3
S_{year}	g/l	1.35	1.5	1.15

2006-2025	Unit	mean	max	min
W_{yr}	km^3/yr	7.77	21.5	3.6
S_{yr}	g/l	1.27	1.95	0.96

Fig. 8.18 Development Scenario: “Business as Usual” – Water Availability Scenario for 2006-2025: “Humid 20-year Period”

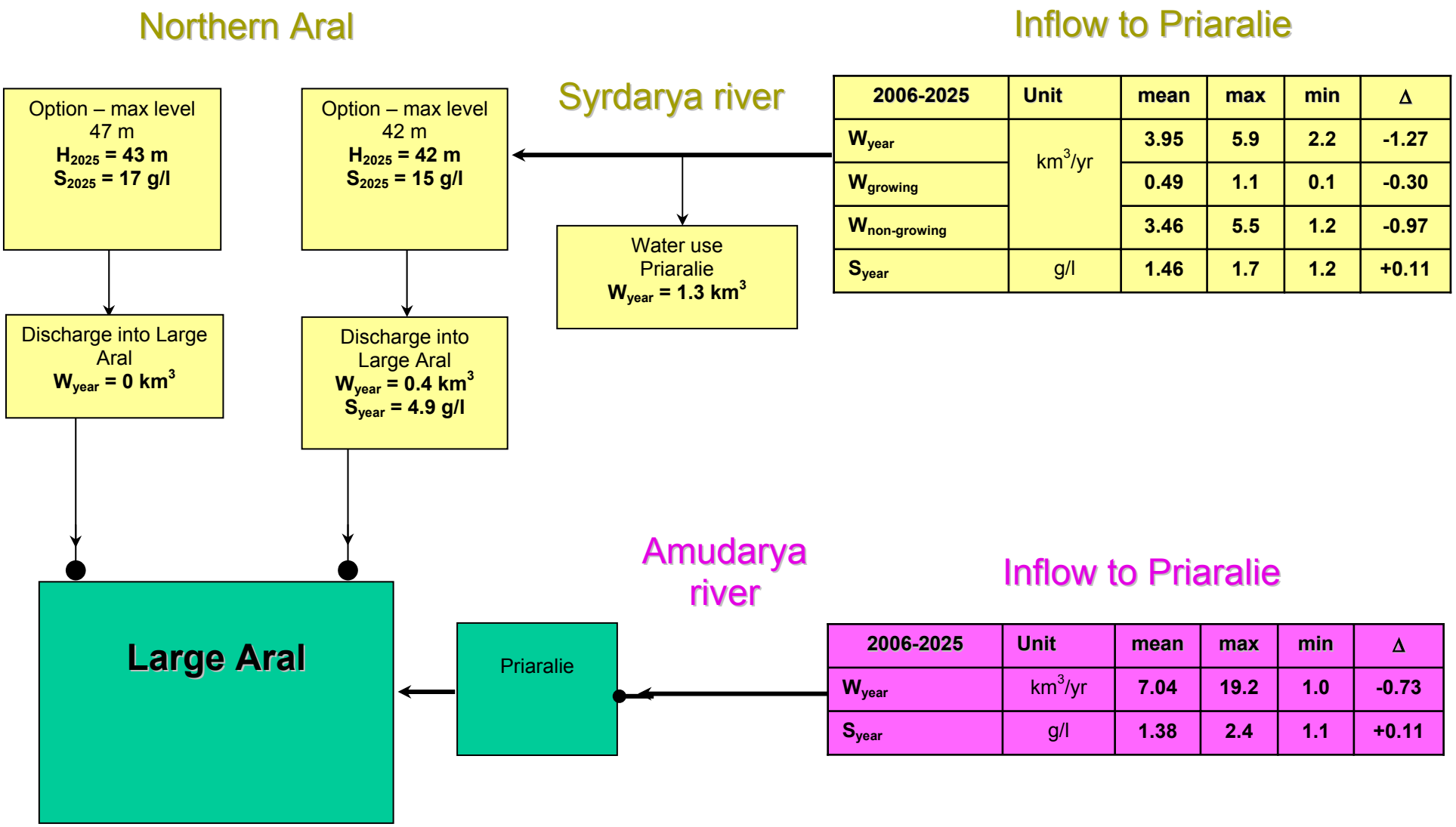

2006-2025	Unit	mean	max	min	Δ
W_{year}	km³/yr	3.95	5.9	2.2	-1.27
$W_{growing}$		0.49	1.1	0.1	-0.30
$W_{non-growing}$		3.46	5.5	1.2	-0.97
S_{year}	g/l	1.46	1.7	1.2	+0.11

2006-2025	Unit	mean	max	min	Δ
W_{year}	km³/yr	7.04	19.2	1.0	-0.73
S_{year}	g/l	1.38	2.4	1.1	+0.11

Fig. 8.19 Development Scenario: “National Vision” – Water Availability Scenario for 2006-2025: “Humid 20-year Period”

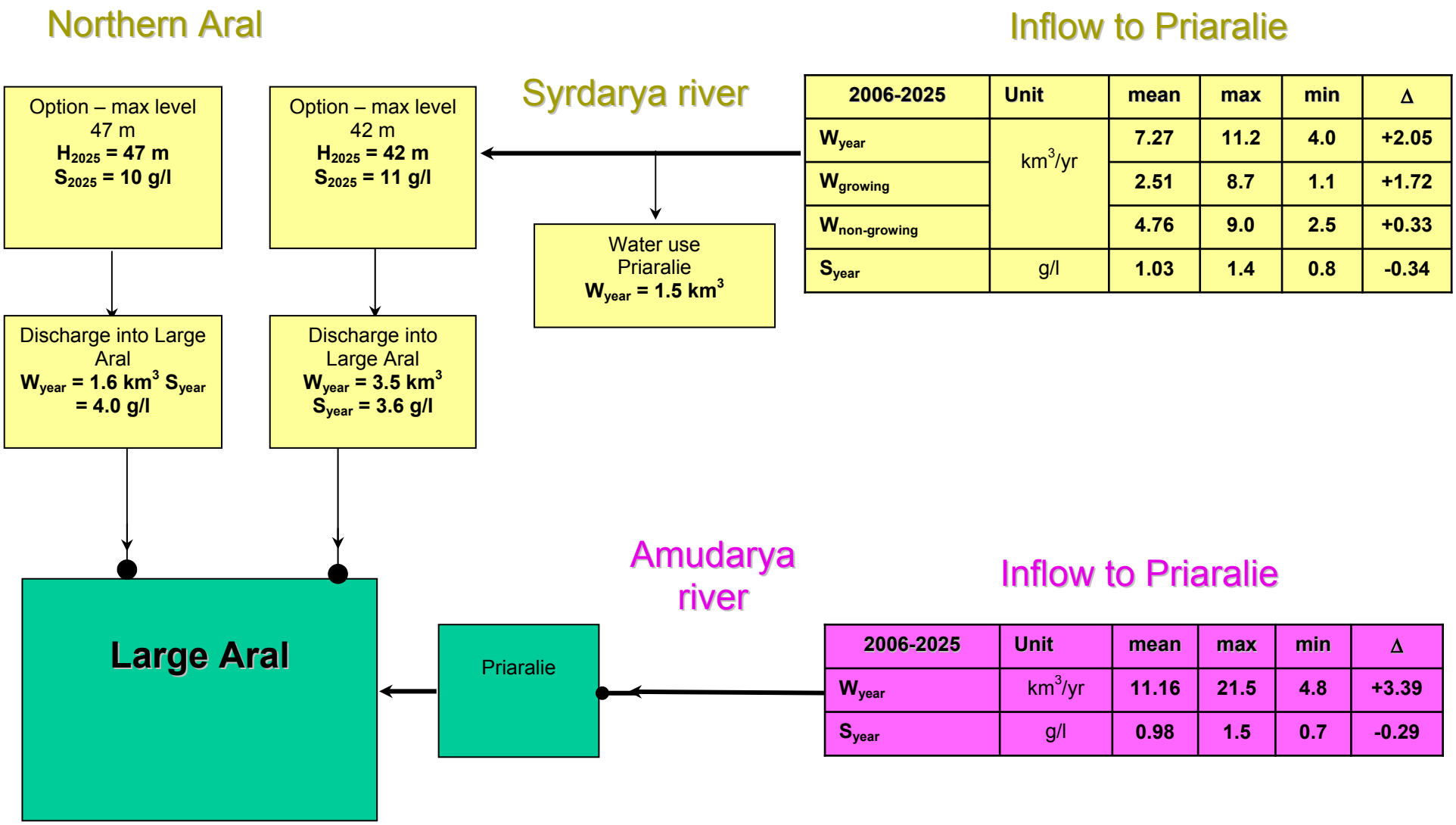

2006-2025	Unit	mean	max	min	Δ
W_{year}	km^3/yr	7.27	11.2	4.0	+2.05
$W_{growing}$		2.51	8.7	1.1	+1.72
$W_{non-growing}$		4.76	9.0	2.5	+0.33
S_{year}	g/l	1.03	1.4	0.8	-0.34

2006-2025	Unit	mean	max	min	Δ
W_{year}	km^3/yr	11.16	21.5	4.8	+3.39
S_{year}	g/l	0.98	1.5	0.7	-0.29

Fig. 8.20 Development Scenario “Optimistic” – Water Availability Scenario for 2006-2025: “Humid 20-year Period”

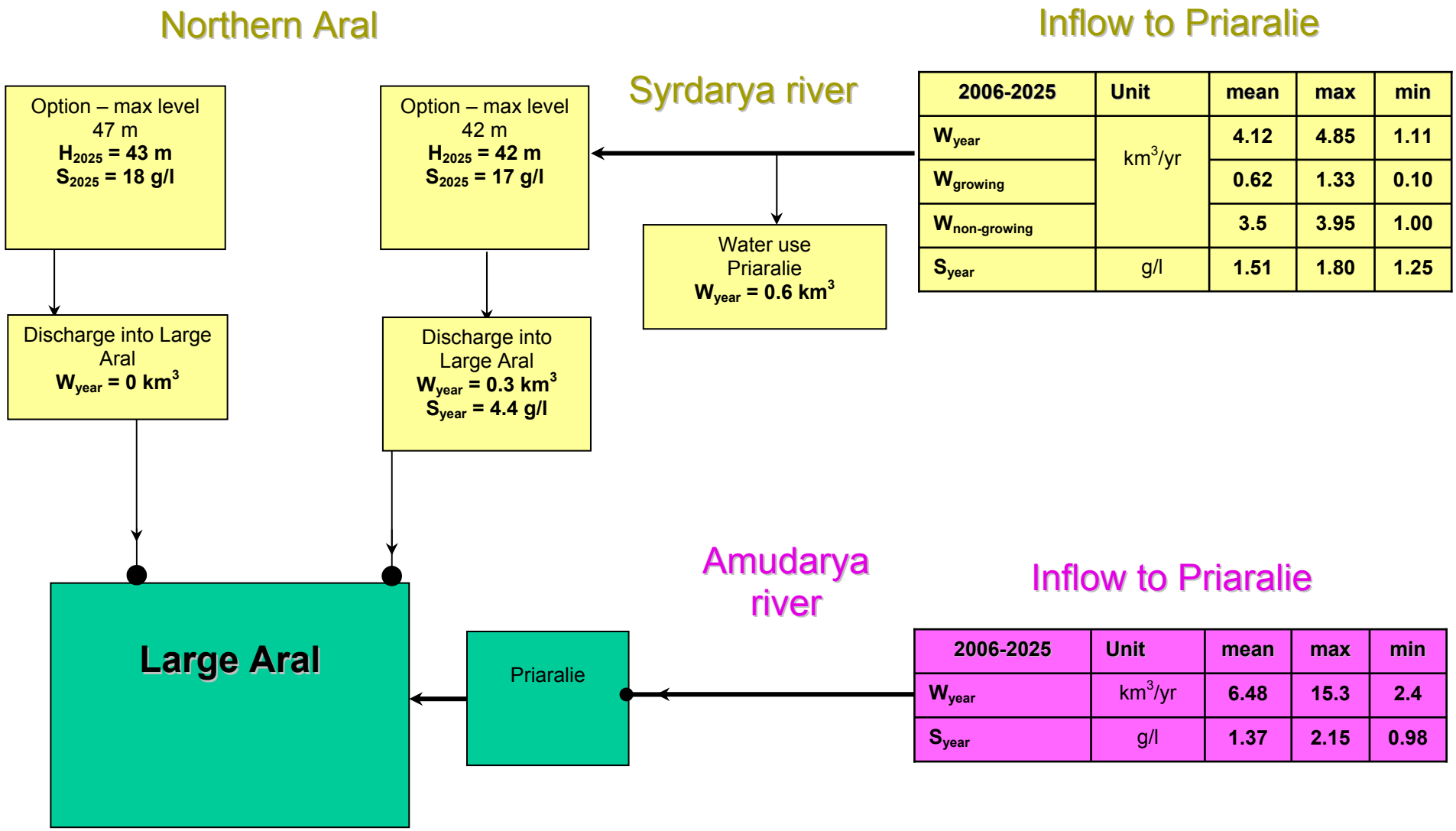

2006-2025	Unit	mean	max	min
W_{year}	km^3/yr	4.12	4.85	1.11
$W_{growing}$		0.62	1.33	0.10
$W_{non-growing}$		3.5	3.95	1.00
S_{year}	g/l	1.51	1.80	1.25

2006-2025	Unit	mean	max	min
W_{year}	km^3/yr	6.48	15.3	2.4
S_{year}	g/l	1.37	2.15	0.98

Fig. 8.21 Development Scenario: “Business as Usual” – Water Availability Scenario for 2006-2025: “Dry 20-year Period”

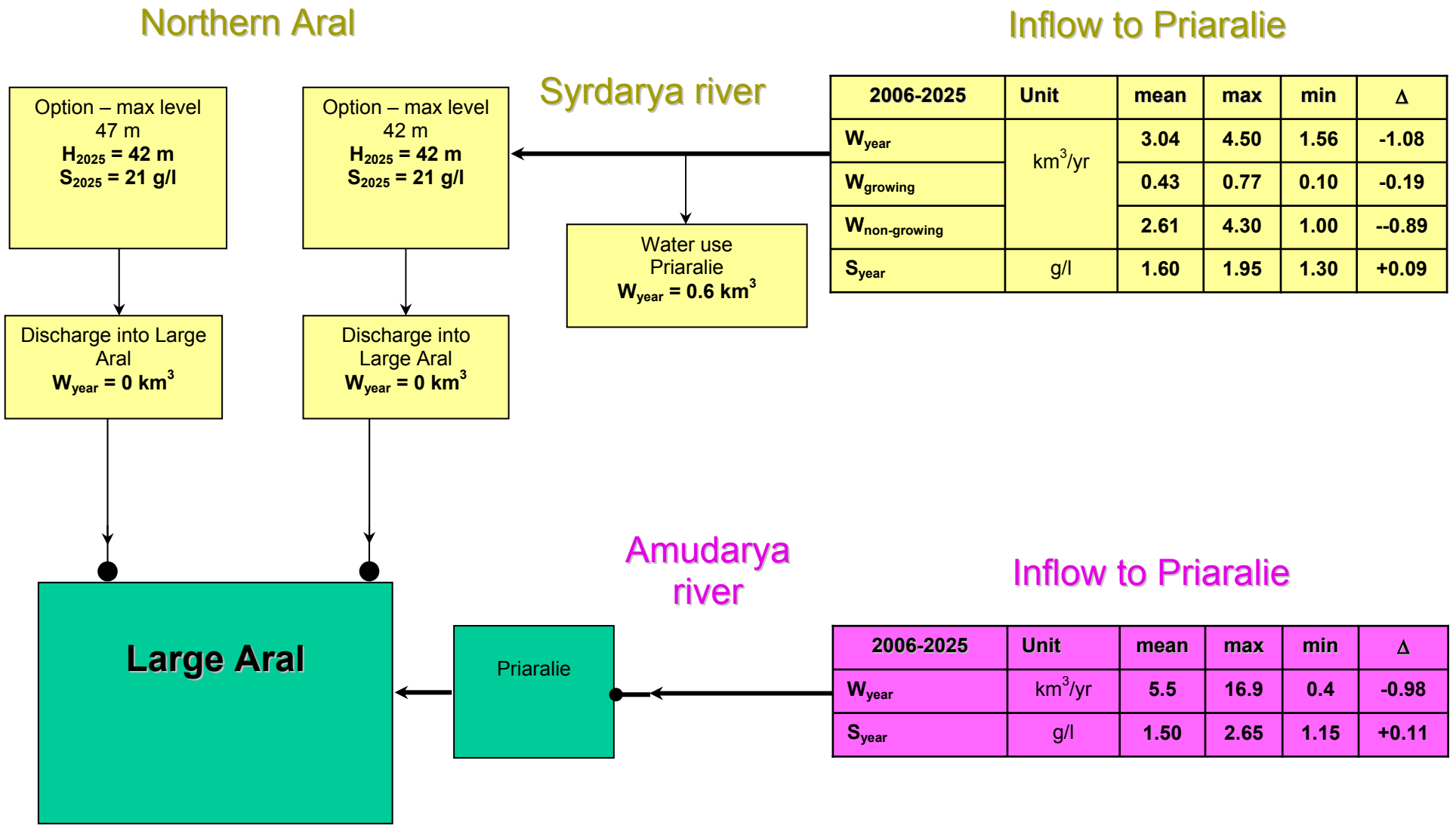

2006-2025	Unit	mean	max	min	Δ
W_{year}	km³/yr	3.04	4.50	1.56	-1.08
$W_{growing}$		0.43	0.77	0.10	-0.19
$W_{non-growing}$		2.61	4.30	1.00	--0.89
S_{year}	g/l	1.60	1.95	1.30	+0.09

2006-2025	Unit	mean	max	min	Δ
W_{year}	km³/yr	5.5	16.9	0.4	-0.98
S_{year}	g/l	1.50	2.65	1.15	+0.11

Fig. 8.22 Development Scenario: “National Vision” – Water Availability Scenario for 2006-2025: “Dry 20-year Period”

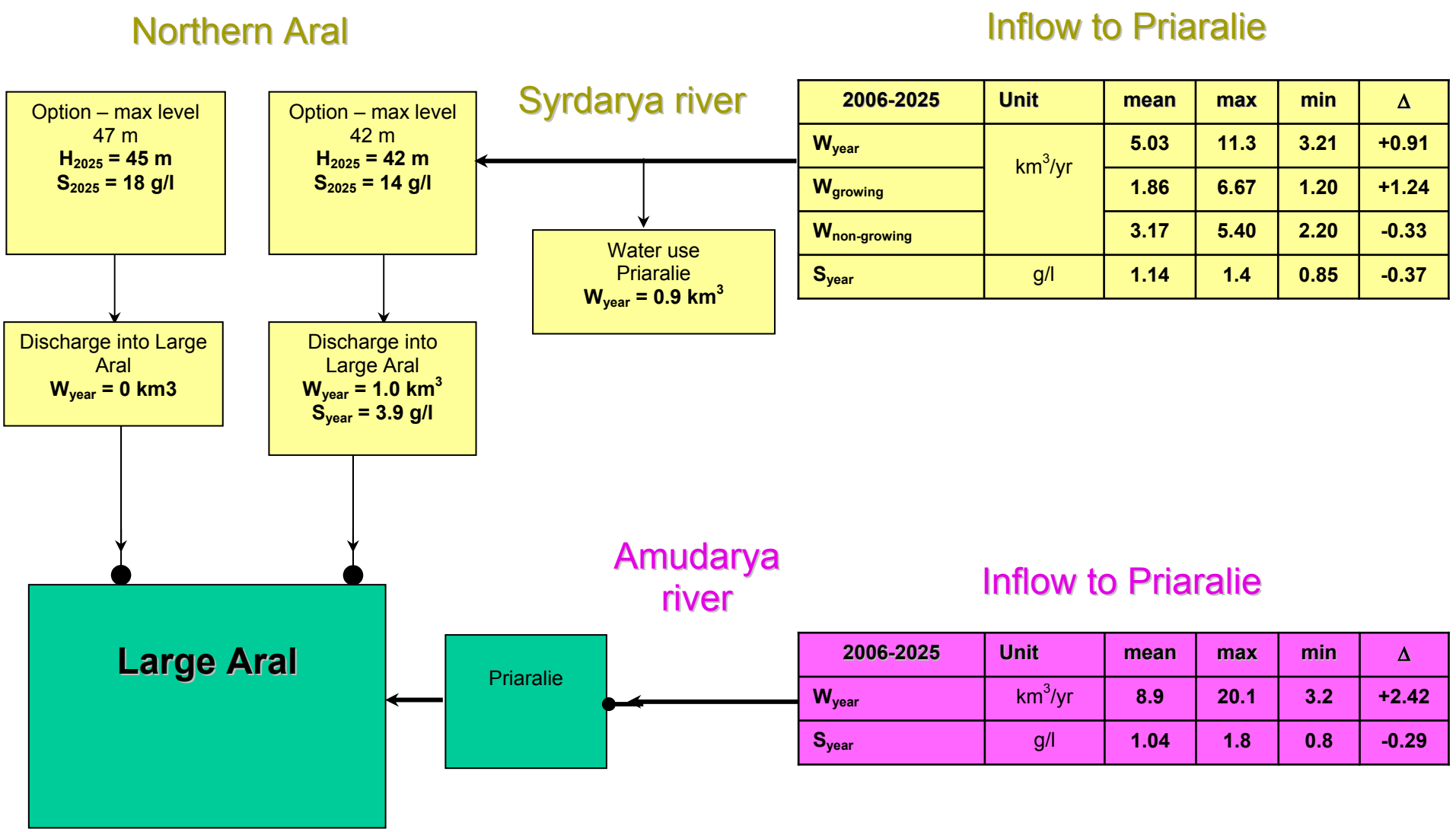

2006-2025	Unit	mean	max	min	Δ
W_{year}	km³/yr	5.03	11.3	3.21	+0.91
$W_{growing}$		1.86	6.67	1.20	+1.24
$W_{non\text{-}growing}$		3.17	5.40	2.20	-0.33
S_{year}	g/l	1.14	1.4	0.85	-0.37

2006-2025	Unit	mean	max	min	Δ
W_{year}	km³/yr	8.9	20.1	3.2	+2.42
S_{year}	g/l	1.04	1.8	0.8	-0.29

Fig. 8.23 Development Scenario: “Optimistic” – Water Availability Scenario for 2006-2025: “Humid 20-year Period”

9. Object infrastructure and the order of model interaction

As a working assumption for modeling an evolution of the Aral Sea a set of three mathematical models is considered, which represents various aspects of the sea behavior and development. Those are hydrological, hydro-dynamical, and environmental models. Each model has its own aim and solves a specific range of problems so that to justify every restoration option, as well as to develop recommendations on water management when operating reservoirs in the Amudarya river delta. Though different spatial and temporal scales are applied in the models to describe processes, the models have common topographic basis through which all modeling (two simulations and one optimization) results at two hierarchical levels are coordinated. At higher hierarchic level the Aral Sea is considered as a system consisting of four interconnected objects: AmuDrya delta, Aral Sea's Western bowl, Aral Sea's Eastern bowl and Aral Sea's Northern bowl referred to as the Small Aral Sea with own economic and ecological indicators. Division of the system into four components is caused by difference between water resources transfer from the Amudarya delta to the Aral Sea's Western part and their transfer firstly to Eastern part and then to the Western part of the Sea. Besides, separate account of filling the sea has both economic and social character. At this level water resources are transferred from the two rivers to appropriate objects depending on reservoir location within the Amudarya delta and filling strategy and only then they are forwarded to the Aral Sea. System feedback to various amounts and options of water resources distribution are average-weighted values of free surface altitude and water salinity. Here mainly the hydrological modeling is undertaken and helps to justify a strategy of water supply and to estimate levels that are stable on long-term basis in Eastern and Western Seas.

The second hierarchic level is comprised of three simulation models, two of which describe water movement and mixing dynamics within Eastern and Western parts, while the third one - formation and development of biological populations under ecological conditions determined by first two models. The mathematical model of CR3 group is based on equations coming out from the laws of mass and momentum conservation for two-phase liquid under the assumption that the volume of solid phase (in this case - salinity) is quite small and only forms ecology of the environment, while momentum conservation equations are written for homogenous liquid with variable density. The boundary conditions for this model are formed at previous hierarchic level and reflect chosen water resources distribution strategy, current situation in Eastern and Western parts of the Aral Sea and external climatic factors of the Aral region. Model outputs (statistical characteristics of Eastern and Western parts) form ecological conditions for further environmental model, which, in turn, based on ordinary differential equations, simulates dynamics of biological populations for considered option of bio-productivity development in the Western part of the sea.

Joint operation of these mathematical models helps to predict integrated development of the Aral Sea under various environmental impacts and to find optimal conditions for natural environment restoration under different national development scenarios in the Central Asian countries. Forecast is based on combination of reservoirs' (maintained and periodically emptied) simulation mode and analysis of consequences of these modes as well as compliance of these conditions with the requirements dictated by the project's ecological concerns.

9.1 Hydrological Modeling

The aim of hydrological modeling is to find permissible water elevations for the lake system and the sea through current and planned water inflows and in light of changes in the infrastructure of feeding canals and collectors and to forecast annual changes in the water levels on the basis of flow probability in the Amudarya and the Syrdarya rivers and chosen water management policy.

Mathematical model, chosen for hydrological modeling, is based on a system of ordinary differential equations describing structural relations within the system of reservoirs and all elements of water balance, with account of water salinity.

Input data for the hydrological model are comprised of a scheme of spatial distribution of reservoirs, with indicated feeder and discharge canals and collectors, curves of free water surface volume and area as a function of water levels for each reservoir, time series of water inflow, reed and cattail coverage of reservoirs, and temperature and rainfall plots.

Model outputs are the sets of reservoir's water level curves in monthly and annual dimensions, amounts of evaporation and filtration, as well as average salinity in each reservoir with regard to flow changes and adopted water allocation policy.

9.2 Hydro-dynamic model

The aim of hydro-dynamic modeling is to find an intensity of water masses mixing inside each reservoir, to determine the main parameters of streams and salinity distribution in time in the Western and Eastern parts of the Aral sea on the basis of hydraulic resistance change due to reed and cattail expansion.
Mathematical models chosen for hydro-dynamical modeling are based on a system of partial differential equations, which follow the laws of mass and momentum conservation for two-phase liquid under the assumption that the volume of solid phase (in this case - salinity) is quite small and only forms ecology of the environment, while momentum conservation equations are written for homogenous liquid with variable density. Boundary conditions of these models are set on the basis of the solution of the first level problem and the physical and climatic characteristics of the year under consideration.
Input data of the hydro-dynamic model include: topographic map of relief, layout of canals and collectors, time series of water inflow, with data on salinity and temperature, reed and cattail areas, temperature and evaporation curves.
Model outputs are presented in form of datasheets comprising parameters of streams within water space, free water surface elevations and salinity depending on state of reservoir and water inflow.

9.3 Environmental Modeling

The aim of environmental modeling is to find permissible depths, salinity and active oxygen content in selected water areas of the Aral Sea based on environmental requirements for projected options of biological and water resources restoration. Using these data, bio-productivity growth will be estimated in selected parts of the Aral Sea.
Mathematical model, chosen for environmental simulation, is based on a system of ordinary differential and algebraic equations describing the processes of bio-resources growth and disappearing depending on water depth and salinity, dynamics of frost penetration into water bodies and presence of active oxygen in summer and winter periods.
Input data of the environmental model include: parameters of water flows and their salinity from hydraulic model, time series of temperature and active oxygen from hydro-dynamic model (groups CR3, CR5) and coefficients of biomass growth as a function of depth, temperature, salinity and active oxygen derived from group CR4 environmental research.
Model outputs are given in the form of sets of maps representing changes in volumes of vegetation and in bio-productivity for various periods of time (for each period its own set of maps), with indication of the most risky periods of time in the Aral Sea evolution.

9.4 Model Contents

Each model (hydrological, hydrodynamic, environmental*)* consists of several blocks (modules) describing evolution of an object and connected with database*.* All blocks are characterized by strict succession of task fulfillment determined by the system's interface (Fig. 9.1).
Hydrological model consists of four GAMS-blocks and the database*:*

RS - Syrdarya river,
RA - Amudarya river,
DA - Amudarya delta,
AS – Aral Sea.

Last block *AS,* in process of the sea evolution, is reduced to three independent blocks:

ASm - Small Aral Sea,
ASe - Eastern bowl of the Large Aral Sea,
ASw - Western bowl of the Large Aral Sea.

Blocks operate in three cycles with the following succession: *(RS, RA)* - simultaneously, $\Rightarrow$ *(DA)* - independently, $\Rightarrow$ *(AS).* Blocks work succession is provided by *database* interface. Layout of objects corresponding to hydrological blocks is presented in Fig. 9.1.

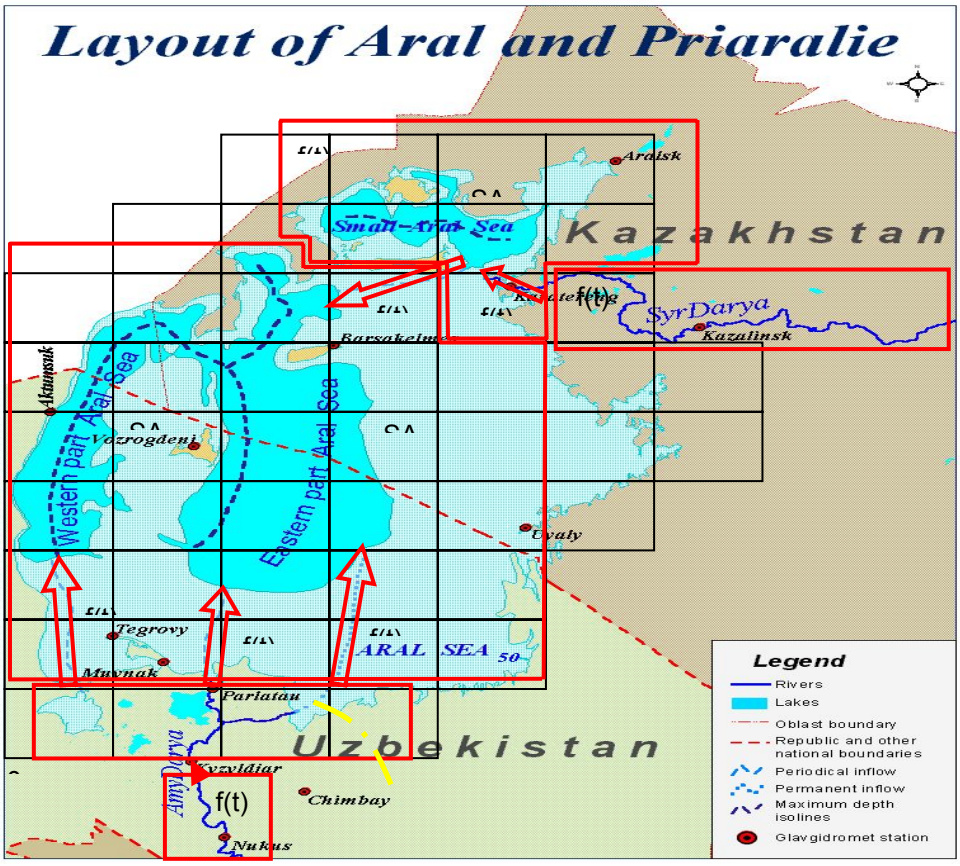

Fig. 9.1 Map of Priaralie and Aral Sea Region

9.5 Model Work Modes

Studies of evolution of an object by mathematical methods require that time series be selected and used to calibrate and evaluate the adequacy of chosen mathematical models and testing and forecast periods. Within given project those periods are distributed rationally in the following way:

- ... 1960 -period of stationary state of the sea (in long-term dimension),
- 1961 - 2002 - reference period of unsteady state of the sea,
- 2000 - 2005 - testing period,
- 2000 – 2025 forecasting period

The first period is characterized by average long-term values of parameters by months combined with affixment to the project site coordinates.
The second period is represented by annual values in monthly profile with coordinate affixment to the objects selected on the project site.
The first two periods form the basis for obtaining values of phenomenological parameters for all groups of mathematical models.
The forecasting period is unlimited since at present one can quite definitely estimate a period of the Aral Sea stabilization through the water factor, i.e. water surface elevation and volume of water body under different water inflows; however, time of stabilization of hydro-chemical and biological processes cannot be determined at the given stage. The testing period within the framework of the given project allows evaluating the accuracy of forecasts in the first approximation and, if necessary, specifying recommendations based on forecast results or rejecting such recommendations.

Thus, all groups of mathematical models should be worked over in three modes:

- calibration of phenomenological parameters,
- short-term forecast (testing period),
- long-term forecast.

9.6 Models of Delta Reservoirs

Taking into account that after water inflow to the delta mouth, water is prone to transformations in reservoirs and water systems, our research gave particular attention to models of the reservoirs. The key principles of such modeling were discussed in work "South Priaralie – new perspectives" (Ecotec Resource Netherlands, SIC ICWC, Central Asia, Tashkent 2003). Nevertheless, from the accumulated experience, certain corrections were made within the given project.

10. Formal Description of the Hydrological Model

10.1 Formal Description of a Reservoir

The formal description of the processes determining evolution of a reservoir is based on a system of three ordinary differential equations, which reflect inflow and outflow of water resources, variation of salinity levels and overgrowing of water areas with reed. Selection of such a list of ecosystem components is determined by the estimated relevance of the components, and by the possibility of making an indirect assessment of other ecological parameters using above-mentioned components. An important element of a reservoir's water balance is evaporation, which amounts to about 300 mm/month from free water surface during summer period in the Aral Sea region. Vegetation covered water surfaces show greater losses. Evapotranspiration of reed and cattail increases evaporation 1.6 - 1.7 times and results in 340 mm/month at an average annual value of 1600 mm/year. Therefore, among the basic parameters that form water-related and environmental balances of lakes are the areas under reeds and the water salinity. For further development of the mathematical model we consider an elementary reservoir, the geometry of which is described by two functions Ω (z) and L(z), where z is the water surface level, Ω(z) is the free water surface at z-level, and *L (z)* is the contour encompassing the free water surface Ω(z) at the same z-level. Both functions depend on the topography of the site where waters are located. Hereinafter, under the term "elementary reservoir" we will understand such a reservoir within which water can be considered with a uniform level *z (t)*, mean salinity *s (t)* and a certain mass of reed *m(t)*. The interaction of the elementary reservoir with an external environment takes place through the free water surface Ω, in the form of evaporation and rainfall, through the bottom in the form of seepage, and through the contour *L* via conjunction with different canals, drains or other elementary reservoirs. Mass conservation equations for water and salts as applied to the elementary reservoir can be re-written as:

$$\frac{dW}{dt} = \int_L Q(l,z,t)dl + Q^0(t) - Q^f(t) - Q^e(t) \quad ; \qquad (10.1)$$

$$\frac{dS}{dt} = \int_L (s(l,t) \times Q(l,z,t))dl - Q^{S,f}(t) \quad ; \qquad (10.2)$$

$$W(z) = \int_{z^d}^{z} \Omega(h)dh \quad ; \qquad (10.3)$$

where: Q(l,z,t), $\forall$ l $\in$ L is water discharge determined by conditions of conjunction at the contour L,
Q^0(t) is precipitation,
Q^f(t) is filtration outflow,
Q^e(t) is evaporation from the free water surface,
$Q^{S,f}$ (t) is salt outflow at the boundary "water – bottom".
The evaporation flux from the free water surface Q^e(t) depends on the percentage of reed coverage; if we express through q^{tr}(t) – reed evapotranspiration intensity, and through q^0(t) – intensity of evaporation from the open water surface, we will receive the expression for Q^e(t) :

$$Q^e(t) = q^0(t) \times \Omega^0 + q^{tr}(t) \times \Omega^{tr} \qquad (10.4)$$

where, Ω^0 , Ω^{tr} are the open water area and the reedy area, respectively; $\Omega^{tr}+\Omega^0 = \Omega$ is the free water surface area.
The process of reed development on water space is conditioned predominately by two factors: depth of the reservoir – h and salinity of water – s. Moreover it was established in experiment that reed in Sudochie lake develops only at depths less then 1 m. If water level increases, reed gradually dies off. Taking into account that such conditions of reed development are kept in Priaralie's water space, we will consider evolution of areas under reed, Let Ω^{tr}(z) be a part of water space under reed and Ω^1(z) be a part of water space with depth less then one meter,

$$\Omega^1(z)= \{ \Omega (z)- \Omega (z - 1) \text{ at } h>1; \Omega (z) \text{ at } h\le 1\} \quad (10.5)$$

Assuming that expansion and reduction of reed are subject to a linear law, we have the equation for $\Omega^{tr}(z)$

$$\frac{d\Omega^{tr}}{dt} = \lambda(T) \times (\Omega^1 - \Omega^{tr}) \quad (10.6)$$

where: $\lambda(T)=\lambda 1(T)$, at $\Omega^1 - \Omega^{tr} >0$ and $\lambda(T)=\lambda 2(T)$, at $\Omega^1 - \Omega^{tr} \le 0$ are rates of expansion and reduction, respectively. The functions q0(t), qf (t) are usually known from the hydrological data, and in addition, values W(0), S(0), $\Omega^{tr}(0)$ are known. Therefore, in order to complete the set of equations (1) - (6) it is necessary to determine discharges along the contour of an elementary reservoir. The contour of an elementary reservoir coincides with typical areas of the relief, for which it is possible to use relationships such as provided by “de Chezy equation” or with hydro-structures, where discharges are determined through the structure’s parameters and the flow parameters by hydraulic formulas; the number of these formulas (equations) is equal to the number of conjunction zones of elementary reservoirs. Practically any water space may be made up of a set of elementary reservoirs. To this end, the contours of prospective reservoirs, which cover the whole possible water area, are selected on a topographic map. Then, for each elementary reservoir we calculate, using this topographic map, the functions Ω (z) (area of the free water surface at the level *z*) and L(z) (contour encompassing the area Ω (z) at the same level *z*). This results in a set of bathymetric curves for all selected contours. By overlapping those curves, along the contour of the minimum bed level, an integral bathymetric curve is plotted for the whole water space and will be used at the first stage. The indicators of water space behavior are comprised of integral characteristics that represent an average weighted state of elements for various periods of time. These indicators are ranked in the following way:

volume of water space W(t) and relative variations of the volume in yearly and long-term profiles $\delta W(t)/W(t)$, measurement parameters: water-surface area - Ω (t), $\forall$ t $\in${t}.

water salinity in the water space – s(t) and relative variation of salinity in terms of time $\delta s(t)/s(t)$, and space $\delta s(X)/s(X)$, measurement parameters: salinity in different points of the water space for various time points: s(X,t), $\forall$ s(X,t), $\forall$ t $\in${t}; X $\in\{\Omega\}$.

area under reed – $\Omega^{tr}(t)$, measurement parameters: water-surface area under reed.

These indicators associate with equations (1), (2), (6). The mathematical model (1) – (6) is implemented on the basis of discrete mesh in time using the finite-difference method.

10.2 Formal Description of the System of Reservoirs

The system of reservoirs is formalized in the form of the oriented graph **G**(J,I), where J = {0, 1, ..., j} is a set of nodes corresponding to reservoir objects, while I = {0, 1, ..., i} is a set of arcs reflecting links as to water distribution within the system. Each element $i \in I$ is characterized by such a pair (j, k) that ($\forall$(j, k), $j \in J$, $k \in J$, $k \ne j$), where j is the starting node and k is the end node of arc i. Thus, each node **G**(J,I) is associated with some object having water volume, while each arc is associated with a structure generating water flow between nodes. Equations that describe functioning of individual reservoirs are based on a system of ordinary differential equations reflecting inflow, outflow, and evaporation of water resources, salinity changes, and reed invasion in water space. The equations are associated with objects from the set of nodes J = {0, 1, ..., j} that are described in detail in previous report. The given section describes formalization of objects relating to the set of I = {0, 1, ..., i} - arcs, which determine conjunctions between reservoirs themselves and the outer boundary of the Aral Sea territory. The equations of water and salt conservation on the graph **G** (J, I) have the following form:

$$\frac{dW_j}{dt} = \sum_{(k,j)\in I_j^+} Q_{k,j} - \sum_{(j,k)\in I_j^-} Q_{j,k} + q_j \quad (10.7)$$

$$\frac{dS_j}{dt} = \sum_{(k,j)\in I_j^+} (s \times Q)_{k,j} - s_j \times \sum_{(j,k)\in I_j^-} Q_{j,k} + q_j^s \quad (10.8)$$

$$Q_{j,k} = Q_{j,k}(a_{j,k}, W_j, W_k, U_{j,k}), \ \forall (j,k) \in \{I^U\} \subset \{I\} \quad (10.9)$$

$$Q_{j,k} = Q_{j,k}(t), \ \forall (j,k) \in \{\partial G\} \quad (10.10)$$

where: W_j is water volume at the node *j* (m^3), I_j^+, I_j^- are sets of arcs coming into the node *j* and coming out of the node *j*, respectively; q_j is cumulative local inflow (outflow) to/from the node in the form of precipitation, evaporation, etc. (m^3/s), q_j^s is cumulative inflow (outflow) to/from the node of salts (kg/s),

S_j is mass of salts (kg), $s_{j,k}$ is salinity (kg/m^3), $Q_{j,k}$ is discharge between j and k (m^3/s), $a_{j,k}$ is a function that characterizes the particular hydraulic structure located on arch (j,k), $U_{j,k}(t)$ is control of arc (j,k), $\{l^U\}$ is a subset of controlled arcs ($\{l^U\} \subset \{l\}$), and $\{\partial G\}$ is the outer boundary of the system. While considering $\boldsymbol{W}$ and $\boldsymbol{S}$ as vectors with lengths of "J", we will get the Cauchy problem for nonlinear equations (11) – (14), solution of which may be found only through numerical integration. Therefore, we consider now discrete space in time. For this purpose time interval $\{t^0:t^K\}$ should be divided into equal intervals Δt in such a way that t can take values from the set $\{t^0, t^0+\Delta t, t^0+2\Delta t, \ldots, t^0+K\Delta t=t^K\}$. We will attribute system parameters in nodes to the points in time $t \in \{t^0, t^0+\Delta t, t^0+2\Delta t, \ldots, t^0+K\Delta t\}$, while system parameters in arcs will be attributed to the points in time $t \in \{t^0+0.5\times\Delta t, t^0+1.5\times\Delta t, t^0+2.5\times\Delta t, \ldots, t^0+(K-0.5)\times\Delta t\}$. Then:

$$W_j^{t+1} = W_j^t + \sum_{(k,j)\in I_j^+} W_{k,j}^{t+1/2} - \sum_{(j,k)\in I_j^-} W_{j,k}^{t+1/2} + w_j^{t+1/2} \qquad (10.11)$$

$$S_j^{t+1} = S_j^t + \sum_{(k,j)\in I_j^+} (s\times W)_{k,j}^{t+1/2} - \sum_{(j,k)\in I_j^-} (s\times W)_{j,k}^{t+1/2} + w_j^{s,t+1/2} \qquad (10.12)$$

$$W_{j,k}^{t+1/2} = \Delta t \times Q_{j,k}(a_{j,k}, W_j^{t+1/2}, W_k^{t+1/2}, U_{j,k}^{t+1/2}),\ \forall (j,k) \in \{l^U\} \subset \{l\} \qquad (10.13)$$

where: $w_j = q_j \times \Delta t$;

Thus, the system of $2\times|\{J\}|$ differential equations on discrete spatial-temporal mesh is reduced to the system of $2\times(K+1)\times|\{J\}|$ nonlinear algebraic equations in variables in nodes connected through $2\times K\times|\{l\}|$ variables on arcs, of which $K\times|\{l\}|$ variables are controls. Here $|\{.\}|$ is a number of elements in the specified set. For discharge on arc we will make translation of formula (17); expression for $Q_{j,k}$ may be written as:

$$Q_{j,k}(a_{j,k}, W_j, U_{j,k}) = Q_{j,k}(f(a_{j,k}, U_{j,k}), W_j), \qquad (10.14)$$

We replace $U_{j,k}$ by $\boldsymbol{U}_{j,k}$ (allowable control space) in function $f(a_{j,k}, U_{j,k})$ and multiply it by Δt; the function $\boldsymbol{W}_{j,k} = \Delta t \times f(a_{j,k}, \boldsymbol{U}_{j,k})$ forms new allowable control space, but now in variable $W_{j,k}$, thus instead of (17) we have:

$$W_{j,k}^{t+1/2} = W_{j,k}(W_j^t, W_j^{t+1}) \in \boldsymbol{W}_{j,k},\ \forall [(j,k) \in \{l^U\},\ t \in \{t^0:t^K\}] \qquad (10.15)$$

To complete the process of formulation, it is necessary to determine formulas for computing discharge at arcs. By analyzing Priaralie infrastructure, we may select three types of conjunction between reservoirs. Every type of conjunction is described by its own equation of hydraulics, depending on characteristics of liquid flow processes.

Flow in an open channel, canal (Chezy formula)

Flow through a broad-crested spillway, (spillway relationship)

Flow out of a gate (formula of flow out of a gate).

The first two types are uncontrollable and the discharge is determined through channel parameters and free surface slope as the function of free surface elevations of conjugated waters, while the latter type is controllable, which besides design parameters and elevations includes the control parameter that specifies a value of the gate opening. The given mathematical model relates to models of the "compartment" type. These models strictly keep to the mass conservation law and use semi-empirical equations of structure hydraulics instead of momentum and energy conservation laws. Models of this type were studied in detail; therefore, here we only note that in modeling the reservoirs with heavy salinity the most complex aspect is taking into account salt sedimentation with further washing out of salts, thus changing both water salinity and capacitance characteristics of compartments themselves.

11. Mathematical Model of the Aral Sea

11.1 Main Equations of Self-Cleaning Factors

Description of water-salt dynamics of the Aral Sea is based on water and salt mass conservation laws that are re-written for our problem as:

$$\frac{dW}{dt} = Q^A + Q^S + q^p - q^f - q^e + q^g; \qquad (11.1)$$

$$\frac{d(W \times s)}{dt} = Q^A \times s^A + Q^S \times s^S - s \times q^f + s^g \times q^g - W \times f(s,...) \quad ; \qquad (11.2)$$

where: W(t), s(t) are volume and salinity of water body of the Aral Sea, QA(t) and QS(t) are inflows from the Amudarya and the Syrdarya, respectively, sA(t) and sS(t) are salinities of these inflows, respectively, qp(t) is precipitation, qe(t,..) is evaporation from free sea's water surface, qf(t,W) is filtration outflow, qg(t) and sg(t) are inflow and salinity from groundwater, f(s, …) is a function of reservoir self-cleaning, which is written as a function of water salinity in the sea and of a range of parameters to be determined. The equations show that amount of salts coming in with precipitation and coming out with evaporation is neglected in the model since numerous studies show that imbalance between salt influx from the atmosphere and salt outflux to the atmosphere is less than 0.5% of the total salt influx into the Aral Sea. Many works were dedicated to individual analysis of equations and their elements, for example [9,10]; however, one of the key questions such as why salinity in the Aral Sea during the stable period (until 1961) was stabilized at values ~ (10.0 ± 0.25) g/l remains unsolved. We will start the analysis of the system of equations just since this period of time and select its last decade 1950 – 1961, as well as mean long-term characteristics for time interval 1911-1960 [8] that are shown in Table 11.1.

Table 11.1 Estimation of Water Balance Components

	Rivers	Precipitation	Evaporation	Filtration	Inflow from groundwater	Actual increase in the sea	Imbalance
Runoff, [km^3 /yr]	56.0	9.1	66.1	-	-	0.1	-1.1
Ion flux, [Mt/yr]	23.79	0.76	0.89	1.5	1.4	23.56	0.0

Negative imbalance means the additional mean annual inflow of 1.1 km^3/yr to the Aral Sea. The Table 11.1 does not meet the system of equations (1), (2), since availability of filtration ion flux requires filtration water outflow in an amount of 0.15km^3/yr under salinity of 10.0g/l. In the previous report, the remaining imbalance was attributed to inflow from groundwater. However, salinity of inflow from groundwater is about 7 g/l and thus, in order to keep salt balance, amount of groundwater inflow should be approximately 0.2 km^3/year under such level of salinity and this fits well the results of groundwater inflow estimations during the stable period [8]. The results of adjusted Table 11.1 are shown in Table 11.2, which will be used as reference one for the first phase of phenomenological parameter adjustment in the model.

Table 11.2 Adjusted Water Balance Components

	Rivers	Precipitation	Evaporation	Filtration	Inflow from groundwater	Actual increase in the sea	Imbalance
Runoff, [km^3 /yr]	56.0	9.1	66.1	0.15	0.2	0.1	-1.05
Ion flux, [Mt/yr]	23.79	0.76	0.89	1.5	1.4	23.56	0.0

Maintenance of constant water salinity at about 10.0g/l in the Aral Sea during this period of time means that amount of water area self-cleaning is equal to actual increase in ion flux in the sea. Taking into account that during the stable period the volume of water body of the Aral Sea was ~1064 km^3 under the free surface area of ~ 66 100 km^2, the numerical estimation of the mean annual water self-cleaning in the Aral Sea is

$$f(s=10,\ldots)=S/W=23{,}56\times1012/1064\times1012 = 0.022143 \ [g/l\times year]=[Mt/km^3\times year] \ ;$$

The mechanism of such self-cleaning was not studied completely, thus generating a number of various hypotheses on its determinants. Self-cleaning caused by periodical outflow has poor agreement with the results of water balance studies.

11.2 Sedimentation

Presently, factor of self-cleaning is doubtless. It is bounded with carbonate salt sedimentation under sea and river water mixing (sedimentation) [2], which contribution in stable period [8] was 10.94 Mt/yr. Hydrochemistry of this process was considered in detail [4],[5],[15], for hydrological model is expedient to suppose that self-cleaning from this factor is proportional to the relative flow volume coming from rivers and the sea salinity. At this stage of study, sedimentation process can be considered as reaction of first order, then self-cleaning function will be as follows:

$$f^{I}(s,\ W^{R}, W) = \alpha^{I} \times \frac{W^{R}}{W} s\ ; \qquad (11.3)$$

where: W^R is the total runoff of Amudarya and Syrdarya, α^I is phenomenological parameter, value of which is derived from self-cleaning conditions during the stable period:

$\alpha^I = f^I(s=10,\ldots) \times (S^I/S) \times (W/WR)/s = 0.019536$ [1/year].

where S^I = 10.94 Mt, s = 10 [g/l]≡ [Mt/km^3], rest explanations correspond to equations (1-2).

11.3 Local Salt Sedimentation

The next self-cleaning factor is the local salt sedimentation in shallow bays and bights. The essence of this factor is periodical filling of closed depressions around sea perimeter due to sea level fluctuation and further full evaporation. With next filling under level increase only a share of precipitated salts is dissolved, thus gradually accumulating salt mass in coastal zone.
According to estimates [7], main part of self-cleaning is due to this factor ~ 12.62 Mt/yr. It is difficult to agree with this because water volume participating in salt accumulation can be evaluated as multiplication of free surface growth and half of sea level fluctuation. For the considered period $\Delta z \approx 0.4m$, and $\Delta F \approx 1500km^2$, thus, water volume is: ∆W ~ 0.5×0.4×1500/1000 = 0.6km3. The total salt mass contained in this water volume is ~ 6 Mt, and if one assumes that all this mass precipitates without repeated dissolution, 6 Mt will be the maximum value of self-cleaning for this factor. The actual volume of sedimentation related to this factor is much less. The share of closed depressions in the coastal zone according to GIS estimates is 20% of estimated water volume. Apart of this, there is reverse dissolution effect. Thus, real contribution of this factor to total self-cleaning can be accepted as ~ 1 Mt/yr (specific value = 0.00094 g/l×yr). More accurate values of this factor will be received during hydrodynamic modeling. Expression for self-cleaning function for this factor is similar to precedent one:

$$f^{II}(s, \Delta W, W) = \alpha^{II} \times \frac{\Delta W}{W} s\ ; \qquad (11.4)$$

$$\Delta W = 0.5 \times (F(zmax) - F(zmin)) \times (zmax - zmin)/1000; \qquad (11.5)$$

where: ∆W is water volume participating in salt mass formation (km^3), zmax and zmin are maximum and minimum altitudes of sea level (m), F(zmax) and F(zmin) are areas of free surface corresponding to these altitudes (km2), α^{II} is second phenomenological parameter, value of which is 0,1667[1/yr].

11.4 Salt Sedimentation under Water Freezing

Third factor of self-cleaning is caused by annual sea freezing. This factor availability is proved by field investigations on Sudochie lake [10], [11] where negative salinity jumps are fixed during water freezing and melting. Water salinity changes due to salt precipitation under freezing and due to another reasons caused by lower ice salinity compared to water. Qualitative explanation of this effect can be given starting from water freezing point decrease under water salinity increase that leads to first freezing of fresh water first and rest water receives additional salts concentrated in the zone of phase change water→ice. Salinity growth leads to galocline formation, which can distort liquid static equilibrium and form vertical flow of high salinity towards bottom. This question is not well studied but is very important for self-cleaning conditions because under small depth ice and water volumes are almost equal. We will consider this question during hydrodynamic modeling in more details. For hydrological model the self-cleaning function will be built like sedimentation using ice volume as determinant:

$$f^{III}(s, WI, W) = \alpha^{III} \times \frac{W^I}{W} s \; ; \qquad (11.6)$$

where: W^I is ice volume ($W^I = \Omega \times h^I$), h^I is average ice thickness in water area, α^{III} is third phenomenological parameter determined though retained salt mass and average long-term Aral sea characteristics (average long-term ice thickness ~ 0.5m). α1II = (23.56-10.94- 1)/(661×0.5)=0.035159 [1/yr].
Assuming independence of distinguished factors, we receive the general self-cleaning function for the Aral Sea:

$$f(\ldots) = \frac{s}{W} \times (\alpha^I \times W^R + \alpha^{II} \times \Delta W + \alpha^{III} \times W^I); \qquad (11.7)$$

The dimension of the self-cleaning function is [g/l×yr]=[Mt/km^3×year].

12. Calibration of Mathematical Model (1950 – 1989)

12.1 Calibration of Water Component

Description of water-salt dynamics of the Aral Sea is based on water and salt mass conservation laws, equations (9.16) – (9.17) in the previous section. For calibration of the mathematical model, volume of the sea's water body W(t) and salt mass (W(t)×s(t)) will be selected as the main variables and equations (9.16) – (9.17) will be re-written as:

$$\delta W(t) = \Delta W(t) + Q^A(t) + Q^S(t) - \Omega(W) \times h^{E-P}(t) \; ; \qquad (12.1)$$

$$\delta[W(t) \times s(t)] = \Delta[W(t) \times s(t)] + s^A(t) \times Q^A(t) + s^S(t) \times Q^S(t) - W \times f(\ldots, \alpha^I, \alpha^{II}, \alpha^{III}) \; ; \qquad (12.2)$$

where: ΔW(t), Δ(W(t)×s (t)) is increase in water volume and salt mass of the Aral Sea, respectively, dimensions [km^3 /year], [Mt/yr], Ω(W) is free water surface area, considered as a well-known function of the sea's water body volume [thousand km^2], h^{E-P}(t) is difference between evaporation and precipitation ($h^{E-P}(t) = h^E(t) - h^P(t)$), h^E(t) is evaporation from free water surface [m], h^P(t) is precipitation [m]. Here the evident equality of dimensions is used [thousand km^2]×[m]= [km^3], δW(t), δ(W(t)×s (t)) are values determined as imbalance, dimensions [km^3/year], [Mt/year], respectively, other notations are the same as in section 11. As the most accurate measurement parameters of the state of the Aral Sea, the mean monthly elevations of the sea surface were taken from the following stations:

- «Barsakel'mes» - measurement period 1950 – 1989.
- «Lazarevskaya» - measurement period 1962 – 1989.

During 1962 – 1989, the mean monthly elevation was calculated as a half-sum of measurements from two stations. By using elevations and bathymetric curves of CR2 group, we reconstructed by Simpson's method the free water surface areas and water body volumes in the Aral Sea in monthly scale for the period of 1950 – 1989 (the results are shown in Annex 2). Incrementations ΔW(t)= W(t, beginning of year) - W(t, end of year) ,$\forall$ t $\in$ {1950, 1951, . . . , 1988, 1989} were calculated by using values of water body volume at the beginning and the end of year. For self-cleaning function, preliminary values of these parameters were taken from average long-term characteristics of quasi-stationary period of the Aral Sea.

α^I =0.019536 , α^{II} =0.1667 , α^{III} =0.035159.

Seawater body volume participating in salt sedimentation on shore and shallow parts is calculated as follows:

$$\Delta W = 0.5 \times (\Omega(z_{max}) - \Omega(z_{min})) \times (z_{max} - z_{min})/1000; \qquad (12.3)$$

Annual ice volume is calculated by formula:

$$W^{Ice} = \Omega \times \beta \times \sqrt{\sum_{\tau} (-T_\tau)} \; , \; \forall \tau \mid T\tau < 0; \qquad (12.4)$$

where: $T\tau$ is mean monthly negative temperature, β is constant equal for the Aral Sea (β = 0.11), derivation of this formula is given in the next section. Inflow to the Aral Sea is calculated with regard to is losses through evaporation in Syrdarya and Amudarya deltas.

$$Q^A(t) = (Q^{AD})^2/(\beta^A + Q^{AD}); \quad Q^S(t)= (Q^{SD})^2/(\beta^S + Q^{SD}) \qquad (12.5)$$

where Q^{AD} , Q^{SD} are annual runoffs of Amudarya river and Syrdarya river, as measured in tail stations (Samanbai and Kazalinsk), respectively, β^A and β^S are parameters characterizing a delta (β^A = 2,2÷ 0,5; β^S = 1,4 ÷ 0,5). Type of function (5) and numerical parameter for Amudarya delta are taken from project [10]; for Syrdarya type of function is taken as analogue. The results of project [10] showed that when water was supplied to the delta, internal reservoirs were filled up quite quickly and then all excess water flew into the Aral Sea. Moreover, irrespective of inflow to the delta, the free surface of all reservoirs tends to some maximum value. Therefore, in order to describe changes in the free surface of reservoirs, depending on inflow, a function of "limited growth" may be used. Let free surface area of reservoirs in the delta and inflow be noted as Ω^D and Q, respectively, then the free surface area as a function of maximum possible area and inflow can by written as:

$$\Omega^D(Q) = \Omega^{max} \frac{Q}{\beta + Q}; \qquad (12.6)$$

where β is some parameter having dimension of inflow, Ωmax is maximum free surface area of reservoirs. Water losses in the delta are:

$$\delta Q = h^{E-P} \times \Omega^D(Q) = h^{E-P} \times \Omega^{max} \frac{Q}{\beta + Q}; \qquad (12.7)$$

Inflow to the sea will be the difference between Q and δQ

$$Q^{Sea} = Q - \delta Q = Q\times[1- h^{E-P} \times \Omega^{max}/(\beta+Q)] \geq 0 \ \forall\ Q, \ 0 \leq Q \leq \infty, \qquad (12.8)$$

$$Q + \beta \geq h^{E-P} \times \Omega^{max} \qquad (12.9)$$

Equation (9) should be fulfilled for any inflows, and therefore when assuming that Q = 0 and selecting β as the minimum equal to $\beta = h^{E-P} \times \Omega^{max}$, we will get the formula (9.27) after simple transformations. While calibrating the model, this formula was adjusted to β, and β was taken as a function of h^{E-P}, i.e.

$$\beta(t) = \beta_0 \times h^{E-P}(t)/ h_0^{E-P} \qquad (12.10)$$

where: β_0 and h_0^{E-P} are the mean values that were derived from inverse problem solution for given period of time, see below.
Aral Sea bathymetric tables prepared by CR2 groups, as well as hydrologic and climatic characteristics presented in "Database" are served as initial data. The mean annual parameters of the Aral Sea are given in Table 12.1.

Table 12.1 Time Series of the Estimated Water Balance Components

Year	Inflow to deltas, [km3/yr]				Precipitation km^3/yr	Evaporation $[km^3/yr]$	Elevation, m (BS)	Water mass volume $[km^3]$	Water surface area $[km^2]$	Salinity (g/l)
	Amudarya		Syrdarya							
	Q	s	Q	s						
1950	41.00	0.47	11.90	0.57	9.22	66.06	52.82	1060.17	65273	10.17
1951	33.40	0.52	13.20	0.65	8.07	59.19	52.72	1054.14	64896	9.74
1952	55.20	0.41	18.80	0.58	8.78	62.62	52.70	1052.93	64822	10.67
1953	54.80	0.41	19.50	0.68	9.63	64.11	52.86	1063.12	65440	9.82
1954	55.10	0.41	21.10	0.64	10.87	62.87	53.12	1081.91	66649	10.21
1955	41.90	0.47	16.70	0.65	9.17	66.13	53.16	1085.27	66837	10.13
1956	48.00	0.44	16.40	0.78	9.30	67.20	53.22	1088.11	67086	10.19
1957	30.90	0.54	9.50	0.92	8.51	68.11	53.19	1087.04	66986	10.01
1958	52.30	0.42	17.90	0.78	7.94	68.93	53.16	1084.63	66821	10.42
1959	46.30	0.45	18.80	0.82	9.92	70.05	53.28	1093.39	67447	10.19
1960	42.00	0.47	20.70	0.79	9.41	71.13	53.40	1101.07	68028	9.93
1961	31.10	0.57	13.40	0.93	6.59	70.43	53.29	1093.67	67468	9.97
1962	38.40	0.51	5.80	1.13	8.63	70.93	52.97	1071.62	65937	10.80
1963	31.80	0.56	10.60	1.34	11.56	70.64	52.63	1046.88	64446	10.58
1964	39.20	0.51	14.90	0.92	8.12	64.04	52.49	1039.06	63962	10.13
1965	25.30	0.62	4.70	1.19	8.48	66.35	52.30	1027.14	63241	10.81
1966	35.60	0.53	9.60	1.01	6.64	71.13	51.87	997.40	61353	11.81
1967	29.30	0.58	8.70	1.14	7.51	57.82	51.56	980.59	60046	11.02
1968	34.40	0.54	7.20	1.11	6.03	67.35	51.23	960.11	58584	11.49
1969	70.60	0.36	17.40	0.73	9.06	62.31	51.28	962.99	58851	10.91
1970	32.40	0.56	9.80	0.98	7.22	62.03	51.41	971.30	59358	11.20
1971	20.60	0.65	8.20	1.22	5.81	59.83	51.06	949.33	58040	11.38
1972	24.20	0.59	7.00	1.27	5.78	55.34	50.55	918.90	57208	11.95
1973	43.50	0.40	8.90	1.16	8.95	56.45	50.22	900.67	57049	11.95
1974	6.90	1.01	4.80	1.58	4.75	60.18	49.86	878.99	56814	13.02
1975	9.20	0.92	0.60	1.52	4.43	59.99	49.01	831.19	55763	13.40
1976	11.30	0.85	0.60	1.46	5.79	51.09	48.27	790.39	54599	14.57
1977	7.20	0.99	0.40	1.11	5.04	45.75	47.64	754.69	53257	15.44
1978	18.90	0.68	0.70	1.39	6.42	52.52	47.05	724.34	52066	14.97
1979	10.90	0.87	2.90	0.89	4.87	52.14	46.45	692.62	51443	15.09
1980	9.30	0.92	2.50	1.81	9.73	50.24	45.75	656.45	51101	16.80
1981	6.90	1.33	2.40	1.62	11.92	47.11	45.19	627.58	50598	17.70
1982	0.30	2.75	1.80	3.32	8.52	38.50	44.39	586.33	48126	18.80
1983	2.40	2.06	0.90	1.94	4.51	47.59	43.56	546.84	46046	20.30
1984	8.00	1.23	0.60	1.83	5.99	44.33	42.76	509.60	45406	21.90
1985	2.20	2.11	0.70	1.18	7.19	42.52	41.94	472.57	44066	22.90
1986	0.50	1.47	0.20	1.94	4.17	41.67	41.03	432.16	41669	23.90
1987	8.70	0.82	1.10	1.83	4.39	37.55	40.20	397.41	39942	25.00
1988	17.80	1.88	7.10	4.18	5.85	37.82	39.67	375.69	38988	28.00
1989	1.50	1.12	4.30	4.62	2.65	39.37	39.10	353.74	37858	30.00

At this stage of calibration, equations (1) and (2) can be solved in sequence since water salinity during this period practically does not have effect on evaporation. Only free surface area $\Omega(W)$ is not known in the equation (2). If one uses mean annual values for calculation of this term, great error occurs due to wide variations of the function hE-P during a year. In order to reduce this error, by using mean long-term characteristics of the Aral Sea, precipitation distribution tables from the Database and B.I.Zaikov's evaporation distribution table ([46], Table 13, p. 87), we will construct an auxiliary function f^{E-h} for within-year distribution of value h^{E-P}. Values of this function are given in Table 12.2 and plotted in Fig. 12.1.

Table 12.2 Monthly Values of f(E)-h(t)

jan	feb	mar	apr	may	jun	jul	aug	sep	oct	nov	dec
-0.012	-0.008	0.032	0.088	0.145	0.172	0.199	0.190	0.128	0.063	0.017	-0.015

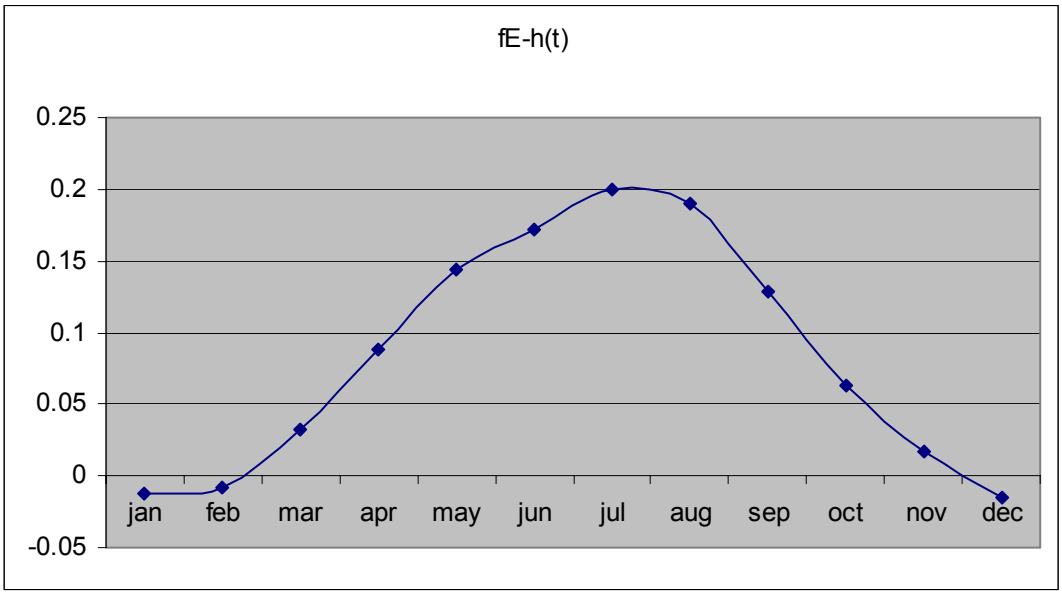

Fig. 12.1 Function of within-year distribution of evaporation-precipitation distribution difference

The distribution function f^{E-h} is subject to normalization requirement:

$$\sum_{\tau} f^{E-h}(\tau) = 1, \quad \tau \in \{\text{jan, feb, . . . ,dec}\} \qquad (12.11)$$

Thus, the last term in equation (1) will be calculated as:

$$\Omega(W) \times h^{E-P}(t) = h^{E-P}(t) \times \sum_{\tau} f^{E-h}(\tau) \times \Omega(t,\tau); \quad \forall\, t \in \{1950, \ldots, 1989\} \qquad (12.12)$$

In initial statement it was proposed to find values of β_0^A, β_0^S that minimize imbalance in equation (2) for given period of time, i.e. it was assumed indirectly that major imbalance is caused by losses in river deltas. However, the analysis of first results identified deviations in evaporation estimations that were next-higher order of errors in estimation of losses in the deltas, for example, balance of the year 1982. Therefore, it was decided to re-formulate the initial problem. We will assume that errors were made during measurements, and, at the same time, the value of error is directly proportional to absolute value of measured parameter. We will consider measurements of sea surface elevation as obtained from gauging stations as the most reliable measurements. For other variables $Q^A(t)$, $Q^S(t)$ and $h^{E-P}(t)$ we introduce deviations $Q^{A\sim}(t)$, $Q^{S\sim}(t)$ and $h^{E-P\sim}(t)$ that meet equations (2) and (5), and based on (10), we will have:

$$\Delta W(t) + \frac{[Q^{A\sim}(t)]^2}{\beta_0^A \dfrac{h^{E-P\sim}(t)}{h_0^{E-P\sim}} + Q^{A\sim}(t)} + \frac{[Q^{S\sim}(t)]^2}{\beta_0^S \dfrac{h^{E-P\sim}(t)}{h_0^{E-P\sim}} + Q^{S\sim}(t)} - h^{E-P\sim}(t) \times \sum_{\tau} f^{E-P}(\tau) \times \Omega(t,\tau) = 0 \qquad (12.13)$$

where $h_0^{E-P\sim}$ is derived from formula:

$$h_0^{E\text{-}P\sim} = \frac{1}{|\{t_1, t_2, \ldots, t_K\}|} \sum_{t \in \{t_k\}} h^{E-P\sim}(t); \qquad (12.14)$$

where |{…}| is number of elements in sequence {…}.
For each of selected variables, we will introduce a degree of deviation by the following formulae:

$$X^A(t) = \frac{Q^A(t) - Q^{A\sim}(t)}{Q^A(t)};$$

$$X^S(t) = \frac{Q^S(t) - Q^{S\sim}(t)}{Q^S(t)}; \qquad (12.15)$$

$$X^E(t) = \frac{h^{E-P}(t) - h^{E-P\sim}(t)}{h^{E-P}(t)} \sum_{\tau} f^{E-P}(\tau) \times \Omega(t, \tau);$$

$$X^W(t) = \frac{W(t) - W^{\sim}(t)}{W(t)};$$

Quadratic functional is used for assessment of solution quality:

$$\Phi(\beta_0^A, \beta_0^S, Q^{A\sim}(t), Q^{S\sim}(t), h^{E\text{-}P\sim}(t)) = \sum_{t \in \{1950,\ldots 1989\}} [X^A(t)]^2 + [X^S(t)]^2 + [X^E(t)]^2 + [X^W(t)]^2 \qquad (12.16)$$

Now, the problem of model calibration regarding water component can be formulated in the following way: to determine a set of variables β_0^A, β_0^S, $Q^{A\sim}(t)$, $Q^{S\sim}(t)$, $h^{E\text{-}P\sim}(t)$ that meet equations (2) and minimize the functional (16). In terms of "GAMS" language, the formulated problem is related to "nlp" type and has direct solution; however, the result analysis identified high sensitivity of parameters β_0^A, β_0^S to measurement errors. Taking into account that these variables are not directly included in the functional (16), only variables $Q^{A\sim}(t)$, $Q^{S\sim}(t)$, $h^{E\text{-}P\sim}(t)$ were changed iteratively.
According to data from Table 12.1 on inflow salinity and water component calibration results, the annual salt influx was calculated to the Aral Sea from Amudarya river and Syrdarya river since 1950 to 1989. The results are shown in Table 12.3.

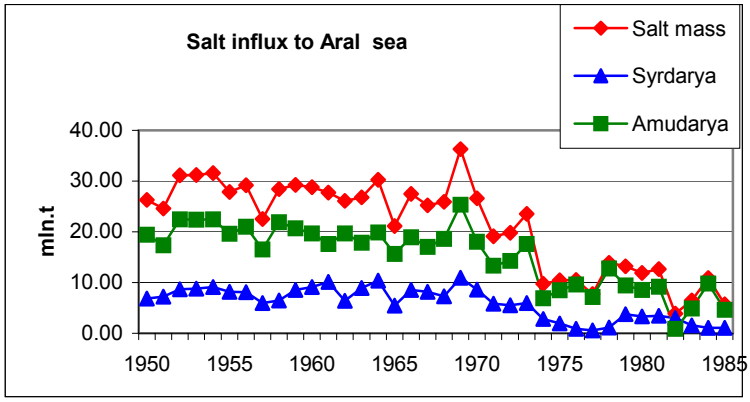

Fig. 12.2 Salt influx to the Aral Sea

Fig. 12.2 "Salt influx to the Aral Sea" gives graphical representation of the results. From the figure is evident that before 1973 salt influx varied between 15-25 Mt from the Amudarya and between 5-10 Mt from the Syrdarya. Then situation changed dramatically: salt influx decreased: to 5-10 Mt from Amudarya; 0-5 Mt from Syrdarya. In the both cases, decrease in salt influx to the Aral Sea is resulted exclusively from drop in water inflow under continuous increase in river water salinity.

Table 12.3 Time Series of Revised Water Balance Components

Year	Initial imbalance km^3/yr	Inflow to deltas, [km^3/yr]				Layer (Evaporation - precipitation) [m]		Inflow to the sea [km^3/yr]	
		Amudarya		Syrdarya				Amu-darya	Syr-darya
		Q_base	Q_calc	Q_base	Q_calc	h_base	h_calc		
1950	1.87	41.0	41.2	11.9	11.9	0.87	0.84	38.4	11.2
1951	-0.02	33.4	33.7	13.2	13.3	0.78	0.74	31.3	12.6
1952	19.52	55.2	51.9	18.8	18.4	0.82	1.00	48.6	17.5
1953	-3.22	54.8	56.4	19.5	19.7	0.83	0.76	53.9	19.0
1954	8.43	55.1	53.8	21.1	20.9	0.78	0.83	51.1	20.2
1955	10.7	41.9	41.0	16.7	16.6	0.85	0.93	38.0	15.7
1956	-7.24	48.0	49.9	16.4	16.6	0.86	0.74	47.5	16.0
1957	-2.37	30.9	31.3	9.5	9.5	0.88	0.81	28.7	8.8
1958	-0.62	52.3	53.0	17.9	18.0	0.91	0.86	50.2	17.2
1959	-8.75	46.3	48.3	18.8	19.1	0.89	0.75	45.8	18.4
1960	0.31	42.0	42.3	20.7	20.8	0.90	0.86	39.6	20.0
1961	-3.62	31.1	31.5	13.4	13.5	0.94	0.85	28.9	12.7
1962	10.94	38.4	37.8	5.8	5.8	0.94	1.04	34.5	4.9
1963	2.83	31.8	31.8	10.6	10.6	0.91	0.90	29.0	9.8
1964	-4.36	39.2	40.2	14.9	15.0	0.87	0.77	37.7	14.3
1965	-2.26	25.3	25.6	4.7	4.7	0.91	0.83	23.0	4.0
1966	4.74	35.6	35.5	9.6	9.6	1.05	1.05	32.2	8.7
1967	1.42	29.3	29.4	8.7	8.7	0.83	0.81	26.9	8.0
1968	5.85	34.4	34.3	7.2	7.2	1.04	1.07	30.9	6.3
1969	5.03	70.6	70.1	17.4	17.4	0.90	0.91	67.1	16.5
1970	4.75	32.4	32.3	9.8	9.8	0.92	0.93	29.3	9.0
1971	2.94	20.6	20.6	8.2	8.2	0.93	0.92	17.8	7.4
1972	11.06	24.2	23.8	7.0	7.0	0.87	0.99	20.9	6.1
1973	11.46	43.5	42.1	8.9	8.8	0.83	0.94	39.0	8.0
1974	-0.45	6.9	6.9	4.8	4.8	0.97	0.92	4.7	4.1
1975	3.03	9.2	9.2	0.6	0.6	0.99	1.00	6.7	0.2
1976	0.26	11.3	11.3	0.6	0.6	0.83	0.79	9.1	0.3
1977	1.33	7.2	7.2	0.4	0.4	0.76	0.75	5.3	0.1
1978	-1.71	18.9	19.1	0.7	0.7	0.88	0.80	16.7	0.3
1979	7.62	10.9	10.9	2.9	2.9	0.92	1.00	8.2	2.2
1980	-2.15	9.3	9.4	2.5	2.5	0.79	0.70	7.4	2.0
1981	2.8	6.9	6.9	2.4	2.4	0.69	0.70	5.1	1.9
1982	27.84	0.3	0.3	1.8	1.8	0.62	1.18	0.0	1.1
1983	-10.64	2.4	2.4	0.9	0.9	0.93	0.67	1.2	0.5
1984	11.06	8.0	8.0	0.6	0.6	0.84	1.02	5.5	0.2
1985	5.7	2.2	2.2	0.7	0.7	0.80	0.89	0.9	0.3
1986	2.11	0.5	0.5	0.2	0.2	0.90	0.94	0.1	0.0
1987	4.65	8.7	8.7	1.1	1.1	0.83	0.88	6.4	0.6
1988	2.75	17.8	17.5	1.6	1.6	0.82	0.82	14.8	6.3
1989	-5.94	1.5	1.5	6.9	7.0	0.97	0.77	0.6	3.8
	117.7 2.9	1079.3 27.0	1079.6 27.0	339.4 8.5	339.9 8.5	0.87 0.08	0.87 0.12	983.1 24.6	316.3 7.9

12.2 Calibration of Salt Component

Despite many studies of the Aral Sea's water-salt balance, salt content was defined approximately (10 billion t). Therefore, to define basic salt mass through known water salinity 11-year period was selected (1950 – 1960), which in turn was divided into groups of 1, 2, …10 years. For each group salt mass was

averaged, results are presented in Table 9.6. In lower line average mass value and its mean-square deviation for each group (column) are presented.

Table 12.4 Development of Salinity (for different groups of years 1-10)

Year	Water mass volume, km3	Salinity (g/l)	Salt mass (Mt)										
1	2	3	4	5	6	7	8	9	10	11	12	13	14
1950	1058	10.17	10760										
1951	1049	9.74	10217	10488									
1952	1050	10.67	11204	10710	10727								
1953	1059	9.82	10399	10803	10607	10645							
1954	1076	10.21	10986	10691	10864	10701	10713						
1955	1079	10.13	10930	10958	10770	10881	10747	10749					
1956	1082	10.19	11026	10978	10981	10834	10910	10793	10789				
1957	1080	10.01	10811	10918	10922	10938	10829	10894	10796	10792			
1958	1078	10.42	11233	11022	11023	11000	10997	10897	10942	10850	10840		
1959	1086	10.19	11066	11150	11037	11034	11013	11009	10921	10958	10874	10863	
1960	1093	9.93	10853	10960	11052	10992	10998	10987	10987	10913	10947	10873	
	1072	**10.13**	**10862**	**10868**	**10887**	**10878**	**10887**	**10888**	**10887**	**10878**	**10887**	**10868**	**10879**
	15	**0.26**	**314**	**194**	**157**	**143**	**125**	**103**	**90**	**63**	**54**	**7**	**10**

The mean long-term value is 10 862 Mt., which is taken for initial salt mass in Aral sea in its quasi-stationary state. It worthy to note, that in result of detail analysis of USSR State Cadastre for 1978, salt mass ~ 10 842 Mt. In column 14 mean and mean-square deviation is presented over groups. Upper part of matrix (Table 9.6) can be filled using cyclical rearrangement; in this case mean deviation for groups will coincide and mean-square deviation will change.

Here truncated rows are maintained to assess averaging impact on salt mass fluctuations; mean salt mass is ~ 10 860 Mt over groups; mean-square deviation is ~ 314 Mt (last line in column 4) when annual salt influx is ~ 30 Mt. Character of mean-square deviation decline with averaging row increase doesn't permit to consider long-term salt mass fluctuations as error of average water salinity measurement. The latter, in turn, make competence of hypothesis about one-side exchange between salt mass in water and on the bed doubtful; part of salt is settled on the bed as insoluble sediment. Process of Aral Sea self-cleaning was described in such approaching in mathematical model. Salt sedimentation in coastal zone and ice were considered as main self-cleaning factors. Each factor, beside physical characteristics, had phenomenological parameter, used for model tuning. Functional was determined as minimum sum of mean-squre deviations in water salinity between simulated and measured data for 1950 – 1985 under real conditions for this period of time.

Taking into account that the mean annual salinity values are used for assessment of salt component, in equation (9.23), water volume values are the mean annual volumes of the Aral Sea water body. Let express, as earlier, variables derived from equation (2) through s(t), while measurements through s~(t). We will form the following functional:

$$\Phi(\alpha^{I},\alpha^{II},\alpha^{III}) = \sum_{t}\{\lambda_1 \times [s(t) - \tilde{s}(t)]^2 + \lambda_2 \times [\frac{\partial s}{\partial t}(t) - \frac{\partial \tilde{s}}{\partial t}(t)]^2\} \rightarrow \frac{\min}{\alpha^{I},\alpha^{II},\alpha^{III}}; \qquad (12,17)$$

Full set of input data with simulation results is given in the next section. Graphs in Figure 12.3 show only comparison results of simulation and measured data on salinity dynamics in Aral Sea waters for given period of time. Each curve was obtained from fundamentally different physical hypotheses which are characterized by phenomenological parameters.

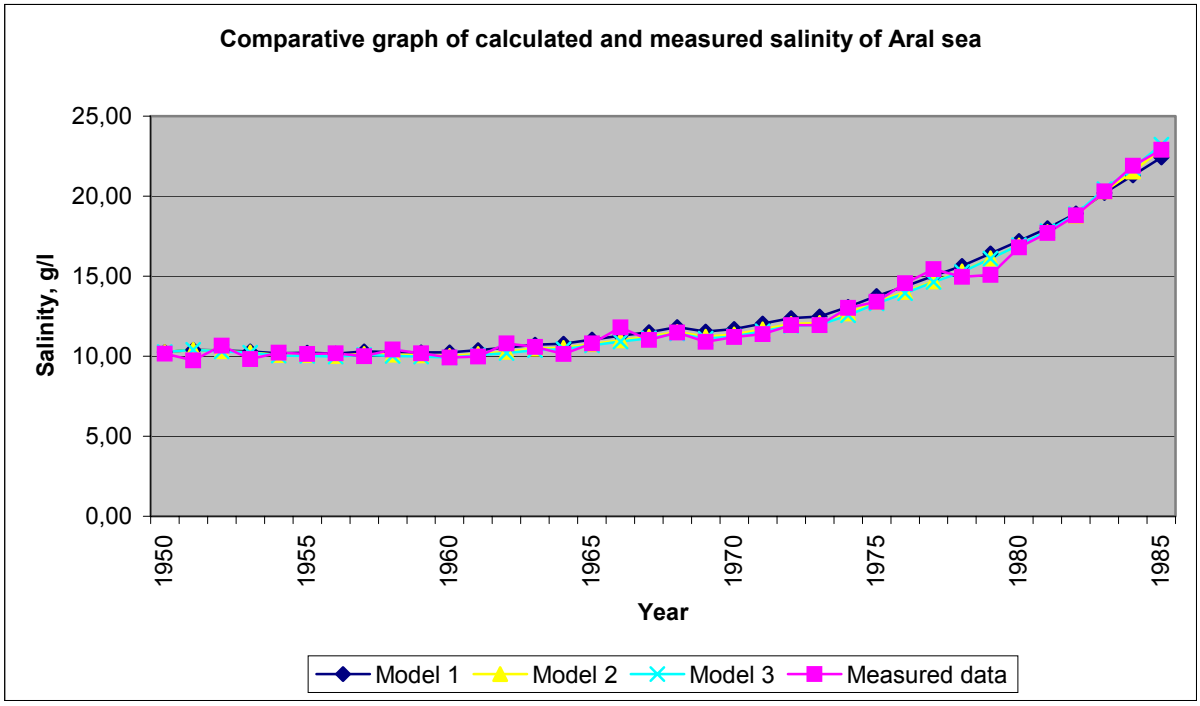

Fig. 12.3 Comparative Graph of Calculated and Measured Salinity of Aral Sea

Model 1: α^{I} = 0,0000 , α^{II} = 5,1136 , α^{III} = 0,0000 .
Model 2: α^{I} = 0,0000, α^{II} = 0,0000 , α^{III} = 0,0502.
Model 3: α^{I} = 0,0511 , α^{II} = 0,0000 , α^{III} = 0,0000 .
where: α^{I} – phenomenological parameter of sedimentation, α^{II} - phenomenological parameter of sedimentation in coastal zone, α^{III} - phenomenological parameter of ice.
The first option (Model 1) corresponds to assumption that water body cleaning occurs exclusively due to salt sedimentation in coastal zone; the second one (Model 2) reflects hypothesis about water self-cleaning exclusively due to freezing, and the third one (Model 3) due to only sedimentation. Such curves similarity indicates that only salinity is well described by ordinary differential equation with one phenomenological parameter. Therefore, it is impossible to define impact of different parameters at this stage with the above-mentioned model. Deviation regularity in total salt mass draws to conclusion that self-cleaning process has minimum two stages. The first stage is connected with mass salt sedimentation and their reverse solution and the second stage is connected within occurrence of insoluble sediment, which doesn't participate in exchange processes. Thus, even in quasi-stationary period the Aral Sea's equilibrium should be considered as dynamic equilibrium close to 1-year period but different from it, and self-cleaning volume as the average annual difference between precipitated and soluble salts. This process can be described schematically as follows: $S \leftrightarrow S^{L} \rightarrow S^{N}$ where S^{N} is insoluble salt mass precipitated, S^{L} is salt mass on sea bed participating in salt exchange with water body, and S is salt mass in water body (S = 10 862 Mt). Water salinity is calculated though S value as s= S/W; where W is sea water body volume.
The Table 12.5. shows the simulated Aral Sea's main parameters. Each column is ended by two values: average for column and mean-square deviation. As it can be seen from Table 12.5 and diagrams, water body volume and salinity dynamics are simulated with good approximation but salt mass in water body is simulated only on average. Simulated and measured data from Table 12.7 reduced to sea parameters of the year 1950 are presented in Fig. 12.4 - Fig. 12.6.
Fig. 12.4 shows visually changes in water volume in the Aral Sea as compared to the volume of the year 1950. Whereas until 1965 the relative volume of the Aral Sea had not changed, since 1965 to 1985 it dropped abruptly to 0,4. That is water volume decreased more then two-fold in the Aral Sea.
Fig. 12.5 shows salt mass dynamics. Average, for the period under consideration, salt influx to the Aral Sea changed negligibly -1000 Mt. But sea water salinity dynamics (Fig. 12.6) shows permanent growth: in the period 1965 -1985, salinity increased 2 times. Since 1950 till 1965, under relatively constant water and salt volumes, salinity did not change. Since1965 till 1985 sharp water volume reduction under relatively stable salt volume led to salinity increase. According to data in Table 12.5 and Fig. 12.5, the mass of soluble salts in the Aral Sea may be considered as constant and equal to 10948+-366 Mt since 1950 to 1985.

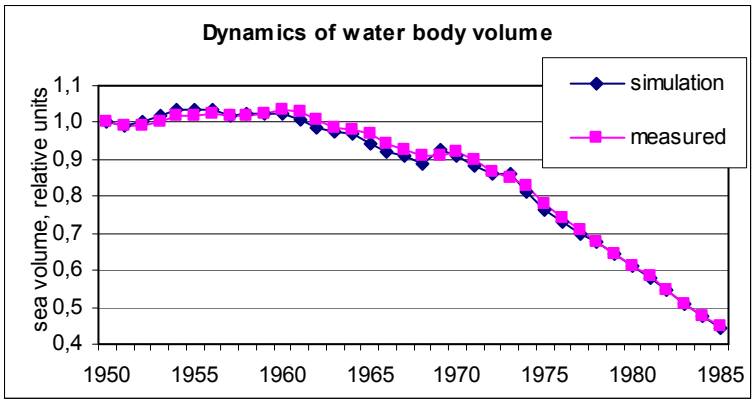

Fig. 12.4 Dynamics of Water Body Volume

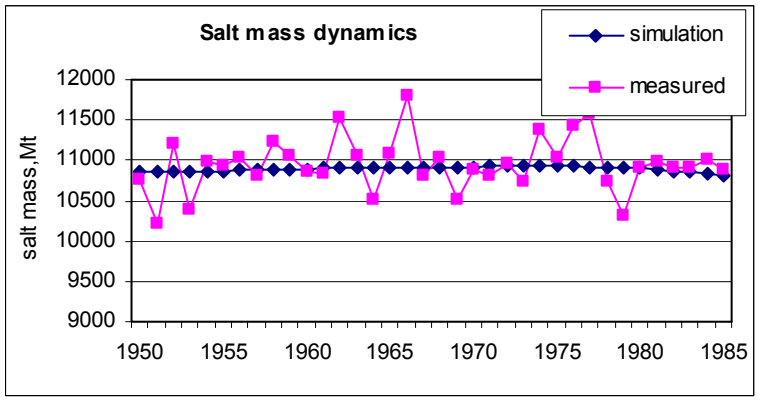

Fig. 12.5 Salt Mass Dynamics

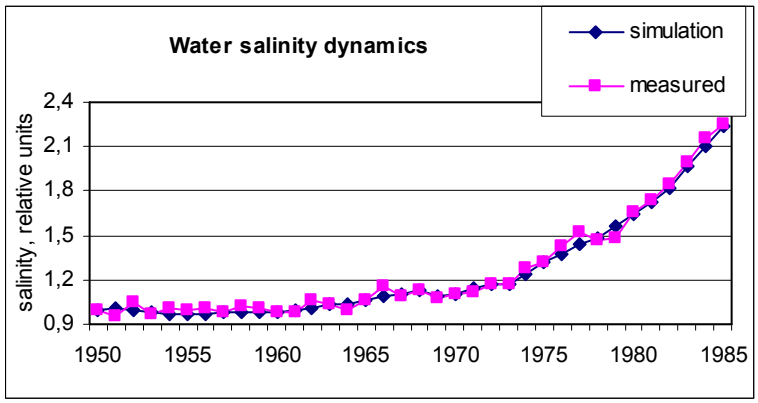

Fig. 12.6 Water Salinity Dynamics

Table 12.5 Simulated Components of the Salt Water Balance

	Volume of water body (km^3)		Salt mass (Mt)		Salinity (g/l)		Mass of precipitated salts (Mt)			
Year	Simulation	Measured data	Simulation	Measured data	Simulation	Measured data	Sedimentation	Sedimentation in coastal zone	Ice	Total
1950	1058	1058	10862	10760	10.27	10.17	9.97	0.00	13.93	23.90
1951	1050	1049	10865	10217	10.35	9.74	8.77	0.08	14.56	23.41
1952	1063	1050	10865	11204	10.22	10.67	14.11	0.03	14.85	28.98
1953	1078	1059	10866	10399	10.08	9.82	13.97	-0.24	16.84	30.56
1954	1097	1076	10865	10986	9.91	10.21	14.10	-0.55	18.64	32.19
1955	1094	1079	10868	10930	9.94	10.13	10.73	-0.01	14.75	25.47
1956	1097	1082	10875	11026	9.91	10.19	11.83	-0.02	12.63	24.45
1957	1075	1080	10879	10811	10.12	10.01	7.37	0.05	14.68	22.10
1958	1082	1078	10883	11233	10.06	10.42	13.14	0.03	14.17	27.34
1959	1086	1086	10888	11066	10.03	10.19	12.10	-0.06	15.89	27.94
1960	1086	1093	10893	10853	10.03	9.93	11.63	-0.01	17.50	29.13
1961	1066	1087	10899	10837	10.22	9.97	8.24	0.28	15.16	23.69
1962	1046	1067	10898	11524	10.42	10.80	8.40	0.80	14.74	23.94
1963	1029	1045	10908	11056	10.60	10.58	8.13	0.69	11.70	20.52
1964	1027	1038	10913	10515	10.63	10.13	10.56	0.03	15.56	26.14
1965	996	1026	10914	11091	10.95	10.81	5.82	0.63	14.40	20.85
1966	974	1000	10915	11810	11.21	11.81	9.21	1.31	14.91	25.42
1967	961	981	10918	10810	11.36	11.02	7.75	0.53	15.30	23.58
1968	939	961	10916	11038	11.63	11.49	8.76	1.06	17.39	27.22
1969	980	964	10917	10514	11.13	10.91	18.42	-0.35	18.50	36.57
1970	964	972	10920	10883	11.33	11.20	8.65	-0.27	14.94	23.32
1971	934	949	10926	10800	11.69	11.38	5.88	1.31	12.89	20.08
1972	910	918	10929	10968	12.01	11.95	6.62	0.70	14.89	22.20
1973	909	899	10931	10742	12.03	11.95	11.58	0.01	14.46	26.04
1974	859	874	10933	11385	12.72	13.02	2.24	0.44	16.98	19.66
1975	810	824	10931	11044	13.49	13.40	2.14	2.08	14.92	19.14
1976	773	785	10925	11442	14.14	14.57	2.81	1.87	17.83	22.52
1977	739	749	10918	11568	14.78	15.44	1.76	2.12	19.23	23.11
1978	715	718	10912	10742	15.27	14.97	5.30	1.39	18.03	24.72
1979	681	683	10908	10313	16.01	15.09	3.54	1.08	18.02	22.64
1980	646	649	10901	10898	16.86	16.80	3.10	0.66	22.08	25.84
1981	614	620	10896	10974	17.75	17.70	2.42	0.95	16.29	19.66
1982	581	580	10867	10900	18.71	18.80	0.32	5.33	21.89	27.53
1983	536	538	10848	10911	20.23	20.30	0.70	6.77	13.62	21.09
1984	502	503	10824	11009	21.54	21.90	2.92	1.71	27.52	32.15
1985	470	475	10798	10878	22.99	22.90	0.68	3.83	21.99	26.50
	904	908	10894	10948	12.80	12.79	7.60	0.95	16.44	24.99
	195	194	32	336	3.60	3.62	4.59	1.55	3.15	3.94

Fig. 12.7 shows salinity dynamics with regard to sedimentation in coastal zone and ice cover. Whereas sedimentation in coastal zone remained constant up to1980, ice impact on salinity has started to increase since 1975.

Salt sedimentation varies around 10 Mt, only in 1969 it reached 18,42 Mt and since 1974 it has sharply decreased.

As it can be seen from diagrams, water body volume and salinity dynamics are simulated with good approximation, and salt mass in Aral Sea's water body can be simulated only on average.

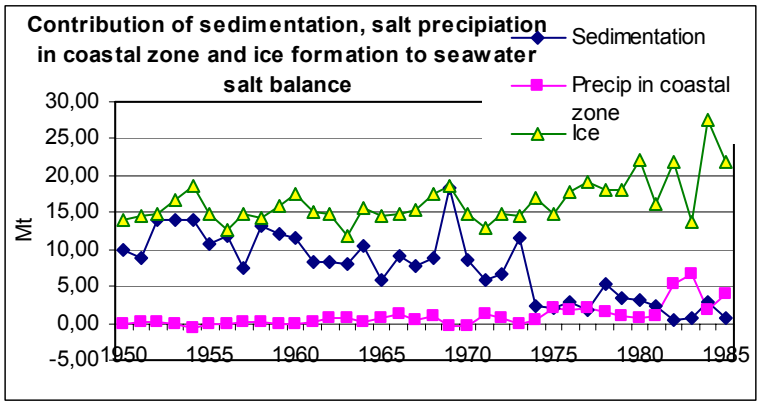

Fig. 12.7 Contribution of Sedimentation, Salt Precipitation in Coastal Zones and Ice Formation to Seawater Salt Balance

13. The Aral Sea in Winter Conditions

13.1 Freezing of the Sea

In terms of physics, dynamics of sea freezing is a heat-and-energy process; therefore, the law of enthalpy conservation and Fourier law are used for its quantitative description. Let consider the three-layered system: «snow + ice + water», Fig. 13.1, where Z^0 is water level in reservoir at the moment of ice cover formation. Further development of snow and ice covers takes place through precipitation and movement of interface «ice – water». Precipitation can be considered in form of set time function, $h^s = h^s(t)$. Then, the main energy of «ice – water» interface movement will result from change in aggregate state of water «water ↔ ice» (first order phase transition) under impact of temperature gradient.

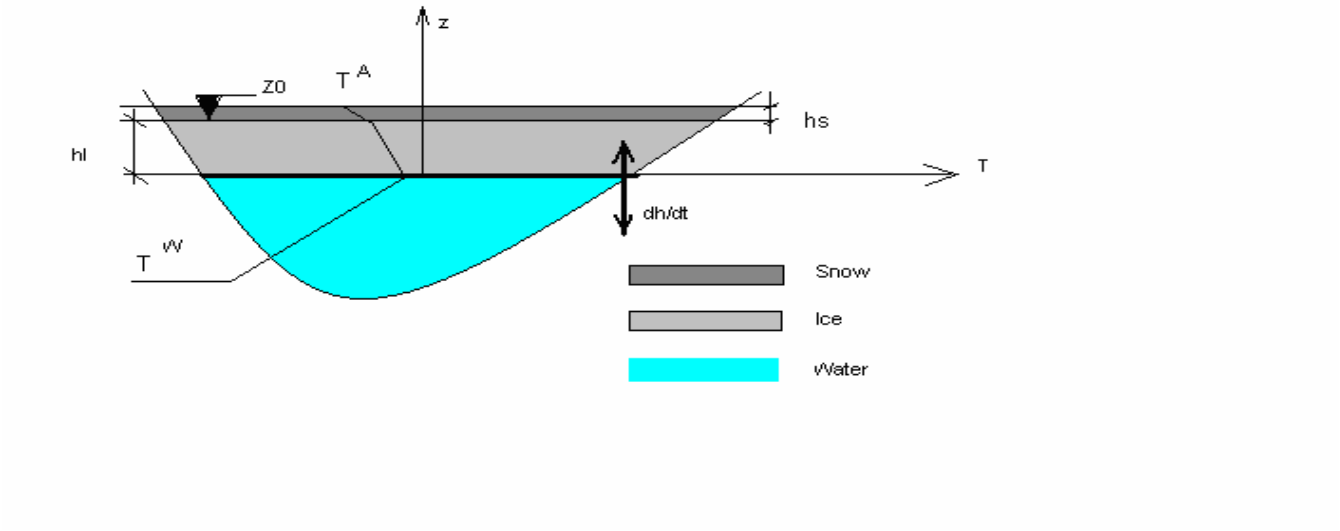

Fig. 13.1 System «water + ice + snow»

By neglecting change in enthalpy of ice and snow cover (usual assumption in hydrology), equation of "ice-water" interface movement may be written for unit surface as:

$$L^{W,I}\rho^{I}\frac{dh^{I}}{dt} = \frac{\lambda^{*}}{h^{I}}(T^{W}(s) - T^{A}); \qquad (13.1)$$

where: h^I is ice layer thickness, ρ^I is ice density (ρ^I = 917kg/m^3), $L^{W,I}$ is specific heat of phase transition «water ↔ ice» ($L^{W,I}$ = 333 ×10^3 J/kg), λ^*(t) is equivalent coefficient of system heat conductivity, T^W(s) is water freezing temperature as a function of water salinity "s", T^A is air temperature. For slightly saline water (s < 3 g/l), value of T^W(s) is taken as constant and equal to 273.15^o K = 0^o C, and these conditions are used in calculating increase of ice cover in river deltas. The equivalent coefficient of system heat

conductivity for the above mentioned two-layer system is determined by summing up the specific thermal resistance of each layer (h^j/λ^j) with its subsequent reduction ice layer thickness:

$$\lambda^*(t) = \frac{\lambda^S \lambda^I}{\lambda^S + \alpha(t)\lambda^I}; \quad (13.2)$$

where: λ^S, λ^I are snow and ice heat conductivity coefficients (λ^I = 2,24 W/(m × °C)), $\alpha(t)$ is zero-dimension parameter characterizing relative thickness of snow cover on ice ($\alpha(t)=h^S/h^I$), which will be considered further as a function of weather conditions. The thickness of snow cover on ice is determined through precipitation layer "h^W" and snow density "ρ^S ".

$$h^S = h^W \times \rho^W / \rho^S; \quad (13.3)$$

Here ρ^W is water density (ρ^W= 1000 kg/m^3), ρ^S is snow density, for the Aral Sea the mean snow density in winter [3] is ~ 280 kg/m^3 and increases to during ~ 450 kg/m^3 peak melting. Practically during the whole period of ice cover growth, snow density is within the limits of G.Abels' formula [2] satisfiability, and therefore, snow heat conductivity is calculated as:

$$\lambda^S = 2{,}85 \times 10^{-6} \times (\rho^S)^2; \quad (13.4)$$

The mean value of snow heat conductivity coefficient for winter period in the Aral Sea is $\lambda^S = 2{,}85 \times 10^{-6} \times (280)^2 = 0{,}2234$ W/(m × °C). Velocity of free water surface movement "z" is connected with velocity of ice limit movement dh^I/dt through the equation:

$$\frac{dz^W}{dt} = -\frac{\rho^I}{\rho^W}\frac{dh^I}{dt}; \quad (13.5)$$

where: z^W and ρ^W are water surface elevation and density, respectively. If follows from inequality $\rho^W > \rho^I$ that during ice cover augmentation at interface «water – ice», an excessive pressure is created and compensated (taking into account practical incompressibility of water) first by increase of elevation "Z0" and then after freezing of ice and ground together by share of water extruded into the ground. Multiplication of free water surface movement velocity "z" and reservoir surface area "Ω(z)" is a flux from water into ice and inversely. By inserting (5) in (1) and considering flux «water → ice» as positive, and taking into account the above comment, we will have:

$$Q^{W,I} = -\Omega(z)\frac{dz^W}{dt} = \Omega(z)\frac{\rho^I}{\rho^W}\frac{dh^I}{dt} = \Omega(z)\frac{\lambda^*}{h^I L^{W,I}\rho^W}(T^W(s) - T^A); \quad (13.6)$$

In equation (3.6), value "z" is calculated as $z = Z0 - h$, and only solution freezing temperature $T^W(s)$ is undefined. Change of the latter, within Raoult law satisfiability and normal atmospheric pressure, may be written as [5]:

$$T^W(s) = T^0 - \frac{N^S}{N^W}\frac{RT^2}{L^{W,I}}; \quad (13.7)$$

where: T^0 is clean water freezing temperature ($T^0 = 273.15\ ^oK$), R is absolute gas constant, N^W , N^S are moles of solvent (water) and dissolved matter, respectively. Taking into account relationship between molar and bulk concentrations of solution [8]:

$$\frac{N^S}{N^W} = \frac{\mu^S N^S \rho^W}{\mu^W N^W}\frac{\mu^W}{\mu^S \rho^W} = \frac{m^S m^W}{m^W V}\frac{\mu^W}{\mu^S \rho^W} = s\frac{\mu^W}{\mu^S \rho^W}; \quad (13.8)$$

where: s is bulk concentration, V is unit volume, m^S, m^W are masses of dissolved matter and water, respectively, μ^S, μ^W are molecular weights of dissolved matter and water, respectively;
we will have final expression for $T^W(s)$:

$$T^W(s) = T^0 - s\frac{\mu^W}{\mu^S \rho^W}\frac{RT^2}{L^{W,I}}; \quad (13.9)$$

For multicomponent solutions usually present in practice, the value μ^S is calculated as the weighted average one:

$$\mu^S = \frac{\sum_{j\in S} \mu^j N^j}{\sum_{j\in S} N^j}; \qquad (13.10)$$

If one assumes conservatism of the process of salinity increase in reservoir, that mainly observed in practice (μ^S = *constanta)*, it follows from equation (9) that freezing temperature lowers linearly, depending on concentration growth, i.e.

$$T^W(s) = T^0 - s(t) \times \text{constanta}; \qquad (13.11)$$

where *constanta* is derived from (9), (10) and may differ for various reservoirs. It needs to be noted that equation (6) is valid only for $T^A < T^0$. For winter conditions, the equation of water mass conservation (10.1) is divided into two:

$$\frac{dV^W}{dt} = \int_L Q(l,z,t)dl - Q^{W,I}(t); \qquad (13.12)$$

$$\frac{dV^I}{dt} = \frac{\rho^W}{\rho^I}[Q^0(t) + Q^{W,I}(t)]; \qquad (13.13)$$

here V^W and V^I are water and ice volumes, respectively.
Similarly salt mass conservation equation is divided:

$$\frac{dS^W}{dt} = \int_L [s^W(t) \times Q(l,z,t)]dl - Q^{S,I}(t) - Q^{S,f}(t); \qquad (13.14)$$

$$\frac{dS^I}{dt} = Q^{S,I}(t); \qquad (13.15)$$

where S^W and S^I are salt masses in water and in ice, respectively, $Q^{S,I}$ is salt flux water ↔ ice.
The process of salt exchange between water and ice is pronounced and non-symmetrical. When ice melts, all salts enter into water; however, when water solution freezes, only minor portion of salts (~ 10%) gets into ice, and therefore this is taken into account in writing equation for salt mass flux «water ↔ ice». Let express water and ice salinities through s^W and s^I, respectively.

$$s^W = S^W/V^W; \quad s^I = S^I/V^I; \qquad (13.16)$$

We consider fluxes from water to ice as positive direction of flux $Q^{W,I}$, thus for $Q^{S,I}$ we have:

$$Q^{S,I} = \begin{cases} s^I Q^{W,I} \dfrac{\rho^I}{\rho^W} & |Q^{W,I} < 0; \\ \beta \times s^W Q^{W,I} & |Q^{W,I} > 0; \end{cases} \qquad (13.17)$$

where β can be considered as coefficient of membrane «water ⇒ ice» according to [3], (β = 0.1).
It is important to note here that despite the condition $T^A < T^0$, flux $Q^{W,I}$ may be both positive and negative, depending on sign of difference ($T^W(s)$ - T^A). Therefore, in case of saline reservoirs, the process of unfreezing may take place from the bottom even under negative air temperatures, unlike freshwater reservoirs, where unfreezing always starts from upper ice surface.

13.2 Unfreezing of the sea (T^A >T).

When positive air temperature period begins, sea unfreezing intensified due to both the abrupt increase of heat conductivity coefficient and the contribution of upper ice layer, area of which is always larger than that of lower one under natural conditions. Melted snow forms thin water layer having temperature ~ 0°C on upper ice layer. During this short period, snow density increases abruptly and thickness of snow layer decreases (at ρ^S > 350 kg/m^3, Abels formula needs adjustment, according to A.Kondratyeva's work, the first coefficient rises from формула Абельса требует корректировки, согласно работе А. Кондратьевой, первый коэффициент 2,85 to 4,85 [3], p.45). Detail modeling of snow melting during this short period is not possible under given project. Therefore, with the beginning of positive

temperatures, the snow layer is completely transferred to equivalent ice layer with clean water heat conductivity coefficient at 0°C :

$$h^{S,*} = h^S \frac{\rho^S}{\rho^I}; \quad (13.18)$$

$\lambda^{S,*} = \lambda^W$; ($\lambda^W$ = 0.569Вт/(м×°С)) (13.19)

Value h^S is counted upward from Z^0 ; therefore, while developing equation for dynamics of this layer by analogy with (1), it is necessary to change direction of temperature gradient, and based on (18) and (19) we will have:

$$\frac{dh^S}{dt} = \frac{\rho^I \lambda^W}{L^{W,I} h^S (\rho^S)^2} (T^0 - T^A); \quad (13.20)$$

At the same time, equation for basic ice layer is changed:

$$\frac{dh^I}{dt} = \frac{\lambda^I}{L^{W,I} \rho^I h^I} (T^W(s) - T^0); \quad (13.21)$$

The general water inflow to reservoir is comprised of surface runoff and ground flow, and by summing up fluxes (20) and (21) and considering respective areas, we will obtain:

$$Q^{W,I} = \Omega(z) \frac{\lambda^I}{L^{W,I} h^I \rho^W} (T^W(s) - T^0) + \Omega(Z0) \frac{\rho^I \lambda^W}{L^{W,I} h^S \rho^W \rho^S} (T^0 - T^A); \quad (13.22)$$

All terms correspond to the above mentioned ones, and the sign of flux in equation (22) is negative, according to mass conservation equations (12), (13).
Using equations (20) and (21), calculation is made until zero value of $h^{S,,*}$ is achieved, and then only equation for basic ice layer remains. This layer melts mainly from upper surface. By neglecting velocity of lower surface movement at final stage of melting, we will have:

$$\frac{dh^I}{dt} = \frac{\lambda^I}{L^{W,I} \rho^I h^I} (T^0 - T^A); \quad (13.23)$$

from which follows the equation of water inflow to reservoir:

$$Q^{W,I} = \Omega(Z0) \times \frac{\lambda^I}{h^I L^{W,I} \rho^W} (T^0 - T^A); \quad (13.24)$$

14. Aral Sea Separation (1986 – 2000)

14.1 Scheme for Modeling

Since 1986, the Aral Sea can be considered as two independent objects - Large Sea and Small Sea - with their own bathymetry and hydrology. Small sea (Northern part of Aral Sea) is recharged by the Syrdarya river from south-east. Volume of Small Sea at 42,0BS is ~ 27km^3 with free water surface of 3105 km^2. Maximum depth equals 18m under average depth of 8,7m. Evaporation rate from the Large Sea is equal to that from the Small Sea because of wind speed compensation. Freezing conditions differ because in Small Sea winter temperatures are 4° C lower compared with Large Sea. The Syrdarya runoff is taken by Small Sea within its capacity, excessive water flows to Large Sea. River and sea water mixing is slow because of Small Sea bed morphology (river water replaces sea water); that's why salinity of water inflowing to Large Sea is lower compared with water salinity in Small Sea. Regarding Large Sea, Small Sea plays a role of pulse source, with salinity depending on volume of release. Replacing the Syrdarya for Small Sea in previous model and excluding the Syrdarya delta function (Small Sea evolution for this period is modeled by team CR2), we receive simulation model of Large Sea evolution for this period. Evaporation during this period can be considered as climatic factor not depending from water salinity (as results from physical experiments with water from the Aral Sea). Thus, there is the following set of objects:
Amudarya => Amudarya delta => Large Sea <= Small Sea

14.2 Input Data

Input data are presented by bathymetric tables of the Large Sea (team CR2) and hydrological and climatic characteristics from the database. Input parameters of the Aral Sea are given in Table 14.1.

Table 14.1 Time Series for the Large Sea

Year	River runoff, km^3/yr				Precipitation, km^3	Evaporation, km^3	Level,H, m	Water mass volume km^3	Water surface area (km^2)	Salinity (g/l)
	Amudarya		Syrdarya							
	s	Q	s	Q						
1986	2.69	0.46	3.73	0.20	0.11	0.98	41.94	448.00	41047	22.9
1987	1.17	8.68	2.58	1.00	0.10	1.00	41.10	432.00	38831	23.9
1988	0.72	17.81	1.01	5.00	0.11	0.94	40.29	401.00	37410	25.0
1989	2.30	1.51	1.42	3.10	0.15	0.97	39.75	380.00	36562	28.0
1990	1.33	6.89	1.67	2.41	0.70	1.04	39.08	354.00	35349	30.0
1991	1.33	10.48	1.89	2.58	0.80	1.06	38.24	323.00	33831	32.0
1992	0.78	24.27	1.73	3.34	0.10	0.92	37.56	299.00	32649	34.0
1993	1.06	15.52	1.17	7.50	0.90	0.83	37.20	286.00	32017	35.0
1994	0.93	18.72	1.09	8.46	0.12	0.97	36.95	278.00	31564	36.0
1995	2.13	3.24	1.52	4.53	0.90	0.98	36.60	266.00	30879	37.0
1996	1.87	4.92	1.47	4.89	0.19	0.97	36.11	250.00	29872	42.0
1997	2.68	0.73	1.64	3.82	0.24	0.93	35.48	230.00	28530	43.5
1998	0.89	20.07	1.18	7.41	0.17	0.88	34.80	210.00	26959	49.8
1999	1.97	4.17	1.32	6.03	0.90	1.00	34.24	194.00	25519	50.6
2000	2.51	1.37	1.83	2.86	0.13	0.96	33.80	181.00	24266	55.8
2001	2.87	0.09	1.79	3.03	0.16	0.95	33.30	169.00	22745	58.6

Based on data from the Table 14.1, salt influx to the Aral Sea from Amudary and Syrdarya were calculated for the period since 1986 till 2001. Calculations are given in Table 14.2.

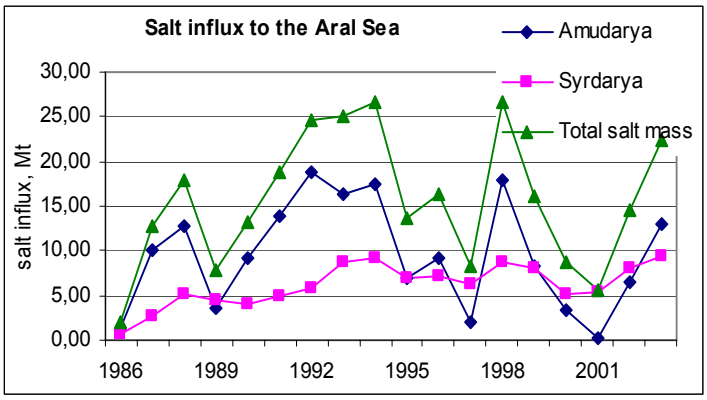

Fig. 14.1 Salt Inflow to the Aral Sea

The diagram “Salt influx to the Aral Sea” gives graphical presentation of the results. Salt influx from Syrdarya river softly increases, while salt influxes from the Amudarya river jump that leads to sharp fluctuations of salt influx in the Aral Sea as a whole.

Table 14.2 Salt Balance for the Large Sea

Year	Salt mass from A-D	Salt mass from SD	Total
1986	1.25	0.75	1.99
1987	10.15	2.58	12.73
1988	12.79	5.07	17.86
1989	3.49	4.42	7.91
1990	9.19	4.03	13.21
1991	13.95	4.88	18.83
1992	18.86	5.77	24.63
1993	16.39	8.76	25.15
1994	17.48	9.20	26.67
1995	6.89	6.88	13.77
1996	9.19	7.17	16.35
1997	1.96	6.25	8.21
1998	17.86	8.72	26.58
1999	8.23	7.95	16.19
2000	3.45	5.22	8.68
2001	0.26	5.42	5.68
2002	6.50	8.15	14.66
2003	12.92	9.41	22.34

14.3 Modeling Results

Table 14.3 presents the main parameters of the Aral Sea derived from the modeling. Each column is ended with two values: mean and mean-square deviation.

Table 14.3 Main Components of the Aral Sea Obtained from Simulations

Year	Water body volume (km^3)		Salt mass (Mt)		Salinity (g/l)		Mass of precipitated salts (Mt)			
	Simulation	Measured data	Simulation	Measured data	Simulation	Measured data	Sedimentation	Sedimentation in coastal zone	Ice	Total
1985	442.60	448.00	10135	10259	22.90	22.90	0.49	0.00	23.16	23.66
1986	407.40	432.00	10096	10325	24.78	23.90	0.04	8.29	23.71	32.05
1987	382.55	401.00	10066	10025	26.31	25.00	3.57	4.14	23.16	30.87
1988	370.09	380.00	10127	10640	27.36	28.00	10.13	1.32	20.40	31.85
1989	336.63	354.00	10122	10620	30.07	30.00	1.07	5.75	20.88	27.70
1990	308.58	323.00	10105	10336	32.75	32.00	3.87	6.87	21.25	31.99
1991	290.12	299.00	10094	10166	34.79	34.00	6.59	3.87	24.14	34.60
1992	286.82	286.00	10070	10010	35.11	35.00	15.28	0.38	23.17	38.83
1993	273.94	278.00	10065	10008	36.74	36.00	11.40	1.13	29.89	42.42
1994	265.59	266.00	10096	9842	38.01	37.00	15.99	1.18	30.28	47.45
1995	242.98	250.00	10084	10500	41.50	42.00	3.00	5.27	25.37	33.64
1996	225.24	230.00	10051	10005	44.63	43.50	3.74	6.20	33.76	43.70
1997	205.02	210.00	10027	10458	48.91	49.80	1.89	9.60	27.18	38.67
1998	197.99	194.00	9994	9816	50.48	50.60	17.86	3.34	33.19	54.40
1999	185.86	181.00	9991	10100	53.75	55.80	10.14	5.61	33.65	49.41
2000	168.78	169.00	9945	9903	58.92	58.60	0.63	11.23	27.43	39.28
	286.89	293.81	10067	10188	37.94	37.76	6.61	4.64	26.29	37.53
	82.83	88.94	54	268	10.89	11.29	6.03	3.36	4.61	8.34

It is clear from the Table 14.3 and diagrams below that similar to previous period the reservoir volume and salinity are well simulated but salt mass is simulated only on average.

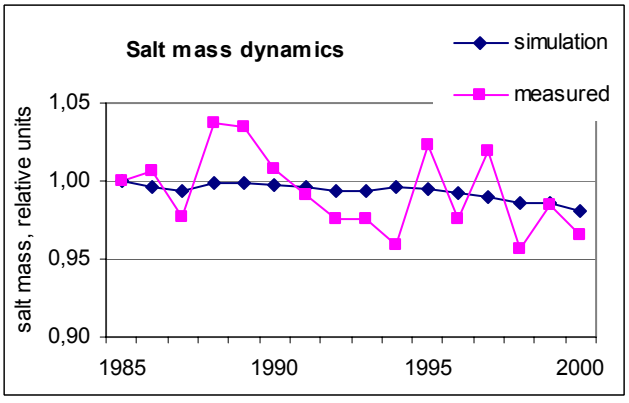

Fig. 14.2 Salt Mass Dynamics

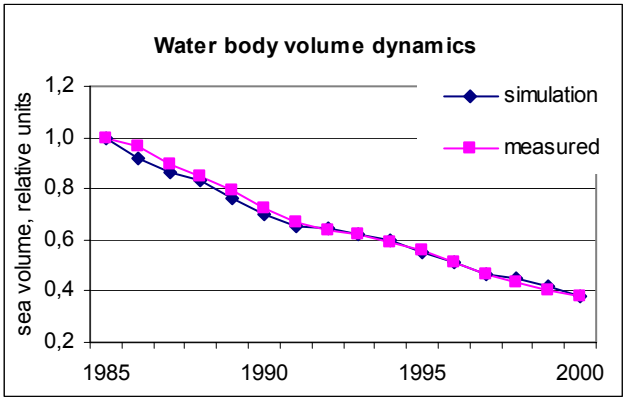

Fig. 14.3 Water Volume Dynamics

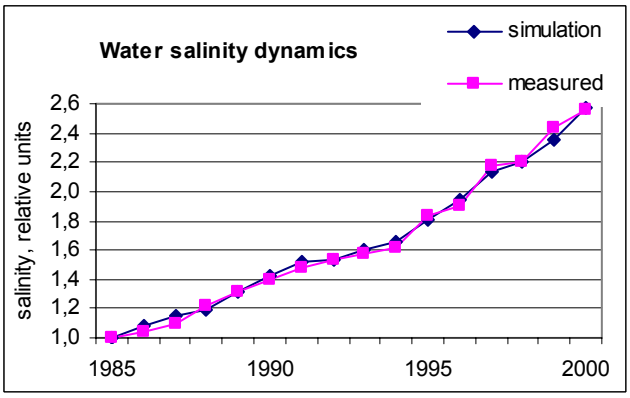

Fig. 14.4 Water Salinity Dynamics

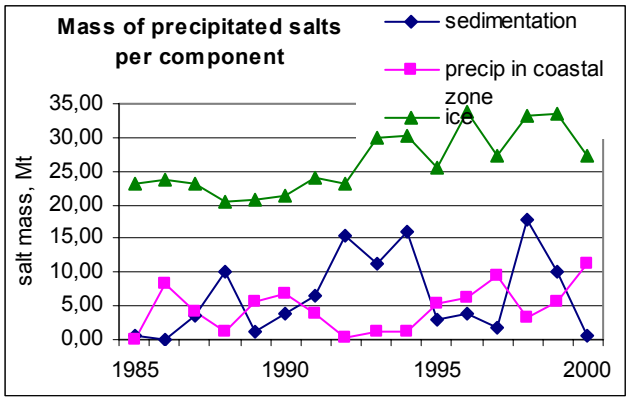

Fig. 14.5 Mass of Precipitated Salts

Fig. 14.6 shows level fluctuations in the Large Sea. Notable difference between simulated and measured data is related to bathymetric error because approximation was made on the basis of water mass maintenance. As CR2 analysis showed, this difference reaches 5%. For instance, simulated Aral Sea body calculated by trapezium method is systematically less by 4-5% of that calculated by Simpson method. This difference is possible since square approximation is used in the program.

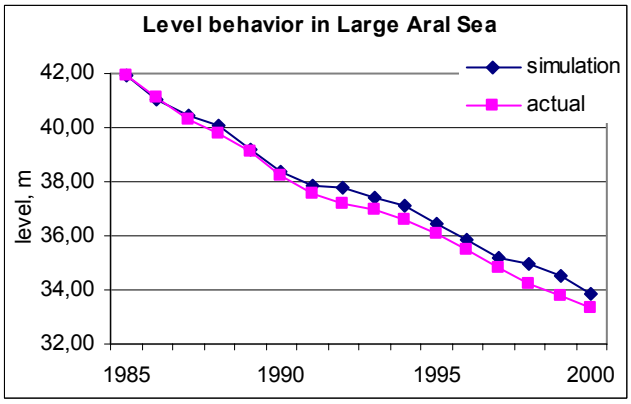

Fig. 14.6 Changes in the Water Level

14.4 Selection of Level Mark for Full Separation of Western and Eastern Bowls

Complete justification of level mark, where water exchange between Western and Eastern bowls stops, requires specific field studies related to erosion of flow passage between these two bowls. Within the framework of given project, single (stationary) level mark was selected. This level was obtained from analysis of maps (Fig. 14.7, Fig. 14.8) for bathymetry of the Aral Sea bed and field studies undertaken in 2003. Bathymetric grid spacing is ~ 500 × 500m, and therefore objects that are less than this spacing are indistinguishable. From Fig. 14.7, Fig. 14.8 follows that the main bed of separating valley is located at 31.5m BS. Inside the valley, there is a flow channel, which is not visible in presented Figures by distinguishable in satellite images with resolution 23 × 23m.

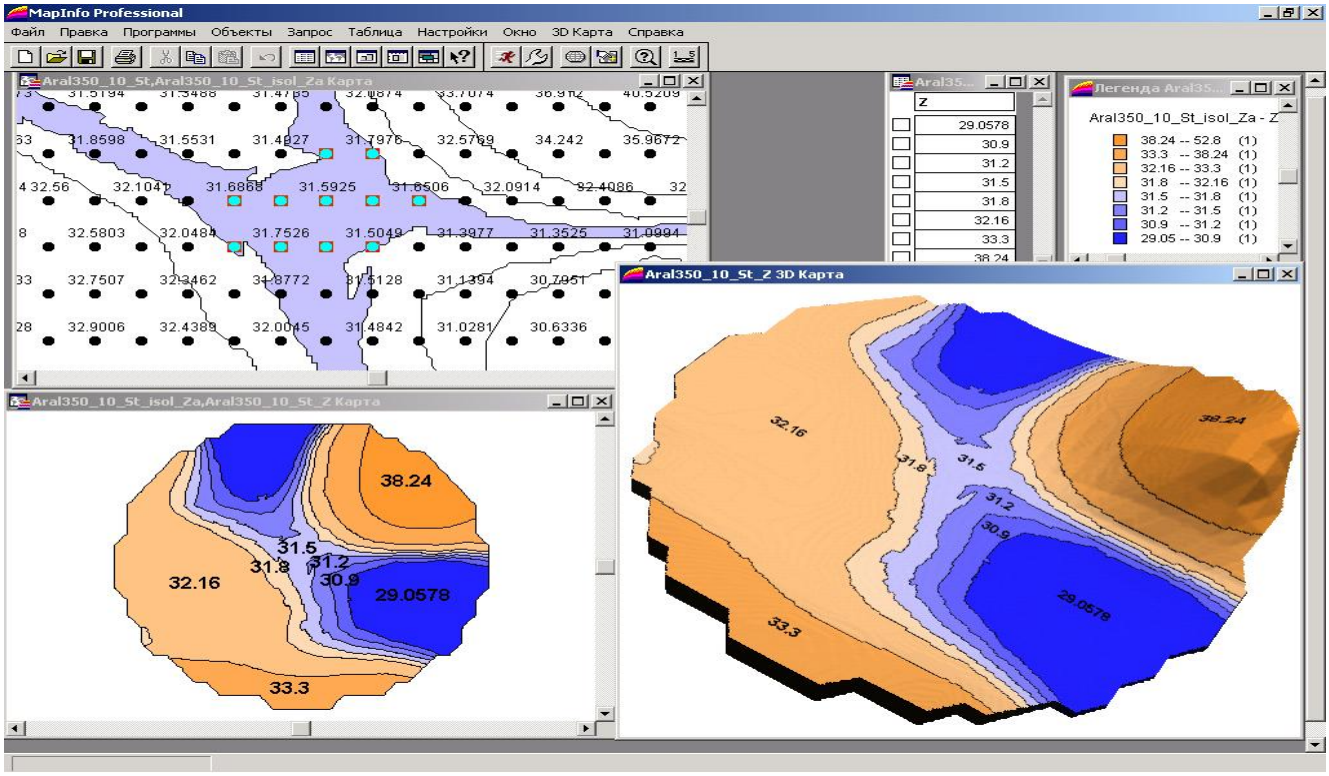

Fig. 14.7 Critical Water Levels for Seperation of Water Bodies

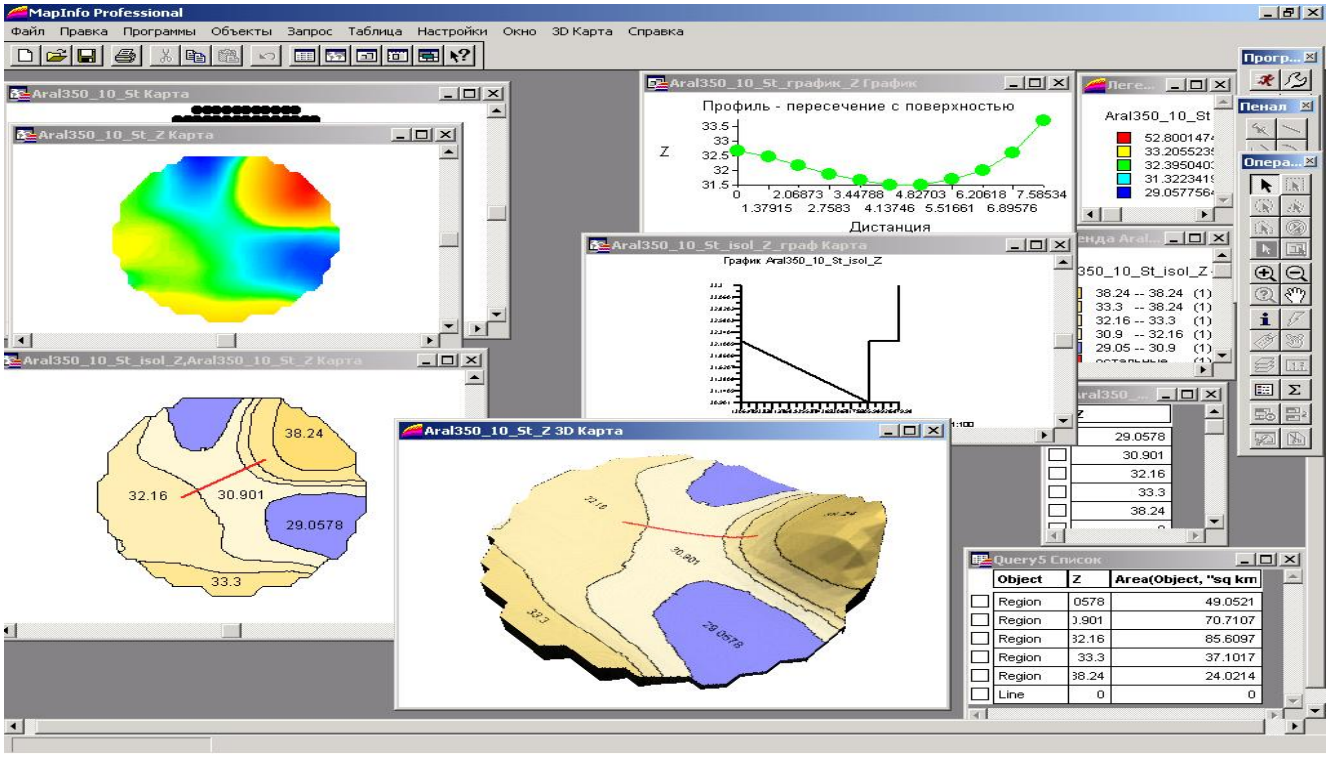

Fig. 14.8 Critical Water Levels for Seperation of the Water Bodies

15. Forecast of the Aral Sea Development

15.1 Calculation Options

Since 2000, an isthmus occurred in the south of the Large Aral Sea flow and separated the water body into Esatern and Western bowls. Circulation of flow in the sea practically stopped, though through flow channel in the North, water horizons are kept at common level in the both bowls. This fact had dramatical effect on salinity dynamics. More than two-fold difference in free surface areas under volumes of the same order has raised intensity of salinity growth in Eastern bowl, even despite the fact that it receives, through Mezhdurechie reservoir and further from the system of Dumalak lakes, practically the whole runoff of the Amudarya river and plus releasses from Small Sea. Under current engineering infrastructure, Western bowl from the side of Amudarya delta is fed only by collector and drainage water released from the system of Sudochie lakes that are quite minor. Thus, at present, Western bowl is filled with water through Northern flow channel, and its only source is Eastern bowl with highly saline water. The basis for separation of the Large Sea into Western and Eastern bowls is the bathymetrical tables, free water surface elevation and volume. At initial moment of time – the year 2000 – salinity is taken as similar for the both bowls; therefore, by the time of separatuin, the salt mass of Large Sea is distributed between the bowls proportionally to their bathymetric volumes. Water surface level at initial moment of time are considered the same in both water areas. Discharge in flow channel and its direction is determined from difference of water surface levels between the bowls and from cross-section area of the channel. According to bathymetric curves, Northern channel disappears at 29.0 BS and the both bowls start to develop independently from each other. For calculation purposes, we form mixed natural + simulated series of input fluxes (inflows from the Amudarya river and from Small Sea), among which the first four years: - 2000, 2001, 2002 and 2003 – are taken from actual data, while the year 2004 is comprized partially of actual data and partially formed by the analog year 1993. Another 20 years are formed by six simulated series (three series for Amudarya river and three series for releases from Small Sea) corresponding to three regional development scenarios (CR2 group). Further, each series of water inflow to Amudarya river delta, corresponding to certain scenario, is applied to three schemes of water distribution in the delta, according to project plan:

1 – Current delta infrastructure,
2 – NATO SFP 974357 Project's delta infrastructure,
3 – Hypothetucal option of inflow to Western bowl.

Since each scheme generates various directions of flows and varios losses in the delta, 9 water inflow options to Eastern and Western bowls of the Aral Sea are formed in general. Description of the first and second schemes for water distribution in the Amudarya river delta is give in [10], slight ~ 5% increase in water volume towards Western bowl (in contrast to project [10]) is due to the fact that under the given project we consider such management option that ensures maximum flow in this direction. Since at present there is no project for the third scheme, the hypothetucal option of inflow to Western bowl proceeds from basic terms of impelementation of the scheme 2, while maintaining current requirements of Amudarya river delta.

Input data
Annex 3 gives climatic characteristics in annual dimension on the basis of previous years, inflows to Amudarya delta and releases from Small Sea according to CR2 group's scenarios. Initial conditions for Eastern and Western bowls are as follows:

- Volumes for the year 2000 follow bathymetric tables
- Salinity and free water surface levels are the same for the both bowls.

15.2 Modeling Results

15.2.1 Current Amudarya Delta Infrastructure

Under current infrastructure, flow from Sudochie lake system is neglected since releases from the last Karateren lake almost completely evaporate in former Adjibay bay (Tables 15.1-15.12, Annex 2).

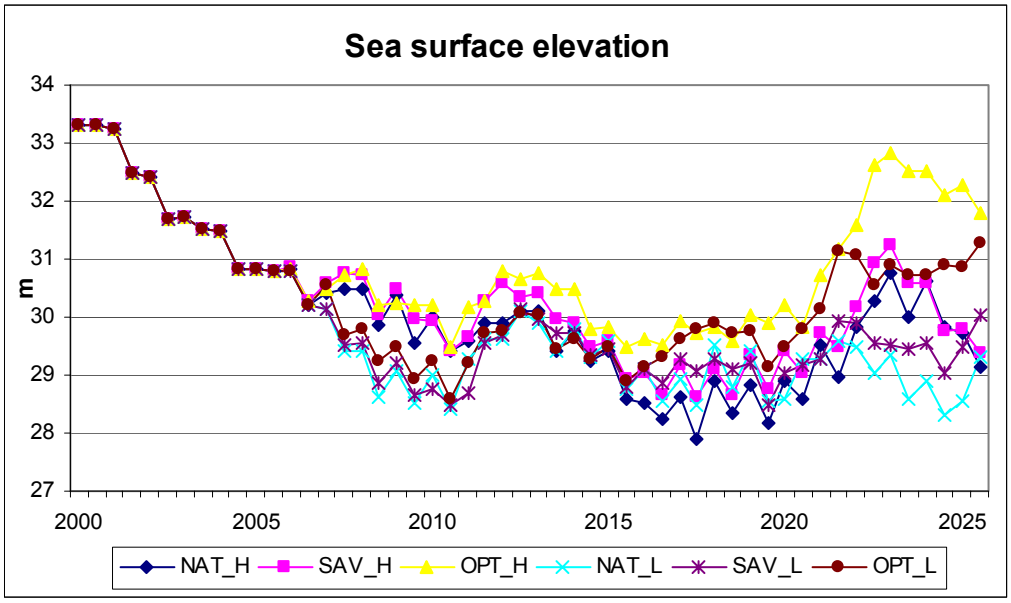

Fig. 15.1 Sea Surface Elevation of Eastern Bowl

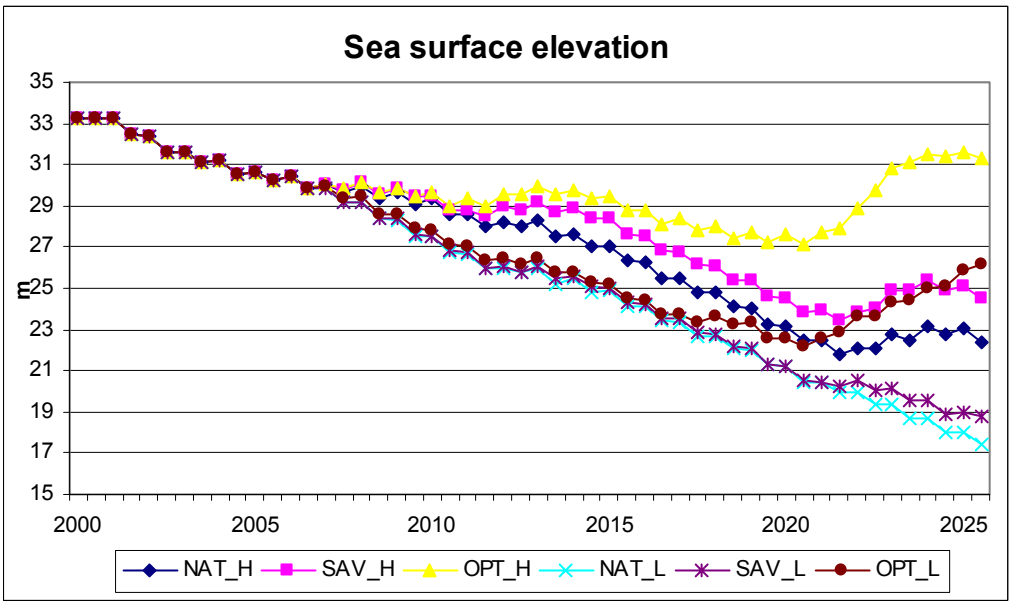

Fig. 15.2 Sea Surface Elevation of Western Bowl

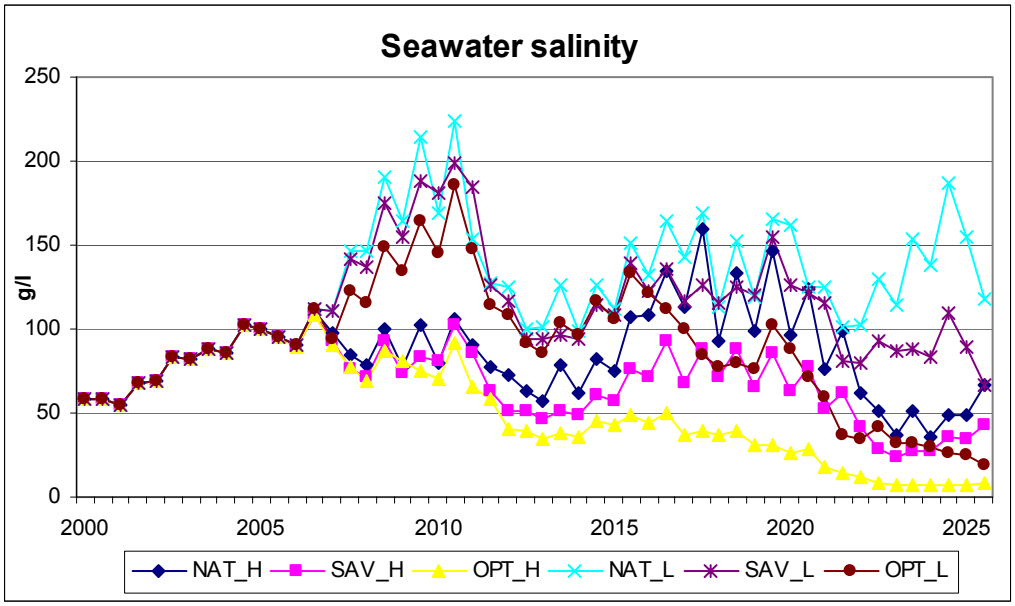

Fig. 15.3 Salinity in Eastern Bowl

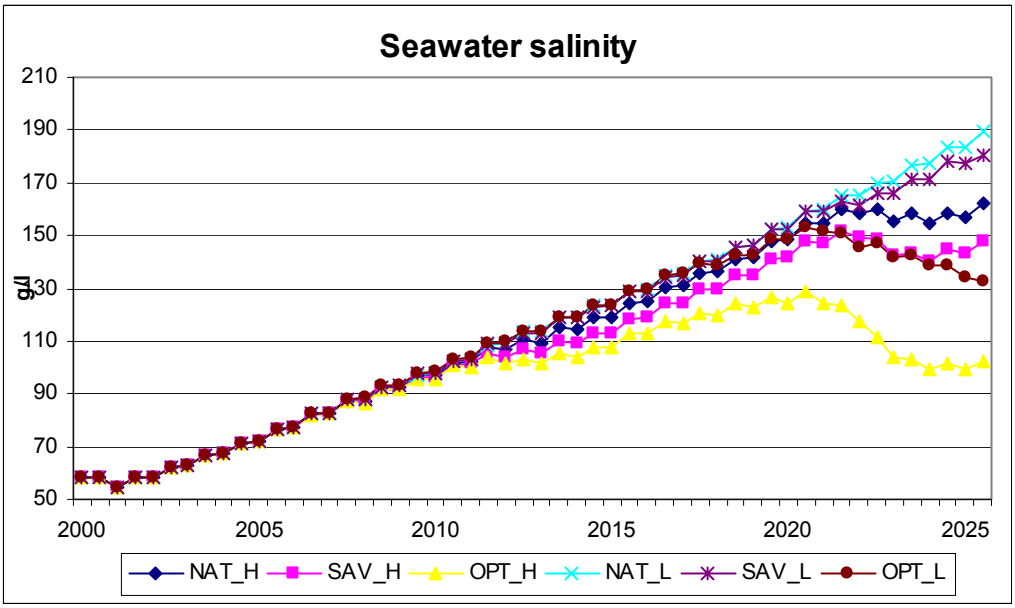

Fig. 15.4 Salinity in Western Bowl

15.2.2 NATO SFP 974357 Project's infrastructure. Water surface elevations.

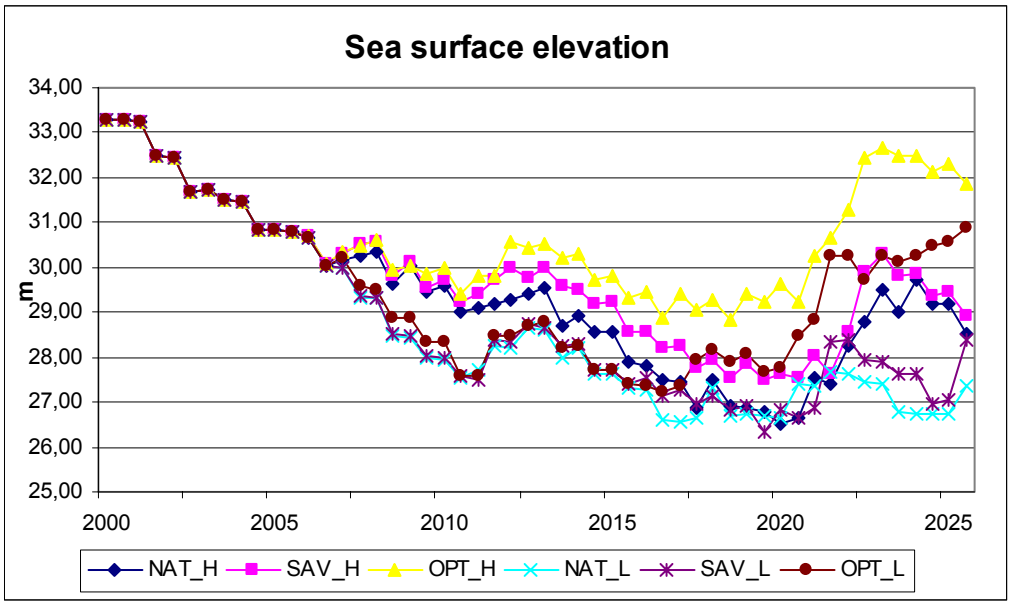

Fig. 15.5 Sea Surface Elevation in Eastern Bowl

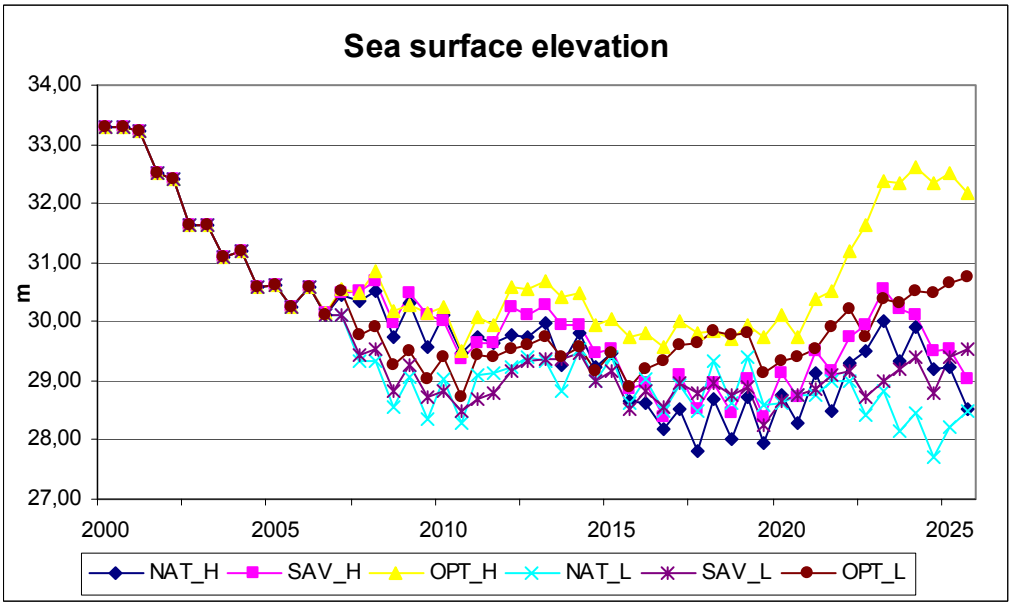

Fig. 15.6 Sea Surface Elevation in Western Bowl

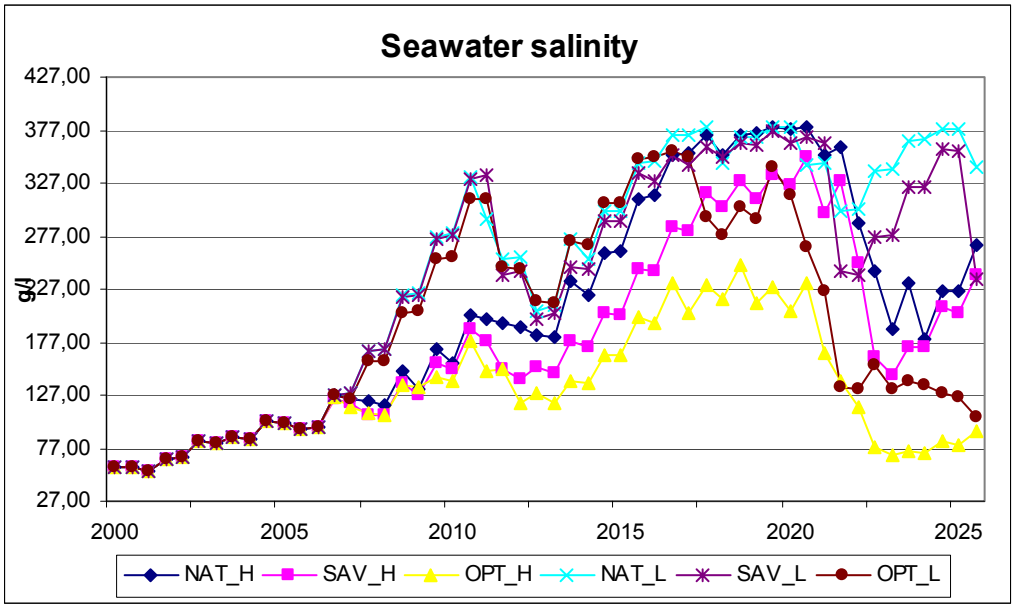

Fig. 15.7 Sea Water Salinity in Eastern Bowl

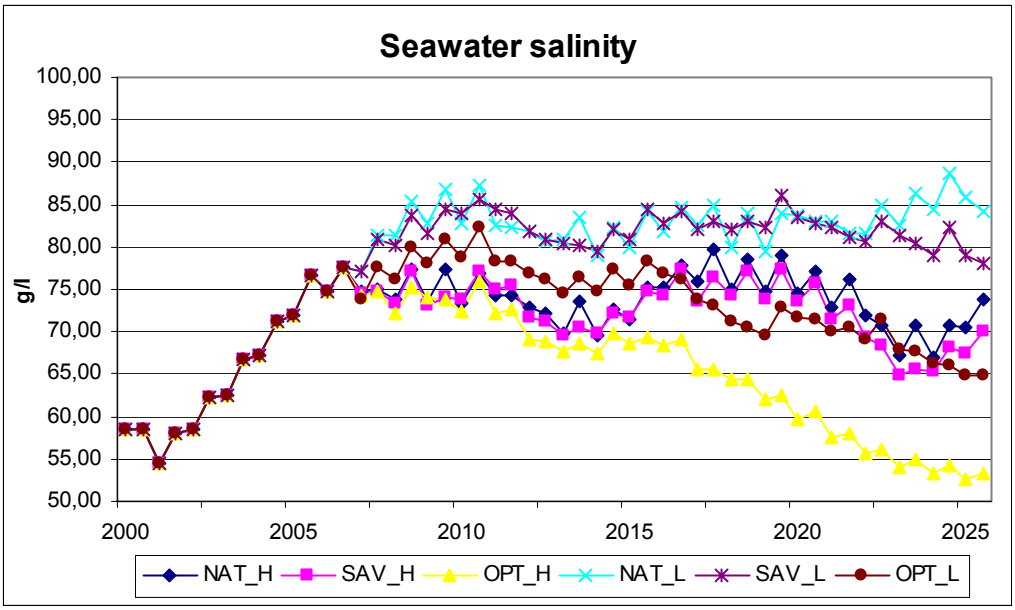

Fig. 15.8 Sea Water Salinity in Western Bowl

15.2.3 Hypothetical Option of Water Inflow to Western Bowl

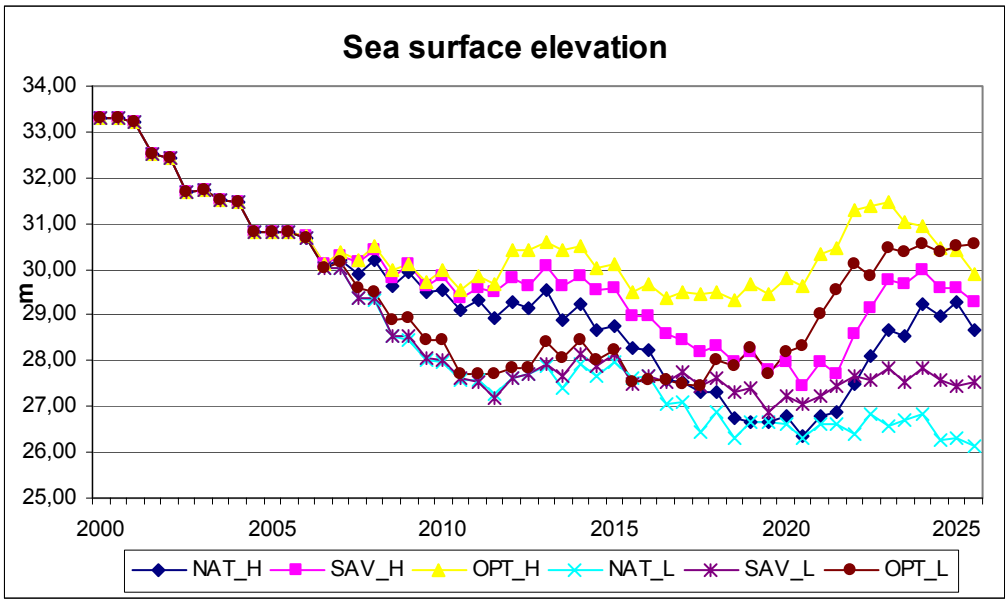

Fig. 15.9 Sea Water Elevation in Eastern Bowl

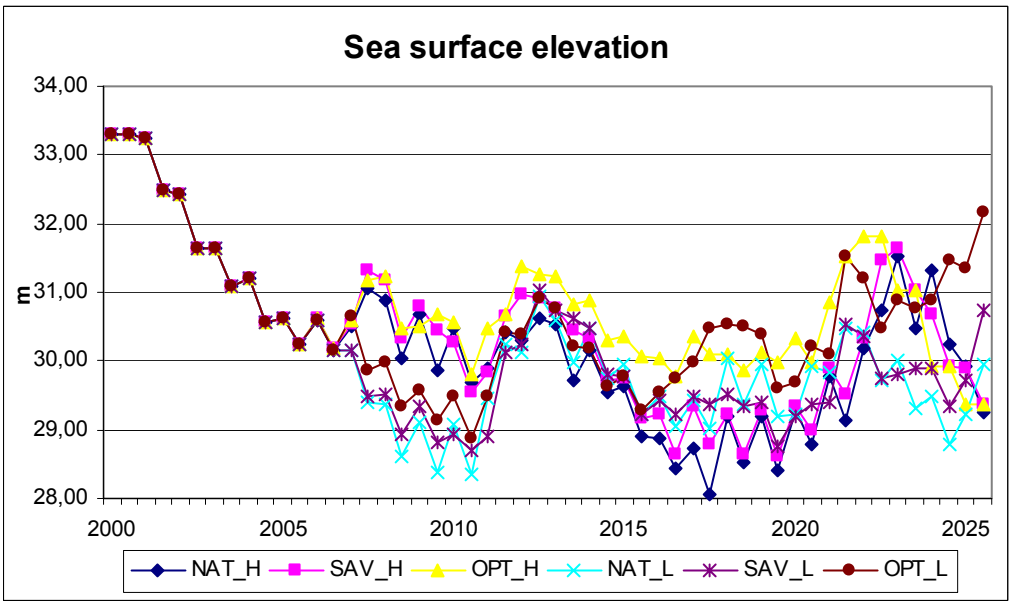

Fig. 15.10 Sea Water Elevation in Western Bowl

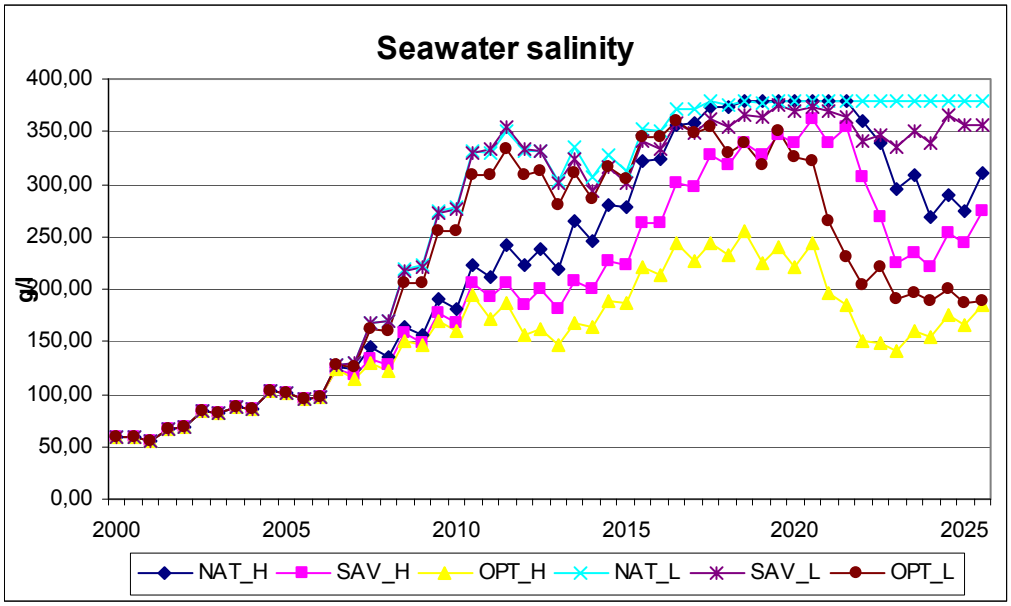

Fig. 15.11 Sea Water Salinity in Eastern Bowl

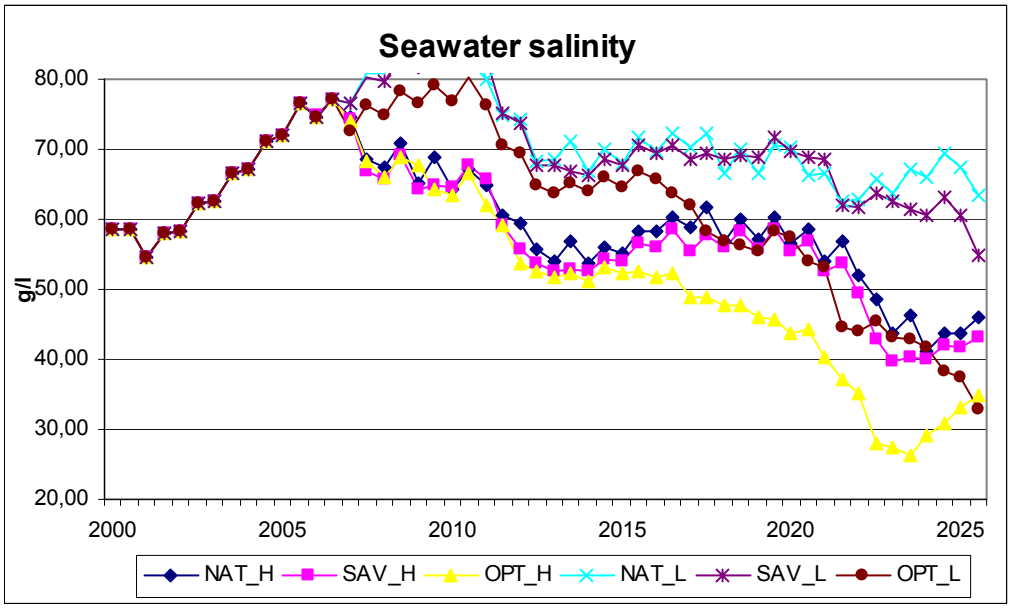

Fig. 15.12 Sea Water Salinity in Western Bowl

15.2.4 Flow Channel Behavior

Positive direction of flow is from Eastern bowl to Western bowl, negative sign indicates to changed direction of flow.

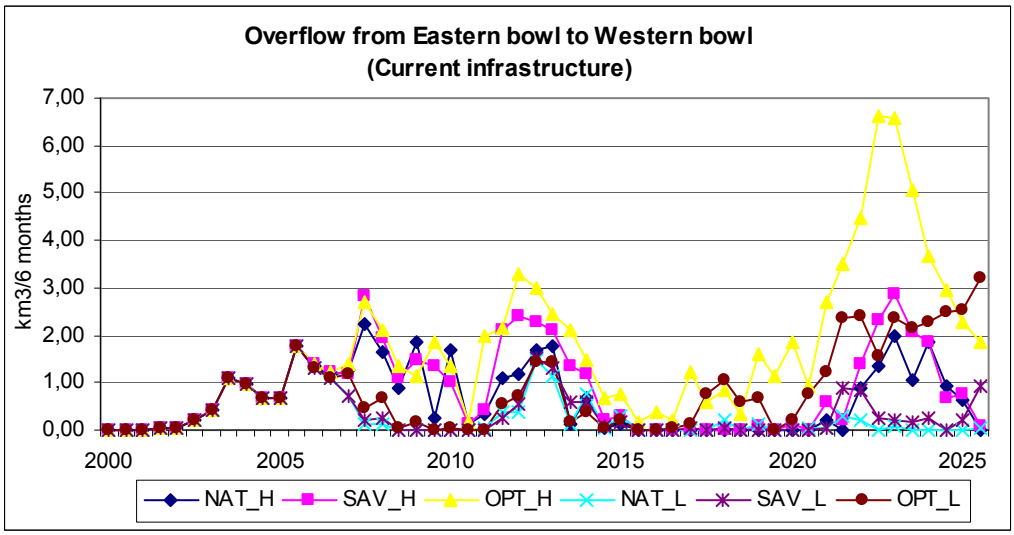

Fig. 15.13 Water Exchange (Flows) among Current Infrastructure

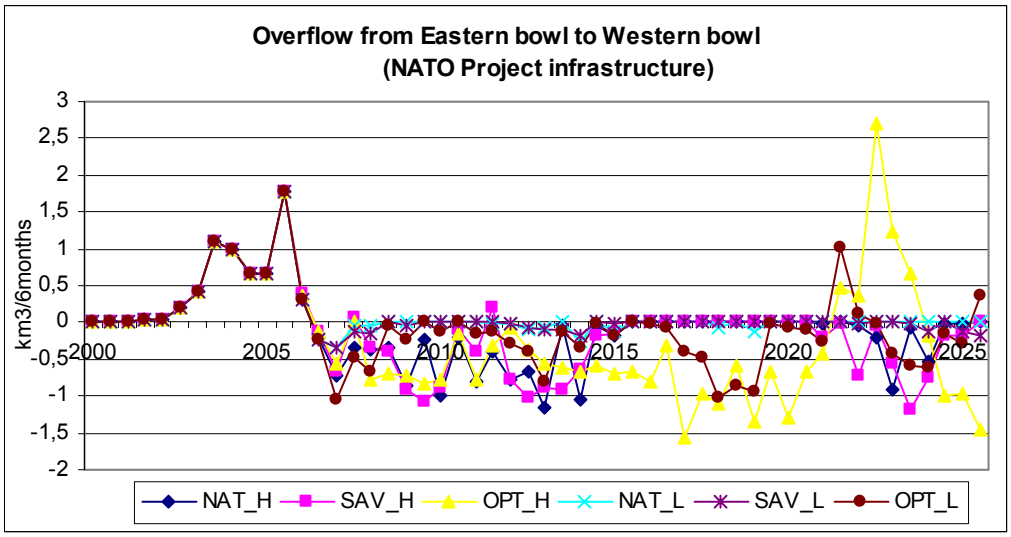

Fig. 15.14 Water Exchange (Flows) among NATO Project Infrastructure

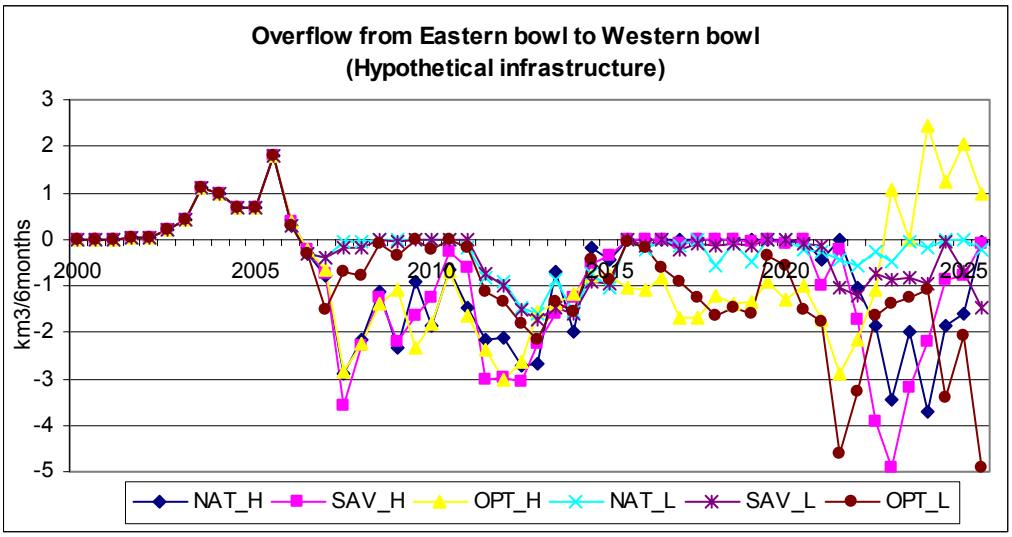

Fig. 15.15 Water Exchange (Flows) among Hypothetical Infrastructures

16. Hydrochemistry of the Aral Sea

During 4 decades research efforts has been undertaken to study consequences of the Aral Sea shrinking and to plan mitigation measures in social, economic and ecologic aspects [18,44]. One of the main factors is salt dissolved in seawater, which remains on dried seabed as well as impacts biological objects in water.

Chemical composition of seawater is determined by the following ions: Ca^{2+}, Mg^{2+}, Na^{+}, K^{+}, HCO^{3-}, SO_4^{2-} и Cl^{-}, and other ions have minor concentrations [1]. Nevertheless, with salinity increase salt content is transformed [3]. In order to develop mathematical model of salt balance in Aral Sea water and mitigation measures on bio-productivity restoration, information about seawater chemical composition and its salinity dynamics is needed.

This work is devoted to study the ion content and salt balance under water mass reduction due to evaporation and the evaporation rate depending on salinity.

Ion content and evaporation rate were studied experimentally in seawater (without visible admixtures). Sample was taken from western part of the Large Sea near Aktumsuk weather station in July 2003.

Water evaporation was observed in chemical vessels with cross-section of 117cm^2 in natural conditions (without artificial heating). Test duration – July-August 2004, maximum temperature was 29^{o}C. Initial sample volume was 200ml. Samples were analyzed each second day at the same time.

Definition of solution's ion composition was performed by classic analytical chemistry method. Results of analyses are presented in Table 16.1. Mean relative error was 10%. Reliability of the analyses was verified by comparing salt solid mass and sum of ion mass determined by analysis under obligatory conditions:

$$m_{ij} = c_{ij} * V_j \le c_{io} * V_o = m_{io},$$

where m_{ij} is i-ion mass in sampling time t_j; c_{ij} is i-ion concentration in sample; Vj is water volume in vessel at the moment of sampling (determined experimentally); c_{io} and V_o are i-ion content in initial sample and initial water volume.

16.1 Chemical Composition

It is evident from the analysis that salt solid and sum of ion mass differ by less than 3,5%. Salt solid and sum of ion in 1liter solution define salinity of water taken for analysis. But salt solid defines dissolved matters content only approximately because during water evaporation under temperature 105-120^{o}C some organic matters oxidize and chemical compositions do not give all water and crystallized water. Sum of ions is accepted as reduced to 1liter of water though not all ions are accounted (e.g. iron, chromium).

Table 16.1 Chemical Composition of Aral Sea Water

Sample	*Analysis date*	*Salt solid g/l*	*Ion content ,g/l*						*Sum of ions, g/l*	*mg/ekv/l*					
			HCO^-_3	Cl^-	SO^{2-}_4	Ca^{2+}	Mg^{2+}	$Na^+ + K^+$		HCO^-_3	Cl^-	SO^{2-}_4	Ca^{2+}	Mg^{2+}	$Na^+ + K^+$
Initial	30.07.04.	85,0	1,2	32,0	24,1	1,5	4,2	23,1	86,1	20,3	902,4	501,3	74,9	345,2	1004,0
	02.08.04.	140,6	1,2	53,5	40,2	1,5	7,5	38,5	142,4	20,3	1508,7	835,2	74,9	616,5	1672,9
	03.08.04.	168,1	1,6	56,0	54,8	3,0	10,2	40,4	165,9	25,4	1579,2	1139,0	149,7	838,4	1755,5
	04.08.04.	303,2	1,7	114,0	80,5	0,8	16,9	80,1	294,0	28,0	3214,8	1673,8	39,9	1390,8	3485,9
	05.08.04.	416,5	2,8	145,6	130,5	1,0	27,6	104,6	412,1	46,1	4105,9	2714,6	49,9	2268,7	4548,0
Data [36], 1947			0,2	3,5	3,3	0,6	0,5	2,3	10,4	3,1	98,7	68,8	27,9	40,3	101,8
Blinov [1,14],1956			0,2	3,1	2,7	0,4	0,5	2,1	8,9	2,8	86,3	56,8	20,5	37,8	89,2

Fig. 16.1 shows results of calculation using data from Table 16.1 during water evaporation:

$$\delta_i = \frac{c_i}{c_{io}},$$

where c_i is i-ion content g/l; c_{io} is i-ion mass in initial water. It can be seen that during water evaporation and salinity increase up to 300g/l δ_i ions Cl^- and $Na^+ + K^+$ are close to δ_i salinity value. It can be supposed that these ions during evaporation did not create stable associations, which can settle or form salts settling but there is dynamic equilibrium between sedimentation and solution process. First assumption is more reliable because salts, which can be formed by these ions have relatively high solubility and don't reach saturation in our tests.

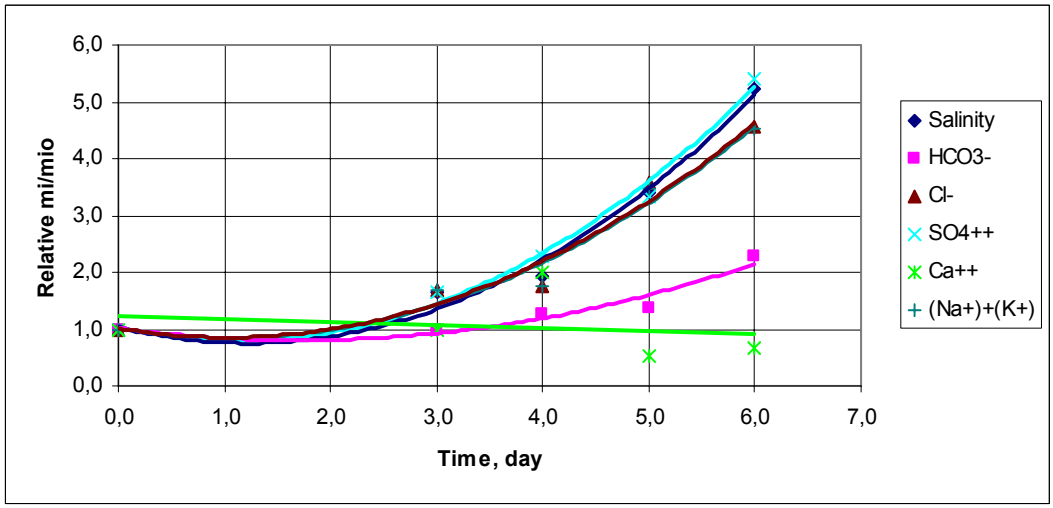

Fig. 16.1 Change in ion content in seawater: c_i/c_{io}, c_i – i-ion content, c_{io} – i-ion content in initial water

Values δ_i of ions HCO_3^- and Ca^{2+} differ significantly from δ_i salinity of water. It may be caused by ion participation in chemical reaction with $CaCO_3$ formation, which settles. i-ion content in total ion mass draws to the same conclusion (Table 16.2). It is clear that share of ions HCO_3^- and Ca^{2+} decreases with water salinity increase.

Table 16.3 presents calculation results of relative ion content in seawater in 1947 and 1956. Calculations were based on data from [1,14,36]. It's obvious that since 1947 till 2003 share of ions Mg^{2+}, $Na^+ + K^+$ and Cl^- didn't change (within measurement error) and ions Ca^{2+}, HCO_3^- and SO_4^{2-} decreased. Decreasing share of ions Ca^{2+} and SO_4^{2-} is clearly traced while considering relations between Mg^{2+}/Ca^{2+} and SO_4^{2-}/Cl^-, which are given in Table 16.3. This table shows that in 1947 under water salinity 10,39g/l Mg^{2+}/Ca^{2+} mass ratio equals 0,88 and for SO_4^{2-}/Cl^- it equals 0,95; in 1956 under salinity 8,88g/l Mg^{2+}/Ca^{2+} mass ratio was 1,1 and SO_4^{2-}/Cl^- -0,89; in 2003 under salinity 86,1g/l Mg^{2+}/Ca^{2+} mass ratio was 2,8 and SO_4^{2-}/Cl^- - 0,75. Taking into account that Mg^{2+} and Cl^- ion share almost didn't change (Table 16.2), Mg^{2+}/Ca^{2+} and SO_4^{2-}/Cl^- mass ratio growth with salinity increase is connected with reduction of Ca^{2+} and SO_4^{2-} share due to $CaSO_4$ sedimentation.

Table 16.2 Share of Main Ions in Aral Sea Water (%)

Sample	Date of analysis	Sum of ions, g/l	*HCO^-_3*	*Cl^-*	*SO^{2-}_4*	*Ca^{2+}*	*Mg^{2+}*	*$Na^+ + K^+$*
Initial	30.07.04.	86,1	1,4	37,2	28,0	1,7	4,9	26,8
	02.08.04.	142,4	0,9	37,6	28,2	1,1	5,3	27,0
	03.08.04.	165,9	0,9	33,8	33,0	1,8	6,1	24,3
	04.08.04.	294,0	0,6	38,8	27,4	0,3	5,8	27,3
	05.08.04.	412,1	0,7	35,3	31,7	0,2	6,7	25,4
Data from [36], 1947		10,4	1,8	33,7	31,9	5,4	4,7	22,5
Blinov [1,14],1956		8,9	1,9	34,5	30,7	4,6	5,2	23,1

Table 16.3 Ratio of Ions in the Aral Sea Water

	Salinity, g/l					1947	1956
Ratio of ions	86,1	142,4	165,9	294,0	449,0	10,39	8,88
Mg^{2+}/Ca^{2+}	2,8	5,0	3,4	21,2	27,6	0,88	1,1
SO_4^{2-}/Cl^-	0,75	0,75	0,98	0,71	0,90	0,95	0,89

For comparison, in ocean water at medium salinity degree of 35 g/l ratio of ion masses Mg^{2+}/Ca^{2+} is equal to 2,93 and SO_4^{2-}/Cl^- is equal to 0,14, for the Black Sea at medium salinity degree of 17,4 g/l ratio of ion masses Mg^{2+}/Ca^{2+} is equal to 2,6 and SO_4^{2-}/Cl^- is equal to 0,14, for the Caspian Sea at medium salinity degree of 13,3 g/l ratio of ion masses Mg^{2+}/Ca^{2+} is equal to 2,03 and SO_4^{2-}/Cl^- is equal to 0,53.
As you know, water contains cations and anions, not molecules of salts. Nevertheless, definition of hypothetical salt composition, which helps to reveal some solution properties, is of interest. Table 16.4 shows hypothetical salt composition. It is obvious that in 2003 as well as during stable period of the Aral Sea, hypothetical salts of sodium chloride and magnesium sulfate were dominating in the water, at that from 1947 to 2003 ratio of $NaCl/MgSO_4$ almost didn't change and was within 2,2-2,5.
Concentration of hypothetical salts of calcium sulfate was 3,71 g/l in the Aral water in 2003. It worth to note that calcium sulfate solubility in clean water is 2,4 g/l at 0^oC and 2,2 g/l at 100^oC. Increased calcium sulfate solubility in water under availability of other ions is caused by electrostatic interaction between ions. Each ion is influenced not only by water dipoles, but also by other ions in solution. The higher ion concentration in solution and the stronger their load, the bigger this influence. Electrostatic ions interacting forces weaken their ability of chemical reactions. Chlorine ions mainly impact on increase of calcium sulfate solubility. It should be noted that at 0^0C solubility of $CaCl_2$ in water is approximately equal to 595 g/l, $MgSO_4$ solubility is about 710 g/l, and Na_2SO_4 solubility – 50 g/l [29], that is ions existing in solution, hindering ions recombination Ca^{2+} and SO_4^{2-} by their charges shielding, can form with these ions easy soluble salts.

Table 16.4 Hypothetical Salts in the Aral Sea Water

Sampling	Analysis date	$Ca(HCO_3)_2$	$CaSO_4$	$MgSO_4$	Na_2SO_4	NaCl	Sum of salts, g/l
Initial	30.07.04.	1,6	3,7	20,8	7,2	52,8	86,1
	02.08.04.	1,6	3,7	37,1	11,7	88,2	142,4
	03.08.04.	2,1	8,5	50,5	12,5	92,4	165,9
	04.08.04.	2,3	0,8	83,7	19,3	188,0	294,1
	05.08.04.	3,7	0,3	136,6	31,4	240,1	412,1
Data [36], 1947		0,3	1,7	2,4	0,2	5,8	10,4
Blinov [1,14],1956		0,2	1,2	2,3	0,2	5,0	9,0

Now let us consider portion of each hypothetical salt in general mass of dissolved salts in water (Table 16.5). Based on comparing data of 1947, 1956 and 2003, it can be noted that portions of NaCl and $MgSO_4$ in the Aral water during 56-year period almost didn't change, although water salinity increased 8,6 times. Portion of Na_2SO_4 for the same period increased 3,5-4 times, and portions of $Ca(HCO_3)_2$ and $CaSO_4$ decreased. Data from Table 9.12 prove once again that under increasing water salinity, because of water evaporation, calcium sulfates and carbonates form sediments on seabed. Portion of $CaSO_4$ in water reduced 3,8 times by 2003 against that in 1956. When the Aral Sea will further shrink, water salinity will be comprised by more than 95% by salts of NaCl, $MgSO_4$ and Na_2SO_4. In testing with Aral water separate chips of calcium carbonate and sulfate can be visually observed, when water salinity reaches ~110-120 g/l.

Table 16.5 Hypothetical Salt Share in the Aral Sea Water, %

Sampling	Analysis date	Sum of salts, g/l	$Ca(HCO_3)_2$	$CaSO_4$	$MgSO_4$	Na_2SO_4	NaCl
Initial	30.07.04.	86,13	1,9	4,3	24,1	8,4	61,3
	02.08.04.	142,07	1,2	2,6	26,1	8,2	62,0
	03.08.04.	165,87	1,2	5,1	30,4	7,5	55,7
	04.08.04.	294,07	0,8	0,3	28,5	6,5	63,9
	05.08.04.	449,02	0,9	0,1	33,1	7,6	58,3
Data [36], 1947		10,36	2,4	16,3	23,4	2,1	55,7
Blinov [1,14],1956		8,96	2,5	13,4	25,4	2,3	56,3

Let us carry out following experiment in mind. Let river water in an amount of W_r, where concentration of sulfate-ions is 0,5 g/l, mix with W_s of seawater with concentration 3,7 g/l of hypothetical salts of calcium sulfate. We will count that 3,7 g/l is a $CaSO_4$ solubility limit in seawater at salinity degree of 86 g/l and ion composition given in Table 8.1 When mixing sea water and river water, sulfate-ions transported by river flow can form $CaSO_4$ in the following amount

$$m_{CaSO_4} = \frac{0{,}5 \times W_r \times 136}{96} = 0{,}71 W_r \text{, г}$$

Then, general mass of calcium sulfate in water mix will be

$$m_{CaSO_4,o} = 0{,}71 \times W_r + 3{,}7 \times W_s \text{, г}$$

Respectively, concentration of hypothetical salts in water mix will be equal to

$$c_{CaSO_4,см} = \frac{m_{CaSO_4,o}}{W_r + W_s} = \frac{0{,}71 \times W_r + 3{,}7 \times W_s}{W_r + W_s} \text{, g/l} \qquad (16.1)$$

Hence, from (1) follows that calcium sulfate concentration in water mix can vary from 0,71 g/l, when large river water amount mixes with smaller seawater amount ($W_r >> W_s$), to 3,7 g/l, when $W_r << W_s$, i.e. 0,71 g/l ≤ $c_{CaSO_4,см}$ ≤ 3,7 g/l. So in this case calcium sulfate content in water mix doesn't exceed $CaSO_4$ content in seawater. In reality, the second situation occurs more often, that is river water mixes with larger amount of seawater.

Thus, when mixing river water with Aral seawater, over-saturation of water with calcium sulfate is not observed. Similarly, mixing of river and seawater doesn't cause over-saturation with calcium carbonate. By the way, under full-scale study calcium carbonate sedimentation was noticed during mixing river water and seawater [45]. One of factors, which cause $CaCO_3$ sedimentation during the process of waters mixing, can be ion imbalance in solution.

In river and seawater the dynamic balance exists between different forms of carbonic acid:

$$2HCO3^- \leftrightarrow CO3^{2-} + CO2 + H2O$$

When waters are mixed, dynamic imbalance can take place. For example, if there is a shortage of CO_2 in water mix against balanced concentration, it will lead to HCO_3 portion decay – and formation of CO_3^{2-} ions, which will react with calcium ions while forming $CaCO_3$.

In experiments, along with study of water ionic composition, dependency of water evaporation rate on its salinity was investigated. As a reference pattern, distilled water that evaporated in similar conditions and in the same container as Aral water was used. Initial amount of distilled water was 200 ml. Calculation of evaporated water mass was made on the basis of daily weighing the container with water at the same time (at moment of water sampling for chemical analysis). Weighing was fulfilled by means of electronic scales (scales accuracy 0,001 g). Average relative error of mass estimation was 5%. The experiment results are shown in Table 5.6. These data show that distilled water evaporates more than 10% faster than Aral water. Difference between water evaporation rates increases with Aral water salinity increase.

16.2 Aral Sea Water Evaporation

Table 16.6 Evaporation Rates from the Sea

Measurement date	Mass of the container with seawater, g	Seawater evaporation, g	Seawater evaporation rate, g/day	Mass of the container with distilled water, g	Distilled water evaporation, g	Distilled water evaporation rate, g/day	Ratio of seawater and distilled water evaporation rates
30.07.2004	211,15	-	-	198,83	-	-	-
02.08.2004	132,58	78,57	26.19	112,55	86,28	28.74-	0.91
03.08.2004	108,80	102,35	23,78	85,82	113,01	26,73	0,89
04.08.2004	72,68	138,47	36,12	42,73	156,10	43,09	0,84
05.08.2004	48,39	162,76	24,29	10,04	188,79	32,69	0,74
06.08.2004	36,30	174,85	12,09	-	198,83	-	-

If salts are available in water, some phenomenon called as pressure decline happens – difference between vapor pressure over pure dissolvent (water) and vapor pressure over solution at given temperature. Decline of dissolvent vapor pressure for diluted solutions can be defined on the basis of Raul's First Law:

$$\frac{P_в - P_p}{P_в} = \frac{\Delta P}{P_в} = \frac{N_1}{N_2}, \qquad (16.2)$$

where $P_в$ and P_p are vapor pressures over pure water and solution, respectively; N_1 and N_2 are numbers of molecules of dissolved salt and water per 1 kg of solution.

The Aral seawater with salinity of 85 g/l can't be considered as diluted solution. However, difference between experiment results and data derived from the Raul's First Law is of research and practical interest.

Taking into account ratios

$$N_1 = N_a \frac{m_1}{\mu_1}; \quad N_2 = N_a \sum_i \frac{m_i}{\mu_i};$$

$$m_1 + \sum_i m_i = 1000;$$

$$m_i = \frac{c_i}{1 + 10^{-3} \sum_i c_i},$$

equation (2) can be presented as:

$$\frac{P_p}{P_в} = 1 - 10^{-3} \mu_1 \sum_i \frac{c_i}{\mu_i}, \qquad (16.3)$$

where N_a is Avogadro number; m_1 and μ_1 are water mass per 1kg of solution and molar water mass, g; Σm_i is sum of i-ion masses per 1kg of solution, g; μ_i–i-ion molar mass; c_i – i-ion concentration per 1 liter of water.

Water evaporation rate is equal to

$$v = \frac{dm_{ev}}{dt}, \qquad (16.4)$$

where m_{ev} is evaporated water mass. Since

$$m_{ev} = \mu_1 \frac{N}{N_a},$$

where N is number of water molecules in vapor, ratio of evaporated seawater and distilled water for some period of time Δt can be expressed as equation

$$\delta_{ev} = \frac{v_p \Delta t}{v_в \Delta t} = \frac{m_p}{m_в} = \frac{N_p}{N_в}, \qquad (16.5)$$

where index «p» belongs to parameters related to solution, and «в»- to distilled water. Taking into account that P = nkT, calculations of ratio of seawater and distilled water evaporation rates were made on the basis of equations (3) - (5) using data from Table 16.6. Calculation results are shown in Fig. 16.2. At the same, the figure shows the experimental data given Table 19.7.

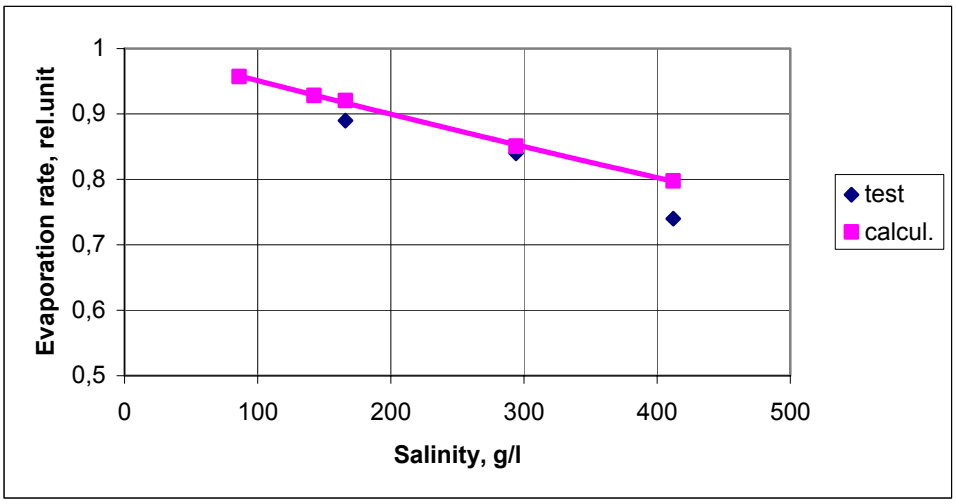

Fig. 16.2 Variation of Ratio of Aral Seawater and Distilled Water Evaporation Rates with Increasing Seawater Salinity

From the comparison of calculation results and experimental data it follows that at water salinity of above 80 g/l solution evaporation can be expressed by equation based on Raul's First Law with accuracy reaching up to 10%.

17. Forecast Options of the Aral Sea Development

Let us consider in sequence the results of each of water inflow options, bearing in mind that inside each of option three scenarios of water use in the basin (national, business as usual, and optimistic) will be considered for two hydrological series – minimal and maximal. In total, 18 particulars were considered and grouped into 3 inflow infrastructure options.

17.1 Maintaining Current Infrastructure in Amudarya Delta without Radical Reconstruction

According to this option – the least capital intensive, Eastern sea will keep lowering to maximum ↓ 28 in national water use scenario under low series of water availability. In case of optimistic scenario and maximum, in terms of water availability, series, the minimum water level in large sea will lower maximally to ↓ 29,5, but in all options the sea level stabilizes between ↓ 29 and ↓ 31. Moreover, water salinity will increase to 150 g/l in all the options by 2008, and then trendline will depend on water use scenarios and water availability – in the worst case salinity jumps to 300 g/l and further stabilizes within 200 g/l. In optimistic scenario, salinity will stabilize within 100 g/l by 2010 and then will decrease to 25 g/l in last five-year period 2020 … 2025. This is solely related to huge releases from Northern Sea (on average 7.3km3/yr, with maximum 12.8 km3/yr in five-year period 2021-2025). In scenarios of "national vision" and "business as usual" salinity will vary from 100 to 250 g/l under low water availability options.
In Western bowl, by 2020, water level will drop at different rates – to 17.5… 18.9BS during low water availability years under national and business as usual scenarios; will raise to 31.34BS in optimistic

scenario during last five years under high water availability and to 27 BS under low water availability (unlikely).
Salinity increases in all the options – to 102 g/l in best case and to 190 g/l in worst case.
Further, two options that start to work since 2006 are considered. Certainly, none of these options can be implemented in one year; therefore, the results should be considered as probable Aral Sea development alternative.

17.2 NATO SFP 974357 Project's Infrastructure in Amudarya Delta

Construction of infrastructure under this project will improve delta productivity and reduce socio-economic and environmental damage but will aggravate state of affair in Large Sea: Eastern sea level lowers to 27,5, Western sea level, to 27,6 in worst cases, while salinity reaches 370 g/l in Eastern sea, though it decreases to 90 … 106 g/l in optimistic scenarios. Better situation will be observed in Western bowl, where water salinity averages 65 … 75 g/l, and decreases to 53 g/l in optimistic scenario by 2025.

17.3 Hypothetical Option

Water supply to Western bowl is suggested through newly constructed system of waterways Amudarya – Sudochie – Adjibai bay. This system is completely focused on deeper reservoir. Eastern bowl is fed only through overflows from Western sea to Eastern sea, plus releases from Northern sea. In all options in Western bowl, water horizon is set within 29 … 31, with short-term minimum of 28 and maximum of 32,3. Eastern bowl is also stabilized at 26 … 27BS. Rise to 30BS in optimistic option should be considered as impossible. Such inflow will allow achieving stable trend towards salinity decrease in Western sea to 45 g/l $\pm$16 g/l by 2025.
However, salinity in Eastern bowl increases to 380 g/l, though under such high salinity, assumptions made in the model will become invalid and require detailed hydrochemical modeling of high-saturated solutions.
While considering report of CR-4 group on bioproductivity, it seems to be rather doubtful and impossible to implement the "hypothetical option" of water supply from the Amudarya to Western sea on such scale so that to achieve cost-effectiveness of Western sea preservation under environmentally active parameters – when salinity less than 20 g/l. This would require the following:

- adoption of optimistic scenario of water use in the basin;
- quite good natural water availability of hydrological series;
- rapid (5 – 6 years) implementation of water supply to Western sea;
- additional supply of collector-drainage water from Ozerny collector, with water pumping to GLK system and further to Sudochie;
- capital investments in an amount of 1,500 – 1,800 million USD.

Undoubtedly, there is one possibility to find such investments – attract funds of gas and oil companies that develop Prearalie, taking into account their interests in developing gas and oil reserves located under Eastern Aral Sea.
Under present conditions, main attention should be paid to establishment of sustainable bioproductivity in Amudarya and Syrdarya deltas according to earlier developed NATO Project.

REFERENCES

1. «Hydrochemistry of the Aral Sea». Blinov L.K., L. Gidrometeoizdat, 1956.
2. Water balance of the Aral Sea, Shultz V.L. //SarNIGMI Transactions – 1975– Issue 23.
3. Present and forecasted changes in hydrological, hydrochemical and hydrobiological conditions of the Aral Sea. Bortnik V.N., Journal "Water Resources", 1983, №5.
4. Salt composition of highly saline water in the Aral Sea. Bortnik V.N., Buynievich N.A., GOIN Transactions, issue 159, 1980, p. 85-93.
5. Aral Sea problem and environmental measures/V.A.Dukhovny, R.M.Rozakov, I.B.Ruziev, K.A.Kosnazarov//Problems of desert development.– 1984.– № 6.
6. Aral Sea Problems: Review and Decisions, Dukhovny V., Report of the Interstate Water Commission to ICID, Varna, 1994.
7. "Hydrometeorological problems in Prearalie zone". L. Gidrometeoizdat, 1990.
8. The Aral Sea basin problems. Annotated bibliography, IFAS, SIC ICWC, 1999, 226p.
9. The Aral Sea: Selected Bibliography. Noosphere, Moscow 2002y. 232pp.
10. SFP NATO № 974357 "Integrated Water Resources Management for Wetlands Restoration in the Aral Sea Basin", 2000.
11. "Sudochye Lake rehabilitation", project GEF, 2000.
12. INTAS/RFBR-1733 Project, Assessment of the social-economic damage under the influence of the Aral Sea Level lowering. SIC ICWC, Tashkent, 2000y.
13. Modeling water balance of the Aral Sea (multidimensional case). Meteorology and hydrology. Homeriki I.V.–1978 – № 9.– p. 70–80.
14. «Ion balance in Aral Sea' waters». Savenko V.S., Shirokov S.R. Journal "Water Resources", issue 3, M. 1982, p. 196-199.
15. Course of chemical kinetics. Emanuel N.M., Knorre D.G., M.: Vyschaya shkola, 1984. – 463 p.
16. Chemistry in action. Frimantle M. Two volumes. V. 1: transl. from English – M.: Mir, 1991. – 528p.
17. Hydrophysics – Vinnikov S.D., Proskuryakov B.V., L.: Gidrometizdat, 1988. – 248p.
18. Proceedings of the NATO Advanced Research Workshop on Dying and Dead Seas – Climatic Versus Anthropic Causes edited by Jacques C.J. Nihoul, Peter O. Zavialov and Philip P. Micklin. Liege, Belgium. 2003.
19. State water cadastre. Annual data on water quality and regime in sea and river mouths. 1978. Vol. II, issue 3
20. Comprehensive mathematical model of Aral Sea's hydrological regime. Kotov S.V. Transactions of Zoological Institute at the USSR Academy of Sciences, 1989, T. 199.
21. Numerical evaluations of future changes in parameters of Aral Sea's hydrological regime. Kotov S.V., Aripov S.L. Transactions of Zoological Institute at the USSR Academy of Sciences, 1989, T. 199.
22. Identification of hydraulics models \Edited by Artsimovich G.V.\-Novosibirsk: Nauka, 1980. - 160 p.
23. Issues of hydrodynamics and their mathematical models - Lavrentiev M.A., Shabat B.V., M.: Nauka, 1973. - 416 p.
24. Atmosphere and ocean dynamics. - Ghill A., M.: Mir, 1986.- v.1. 397 p.
25. Atmosphere and ocean dynamics. - Ghill A., M.: Mir, 1986.- v.2. 415p.
26. Self-purification and diffusion in inland reservoirs. USSR Academy of Sciences, Nauka, Novosibirsk 1980. -189 p.
27. Statistical physics, L.D.Landau, Ye.M.Lifshits.V.1, Theoretical physics v.V, M, Nauka 1978 – 583p.
28. Reference manual for hydrologist. Volume1/edited by V.M.Maksimov, L.:."Nedra", 1967.
29. Tables of physical and chemical constants. J.Kei, T.Labi. M.: State publishing house of physical and mathematical literature, 1962.
30. Multidisciplinary marine environmental database for the Aral Sea V.G. Lyubartsev, V.L. Vladymyrov and V.V. Myroshnychenko. Journal of Marine systems. Special Issue: The Dying Aral Sea edited by A.Kostyanov and W.Wiseman June 2004.
31. The recent evolution of the Aral Sea level and water properties: analysis of satellite, gauge and hydromctcorological data E.L. Peneva, E.V. Stanev, S.V Stanychni, A. Salokhiddinov and G. Stulina. Special Issue: The Dying Aral Sea edited by A.Kostyanov and W.Wiseman June 2004.
32. Long-term variability of air temperature in the Aral sea region V.M. Khan, R.M. Vilfand and P.O. Zavialov. Special Issue: The Dying Aral Sea edited by A.Kostyanov and W.Wiseman June 2004.
33. A dynamic model of the Aral Sea water and salt balance F.Benduhn and P. Renard. Special Issue: The Dying Aral Sea edited by A.Kostyanov and W.Wiseman June 2004.
34. Influence of the Aral Sea negative water balance on its seasonal circulation patterns: use of a 3D hydrodynamic model D.Sirjacobs, M. Gregoirc, E. Delhez and J.C.J. Nihoul. Special Issue: The Dying Aral Sea edited by A.Kostyanov and W.Wiseman June 2004.

35. Interannual variations of the discharge of Amu Darya and Syr Darya estimated from global atmospheric precipitation N-P, Nezlin, A.G. Kostianoy and S.A. Lebedev. Special Issue: The Dying Aral Sea edited by A.Kostyanov and W.Wiseman June 2004.
36. Hydrochemical properties of the Aral Sea water in summer 2002 J. Friedrich and H. Oberhansii
37. Sea ice cover in the Caspian and Aral Seas from historical and satellite data A.V. Kouraev, F. Papa, N.M. Mognard. P.I. Buharizin, A. Cazenave, J.-F. Cretaux, .1. Dozortseva and F. Remy
38. Succession of the ecosystems of the Aral Sea during its transition from oligohaline to polyhaline water body. I.M. Mirabdullayev, J.M. Joldasova, Z.A. Mustafaeva. S. Kazakhbaev, S.A. Lyubimova and B.A. Tashmukhamedov
39. Groundwater discharge into the Aral Sea after 1 %. J. Jarsjo and G. Destouni
40. The change in soil cover on the exposed bed of the Aral Sea G.Stulma and V. Sektimcnko
41. Ways the Aral Sea behaves A.T Salokhiddinnov and Z.M. Khakimov
42. Analysis of water resources variability of the Caspian and Aral sea basins on the basis of solar aetivity E.Shcrmatov, B. Nurtayev. U. Muhamedgalicva and U. Shermatov
43. The share of a glacial feeding in water balance of Aral Sea and Karakul Lake A. Ni, B. Nurtayev, M. Petrov, A. Tikhanovskaya and I. Tomashevskaya
44. Southern Prearalie-new prospects/Edited by Prof. V.A.Dukhovny and Eng. Y.de Schutter, Tashkent, 2003.
45. Calculation of salt sedimentation in Aral Sea waters under conditions of its progressive drying. Bortnik V.N. in book “Studying man impact on hydrological regime of water reservoirs. Transactions of Kazakh regional hydrometeorological research institute, issue101. M.:Gidrometeoizdat, pp.115-119,

ANNEX I

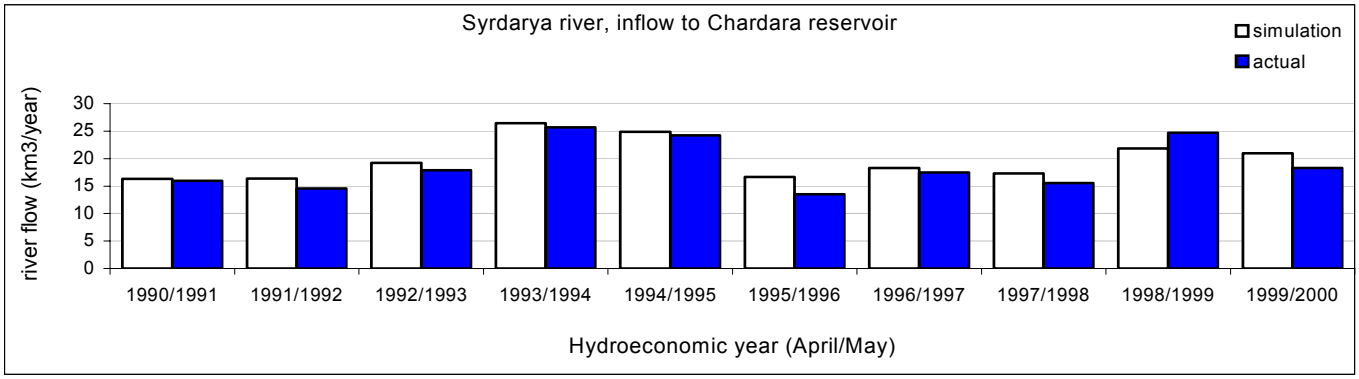
Syrdarya river, inflow to Chardara reservoir
simulation
actual
river flow (km3/year)
30
25
20
15
10
5
0
1990/1991
1991/1992
1992/1993
1993/1994
1994/1995
1995/1996
1996/1997
1997/1998
1998/1999
1999/2000
Hydroeconomic year (April/May)

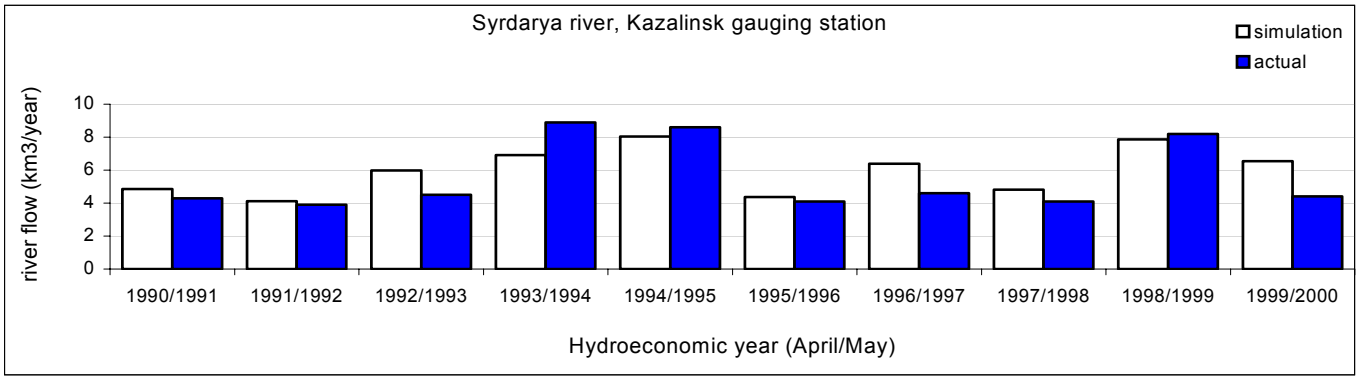
Syrdarya river, Kazalinsk gauging station
simulation
actual
river flow (km3/year)
10
8
6
4
2
0
1990/1991
1991/1992
1992/1993
1993/1994
1994/1995
1995/1996
1996/1997
1997/1998
1998/1999
1999/2000
Hydroeconomic year (April/May)

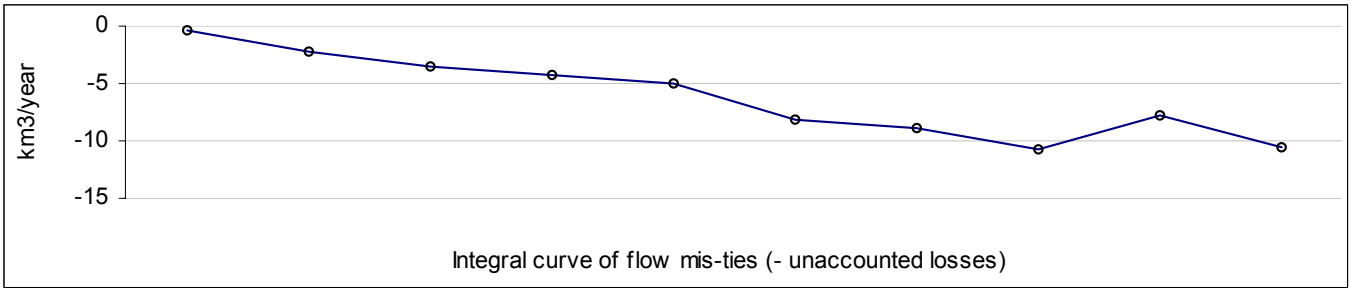
km3/year
0
-5
-10
-15
Integral curve of flow mis-ties (- unaccounted losses)

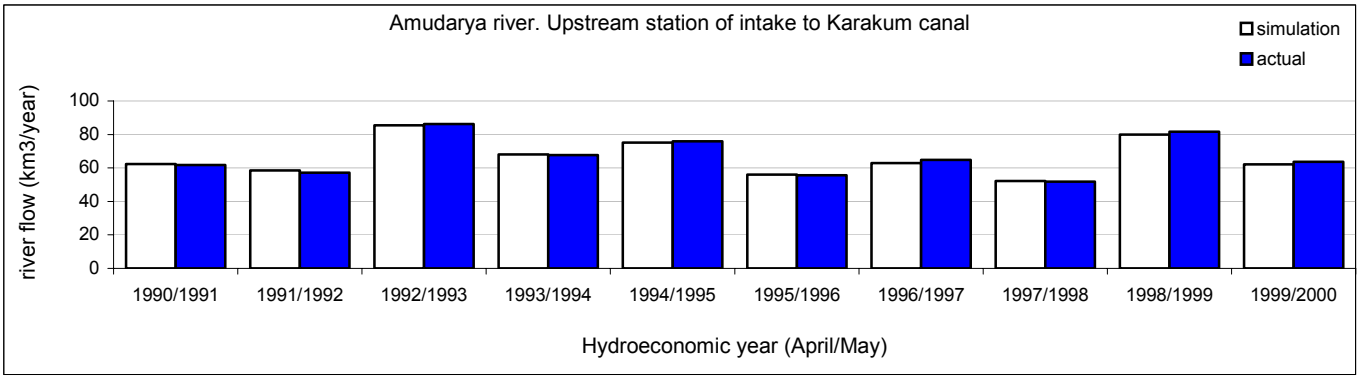
Amudarya river. Upstream station of intake to Karakum canal
simulation
actual
river flow (km3/year)
100
80
60
40
20
0
1990/1991
1991/1992
1992/1993
1993/1994
1994/1995
1995/1996
1996/1997
1997/1998
1998/1999
1999/2000
Hydroeconomic year (April/May)

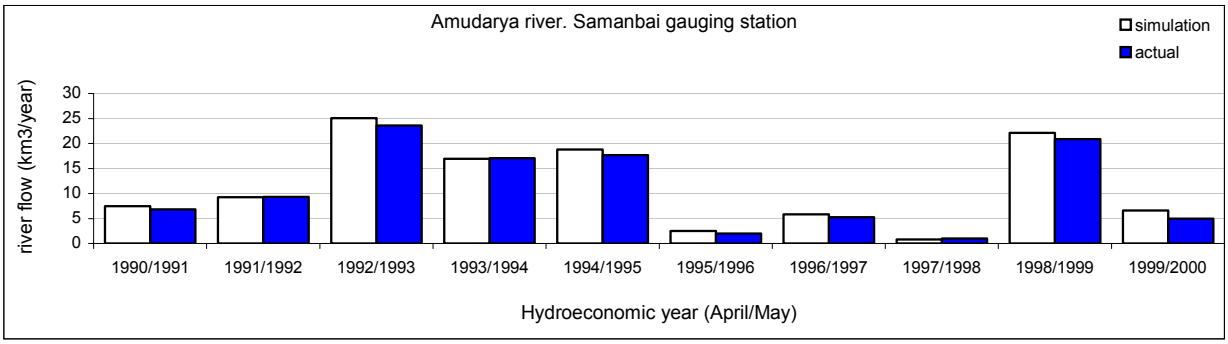
Amudarya river. Samanbai gauging station
simulation
actual
river flow (km3/year)
30
25
20
15
10
5
0
1990/1991
1991/1992
1992/1993
1993/1994
1994/1995
1995/1996
1996/1997
1997/1998
1998/1999
1999/2000
Hydroeconomic year (April/May)

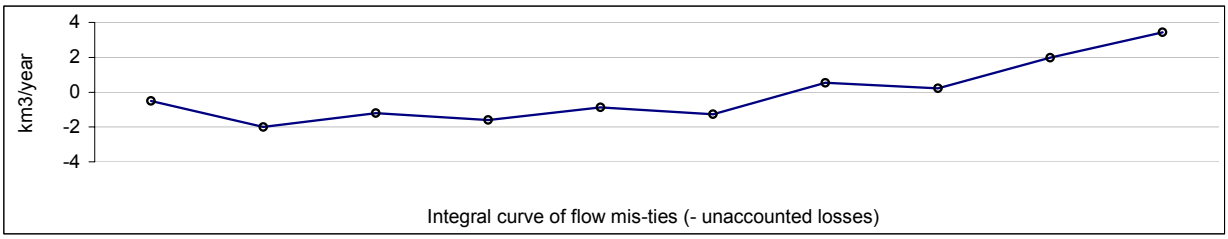
km3/year
4
2
0
-2
-4
Integral curve of flow mis-ties (- unaccounted losses)

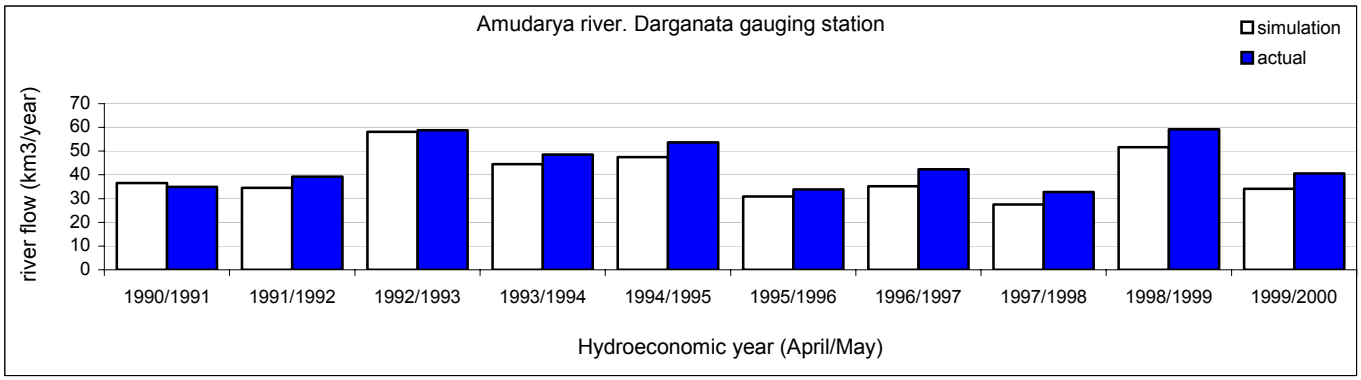
Amudarya river. Darganata gauging station
simulation
actual
river flow (km3/year)
70
60
50
40
30
20
10
0
1990/1991
1991/1992
1992/1993
1993/1994
1994/1995
1995/1996
1996/1997
1997/1998
1998/1999
1999/2000
Hydroeconomic year (April/May)

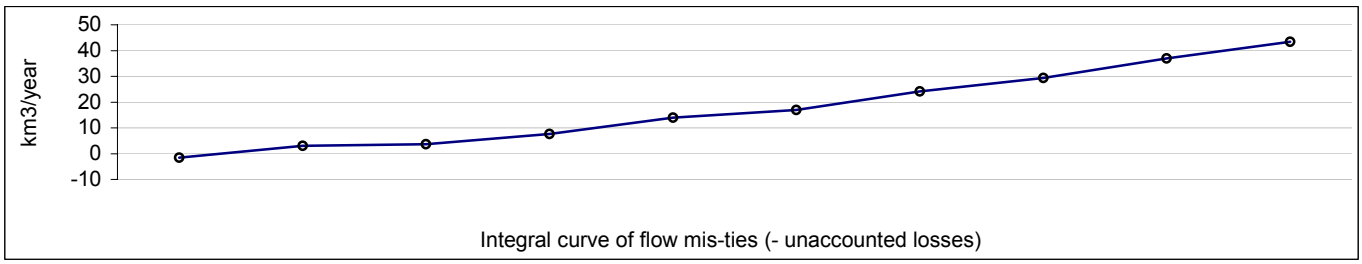
km3/year
50
40
30
20
10
0
-10
Integral curve of flow mis-ties (- unaccounted losses)

Рис 3.1 Сравнение расчетных и измеренных уровней Северного Моря

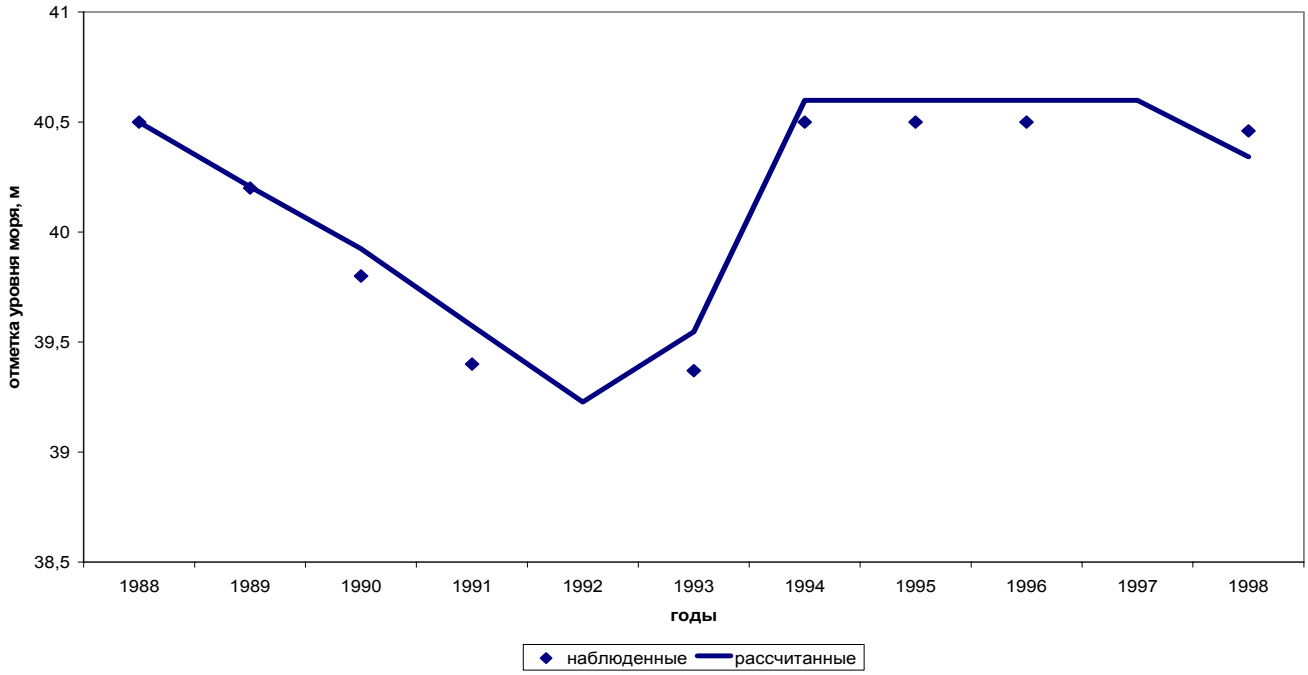

Площадь Северного Моря

Сравнение расчетной и измеренной минерализации воды Северного моря

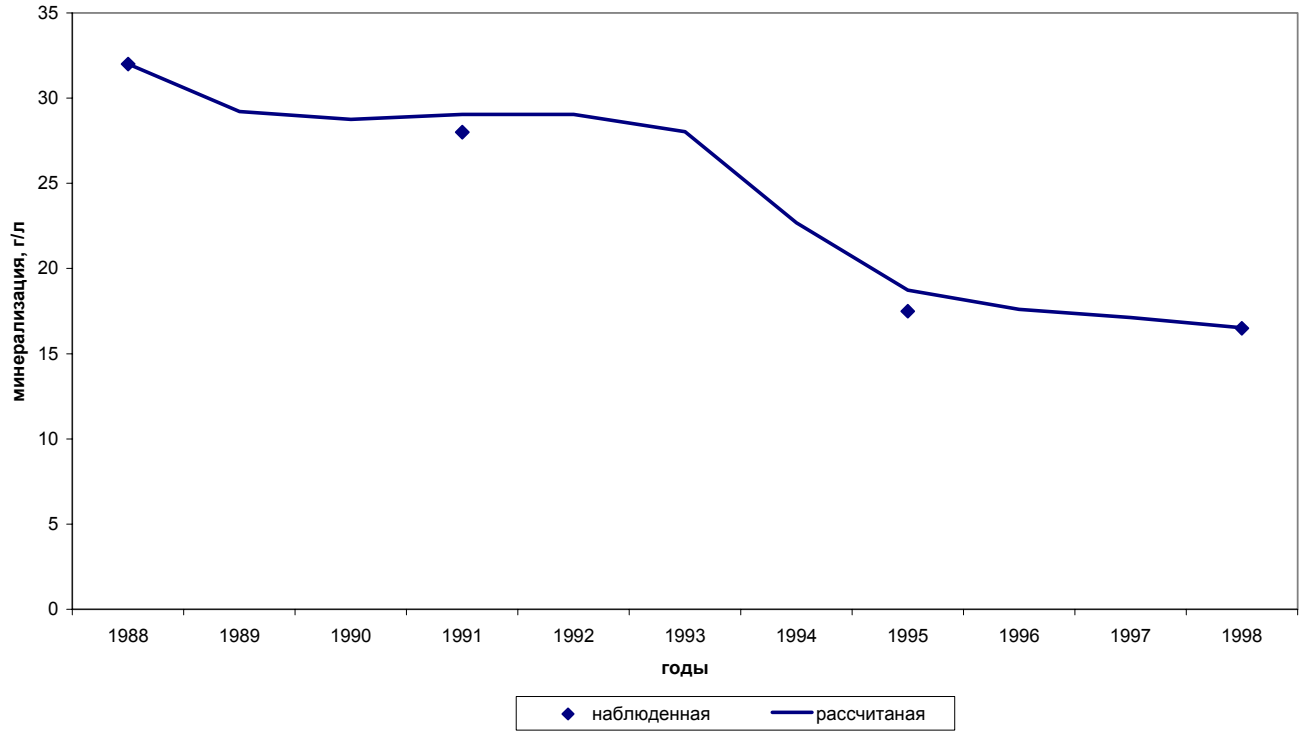

ANNEX II

Current infrastructure in Amudarya river delta. Runoff volume. National vision (maximum).

	OCT	NOV	DEC	JAN	FEB	MAR	APR	MAY	JUN	JUL	AUG	SEP	TMG	TVG	Total
1990	0.19	0.13	0.12	0.12	0.15	0.14	0.21	0.37	1.01	1.13	0.61	0.77	0.84	4.09	4.94
1991	1.43	0.67	0.62	1.08	0.51	0.53	0.33	0.60	1.22	1.16	0.88	1.18	4.83	5.36	10.19
1992	1.62	0.74	0.64	1.14	0.53	0.61	0.38	3.14	4.79	5.11	3.68	2.08	5.29	19.18	24.47
1993	1.77	0.80	0.67	1.17	0.57	0.69	0.81	1.03	2.23	4.07	1.48	1.38	5.66	11.00	16.66
1994	1.91	0.86	0.78	1.26	0.69	0.85	1.00	0.85	1.67	4.47	2.51	1.88	6.34	12.37	18.72
1995	1.73	0.79	0.66	1.16	0.55	0.67	0.09	0.10	0.11	0.12	0.12	0.16	5.57	0.70	6.26
1996	0.20	0.14	0.13	0.13	0.16	0.14	0.17	0.26	0.84	0.96	0.38	0.53	0.90	3.14	4.04
1997	0.38	0.24	0.25	0.26	0.24	0.23	0.04	0.04	0.04	0.04	0.04	0.05	1.60	0.26	1.86
1998	0.14	0.09	0.09	0.09	0.11	0.10	0.30	2.94	4.83	4.52	3.35	1.76	0.60	17.69	18.29
1999	1.03	0.51	0.53	0.65	0.38	0.37	0.15	0.16	0.26	0.30	0.24	0.36	3.46	1.45	4.91
2000	0.70	0.39	0.45	0.51	0.32	0.29	0.03	0.04	0.04	0.04	0.04	0.05	2.66	0.22	2.88
2001	0.01	0.01	0.01	0.01	0.01	0.01	0.01	0.01	0.01	0.01	0.01	0.01	0.04	0.05	0.09
2002	0.01	0.01	0.01	0.01	0.01	0.01	0.15	0.20	0.67	0.78	0.32	0.48	0.05	2.60	2.65
2003	0.45	0.27	0.30	0.32	0.26	0.25	0.63	1.66	2.39	2.55	0.60	0.74	1.85	8.57	10.42
2004	0.29	0.19	0.19	0.20	0.21	0.20	0.18	0.28	0.88	1.01	0.41	0.56	1.27	3.32	4.59
2005	0.28	0.18	0.18	0.19	0.20	0.19	0.86	1.00	2.11	4.26	1.64	1.44	1.22	11.32	12.55
2006	0.63	0.36	0.41	0.46	0.31	0.28	0.17	0.27	0.86	0.99	0.39	0.54	2.45	3.22	5.67
2007	0.87	0.45	0.49	0.58	0.35	0.33	1.02	0.85	1.66	4.50	2.64	1.95	3.07	12.62	15.69
2008	0.37	0.23	0.25	0.26	0.24	0.23	0.16	0.16	0.32	0.37	0.26	0.40	1.57	1.67	3.24
2009	1.93	0.88	0.81	1.29	0.72	0.88	0.12	0.12	0.15	0.17	0.16	0.22	6.51	0.93	7.44
2010	1.68	0.77	0.65	1.15	0.54	0.64	0.16	0.17	0.41	0.48	0.29	0.43	5.44	1.94	7.38
2011	0.86	0.45	0.49	0.58	0.35	0.33	0.86	1.00	2.13	4.25	1.62	1.44	3.04	11.29	14.33
2012	0.45	0.28	0.30	0.32	0.26	0.25	0.74	1.14	2.32	3.60	1.25	1.25	1.86	10.30	12.16
2013	0.80	0.43	0.48	0.56	0.34	0.32	0.16	0.18	0.42	0.49	0.29	0.44	2.92	1.97	4.89
2014	1.30	0.62	0.60	0.95	0.47	0.47	0.03	0.03	0.03	0.03	0.03	0.04	4.41	0.20	4.61
2015	0.39	0.24	0.26	0.27	0.25	0.23	0.04	0.04	0.04	0.04	0.04	0.05	1.65	0.24	1.89
2016	0.05	0.03	0.03	0.03	0.03	0.03	0.15	0.19	0.57	0.66	0.30	0.46	0.20	2.34	2.54
2017	0.46	0.28	0.31	0.33	0.27	0.25	0.03	0.03	0.03	0.03	0.03	0.04	1.90	0.18	2.08
2018	1.67	0.76	0.65	1.15	0.54	0.64	0.03	0.04	0.04	0.04	0.03	0.05	5.40	0.22	5.62
2019	1.11	0.54	0.55	0.70	0.39	0.40	0.03	0.04	0.04	0.03	0.03	0.04	3.68	0.21	3.89
2020	1.35	0.64	0.61	1.01	0.49	0.49	0.16	0.23	0.77	0.89	0.35	0.50	4.59	2.91	7.50
2021	1.79	0.82	0.68	1.17	0.58	0.71	0.05	0.06	0.06	0.06	0.06	0.08	5.75	0.38	6.13
2022	1.97	0.89	0.85	1.33	0.75	0.91	0.72	1.25	2.34	3.36	1.13	1.15	6.69	9.95	16.64
2023	2.49	1.19	1.14	1.70	1.00	1.14	0.03	0.04	0.04	0.04	0.04	0.05	8.65	0.23	8.88
2024	2.71	1.33	1.26	1.85	1.11	1.24	0.03	0.04	0.04	0.04	0.03	0.05	9.50	0.22	9.72
2025	0.06	0.04	0.04	0.04	0.04	0.04	0.02	0.03	0.03	0.02	0.02	0.03	0.25	0.15	0.40

Current infrastructure in Amudarya river delta. Runoff volume. Business as usual (maximum).

	OCT	NOV	DEC	JAN	FEB	MAR	APR	MAY	JUN	JUL	AUG	SEP	TMG	TVG	Total
1990	0.19	0.13	0.12	0.12	0.15	0.14	0.21	0.37	1.01	1.13	0.61	0.77	0.84	4.09	4.94
1991	1.43	0.67	0.62	1.08	0.51	0.53	0.33	0.60	1.22	1.16	0.88	1.18	4.83	5.36	10.19
1992	1.62	0.74	0.64	1.14	0.53	0.61	0.38	3.14	4.79	5.11	3.68	2.08	5.29	19.18	24.47
1993	1.77	0.80	0.67	1.17	0.57	0.69	0.81	1.03	2.23	4.07	1.48	1.38	5.66	11.00	16.66
1994	1.91	0.86	0.78	1.26	0.69	0.85	1.00	0.85	1.67	4.47	2.51	1.88	6.34	12.37	18.72
1995	1.73	0.79	0.66	1.16	0.55	0.67	0.09	0.10	0.11	0.12	0.12	0.16	5.57	0.70	6.26
1996	0.20	0.14	0.13	0.13	0.16	0.14	0.17	0.26	0.84	0.96	0.38	0.53	0.90	3.14	4.04
1997	0.38	0.24	0.25	0.26	0.24	0.23	0.04	0.04	0.04	0.04	0.04	0.05	1.60	0.26	1.86
1998	0.14	0.09	0.09	0.09	0.11	0.10	0.30	2.94	4.83	4.52	3.35	1.76	0.60	17.69	18.29
1999	1.03	0.51	0.53	0.65	0.38	0.37	0.15	0.16	0.26	0.30	0.24	0.36	3.46	1.45	4.91
2000	0.70	0.39	0.45	0.51	0.32	0.29	0.03	0.04	0.04	0.04	0.04	0.05	2.66	0.22	2.88
2001	0.01	0.01	0.01	0.01	0.01	0.01	0.01	0.01	0.01	0.01	0.01	0.01	0.04	0.05	0.09
2002	0.01	0.01	0.01	0.01	0.01	0.01	0.15	0.20	0.67	0.78	0.32	0.48	0.05	2.60	2.65
2003	0.45	0.27	0.30	0.32	0.26	0.25	0.63	1.66	2.39	2.55	0.60	0.74	1.85	8.57	10.42
2004	0.29	0.19	0.19	0.20	0.21	0.20	0.18	0.28	0.88	1.01	0.41	0.56	1.27	3.32	4.59
2005	0.28	0.18	0.18	0.19	0.20	0.19	0.86	1.00	2.11	4.26	1.64	1.44	1.22	11.32	12.55
2006	0.63	0.36	0.41	0.46	0.31	0.28	0.17	0.27	0.86	0.99	0.39	0.54	2.45	3.22	5.67
2007	1.01	0.50	0.52	0.64	0.37	0.37	0.97	1.39	2.53	4.70	2.72	2.04	3.40	14.35	17.75
2008	0.46	0.28	0.31	0.33	0.27	0.25	0.16	0.17	0.34	0.39	0.27	0.41	1.88	1.73	3.61
2009	1.76	0.80	0.67	1.17	0.56	0.69	0.29	0.53	1.16	1.15	0.82	1.08	5.64	5.02	10.66
2010	0.18	0.12	0.11	0.11	0.14	0.13	0.16	0.16	0.30	0.35	0.26	0.39	0.79	1.61	2.40
2011	0.65	0.37	0.42	0.48	0.31	0.28	0.98	1.33	2.44	4.70	2.72	2.05	2.51	14.21	16.72
2012	1.60	0.74	0.64	1.14	0.53	0.61	0.62	1.60	2.32	2.45	0.60	0.74	5.25	8.33	13.58
2013	0.59	0.34	0.39	0.43	0.30	0.27	0.40	0.73	1.39	1.34	0.94	1.27	2.33	6.06	8.39
2014	0.20	0.14	0.13	0.13	0.16	0.14	0.15	0.16	0.27	0.31	0.25	0.37	0.90	1.50	2.40
2015	0.19	0.13	0.12	0.12	0.15	0.14	0.15	0.16	0.28	0.33	0.25	0.38	0.85	1.55	2.40
2016	0.18	0.12	0.12	0.12	0.14	0.13	0.16	0.17	0.32	0.38	0.27	0.40	0.80	1.69	2.49
2017	1.11	0.54	0.55	0.70	0.39	0.40	0.15	0.16	0.30	0.35	0.26	0.39	3.68	1.60	5.28
2018	0.53	0.32	0.36	0.39	0.29	0.26	0.16	0.16	0.31	0.36	0.26	0.39	2.15	1.63	3.78
2019	0.99	0.49	0.52	0.63	0.37	0.36	0.16	0.16	0.30	0.35	0.26	0.39	3.36	1.62	4.98
2020	1.17	0.56	0.56	0.77	0.42	0.42	0.19	0.32	0.96	1.08	0.49	0.64	3.90	3.67	7.57
2021	1.83	0.83	0.70	1.19	0.60	0.75	0.17	0.25	0.82	0.94	0.37	0.52	5.89	3.06	8.95
2022	1.88	0.85	0.75	1.23	0.65	0.81	0.57	2.32	3.92	4.50	2.98	1.86	6.17	16.14	22.31
2023	1.92	0.87	0.80	1.28	0.71	0.87	0.32	0.58	1.20	1.15	0.86	1.15	6.46	5.27	11.73
2024	0.18	0.12	0.12	0.12	0.14	0.13	0.15	0.16	0.30	0.35	0.26	0.39	0.80	1.60	2.40
2025	0.18	0.12	0.12	0.12	0.14	0.13	0.15	0.16	0.30	0.35	0.26	0.39	0.80	1.60	2.40

Current infrastructure in Amudarya river delta. Runoff volume. Optimistic scenario (maximum).

	OCT	NOV	DEC	JAN	FEB	MAR	APR	MAY	JUN	JUL	AUG	SEP	TMG	TVG	Total
1990	0.19	0.13	0.12	0.12	0.15	0.14	0.21	0.37	1.01	1.13	0.61	0.77	0.84	4.09	4.94
1991	1.43	0.67	0.62	1.08	0.51	0.53	0.33	0.60	1.22	1.16	0.88	1.18	4.83	5.36	10.19
1992	1.62	0.74	0.64	1.14	0.53	0.61	0.38	3.14	4.79	5.11	3.68	2.08	5.29	19.18	24.47
1993	1.77	0.80	0.67	1.17	0.57	0.69	0.81	1.03	2.23	4.07	1.48	1.38	5.66	11.00	16.66
1994	1.91	0.86	0.78	1.26	0.69	0.85	1.00	0.85	1.67	4.47	2.51	1.88	6.34	12.37	18.72
1995	1.73	0.79	0.66	1.16	0.55	0.67	0.09	0.10	0.11	0.12	0.12	0.16	5.57	0.70	6.26
1996	0.20	0.14	0.13	0.13	0.16	0.14	0.17	0.26	0.84	0.96	0.38	0.53	0.90	3.14	4.04
1997	0.38	0.24	0.25	0.26	0.24	0.23	0.04	0.04	0.04	0.04	0.04	0.05	1.60	0.26	1.86
1998	0.14	0.09	0.09	0.09	0.11	0.10	0.30	2.94	4.83	4.52	3.35	1.76	0.60	17.69	18.29
1999	1.03	0.51	0.53	0.65	0.38	0.37	0.15	0.16	0.26	0.30	0.24	0.36	3.46	1.45	4.91
2000	0.70	0.39	0.45	0.51	0.32	0.29	0.03	0.04	0.04	0.04	0.04	0.05	2.66	0.22	2.88
2001	0.01	0.01	0.01	0.01	0.01	0.01	0.01	0.01	0.01	0.01	0.01	0.01	0.04	0.05	0.09
2002	0.01	0.01	0.01	0.01	0.01	0.01	0.15	0.20	0.67	0.78	0.32	0.48	0.05	2.60	2.65
2003	0.45	0.27	0.30	0.32	0.26	0.25	0.63	1.66	2.39	2.55	0.60	0.74	1.85	8.57	10.42
2004	0.29	0.19	0.19	0.20	0.21	0.20	0.18	0.28	0.88	1.01	0.41	0.56	1.27	3.32	4.59
2005	0.28	0.18	0.18	0.19	0.20	0.19	0.86	1.00	2.11	4.26	1.64	1.44	1.22	11.32	12.55
2006	0.63	0.36	0.41	0.46	0.31	0.28	0.17	0.27	0.86	0.99	0.39	0.54	2.45	3.22	5.67
2007	1.08	0.53	0.54	0.68	0.39	0.39	1.01	0.85	1.65	4.48	2.58	1.92	3.60	12.48	16.08
2008	0.86	0.45	0.49	0.58	0.35	0.33	0.16	0.21	0.71	0.83	0.33	0.49	3.04	2.72	5.76
2009	0.38	0.24	0.25	0.26	0.24	0.23	0.69	1.48	2.40	3.01	0.89	0.97	1.60	9.44	11.04
2010	0.39	0.24	0.26	0.27	0.25	0.23	0.15	0.16	0.29	0.34	0.25	0.38	1.65	1.58	3.23
2011	1.75	0.80	0.66	1.16	0.56	0.68	0.77	1.07	2.30	3.83	1.36	1.31	5.61	10.64	16.25
2012	2.19	1.01	0.98	1.49	0.86	1.02	0.58	1.44	2.15	2.27	0.66	0.83	7.55	7.93	15.48
2013	0.49	0.29	0.33	0.35	0.27	0.26	0.40	0.73	1.39	1.34	0.94	1.27	1.99	6.06	8.05
2014	0.40	0.25	0.26	0.27	0.25	0.24	0.15	0.16	0.28	0.33	0.25	0.37	1.66	1.54	3.20
2015	0.38	0.24	0.25	0.26	0.24	0.23	0.31	0.56	1.18	1.15	0.84	1.11	1.60	5.13	6.73
2016	0.37	0.23	0.24	0.25	0.24	0.23	0.28	0.51	1.14	1.15	0.79	1.04	1.55	4.91	6.46
2017	1.53	0.71	0.63	1.12	0.52	0.57	0.34	0.63	1.25	1.17	0.89	1.21	5.08	5.49	10.57
2018	0.38	0.24	0.25	0.26	0.24	0.23	0.33	0.60	1.22	1.16	0.88	1.18	1.61	5.36	6.97
2019	0.96	0.48	0.51	0.61	0.36	0.35	0.38	0.70	1.35	1.28	0.93	1.26	3.28	5.91	9.19
2020	1.14	0.55	0.55	0.73	0.40	0.41	0.32	0.58	1.20	1.15	0.86	1.15	3.78	5.26	9.04
2021	2.09	0.96	0.92	1.43	0.82	0.98	1.02	0.85	1.65	4.50	2.63	1.95	7.19	12.59	19.78
2022	1.47	0.69	0.62	1.10	0.51	0.54	1.24	3.60	5.99	7.16	4.46	3.44	4.93	25.88	30.81
2023	2.29	1.07	1.03	1.56	0.91	1.06	0.92	0.95	1.93	4.40	1.94	1.58	7.92	11.72	19.64
2024	0.91	0.47	0.50	0.60	0.35	0.34	0.54	1.25	1.97	2.08	0.75	0.96	3.17	7.55	10.72
2025	0.79	0.43	0.47	0.55	0.34	0.31	0.35	0.64	1.27	1.19	0.91	1.23	2.89	5.59	8.48

Current infrastructure in Amudarya river delta. Runoff volume. National vision (minimum).

	OCT	NOV	DEC	JAN	FEB	MAR	APR	MAY	JUN	JUL	AUG	SEP	TMG	TVG	Total
1990	0.19	0.13	0.12	0.12	0.15	0.14	0.21	0.37	1.01	1.13	0.61	0.77	0.84	4.09	4.94
1991	1.43	0.67	0.62	1.08	0.51	0.53	0.33	0.60	1.22	1.16	0.88	1.18	4.83	5.36	10.19
1992	1.62	0.74	0.64	1.14	0.53	0.61	0.38	3.14	4.79	5.11	3.68	2.08	5.29	19.18	24.47
1993	1.77	0.80	0.67	1.17	0.57	0.69	0.81	1.03	2.23	4.07	1.48	1.38	5.66	11.00	16.66
1994	1.91	0.86	0.78	1.26	0.69	0.85	1.00	0.85	1.67	4.47	2.51	1.88	6.34	12.37	18.72
1995	1.73	0.79	0.66	1.16	0.55	0.67	0.09	0.10	0.11	0.12	0.12	0.16	5.57	0.70	6.26
1996	0.20	0.14	0.13	0.13	0.16	0.14	0.17	0.26	0.84	0.96	0.38	0.53	0.90	3.14	4.04
1997	0.38	0.24	0.25	0.26	0.24	0.23	0.04	0.04	0.04	0.04	0.04	0.05	1.60	0.26	1.86
1998	0.14	0.09	0.09	0.09	0.11	0.10	0.30	2.94	4.83	4.52	3.35	1.76	0.60	17.69	18.29
1999	1.03	0.51	0.53	0.65	0.38	0.37	0.15	0.16	0.26	0.30	0.24	0.36	3.46	1.45	4.91
2000	0.70	0.39	0.45	0.51	0.32	0.29	0.03	0.04	0.04	0.04	0.04	0.05	2.66	0.22	2.88
2001	0.01	0.01	0.01	0.01	0.01	0.01	0.01	0.01	0.01	0.01	0.01	0.01	0.04	0.05	0.09
2002	0.01	0.01	0.01	0.01	0.01	0.01	0.15	0.20	0.67	0.78	0.32	0.48	0.05	2.60	2.65
2003	0.45	0.27	0.30	0.32	0.26	0.25	0.63	1.66	2.39	2.55	0.60	0.74	1.85	8.57	10.42
2004	0.29	0.19	0.19	0.20	0.21	0.20	0.18	0.28	0.88	1.01	0.41	0.56	1.27	3.32	4.59
2005	0.28	0.18	0.18	0.19	0.20	0.19	0.86	1.00	2.11	4.26	1.64	1.44	1.22	11.32	12.55
2006	0.63	0.36	0.41	0.46	0.31	0.28	0.17	0.27	0.86	0.99	0.39	0.54	2.45	3.22	5.67
2007	0.19	0.13	0.12	0.12	0.15	0.14	0.03	0.03	0.03	0.03	0.03	0.04	0.85	0.20	1.05
2008	0.06	0.04	0.04	0.04	0.04	0.04	0.10	0.11	0.12	0.13	0.12	0.17	0.25	0.74	0.99
2009	0.63	0.36	0.42	0.47	0.31	0.28	0.03	0.03	0.03	0.03	0.03	0.04	2.47	0.18	2.65
2010	1.08	0.53	0.54	0.68	0.39	0.39	0.04	0.04	0.04	0.04	0.04	0.05	3.60	0.26	3.86
2011	1.82	0.83	0.70	1.19	0.60	0.74	0.82	1.02	2.21	4.12	1.51	1.39	5.87	11.08	16.95
2012	0.16	0.11	0.10	0.10	0.13	0.12	0.90	0.97	2.00	4.37	1.81	1.52	0.72	11.57	12.29
2013	0.07	0.05	0.05	0.05	0.06	0.05	0.18	0.28	0.88	1.01	0.41	0.56	0.32	3.32	3.64
2014	1.42	0.67	0.62	1.07	0.50	0.52	0.03	0.04	0.04	0.04	0.04	0.05	4.80	0.23	5.03
2015	0.63	0.36	0.41	0.46	0.31	0.28	0.03	0.03	0.03	0.03	0.03	0.04	2.45	0.20	2.65
2016	0.58	0.34	0.39	0.43	0.30	0.27	0.16	0.18	0.52	0.61	0.30	0.45	2.31	2.22	4.53
2017	0.55	0.33	0.37	0.41	0.29	0.27	0.15	0.20	0.63	0.73	0.31	0.47	2.21	2.49	4.70
2018	1.85	0.84	0.72	1.21	0.62	0.77	0.03	0.04	0.04	0.04	0.03	0.05	6.01	0.22	6.23
2019	1.25	0.60	0.58	0.87	0.45	0.45	0.03	0.04	0.04	0.03	0.03	0.04	4.20	0.21	4.41
2020	0.15	0.10	0.10	0.10	0.12	0.11	0.69	1.47	2.40	3.03	0.90	0.98	0.68	9.46	10.14
2021	0.06	0.04	0.04	0.04	0.05	0.05	0.68	1.57	2.43	2.87	0.78	0.88	0.28	9.20	9.48
2022	0.03	0.02	0.02	0.02	0.03	0.02	0.04	0.04	0.04	0.04	0.04	0.05	0.15	0.25	0.40
2023	0.58	0.34	0.39	0.43	0.30	0.27	0.04	0.04	0.04	0.04	0.04	0.05	2.30	0.26	2.56
2024	0.43	0.26	0.29	0.30	0.26	0.24	0.03	0.03	0.03	0.03	0.03	0.04	1.77	0.20	1.97
2025	0.53	0.32	0.36	0.39	0.29	0.26	0.65	1.66	2.42	2.62	0.62	0.75	2.15	8.73	10.88

Current infrastructure in Amudarya river delta. Runoff volume. Business as usual (minimum).

	OCT	NOV	DEC	JAN	FEB	MAR	APR	MAY	JUN	JUL	AUG	SEP	TMG	TVG	Total
1990	0.19	0.13	0.12	0.12	0.15	0.14	0.21	0.37	1.01	1.13	0.61	0.77	0.84	4.09	4.94
1991	1.43	0.67	0.62	1.08	0.51	0.53	0.33	0.60	1.22	1.16	0.88	1.18	4.83	5.36	10.19
1992	1.62	0.74	0.64	1.14	0.53	0.61	0.38	3.14	4.79	5.11	3.68	2.08	5.29	19.18	24.47
1993	1.77	0.80	0.67	1.17	0.57	0.69	0.81	1.03	2.23	4.07	1.48	1.38	5.66	11.00	16.66
1994	1.91	0.86	0.78	1.26	0.69	0.85	1.00	0.85	1.67	4.47	2.51	1.88	6.34	12.37	18.72
1995	1.73	0.79	0.66	1.16	0.55	0.67	0.09	0.10	0.11	0.12	0.12	0.16	5.57	0.70	6.26
1996	0.20	0.14	0.13	0.13	0.16	0.14	0.17	0.26	0.84	0.96	0.38	0.53	0.90	3.14	4.04
1997	0.38	0.24	0.25	0.26	0.24	0.23	0.04	0.04	0.04	0.04	0.04	0.05	1.60	0.26	1.86
1998	0.14	0.09	0.09	0.09	0.11	0.10	0.30	2.94	4.83	4.52	3.35	1.76	0.60	17.69	18.29
1999	1.03	0.51	0.53	0.65	0.38	0.37	0.15	0.16	0.26	0.30	0.24	0.36	3.46	1.45	4.91
2000	0.70	0.39	0.45	0.51	0.32	0.29	0.03	0.04	0.04	0.04	0.04	0.05	2.66	0.22	2.88
2001	0.01	0.01	0.01	0.01	0.01	0.01	0.01	0.01	0.01	0.01	0.01	0.01	0.04	0.05	0.09
2002	0.01	0.01	0.01	0.01	0.01	0.01	0.15	0.20	0.67	0.78	0.32	0.48	0.05	2.60	2.65
2003	0.45	0.27	0.30	0.32	0.26	0.25	0.63	1.66	2.39	2.55	0.60	0.74	1.85	8.57	10.42
2004	0.29	0.19	0.19	0.20	0.21	0.20	0.18	0.28	0.88	1.01	0.41	0.56	1.27	3.32	4.59
2005	0.28	0.18	0.18	0.19	0.20	0.19	0.86	1.00	2.11	4.26	1.64	1.44	1.22	11.32	12.55
2006	0.63	0.36	0.41	0.46	0.31	0.28	0.17	0.27	0.86	0.99	0.39	0.54	2.45	3.22	5.67
2007	0.18	0.12	0.12	0.12	0.14	0.13	0.15	0.16	0.30	0.35	0.26	0.39	0.80	1.60	2.40
2008	0.19	0.13	0.12	0.12	0.15	0.14	0.15	0.16	0.29	0.33	0.25	0.38	0.84	1.56	2.40
2009	0.57	0.34	0.38	0.42	0.29	0.27	0.16	0.18	0.47	0.55	0.29	0.45	2.27	2.10	4.37
2010	0.18	0.12	0.12	0.12	0.14	0.13	0.20	0.33	0.97	1.09	0.52	0.67	0.80	3.77	4.57
2011	0.33	0.21	0.21	0.22	0.22	0.21	1.02	0.86	1.66	4.51	2.67	1.97	1.40	12.69	14.09
2012	0.49	0.29	0.33	0.35	0.27	0.26	0.89	0.98	2.03	4.35	1.77	1.50	1.99	11.51	13.50
2013	0.17	0.11	0.11	0.11	0.13	0.12	0.53	1.22	1.94	2.05	0.77	0.98	0.75	7.48	8.23
2014	0.17	0.12	0.11	0.11	0.13	0.12	0.16	0.16	0.31	0.36	0.26	0.39	0.77	1.63	2.40
2015	0.27	0.18	0.18	0.18	0.20	0.19	0.15	0.16	0.30	0.35	0.26	0.39	1.18	1.60	2.78
2016	0.40	0.25	0.27	0.28	0.25	0.24	0.20	0.33	0.97	1.09	0.52	0.67	1.68	3.78	5.46
2017	0.56	0.33	0.38	0.42	0.29	0.27	0.20	0.35	0.98	1.10	0.54	0.70	2.26	3.87	6.13
2018	0.25	0.16	0.16	0.16	0.19	0.17	0.20	0.34	0.98	1.10	0.54	0.69	1.10	3.85	4.95
2019	0.22	0.14	0.14	0.14	0.16	0.15	0.16	0.16	0.30	0.35	0.26	0.39	0.96	1.62	2.58
2020	0.64	0.37	0.42	0.47	0.31	0.28	0.42	0.79	1.48	1.46	0.94	1.25	2.48	6.34	8.82
2021	0.16	0.11	0.10	0.10	0.12	0.11	0.95	0.92	1.84	4.43	2.11	1.67	0.70	11.90	12.60
2022	0.13	0.09	0.09	0.09	0.11	0.10	0.16	0.17	0.36	0.42	0.28	0.42	0.60	1.80	2.40
2023	0.38	0.24	0.25	0.26	0.24	0.23	0.42	0.78	1.46	1.44	0.94	1.26	1.60	6.29	7.89
2024	0.35	0.22	0.23	0.24	0.23	0.22	0.15	0.16	0.30	0.35	0.26	0.39	1.50	1.60	3.10
2025	0.86	0.45	0.49	0.58	0.35	0.33	0.97	0.88	1.74	4.44	2.32	1.78	3.06	12.13	15.19

Current infrastructure in Amudarya river delta. Runoff volume. Optimistic scenario (minimum).

	OCT	NOV	DEC	JAN	FEB	MAR	APR	MAY	JUN	JUL	AUG	SEP	TMG	TVG	Total
1990	0.19	0.13	0.12	0.12	0.15	0.14	0.21	0.37	1.01	1.13	0.61	0.77	0.84	4.09	4.94
1991	1.43	0.67	0.62	1.08	0.51	0.53	0.33	0.60	1.22	1.16	0.88	1.18	4.83	5.36	10.19
1992	1.62	0.74	0.64	1.14	0.53	0.61	0.38	3.14	4.79	5.11	3.68	2.08	5.29	19.18	24.47
1993	1.77	0.80	0.67	1.17	0.57	0.69	0.81	1.03	2.23	4.07	1.48	1.38	5.66	11.00	16.66
1994	1.91	0.86	0.78	1.26	0.69	0.85	1.00	0.85	1.67	4.47	2.51	1.88	6.34	12.37	18.72
1995	1.73	0.79	0.66	1.16	0.55	0.67	0.09	0.10	0.11	0.12	0.12	0.16	5.57	0.70	6.26
1996	0.20	0.14	0.13	0.13	0.16	0.14	0.17	0.26	0.84	0.96	0.38	0.53	0.90	3.14	4.04
1997	0.38	0.24	0.25	0.26	0.24	0.23	0.04	0.04	0.04	0.04	0.04	0.05	1.60	0.26	1.86
1998	0.14	0.09	0.09	0.09	0.11	0.10	0.30	2.94	4.83	4.52	3.35	1.76	0.60	17.69	18.29
1999	1.03	0.51	0.53	0.65	0.38	0.37	0.15	0.16	0.26	0.30	0.24	0.36	3.46	1.45	4.91
2000	0.70	0.39	0.45	0.51	0.32	0.29	0.03	0.04	0.04	0.04	0.04	0.05	2.66	0.22	2.88
2001	0.01	0.01	0.01	0.01	0.01	0.01	0.01	0.01	0.01	0.01	0.01	0.01	0.04	0.05	0.09
2002	0.01	0.01	0.01	0.01	0.01	0.01	0.15	0.20	0.67	0.78	0.32	0.48	0.05	2.60	2.65
2003	0.45	0.27	0.30	0.32	0.26	0.25	0.63	1.66	2.39	2.55	0.60	0.74	1.85	8.57	10.42
2004	0.29	0.19	0.19	0.20	0.21	0.20	0.18	0.28	0.88	1.01	0.41	0.56	1.27	3.32	4.59
2005	0.28	0.18	0.18	0.19	0.20	0.19	0.86	1.00	2.11	4.26	1.64	1.44	1.22	11.32	12.55
2006	0.63	0.36	0.41	0.46	0.31	0.28	0.17	0.27	0.86	0.99	0.39	0.54	2.45	3.22	5.67
2007	1.52	0.71	0.63	1.12	0.52	0.57	0.15	0.16	0.28	0.33	0.25	0.38	5.05	1.55	6.60
2008	0.39	0.24	0.26	0.27	0.25	0.23	0.15	0.16	0.29	0.34	0.25	0.38	1.63	1.57	3.20
2009	0.51	0.31	0.35	0.37	0.28	0.26	0.16	0.19	0.53	0.62	0.30	0.46	2.07	2.24	4.31
2010	0.56	0.33	0.38	0.41	0.29	0.27	0.16	0.16	0.30	0.35	0.26	0.39	2.24	1.62	3.86
2011	1.17	0.56	0.56	0.76	0.42	0.42	0.97	0.89	1.76	4.44	2.28	1.76	3.88	12.08	15.96
2012	0.38	0.24	0.25	0.26	0.24	0.23	0.75	1.10	2.31	3.70	1.30	1.28	1.60	10.44	12.04
2013	0.51	0.31	0.35	0.38	0.28	0.26	0.23	0.42	1.06	1.15	0.69	0.87	2.09	4.42	6.51
2014	0.40	0.25	0.26	0.27	0.25	0.24	0.15	0.16	0.28	0.33	0.25	0.37	1.66	1.54	3.20
2015	0.50	0.30	0.34	0.37	0.28	0.26	0.16	0.19	0.54	0.62	0.30	0.46	2.05	2.26	4.31
2016	0.43	0.27	0.29	0.31	0.26	0.24	0.50	1.07	1.79	1.88	0.84	1.08	1.80	7.17	8.97
2017	0.64	0.37	0.42	0.47	0.31	0.28	0.70	1.43	2.38	3.08	0.94	1.01	2.48	9.54	12.02
2018	0.57	0.34	0.39	0.42	0.30	0.27	0.41	0.78	1.46	1.43	0.94	1.26	2.28	6.27	8.55
2019	0.39	0.24	0.26	0.27	0.24	0.23	0.15	0.16	0.29	0.34	0.25	0.38	1.62	1.58	3.20
2020	0.38	0.24	0.25	0.26	0.24	0.23	0.72	1.23	2.33	3.41	1.16	1.17	1.60	10.02	11.62
2021	0.41	0.25	0.27	0.28	0.25	0.24	0.33	3.03	4.83	4.77	3.49	1.89	1.70	18.35	20.05
2022	0.44	0.27	0.30	0.32	0.26	0.25	0.16	0.17	0.33	0.38	0.27	0.40	1.84	1.70	3.54
2023	1.30	0.63	0.60	0.96	0.47	0.48	0.43	0.82	1.52	1.51	0.93	1.24	4.44	6.45	10.89
2024	0.56	0.33	0.38	0.42	0.29	0.27	1.03	0.92	1.78	4.58	2.73	2.02	2.26	13.07	15.33
2025	0.40	0.25	0.26	0.27	0.25	0.24	0.49	2.47	4.14	4.46	3.05	1.82	1.66	16.42	18.08

Current infrastructure in Amudarya river delta. Water salinity. National vision (maximum).

	OCT	NOV	DEC	JAN	FEB	MAR	APR	MAY	JUN	JUL	AUG	SEP
1990	1.883	2.098	2.121	2.122	2.027	2.068	1.831	1.523	1.109	1.076	1.295	1.204
1991	0.944	1.207	1.242	1.033	1.325	1.307	1.502	1.253	0.992	1.009	1.106	1.003
1992	0.934	1.183	1.231	1.045	1.286	1.243	1.382	0.751	0.66	0.648	0.714	0.86
1993	0.882	1.142	1.208	1.012	1.268	1.195	1.138	1.055	0.818	0.686	0.935	0.959
1994	0.866	1.121	1.156	0.993	1.201	1.127	1.071	1.127	0.905	0.669	0.791	0.87
1995	0.933	1.169	1.24	1.039	1.313	1.232	2.153	2.118	2.075	2.051	2.066	1.925
1996	1.88	2.121	2.144	2.142	2.042	2.086	1.987	1.74	1.197	1.152	1.533	1.373
1997	1.606	1.853	1.818	1.796	1.838	1.868	3.205	3.118	3.112	3.129	3.149	2.949
1998	1.652	1.71	1.718	1.721	1.692	1.704	1.47	0.753	0.656	0.667	0.725	0.888
1999	1.103	1.374	1.356	1.269	1.519	1.524	2.017	1.998	1.718	1.638	1.759	1.546
2000	1.309	1.548	1.488	1.43	1.65	1.7	3.053	2.995	2.994	3.008	3.021	2.887
2001	3.172	3.535	3.627	3.699	3.504	3.534	3.39	3.249	3.258	3.309	3.348	3.08
2002	3.492	3.559	3.573	3.582	3.554	3.559	2.114	1.927	1.336	1.288	1.661	1.467
2003	1.375	1.575	1.536	1.515	1.59	1.614	1.23	0.9	0.81	0.797	1.254	1.172
2004	1.652	1.903	1.896	1.882	1.847	1.876	1.934	1.679	1.161	1.119	1.481	1.337
2005	1.536	1.681	1.68	1.673	1.649	1.665	1.111	1.057	0.831	0.692	0.899	0.936
2006	1.27	1.522	1.456	1.403	1.605	1.652	1.901	1.675	1.147	1.101	1.483	1.331
2007	1.113	1.348	1.317	1.259	1.438	1.456	1.056	1.12	0.899	0.671	0.775	0.852
2008	1.564	1.828	1.795	1.772	1.809	1.839	2.078	2.046	1.646	1.566	1.751	1.529
2009	0.887	1.119	1.146	0.991	1.195	1.116	1.997	1.973	1.893	1.852	1.879	1.729
2010	0.92	1.168	1.236	1.026	1.312	1.238	1.874	1.834	1.436	1.368	1.608	1.412
2011	1.116	1.356	1.323	1.263	1.448	1.469	1.115	1.058	0.828	0.684	0.903	0.94
2012	1.363	1.549	1.514	1.494	1.565	1.586	1.167	1.013	0.809	0.721	0.981	0.983
2013	1.187	1.451	1.401	1.333	1.571	1.61	1.985	1.931	1.459	1.389	1.66	1.444
2014	1.049	1.291	1.309	1.137	1.413	1.413	2.724	2.69	2.69	2.699	2.707	2.628
2015	1.588	1.832	1.793	1.77	1.826	1.856	3.253	3.169	3.165	3.184	3.204	3.012
2016	2.965	3.15	3.188	3.212	3.119	3.143	2.116	1.98	1.399	1.347	1.692	1.487
2017	1.51	1.747	1.692	1.662	1.776	1.813	3.375	3.305	3.305	3.325	3.342	3.184
2018	0.957	1.192	1.257	1.054	1.334	1.263	2.542	2.514	2.513	2.52	2.527	2.459
2019	1.118	1.372	1.365	1.266	1.516	1.514	2.848	2.806	2.806	2.816	2.826	2.729
2020	0.978	1.238	1.263	1.067	1.358	1.352	1.863	1.701	1.166	1.111	1.511	1.344
2021	0.928	1.159	1.229	1.038	1.298	1.21	2.347	2.312	2.304	2.306	2.314	2.219
2022	0.852	1.105	1.124	0.97	1.168	1.097	1.181	0.989	0.806	0.723	1.024	1.016
2023	0.815	1.004	1.019	0.902	1.063	1.018	2.201	2.184	2.183	2.187	2.191	2.149
2024	0.79	0.967	0.982	0.875	1.024	0.987	2.147	2.132	2.132	2.135	2.139	2.103
2025	2.559	2.854	2.928	2.975	2.789	2.84	3.461	3.324	3.326	3.367	3.402	3.124

Current infrastructure in Amudarya river delta. Water salinity. Business as usual (maximum).

	OCT	NOV	DEC	JAN	FEB	MAR	APR	MAY	JUN	JUL	AUG	SEP
1990	1.883	2.098	2.121	2.122	2.027	2.068	1.831	1.523	1.109	1.076	1.295	1.204
1991	0.944	1.207	1.242	1.033	1.325	1.307	1.502	1.253	0.992	1.009	1.106	1.003
1992	0.934	1.183	1.231	1.045	1.286	1.243	1.382	0.751	0.66	0.648	0.714	0.86
1993	0.882	1.142	1.208	1.012	1.268	1.195	1.138	1.055	0.818	0.686	0.935	0.959
1994	0.866	1.121	1.156	0.993	1.201	1.127	1.071	1.127	0.905	0.669	0.791	0.87
1995	0.933	1.169	1.24	1.039	1.313	1.232	2.153	2.118	2.075	2.051	2.066	1.925
1996	1.88	2.121	2.144	2.142	2.042	2.086	1.987	1.74	1.197	1.152	1.533	1.373
1997	1.606	1.853	1.818	1.796	1.838	1.868	3.205	3.118	3.112	3.129	3.149	2.949
1998	1.652	1.71	1.718	1.721	1.692	1.704	1.47	0.753	0.656	0.667	0.725	0.888
1999	1.103	1.374	1.356	1.269	1.519	1.524	2.017	1.998	1.718	1.638	1.759	1.546
2000	1.309	1.548	1.488	1.43	1.65	1.7	3.053	2.995	2.994	3.008	3.021	2.887
2001	3.172	3.535	3.627	3.699	3.504	3.534	3.39	3.249	3.258	3.309	3.348	3.08
2002	3.492	3.559	3.573	3.582	3.554	3.559	2.114	1.927	1.336	1.288	1.661	1.467
2003	1.375	1.575	1.536	1.515	1.59	1.614	1.23	0.9	0.81	0.797	1.254	1.172
2004	1.652	1.903	1.896	1.882	1.847	1.876	1.934	1.679	1.161	1.119	1.481	1.337
2005	1.536	1.681	1.68	1.673	1.649	1.665	1.111	1.057	0.831	0.692	0.899	0.936
2006	1.27	1.522	1.456	1.403	1.605	1.652	1.901	1.675	1.147	1.101	1.483	1.331
2007	1.065	1.31	1.294	1.227	1.408	1.412	1.08	0.959	0.788	0.661	0.77	0.843
2008	1.454	1.71	1.654	1.624	1.737	1.774	2.055	2.02	1.604	1.526	1.728	1.506
2009	0.883	1.139	1.21	1.006	1.278	1.198	1.544	1.3	1.009	1.01	1.132	1.033
2010	2.024	2.298	2.335	2.338	2.202	2.259	2.119	2.089	1.702	1.623	1.789	1.571
2011	1.22	1.412	1.368	1.328	1.467	1.494	1.072	0.97	0.796	0.662	0.769	0.841
2012	0.905	1.169	1.225	1.014	1.296	1.244	1.238	0.906	0.806	0.794	1.25	1.166
2013	1.271	1.506	1.445	1.401	1.569	1.608	1.444	1.181	0.96	0.972	1.087	0.989
2014	1.934	2.21	2.238	2.236	2.117	2.168	2.135	2.11	1.763	1.68	1.82	1.599
2015	1.973	2.249	2.281	2.281	2.153	2.208	2.127	2.1	1.735	1.654	1.805	1.586
2016	2.012	2.285	2.321	2.324	2.19	2.246	2.108	2.073	1.658	1.581	1.768	1.551
2017	1.072	1.342	1.334	1.231	1.486	1.485	1.98	1.958	1.631	1.553	1.709	1.497
2018	1.379	1.631	1.564	1.523	1.691	1.735	2.054	2.027	1.652	1.571	1.745	1.522
2019	1.114	1.385	1.362	1.28	1.527	1.538	1.993	1.969	1.628	1.549	1.713	1.498
2020	1.019	1.293	1.294	1.168	1.428	1.425	1.783	1.548	1.087	1.046	1.357	1.241
2021	0.883	1.129	1.196	1.004	1.259	1.171	1.799	1.638	1.136	1.083	1.47	1.319
2022	0.881	1.135	1.177	1.013	1.222	1.151	1.266	0.822	0.696	0.67	0.758	0.885
2023	0.856	1.107	1.137	0.973	1.185	1.107	1.497	1.261	0.995	1.009	1.111	1.008
2024	2.015	2.29	2.326	2.329	2.193	2.25	2.12	2.091	1.708	1.628	1.791	1.573
2025	2.015	2.29	2.326	2.329	2.193	2.25	2.12	2.091	1.708	1.628	1.791	1.573

Current infrastructure in Amudarya river delta. Water salinity. Optimistic scenario (maximum).

	OCT	NOV	DEC	JAN	FEB	MAR	APR	MAY	JUN	JUL	AUG	SEP
1990	1.883	2.098	2.121	2.122	2.027	2.068	1.831	1.523	1.109	1.076	1.295	1.204
1991	0.944	1.207	1.242	1.033	1.325	1.307	1.502	1.253	0.992	1.009	1.106	1.003
1992	0.934	1.183	1.231	1.045	1.286	1.243	1.382	0.751	0.66	0.648	0.714	0.86
1993	0.882	1.142	1.208	1.012	1.268	1.195	1.138	1.055	0.818	0.686	0.935	0.959
1994	0.866	1.121	1.156	0.993	1.201	1.127	1.071	1.127	0.905	0.669	0.791	0.87
1995	0.933	1.169	1.24	1.039	1.313	1.232	2.153	2.118	2.075	2.051	2.066	1.925
1996	1.88	2.121	2.144	2.142	2.042	2.086	1.987	1.74	1.197	1.152	1.533	1.373
1997	1.606	1.853	1.818	1.796	1.838	1.868	3.205	3.118	3.112	3.129	3.149	2.949
1998	1.652	1.71	1.718	1.721	1.692	1.704	1.47	0.753	0.656	0.667	0.725	0.888
1999	1.103	1.374	1.356	1.269	1.519	1.524	2.017	1.998	1.718	1.638	1.759	1.546
2000	1.309	1.548	1.488	1.43	1.65	1.7	3.053	2.995	2.994	3.008	3.021	2.887
2001	3.172	3.535	3.627	3.699	3.504	3.534	3.39	3.249	3.258	3.309	3.348	3.08
2002	3.492	3.559	3.573	3.582	3.554	3.559	2.114	1.927	1.336	1.288	1.661	1.467
2003	1.375	1.575	1.536	1.515	1.59	1.614	1.23	0.9	0.81	0.797	1.254	1.172
2004	1.652	1.903	1.896	1.882	1.847	1.876	1.934	1.679	1.161	1.119	1.481	1.337
2005	1.536	1.681	1.68	1.673	1.649	1.665	1.111	1.057	0.831	0.692	0.899	0.936
2006	1.27	1.522	1.456	1.403	1.605	1.652	1.901	1.675	1.147	1.101	1.483	1.331
2007	1.036	1.294	1.285	1.202	1.401	1.401	1.061	1.123	0.9	0.671	0.781	0.858
2008	1.148	1.417	1.375	1.304	1.543	1.573	1.953	1.792	1.216	1.16	1.568	1.379
2009	1.437	1.621	1.599	1.584	1.612	1.63	1.195	0.931	0.806	0.76	1.098	1.068
2010	1.536	1.798	1.758	1.734	1.791	1.823	2.088	2.062	1.695	1.612	1.773	1.55
2011	0.884	1.145	1.21	1.012	1.272	1.201	1.157	1.041	0.809	0.698	0.962	0.972
2012	0.821	1.057	1.071	0.93	1.115	1.056	1.26	0.941	0.825	0.812	1.213	1.129
2013	1.355	1.581	1.529	1.5	1.614	1.645	1.447	1.183	0.963	0.975	1.089	0.991
2014	1.534	1.795	1.754	1.73	1.79	1.822	2.095	2.07	1.718	1.635	1.785	1.561
2015	1.482	1.712	1.683	1.664	1.7	1.725	1.586	1.307	1.028	1.035	1.142	1.045
2016	1.503	1.735	1.709	1.691	1.717	1.741	1.633	1.347	1.042	1.038	1.165	1.071
2017	0.922	1.185	1.233	1.019	1.311	1.272	1.482	1.236	0.984	1.003	1.098	0.994
2018	1.476	1.703	1.673	1.654	1.692	1.717	1.545	1.271	1.014	1.029	1.123	1.024
2019	1.076	1.349	1.324	1.248	1.474	1.487	1.451	1.194	0.964	0.98	1.086	0.985
2020	1.018	1.295	1.292	1.18	1.427	1.425	1.529	1.271	1.001	1.015	1.117	1.015
2021	0.843	1.089	1.101	0.957	1.143	1.081	1.068	1.13	0.911	0.668	0.782	0.863
2022	0.989	1.216	1.244	1.078	1.296	1.28	1.04	0.737	0.63	0.6	0.688	0.748
2023	0.817	1.049	1.064	0.928	1.107	1.054	1.102	1.091	0.865	0.671	0.863	0.923
2024	1.091	1.355	1.324	1.255	1.467	1.485	1.294	0.983	0.854	0.84	1.163	1.074
2025	1.15	1.409	1.362	1.297	1.514	1.548	1.493	1.232	0.987	1.006	1.099	0.998

Current infrastructure in Amudarya river delta. Water salinity. National vision (minimum).

	OCT	NOV	DEC	JAN	FEB	MAR	APR	MAY	JUN	JUL	AUG	SEP
1990	1.883	2.098	2.121	2.122	2.027	2.068	1.831	1.523	1.109	1.076	1.295	1.204
1991	0.944	1.207	1.242	1.033	1.325	1.307	1.502	1.253	0.992	1.009	1.106	1.003
1992	0.934	1.183	1.231	1.045	1.286	1.243	1.382	0.751	0.66	0.648	0.714	0.86
1993	0.882	1.142	1.208	1.012	1.268	1.195	1.138	1.055	0.818	0.686	0.935	0.959
1994	0.866	1.121	1.156	0.993	1.201	1.127	1.071	1.127	0.905	0.669	0.791	0.87
1995	0.933	1.169	1.24	1.039	1.313	1.232	2.153	2.118	2.075	2.051	2.066	1.925
1996	1.88	2.121	2.144	2.142	2.042	2.086	1.987	1.74	1.197	1.152	1.533	1.373
1997	1.606	1.853	1.818	1.796	1.838	1.868	3.205	3.118	3.112	3.129	3.149	2.949
1998	1.652	1.71	1.718	1.721	1.692	1.704	1.47	0.753	0.656	0.667	0.725	0.888
1999	1.103	1.374	1.356	1.269	1.519	1.524	2.017	1.998	1.718	1.638	1.759	1.546
2000	1.309	1.548	1.488	1.43	1.65	1.7	3.053	2.995	2.994	3.008	3.021	2.887
2001	3.172	3.535	3.627	3.699	3.504	3.534	3.39	3.249	3.258	3.309	3.348	3.08
2002	3.492	3.559	3.573	3.582	3.554	3.559	2.114	1.927	1.336	1.288	1.661	1.467
2003	1.375	1.575	1.536	1.515	1.59	1.614	1.23	0.9	0.81	0.797	1.254	1.172
2004	1.652	1.903	1.896	1.882	1.847	1.876	1.934	1.679	1.161	1.119	1.481	1.337
2005	1.536	1.681	1.68	1.673	1.649	1.665	1.111	1.057	0.831	0.692	0.899	0.936
2006	1.27	1.522	1.456	1.403	1.605	1.652	1.901	1.675	1.147	1.101	1.483	1.331
2007	1.961	2.218	2.25	2.251	2.125	2.178	3.52	3.407	3.406	3.435	3.463	3.218
2008	2.911	3.232	3.306	3.351	3.165	3.217	2.42	2.354	2.264	2.217	2.245	2.033
2009	1.356	1.592	1.527	1.476	1.679	1.731	3.207	3.151	3.151	3.167	3.181	3.053
2010	1.126	1.382	1.371	1.278	1.526	1.526	2.782	2.735	2.731	2.741	2.752	2.639
2011	0.874	1.132	1.194	1.007	1.249	1.172	1.134	1.058	0.821	0.684	0.929	0.956
2012	1.721	1.819	1.832	1.834	1.788	1.808	1.096	1.067	0.845	0.69	0.871	0.92
2013	2.526	2.699	2.734	2.752	2.659	2.689	1.976	1.705	1.195	1.156	1.504	1.362
2014	1.013	1.252	1.286	1.089	1.375	1.358	2.619	2.585	2.584	2.592	2.6	2.52
2015	1.36	1.596	1.531	1.481	1.682	1.733	3.161	3.101	3.1	3.116	3.13	2.994
2016	1.322	1.575	1.507	1.459	1.649	1.696	2.013	1.919	1.367	1.304	1.647	1.432
2017	1.342	1.594	1.527	1.484	1.658	1.702	2.013	1.874	1.284	1.227	1.619	1.413
2018	0.919	1.146	1.206	1.028	1.265	1.178	2.463	2.437	2.437	2.443	2.449	2.388
2019	1.067	1.312	1.323	1.171	1.439	1.439	2.747	2.711	2.71	2.719	2.728	2.643
2020	1.794	1.906	1.922	1.926	1.87	1.894	1.196	0.935	0.812	0.766	1.095	1.067
2021	2.059	2.119	2.131	2.138	2.107	2.117	1.207	0.919	0.814	0.782	1.152	1.107
2022	3.023	3.373	3.458	3.519	3.319	3.364	2.936	2.82	2.814	2.838	2.864	2.626
2023	1.395	1.631	1.564	1.52	1.704	1.753	3.053	2.985	2.98	2.994	3.01	2.849
2024	1.55	1.79	1.742	1.716	1.801	1.835	3.347	3.27	3.269	3.29	3.308	3.135
2025	1.301	1.51	1.459	1.427	1.552	1.582	1.222	0.897	0.805	0.788	1.237	1.163

Current infrastructure in Amudarya river delta. Water salinity. Business as usual (minimum).

	OCT	NOV	DEC	JAN	FEB	MAR	APR	MAY	JUN	JUL	AUG	SEP
1990	1.883	2.098	2.121	2.122	2.027	2.068	1.831	1.523	1.109	1.076	1.295	1.204
1991	0.944	1.207	1.242	1.033	1.325	1.307	1.502	1.253	0.992	1.009	1.106	1.003
1992	0.934	1.183	1.231	1.045	1.286	1.243	1.382	0.751	0.66	0.648	0.714	0.86
1993	0.882	1.142	1.208	1.012	1.268	1.195	1.138	1.055	0.818	0.686	0.935	0.959
1994	0.866	1.121	1.156	0.993	1.201	1.127	1.071	1.127	0.905	0.669	0.791	0.87
1995	0.933	1.169	1.24	1.039	1.313	1.232	2.153	2.118	2.075	2.051	2.066	1.925
1996	1.88	2.121	2.144	2.142	2.042	2.086	1.987	1.74	1.197	1.152	1.533	1.373
1997	1.606	1.853	1.818	1.796	1.838	1.868	3.205	3.118	3.112	3.129	3.149	2.949
1998	1.652	1.71	1.718	1.721	1.692	1.704	1.47	0.753	0.656	0.667	0.725	0.888
1999	1.103	1.374	1.356	1.269	1.519	1.524	2.017	1.998	1.718	1.638	1.759	1.546
2000	1.309	1.548	1.488	1.43	1.65	1.7	3.053	2.995	2.994	3.008	3.021	2.887
2001	3.172	3.535	3.627	3.699	3.504	3.534	3.39	3.249	3.258	3.309	3.348	3.08
2002	3.492	3.559	3.573	3.582	3.554	3.559	2.114	1.927	1.336	1.288	1.661	1.467
2003	1.375	1.575	1.536	1.515	1.59	1.614	1.23	0.9	0.81	0.797	1.254	1.172
2004	1.652	1.903	1.896	1.882	1.847	1.876	1.934	1.679	1.161	1.119	1.481	1.337
2005	1.536	1.681	1.68	1.673	1.649	1.665	1.111	1.057	0.831	0.692	0.899	0.936
2006	1.27	1.522	1.456	1.403	1.605	1.652	1.901	1.675	1.147	1.101	1.483	1.331
2007	2.015	2.29	2.326	2.329	2.193	2.25	2.12	2.091	1.708	1.628	1.791	1.573
2008	1.981	2.257	2.29	2.29	2.161	2.216	2.125	2.098	1.73	1.648	1.802	1.583
2009	1.335	1.588	1.519	1.474	1.658	1.705	2.016	1.939	1.415	1.349	1.661	1.444
2010	1.929	2.148	2.175	2.177	2.074	2.118	1.881	1.587	1.132	1.097	1.373	1.265
2011	1.47	1.616	1.608	1.599	1.595	1.609	1.052	1.115	0.895	0.676	0.774	0.848
2012	1.328	1.511	1.471	1.448	1.536	1.559	1.1	1.065	0.841	0.684	0.878	0.925
2013	1.818	1.961	1.98	1.982	1.915	1.944	1.311	1.002	0.876	0.864	1.162	1.073
2014	2.042	2.316	2.354	2.358	2.219	2.277	2.116	2.085	1.692	1.613	1.784	1.567
2015	1.749	2.022	2.024	2.01	1.949	1.984	2.106	2.078	1.697	1.615	1.781	1.559
2016	1.475	1.721	1.683	1.66	1.719	1.748	1.846	1.566	1.11	1.073	1.355	1.246
2017	1.307	1.554	1.489	1.445	1.618	1.661	1.813	1.538	1.093	1.056	1.324	1.22
2018	1.729	1.964	1.972	1.963	1.898	1.931	1.858	1.564	1.118	1.083	1.347	1.243
2019	1.887	2.161	2.183	2.178	2.071	2.118	2.111	2.082	1.692	1.612	1.782	1.562
2020	1.235	1.473	1.414	1.364	1.547	1.587	1.412	1.148	0.94	0.944	1.085	0.989
2021	1.722	1.816	1.829	1.831	1.786	1.805	1.078	1.088	0.867	0.686	0.832	0.894
2022	2.22	2.487	2.535	2.55	2.396	2.457	2.103	2.058	1.606	1.535	1.75	1.536
2023	1.467	1.683	1.656	1.639	1.672	1.695	1.425	1.159	0.951	0.956	1.09	0.995
2024	1.594	1.861	1.833	1.812	1.83	1.86	2.092	2.064	1.688	1.606	1.772	1.549
2025	1.114	1.351	1.319	1.26	1.441	1.46	1.071	1.108	0.884	0.674	0.806	0.877

Current infrastructure in Amudarya river delta. Water salinity. Optimistic scenario (minimum).

	OCT	NOV	DEC	JAN	FEB	MAR	APR	MAY	JUN	JUL	AUG	SEP
1990	1.883	2.098	2.121	2.122	2.027	2.068	1.831	1.523	1.109	1.076	1.295	1.204
1991	0.944	1.207	1.242	1.033	1.325	1.307	1.502	1.253	0.992	1.009	1.106	1.003
1992	0.934	1.183	1.231	1.045	1.286	1.243	1.382	0.751	0.66	0.648	0.714	0.86
1993	0.882	1.142	1.208	1.012	1.268	1.195	1.138	1.055	0.818	0.686	0.935	0.959
1994	0.866	1.121	1.156	0.993	1.201	1.127	1.071	1.127	0.905	0.669	0.791	0.87
1995	0.933	1.169	1.24	1.039	1.313	1.232	2.153	2.118	2.075	2.051	2.066	1.925
1996	1.88	2.121	2.144	2.142	2.042	2.086	1.987	1.74	1.197	1.152	1.533	1.373
1997	1.606	1.853	1.818	1.796	1.838	1.868	3.205	3.118	3.112	3.129	3.149	2.949
1998	1.652	1.71	1.718	1.721	1.692	1.704	1.47	0.753	0.656	0.667	0.725	0.888
1999	1.103	1.374	1.356	1.269	1.519	1.524	2.017	1.998	1.718	1.638	1.759	1.546
2000	1.309	1.548	1.488	1.43	1.65	1.7	3.053	2.995	2.994	3.008	3.021	2.887
2001	3.172	3.535	3.627	3.699	3.504	3.534	3.39	3.249	3.258	3.309	3.348	3.08
2002	3.492	3.559	3.573	3.582	3.554	3.559	2.114	1.927	1.336	1.288	1.661	1.467
2003	1.375	1.575	1.536	1.515	1.59	1.614	1.23	0.9	0.81	0.797	1.254	1.172
2004	1.652	1.903	1.896	1.882	1.847	1.876	1.934	1.679	1.161	1.119	1.481	1.337
2005	1.536	1.681	1.68	1.673	1.649	1.665	1.111	1.057	0.831	0.692	0.899	0.936
2006	1.27	1.522	1.456	1.403	1.605	1.652	1.901	1.675	1.147	1.101	1.483	1.331
2007	0.959	1.209	1.256	1.045	1.34	1.301	1.922	1.905	1.627	1.554	1.687	1.488
2008	1.544	1.806	1.768	1.744	1.796	1.827	2.091	2.065	1.701	1.618	1.777	1.553
2009	1.385	1.638	1.574	1.537	1.688	1.729	2.026	1.926	1.365	1.303	1.651	1.436
2010	1.356	1.608	1.539	1.494	1.676	1.723	2.051	2.025	1.656	1.574	1.745	1.522
2011	1.01	1.271	1.271	1.161	1.377	1.376	1.075	1.106	0.882	0.673	0.812	0.882
2012	1.43	1.605	1.584	1.57	1.596	1.614	1.162	1.023	0.81	0.717	0.97	0.975
2013	1.344	1.585	1.525	1.49	1.632	1.669	1.729	1.439	1.064	1.037	1.219	1.13
2014	1.534	1.795	1.754	1.73	1.79	1.822	2.095	2.07	1.718	1.635	1.785	1.561
2015	1.39	1.644	1.579	1.543	1.691	1.732	2.027	1.923	1.359	1.297	1.649	1.435
2016	1.398	1.609	1.571	1.549	1.621	1.646	1.333	1.039	0.887	0.875	1.125	1.035
2017	1.227	1.444	1.392	1.347	1.508	1.542	1.191	0.939	0.803	0.75	1.079	1.054
2018	1.281	1.513	1.454	1.412	1.572	1.609	1.421	1.157	0.946	0.952	1.086	0.989
2019	1.547	1.81	1.773	1.749	1.799	1.829	2.089	2.063	1.696	1.613	1.774	1.551
2020	1.433	1.611	1.59	1.576	1.603	1.62	1.176	0.988	0.81	0.733	1.008	1.002
2021	1.371	1.502	1.483	1.472	1.502	1.515	1.433	0.749	0.655	0.657	0.717	0.872
2022	1.468	1.724	1.671	1.642	1.746	1.782	2.06	2.028	1.622	1.542	1.736	1.514
2023	0.969	1.235	1.253	1.071	1.347	1.346	1.386	1.13	0.924	0.925	1.082	0.985
2024	1.269	1.454	1.409	1.378	1.495	1.522	1.05	1.09	0.878	0.669	0.768	0.842
2025	1.386	1.524	1.505	1.494	1.521	1.535	1.314	0.794	0.683	0.669	0.745	0.878

NATO SFP 974357 Project infrastructure. Runoff volume. National vision (maximum).

	OCT	NOV	DEC	JAN	FEB	MAR	APR	MAY	JUN	JUL	AUG	SEP	TMG	TVG	Total
1990	0.19	0.13	0.12	0.12	0.15	0.14	0.21	0.37	1.01	1.13	0.61	0.77	0.84	4.09	4.94
1991	1.43	0.67	0.62	1.08	0.51	0.53	0.33	0.60	1.22	1.16	0.88	1.18	4.83	5.36	10.19
1992	1.62	0.74	0.64	1.14	0.53	0.61	0.38	3.14	4.79	5.11	3.68	2.08	5.29	19.18	24.47
1993	1.77	0.80	0.67	1.17	0.57	0.69	0.81	1.03	2.23	4.07	1.48	1.38	5.66	11.00	16.66
1994	1.91	0.86	0.78	1.26	0.69	0.85	1.00	0.85	1.67	4.47	2.51	1.88	6.34	12.37	18.72
1995	1.73	0.79	0.66	1.16	0.55	0.67	0.09	0.10	0.11	0.12	0.12	0.16	5.57	0.70	6.26
1996	0.20	0.14	0.13	0.13	0.16	0.14	0.17	0.26	0.84	0.96	0.38	0.53	0.90	3.14	4.04
1997	0.38	0.24	0.25	0.26	0.24	0.23	0.04	0.04	0.04	0.04	0.04	0.05	1.60	0.26	1.86
1998	0.14	0.09	0.09	0.09	0.11	0.10	0.30	2.94	4.83	4.52	3.35	1.76	0.60	17.69	18.29
1999	1.03	0.51	0.53	0.65	0.38	0.37	0.15	0.16	0.26	0.30	0.24	0.36	3.46	1.45	4.91
2000	0.70	0.39	0.45	0.51	0.32	0.29	0.03	0.04	0.04	0.04	0.04	0.05	2.66	0.22	2.88
2001	0.01	0.01	0.01	0.01	0.01	0.01	0.01	0.01	0.01	0.01	0.01	0.01	0.04	0.05	0.09
2002	0.01	0.01	0.01	0.01	0.01	0.01	0.15	0.20	0.67	0.78	0.32	0.48	0.05	2.60	2.65
2003	0.45	0.27	0.30	0.32	0.26	0.25	0.63	1.66	2.39	2.55	0.60	0.74	1.85	8.57	10.42
2004	0.29	0.19	0.19	0.20	0.21	0.20	0.18	0.28	0.88	1.01	0.41	0.56	1.27	3.32	4.59
2005	0.28	0.18	0.18	0.19	0.20	0.19	0.86	1.00	2.11	4.26	1.64	1.44	1.22	11.32	12.55
2006	0.63	0.36	0.41	0.46	0.31	0.28	0.17	0.27	0.86	0.99	0.39	0.54	2.45	3.22	5.67
2007	0.87	0.45	0.49	0.58	0.35	0.33	1.02	0.85	1.66	4.50	2.64	1.95	3.07	12.62	15.69
2008	0.37	0.23	0.25	0.26	0.24	0.23	0.16	0.16	0.32	0.37	0.26	0.40	1.57	1.67	3.24
2009	1.93	0.88	0.81	1.29	0.72	0.88	0.12	0.12	0.15	0.17	0.16	0.22	6.51	0.93	7.44
2010	1.68	0.77	0.65	1.15	0.54	0.64	0.16	0.17	0.41	0.48	0.29	0.43	5.44	1.94	7.38
2011	0.86	0.45	0.49	0.58	0.35	0.33	0.86	1.00	2.13	4.25	1.62	1.44	3.04	11.29	14.33
2012	0.45	0.28	0.30	0.32	0.26	0.25	0.74	1.14	2.32	3.60	1.25	1.25	1.86	10.30	12.16
2013	0.80	0.43	0.48	0.56	0.34	0.32	0.16	0.18	0.42	0.49	0.29	0.44	2.92	1.97	4.89
2014	1.30	0.62	0.60	0.95	0.47	0.47	0.03	0.03	0.03	0.03	0.03	0.04	4.41	0.20	4.61
2015	0.39	0.24	0.26	0.27	0.25	0.23	0.04	0.04	0.04	0.04	0.04	0.05	1.65	0.24	1.89
2016	0.05	0.03	0.03	0.03	0.03	0.03	0.15	0.19	0.57	0.66	0.30	0.46	0.20	2.34	2.54
2017	0.46	0.28	0.31	0.33	0.27	0.25	0.03	0.03	0.03	0.03	0.03	0.04	1.90	0.18	2.08
2018	1.67	0.76	0.65	1.15	0.54	0.64	0.03	0.04	0.04	0.04	0.03	0.05	5.40	0.22	5.62
2019	1.11	0.54	0.55	0.70	0.39	0.40	0.03	0.04	0.04	0.03	0.03	0.04	3.68	0.21	3.89
2020	1.35	0.64	0.61	1.01	0.49	0.49	0.16	0.23	0.77	0.89	0.35	0.50	4.59	2.91	7.50
2021	1.79	0.82	0.68	1.17	0.58	0.71	0.05	0.06	0.06	0.06	0.06	0.08	5.75	0.38	6.13
2022	1.97	0.89	0.85	1.33	0.75	0.91	0.72	1.25	2.34	3.36	1.13	1.15	6.69	9.95	16.64
2023	2.49	1.19	1.14	1.70	1.00	1.14	0.03	0.04	0.04	0.04	0.04	0.05	8.65	0.23	8.88
2024	2.71	1.33	1.26	1.85	1.11	1.24	0.03	0.04	0.04	0.04	0.03	0.05	9.50	0.22	9.72
2025	0.06	0.04	0.04	0.04	0.04	0.04	0.02	0.03	0.03	0.02	0.02	0.03	0.25	0.15	0.40

NATO SFP 974357 Project infrastructure. Runoff volume. Business as usual (maximum).

	OCT	NOV	DEC	JAN	FEB	MAR	APR	MAY	JUN	JUL	AUG	SEP	TMG	TVG	Total
1990	0.19	0.13	0.12	0.12	0.15	0.14	0.21	0.37	1.01	1.13	0.61	0.77	0.84	4.09	4.94
1991	1.43	0.67	0.62	1.08	0.51	0.53	0.33	0.60	1.22	1.16	0.88	1.18	4.83	5.36	10.19
1992	1.62	0.74	0.64	1.14	0.53	0.61	0.38	3.14	4.79	5.11	3.68	2.08	5.29	19.18	24.47
1993	1.77	0.80	0.67	1.17	0.57	0.69	0.81	1.03	2.23	4.07	1.48	1.38	5.66	11.00	16.66
1994	1.91	0.86	0.78	1.26	0.69	0.85	1.00	0.85	1.67	4.47	2.51	1.88	6.34	12.37	18.72
1995	1.73	0.79	0.66	1.16	0.55	0.67	0.09	0.10	0.11	0.12	0.12	0.16	5.57	0.70	6.26
1996	0.20	0.14	0.13	0.13	0.16	0.14	0.17	0.26	0.84	0.96	0.38	0.53	0.90	3.14	4.04
1997	0.38	0.24	0.25	0.26	0.24	0.23	0.04	0.04	0.04	0.04	0.04	0.05	1.60	0.26	1.86
1998	0.14	0.09	0.09	0.09	0.11	0.10	0.30	2.94	4.83	4.52	3.35	1.76	0.60	17.69	18.29
1999	1.03	0.51	0.53	0.65	0.38	0.37	0.15	0.16	0.26	0.30	0.24	0.36	3.46	1.45	4.91
2000	0.70	0.39	0.45	0.51	0.32	0.29	0.03	0.04	0.04	0.04	0.04	0.05	2.66	0.22	2.88
2001	0.01	0.01	0.01	0.01	0.01	0.01	0.01	0.01	0.01	0.01	0.01	0.01	0.04	0.05	0.09
2002	0.01	0.01	0.01	0.01	0.01	0.01	0.15	0.20	0.67	0.78	0.32	0.48	0.05	2.60	2.65
2003	0.45	0.27	0.30	0.32	0.26	0.25	0.63	1.66	2.39	2.55	0.60	0.74	1.85	8.57	10.42
2004	0.29	0.19	0.19	0.20	0.21	0.20	0.18	0.28	0.88	1.01	0.41	0.56	1.27	3.32	4.59
2005	0.28	0.18	0.18	0.19	0.20	0.19	0.86	1.00	2.11	4.26	1.64	1.44	1.22	11.32	12.55
2006	0.63	0.36	0.41	0.46	0.31	0.28	0.17	0.27	0.86	0.99	0.39	0.54	2.45	3.22	5.67
2007	1.01	0.50	0.52	0.64	0.37	0.37	0.97	1.39	2.53	4.70	2.72	2.04	3.40	14.35	17.75
2008	0.46	0.28	0.31	0.33	0.27	0.25	0.16	0.17	0.34	0.39	0.27	0.41	1.88	1.73	3.61
2009	1.76	0.80	0.67	1.17	0.56	0.69	0.29	0.53	1.16	1.15	0.82	1.08	5.64	5.02	10.66
2010	0.18	0.12	0.11	0.11	0.14	0.13	0.16	0.16	0.30	0.35	0.26	0.39	0.79	1.61	2.40
2011	0.65	0.37	0.42	0.48	0.31	0.28	0.98	1.33	2.44	4.70	2.72	2.05	2.51	14.21	16.72
2012	1.60	0.74	0.64	1.14	0.53	0.61	0.62	1.60	2.32	2.45	0.60	0.74	5.25	8.33	13.58
2013	0.59	0.34	0.39	0.43	0.30	0.27	0.40	0.73	1.39	1.34	0.94	1.27	2.33	6.06	8.39
2014	0.20	0.14	0.13	0.13	0.16	0.14	0.15	0.16	0.27	0.31	0.25	0.37	0.90	1.50	2.40
2015	0.19	0.13	0.12	0.12	0.15	0.14	0.15	0.16	0.28	0.33	0.25	0.38	0.85	1.55	2.40
2016	0.18	0.12	0.12	0.12	0.14	0.13	0.16	0.17	0.32	0.38	0.27	0.40	0.80	1.69	2.49
2017	1.11	0.54	0.55	0.70	0.39	0.40	0.15	0.16	0.30	0.35	0.26	0.39	3.68	1.60	5.28
2018	0.53	0.32	0.36	0.39	0.29	0.26	0.16	0.16	0.31	0.36	0.26	0.39	2.15	1.63	3.78
2019	0.99	0.49	0.52	0.63	0.37	0.36	0.16	0.16	0.30	0.35	0.26	0.39	3.36	1.62	4.98
2020	1.17	0.56	0.56	0.77	0.42	0.42	0.19	0.32	0.96	1.08	0.49	0.64	3.90	3.67	7.57
2021	1.83	0.83	0.70	1.19	0.60	0.75	0.17	0.25	0.82	0.94	0.37	0.52	5.89	3.06	8.95
2022	1.88	0.85	0.75	1.23	0.65	0.81	0.57	2.32	3.92	4.50	2.98	1.86	6.17	16.14	22.31
2023	1.92	0.87	0.80	1.28	0.71	0.87	0.32	0.58	1.20	1.15	0.86	1.15	6.46	5.27	11.73
2024	0.18	0.12	0.12	0.12	0.14	0.13	0.15	0.16	0.30	0.35	0.26	0.39	0.80	1.60	2.40
2025	0.18	0.12	0.12	0.12	0.14	0.13	0.15	0.16	0.30	0.35	0.26	0.39	0.80	1.60	2.40

NATO SFP 974357 Project infrastructure. Runoff volume. Optimistic scenario (maximum).

	OCT	NOV	DEC	JAN	FEB	MAR	APR	MAY	JUN	JUL	AUG	SEP	TMG	TVG	Total
1990	0.19	0.13	0.12	0.12	0.15	0.14	0.21	0.37	1.01	1.13	0.61	0.77	0.84	4.09	4.94
1991	1.43	0.67	0.62	1.08	0.51	0.53	0.33	0.60	1.22	1.16	0.88	1.18	4.83	5.36	10.19
1992	1.62	0.74	0.64	1.14	0.53	0.61	0.38	3.14	4.79	5.11	3.68	2.08	5.29	19.18	24.47
1993	1.77	0.80	0.67	1.17	0.57	0.69	0.81	1.03	2.23	4.07	1.48	1.38	5.66	11.00	16.66
1994	1.91	0.86	0.78	1.26	0.69	0.85	1.00	0.85	1.67	4.47	2.51	1.88	6.34	12.37	18.72
1995	1.73	0.79	0.66	1.16	0.55	0.67	0.09	0.10	0.11	0.12	0.12	0.16	5.57	0.70	6.26
1996	0.20	0.14	0.13	0.13	0.16	0.14	0.17	0.26	0.84	0.96	0.38	0.53	0.90	3.14	4.04
1997	0.38	0.24	0.25	0.26	0.24	0.23	0.04	0.04	0.04	0.04	0.04	0.05	1.60	0.26	1.86
1998	0.14	0.09	0.09	0.09	0.11	0.10	0.30	2.94	4.83	4.52	3.35	1.76	0.60	17.69	18.29
1999	1.03	0.51	0.53	0.65	0.38	0.37	0.15	0.16	0.26	0.30	0.24	0.36	3.46	1.45	4.91
2000	0.70	0.39	0.45	0.51	0.32	0.29	0.03	0.04	0.04	0.04	0.04	0.05	2.66	0.22	2.88
2001	0.01	0.01	0.01	0.01	0.01	0.01	0.01	0.01	0.01	0.01	0.01	0.01	0.04	0.05	0.09
2002	0.01	0.01	0.01	0.01	0.01	0.01	0.15	0.20	0.67	0.78	0.32	0.48	0.05	2.60	2.65
2003	0.45	0.27	0.30	0.32	0.26	0.25	0.63	1.66	2.39	2.55	0.60	0.74	1.85	8.57	10.42
2004	0.29	0.19	0.19	0.20	0.21	0.20	0.18	0.28	0.88	1.01	0.41	0.56	1.27	3.32	4.59
2005	0.28	0.18	0.18	0.19	0.20	0.19	0.86	1.00	2.11	4.26	1.64	1.44	1.22	11.32	12.55
2006	0.63	0.36	0.41	0.46	0.31	0.28	0.17	0.27	0.86	0.99	0.39	0.54	2.45	3.22	5.67
2007	1.08	0.53	0.54	0.68	0.39	0.39	1.01	0.85	1.65	4.48	2.58	1.92	3.60	12.48	16.08
2008	0.86	0.45	0.49	0.58	0.35	0.33	0.16	0.21	0.71	0.83	0.33	0.49	3.04	2.72	5.76
2009	0.38	0.24	0.25	0.26	0.24	0.23	0.69	1.48	2.40	3.01	0.89	0.97	1.60	9.44	11.04
2010	0.39	0.24	0.26	0.27	0.25	0.23	0.15	0.16	0.29	0.34	0.25	0.38	1.65	1.58	3.23
2011	1.75	0.80	0.66	1.16	0.56	0.68	0.77	1.07	2.30	3.83	1.36	1.31	5.61	10.64	16.25
2012	2.19	1.01	0.98	1.49	0.86	1.02	0.58	1.44	2.15	2.27	0.66	0.83	7.55	7.93	15.48
2013	0.49	0.29	0.33	0.35	0.27	0.26	0.40	0.73	1.39	1.34	0.94	1.27	1.99	6.06	8.05
2014	0.40	0.25	0.26	0.27	0.25	0.24	0.15	0.16	0.28	0.33	0.25	0.37	1.66	1.54	3.20
2015	0.38	0.24	0.25	0.26	0.24	0.23	0.31	0.56	1.18	1.15	0.84	1.11	1.60	5.13	6.73
2016	0.37	0.23	0.24	0.25	0.24	0.23	0.28	0.51	1.14	1.15	0.79	1.04	1.55	4.91	6.46
2017	1.53	0.71	0.63	1.12	0.52	0.57	0.34	0.63	1.25	1.17	0.89	1.21	5.08	5.49	10.57
2018	0.38	0.24	0.25	0.26	0.24	0.23	0.33	0.60	1.22	1.16	0.88	1.18	1.61	5.36	6.97
2019	0.96	0.48	0.51	0.61	0.36	0.35	0.38	0.70	1.35	1.28	0.93	1.26	3.28	5.91	9.19
2020	1.14	0.55	0.55	0.73	0.40	0.41	0.32	0.58	1.20	1.15	0.86	1.15	3.78	5.26	9.04
2021	2.09	0.96	0.92	1.43	0.82	0.98	1.02	0.85	1.65	4.50	2.63	1.95	7.19	12.59	19.78
2022	1.47	0.69	0.62	1.10	0.51	0.54	1.24	3.60	5.99	7.16	4.46	3.44	4.93	25.88	30.81
2023	2.29	1.07	1.03	1.56	0.91	1.06	0.92	0.95	1.93	4.40	1.94	1.58	7.92	11.72	19.64
2024	0.91	0.47	0.50	0.60	0.35	0.34	0.54	1.25	1.97	2.08	0.75	0.96	3.17	7.55	10.72
2025	0.79	0.43	0.47	0.55	0.34	0.31	0.35	0.64	1.27	1.19	0.91	1.23	2.89	5.59	8.48

NATO SFP 974357 Project infrastructure. Runoff volume. National vision (minimum).

	OCT	NOV	DEC	JAN	FEB	MAR	APR	MAY	JUN	JUL	AUG	SEP	TMG	TVG	Total
1990	0.19	0.13	0.12	0.12	0.15	0.14	0.21	0.37	1.01	1.13	0.61	0.77	0.84	4.09	4.94
1991	1.43	0.67	0.62	1.08	0.51	0.53	0.33	0.60	1.22	1.16	0.88	1.18	4.83	5.36	10.19
1992	1.62	0.74	0.64	1.14	0.53	0.61	0.38	3.14	4.79	5.11	3.68	2.08	5.29	19.18	24.47
1993	1.77	0.80	0.67	1.17	0.57	0.69	0.81	1.03	2.23	4.07	1.48	1.38	5.66	11.00	16.66
1994	1.91	0.86	0.78	1.26	0.69	0.85	1.00	0.85	1.67	4.47	2.51	1.88	6.34	12.37	18.72
1995	1.73	0.79	0.66	1.16	0.55	0.67	0.09	0.10	0.11	0.12	0.12	0.16	5.57	0.70	6.26
1996	0.20	0.14	0.13	0.13	0.16	0.14	0.17	0.26	0.84	0.96	0.38	0.53	0.90	3.14	4.04
1997	0.38	0.24	0.25	0.26	0.24	0.23	0.04	0.04	0.04	0.04	0.04	0.05	1.60	0.26	1.86
1998	0.14	0.09	0.09	0.09	0.11	0.10	0.30	2.94	4.83	4.52	3.35	1.76	0.60	17.69	18.29
1999	1.03	0.51	0.53	0.65	0.38	0.37	0.15	0.16	0.26	0.30	0.24	0.36	3.46	1.45	4.91
2000	0.70	0.39	0.45	0.51	0.32	0.29	0.03	0.04	0.04	0.04	0.04	0.05	2.66	0.22	2.88
2001	0.01	0.01	0.01	0.01	0.01	0.01	0.01	0.01	0.01	0.01	0.01	0.01	0.04	0.05	0.09
2002	0.01	0.01	0.01	0.01	0.01	0.01	0.15	0.20	0.67	0.78	0.32	0.48	0.05	2.60	2.65
2003	0.45	0.27	0.30	0.32	0.26	0.25	0.63	1.66	2.39	2.55	0.60	0.74	1.85	8.57	10.42
2004	0.29	0.19	0.19	0.20	0.21	0.20	0.18	0.28	0.88	1.01	0.41	0.56	1.27	3.32	4.59
2005	0.28	0.18	0.18	0.19	0.20	0.19	0.86	1.00	2.11	4.26	1.64	1.44	1.22	11.32	12.55
2006	0.63	0.36	0.41	0.46	0.31	0.28	0.17	0.27	0.86	0.99	0.39	0.54	2.45	3.22	5.67
2007	0.19	0.13	0.12	0.12	0.15	0.14	0.03	0.03	0.03	0.03	0.03	0.04	0.85	0.20	1.05
2008	0.06	0.04	0.04	0.04	0.04	0.04	0.10	0.11	0.12	0.13	0.12	0.17	0.25	0.74	0.99
2009	0.63	0.36	0.42	0.47	0.31	0.28	0.03	0.03	0.03	0.03	0.03	0.04	2.47	0.18	2.65
2010	1.08	0.53	0.54	0.68	0.39	0.39	0.04	0.04	0.04	0.04	0.04	0.05	3.60	0.26	3.86
2011	1.82	0.83	0.70	1.19	0.60	0.74	0.82	1.02	2.21	4.12	1.51	1.39	5.87	11.08	16.95
2012	0.16	0.11	0.10	0.10	0.13	0.12	0.90	0.97	2.00	4.37	1.81	1.52	0.72	11.57	12.29
2013	0.07	0.05	0.05	0.05	0.06	0.05	0.18	0.28	0.88	1.01	0.41	0.56	0.32	3.32	3.64
2014	1.42	0.67	0.62	1.07	0.50	0.52	0.03	0.04	0.04	0.04	0.04	0.05	4.80	0.23	5.03
2015	0.63	0.36	0.41	0.46	0.31	0.28	0.03	0.03	0.03	0.03	0.03	0.04	2.45	0.20	2.65
2016	0.58	0.34	0.39	0.43	0.30	0.27	0.16	0.18	0.52	0.61	0.30	0.45	2.31	2.22	4.53
2017	0.55	0.33	0.37	0.41	0.29	0.27	0.15	0.20	0.63	0.73	0.31	0.47	2.21	2.49	4.70
2018	1.85	0.84	0.72	1.21	0.62	0.77	0.03	0.04	0.04	0.04	0.03	0.05	6.01	0.22	6.23
2019	1.25	0.60	0.58	0.87	0.45	0.45	0.03	0.04	0.04	0.03	0.03	0.04	4.20	0.21	4.41
2020	0.15	0.10	0.10	0.10	0.12	0.11	0.69	1.47	2.40	3.03	0.90	0.98	0.68	9.46	10.14
2021	0.06	0.04	0.04	0.04	0.05	0.05	0.68	1.57	2.43	2.87	0.78	0.88	0.28	9.20	9.48
2022	0.03	0.02	0.02	0.02	0.03	0.02	0.04	0.04	0.04	0.04	0.04	0.05	0.15	0.25	0.40
2023	0.58	0.34	0.39	0.43	0.30	0.27	0.04	0.04	0.04	0.04	0.04	0.05	2.30	0.26	2.56
2024	0.43	0.26	0.29	0.30	0.26	0.24	0.03	0.03	0.03	0.03	0.03	0.04	1.77	0.20	1.97
2025	0.53	0.32	0.36	0.39	0.29	0.26	0.65	1.66	2.42	2.62	0.62	0.75	2.15	8.73	10.88

NATO SFP 974357 Project infrastructure. Runoff volume. Business as usual (minimum).

	OCT	NOV	DEC	JAN	FEB	MAR	APR	MAY	JUN	JUL	AUG	SEP	TMG	TVG	Total
1990	0.19	0.13	0.12	0.12	0.15	0.14	0.21	0.37	1.01	1.13	0.61	0.77	0.84	4.09	4.94
1991	1.43	0.67	0.62	1.08	0.51	0.53	0.33	0.60	1.22	1.16	0.88	1.18	4.83	5.36	10.19
1992	1.62	0.74	0.64	1.14	0.53	0.61	0.38	3.14	4.79	5.11	3.68	2.08	5.29	19.18	24.47
1993	1.77	0.80	0.67	1.17	0.57	0.69	0.81	1.03	2.23	4.07	1.48	1.38	5.66	11.00	16.66
1994	1.91	0.86	0.78	1.26	0.69	0.85	1.00	0.85	1.67	4.47	2.51	1.88	6.34	12.37	18.72
1995	1.73	0.79	0.66	1.16	0.55	0.67	0.09	0.10	0.11	0.12	0.12	0.16	5.57	0.70	6.26
1996	0.20	0.14	0.13	0.13	0.16	0.14	0.17	0.26	0.84	0.96	0.38	0.53	0.90	3.14	4.04
1997	0.38	0.24	0.25	0.26	0.24	0.23	0.04	0.04	0.04	0.04	0.04	0.05	1.60	0.26	1.86
1998	0.14	0.09	0.09	0.09	0.11	0.10	0.30	2.94	4.83	4.52	3.35	1.76	0.60	17.69	18.29
1999	1.03	0.51	0.53	0.65	0.38	0.37	0.15	0.16	0.26	0.30	0.24	0.36	3.46	1.45	4.91
2000	0.70	0.39	0.45	0.51	0.32	0.29	0.03	0.04	0.04	0.04	0.04	0.05	2.66	0.22	2.88
2001	0.01	0.01	0.01	0.01	0.01	0.01	0.01	0.01	0.01	0.01	0.01	0.01	0.04	0.05	0.09
2002	0.01	0.01	0.01	0.01	0.01	0.01	0.15	0.20	0.67	0.78	0.32	0.48	0.05	2.60	2.65
2003	0.45	0.27	0.30	0.32	0.26	0.25	0.63	1.66	2.39	2.55	0.60	0.74	1.85	8.57	10.42
2004	0.29	0.19	0.19	0.20	0.21	0.20	0.18	0.28	0.88	1.01	0.41	0.56	1.27	3.32	4.59
2005	0.28	0.18	0.18	0.19	0.20	0.19	0.86	1.00	2.11	4.26	1.64	1.44	1.22	11.32	12.55
2006	0.63	0.36	0.41	0.46	0.31	0.28	0.17	0.27	0.86	0.99	0.39	0.54	2.45	3.22	5.67
2007	0.18	0.12	0.12	0.12	0.14	0.13	0.15	0.16	0.30	0.35	0.26	0.39	0.80	1.60	2.40
2008	0.19	0.13	0.12	0.12	0.15	0.14	0.15	0.16	0.29	0.33	0.25	0.38	0.84	1.56	2.40
2009	0.57	0.34	0.38	0.42	0.29	0.27	0.16	0.18	0.47	0.55	0.29	0.45	2.27	2.10	4.37
2010	0.18	0.12	0.12	0.12	0.14	0.13	0.20	0.33	0.97	1.09	0.52	0.67	0.80	3.77	4.57
2011	0.33	0.21	0.21	0.22	0.22	0.21	1.02	0.86	1.66	4.51	2.67	1.97	1.40	12.69	14.09
2012	0.49	0.29	0.33	0.35	0.27	0.26	0.89	0.98	2.03	4.35	1.77	1.50	1.99	11.51	13.50
2013	0.17	0.11	0.11	0.11	0.13	0.12	0.53	1.22	1.94	2.05	0.77	0.98	0.75	7.48	8.23
2014	0.17	0.12	0.11	0.11	0.13	0.12	0.16	0.16	0.31	0.36	0.26	0.39	0.77	1.63	2.40
2015	0.27	0.18	0.18	0.18	0.20	0.19	0.15	0.16	0.30	0.35	0.26	0.39	1.18	1.60	2.78
2016	0.40	0.25	0.27	0.28	0.25	0.24	0.20	0.33	0.97	1.09	0.52	0.67	1.68	3.78	5.46
2017	0.56	0.33	0.38	0.42	0.29	0.27	0.20	0.35	0.98	1.10	0.54	0.70	2.26	3.87	6.13
2018	0.25	0.16	0.16	0.16	0.19	0.17	0.20	0.34	0.98	1.10	0.54	0.69	1.10	3.85	4.95
2019	0.22	0.14	0.14	0.14	0.16	0.15	0.16	0.16	0.30	0.35	0.26	0.39	0.96	1.62	2.58
2020	0.64	0.37	0.42	0.47	0.31	0.28	0.42	0.79	1.48	1.46	0.94	1.25	2.48	6.34	8.82
2021	0.16	0.11	0.10	0.10	0.12	0.11	0.95	0.92	1.84	4.43	2.11	1.67	0.70	11.90	12.60
2022	0.13	0.09	0.09	0.09	0.11	0.10	0.16	0.17	0.36	0.42	0.28	0.42	0.60	1.80	2.40
2023	0.38	0.24	0.25	0.26	0.24	0.23	0.42	0.78	1.46	1.44	0.94	1.26	1.60	6.29	7.89
2024	0.35	0.22	0.23	0.24	0.23	0.22	0.15	0.16	0.30	0.35	0.26	0.39	1.50	1.60	3.10
2025	0.86	0.45	0.49	0.58	0.35	0.33	0.97	0.88	1.74	4.44	2.32	1.78	3.06	12.13	15.19

NATO SFP 974357 Project infrastructure. Runoff volume. Optimistic scenario (minimum).

	OCT	NOV	DEC	JAN	FEB	MAR	APR	MAY	JUN	JUL	AUG	SEP	TMG	TVG	Total
1990	0.19	0.13	0.12	0.12	0.15	0.14	0.21	0.37	1.01	1.13	0.61	0.77	0.84	4.09	4.94
1991	1.43	0.67	0.62	1.08	0.51	0.53	0.33	0.60	1.22	1.16	0.88	1.18	4.83	5.36	10.19
1992	1.62	0.74	0.64	1.14	0.53	0.61	0.38	3.14	4.79	5.11	3.68	2.08	5.29	19.18	24.47
1993	1.77	0.80	0.67	1.17	0.57	0.69	0.81	1.03	2.23	4.07	1.48	1.38	5.66	11.00	16.66
1994	1.91	0.86	0.78	1.26	0.69	0.85	1.00	0.85	1.67	4.47	2.51	1.88	6.34	12.37	18.72
1995	1.73	0.79	0.66	1.16	0.55	0.67	0.09	0.10	0.11	0.12	0.12	0.16	5.57	0.70	6.26
1996	0.20	0.14	0.13	0.13	0.16	0.14	0.17	0.26	0.84	0.96	0.38	0.53	0.90	3.14	4.04
1997	0.38	0.24	0.25	0.26	0.24	0.23	0.04	0.04	0.04	0.04	0.04	0.05	1.60	0.26	1.86
1998	0.14	0.09	0.09	0.09	0.11	0.10	0.30	2.94	4.83	4.52	3.35	1.76	0.60	17.69	18.29
1999	1.03	0.51	0.53	0.65	0.38	0.37	0.15	0.16	0.26	0.30	0.24	0.36	3.46	1.45	4.91
2000	0.70	0.39	0.45	0.51	0.32	0.29	0.03	0.04	0.04	0.04	0.04	0.05	2.66	0.22	2.88
2001	0.01	0.01	0.01	0.01	0.01	0.01	0.01	0.01	0.01	0.01	0.01	0.01	0.04	0.05	0.09
2002	0.01	0.01	0.01	0.01	0.01	0.01	0.15	0.20	0.67	0.78	0.32	0.48	0.05	2.60	2.65
2003	0.45	0.27	0.30	0.32	0.26	0.25	0.63	1.66	2.39	2.55	0.60	0.74	1.85	8.57	10.42
2004	0.29	0.19	0.19	0.20	0.21	0.20	0.18	0.28	0.88	1.01	0.41	0.56	1.27	3.32	4.59
2005	0.28	0.18	0.18	0.19	0.20	0.19	0.86	1.00	2.11	4.26	1.64	1.44	1.22	11.32	12.55
2006	0.63	0.36	0.41	0.46	0.31	0.28	0.17	0.27	0.86	0.99	0.39	0.54	2.45	3.22	5.67
2007	1.52	0.71	0.63	1.12	0.52	0.57	0.15	0.16	0.28	0.33	0.25	0.38	5.05	1.55	6.60
2008	0.39	0.24	0.26	0.27	0.25	0.23	0.15	0.16	0.29	0.34	0.25	0.38	1.63	1.57	3.20
2009	0.51	0.31	0.35	0.37	0.28	0.26	0.16	0.19	0.53	0.62	0.30	0.46	2.07	2.24	4.31
2010	0.56	0.33	0.38	0.41	0.29	0.27	0.16	0.16	0.30	0.35	0.26	0.39	2.24	1.62	3.86
2011	1.17	0.56	0.56	0.76	0.42	0.42	0.97	0.89	1.76	4.44	2.28	1.76	3.88	12.08	15.96
2012	0.38	0.24	0.25	0.26	0.24	0.23	0.75	1.10	2.31	3.70	1.30	1.28	1.60	10.44	12.04
2013	0.51	0.31	0.35	0.38	0.28	0.26	0.23	0.42	1.06	1.15	0.69	0.87	2.09	4.42	6.51
2014	0.40	0.25	0.26	0.27	0.25	0.24	0.15	0.16	0.28	0.33	0.25	0.37	1.66	1.54	3.20
2015	0.50	0.30	0.34	0.37	0.28	0.26	0.16	0.19	0.54	0.62	0.30	0.46	2.05	2.26	4.31
2016	0.43	0.27	0.29	0.31	0.26	0.24	0.50	1.07	1.79	1.88	0.84	1.08	1.80	7.17	8.97
2017	0.64	0.37	0.42	0.47	0.31	0.28	0.70	1.43	2.38	3.08	0.94	1.01	2.48	9.54	12.02
2018	0.57	0.34	0.39	0.42	0.30	0.27	0.41	0.78	1.46	1.43	0.94	1.26	2.28	6.27	8.55
2019	0.39	0.24	0.26	0.27	0.24	0.23	0.15	0.16	0.29	0.34	0.25	0.38	1.62	1.58	3.20
2020	0.38	0.24	0.25	0.26	0.24	0.23	0.72	1.23	2.33	3.41	1.16	1.17	1.60	10.02	11.62
2021	0.41	0.25	0.27	0.28	0.25	0.24	0.33	3.03	4.83	4.77	3.49	1.89	1.70	18.35	20.05
2022	0.44	0.27	0.30	0.32	0.26	0.25	0.16	0.17	0.33	0.38	0.27	0.40	1.84	1.70	3.54
2023	1.30	0.63	0.60	0.96	0.47	0.48	0.43	0.82	1.52	1.51	0.93	1.24	4.44	6.45	10.89
2024	0.56	0.33	0.38	0.42	0.29	0.27	1.03	0.92	1.78	4.58	2.73	2.02	2.26	13.07	15.33
2025	0.40	0.25	0.26	0.27	0.25	0.24	0.49	2.47	4.14	4.46	3.05	1.82	1.66	16.42	18.08

NATO SFP 974357 Project infrastructure. Water salinity. National vision (maximum).

	OCT	NOV	DEC	JAN	FEB	MAR	APR	MAY	JUN	JUL	AUG	SEP
1990	1.883	2.098	2.121	2.122	2.027	2.068	1.831	1.523	1.109	1.076	1.295	1.204
1991	0.944	1.207	1.242	1.033	1.325	1.307	1.502	1.253	0.992	1.009	1.106	1.003
1992	0.934	1.183	1.231	1.045	1.286	1.243	1.382	0.751	0.66	0.648	0.714	0.86
1993	0.882	1.142	1.208	1.012	1.268	1.195	1.138	1.055	0.818	0.686	0.935	0.959
1994	0.866	1.121	1.156	0.993	1.201	1.127	1.071	1.127	0.905	0.669	0.791	0.87
1995	0.933	1.169	1.24	1.039	1.313	1.232	2.153	2.118	2.075	2.051	2.066	1.925
1996	1.88	2.121	2.144	2.142	2.042	2.086	1.987	1.74	1.197	1.152	1.533	1.373
1997	1.606	1.853	1.818	1.796	1.838	1.868	3.205	3.118	3.112	3.129	3.149	2.949
1998	1.652	1.71	1.718	1.721	1.692	1.704	1.47	0.753	0.656	0.667	0.725	0.888
1999	1.103	1.374	1.356	1.269	1.519	1.524	2.017	1.998	1.718	1.638	1.759	1.546
2000	1.309	1.548	1.488	1.43	1.65	1.7	3.053	2.995	2.994	3.008	3.021	2.887
2001	3.172	3.535	3.627	3.699	3.504	3.534	3.39	3.249	3.258	3.309	3.348	3.08
2002	3.492	3.559	3.573	3.582	3.554	3.559	2.114	1.927	1.336	1.288	1.661	1.467
2003	1.375	1.575	1.536	1.515	1.59	1.614	1.23	0.9	0.81	0.797	1.254	1.172
2004	1.652	1.903	1.896	1.882	1.847	1.876	1.934	1.679	1.161	1.119	1.481	1.337
2005	1.536	1.681	1.68	1.673	1.649	1.665	1.111	1.057	0.831	0.692	0.899	0.936
2006	1.27	1.522	1.456	1.403	1.605	1.652	1.901	1.675	1.147	1.101	1.483	1.331
2007	1.113	1.348	1.317	1.259	1.438	1.456	1.056	1.12	0.899	0.671	0.775	0.852
2008	1.564	1.828	1.795	1.772	1.809	1.839	2.078	2.046	1.646	1.566	1.751	1.529
2009	0.887	1.119	1.146	0.991	1.195	1.116	1.997	1.973	1.893	1.852	1.879	1.729
2010	0.92	1.168	1.236	1.026	1.312	1.238	1.874	1.834	1.436	1.368	1.608	1.412
2011	1.116	1.356	1.323	1.263	1.448	1.469	1.115	1.058	0.828	0.684	0.903	0.94
2012	1.363	1.549	1.514	1.494	1.565	1.586	1.167	1.013	0.809	0.721	0.981	0.983
2013	1.187	1.451	1.401	1.333	1.571	1.61	1.985	1.931	1.459	1.389	1.66	1.444
2014	1.049	1.291	1.309	1.137	1.413	1.413	2.724	2.69	2.69	2.699	2.707	2.628
2015	1.588	1.832	1.793	1.77	1.826	1.856	3.253	3.169	3.165	3.184	3.204	3.012
2016	2.965	3.15	3.188	3.212	3.119	3.143	2.116	1.98	1.399	1.347	1.692	1.487
2017	1.51	1.747	1.692	1.662	1.776	1.813	3.375	3.305	3.305	3.325	3.342	3.184
2018	0.957	1.192	1.257	1.054	1.334	1.263	2.542	2.514	2.513	2.52	2.527	2.459
2019	1.118	1.372	1.365	1.266	1.516	1.514	2.848	2.806	2.806	2.816	2.826	2.729
2020	0.978	1.238	1.263	1.067	1.358	1.352	1.863	1.701	1.166	1.111	1.511	1.344
2021	0.928	1.159	1.229	1.038	1.298	1.21	2.347	2.312	2.304	2.306	2.314	2.219
2022	0.852	1.105	1.124	0.97	1.168	1.097	1.181	0.989	0.806	0.723	1.024	1.016
2023	0.815	1.004	1.019	0.902	1.063	1.018	2.201	2.184	2.183	2.187	2.191	2.149
2024	0.79	0.967	0.982	0.875	1.024	0.987	2.147	2.132	2.132	2.135	2.139	2.103
2025	2.559	2.854	2.928	2.975	2.789	2.84	3.461	3.324	3.326	3.367	3.402	3.124

NATO SFP 974357 Project infrastructure. Water salinity. Business as usual (maximum).

	OCT	NOV	DEC	JAN	FEB	MAR	APR	MAY	JUN	JUL	AUG	SEP
1990	1.883	2.098	2.121	2.122	2.027	2.068	1.831	1.523	1.109	1.076	1.295	1.204
1991	0.944	1.207	1.242	1.033	1.325	1.307	1.502	1.253	0.992	1.009	1.106	1.003
1992	0.934	1.183	1.231	1.045	1.286	1.243	1.382	0.751	0.66	0.648	0.714	0.86
1993	0.882	1.142	1.208	1.012	1.268	1.195	1.138	1.055	0.818	0.686	0.935	0.959
1994	0.866	1.121	1.156	0.993	1.201	1.127	1.071	1.127	0.905	0.669	0.791	0.87
1995	0.933	1.169	1.24	1.039	1.313	1.232	2.153	2.118	2.075	2.051	2.066	1.925
1996	1.88	2.121	2.144	2.142	2.042	2.086	1.987	1.74	1.197	1.152	1.533	1.373
1997	1.606	1.853	1.818	1.796	1.838	1.868	3.205	3.118	3.112	3.129	3.149	2.949
1998	1.652	1.71	1.718	1.721	1.692	1.704	1.47	0.753	0.656	0.667	0.725	0.888
1999	1.103	1.374	1.356	1.269	1.519	1.524	2.017	1.998	1.718	1.638	1.759	1.546
2000	1.309	1.548	1.488	1.43	1.65	1.7	3.053	2.995	2.994	3.008	3.021	2.887
2001	3.172	3.535	3.627	3.699	3.504	3.534	3.39	3.249	3.258	3.309	3.348	3.08
2002	3.492	3.559	3.573	3.582	3.554	3.559	2.114	1.927	1.336	1.288	1.661	1.467
2003	1.375	1.575	1.536	1.515	1.59	1.614	1.23	0.9	0.81	0.797	1.254	1.172
2004	1.652	1.903	1.896	1.882	1.847	1.876	1.934	1.679	1.161	1.119	1.481	1.337
2005	1.536	1.681	1.68	1.673	1.649	1.665	1.111	1.057	0.831	0.692	0.899	0.936
2006	1.27	1.522	1.456	1.403	1.605	1.652	1.901	1.675	1.147	1.101	1.483	1.331
2007	1.065	1.31	1.294	1.227	1.408	1.412	1.08	0.959	0.788	0.661	0.77	0.843
2008	1.454	1.71	1.654	1.624	1.737	1.774	2.055	2.02	1.604	1.526	1.728	1.506
2009	0.883	1.139	1.21	1.006	1.278	1.198	1.544	1.3	1.009	1.01	1.132	1.033
2010	2.024	2.298	2.335	2.338	2.202	2.259	2.119	2.089	1.702	1.623	1.789	1.571
2011	1.22	1.412	1.368	1.328	1.467	1.494	1.072	0.97	0.796	0.662	0.769	0.841
2012	0.905	1.169	1.225	1.014	1.296	1.244	1.238	0.906	0.806	0.794	1.25	1.166
2013	1.271	1.506	1.445	1.401	1.569	1.608	1.444	1.181	0.96	0.972	1.087	0.989
2014	1.934	2.21	2.238	2.236	2.117	2.168	2.135	2.11	1.763	1.68	1.82	1.599
2015	1.973	2.249	2.281	2.281	2.153	2.208	2.127	2.1	1.735	1.654	1.805	1.586
2016	2.012	2.285	2.321	2.324	2.19	2.246	2.108	2.073	1.658	1.581	1.768	1.551
2017	1.072	1.342	1.334	1.231	1.486	1.485	1.98	1.958	1.631	1.553	1.709	1.497
2018	1.379	1.631	1.564	1.523	1.691	1.735	2.054	2.027	1.652	1.571	1.745	1.522
2019	1.114	1.385	1.362	1.28	1.527	1.538	1.993	1.969	1.628	1.549	1.713	1.498
2020	1.019	1.293	1.294	1.168	1.428	1.425	1.783	1.548	1.087	1.046	1.357	1.241
2021	0.883	1.129	1.196	1.004	1.259	1.171	1.799	1.638	1.136	1.083	1.47	1.319
2022	0.881	1.135	1.177	1.013	1.222	1.151	1.266	0.822	0.696	0.67	0.758	0.885
2023	0.856	1.107	1.137	0.973	1.185	1.107	1.497	1.261	0.995	1.009	1.111	1.008
2024	2.015	2.29	2.326	2.329	2.193	2.25	2.12	2.091	1.708	1.628	1.791	1.573
2025	2.015	2.29	2.326	2.329	2.193	2.25	2.12	2.091	1.708	1.628	1.791	1.573

NATO SFP 974357 Project infrastructure. Water salinity. Optimistic scenario (maximum).

	OCT	NOV	DEC	JAN	FEB	MAR	APR	MAY	JUN	JUL	AUG	SEP
1990	1.883	2.098	2.121	2.122	2.027	2.068	1.831	1.523	1.109	1.076	1.295	1.204
1991	0.944	1.207	1.242	1.033	1.325	1.307	1.502	1.253	0.992	1.009	1.106	1.003
1992	0.934	1.183	1.231	1.045	1.286	1.243	1.382	0.751	0.66	0.648	0.714	0.86
1993	0.882	1.142	1.208	1.012	1.268	1.195	1.138	1.055	0.818	0.686	0.935	0.959
1994	0.866	1.121	1.156	0.993	1.201	1.127	1.071	1.127	0.905	0.669	0.791	0.87
1995	0.933	1.169	1.24	1.039	1.313	1.232	2.153	2.118	2.075	2.051	2.066	1.925
1996	1.88	2.121	2.144	2.142	2.042	2.086	1.987	1.74	1.197	1.152	1.533	1.373
1997	1.606	1.853	1.818	1.796	1.838	1.868	3.205	3.118	3.112	3.129	3.149	2.949
1998	1.652	1.71	1.718	1.721	1.692	1.704	1.47	0.753	0.656	0.667	0.725	0.888
1999	1.103	1.374	1.356	1.269	1.519	1.524	2.017	1.998	1.718	1.638	1.759	1.546
2000	1.309	1.548	1.488	1.43	1.65	1.7	3.053	2.995	2.994	3.008	3.021	2.887
2001	3.172	3.535	3.627	3.699	3.504	3.534	3.39	3.249	3.258	3.309	3.348	3.08
2002	3.492	3.559	3.573	3.582	3.554	3.559	2.114	1.927	1.336	1.288	1.661	1.467
2003	1.375	1.575	1.536	1.515	1.59	1.614	1.23	0.9	0.81	0.797	1.254	1.172
2004	1.652	1.903	1.896	1.882	1.847	1.876	1.934	1.679	1.161	1.119	1.481	1.337
2005	1.536	1.681	1.68	1.673	1.649	1.665	1.111	1.057	0.831	0.692	0.899	0.936
2006	1.27	1.522	1.456	1.403	1.605	1.652	1.901	1.675	1.147	1.101	1.483	1.331
2007	1.036	1.294	1.285	1.202	1.401	1.401	1.061	1.123	0.9	0.671	0.781	0.858
2008	1.148	1.417	1.375	1.304	1.543	1.573	1.953	1.792	1.216	1.16	1.568	1.379
2009	1.437	1.621	1.599	1.584	1.612	1.63	1.195	0.931	0.806	0.76	1.098	1.068
2010	1.536	1.798	1.758	1.734	1.791	1.823	2.088	2.062	1.695	1.612	1.773	1.55
2011	0.884	1.145	1.21	1.012	1.272	1.201	1.157	1.041	0.809	0.698	0.962	0.972
2012	0.821	1.057	1.071	0.93	1.115	1.056	1.26	0.941	0.825	0.812	1.213	1.129
2013	1.355	1.581	1.529	1.5	1.614	1.645	1.447	1.183	0.963	0.975	1.089	0.991
2014	1.534	1.795	1.754	1.73	1.79	1.822	2.095	2.07	1.718	1.635	1.785	1.561
2015	1.482	1.712	1.683	1.664	1.7	1.725	1.586	1.307	1.028	1.035	1.142	1.045
2016	1.503	1.735	1.709	1.691	1.717	1.741	1.633	1.347	1.042	1.038	1.165	1.071
2017	0.922	1.185	1.233	1.019	1.311	1.272	1.482	1.236	0.984	1.003	1.098	0.994
2018	1.476	1.703	1.673	1.654	1.692	1.717	1.545	1.271	1.014	1.029	1.123	1.024
2019	1.076	1.349	1.324	1.248	1.474	1.487	1.451	1.194	0.964	0.98	1.086	0.985
2020	1.018	1.295	1.292	1.18	1.427	1.425	1.529	1.271	1.001	1.015	1.117	1.015
2021	0.843	1.089	1.101	0.957	1.143	1.081	1.068	1.13	0.911	0.668	0.782	0.863
2022	0.989	1.216	1.244	1.078	1.296	1.28	1.04	0.737	0.63	0.6	0.688	0.748
2023	0.817	1.049	1.064	0.928	1.107	1.054	1.102	1.091	0.865	0.671	0.863	0.923
2024	1.091	1.355	1.324	1.255	1.467	1.485	1.294	0.983	0.854	0.84	1.163	1.074
2025	1.15	1.409	1.362	1.297	1.514	1.548	1.493	1.232	0.987	1.006	1.099	0.998

NATO SFP 974357 Project infrastructure. Water salinity. National vision (minimum).

	OCT	NOV	DEC	JAN	FEB	MAR	APR	MAY	JUN	JUL	AUG	SEP
1990	1.883	2.098	2.121	2.122	2.027	2.068	1.831	1.523	1.109	1.076	1.295	1.204
1991	0.944	1.207	1.242	1.033	1.325	1.307	1.502	1.253	0.992	1.009	1.106	1.003
1992	0.934	1.183	1.231	1.045	1.286	1.243	1.382	0.751	0.66	0.648	0.714	0.86
1993	0.882	1.142	1.208	1.012	1.268	1.195	1.138	1.055	0.818	0.686	0.935	0.959
1994	0.866	1.121	1.156	0.993	1.201	1.127	1.071	1.127	0.905	0.669	0.791	0.87
1995	0.933	1.169	1.24	1.039	1.313	1.232	2.153	2.118	2.075	2.051	2.066	1.925
1996	1.88	2.121	2.144	2.142	2.042	2.086	1.987	1.74	1.197	1.152	1.533	1.373
1997	1.606	1.853	1.818	1.796	1.838	1.868	3.205	3.118	3.112	3.129	3.149	2.949
1998	1.652	1.71	1.718	1.721	1.692	1.704	1.47	0.753	0.656	0.667	0.725	0.888
1999	1.103	1.374	1.356	1.269	1.519	1.524	2.017	1.998	1.718	1.638	1.759	1.546
2000	1.309	1.548	1.488	1.43	1.65	1.7	3.053	2.995	2.994	3.008	3.021	2.887
2001	3.172	3.535	3.627	3.699	3.504	3.534	3.39	3.249	3.258	3.309	3.348	3.08
2002	3.492	3.559	3.573	3.582	3.554	3.559	2.114	1.927	1.336	1.288	1.661	1.467
2003	1.375	1.575	1.536	1.515	1.59	1.614	1.23	0.9	0.81	0.797	1.254	1.172
2004	1.652	1.903	1.896	1.882	1.847	1.876	1.934	1.679	1.161	1.119	1.481	1.337
2005	1.536	1.681	1.68	1.673	1.649	1.665	1.111	1.057	0.831	0.692	0.899	0.936
2006	1.27	1.522	1.456	1.403	1.605	1.652	1.901	1.675	1.147	1.101	1.483	1.331
2007	1.961	2.218	2.25	2.251	2.125	2.178	3.52	3.407	3.406	3.435	3.463	3.218
2008	2.911	3.232	3.306	3.351	3.165	3.217	2.42	2.354	2.264	2.217	2.245	2.033
2009	1.356	1.592	1.527	1.476	1.679	1.731	3.207	3.151	3.151	3.167	3.181	3.053
2010	1.126	1.382	1.371	1.278	1.526	1.526	2.782	2.735	2.731	2.741	2.752	2.639
2011	0.874	1.132	1.194	1.007	1.249	1.172	1.134	1.058	0.821	0.684	0.929	0.956
2012	1.721	1.819	1.832	1.834	1.788	1.808	1.096	1.067	0.845	0.69	0.871	0.92
2013	2.526	2.699	2.734	2.752	2.659	2.689	1.976	1.705	1.195	1.156	1.504	1.362
2014	1.013	1.252	1.286	1.089	1.375	1.358	2.619	2.585	2.584	2.592	2.6	2.52
2015	1.36	1.596	1.531	1.481	1.682	1.733	3.161	3.101	3.1	3.116	3.13	2.994
2016	1.322	1.575	1.507	1.459	1.649	1.696	2.013	1.919	1.367	1.304	1.647	1.432
2017	1.342	1.594	1.527	1.484	1.658	1.702	2.013	1.874	1.284	1.227	1.619	1.413
2018	0.919	1.146	1.206	1.028	1.265	1.178	2.463	2.437	2.437	2.443	2.449	2.388
2019	1.067	1.312	1.323	1.171	1.439	1.439	2.747	2.711	2.71	2.719	2.728	2.643
2020	1.794	1.906	1.922	1.926	1.87	1.894	1.196	0.935	0.812	0.766	1.095	1.067
2021	2.059	2.119	2.131	2.138	2.107	2.117	1.207	0.919	0.814	0.782	1.152	1.107
2022	3.023	3.373	3.458	3.519	3.319	3.364	2.936	2.82	2.814	2.838	2.864	2.626
2023	1.395	1.631	1.564	1.52	1.704	1.753	3.053	2.985	2.98	2.994	3.01	2.849
2024	1.55	1.79	1.742	1.716	1.801	1.835	3.347	3.27	3.269	3.29	3.308	3.135
2025	1.301	1.51	1.459	1.427	1.552	1.582	1.222	0.897	0.805	0.788	1.237	1.163

NATO SFP 974357 Project infrastructure. Water salinity. Business as usual (minimum).

	OCT	NOV	DEC	JAN	FEB	MAR	APR	MAY	JUN	JUL	AUG	SEP
1990	1.883	2.098	2.121	2.122	2.027	2.068	1.831	1.523	1.109	1.076	1.295	1.204
1991	0.944	1.207	1.242	1.033	1.325	1.307	1.502	1.253	0.992	1.009	1.106	1.003
1992	0.934	1.183	1.231	1.045	1.286	1.243	1.382	0.751	0.66	0.648	0.714	0.86
1993	0.882	1.142	1.208	1.012	1.268	1.195	1.138	1.055	0.818	0.686	0.935	0.959
1994	0.866	1.121	1.156	0.993	1.201	1.127	1.071	1.127	0.905	0.669	0.791	0.87
1995	0.933	1.169	1.24	1.039	1.313	1.232	2.153	2.118	2.075	2.051	2.066	1.925
1996	1.88	2.121	2.144	2.142	2.042	2.086	1.987	1.74	1.197	1.152	1.533	1.373
1997	1.606	1.853	1.818	1.796	1.838	1.868	3.205	3.118	3.112	3.129	3.149	2.949
1998	1.652	1.71	1.718	1.721	1.692	1.704	1.47	0.753	0.656	0.667	0.725	0.888
1999	1.103	1.374	1.356	1.269	1.519	1.524	2.017	1.998	1.718	1.638	1.759	1.546
2000	1.309	1.548	1.488	1.43	1.65	1.7	3.053	2.995	2.994	3.008	3.021	2.887
2001	3.172	3.535	3.627	3.699	3.504	3.534	3.39	3.249	3.258	3.309	3.348	3.08
2002	3.492	3.559	3.573	3.582	3.554	3.559	2.114	1.927	1.336	1.288	1.661	1.467
2003	1.375	1.575	1.536	1.515	1.59	1.614	1.23	0.9	0.81	0.797	1.254	1.172
2004	1.652	1.903	1.896	1.882	1.847	1.876	1.934	1.679	1.161	1.119	1.481	1.337
2005	1.536	1.681	1.68	1.673	1.649	1.665	1.111	1.057	0.831	0.692	0.899	0.936
2006	1.27	1.522	1.456	1.403	1.605	1.652	1.901	1.675	1.147	1.101	1.483	1.331
2007	2.015	2.29	2.326	2.329	2.193	2.25	2.12	2.091	1.708	1.628	1.791	1.573
2008	1.981	2.257	2.29	2.29	2.161	2.216	2.125	2.098	1.73	1.648	1.802	1.583
2009	1.335	1.588	1.519	1.474	1.658	1.705	2.016	1.939	1.415	1.349	1.661	1.444
2010	1.929	2.148	2.175	2.177	2.074	2.118	1.881	1.587	1.132	1.097	1.373	1.265
2011	1.47	1.616	1.608	1.599	1.595	1.609	1.052	1.115	0.895	0.676	0.774	0.848
2012	1.328	1.511	1.471	1.448	1.536	1.559	1.1	1.065	0.841	0.684	0.878	0.925
2013	1.818	1.961	1.98	1.982	1.915	1.944	1.311	1.002	0.876	0.864	1.162	1.073
2014	2.042	2.316	2.354	2.358	2.219	2.277	2.116	2.085	1.692	1.613	1.784	1.567
2015	1.749	2.022	2.024	2.01	1.949	1.984	2.106	2.078	1.697	1.615	1.781	1.559
2016	1.475	1.721	1.683	1.66	1.719	1.748	1.846	1.566	1.11	1.073	1.355	1.246
2017	1.307	1.554	1.489	1.445	1.618	1.661	1.813	1.538	1.093	1.056	1.324	1.22
2018	1.729	1.964	1.972	1.963	1.898	1.931	1.858	1.564	1.118	1.083	1.347	1.243
2019	1.887	2.161	2.183	2.178	2.071	2.118	2.111	2.082	1.692	1.612	1.782	1.562
2020	1.235	1.473	1.414	1.364	1.547	1.587	1.412	1.148	0.94	0.944	1.085	0.989
2021	1.722	1.816	1.829	1.831	1.786	1.805	1.078	1.088	0.867	0.686	0.832	0.894
2022	2.22	2.487	2.535	2.55	2.396	2.457	2.103	2.058	1.606	1.535	1.75	1.536
2023	1.467	1.683	1.656	1.639	1.672	1.695	1.425	1.159	0.951	0.956	1.09	0.995
2024	1.594	1.861	1.833	1.812	1.83	1.86	2.092	2.064	1.688	1.606	1.772	1.549
2025	1.114	1.351	1.319	1.26	1.441	1.46	1.071	1.108	0.884	0.674	0.806	0.877

NATO SFP 974357 Project infrastructure. Water salinity. Optimistic scenario (minimum).

	OCT	NOV	DEC	JAN	FEB	MAR	APR	MAY	JUN	JUL	AUG	SEP
1990	1.883	2.098	2.121	2.122	2.027	2.068	1.831	1.523	1.109	1.076	1.295	1.204
1991	0.944	1.207	1.242	1.033	1.325	1.307	1.502	1.253	0.992	1.009	1.106	1.003
1992	0.934	1.183	1.231	1.045	1.286	1.243	1.382	0.751	0.66	0.648	0.714	0.86
1993	0.882	1.142	1.208	1.012	1.268	1.195	1.138	1.055	0.818	0.686	0.935	0.959
1994	0.866	1.121	1.156	0.993	1.201	1.127	1.071	1.127	0.905	0.669	0.791	0.87
1995	0.933	1.169	1.24	1.039	1.313	1.232	2.153	2.118	2.075	2.051	2.066	1.925
1996	1.88	2.121	2.144	2.142	2.042	2.086	1.987	1.74	1.197	1.152	1.533	1.373
1997	1.606	1.853	1.818	1.796	1.838	1.868	3.205	3.118	3.112	3.129	3.149	2.949
1998	1.652	1.71	1.718	1.721	1.692	1.704	1.47	0.753	0.656	0.667	0.725	0.888
1999	1.103	1.374	1.356	1.269	1.519	1.524	2.017	1.998	1.718	1.638	1.759	1.546
2000	1.309	1.548	1.488	1.43	1.65	1.7	3.053	2.995	2.994	3.008	3.021	2.887
2001	3.172	3.535	3.627	3.699	3.504	3.534	3.39	3.249	3.258	3.309	3.348	3.08
2002	3.492	3.559	3.573	3.582	3.554	3.559	2.114	1.927	1.336	1.288	1.661	1.467
2003	1.375	1.575	1.536	1.515	1.59	1.614	1.23	0.9	0.81	0.797	1.254	1.172
2004	1.652	1.903	1.896	1.882	1.847	1.876	1.934	1.679	1.161	1.119	1.481	1.337
2005	1.536	1.681	1.68	1.673	1.649	1.665	1.111	1.057	0.831	0.692	0.899	0.936
2006	1.27	1.522	1.456	1.403	1.605	1.652	1.901	1.675	1.147	1.101	1.483	1.331
2007	0.959	1.209	1.256	1.045	1.34	1.301	1.922	1.905	1.627	1.554	1.687	1.488
2008	1.544	1.806	1.768	1.744	1.796	1.827	2.091	2.065	1.701	1.618	1.777	1.553
2009	1.385	1.638	1.574	1.537	1.688	1.729	2.026	1.926	1.365	1.303	1.651	1.436
2010	1.356	1.608	1.539	1.494	1.676	1.723	2.051	2.025	1.656	1.574	1.745	1.522
2011	1.01	1.271	1.271	1.161	1.377	1.376	1.075	1.106	0.882	0.673	0.812	0.882
2012	1.43	1.605	1.584	1.57	1.596	1.614	1.162	1.023	0.81	0.717	0.97	0.975
2013	1.344	1.585	1.525	1.49	1.632	1.669	1.729	1.439	1.064	1.037	1.219	1.13
2014	1.534	1.795	1.754	1.73	1.79	1.822	2.095	2.07	1.718	1.635	1.785	1.561
2015	1.39	1.644	1.579	1.543	1.691	1.732	2.027	1.923	1.359	1.297	1.649	1.435
2016	1.398	1.609	1.571	1.549	1.621	1.646	1.333	1.039	0.887	0.875	1.125	1.035
2017	1.227	1.444	1.392	1.347	1.508	1.542	1.191	0.939	0.803	0.75	1.079	1.054
2018	1.281	1.513	1.454	1.412	1.572	1.609	1.421	1.157	0.946	0.952	1.086	0.989
2019	1.547	1.81	1.773	1.749	1.799	1.829	2.089	2.063	1.696	1.613	1.774	1.551
2020	1.433	1.611	1.59	1.576	1.603	1.62	1.176	0.988	0.81	0.733	1.008	1.002
2021	1.371	1.502	1.483	1.472	1.502	1.515	1.433	0.749	0.655	0.657	0.717	0.872
2022	1.468	1.724	1.671	1.642	1.746	1.782	2.06	2.028	1.622	1.542	1.736	1.514
2023	0.969	1.235	1.253	1.071	1.347	1.346	1.386	1.13	0.924	0.925	1.082	0.985
2024	1.269	1.454	1.409	1.378	1.495	1.522	1.05	1.09	0.878	0.669	0.768	0.842
2025	1.386	1.524	1.505	1.494	1.521	1.535	1.314	0.794	0.683	0.669	0.745	0.878

Hypothetical option of inflow to Western part. Runoff volume. National vision (maximum).

	OCT	NOV	DEC	JAN	FEB	MAR	APR	MAY	JUN	JUL	AUG	SEP	TMG	TVG	Total
1990	0.19	0.13	0.12	0.12	0.15	0.14	0.21	0.37	1.01	1.13	0.61	0.77	0.84	4.09	4.94
1991	1.43	0.67	0.62	1.08	0.51	0.53	0.33	0.60	1.22	1.16	0.88	1.18	4.83	5.36	10.19
1992	1.62	0.74	0.64	1.14	0.53	0.61	0.38	3.14	4.79	5.11	3.68	2.08	5.29	19.18	24.47
1993	1.77	0.80	0.67	1.17	0.57	0.69	0.81	1.03	2.23	4.07	1.48	1.38	5.66	11.00	16.66
1994	1.91	0.86	0.78	1.26	0.69	0.85	1.00	0.85	1.67	4.47	2.51	1.88	6.34	12.37	18.72
1995	1.73	0.79	0.66	1.16	0.55	0.67	0.09	0.10	0.11	0.12	0.12	0.16	5.57	0.70	6.26
1996	0.20	0.14	0.13	0.13	0.16	0.14	0.17	0.26	0.84	0.96	0.38	0.53	0.90	3.14	4.04
1997	0.38	0.24	0.25	0.26	0.24	0.23	0.04	0.04	0.04	0.04	0.04	0.05	1.60	0.26	1.86
1998	0.14	0.09	0.09	0.09	0.11	0.10	0.30	2.94	4.83	4.52	3.35	1.76	0.60	17.69	18.29
1999	1.03	0.51	0.53	0.65	0.38	0.37	0.15	0.16	0.26	0.30	0.24	0.36	3.46	1.45	4.91
2000	0.70	0.39	0.45	0.51	0.32	0.29	0.03	0.04	0.04	0.04	0.04	0.05	2.66	0.22	2.88
2001	0.01	0.01	0.01	0.01	0.01	0.01	0.01	0.01	0.01	0.01	0.01	0.01	0.04	0.05	0.09
2002	0.01	0.01	0.01	0.01	0.01	0.01	0.15	0.20	0.67	0.78	0.32	0.48	0.05	2.60	2.65
2003	0.45	0.27	0.30	0.32	0.26	0.25	0.63	1.66	2.39	2.55	0.60	0.74	1.85	8.57	10.42
2004	0.29	0.19	0.19	0.20	0.21	0.20	0.18	0.28	0.88	1.01	0.41	0.56	1.27	3.32	4.59
2005	0.28	0.18	0.18	0.19	0.20	0.19	0.86	1.00	2.11	4.26	1.64	1.44	1.22	11.32	12.55
2006	0.63	0.36	0.41	0.46	0.31	0.28	0.17	0.27	0.86	0.99	0.39	0.54	2.45	3.22	5.67
2007	0.87	0.45	0.49	0.58	0.35	0.33	1.02	0.85	1.66	4.50	2.64	1.95	3.07	12.62	15.69
2008	0.37	0.23	0.25	0.26	0.24	0.23	0.16	0.16	0.32	0.37	0.26	0.40	1.57	1.67	3.24
2009	1.93	0.88	0.81	1.29	0.72	0.88	0.12	0.12	0.15	0.17	0.16	0.22	6.51	0.93	7.44
2010	1.68	0.77	0.65	1.15	0.54	0.64	0.16	0.17	0.41	0.48	0.29	0.43	5.44	1.94	7.38
2011	0.86	0.45	0.49	0.58	0.35	0.33	0.86	1.00	2.13	4.25	1.62	1.44	3.04	11.29	14.33
2012	0.45	0.28	0.30	0.32	0.26	0.25	0.74	1.14	2.32	3.60	1.25	1.25	1.86	10.30	12.16
2013	0.80	0.43	0.48	0.56	0.34	0.32	0.16	0.18	0.42	0.49	0.29	0.44	2.92	1.97	4.89
2014	1.30	0.62	0.60	0.95	0.47	0.47	0.03	0.03	0.03	0.03	0.03	0.04	4.41	0.20	4.61
2015	0.39	0.24	0.26	0.27	0.25	0.23	0.04	0.04	0.04	0.04	0.04	0.05	1.65	0.24	1.89
2016	0.05	0.03	0.03	0.03	0.03	0.03	0.15	0.19	0.57	0.66	0.30	0.46	0.20	2.34	2.54
2017	0.46	0.28	0.31	0.33	0.27	0.25	0.03	0.03	0.03	0.03	0.03	0.04	1.90	0.18	2.08
2018	1.67	0.76	0.65	1.15	0.54	0.64	0.03	0.04	0.04	0.04	0.03	0.05	5.40	0.22	5.62
2019	1.11	0.54	0.55	0.70	0.39	0.40	0.03	0.04	0.04	0.03	0.03	0.04	3.68	0.21	3.89
2020	1.35	0.64	0.61	1.01	0.49	0.49	0.16	0.23	0.77	0.89	0.35	0.50	4.59	2.91	7.50
2021	1.79	0.82	0.68	1.17	0.58	0.71	0.05	0.06	0.06	0.06	0.06	0.08	5.75	0.38	6.13
2022	1.97	0.89	0.85	1.33	0.75	0.91	0.72	1.25	2.34	3.36	1.13	1.15	6.69	9.95	16.64
2023	2.49	1.19	1.14	1.70	1.00	1.14	0.03	0.04	0.04	0.04	0.04	0.05	8.65	0.23	8.88
2024	2.71	1.33	1.26	1.85	1.11	1.24	0.03	0.04	0.04	0.04	0.03	0.05	9.50	0.22	9.72
2025	0.06	0.04	0.04	0.04	0.04	0.04	0.02	0.03	0.03	0.02	0.02	0.03	0.25	0.15	0.40

Hypothetical option of inflow to Western part. Runoff volume. Business as usual (maximum).

	OCT	NOV	DEC	JAN	FEB	MAR	APR	MAY	JUN	JUL	AUG	SEP	TMG	TVG	Total
1990	0.19	0.13	0.12	0.12	0.15	0.14	0.21	0.37	1.01	1.13	0.61	0.77	0.84	4.09	4.94
1991	1.43	0.67	0.62	1.08	0.51	0.53	0.33	0.60	1.22	1.16	0.88	1.18	4.83	5.36	10.19
1992	1.62	0.74	0.64	1.14	0.53	0.61	0.38	3.14	4.79	5.11	3.68	2.08	5.29	19.18	24.47
1993	1.77	0.80	0.67	1.17	0.57	0.69	0.81	1.03	2.23	4.07	1.48	1.38	5.66	11.00	16.66
1994	1.91	0.86	0.78	1.26	0.69	0.85	1.00	0.85	1.67	4.47	2.51	1.88	6.34	12.37	18.72
1995	1.73	0.79	0.66	1.16	0.55	0.67	0.09	0.10	0.11	0.12	0.12	0.16	5.57	0.70	6.26
1996	0.20	0.14	0.13	0.13	0.16	0.14	0.17	0.26	0.84	0.96	0.38	0.53	0.90	3.14	4.04
1997	0.38	0.24	0.25	0.26	0.24	0.23	0.04	0.04	0.04	0.04	0.04	0.05	1.60	0.26	1.86
1998	0.14	0.09	0.09	0.09	0.11	0.10	0.30	2.94	4.83	4.52	3.35	1.76	0.60	17.69	18.29
1999	1.03	0.51	0.53	0.65	0.38	0.37	0.15	0.16	0.26	0.30	0.24	0.36	3.46	1.45	4.91
2000	0.70	0.39	0.45	0.51	0.32	0.29	0.03	0.04	0.04	0.04	0.04	0.05	2.66	0.22	2.88
2001	0.01	0.01	0.01	0.01	0.01	0.01	0.01	0.01	0.01	0.01	0.01	0.01	0.04	0.05	0.09
2002	0.01	0.01	0.01	0.01	0.01	0.01	0.15	0.20	0.67	0.78	0.32	0.48	0.05	2.60	2.65
2003	0.45	0.27	0.30	0.32	0.26	0.25	0.63	1.66	2.39	2.55	0.60	0.74	1.85	8.57	10.42
2004	0.29	0.19	0.19	0.20	0.21	0.20	0.18	0.28	0.88	1.01	0.41	0.56	1.27	3.32	4.59
2005	0.28	0.18	0.18	0.19	0.20	0.19	0.86	1.00	2.11	4.26	1.64	1.44	1.22	11.32	12.55
2006	0.63	0.36	0.41	0.46	0.31	0.28	0.17	0.27	0.86	0.99	0.39	0.54	2.45	3.22	5.67
2007	1.01	0.50	0.52	0.64	0.37	0.37	0.97	1.39	2.53	4.70	2.72	2.04	3.40	14.35	17.75
2008	0.46	0.28	0.31	0.33	0.27	0.25	0.16	0.17	0.34	0.39	0.27	0.41	1.88	1.73	3.61
2009	1.76	0.80	0.67	1.17	0.56	0.69	0.29	0.53	1.16	1.15	0.82	1.08	5.64	5.02	10.66
2010	0.18	0.12	0.11	0.11	0.14	0.13	0.16	0.16	0.30	0.35	0.26	0.39	0.79	1.61	2.40
2011	0.65	0.37	0.42	0.48	0.31	0.28	0.98	1.33	2.44	4.70	2.72	2.05	2.51	14.21	16.72
2012	1.60	0.74	0.64	1.14	0.53	0.61	0.62	1.60	2.32	2.45	0.60	0.74	5.25	8.33	13.58
2013	0.59	0.34	0.39	0.43	0.30	0.27	0.40	0.73	1.39	1.34	0.94	1.27	2.33	6.06	8.39
2014	0.20	0.14	0.13	0.13	0.16	0.14	0.15	0.16	0.27	0.31	0.25	0.37	0.90	1.50	2.40
2015	0.19	0.13	0.12	0.12	0.15	0.14	0.15	0.16	0.28	0.33	0.25	0.38	0.85	1.55	2.40
2016	0.18	0.12	0.12	0.12	0.14	0.13	0.16	0.17	0.32	0.38	0.27	0.40	0.80	1.69	2.49
2017	1.11	0.54	0.55	0.70	0.39	0.40	0.15	0.16	0.30	0.35	0.26	0.39	3.68	1.60	5.28
2018	0.53	0.32	0.36	0.39	0.29	0.26	0.16	0.16	0.31	0.36	0.26	0.39	2.15	1.63	3.78
2019	0.99	0.49	0.52	0.63	0.37	0.36	0.16	0.16	0.30	0.35	0.26	0.39	3.36	1.62	4.98
2020	1.17	0.56	0.56	0.77	0.42	0.42	0.19	0.32	0.96	1.08	0.49	0.64	3.90	3.67	7.57
2021	1.83	0.83	0.70	1.19	0.60	0.75	0.17	0.25	0.82	0.94	0.37	0.52	5.89	3.06	8.95
2022	1.88	0.85	0.75	1.23	0.65	0.81	0.57	2.32	3.92	4.50	2.98	1.86	6.17	16.14	22.31
2023	1.92	0.87	0.80	1.28	0.71	0.87	0.32	0.58	1.20	1.15	0.86	1.15	6.46	5.27	11.73
2024	0.18	0.12	0.12	0.12	0.14	0.13	0.15	0.16	0.30	0.35	0.26	0.39	0.80	1.60	2.40
2025	0.18	0.12	0.12	0.12	0.14	0.13	0.15	0.16	0.30	0.35	0.26	0.39	0.80	1.60	2.40

Hypothetical option of inflow to Western part. Runoff volume. Optimistic scenario (maximum).

	OCT	NOV	DEC	JAN	FEB	MAR	APR	MAY	JUN	JUL	AUG	SEP	TMG	TVG	Total
1990	0.19	0.13	0.12	0.12	0.15	0.14	0.21	0.37	1.01	1.13	0.61	0.77	0.84	4.09	4.94
1991	1.43	0.67	0.62	1.08	0.51	0.53	0.33	0.60	1.22	1.16	0.88	1.18	4.83	5.36	10.19
1992	1.62	0.74	0.64	1.14	0.53	0.61	0.38	3.14	4.79	5.11	3.68	2.08	5.29	19.18	24.47
1993	1.77	0.80	0.67	1.17	0.57	0.69	0.81	1.03	2.23	4.07	1.48	1.38	5.66	11.00	16.66
1994	1.91	0.86	0.78	1.26	0.69	0.85	1.00	0.85	1.67	4.47	2.51	1.88	6.34	12.37	18.72
1995	1.73	0.79	0.66	1.16	0.55	0.67	0.09	0.10	0.11	0.12	0.12	0.16	5.57	0.70	6.26
1996	0.20	0.14	0.13	0.13	0.16	0.14	0.17	0.26	0.84	0.96	0.38	0.53	0.90	3.14	4.04
1997	0.38	0.24	0.25	0.26	0.24	0.23	0.04	0.04	0.04	0.04	0.04	0.05	1.60	0.26	1.86
1998	0.14	0.09	0.09	0.09	0.11	0.10	0.30	2.94	4.83	4.52	3.35	1.76	0.60	17.69	18.29
1999	1.03	0.51	0.53	0.65	0.38	0.37	0.15	0.16	0.26	0.30	0.24	0.36	3.46	1.45	4.91
2000	0.70	0.39	0.45	0.51	0.32	0.29	0.03	0.04	0.04	0.04	0.04	0.05	2.66	0.22	2.88
2001	0.01	0.01	0.01	0.01	0.01	0.01	0.01	0.01	0.01	0.01	0.01	0.01	0.04	0.05	0.09
2002	0.01	0.01	0.01	0.01	0.01	0.01	0.15	0.20	0.67	0.78	0.32	0.48	0.05	2.60	2.65
2003	0.45	0.27	0.30	0.32	0.26	0.25	0.63	1.66	2.39	2.55	0.60	0.74	1.85	8.57	10.42
2004	0.29	0.19	0.19	0.20	0.21	0.20	0.18	0.28	0.88	1.01	0.41	0.56	1.27	3.32	4.59
2005	0.28	0.18	0.18	0.19	0.20	0.19	0.86	1.00	2.11	4.26	1.64	1.44	1.22	11.32	12.55
2006	0.63	0.36	0.41	0.46	0.31	0.28	0.17	0.27	0.86	0.99	0.39	0.54	2.45	3.22	5.67
2007	1.08	0.53	0.54	0.68	0.39	0.39	1.01	0.85	1.65	4.48	2.58	1.92	3.60	12.48	16.08
2008	0.86	0.45	0.49	0.58	0.35	0.33	0.16	0.21	0.71	0.83	0.33	0.49	3.04	2.72	5.76
2009	0.38	0.24	0.25	0.26	0.24	0.23	0.69	1.48	2.40	3.01	0.89	0.97	1.60	9.44	11.04
2010	0.39	0.24	0.26	0.27	0.25	0.23	0.15	0.16	0.29	0.34	0.25	0.38	1.65	1.58	3.23
2011	1.75	0.80	0.66	1.16	0.56	0.68	0.77	1.07	2.30	3.83	1.36	1.31	5.61	10.64	16.25
2012	2.19	1.01	0.98	1.49	0.86	1.02	0.58	1.44	2.15	2.27	0.66	0.83	7.55	7.93	15.48
2013	0.49	0.29	0.33	0.35	0.27	0.26	0.40	0.73	1.39	1.34	0.94	1.27	1.99	6.06	8.05
2014	0.40	0.25	0.26	0.27	0.25	0.24	0.15	0.16	0.28	0.33	0.25	0.37	1.66	1.54	3.20
2015	0.38	0.24	0.25	0.26	0.24	0.23	0.31	0.56	1.18	1.15	0.84	1.11	1.60	5.13	6.73
2016	0.37	0.23	0.24	0.25	0.24	0.23	0.28	0.51	1.14	1.15	0.79	1.04	1.55	4.91	6.46
2017	1.53	0.71	0.63	1.12	0.52	0.57	0.34	0.63	1.25	1.17	0.89	1.21	5.08	5.49	10.57
2018	0.38	0.24	0.25	0.26	0.24	0.23	0.33	0.60	1.22	1.16	0.88	1.18	1.61	5.36	6.97
2019	0.96	0.48	0.51	0.61	0.36	0.35	0.38	0.70	1.35	1.28	0.93	1.26	3.28	5.91	9.19
2020	1.14	0.55	0.55	0.73	0.40	0.41	0.32	0.58	1.20	1.15	0.86	1.15	3.78	5.26	9.04
2021	2.09	0.96	0.92	1.43	0.82	0.98	1.02	0.85	1.65	4.50	2.63	1.95	7.19	12.59	19.78
2022	1.47	0.69	0.62	1.10	0.51	0.54	1.24	3.60	5.99	7.16	4.46	3.44	4.93	25.88	30.81
2023	2.29	1.07	1.03	1.56	0.91	1.06	0.92	0.95	1.93	4.40	1.94	1.58	7.92	11.72	19.64
2024	0.91	0.47	0.50	0.60	0.35	0.34	0.54	1.25	1.97	2.08	0.75	0.96	3.17	7.55	10.72
2025	0.79	0.43	0.47	0.55	0.34	0.31	0.35	0.64	1.27	1.19	0.91	1.23	2.89	5.59	8.48

Hypothetical option of inflow to Western part. Runoff volume. National vision (minimum).

	OCT	NOV	DEC	JAN	FEB	MAR	APR	MAY	JUN	JUL	AUG	SEP	TMG	TVG	Total
1990	0.19	0.13	0.12	0.12	0.15	0.14	0.21	0.37	1.01	1.13	0.61	0.77	0.84	4.09	4.94
1991	1.43	0.67	0.62	1.08	0.51	0.53	0.33	0.60	1.22	1.16	0.88	1.18	4.83	5.36	10.19
1992	1.62	0.74	0.64	1.14	0.53	0.61	0.38	3.14	4.79	5.11	3.68	2.08	5.29	19.18	24.47
1993	1.77	0.80	0.67	1.17	0.57	0.69	0.81	1.03	2.23	4.07	1.48	1.38	5.66	11.00	16.66
1994	1.91	0.86	0.78	1.26	0.69	0.85	1.00	0.85	1.67	4.47	2.51	1.88	6.34	12.37	18.72
1995	1.73	0.79	0.66	1.16	0.55	0.67	0.09	0.10	0.11	0.12	0.12	0.16	5.57	0.70	6.26
1996	0.20	0.14	0.13	0.13	0.16	0.14	0.17	0.26	0.84	0.96	0.38	0.53	0.90	3.14	4.04
1997	0.38	0.24	0.25	0.26	0.24	0.23	0.04	0.04	0.04	0.04	0.04	0.05	1.60	0.26	1.86
1998	0.14	0.09	0.09	0.09	0.11	0.10	0.30	2.94	4.83	4.52	3.35	1.76	0.60	17.69	18.29
1999	1.03	0.51	0.53	0.65	0.38	0.37	0.15	0.16	0.26	0.30	0.24	0.36	3.46	1.45	4.91
2000	0.70	0.39	0.45	0.51	0.32	0.29	0.03	0.04	0.04	0.04	0.04	0.05	2.66	0.22	2.88
2001	0.01	0.01	0.01	0.01	0.01	0.01	0.01	0.01	0.01	0.01	0.01	0.01	0.04	0.05	0.09
2002	0.01	0.01	0.01	0.01	0.01	0.01	0.15	0.20	0.67	0.78	0.32	0.48	0.05	2.60	2.65
2003	0.45	0.27	0.30	0.32	0.26	0.25	0.63	1.66	2.39	2.55	0.60	0.74	1.85	8.57	10.42
2004	0.29	0.19	0.19	0.20	0.21	0.20	0.18	0.28	0.88	1.01	0.41	0.56	1.27	3.32	4.59
2005	0.28	0.18	0.18	0.19	0.20	0.19	0.86	1.00	2.11	4.26	1.64	1.44	1.22	11.32	12.55
2006	0.63	0.36	0.41	0.46	0.31	0.28	0.17	0.27	0.86	0.99	0.39	0.54	2.45	3.22	5.67
2007	0.19	0.13	0.12	0.12	0.15	0.14	0.03	0.03	0.03	0.03	0.03	0.04	0.85	0.20	1.05
2008	0.06	0.04	0.04	0.04	0.04	0.04	0.10	0.11	0.12	0.13	0.12	0.17	0.25	0.74	0.99
2009	0.63	0.36	0.42	0.47	0.31	0.28	0.03	0.03	0.03	0.03	0.03	0.04	2.47	0.18	2.65
2010	1.08	0.53	0.54	0.68	0.39	0.39	0.04	0.04	0.04	0.04	0.04	0.05	3.60	0.26	3.86
2011	1.82	0.83	0.70	1.19	0.60	0.74	0.82	1.02	2.21	4.12	1.51	1.39	5.87	11.08	16.95
2012	0.16	0.11	0.10	0.10	0.13	0.12	0.90	0.97	2.00	4.37	1.81	1.52	0.72	11.57	12.29
2013	0.07	0.05	0.05	0.05	0.06	0.05	0.18	0.28	0.88	1.01	0.41	0.56	0.32	3.32	3.64
2014	1.42	0.67	0.62	1.07	0.50	0.52	0.03	0.04	0.04	0.04	0.04	0.05	4.80	0.23	5.03
2015	0.63	0.36	0.41	0.46	0.31	0.28	0.03	0.03	0.03	0.03	0.03	0.04	2.45	0.20	2.65
2016	0.58	0.34	0.39	0.43	0.30	0.27	0.16	0.18	0.52	0.61	0.30	0.45	2.31	2.22	4.53
2017	0.55	0.33	0.37	0.41	0.29	0.27	0.15	0.20	0.63	0.73	0.31	0.47	2.21	2.49	4.70
2018	1.85	0.84	0.72	1.21	0.62	0.77	0.03	0.04	0.04	0.04	0.03	0.05	6.01	0.22	6.23
2019	1.25	0.60	0.58	0.87	0.45	0.45	0.03	0.04	0.04	0.03	0.03	0.04	4.20	0.21	4.41
2020	0.15	0.10	0.10	0.10	0.12	0.11	0.69	1.47	2.40	3.03	0.90	0.98	0.68	9.46	10.14
2021	0.06	0.04	0.04	0.04	0.05	0.05	0.68	1.57	2.43	2.87	0.78	0.88	0.28	9.20	9.48
2022	0.03	0.02	0.02	0.02	0.03	0.02	0.04	0.04	0.04	0.04	0.04	0.05	0.15	0.25	0.40
2023	0.58	0.34	0.39	0.43	0.30	0.27	0.04	0.04	0.04	0.04	0.04	0.05	2.30	0.26	2.56
2024	0.43	0.26	0.29	0.30	0.26	0.24	0.03	0.03	0.03	0.03	0.03	0.04	1.77	0.20	1.97
2025	0.53	0.32	0.36	0.39	0.29	0.26	0.65	1.66	2.42	2.62	0.62	0.75	2.15	8.73	10.88

Hypothetical option of inflow to Western part. Runoff volume. Business as usual (minimum).

	OCT	NOV	DEC	JAN	FEB	MAR	APR	MAY	JUN	JUL	AUG	SEP	TMG	TVG	Total
1990	0.19	0.13	0.12	0.12	0.15	0.14	0.21	0.37	1.01	1.13	0.61	0.77	0.84	4.09	4.94
1991	1.43	0.67	0.62	1.08	0.51	0.53	0.33	0.60	1.22	1.16	0.88	1.18	4.83	5.36	10.19
1992	1.62	0.74	0.64	1.14	0.53	0.61	0.38	3.14	4.79	5.11	3.68	2.08	5.29	19.18	24.47
1993	1.77	0.80	0.67	1.17	0.57	0.69	0.81	1.03	2.23	4.07	1.48	1.38	5.66	11.00	16.66
1994	1.91	0.86	0.78	1.26	0.69	0.85	1.00	0.85	1.67	4.47	2.51	1.88	6.34	12.37	18.72
1995	1.73	0.79	0.66	1.16	0.55	0.67	0.09	0.10	0.11	0.12	0.12	0.16	5.57	0.70	6.26
1996	0.20	0.14	0.13	0.13	0.16	0.14	0.17	0.26	0.84	0.96	0.38	0.53	0.90	3.14	4.04
1997	0.38	0.24	0.25	0.26	0.24	0.23	0.04	0.04	0.04	0.04	0.04	0.05	1.60	0.26	1.86
1998	0.14	0.09	0.09	0.09	0.11	0.10	0.30	2.94	4.83	4.52	3.35	1.76	0.60	17.69	18.29
1999	1.03	0.51	0.53	0.65	0.38	0.37	0.15	0.16	0.26	0.30	0.24	0.36	3.46	1.45	4.91
2000	0.70	0.39	0.45	0.51	0.32	0.29	0.03	0.04	0.04	0.04	0.04	0.05	2.66	0.22	2.88
2001	0.01	0.01	0.01	0.01	0.01	0.01	0.01	0.01	0.01	0.01	0.01	0.01	0.04	0.05	0.09
2002	0.01	0.01	0.01	0.01	0.01	0.01	0.15	0.20	0.67	0.78	0.32	0.48	0.05	2.60	2.65
2003	0.45	0.27	0.30	0.32	0.26	0.25	0.63	1.66	2.39	2.55	0.60	0.74	1.85	8.57	10.42
2004	0.29	0.19	0.19	0.20	0.21	0.20	0.18	0.28	0.88	1.01	0.41	0.56	1.27	3.32	4.59
2005	0.28	0.18	0.18	0.19	0.20	0.19	0.86	1.00	2.11	4.26	1.64	1.44	1.22	11.32	12.55
2006	0.63	0.36	0.41	0.46	0.31	0.28	0.17	0.27	0.86	0.99	0.39	0.54	2.45	3.22	5.67
2007	0.18	0.12	0.12	0.12	0.14	0.13	0.15	0.16	0.30	0.35	0.26	0.39	0.80	1.60	2.40
2008	0.19	0.13	0.12	0.12	0.15	0.14	0.15	0.16	0.29	0.33	0.25	0.38	0.84	1.56	2.40
2009	0.57	0.34	0.38	0.42	0.29	0.27	0.16	0.18	0.47	0.55	0.29	0.45	2.27	2.10	4.37
2010	0.18	0.12	0.12	0.12	0.14	0.13	0.20	0.33	0.97	1.09	0.52	0.67	0.80	3.77	4.57
2011	0.33	0.21	0.21	0.22	0.22	0.21	1.02	0.86	1.66	4.51	2.67	1.97	1.40	12.69	14.09
2012	0.49	0.29	0.33	0.35	0.27	0.26	0.89	0.98	2.03	4.35	1.77	1.50	1.99	11.51	13.50
2013	0.17	0.11	0.11	0.11	0.13	0.12	0.53	1.22	1.94	2.05	0.77	0.98	0.75	7.48	8.23
2014	0.17	0.12	0.11	0.11	0.13	0.12	0.16	0.16	0.31	0.36	0.26	0.39	0.77	1.63	2.40
2015	0.27	0.18	0.18	0.18	0.20	0.19	0.15	0.16	0.30	0.35	0.26	0.39	1.18	1.60	2.78
2016	0.40	0.25	0.27	0.28	0.25	0.24	0.20	0.33	0.97	1.09	0.52	0.67	1.68	3.78	5.46
2017	0.56	0.33	0.38	0.42	0.29	0.27	0.20	0.35	0.98	1.10	0.54	0.70	2.26	3.87	6.13
2018	0.25	0.16	0.16	0.16	0.19	0.17	0.20	0.34	0.98	1.10	0.54	0.69	1.10	3.85	4.95
2019	0.22	0.14	0.14	0.14	0.16	0.15	0.16	0.16	0.30	0.35	0.26	0.39	0.96	1.62	2.58
2020	0.64	0.37	0.42	0.47	0.31	0.28	0.42	0.79	1.48	1.46	0.94	1.25	2.48	6.34	8.82
2021	0.16	0.11	0.10	0.10	0.12	0.11	0.95	0.92	1.84	4.43	2.11	1.67	0.70	11.90	12.60
2022	0.13	0.09	0.09	0.09	0.11	0.10	0.16	0.17	0.36	0.42	0.28	0.42	0.60	1.80	2.40
2023	0.38	0.24	0.25	0.26	0.24	0.23	0.42	0.78	1.46	1.44	0.94	1.26	1.60	6.29	7.89
2024	0.35	0.22	0.23	0.24	0.23	0.22	0.15	0.16	0.30	0.35	0.26	0.39	1.50	1.60	3.10
2025	0.86	0.45	0.49	0.58	0.35	0.33	0.97	0.88	1.74	4.44	2.32	1.78	3.06	12.13	15.19

Hypothetical option of inflow to Western part. Runoff volume. Optimistic scenario (minimum).

	OCT	NOV	DEC	JAN	FEB	MAR	APR	MAY	JUN	JUL	AUG	SEP	TMG	TVG	Total
1990	0.19	0.13	0.12	0.12	0.15	0.14	0.21	0.37	1.01	1.13	0.61	0.77	0.84	4.09	4.94
1991	1.43	0.67	0.62	1.08	0.51	0.53	0.33	0.60	1.22	1.16	0.88	1.18	4.83	5.36	10.19
1992	1.62	0.74	0.64	1.14	0.53	0.61	0.38	3.14	4.79	5.11	3.68	2.08	5.29	19.18	24.47
1993	1.77	0.80	0.67	1.17	0.57	0.69	0.81	1.03	2.23	4.07	1.48	1.38	5.66	11.00	16.66
1994	1.91	0.86	0.78	1.26	0.69	0.85	1.00	0.85	1.67	4.47	2.51	1.88	6.34	12.37	18.72
1995	1.73	0.79	0.66	1.16	0.55	0.67	0.09	0.10	0.11	0.12	0.12	0.16	5.57	0.70	6.26
1996	0.20	0.14	0.13	0.13	0.16	0.14	0.17	0.26	0.84	0.96	0.38	0.53	0.90	3.14	4.04
1997	0.38	0.24	0.25	0.26	0.24	0.23	0.04	0.04	0.04	0.04	0.04	0.05	1.60	0.26	1.86
1998	0.14	0.09	0.09	0.09	0.11	0.10	0.30	2.94	4.83	4.52	3.35	1.76	0.60	17.69	18.29
1999	1.03	0.51	0.53	0.65	0.38	0.37	0.15	0.16	0.26	0.30	0.24	0.36	3.46	1.45	4.91
2000	0.70	0.39	0.45	0.51	0.32	0.29	0.03	0.04	0.04	0.04	0.04	0.05	2.66	0.22	2.88
2001	0.01	0.01	0.01	0.01	0.01	0.01	0.01	0.01	0.01	0.01	0.01	0.01	0.04	0.05	0.09
2002	0.01	0.01	0.01	0.01	0.01	0.01	0.15	0.20	0.67	0.78	0.32	0.48	0.05	2.60	2.65
2003	0.45	0.27	0.30	0.32	0.26	0.25	0.63	1.66	2.39	2.55	0.60	0.74	1.85	8.57	10.42
2004	0.29	0.19	0.19	0.20	0.21	0.20	0.18	0.28	0.88	1.01	0.41	0.56	1.27	3.32	4.59
2005	0.28	0.18	0.18	0.19	0.20	0.19	0.86	1.00	2.11	4.26	1.64	1.44	1.22	11.32	12.55
2006	0.63	0.36	0.41	0.46	0.31	0.28	0.17	0.27	0.86	0.99	0.39	0.54	2.45	3.22	5.67
2007	1.52	0.71	0.63	1.12	0.52	0.57	0.15	0.16	0.28	0.33	0.25	0.38	5.05	1.55	6.60
2008	0.39	0.24	0.26	0.27	0.25	0.23	0.15	0.16	0.29	0.34	0.25	0.38	1.63	1.57	3.20
2009	0.51	0.31	0.35	0.37	0.28	0.26	0.16	0.19	0.53	0.62	0.30	0.46	2.07	2.24	4.31
2010	0.56	0.33	0.38	0.41	0.29	0.27	0.16	0.16	0.30	0.35	0.26	0.39	2.24	1.62	3.86
2011	1.17	0.56	0.56	0.76	0.42	0.42	0.97	0.89	1.76	4.44	2.28	1.76	3.88	12.08	15.96
2012	0.38	0.24	0.25	0.26	0.24	0.23	0.75	1.10	2.31	3.70	1.30	1.28	1.60	10.44	12.04
2013	0.51	0.31	0.35	0.38	0.28	0.26	0.23	0.42	1.06	1.15	0.69	0.87	2.09	4.42	6.51
2014	0.40	0.25	0.26	0.27	0.25	0.24	0.15	0.16	0.28	0.33	0.25	0.37	1.66	1.54	3.20
2015	0.50	0.30	0.34	0.37	0.28	0.26	0.16	0.19	0.54	0.62	0.30	0.46	2.05	2.26	4.31
2016	0.43	0.27	0.29	0.31	0.26	0.24	0.50	1.07	1.79	1.88	0.84	1.08	1.80	7.17	8.97
2017	0.64	0.37	0.42	0.47	0.31	0.28	0.70	1.43	2.38	3.08	0.94	1.01	2.48	9.54	12.02
2018	0.57	0.34	0.39	0.42	0.30	0.27	0.41	0.78	1.46	1.43	0.94	1.26	2.28	6.27	8.55
2019	0.39	0.24	0.26	0.27	0.24	0.23	0.15	0.16	0.29	0.34	0.25	0.38	1.62	1.58	3.20
2020	0.38	0.24	0.25	0.26	0.24	0.23	0.72	1.23	2.33	3.41	1.16	1.17	1.60	10.02	11.62
2021	0.41	0.25	0.27	0.28	0.25	0.24	0.33	3.03	4.83	4.77	3.49	1.89	1.70	18.35	20.05
2022	0.44	0.27	0.30	0.32	0.26	0.25	0.16	0.17	0.33	0.38	0.27	0.40	1.84	1.70	3.54
2023	1.30	0.63	0.60	0.96	0.47	0.48	0.43	0.82	1.52	1.51	0.93	1.24	4.44	6.45	10.89
2024	0.56	0.33	0.38	0.42	0.29	0.27	1.03	0.92	1.78	4.58	2.73	2.02	2.26	13.07	15.33
2025	0.40	0.25	0.26	0.27	0.25	0.24	0.49	2.47	4.14	4.46	3.05	1.82	1.66	16.42	18.08

Hypothetical option of inflow to Western part. Water salinity. National vision (maximum).

	OCT	NOV	DEC	JAN	FEB	MAR	APR	MAY	JUN	JUL	AUG	SEP
1990	1.883	2.098	2.121	2.122	2.027	2.068	1.831	1.523	1.109	1.076	1.295	1.204
1991	0.944	1.207	1.242	1.033	1.325	1.307	1.502	1.253	0.992	1.009	1.106	1.003
1992	0.934	1.183	1.231	1.045	1.286	1.243	1.382	0.751	0.66	0.648	0.714	0.86
1993	0.882	1.142	1.208	1.012	1.268	1.195	1.138	1.055	0.818	0.686	0.935	0.959
1994	0.866	1.121	1.156	0.993	1.201	1.127	1.071	1.127	0.905	0.669	0.791	0.87
1995	0.933	1.169	1.24	1.039	1.313	1.232	2.153	2.118	2.075	2.051	2.066	1.925
1996	1.88	2.121	2.144	2.142	2.042	2.086	1.987	1.74	1.197	1.152	1.533	1.373
1997	1.606	1.853	1.818	1.796	1.838	1.868	3.205	3.118	3.112	3.129	3.149	2.949
1998	1.652	1.71	1.718	1.721	1.692	1.704	1.47	0.753	0.656	0.667	0.725	0.888
1999	1.103	1.374	1.356	1.269	1.519	1.524	2.017	1.998	1.718	1.638	1.759	1.546
2000	1.309	1.548	1.488	1.43	1.65	1.7	3.053	2.995	2.994	3.008	3.021	2.887
2001	3.172	3.535	3.627	3.699	3.504	3.534	3.39	3.249	3.258	3.309	3.348	3.08
2002	3.492	3.559	3.573	3.582	3.554	3.559	2.114	1.927	1.336	1.288	1.661	1.467
2003	1.375	1.575	1.536	1.515	1.59	1.614	1.23	0.9	0.81	0.797	1.254	1.172
2004	1.652	1.903	1.896	1.882	1.847	1.876	1.934	1.679	1.161	1.119	1.481	1.337
2005	1.536	1.681	1.68	1.673	1.649	1.665	1.111	1.057	0.831	0.692	0.899	0.936
2006	1.27	1.522	1.456	1.403	1.605	1.652	1.901	1.675	1.147	1.101	1.483	1.331
2007	1.113	1.348	1.317	1.259	1.438	1.456	1.056	1.12	0.899	0.671	0.775	0.852
2008	1.564	1.828	1.795	1.772	1.809	1.839	2.078	2.046	1.646	1.566	1.751	1.529
2009	0.887	1.119	1.146	0.991	1.195	1.116	1.997	1.973	1.893	1.852	1.879	1.729
2010	0.92	1.168	1.236	1.026	1.312	1.238	1.874	1.834	1.436	1.368	1.608	1.412
2011	1.116	1.356	1.323	1.263	1.448	1.469	1.115	1.058	0.828	0.684	0.903	0.94
2012	1.363	1.549	1.514	1.494	1.565	1.586	1.167	1.013	0.809	0.721	0.981	0.983
2013	1.187	1.451	1.401	1.333	1.571	1.61	1.985	1.931	1.459	1.389	1.66	1.444
2014	1.049	1.291	1.309	1.137	1.413	1.413	2.724	2.69	2.69	2.699	2.707	2.628
2015	1.588	1.832	1.793	1.77	1.826	1.856	3.253	3.169	3.165	3.184	3.204	3.012
2016	2.965	3.15	3.188	3.212	3.119	3.143	2.116	1.98	1.399	1.347	1.692	1.487
2017	1.51	1.747	1.692	1.662	1.776	1.813	3.375	3.305	3.305	3.325	3.342	3.184
2018	0.957	1.192	1.257	1.054	1.334	1.263	2.542	2.514	2.513	2.52	2.527	2.459
2019	1.118	1.372	1.365	1.266	1.516	1.514	2.848	2.806	2.806	2.816	2.826	2.729
2020	0.978	1.238	1.263	1.067	1.358	1.352	1.863	1.701	1.166	1.111	1.511	1.344
2021	0.928	1.159	1.229	1.038	1.298	1.21	2.347	2.312	2.304	2.306	2.314	2.219
2022	0.852	1.105	1.124	0.97	1.168	1.097	1.181	0.989	0.806	0.723	1.024	1.016
2023	0.815	1.004	1.019	0.902	1.063	1.018	2.201	2.184	2.183	2.187	2.191	2.149
2024	0.79	0.967	0.982	0.875	1.024	0.987	2.147	2.132	2.132	2.135	2.139	2.103
2025	2.559	2.854	2.928	2.975	2.789	2.84	3.461	3.324	3.326	3.367	3.402	3.124

Hypothetical option of inflow to Western part. Water salinity. Business as usual (maximum).

	OCT	NOV	DEC	JAN	FEB	MAR	APR	MAY	JUN	JUL	AUG	SEP
1990	1.883	2.098	2.121	2.122	2.027	2.068	1.831	1.523	1.109	1.076	1.295	1.204
1991	0.944	1.207	1.242	1.033	1.325	1.307	1.502	1.253	0.992	1.009	1.106	1.003
1992	0.934	1.183	1.231	1.045	1.286	1.243	1.382	0.751	0.66	0.648	0.714	0.86
1993	0.882	1.142	1.208	1.012	1.268	1.195	1.138	1.055	0.818	0.686	0.935	0.959
1994	0.866	1.121	1.156	0.993	1.201	1.127	1.071	1.127	0.905	0.669	0.791	0.87
1995	0.933	1.169	1.24	1.039	1.313	1.232	2.153	2.118	2.075	2.051	2.066	1.925
1996	1.88	2.121	2.144	2.142	2.042	2.086	1.987	1.74	1.197	1.152	1.533	1.373
1997	1.606	1.853	1.818	1.796	1.838	1.868	3.205	3.118	3.112	3.129	3.149	2.949
1998	1.652	1.71	1.718	1.721	1.692	1.704	1.47	0.753	0.656	0.667	0.725	0.888
1999	1.103	1.374	1.356	1.269	1.519	1.524	2.017	1.998	1.718	1.638	1.759	1.546
2000	1.309	1.548	1.488	1.43	1.65	1.7	3.053	2.995	2.994	3.008	3.021	2.887
2001	3.172	3.535	3.627	3.699	3.504	3.534	3.39	3.249	3.258	3.309	3.348	3.08
2002	3.492	3.559	3.573	3.582	3.554	3.559	2.114	1.927	1.336	1.288	1.661	1.467
2003	1.375	1.575	1.536	1.515	1.59	1.614	1.23	0.9	0.81	0.797	1.254	1.172
2004	1.652	1.903	1.896	1.882	1.847	1.876	1.934	1.679	1.161	1.119	1.481	1.337
2005	1.536	1.681	1.68	1.673	1.649	1.665	1.111	1.057	0.831	0.692	0.899	0.936
2006	1.27	1.522	1.456	1.403	1.605	1.652	1.901	1.675	1.147	1.101	1.483	1.331
2007	1.065	1.31	1.294	1.227	1.408	1.412	1.08	0.959	0.788	0.661	0.77	0.843
2008	1.454	1.71	1.654	1.624	1.737	1.774	2.055	2.02	1.604	1.526	1.728	1.506
2009	0.883	1.139	1.21	1.006	1.278	1.198	1.544	1.3	1.009	1.01	1.132	1.033
2010	2.024	2.298	2.335	2.338	2.202	2.259	2.119	2.089	1.702	1.623	1.789	1.571
2011	1.22	1.412	1.368	1.328	1.467	1.494	1.072	0.97	0.796	0.662	0.769	0.841
2012	0.905	1.169	1.225	1.014	1.296	1.244	1.238	0.906	0.806	0.794	1.25	1.166
2013	1.271	1.506	1.445	1.401	1.569	1.608	1.444	1.181	0.96	0.972	1.087	0.989
2014	1.934	2.21	2.238	2.236	2.117	2.168	2.135	2.11	1.763	1.68	1.82	1.599
2015	1.973	2.249	2.281	2.281	2.153	2.208	2.127	2.1	1.735	1.654	1.805	1.586
2016	2.012	2.285	2.321	2.324	2.19	2.246	2.108	2.073	1.658	1.581	1.768	1.551
2017	1.072	1.342	1.334	1.231	1.486	1.485	1.98	1.958	1.631	1.553	1.709	1.497
2018	1.379	1.631	1.564	1.523	1.691	1.735	2.054	2.027	1.652	1.571	1.745	1.522
2019	1.114	1.385	1.362	1.28	1.527	1.538	1.993	1.969	1.628	1.549	1.713	1.498
2020	1.019	1.293	1.294	1.168	1.428	1.425	1.783	1.548	1.087	1.046	1.357	1.241
2021	0.883	1.129	1.196	1.004	1.259	1.171	1.799	1.638	1.136	1.083	1.47	1.319
2022	0.881	1.135	1.177	1.013	1.222	1.151	1.266	0.822	0.696	0.67	0.758	0.885
2023	0.856	1.107	1.137	0.973	1.185	1.107	1.497	1.261	0.995	1.009	1.111	1.008
2024	2.015	2.29	2.326	2.329	2.193	2.25	2.12	2.091	1.708	1.628	1.791	1.573
2025	2.015	2.29	2.326	2.329	2.193	2.25	2.12	2.091	1.708	1.628	1.791	1.573

Hypothetical option of inflow to Western part. Water salinity. Optimistic scenario (maximum).

	OCT	NOV	DEC	JAN	FEB	MAR	APR	MAY	JUN	JUL	AUG	SEP
1990	1.883	2.098	2.121	2.122	2.027	2.068	1.831	1.523	1.109	1.076	1.295	1.204
1991	0.944	1.207	1.242	1.033	1.325	1.307	1.502	1.253	0.992	1.009	1.106	1.003
1992	0.934	1.183	1.231	1.045	1.286	1.243	1.382	0.751	0.66	0.648	0.714	0.86
1993	0.882	1.142	1.208	1.012	1.268	1.195	1.138	1.055	0.818	0.686	0.935	0.959
1994	0.866	1.121	1.156	0.993	1.201	1.127	1.071	1.127	0.905	0.669	0.791	0.87
1995	0.933	1.169	1.24	1.039	1.313	1.232	2.153	2.118	2.075	2.051	2.066	1.925
1996	1.88	2.121	2.144	2.142	2.042	2.086	1.987	1.74	1.197	1.152	1.533	1.373
1997	1.606	1.853	1.818	1.796	1.838	1.868	3.205	3.118	3.112	3.129	3.149	2.949
1998	1.652	1.71	1.718	1.721	1.692	1.704	1.47	0.753	0.656	0.667	0.725	0.888
1999	1.103	1.374	1.356	1.269	1.519	1.524	2.017	1.998	1.718	1.638	1.759	1.546
2000	1.309	1.548	1.488	1.43	1.65	1.7	3.053	2.995	2.994	3.008	3.021	2.887
2001	3.172	3.535	3.627	3.699	3.504	3.534	3.39	3.249	3.258	3.309	3.348	3.08
2002	3.492	3.559	3.573	3.582	3.554	3.559	2.114	1.927	1.336	1.288	1.661	1.467
2003	1.375	1.575	1.536	1.515	1.59	1.614	1.23	0.9	0.81	0.797	1.254	1.172
2004	1.652	1.903	1.896	1.882	1.847	1.876	1.934	1.679	1.161	1.119	1.481	1.337
2005	1.536	1.681	1.68	1.673	1.649	1.665	1.111	1.057	0.831	0.692	0.899	0.936
2006	1.27	1.522	1.456	1.403	1.605	1.652	1.901	1.675	1.147	1.101	1.483	1.331
2007	1.036	1.294	1.285	1.202	1.401	1.401	1.061	1.123	0.9	0.671	0.781	0.858
2008	1.148	1.417	1.375	1.304	1.543	1.573	1.953	1.792	1.216	1.16	1.568	1.379
2009	1.437	1.621	1.599	1.584	1.612	1.63	1.195	0.931	0.806	0.76	1.098	1.068
2010	1.536	1.798	1.758	1.734	1.791	1.823	2.088	2.062	1.695	1.612	1.773	1.55
2011	0.884	1.145	1.21	1.012	1.272	1.201	1.157	1.041	0.809	0.698	0.962	0.972
2012	0.821	1.057	1.071	0.93	1.115	1.056	1.26	0.941	0.825	0.812	1.213	1.129
2013	1.355	1.581	1.529	1.5	1.614	1.645	1.447	1.183	0.963	0.975	1.089	0.991
2014	1.534	1.795	1.754	1.73	1.79	1.822	2.095	2.07	1.718	1.635	1.785	1.561
2015	1.482	1.712	1.683	1.664	1.7	1.725	1.586	1.307	1.028	1.035	1.142	1.045
2016	1.503	1.735	1.709	1.691	1.717	1.741	1.633	1.347	1.042	1.038	1.165	1.071
2017	0.922	1.185	1.233	1.019	1.311	1.272	1.482	1.236	0.984	1.003	1.098	0.994
2018	1.476	1.703	1.673	1.654	1.692	1.717	1.545	1.271	1.014	1.029	1.123	1.024
2019	1.076	1.349	1.324	1.248	1.474	1.487	1.451	1.194	0.964	0.98	1.086	0.985
2020	1.018	1.295	1.292	1.18	1.427	1.425	1.529	1.271	1.001	1.015	1.117	1.015
2021	0.843	1.089	1.101	0.957	1.143	1.081	1.068	1.13	0.911	0.668	0.782	0.863
2022	0.989	1.216	1.244	1.078	1.296	1.28	1.04	0.737	0.63	0.6	0.688	0.748
2023	0.817	1.049	1.064	0.928	1.107	1.054	1.102	1.091	0.865	0.671	0.863	0.923
2024	1.091	1.355	1.324	1.255	1.467	1.485	1.294	0.983	0.854	0.84	1.163	1.074
2025	1.15	1.409	1.362	1.297	1.514	1.548	1.493	1.232	0.987	1.006	1.099	0.998

Hypothetical option of inflow to Western part. Water salinity. National vision (minimum).

	OCT	NOV	DEC	JAN	FEB	MAR	APR	MAY	JUN	JUL	AUG	SEP
1990	1.883	2.098	2.121	2.122	2.027	2.068	1.831	1.523	1.109	1.076	1.295	1.204
1991	0.944	1.207	1.242	1.033	1.325	1.307	1.502	1.253	0.992	1.009	1.106	1.003
1992	0.934	1.183	1.231	1.045	1.286	1.243	1.382	0.751	0.66	0.648	0.714	0.86
1993	0.882	1.142	1.208	1.012	1.268	1.195	1.138	1.055	0.818	0.686	0.935	0.959
1994	0.866	1.121	1.156	0.993	1.201	1.127	1.071	1.127	0.905	0.669	0.791	0.87
1995	0.933	1.169	1.24	1.039	1.313	1.232	2.153	2.118	2.075	2.051	2.066	1.925
1996	1.88	2.121	2.144	2.142	2.042	2.086	1.987	1.74	1.197	1.152	1.533	1.373
1997	1.606	1.853	1.818	1.796	1.838	1.868	3.205	3.118	3.112	3.129	3.149	2.949
1998	1.652	1.71	1.718	1.721	1.692	1.704	1.47	0.753	0.656	0.667	0.725	0.888
1999	1.103	1.374	1.356	1.269	1.519	1.524	2.017	1.998	1.718	1.638	1.759	1.546
2000	1.309	1.548	1.488	1.43	1.65	1.7	3.053	2.995	2.994	3.008	3.021	2.887
2001	3.172	3.535	3.627	3.699	3.504	3.534	3.39	3.249	3.258	3.309	3.348	3.08
2002	3.492	3.559	3.573	3.582	3.554	3.559	2.114	1.927	1.336	1.288	1.661	1.467
2003	1.375	1.575	1.536	1.515	1.59	1.614	1.23	0.9	0.81	0.797	1.254	1.172
2004	1.652	1.903	1.896	1.882	1.847	1.876	1.934	1.679	1.161	1.119	1.481	1.337
2005	1.536	1.681	1.68	1.673	1.649	1.665	1.111	1.057	0.831	0.692	0.899	0.936
2006	1.27	1.522	1.456	1.403	1.605	1.652	1.901	1.675	1.147	1.101	1.483	1.331
2007	1.961	2.218	2.25	2.251	2.125	2.178	3.52	3.407	3.406	3.435	3.463	3.218
2008	2.911	3.232	3.306	3.351	3.165	3.217	2.42	2.354	2.264	2.217	2.245	2.033
2009	1.356	1.592	1.527	1.476	1.679	1.731	3.207	3.151	3.151	3.167	3.181	3.053
2010	1.126	1.382	1.371	1.278	1.526	1.526	2.782	2.735	2.731	2.741	2.752	2.639
2011	0.874	1.132	1.194	1.007	1.249	1.172	1.134	1.058	0.821	0.684	0.929	0.956
2012	1.721	1.819	1.832	1.834	1.788	1.808	1.096	1.067	0.845	0.69	0.871	0.92
2013	2.526	2.699	2.734	2.752	2.659	2.689	1.976	1.705	1.195	1.156	1.504	1.362
2014	1.013	1.252	1.286	1.089	1.375	1.358	2.619	2.585	2.584	2.592	2.6	2.52
2015	1.36	1.596	1.531	1.481	1.682	1.733	3.161	3.101	3.1	3.116	3.13	2.994
2016	1.322	1.575	1.507	1.459	1.649	1.696	2.013	1.919	1.367	1.304	1.647	1.432
2017	1.342	1.594	1.527	1.484	1.658	1.702	2.013	1.874	1.284	1.227	1.619	1.413
2018	0.919	1.146	1.206	1.028	1.265	1.178	2.463	2.437	2.437	2.443	2.449	2.388
2019	1.067	1.312	1.323	1.171	1.439	1.439	2.747	2.711	2.71	2.719	2.728	2.643
2020	1.794	1.906	1.922	1.926	1.87	1.894	1.196	0.935	0.812	0.766	1.095	1.067
2021	2.059	2.119	2.131	2.138	2.107	2.117	1.207	0.919	0.814	0.782	1.152	1.107
2022	3.023	3.373	3.458	3.519	3.319	3.364	2.936	2.82	2.814	2.838	2.864	2.626
2023	1.395	1.631	1.564	1.52	1.704	1.753	3.053	2.985	2.98	2.994	3.01	2.849
2024	1.55	1.79	1.742	1.716	1.801	1.835	3.347	3.27	3.269	3.29	3.308	3.135
2025	1.301	1.51	1.459	1.427	1.552	1.582	1.222	0.897	0.805	0.788	1.237	1.163

Hypothetical option of inflow to Western part. Water salinity. Business as usual (minimum).

	OCT	NOV	DEC	JAN	FEB	MAR	APR	MAY	JUN	JUL	AUG	SEP
1990	1.883	2.098	2.121	2.122	2.027	2.068	1.831	1.523	1.109	1.076	1.295	1.204
1991	0.944	1.207	1.242	1.033	1.325	1.307	1.502	1.253	0.992	1.009	1.106	1.003
1992	0.934	1.183	1.231	1.045	1.286	1.243	1.382	0.751	0.66	0.648	0.714	0.86
1993	0.882	1.142	1.208	1.012	1.268	1.195	1.138	1.055	0.818	0.686	0.935	0.959
1994	0.866	1.121	1.156	0.993	1.201	1.127	1.071	1.127	0.905	0.669	0.791	0.87
1995	0.933	1.169	1.24	1.039	1.313	1.232	2.153	2.118	2.075	2.051	2.066	1.925
1996	1.88	2.121	2.144	2.142	2.042	2.086	1.987	1.74	1.197	1.152	1.533	1.373
1997	1.606	1.853	1.818	1.796	1.838	1.868	3.205	3.118	3.112	3.129	3.149	2.949
1998	1.652	1.71	1.718	1.721	1.692	1.704	1.47	0.753	0.656	0.667	0.725	0.888
1999	1.103	1.374	1.356	1.269	1.519	1.524	2.017	1.998	1.718	1.638	1.759	1.546
2000	1.309	1.548	1.488	1.43	1.65	1.7	3.053	2.995	2.994	3.008	3.021	2.887
2001	3.172	3.535	3.627	3.699	3.504	3.534	3.39	3.249	3.258	3.309	3.348	3.08
2002	3.492	3.559	3.573	3.582	3.554	3.559	2.114	1.927	1.336	1.288	1.661	1.467
2003	1.375	1.575	1.536	1.515	1.59	1.614	1.23	0.9	0.81	0.797	1.254	1.172
2004	1.652	1.903	1.896	1.882	1.847	1.876	1.934	1.679	1.161	1.119	1.481	1.337
2005	1.536	1.681	1.68	1.673	1.649	1.665	1.111	1.057	0.831	0.692	0.899	0.936
2006	1.27	1.522	1.456	1.403	1.605	1.652	1.901	1.675	1.147	1.101	1.483	1.331
2007	2.015	2.29	2.326	2.329	2.193	2.25	2.12	2.091	1.708	1.628	1.791	1.573
2008	1.981	2.257	2.29	2.29	2.161	2.216	2.125	2.098	1.73	1.648	1.802	1.583
2009	1.335	1.588	1.519	1.474	1.658	1.705	2.016	1.939	1.415	1.349	1.661	1.444
2010	1.929	2.148	2.175	2.177	2.074	2.118	1.881	1.587	1.132	1.097	1.373	1.265
2011	1.47	1.616	1.608	1.599	1.595	1.609	1.052	1.115	0.895	0.676	0.774	0.848
2012	1.328	1.511	1.471	1.448	1.536	1.559	1.1	1.065	0.841	0.684	0.878	0.925
2013	1.818	1.961	1.98	1.982	1.915	1.944	1.311	1.002	0.876	0.864	1.162	1.073
2014	2.042	2.316	2.354	2.358	2.219	2.277	2.116	2.085	1.692	1.613	1.784	1.567
2015	1.749	2.022	2.024	2.01	1.949	1.984	2.106	2.078	1.697	1.615	1.781	1.559
2016	1.475	1.721	1.683	1.66	1.719	1.748	1.846	1.566	1.11	1.073	1.355	1.246
2017	1.307	1.554	1.489	1.445	1.618	1.661	1.813	1.538	1.093	1.056	1.324	1.22
2018	1.729	1.964	1.972	1.963	1.898	1.931	1.858	1.564	1.118	1.083	1.347	1.243
2019	1.887	2.161	2.183	2.178	2.071	2.118	2.111	2.082	1.692	1.612	1.782	1.562
2020	1.235	1.473	1.414	1.364	1.547	1.587	1.412	1.148	0.94	0.944	1.085	0.989
2021	1.722	1.816	1.829	1.831	1.786	1.805	1.078	1.088	0.867	0.686	0.832	0.894
2022	2.22	2.487	2.535	2.55	2.396	2.457	2.103	2.058	1.606	1.535	1.75	1.536
2023	1.467	1.683	1.656	1.639	1.672	1.695	1.425	1.159	0.951	0.956	1.09	0.995
2024	1.594	1.861	1.833	1.812	1.83	1.86	2.092	2.064	1.688	1.606	1.772	1.549
2025	1.114	1.351	1.319	1.26	1.441	1.46	1.071	1.108	0.884	0.674	0.806	0.877

Hypothetical option of inflow to Western part. Water salinity. Optimistic scenario (minimum).

	OCT	NOV	DEC	JAN	FEB	MAR	APR	MAY	JUN	JUL	AUG	SEP
1990	1.883	2.098	2.121	2.122	2.027	2.068	1.831	1.523	1.109	1.076	1.295	1.204
1991	0.944	1.207	1.242	1.033	1.325	1.307	1.502	1.253	0.992	1.009	1.106	1.003
1992	0.934	1.183	1.231	1.045	1.286	1.243	1.382	0.751	0.66	0.648	0.714	0.86
1993	0.882	1.142	1.208	1.012	1.268	1.195	1.138	1.055	0.818	0.686	0.935	0.959
1994	0.866	1.121	1.156	0.993	1.201	1.127	1.071	1.127	0.905	0.669	0.791	0.87
1995	0.933	1.169	1.24	1.039	1.313	1.232	2.153	2.118	2.075	2.051	2.066	1.925
1996	1.88	2.121	2.144	2.142	2.042	2.086	1.987	1.74	1.197	1.152	1.533	1.373
1997	1.606	1.853	1.818	1.796	1.838	1.868	3.205	3.118	3.112	3.129	3.149	2.949
1998	1.652	1.71	1.718	1.721	1.692	1.704	1.47	0.753	0.656	0.667	0.725	0.888
1999	1.103	1.374	1.356	1.269	1.519	1.524	2.017	1.998	1.718	1.638	1.759	1.546
2000	1.309	1.548	1.488	1.43	1.65	1.7	3.053	2.995	2.994	3.008	3.021	2.887
2001	3.172	3.535	3.627	3.699	3.504	3.534	3.39	3.249	3.258	3.309	3.348	3.08
2002	3.492	3.559	3.573	3.582	3.554	3.559	2.114	1.927	1.336	1.288	1.661	1.467
2003	1.375	1.575	1.536	1.515	1.59	1.614	1.23	0.9	0.81	0.797	1.254	1.172
2004	1.652	1.903	1.896	1.882	1.847	1.876	1.934	1.679	1.161	1.119	1.481	1.337
2005	1.536	1.681	1.68	1.673	1.649	1.665	1.111	1.057	0.831	0.692	0.899	0.936
2006	1.27	1.522	1.456	1.403	1.605	1.652	1.901	1.675	1.147	1.101	1.483	1.331
2007	0.959	1.209	1.256	1.045	1.34	1.301	1.922	1.905	1.627	1.554	1.687	1.488
2008	1.544	1.806	1.768	1.744	1.796	1.827	2.091	2.065	1.701	1.618	1.777	1.553
2009	1.385	1.638	1.574	1.537	1.688	1.729	2.026	1.926	1.365	1.303	1.651	1.436
2010	1.356	1.608	1.539	1.494	1.676	1.723	2.051	2.025	1.656	1.574	1.745	1.522
2011	1.01	1.271	1.271	1.161	1.377	1.376	1.075	1.106	0.882	0.673	0.812	0.882
2012	1.43	1.605	1.584	1.57	1.596	1.614	1.162	1.023	0.81	0.717	0.97	0.975
2013	1.344	1.585	1.525	1.49	1.632	1.669	1.729	1.439	1.064	1.037	1.219	1.13
2014	1.534	1.795	1.754	1.73	1.79	1.822	2.095	2.07	1.718	1.635	1.785	1.561
2015	1.39	1.644	1.579	1.543	1.691	1.732	2.027	1.923	1.359	1.297	1.649	1.435
2016	1.398	1.609	1.571	1.549	1.621	1.646	1.333	1.039	0.887	0.875	1.125	1.035
2017	1.227	1.444	1.392	1.347	1.508	1.542	1.191	0.939	0.803	0.75	1.079	1.054
2018	1.281	1.513	1.454	1.412	1.572	1.609	1.421	1.157	0.946	0.952	1.086	0.989
2019	1.547	1.81	1.773	1.749	1.799	1.829	2.089	2.063	1.696	1.613	1.774	1.551
2020	1.433	1.611	1.59	1.576	1.603	1.62	1.176	0.988	0.81	0.733	1.008	1.002
2021	1.371	1.502	1.483	1.472	1.502	1.515	1.433	0.749	0.655	0.657	0.717	0.872
2022	1.468	1.724	1.671	1.642	1.746	1.782	2.06	2.028	1.622	1.542	1.736	1.514
2023	0.969	1.235	1.253	1.071	1.347	1.346	1.386	1.13	0.924	0.925	1.082	0.985
2024	1.269	1.454	1.409	1.378	1.495	1.522	1.05	1.09	0.878	0.669	0.768	0.842
2025	1.386	1.524	1.505	1.494	1.521	1.535	1.314	0.794	0.683	0.669	0.745	0.878

CR-4
Institute of Physiology and Biophysics & Institute of Zoology at the Academy of Sciences, the Republic of Uzbekistan

18. Ecological Degradation of the Aral Sea

Due to a dramatic drop in the influx of water into the Aral Sea, its area has dwindled by more than 4 fold, the volume by more than 10 fold, the level dropped by 23 m – and the Aral Sea has eventually split into two waterbodies, the Small Aral and the Large Aral. As a result, the water salinity in the Large Aral has grown more than 7 fold reaching over 80 ppt in the western basin and 100 ppt in the eastern basin, i.e. the Large Aral has turned into a polyhaline lake. As a result, this has brought about cardinal changes in the composition of the Aral biota.
Changes in the biota composition in the Aral at the initial stages of its salinization (1970-1980) were described in the works by Aladin and Kotov (1989), Andreev (1989), and Andreeva (1989). The later stages of succession (1985-1994) of the ecosystem of the Aral Sea are known mainly for the Small Aral and the northern part of the Large Aral (Aladin et al., 1998).

18.1 Plant communities

Due to high water transparency and shallow depths in the Aral Sea, most organics have been produced by phytobenthos, not phytoplankton, which made the ecosystem of this waterbody different from the ecosystems of other seas. In general, the stet biomass of phytobenthos reached 90%, while phytoplankton reached 10% (Karpevich, 1975). Charophytes (mainly *Tolypella aralica*) yielded ca. 75% and the chlorophyte *Vauscheria dichotoma* ca. 13% of the phytobenthos biomass. Other important benthic algae were the chlorophyte *Cladophora gracilis* and the rhodophyte *Polysiphonia violaceae* (Karpevich, 1975). In 1990's almost all of these species, as well as *Zostera*, the growth of which was recorded in the western basin as early as 1995 became extinct in the Aral Sea. Presently the only benthic macroscopic plants in the Aral are *Cladophora fracta* and *Vauscheria sp.*
In 1950-60's, in phytoplankton diatoms were dominant in the Aral Sea, with *Actinocyclus ehrenbergii var. crassa* as the dominant species (Zenkevich, 1963). According to Aladin and Kotov (1989) from 1972 to 1983 most species of brackishwater planktonic algae vanished from the Aral Sea, including such dominants as the cyanophyte *Microcystis pulveria* and the diatoms *Gyrosigma spencerii* and *Rhopalodia gibba*. In the 1980's, when salinity reached 24 ppt not only brackishwater species, but also some marine euryhaline species of algae like *Anabaena bergii, Entomoneis paludosa* etc. began disappearing (Elmuratov, 1981).
In 1999-2002, we recorded 159 species of algae in the periphyton and 167 species in the plankton. This is approximately half as much as recorded previously. So, in the 1920's, Kiselev (1927) recorded 375 species in the plankton of the Aral Sea, while in 1960-70's Pichkily (1981) and Elmuratov (1981) recorded 306 and 278 species, respectively.
In the last few years, most notably the diversity of Cyanophyta, Pyrrhophyta and Chlorophyta decreased (Table 18.1).
As before Bacillariophyta are most diverse in the plankton. However, the composition of the dominants has changed. Previously, *Actinocyclus ehrenbergi* dominated, but has vanished from the plankton being replaced by such diatoms as *Amphora coffeaformis, A. coffeaformis var. acutiuscula,* and *Synedra tabulata var. parva*. Not all recorded species are true plankters. A significant number of species may be inhabitants of the periphyton and phytobenthos by their origin.

Table 18.1 Succession of taxonomic structure of phytoplankton [*according Kiselev (1927); **according Pichkily (1981), ***Orlova et al., (1998), ****Mirabdullayev et al., 2003]

TAXA	1925*	1967 – 1974**	1993-1995***	1999-2001****
Cyanophyta	41	79	29	30
Bacillariophyta	210	104	115	115
Pyrrhophyta	15	28	31	3
Euglenophyta	-	3	2	2
Chlorophyta	109	60	62	9
Total number of taxa	375	306	245	159

18.2 Zooplankton

Until the 1970's, the composition of zooplankton in the Aral Sea was stable, comprising over 40 species in pelagial (Atlas…, 1974). The basis of the zooplankton was formed by *Arctodiaptomus salinus, Ceriodaphnia reticulata, Moina salina*, Podonidae. In the 1960's a copepod *Calanipeda aquaedulcis* Kritchagin was released into the Aral Sea. In the 1970-80's this species was dominant in the zooplankton of the Aral Sea, which resulted in the disappearance of the former dominants, *A. salinus, C. reticulata, M. salina* (Aladin and Andreev, 1984).

A drop in the inflow of the rivers and progressive salinization of the waters of the Aral Sea produced an adverse impact on the freshwater and brackish-water species, and they quickly vanished from the fauna. A quick decrease in the biodiversity of zooplankton was recorded in the first half of the 1970's. By 1976, the species composition became stable as the average salinity of the Aral Sea reached 14 ppt (Andreev, 1989). Later, a gradual decrease in the zooplankton diversity took place (Table 18.2). Since 1997, the former dominant, *C. aquaedulcis*, vanished from the plankton, which was apparently the reason for the emergence of *Moina salina* and *Artemia parthenogenetica* in the plankton.

Artemia was not known for the open part of the Aral Sea, although it was reported from the saline lakes of the southern Aral Sea region. In the 1980-1990's, artemia was repeatedly recorded in shallow coastal water bodies separated from the Aral Sea and in small lakes in the eastern margin of the Ustyurt Plateau. In October 1998 artemia was recorded in the Aral Sea – near the NE coast of Island Vozrozhdeniya (Joldasova et al., 1999). However, the population of artemia was not stable at that time. Since then, a break in the dam separating the Small and Large Aral resulted in the inflow of a significant volume of less saline water (ca. 21 ppt) and the fish, atherina, into the Large Aral Sea. As a result, no artemia were observed in the Aral Sea in 1999. Since 2000, artemia has been dominant there, constituting over 99% of the zooplankton biomass (Mirabdullayev et al., 2001).

Table 18.2 Species composition of zooplankton of the Aral Sea

Taxa	1971	1981	1989	1994	2000	2001
CILIOPHORA						
1. Tintinnopsis cylindrata	+	-	-	-	-	-
2. T. meunieri	+	-	-	-	-	-
3. T. tubulosa	+	-	-	-	-	-
ROTIFERA						
4. Keratella tropica	+	-	-	-	-	-
5. K. quadrata	+	-	-	-	-	-
6. Notholca squamula	+	-	-	-	-	-
7. N. acuminate	+	-	-	-	-	-
8. Hexarthra fennica	+	+	+	–	+	+
9. H. oxyuris	+	+	-	-	-	-
10. Testudinella patina	+	-	-	-	-	-
11. Lecane bulla	+	-	-	-	-	-
12. Synchaeta vorax	+	+	+	+	–	–
13. Brachionus hyphalmyros	+	+	-	-	-	-
14. B. plicatilis	+	+	-	-	-	-
ANNELLIDA (larvae)						
15. Nereis diversicolor	+	+	+	+	+	–
MOLLUSCA (larvae)						
16. Cerastoderma isthmicum	+	+	+	+	+	–
17. *Syndosmya segmentum*	+	+	+	+	+	+
CRUSTACEA						
18. Artemia parthenogenetica	–	–	–	–	+	+
19. Ceriodaphnia reticulata	+	-	-	-	-	-
20. Alona rectangular	+	-	-	-	-	-
21. Moina salina	+	–	+	–	+	–
22. Podonevadne camptonyx	+	+	+	–	–	–
23. P. angusta	+	-	-	-	-	-
24. Evadne anonyx	+	+	-	-	-	-
25. Cercopagis pengoi aralensis	+	-	-	-	-	-
26. Halicyclops rotundipes	+	+	+	+	–	–
27. *Cletocamptus retrogressus*	+	+	+	+	+	+

28. Cyclops vicinus	+	-	-	-	-	-
29. Megacyclops viridis	+	-	-	-	-	-
30. Apocyclops dengizicus	+	+	+	–	–	–
31. Mesocyclops leuckarti	+	-	-	-	-	-
32. Ergasilus sieboldi	+	-	-	-	-	-
33. Halectinosoma abrau	+	+	+	+	–	–
34. Schizopera aralensis	+	+	-	-	-	-
35. S. reducta	+	-	-	-	-	-
36. Onychocamptus mohammed	+	-	-	-	-	-
37. Mesochra aestuarii	+	-	-	-	-	-
38. Nitocra lacustris	+	-	-	-	-	-
39. Limnocletodes behningi	+	-	-	-	-	-
40. Nannopus palustris	+	-	-	-	-	-
41. Arctodiaptomus salinus	+	+	-	-	-	-
42. *Calanipeda aquaedulcis*	+	+	+	+	–	–
INSECTA (larvae)						
43. Chironomus salinarius	+	+	+	+	+	+
Number of species	43	18	13	9	8	5
Salinity, ppt	12	18	30	37	60	65

18.3 Zoobenthos

The biodiversity of the Aral bottom fauna was originally relatively low and comprised about 75 species. Later, it a little grew to reach 82 species in 1970 as a result of planned and accidental introductions (Andreeva, 1989). Dominants were mollusks *Dreissena spp., Hypanis spp*. and larvae of dipteran Chironomidae. Mollusks *Cerastoderma spp.* and *Caspiohydrobia* inhabited mainly more saline gulfs.
Changes in quantitative development of zoobenthos started already at slight increasing of mineralization of water. Further increasing of mineralization resulted in changes of species composition. In particular, in open part of the Aral Sea have been recorded 18 new for the waterbody gastropod species of the genus Caspiohydrobia. These mollusks inhabited previously more saline gulfs и по мере роста солености в Арале стали активно расселяться в нем (Andreeva, 1989).
In the 1970-80's, a rapid decrease took place in the biodiversity of the zoobenthos (Andreev et al., 1992a). So, if in 1970 diversity of Annellida, Crustacea, Insecta and Mollusca was comparable, in 1980 till 75% of zoobenthos diversity fell on mollusks. Completely vanished Oligochaeta (Annellida) and Insecta (only 2 species of chironomids remained).
Especially fast changes in zoobenthos happened in 1980's, when its diversity decreased about three times. About 60% of zoobenthos diversity belonged to mollusks.
In the 1990's most aboriginal and introduced species vanished (Table 18.3).
Since 1980's most of zoobenthos biomass constituted by seaworm *Nereis diversicolor,* crustaceans *Paleomon elegans* and *Rhithropanopeus harrisii,* mollusks *Cerastoderma ishtmicum* and *Syndosmya segmentum.*
As the analysis has suggested, the decline of the zoobenthos species composition in the Aral Sea resulting from the growing salinization of its waters (for *Turkogammarus aralensis* the competition with *Palaemon elegans* can also be the case) mainly occurred as the salinity reached 14 and 25–28 ‰. Only euryhaline marine species (*Nereis diversicolor, Syndosmya segmentum, Cerastoderma isthmicum, Palaemon elegans,* and *Rhithropanopeus harrisii tridentatus*) and halophylic species inhabiting mainland waters (species of genus *Caspiohydrobia*) have been preserved in them.
Taking into consideration all data on the Aral Sea benthic biomass (Andreev, Andreeva, 2003), it can readily be noted that until 1960s the general zoobenthic biomass and that of individuals groups of organisms had been relatively steady. Insignificant fluctuations of zoobenthic biomass showed a true correlative link to the river flow; with a growing transport of suspended substances to the sea, an increase in the biomass of pelophylic (pelophylous) Chironomidae larvae and a decrease in the biomass of species (*Dreissena*, *Dikerogammarus aralensis*), which prefer a denser bottom, took place (Nikolsky, Fortunatov, 1950; Yablonskaya, 1960).
Introduced fishes were the first reason of the decrease in the biomass of the Aral zoobenthos and zooplankton. Hering, atherina and six bullhead species were first recorded in 1957-1959, while their maximal numbers were recorded in 1960-1962 (Karpevich, 1975).
The emergence of a great number of new benthophage consumers resulted in a significant decline in the biomass of benthic organisms at the depths of up to 10 m recorded in 1961. In the same year, a sharp drop in the volume of river stocks occurred. In subsequent years the biomass of brackish-water

"Caspian" mollusks and Chironomidae larvae significantly declined in deeper areas. In 1964, a permanent decline of the total zoobetnhos biomass throughout the Aral Sea began (Yablonskaya et al., 1973).

In 1967-1968, the lowest values of zoobenthos biomass in the entire period of zoobenthos monitoring in the Aral Sea were recorded. Despite the general decline of the zoobenthos biomass, that of the euryhaline *Cerastoderma* and halophylic *Caspiohydrobia* increased and since 1967 the dynamics of the biomass of brackish-water and fresh-water species stopped determining the dynamics of the general biomass of zoobenthos in the Aral Sea, as the euryhaline species began to play the determining role.

The increase in the total zoobenthos biomass in 1968-1974 was connected to a successful acclimatization of euryhaline marine species, *Nereis diversicolor* and *Syndosmya segmentum*, which quickly became dominant species and settled across the water area. As early as 1970, the biomass of zoobenthos reached the level prior to the decline; it was predetermined by acclimatized species, mainly *S. segmentum*. The total biomass of aboriginal species in those years changed little, but the process of the withdrawal of fresh-water and brackish-water species was almost completed.

The further growth of zoobenthos biomass in 1975 to 1981 was caused by the growth of the biomass of all euryhaline species inhabiting the Aral Sea by that time. In late 1970s, an average biomass of 196 g per sq. m, which 8.5 times exceeded the average long-term value recorded prior to the regulation of the river flow, was recorded. It was obvious that a sharp decline of benthophage fishes, which was recorded by R.M. Lim and E.L. Markova (1981), contributed to this process. The more so, the sharp growth of the numbers and biomass of non-predator species in response to the withdrawal of predators was recorded several times (Holland et al., 1980; Person, 1981; others).

In the years of late, a sharp decrease in the benthic biomass has been observed. In 2000, it varied within 6.3-9.8 g per sq. m. The biomass of nereis and mollusks remained at the same level during the year. *Ch. salinarius* was unavailable in May but showed the peak of development in September (Mirabdullaev et al., 2001).

Table 18.3 Species composition of zoobenthos of the Aral sea [data for 1950-1980 after Andreev et al. (1992b); data for 1990 after Filippov (1996)]

	Taxa	1970	1980	1990	1995	2000
	ANNELIDA					
1.	Nereis diversicolor	+	+	+	+	+
2.	Aelosoma hemprici	+	-	-	-	-
3.	Nais elinguis	+	-	-	-	-
4.	N. communis	+	-	-	-	-
5.	Paranais simplex	+	-	-	-	-
6.	Amphichaeta sannio	+	-	-	-	-
7.	Chaetogaster sp.	+		-	-	-
8.	Potamothrix bavaricus	+	-	-	-	-
9.	Psammorictides albicola	+	-	-	-	-
10.	Lumbriculus lineatus	+	-	-	-	-
11.	Limnodrilus helveticus	+	-	-	-	-
	CRUSTACEA					
12.	Cyprideis torosa	+	+	+	+	+
13.	Darwinula stevensoni	+	-	-	-	-
14.	Candona marchica	+	-	-	-	-
15.	Cyclocypris leavis	+	-	-	-	-
16.	Plesiocypridopsis newtomi	+	-	-	-	-
17.	Amnicythere cymbula	+	-	-	-	-
18.	Tyrrhenocythere amnicola	+	-	-	-	-
19.	Limnocythere dubiosa	+	+	-	-	-
20.	L. inopinata	+	-	-	-	-
21.	L. aralensis	+	-	-	-	-
22.	Galolimnocythere aralensis	+	+	+	-	-
23.	Loxoconchissa immodulata	+	-	-	-	-
24.	Paramysis intermedia	+	+	-	-	-
25.	P. lacustris	+	-	-	-	-
26.	Paleomon elegans	+	+	+	+	–
27.	Rhithropanopeus harrisii	+	+	+	+	–
28.	Turkogammarus aralensis	+	+	-	-	-

	ARACHNOIDEA					
29.	Hydryphantes crassipalpis	+	-	-	-	-
30.	H. flexuosus	+	-	-	-	-
31.	Hydrodroma despiciens	+	-	-	-	-
32.	Limnesia undulate	+	-	-	-	-
33.	Arrenurus tricuspidatur	+	-	-	-	-
34.	Copidognathus oxianus	+	+	-	-	-
	INSECTA					
35.	Agrypnetes crassicornis	+	-	-	-	-
36.	Oecetis intima	+	-	-	-	-
37.	Pelopia villipennis	+	-	-	-	-
38.	Procladius ferrugineus	+	-	-	-	-
39.	Tanytarsus lobatifrons	+	-	-	-	-
40.	T. gregarious	+	-	-	-	-
41.	T. lauterborni	+	-	-	-	-
42.	T. exiguous	+	-	-	-	-
43.	Polypedilum scalaenum	+	-	-	-	-
44.	Cryptochironomus supplicans	+	-	-	-	-
45.	C. defectus	+	-	-	-	-
46.	C. conjugens	+	-	-	-	-
47.	C. viridulus	+	-	-	-	-
48.	Chironomus behningi	+	-	-	-	-
49.	Chironomus salinarius	+	+	+	+	+
50.	C. halophilus	+	+	-	-	-
51.	Cricotopus silvestris	+	-	-	-	-
	MOLLUSCA					
52.	Dreissena polymorpha aralensis	+	-	-	-	-
53.	D. caspia pallasi	+	+	-	-	-
54.	Syndosmya segmentum	+	+	+	+	+
55.	Hypanis vitrea	+	+	-	-	-
56.	H. minima	+	+	-	-	-
57.	Cerastoderma ishtmicum	+	+	+	+	+
58.	C. umbonatum	+	+	-	-	-
59.	C. lamarcki	+	+	-	-	-
60.	Caspiohydrobia conica	+	+	+	-	-
61.	C. husainovae	+	+	-	-	-
62.	C. kazakhstanica	+	+	-	-	-
63.	C. aralensis	+	+	+	-	-
64.	C. obrutchevi	+	+	-	-	-
65.	C. parva	+	+	-	-	-
66.	C. dubia	+	+	-	-	-
67.	C. curta	+	+	+	-	-
68.	C. gemmata	+	+	-	-	-
69.	C. nikolskii	+	+	-	-	-
70.	C. behningi	+	+	+	-	-
71.	C. bergi	+	+	-	-	-
72.	C. oviformis	+	+	-	-	-
73.	C. subconvexa	+	+	-	-	-
74.	C. grimmi	+	+	+	-	-
75.	C. chrysopsis	+	+	-	-	-
76.	C. cylindrical	+	+	-	-	-
77.	C. sidorovi	+	+	-	-	-
78.	C. nikitinskii	+	+	+	-	-
79.	C. pavlovskii	+	+	-	-	-
80.	C. tadzhikistanica	+	+	-	-	-
81.	C. sogdiana	+	+	-	-	-
82.	Thedoxus pallasi	+	+	-	-	-
	Number of species	82	51	14	7	5
	Salinity, ppt	12	17	30	42	60

18.4 Fishes

The ichthyofauna of the Aral Sea originally was relatively poor. There were only 20 species of fishes from 7 families (for comparison, in a similarly landlocked Caspian Sea, the fish fauna comprised 130 species of 19 families). Of 20 Aral fish species, 10 or 12 were commercial; these were mainly valuable large fishes of high commercial quality, such as barbel Barbus brachycephalus, bream Abramis brama aralensis, carp Cyprinus carpio, asp Aspius aspius, Rutilus rutilus aralensis, pike Esox lucius, cat fish Silurus glanis, and some others. From 80 to 85% of catches consisted of these species.
Later, due to introductions in 1950-1960's, the number of species rose up to ca. 30 species (Table 18.4). Owing to acclimatization, the fish fauna was significantly enriched. Acclimatization was initiated in 1927-1929 (Karpevich, 1975). The goal was to increase catches through enriching the fish fauna. As time passed, the trend of perspective formation of euryhaline (salt-resistant) fish fauna prevailed. A total of 18 species of 8 families were introduced into the Aral Sea. Of nine species introduced according to the schedule, only two species, salaka *Clupea harengas membras* and flounder *Plathichtis flesus luscus*, got adapted to the Aral Sea conditions. On the contrary, nine accidentally introduced species all got adapted to inhabiting the Aral Sea. All these species almost at the same time got to the Aral Sea in mid-1950s, when grey mullet was brought from the SE part of the Caspian Sea to the Aral Sea. Undemanding eurybiont species, most of them grew in numbers in a short period of time. As salinity raised in 1970's most aboriginal freshwater species vanished. In 1981 fishery was stopped in the Aral Sea. During 1980's all aboriginal and most introduced species became extinct in the Aral Sea due high salinity.
By 1990, only 5 species survived in the Large Aral: baltic herring *Clupea harengus membras* (Linnaeus), flounder *Platichthys flesus luscus* (Pallas), atherine *Atherina boyeri caspia* (Eichwald), and bullheads *Neogobius fluviatilis* Berg and *Potamoschistus caucasicus* (Kewrajsky). During 1990's both bullheads vanished.
In 1990's the feeding of flounder consisted mainly on shrimp, crabs, nereis, mollusks and bullheads. Currently, artemia constitutes the main food source for flounder.
In 2001 only 2 species of fishes survived in the Aral Sea: atherine and flounder.

Table 18.4 Ichthyofauna of the Aral Sea

	Species	1920	1970	1980	1990	2000
1.	Acipenser nudiventris	+	+	-	-	-
2.	Acipenser stellatus	-	+	-	-	-
3.	Clupea harengus membras	-	+	+	+	+
4.	Salmo trutta aralensis	+	-	-	-	-
5.	Barbus brachycephalus	+	+	-	-	-
6.	Barbus capito conocephalus	+	+	-	-	-
7.	Rutilus rutilus aralensis	+	+	+	-	-
8.	Leuciscus idus oxianus	+	+	-	-	-
9.	Scardinius erythrophthalmus	+	+	-	-	
10.	Aspius aspius	+	+	-	-	-
11.	Chalcalburnus chalcoides aralensis	+	+	+	-	-
12.	Aristichtys nobilis	-	+	-	-	-
13.	Abramis sapa aralensis	+	+	-	-	-
14.	Abramis brama orientalis	+	+	+	-	-
15.	Pelecus cultratus	+	+	+	-	-
16.	Cyprinus carpio	+	+	+	-	-
17.	Carassius auratus	+	-	-	-	-
18.	Gobio gobio laepidolaemus	+	+	-	-	-
19.	Cobitis aurata aralensis	+	+	-	-	-
20.	Silurus glanis	+	+	+	-	-
21.	Pungitius platygaster aralensis	+	+	+	-	-
22.	Stezostedion lucioperca	+	+	+	-	-
23.	Channa argus	-	+	-	-	-
24.	Esox lucius	+	+	-	-	-
25.	Atherina boyeri caspia	-	+	+	+	+
26.	Platichthys flesus luscus	-	+	+	+	+
27.	Neogobius fluviatilis	-	+	+	+	–
28.	Neogobius melanostomus	-	+	+	-	-
29.	Neogobius syrman	-	+	+	-	-
30.	Neogobius kessleri	-	+	+	-	-
31.	Proterorhynus marmoratus	-	+	+	-	-
32.	Potamoschistus caucasicus	-	+	+	+	–
	Total number of species	20	30	17	5	3
	Salinity, ppt	11	12	17	30	60

19. Biological Aspects of the Project

With increasing salinity and transition of the Aral Sea from an oligohaline to a polyhaline water body its biota is becoming drastically poorer. Almost all aboriginal species became extinct in the Large Aral, some still surviving (including some endemics) in some lakes (refugia) around the Aral Sea (Mirabdullayev et al., 2001).

As the main goal of this project is the determination of optimal ways of the management of water resources for the rehabilitation of the original ecosystem of the Aral Sea, the biological aspects of the project consist in the following:

- Description of the current state of biota in the Aral Sea;
- Assessment of the ecological range of the representatives of the Aral biota;
- Forecast of the succession of the biota upon different variants of the water body transformation;
- Revealing the refugia of the Aral biota;
- Elaborate measures aimed at the conservation of the Aral biota.

The description of the current state of the Aral biota is an absolutely necessary stage for the project development, as some modern data on the Aral biota are extremely scarce and patchy (Joldasova et al., 1999; 2000; Mirabdullaev et al., 2001; Zavyalov et al., 2003). There are almost no data on eastern basin of the Aral Sea. Within the project frames, a number of field trips have been made to western coast of Western Aral basin, which resulted in collection of materials on all major components of the biota: phytoplankton, zooplankton, zoobenthos and fish fauna.

The assessment of the ecological range of the representatives of the Aral biota is also crucial for project development as it is the changing abiotic parameters of the Aral Sea ecosystem that bring about radical changes in its biota. Of abiotic parameters, water mineralization, which has increased 10-fold in the last 50 years, is most important for living organisms. Only knowing the limits of salt tolerance of the Aral biota representatives, can we make a prognosis of its composition under some transformations of the Aral ecosystem, and evaluate opportunities and parameters of the rehabilitation of the Aral Sea ecosystem. To evaluate the salt tolerance of the Aral biota representatives (both former and current), literature sources and scientific reports have been collected and analyzed; likewise, a number of laboratory experiments have been conducted. Findings on the state of animal populations at certain levels of salinization (both in the Aral and other water bodies) enabled the assessment of the range of their salt resistance, while experimental data helped to make this information more exact.
Data obtained form the basis for the prognosis of the state and succession of the biota at various levels of water salinity, which will be calculated within the frames of the Aral Sea state modeling, implying different variants of its transformation assessed within this project.
As the modern biota of the Aral Sea is extremely poor and specific, i.e. represented by exclusively extreme halophilic organisms; its composition is not sufficient at all for the planned rehabilitation of the original ecosystems of the Aral Sea. To restore the Aral biota it is crucial to apply reintroduction, which, in turn, requires searches for potential donors – ecosystems that have preserved species of the original Aral ecosystem. Such donors are in particular refugia of the Aral biota, namely, brackish water bodies harboring remaining species of the Aral fauna. To reveal such refugia we both collected and analyzed literature data (Kazakhbaev, 1988; Mirabdullaev et al., 2001), and made a number of field trips to water bodies in southern Aral Sea region.
Revealing the remaining Aral biota in lakes of southern Aral Sea region is important not only from the view point of biodiversity conservation, but also for the increase of biological productivity of water bodies lying in Central Asia. The water used for irrigation in Central Asia is mainly collected in enclosed terminal water bodies such as Aidarkul, Sarykamysh, Ulli-Shorkul, Karakyr et al. Most aquaculture ponds are such brackish water bodies that have emerged in the last 30 to 40 years. This brackish water bodies are usually poor in terms of biota, which was formed, as a rule, on the basis of a freshwater river biota. Mollusks or benthic crustaceans, which form the foraging basis for fishes in water bodies with similar abiotic conditions (the Aral Sea, the Caspian Sea and the Sea of Azov), are almost unavailable in them. As a result, the benthic biomass forming the foraging basis for most commercial fishes, e.g., in Aidar-Arnasai lake system is dozens times as low as in these above water bodies. Gaps in ecological niches in most of considered lakes result in their decreased biological productivity and eventually in lower fish yields. In this case, the introduction of some representatives of the Aral biota could prove an effective means for an increase of fish yields of major aquaculture ponds in Uzbekistan (Mirabdullayev et al., 1999). Studies conducted within the project enabled suggesting a number of steps aimed at the conservation of the unique biota of the Aral Sea region.

19.1 Hydrobiological Database and Related Issues

19.1.1 Material

During the project researches, only the western basin of the Aral Sea was studied. The eastern part of the Aral Sea was inaccessible due to vast coastal marshlands, for the survey of which special equipment is necessary. During eight expeditions, the samples of phytoplankton, zooplankton, and zoobenthos have been collected (Table 19.1 and Table 19.2) and processed at the Laboratory of Hydrobiology of the Institute of Zoology (Tashkent).

Table 19.1 Field trips and hydrobiological material collected

Date	Field sites	Samples collected
2002, August	Asphalt Kulau, Judeli Bulak, Aktumsuk	Phytoplankton, zooplankton, zoobenthos
2002, September	Jideli Bulak, Aktumsuk	Phytoplankton, zooplankton, zoobenthos
2003, July	Jideli Bulak, Aktumsuk	Phytoplankton, zooplankton, zoobenthos
2003, September	Jideli Bulak, Aktumsuk	Phytoplankton, zooplankton, zoobenthos
2004, June	Aktumsuk	Phytoplankton, zooplankton, zoobenthos
2004, August	Jideli Bulak, Aktumsuk	Phytoplankton, zooplankton, zoobenthos
2005, June	Jideli Bulak, Aktumsuk	Phytoplankton, zooplankton, zoobenthos
2005, September	Jideli Bulak, Aktumsuk	Phytoplankton, zooplankton, zoobenthos

Phytoplankton

The diversity of phytoplankton was stable in 2002-2005, but significantly lower than in the preceding period. In these years it continued to decline: if 159 algae species were recorded in 1999-2001, only 81 species were recorded in 2002-2005, less than 60 species being recorded per each year. In the water body, practically only marine and halophilous species remained. Not all recorded algal species are truly planktonic. As the collection sites were shallow (2-4 m), a significant number of algal species are representatives of phytobenthos and peryphyton.

Table 19.2 Species composition of phytoplankton of the Aral Sea in 2002-2005

Year	2002		2003		2004		2005	
Month	08	09	07	09	06	08	06	09
Mineralization, ppt	70	72	75	78	86	90	96	92
CYANOPHYCEAE								
1. Tetrarcus lesteri	+	+	+	-	-	+	-	-
2. Merismopedia tenuissima	+	-	+	+	-	-	-	-
3. Merismopedia glauca	-	-	+	-	-	+	+	+
4. Microcystis pulveria	+	+	+	+	+	-	-	-
5. Microcystis aeruginosa	-	-	-	-	-	+	+	+
6. M. aeruginosa	+	+	+	+	+	-	-	-
7. Gloeocapsa sp.	+	-	-	+	-	+	-	-
8. G. alpina f. Lignicola	+	+	+	-	+	+	+	+
9. G. Turgida	+	+	+	+	+	+	+	+
10. Gomphospherium sp.	+	+	+	+	+	-	-	-
11. G. Aponina	+	+	+	+	-	+	-	-
12. G. aponina f. delicatula	+	+	+	+	+	-	-	-
13. Anabaena sp.	+	+	+	+	+	+	+	+
14. Oscillatoria sp.	+	+	+	+	-	-	-	+
15. Osc.chlorina (Kutz) G.	-	-	-	+	+	+	+	-
16. Phormidium ambiguum	-	-	-	-	+	+	+	+
17. Phormidium mucicola	+	+	+	+	+	-	-	-
18. Phormidium ambiguum Kissel	-	-	-	-	-	+	+	+
19. Phormidium sp.	+	+	+	+	+	+	+	-
20. Synechococcus sp.(salina?)	-	-	-	-	+	+	+	+
21. Spirulina sp.	-	-	-	-	+	+	+	+
22. L.Kuetzingii (Kutz) Schmidle	-	+	-	-	-	+	+	+
23. Lyngbya sp.	+	+	+	+	+	+	+	+
BACILLARIOPHYCEAE								
24. Cyclotella sp.	+	+	+	+	+	+	+	+
25. C. Meneghiniana Kutz.	+	+	-	+	+	-	-	-
26. Grammatophora sp.	+	+	+	+	-	+	-	-
27. Synedra minuscule	+	+	+	+	+	+	+	+
28. S. tabulata	+	+	+	+	+	+	+	+
29. S. tabulata v.acuminata	+	+	+	+	+	+	+	+
30. S. tabulata v.fasciculata	+	+	-	+	+	+	+	+
31. Syn. tabulata v. Parva	+	+	+	+	+	-	-	-
32. Fragilaria construens	-	-	-	-	-	-	+	-
33. Cocconeis plancentula	+	+	+	+	+	+	+	+
34. Achnanthes brevipes	+	+	+	+	+	-	-	-
35. Achnanthes minutissima Kutz.	-	-	-	-	-	+	+	+
36. A. affinis Grun.	-	-	-	-	+	+	+	+
37. Actinocyclus sp.	-	-	-	+	-	+	+	+
38. Diploneis Smithii v.pumilla	+	+	+	+	+	-	-	-
39. Diploneis intterupta	-	-	-	-	+	+	+	+
40. Entomoneis paludosa Reimer	-	-	-	-	-	-	+	+
41. Navicula sp. (lanceolata?)	+	+	+	+	+	-	-	-
42. N.cryptocephala	+	+	+	+	+	+	+	+
43. N.cryptocephala v.intermedia	+	+	+	+	+	-	-	-
44. N.cryptocephala v.veneta	+	+	+	+	+	+	+	+

45. N.cincta	+	+	+	+	+	+	+	+
46. N.halophila	+	+	+	+	+	-	-	-
47. N.Kolbei	+	+	+	+	+	+	+	+
48. N.salinarum	+	+	+	+	+	-	-	-
49. Amphora coffeaformis	+	+	+	+	+	+	+	+
50. Amp.coffeaformis v.pediculus	+	+	+	+	+	-	-	-
51. Amphora .holsatica Hust.	-	-	-	-	-	-	+	+
52. A. ovalis Kutz.	-	-	-	-	+	+	+	-
53. A.robusta Greg.	-	-	-	-	-	+	+	+
54. Amp. veneta	+	+	+	+	+	+	+	+
55. Amphiprora paludosa	+	+	+	-	+	-	-	-
56. Mastogloia Smithii	+	+	+	+	+	-	-	-
57. Hantzschia virgata v.capitellata	+	+	+	+	+	+	+	+
58. Nitzschia sp.	+	+	+	+	+	+	+	+
59. N. acicularis	+	+	+	+	+	+	+	+
60. N. amphibia	+	+	+	+	+	-	-	-
61. N. Closterium	+	+	+	+	+	+	+	+
62. N. Microcephala	+	+	+	+	+	+	+	+
63. N. punctata v. Aralensis	+	+	+	-	+	+	+	+
64. N.cf.sigma (Kutz.)	-	-	-	-	-	+	+	+
65. N. tryblionella v. Levidensis	+	+	+	+	+	+	+	+
66. Gyrosigma scalproides	-	-	-	-	-	+	+	+
67. G. acuminatum (kutz.)Raben.	-	-	-	-	-	-	+	+
68. Surirella cf.ovata Kutz.	-	-	-	-	-	+	+	+
PYRROPHYCEAE								
69. Glenodinium sp.	-	-	-	-	-	+	+	+
70. Peridinium sp.	+	+	+	+	+	-	-	-
EUGLENOPHYCEAE								
71. Euglena sp.	+	+	+	+	+	-	-	-
CLOROPHYCEAE								
72. Chlorella sp.	-	-	-	-	-	+	+	+
73. Dunaliella sp.	-	-	-	-	+	+	+	+
74. Chlamydomonas sp.	+	+	+	+	+	-	-	-
75. Dictyosphaerium pulchellum	+	+	+	+	+	-	-	-
76. Oocystalis sp.	+	+	+	+	+	-	-	-
77. O. marssonii Lemm.	-	-	-	-	-	+	+	+
78. Oocystis borgei	-	-	+	-	-	-	+	+
79. Chloroccocum sp.	-	-	-	-	+	+	+	+
80. Ankistrodesmus.minutissima	-	-	-	-	-	-	+	+
81. Chlorococcoccus turgida	-	-	-	-	+	+	+	+
Total number of species	54	55	56	53	53	54	53	53

Zooplankton

In the last five years, four species have represented permanent elements of the Aral Sea zooplankton: rotiferan *Hexarthra fennica,* branchiopod crustacean *Artemia parthenogenetica,* harpacticoid copepod crustacean *Cletocamptus retrogressus* and larvae of dipteran *Chironomus salinus* (Table 19.3). Surprisingly, in 2004-2005 cyclopoid *Apocyclops dengizicus* and in 2005 rotiferan *Brachionus plicatilis* were recorded, the species which were not observed since mid-1990s. All the species recorded are strict halobionts.

Since 2000, brine shrimp *Artemia* has been dominant in the Aral Sea zooplankton, constituting over 99% of the zooplankton biomass. *Artemia* numbers in western Aral are relatively low, normally at the range of 1000-1500 specimens/m^3, which reflects the oligotrophic state of the waterbody. Adult crustaceans were represented by almost females only, which is characteristic for *Artemia parthenogenetica*, a species widely distributed in hyperhaline waterbodies in Uzbekistan and Central Asia (Mirabdullayev et al., 2002).

Table 19.3 Species composition of zooplankton of the Aral Sea in 2002-2005

Years	2002		2003		2004		2005	
Months	07	09	05	09	06	08	06	09
TAXA								
ROTIFERA:								
1. Hexarthra fennica	+	+	+	+	+	+	+	+
2. Brachionus plicatilis	-	-	-	-	-	-	+	+
CRUSTACEA:								
3. Artemia parthenogenetica	+	+	+	+	+	+	+	+
4. Apocyclops dengizicus	-	-	-	-	+	+	+	+
5. Cletocamptus retrogressus	+	+	+	+	+	+	+	+
INSECTA:								
6. Chironomus salinarius	+	+	+	+	+	+	+	+
Mineralization, ppt	68	72	75	78	86	90	96	92

Zoobenthos

Zoobenthos continued to decrease in 2002-2005. Bivalvian mollusk *Cerastoderma isthmicum* and annelid seaworm *Nereis diversicolor* have not been recorded since 2003. In 2002- 2003 the only benthic animals were ostracod *Cyprideis torosa*, larvae of dipteran *Chironomus salinarius* and bivalvian mollusk *Syndosmya segmentum* (= *Abra ovata*). The latter species inhabits the bottom at the depth of 6-10 m. Zavialov et al. (2003) recorded *S. segmentum* at depths as low as 17 m.

Since 2004, ostracod vanished from samples, so now the only bottom animals in the Big Aral are *Chironomus salinarius* and *Syndosmya segmentum.*

Table 19.4 Species composition of zoobenthos of the Aral Sea in 2002-2005.

Years	2002		2003		2004		2005	
Months	07	09	05	09	06	08	06	09
TAXA								
1. Nereis diversicolor	+	+	-	-	-	-	-	-
2. Cyprideis torosa	+	+	+	+	-	-	-	-
3. Chironomus salinarius	+	+	+	+	+	+	+	+
4. Cerastoderma isthmicum	+	+	-	-	-	-	-	-
5. Syndosmya segmentum	+	+	+	+	+	+	+	+
Mineralization, ppt	68	72	75	78	86	90	96	92

Fishes

Two species of fishes were recorded in 2002, namely, atherine *Atherina boyieri caspia* and flounder *Platichthys flesus luscus.*

Juveniles of atherine in the western basin were recorded in 2002, which is an indication of breeding. In the last years, atherine appear not to have survived the cold winters in the Big Aral. This is confirmed by mass groundings in winter and by the fact that this fish is recorded in the Uzbekistani part of the Big Aral only in the second half of the year. The atherine population may be replenished by the annual spring migrations from the Small Sea.

Dead specimens of flounder were recorded near Jideli Bulak. Flounder was also recorded in 2002 by other researchers (Zavialov et al., 2003). However, later, in 2003-2005 we could not find any fishes. So, probably the fish vanished from the Big Aral.

Два вида рыб были отмечены в 2002: atherina *Atherina boyieri caspia* and flounder *Platichthys flesus luscus.*

19.2 Halotholerance of Components of Autochthonous Biota of the Aral Sea

The most important factor that has catastrophically transformed the biota is the salinity of water-body (from 10 ppt to over 80 ppt). Therefore, to assess the adaptive opportunities of autochthonous biota, we, first and foremost, reviewed its adaptation to salinity.

Methodology. The assessment of hydrobiont tolerance to salinity was made mainly phenomenologically – on the basis of literature and reports, as well as data obtained during the implementation of this project; we recorded the state of the hydrobiont populations in water bodies showing different levels of salinity.
We also conducted a number of experiments aimed at rearing of the Aral aquatic species at different levels of salinity, as well as the effect of varying NaCl concentrations on the respiration as one of the integral values of the bioenergetics of the larvae of shrimp *Artemia parthenogenetica* and fecundated ova of carp *Cyprinus carpio*.
The analysis of literature and our own data enabled us to assess the limits of tolerance to salinity in major representatives of the Aral Sea biota (Table 19.5).

Table 19.5 Limits of halotolerance in major representatives of the Aral Sea biota.

Species	Mineralization, ppt
ROTIFERA	
Brachionus plicatilis	10-80
Hexarthra oxyuris	10-80
ANNELLIDA:	
Nereis diversicolor	10-60
MOLLUSCA:	
Theodoxus pallasi	10-25
Caspiohydrobia spp.	10-35
Dreissena polymorpha aralensis	0-5
Syndosmya segmentum	10-70
Cerastoderma isthmicum	10-60
CRUSTACEA	
Artemia parthenogenetica	60-300
Moina salina	10-80
Ceriodaphnia turkestanica	0-15
Podonevadne camptonyx	10-30
Cyprideis torosa	10-70
Arctodiaptomus salinus	5-60
Calanipeda aquaedulcis	10-45
Halicyclops aralensis	10-40
Cletocamptus retrogressus	10-80
Turkogammarus aralensis	5-20
Palaemon elegans	10-45
Rhithropanopeus harrisii	10-45
INSECTA:	
Chironomus salinarius	10-100
FISHES:	
Pungitius aralensis	5-30
Abramis brama	0-15 (reproduction: 0-8)
Acipenser nudiventris	0-30
Aspius aspius aralensis	0-15 (reproduction: 0-8)
Atherina boyeri caspia	10-80
Barbus brachycephalus	0-15 (reproduction: 0-8)
Chalcalburnus chalcoides aralensis	0-20 (reproduction: 0-15)
Cyprinus carpio	0-15 (reproduction: 0-8)
Clupea harengus	10-40
Neogobius fluviatilis (Pallas)	10-50
Platichthys flesus luscus	10-70
Potamoschistus caucasicus	10-50
Rutilus rutilus aralensis	0-20 (reproduction: 0-10)
Silurus glanis	0-20 (reproduction: 0-8)
Stizostedion lucioperca	0-20 (reproduction: 0-10)
PLANTS	
Chara	0-15
Najas	0-15
Zostera	10-40
Ruppia	10-40
Phragmites	0-20 (reproduction: 0-10)

Study on rearing of hydrobionts at different mineralization.
Mollusks *Theodoxus pallasi*, crustaceans *Turkogammarus aralensis, Artemia parthenogenetica, Arctodiaptomus salinus*, *Halicyclops aralensis,* fish *Pungitius aralensis, Chalcalburnus chalcoides aralensis* (in a pond) have been maintained in laboratory cultures. They were reared at water salinity ranging from 1 to 300 ppt.
The results are given in Table 19.6. It shows that most of the hydrobionts under study have been successfully developing at salinity levels reaching 10-30 ppt. The highest tolerance to salinity was characteristic of copepoda *Arctodiaptomus salinus* and anostracan branchiopod *Artemia parthenogenetica.*

Table 19.6 Results of experiments on rearing of aquatic animals in different conditions of mineralization (D – normal development, d – slow development, R – reproduction, r - slow reproduction, 0 - mortality).

Species	Mineralisation, ppt											
	1	10	20	30	40	50	80	100	150	200	250	300
Theodoxus pallasi	DR	DR	DR	d	0	-	-	-	-	-	-	-
Artemia parthenogenetica	0	D	D	DR	DR	DR	DR	DR	DR	DR	Dr	d
Arctodiaptomus salinus	DR	DR	DR	DR	DR	DR	dr	0	-	-	-	-
Halicyclops aralensis	0	DR	DR	DR	Dr	d	0	0	-	-	-	-
Turkogammarus aralensis	dr	DR	DR	DR	Dr	d	0	-	-	-	-	-
Pungitius aralensis	dr	DR	DR	DR	D	0	0	-	-	-	-	-
Chalcalburnus chalcoides aralensis	DR	DR	Dr	d	0	0	-	-	-	-	-	-

We also studied on the effect of different concentration of NaCl on respiration of the fecundated ova of carp *Cyprinus carpio*. Polarographically, we recorded the O_2 consumption by the fish eggs (roe) after placing them into solutions with different NaCl contents at the temperature 23^{o}C.
Under experimental conditions, salt concentration of 10 ppt did not cause significant changes in the intensity of O_2 consumption by fish eggs; however, the survival rate of the roe significantly decreased. The inhibiting effect of salt on the respiration of fish eggs was recorded beginning with the concentration of 25 ppt (Table 19.7).

Table 19.7 O_2 consumption (J_o) by fertilized eggs of *Cyprinus carpio* and eggs survival in water of different mineralization.

NaCl, Ppt	N	% live eggs	J_o (ng-at. O /min/100 eggs)	live eggs before experiment, %	live eggs after experiment, %
0	*21*	47,8±1,98	79,4±9,52	100	95,2
10	*13*	50,9±2,51	73,4±9,18	100	72,7
25	*10*	51,1±1,97	51,1±3,93	100	68,9
50	*12*	49,4±2,99	45,7±5,54	100	18,2
100	*13*	46,5±3,33	40,4±7,19	100	2,4
150	*9*	54,4±2,03	37,1±1,84	100	1,7

19.3 Review of Bioproductivity Models in the Aral Sea

The original ecosystem of the Aral Sea was relatively poor and biologically low productive, which is connected with the oligotrophic nature of this water body. Nevertheless, until 1960s this is was the largest aquacultural water body in Central Asia with annual catches reaching 40,000 tons of fish (mainly Cyprinidae, but also Acipenseridae). For comparison: all water bodies in Uzbekistan (except aquaculture ponds) produce about 8,000 tons of fish annually. However, by late 1970s, the fisheries on the Aral Sea had ceased as fish stopped breeding. Since 1980s, the Large Aral completely lost its importance in terms of fisheries.
Data obtained on salt resistance of hydrobionts enable the forecast of the biota composition of the Aral Sea at different levels of mineralization (Table 19.8). A decrease in water mineralization and respective reintroduction will contribute to the growth of fish productivity. Fisheries based mainly on flounder and Acipenseridae on the Aral Sea are already possible at the level of water mineralization of 35-40 ppt. However, this is only possible in case of regular stocking of water bodies with juveniles of the Acipenseridae and the use of the Aral Sea as the fattening water body (the so-called pasture

aquaculture). Developed fisheries based on freshwater species (mainly Cyprinidae) is only possible at levels of mineralization of 6-15 ppt (Table 19.9). To implement the project of turning the Aral into a fattening water body of the pasture aquaculture it is necessary to build fish plants.
At mineralization levels within 40-75 ppt, using bioresources of the Aral renders impossible to. However, if the mineralization levels grow higher than 75 ppt, a new type of bioresource, namely brine shrimp *Artemia*, will emerge. Cysts of artemia are widely used in aquaculture and are of commercial importance. Main factors limiting the development of artemia are forage (microalgae of phytoplankton), competitors (zooplankton) and predators (fishes). The development of phytoplankton is largely determined by the number of biogenes (N, P) in the sea. The availability of competitors and predators is mainly determined by their salt resistance. At mineralization reaching 70-80 ppt fishes vanish and the development of zooplankton significantly drops, which helps the artemia population to dominate in the water body ecosystem. This, in turn, enables the commercialization of catches of artemia cysts. The population of artemia preserves productivity at mineralization as high as 200-250 ppt. Artemia is capable of surviving at highest levels of mineralization (up to 300 ppt); however, its productivity is low enough to sustain commercial catches.

Table 19.8 Dependence between mineralization of the Aral Sea and biota composition

Salinity, ppt	Fishes	Fishes (reproduction)	Zooplankton	Zoobenthos	Plants
0-5	Freshwater fishes	Freshwater fishes	Freshwater species	Freshwater species, Dreissena spp., Oligochaeta, Turkogammarus aralensis	Phragmites, Typha, Potamogeton, Chara, Myriophyllum, Ceratophyllum, freshwater microalgae
6-10	cyprinids, Acipenser, Silurus, Stizostedion, Pungitius, Atherina, gobiids,	Atherina, gobiids,	Arctodiaptomus, Moina salina, Hexarthra oxyuris, Brachionus plicatilis	Turkogammarus aralensis, Oligochaeta, Mysidaceae, Dreissena spp., Chironomidae,	Phragmites, Potamogeton, Chara, Najas, Myriophyllum, Ceratophyllum, microalgae
11-15	cyprinids, Stizostedion, Acipenser, Clupea, Atherina, Plathichtys, Pungitius, gobiids,	Plathichtys, Clupea, Atherina, gobiids,	Calanipeda, Polyphemidae, Arctodiaptomus, Moina salina, Hexarthra oxyuris, Brachionus plicatilis, Halicyclops Clethocamptus	Turkogammarus aralensis, Palaemon spp., Mysidaceae, Nereis diversicolor, Abra ovata, Cerastoderma isthmicum, Syndosmya segmentum, Theodoxus pallasi, Caspiohydrobia spp., Oligochaeta, Chironomidae, Cyprideis torosa	Phragmites, Zostera, Chara, Najas, Ruppia, microalgae
16-20	Acipenser, Clupea, Plathichtys, Pungitius, Atherina, Gobiids	Clupea, Atherina, Plathichtys, gobiids	Calanipeda, Polyphemidae, Moina salina, Arctodiaptomus, Hexarthra oxyuris, Brachionus plicatilis, Halicyclops Clethocamptus	Palaemon spp., Nereis diversicolor, Abra ovata, Cerastoderma isthmicum, Syndosmya segmentum, Caspiohydrobia spp., Theodoxus pallasi, Chironomus salinarius, Cyprideis torosa	Phragmites, Zostera, Ruppia, microalgae
21-25	Clupea, Atherina, Plathichtys, gobiids	Clupea, Atherina, Plathichtys, gobiids	Calanipeda, Moina salina, Arctodiaptomus, Hexarthra oxyuris, Brachionus plicatilis, Halicyclops Clethocamptus	Palaemon spp., Nereis diversicolor, Abra ovata, Cerastoderma isthmicum, Syndosmya segmentum, Caspiohydrobia spp., Theodoxus pallasi, Chironomus salinarius, Cyprideis torosa	Zostera, Ruppia, microalgae
26-30	Clupea, Atherina, Plathichtys, gobiids	Clupea, Atherina, Plathichtys, gobiids	Calanipeda, Moina salina, Arctodiaptomus, Hexarthra oxyuris, Brachionus plicatilis, Halicyclops Clethocamptus	Palaemon spp., Nereis diversicolor, Abra ovata, Cerastoderma isthmicum, Syndesmya segmentum, Caspiohydrobia spp., Chironomus salinarius, Cyprideis torosa	Zostera, Ruppia, microalgae

31-40	Acipenser, Clupea, Atherina, Plathichtys, gobiids	Clupea, Atherina, Plathichtys, gobiids	Moina salina, Arctodiaptomus, Hexarthra oxyuris, Halicyclops, Clethocamptus,	Palaemon spp., Nereis diversicolor, Abra ovata, Cerastoderma isthmicum, Syndesmya segmentum, Caspiohydrobia spp., Chironomus salinarius, Cyprideis torosa	Zostera, Ruppia, microalgae
41-50	Atherina, Plathichtys, gobiids	Atherina, Plathichtys	Moina salina, Arctodiaptomus, Hexarthra oxyuris, Clethocamptus,	Palaemon spp., Nereis diversicolor, Abra ovata, Cerastoderma isthmicum, Chironomus salinarius, Cyprideis torosa	microalgae
51-60	Atherina, Plathichtys	Atherina, Plathichtys	Moina salina, Arctodiaptomus, Hexarthra oxyuris, Clethocamptus, Artemia	Nereis diversicolor, Abra ovata, Cerastoderma isthmicum, Chironomus salinarius, Cyprideis torosa	microalgae
61-70	Atherina, Plathichtys	-	Artemia, Moina salina, Arctodiaptomus, Hexarthra oxyuris	Nereis diversicolor, Abra ovata, Cerastoderma isthmicum, Chironomus salinarius Cyprideis torosa	microalgae
71-80	Atherina, Plathichtys	–	Artemia, Clethocamptus	Chironomus salinarius, Abra ovata, Cyprideis torosa	microalgae
81-90	–	–	Artemia, Clethocamptus	Chironomus salinarius, Cyprideis torosa	microalgae
91-100	–	–	Artemia, Clethocamptus	Chironomus salinarius, Cyprideis torosa	microalgae

Table 19.9 Dependence between mineralization of the Aral sea and its biota state

Salini-ty, ppt	Fishery, harvesting	Fishes	Food resources for fish	Plants
11-15	Fishery (artificial reproduction)	Reproduction of a few species in the sea; reproduction of other species in the rivers	Well developed benthos and plankton	Reeds, marine and brackish-water macrophytes, microalgae
16-40	Fishery of flatfish and sturgeons (artificial reproduction)	Reproduction of flatfish and non commercial species	Well developed benthos and plankton	Marine macrophytes, microalgae
41-50	No fishery	Weak reproduction of flatfish, reproduction of non commercial species	Well developed benthos and plankton	Microalgae
51-75	No fishery	reproduction of non commercial species (?)	Plankton, poor benthos	Microalgae
75-200	Harvesting of artemia	-	Plankton	Microalgae
>250	No harvesting of artemia	-	-	Microalgae

19.4 Refugia of the Aral Sea Biota

The Aral Sea has almost completely lost its aboriginal and introduced biota. With the aim of clarifying whether the refugees of the Aral Sea have survived, we identified a number of water bodies in southern Aral Sea basin. Данные о рефугиумах Аральской биоты необходимы для разработки мер по восстановлению исходной экосистемы Аральского моря, а также для сохранения уникального биоразнообразия Аральского моря.

In 2002-2004 data was collected during 4 field trips:
1. 05-15.08.2002. Lakes Saykul, Ayazkala, Aksha;
2. 10-20.09.2003. Lakes Sarykamysh, Muynaksky Zaliv, Mezhdurechie;
3. 08-25.05.2004. Lakes Sudochie; Sarybas;
4. 20-30.05.2004. Lakes Eastern Karatereng, Atakul.

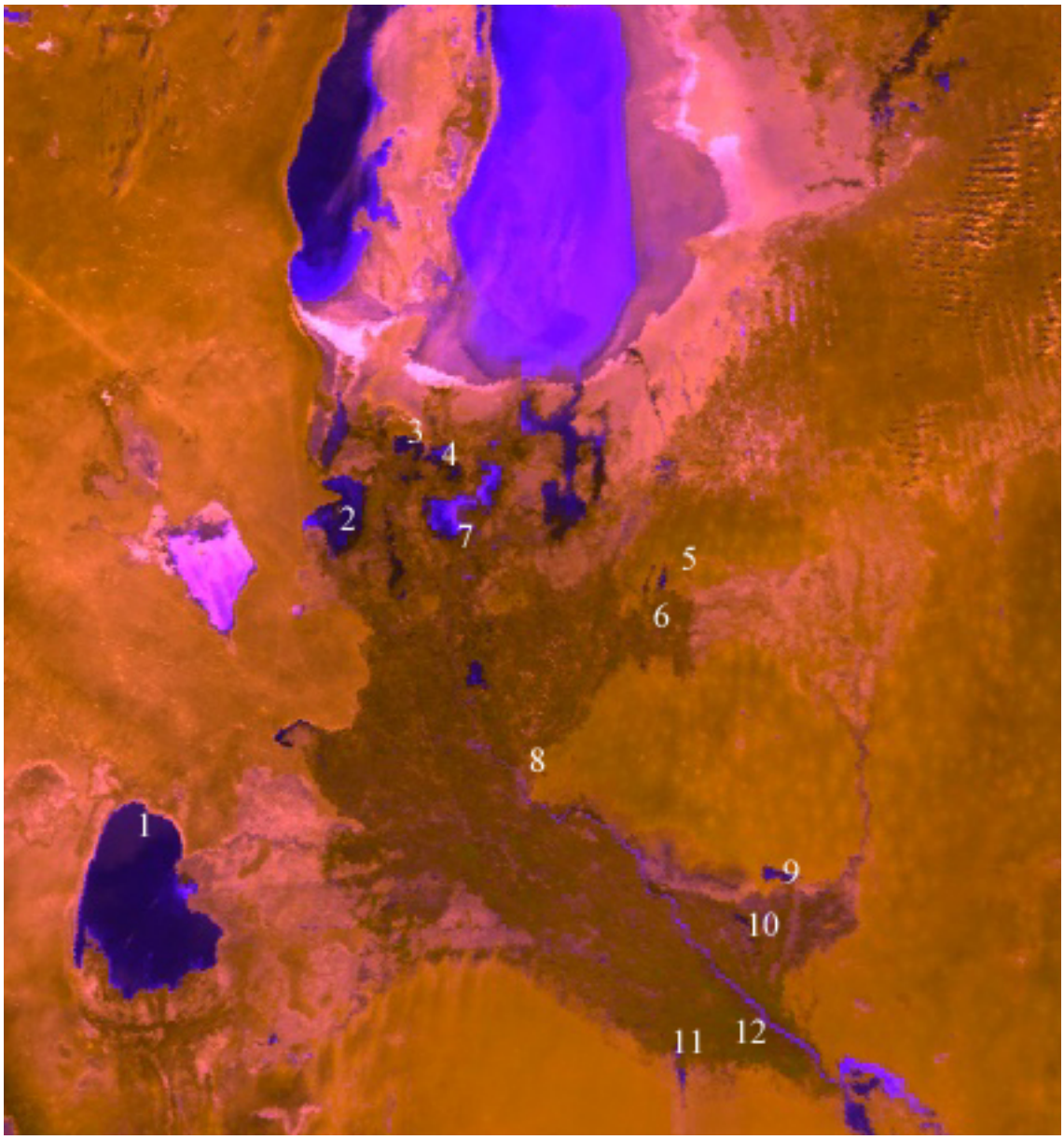

Fig. 19.1 Sites sampled in the Aral Sea Region.

1, Lake Sarykamysh; 2, Lake Sudochie; 3, Lake Muynaksky Zaliv; 4, Lake Sarybas; 5, Lake Eastern Karatereng; 6, Lake Atakul; 7, Lake Mezhdurechie; 8, Lake Saykul; 9, Lake Ayazkala; 10, Lake Akshakul; 11, Lake Ully-Shorkul; 12, Lake Kalajik.

Our researches have revealed however that some elements of Aral biota still exist in some waterbodies lying in southern Aral Sea area, which also are refugees of the Aral Sea biota. The most important refugees are lakes Sarykamysh, Sudochie, and Eastern Karatereng (Fig. 19.1, Table 19.10).
The most diverse community of aquatic animals originating from the Aral were recorded in lake Sudochie. Surveys discovered a number of aquatic animals of the marine origin in the fauna of this lake, namely, marine shell ciliophoran *Folliculina*, bryozoans, marine annelid *Nereis*, marine copepods and ostracods, Aral amphipod, mollusk *Caspiohydrobia*, and fish atherina. The Aral mollusks *Cerastoderma* and *Theodoxus,* crustaceans *Podonevadne camptonyx* and *Turkogammarus aralensis* are recorded in Lake Sarykamysh.

Table 19.10 Biodiversity of the Aral Sea (SU – Lake Sudochie; SK – Lake Sarykamysh; EK – Lake Eastern Karatereng; SB – Lake Sarybas; JB – Lake Jiltirbas).

Representatives of the Aral Sea biota	Su	SK	EK	SB	JB
Zooplankton:					
1. *Podonevadne camptonyx*	-	+	-	-	-
2. *Halicyclops aralensis*	+	-	+	+	-
3. Leptocaris brevicornis	+	-	-	-	-
4. Mesochra aestuarii aralensis	+	-	-	-	-
5. *Schizopera aralensis*	+	-	-	-	-
6. Nitocra lacustris	+	-	-	-	-
Total zooplankton species	76	23	26	24	27
Zoobenthos:					
1. *Nereis diversicolor*	+	+	-	-	-
2. *Turkogammarus aralensis*	+	+	+	+	-
3. Cerastoderma isthmicum	-	+	-	-	-
4. Dreissena polymorpha	-	-	+	-	-
5. Theodoxus pallasi	-	+	-	-	-
6. *Caspiohydrobia spp.*	+	+	-	-	-
Total zoobenthos species	94	27	14	16	18
Fishes:					
1. *Abramis sapa aralensis*	-	+	+	+	+
2. *Barbus brachicephalus*	-	+	+	-	-
3. *Chalcalburnus chalcoides aralensis*	+	+	+	+	+
4. Pungitius aralensis	-	+	-	-	-
Total fish species	24	32	27	26	25
Aquatic plants:					
1. *Polysiphonia violaceae*	-	+	-	-	-
2. *Ruppia maritime*	+	-	-	-	-

It is important that drought 2000-2001 revealed that ecosystems of most lakes of the Aral Sea area (e.g., lakes Sudochie, Sarbas, Shegekul, Khodjakul etc.) in conditions of water scarcity are very unstable, what create a risk disappearance of some refugees (Mirabdullayev et al., 2004).
Instability of the ecosystems depends on shallow condition of the lakes (depths mainly 1-2 m) and high transpiration (more than 1 m per year). In case of drought it causes sharp decreasing of lake size and increasing of water salinity.
Other risk factors are anthropogenic change of hydrological regime and increase in pollution. For example, deviation of significant water resource from Lake Ayazkul caused an increase in its mineralization and disappearance from its plankton most of elements of the Aral fauna revealed in this lake early in 1990s (Mirabdullayev, Getz, 1996) (Table 19.11). Moreover, for the remaining the Aral Sea biota not only droughts but also a significant decrease in the mineralization are dangerous.

Table 19.11 Changes in planktonic Crustacea species composition in Lake Ayazkul

Species	1990	2002
1. *Alona rectangular*	+	-
2. *Moina salina*	-	+
3. *Halicyclops spinifer*	+	-
4. *Onychocamptus mochammed*	+	-
5. *Mesochra aestuarii aralensis*	+	-
6. *Schizopera aralensis*	+	-
7. *Nitocra lacustris*	+	-
8. *Clethocamptus retrogressus*	-	+
9. *Arctodiaptomus salinus*	+	-

Thus, a number of species of the Aral biota inhabit the water bodies lying in the Aral Sea region, which can be used for the reintroduction into the Aral Sea, provided that abiotic parameters of its original ecosystem are restored, and for the introduction into brackish water bodies of Central Asia.
At the same time, no such typical inhabitants of the Aral Sea as crustaceans *Cercopagis pengoi aralensis, Schizopera reducta, Podonevadne angusta, Evadne anonyx, Galolimnocythere aralensis*, моллюски *Hypanis vitrea, H. minima, Cerastoderma umbonatum, C. lamarcki,* and fishes *Acipenser nudiventris,* and *Salmo trutta aralensis* have been recorded there. These species appear to have become extinct in the basin of the Aral Sea. At the same time, many of these have been preserved in the basins of the Caspian Sea and the Sea of Azov, which can be potential waterbody-donors for the introduction of organisms, aimed at the rehabilitation of the original ecosystem of the Aral Sea.

Measures on conservation of refugiums of Aral biota in the waterbodies of the Aral Sea area

1. Provision of a stable water regime in lakes Sudochie, Karateren, Sarykamysh. Salinity in these lakes (or their parts) must range within 10-15 g/l. to that end, stable water supply and flowing regime are necessary.
2. Increasing of biodiversity of refugiums. For this reason, it would be reasonable to introduce some species from one refugium to another one. In particular it could be recommended to introduce some hydrobiont (mollusks *Caspihydrobia spp.*, *Syndosmya segmentum,* flounder *Platychthys flesus*) from Small Aral (Kazakhstan) to waterbodies of souther Aral Sea area.
3. Increasing number of refugiums: introduction representatives of Aral Sea biota to stable waterbodies with near ecological (especially mineralization) conditions. In particular it could be recommend to introduce representatives of Aral biota to such brackish lakes as Ashikul, Aydarkul, Dengizkul, Kara-Kir.

20. Development of Actions on Maintenance of Spawning of Fishes

Even natural, the fish fauna in the Aral Sea was qualitatively poor. In general, by the diversity of flora and fauna the Aral Sea was the last of the brackish-water seas of the USSR (Karpevich, 1975). The local fish fauna of the Aral Sea comprised twenty species of 7 families (for comparison, in a similarly landlocked Caspian Sea, the fish fauna comprised 130 species of 19 families, Nikolsky, 1940). Of 20 Aral fish species, 10 or 12 were commercial; these were mainly valuable large fishes of high commercial quality, such as Aral barbell *Barbus brachycephalus*, Aral bream *Abramis brama aralensis*, carp *Cyprinus carpio*, asp *Aspius aspius*, roach *Rutilus rutilus aralensis*, pike *Esox lucius*, catfish *Silurus glanis*, and some others. From 80 to 85% of catches consisted of these species.
Owing to acclimatization, the fish fauna was significantly enriched. Acclimatization was initiated in 1927-1929 (Karpevich, 1975). The goal was to increase catches through enriching the fish fauna. As time passed, the trend of perspective formation of euryhaline (salt-resistant) fish fauna prevailed. A total of 18 species of 8 families were introduced into the Aral Sea. All of them, excluding ship sturgeon *Acipenser nudiventris*, i.e. 95% were new to the Aral Sea. Of nine species introduced according to the schedule, only two species, salaka *Clupea harengas membras* and flounder *Plathichtis flesus luscus*, got adapted to the Aral Sea conditions. On the contrary, nine accidentally introduced species all got adapted to inhabiting the Aral Sea. All these species almost at the same time got to the Aral Sea in mid-1950s, when grey mullet was brought from the SE part of the Caspian Sea to the Aral Sea. Undemanding eurybiont species, most of them grew in numbers in a short period of time.
However, as the conditions in the Aral Sea grew increasingly harder, fishes vanished from the sea fauna. Currently, there are no fishes in the greater Aral Sea. Sole dead individuals of atherina were recorded on

the coast in the north zone of this part of the Aral Sea. Apparently, these individuals had migrated there from the smaller part of the Aral Sea during the escapes of water in the area of the dyke constriction in the Strait of Berg.

Peculiarities of the migration behavior of local fish species in the Aral Sea are naturally connected to their breeding biology, feeding and confinement to certain biotopes. In this respect of interest is a review made by G.V. Nikolsky (1940), who distinguished the Aral Sea fish species into seven groups by the pattern of their migrations. It is noteworthy that all aboriginal species are freshwater, brackish-water generative and spring-spawning species.

The first group comprises such fish species *Acipenser nudiventris* and *Barbus brachycephalus*, which spawned in the plain-land part of the Amudarya and Syrdarya and migrated more than thousand km upstream from the river mouth. They moved into rivers mainly in summer having immature sexual products and spawned the following year. The fattening of these fish species in the Aral Sea took place beyond the desalinized zone.

Nikolsky (1940) assigned to the second group those fishes that also moved into the rivers, but spawned in the same year and did not migrate a long distance. These are white-eyed bream *Abramis sapa* and asp *Aspius aspius*. In the sea, they had different areas of fattening: that of Abramis sapa was in the deep part of the sea far from the coast; asp, on the contrary, inhabited the coastal zone, in areas shallower than 10 isobaths.

The fish of the 3rd group, the main commercial species, such as roach, bream, sabrefish *Pelecus cultratus* and pike perch twice approached the coast: in spring for spawning and in autumn after the summer fattening season in deep parts, whose depth reached 15 to 30 m. The spawning grounds of these species are confined to both desalinized parts of the sea and those with the increased salinity.

Carp and catfish belong to the fourth group. These two fish species approach the coastal zone two times: in spring for spawning and in autumn for fattening. In contrast to the 3rd group, their fattening grounds lie near the coast, as a rule, less than 10-12 m in depth.

By the character of migrations, Shemaya is in the 5th group. Once a year it approached the coastal zone, but this approach was not confined to the desalinized zone. After spawning, this fish moved away from the coastal zone to the open sea.

Nikolsky (1940) assigned the so-called reed forms of roach, carp, catfish, redeye *Scardinius erythrophthalmus*, pike, perch and ruff to the sixth group. During their life cycle, these fish species inhabited the coastal zone without moving farther than the coastal reeds both in saline bays and desalinized pre-mouth parts of the Amudarya and Syrdarya.

The fishes of the seventh group, ide and crucian carp Carassius auratus, also inhabited the coastal zone, but in exclusively desalinized pre-mouth waters.

This, the most specific are demands for supporting the spawning migrations of Barbus brachicephalus and Acipenser nudiventris that moved upriver for more than 1000 km from the river mouth. There must be an opportunity for asp and *Abramis sapa* to move short distances into the rivers. In desalinized pre-mouth parts and beyond them in more saline waters, roach, bream, sabrefish, sander, carp, catfish, redeye, pike, perch и ruffe, ide and crucian carp can spawn.

The maintenance of spawning migrations of *Barbus brachicephalus* and *Acipenser nudiventris* under modern conditions of the River Amudarya is most problematic as the migratory routes of these species are blocked by Tahiatash and Tuyamuyun dykes and non-operating fish farms. To restore conditions for the movement of fishes to the spawning grounds, two fish-passes must be made in Tahiatash dyke. If there is a pass for migratory fishes through Tahiatash waterworks facility, spawning of *Barbus brachicephalus* will be possible in the area lying between it and Tuyamuyun (Pavlovsky, 1982). Formerly, about 25% of spawning grounds of this species were situated in this area.

However, to provide a fish-pass for Aral barbel and Aral sturgeon to spawning grounds above Tuyamuyun waterworks facility is practically impossible in current conditions, since no fish-passes were designed during the construction of Tuyamuyun dyke. Therefore, to restore and support the population of Aral barbel in the Aral Sea, it will be necessary to set up artificial rearing and regular releases of juveniles into the River Amudarya.

The conditions for spawning and spawning migrations of the other Aral Sea fishes, such as asp, *Abramis sapa*, *Pelecus cultratus*, pike perch, carp, catfish, roach, bream, redeye, pike, ide, and crucian carp can be provided if a permanent functioning of the part of the Amudarya lying lower than Tahiatash waterworks facility and its connection to the Aral Sea are provided. For such fishes as asp, white-eyed bream, pike perch, carp, catfish, etc., the length of this part of the river is sufficient for spawning.

A peculiarity of the site lying between Tahiatash dyke and the Aral Sea is that the river flow in the area of Mezhdurechensky reservoir is broken at the stretch of 12 km. Part of a river bed called Olidarya is no longer a river flow (note: Olidarya is Uzbek for Dead River), because its bed was blocked by dams in the area of Shuak (1977) and Porlytau. The flow of the river before the upper dam Shuak is diverted into Mezhdurechensky reservoir, which has been in operation since 1986. The outflow of the water from the lake is regulated by a spillway dam at the point of 56 m above sea level. This spillway is a non-

reinforced water-eroded cut. Its width during significant water discharges reaches 450-500 m and the length, 500 m. In Mezhdurechensky reservoir, water inflow and outflow are not regulated; this water body is not regulated now. Part of the waters of Mezhdurechensky reservoir runs along discharge outlets Glavmyaso into the Muinak bay and Marinkin (Bay Rybachiy, Sarybas). During floods and in high-water years, the waters of Mezhdurechensky reservoir are discharged into a lateral spillway and get into the Amudarya river through a system of canals and lakes situated along its right bank. Since 2004, a construction of a large regulator-spillway of water reaching 360 cubic meters per sec to the system Maypost-Domalak has been under way. The construction must be completed this year. From Rybachiy bay (Sarybas) waters can be discharged along canal Gonchar-Uzyak to the Aral Sea. From it, waters can reach the Amudarya through an unsteady canal Inzhener-Uzyak.

Water surplus flowing into the system of Mezhdurechensky reservoir after the completion of the construction of water-regulating facilities (planned in 2005) in low-water and average-water years will be diverted into the Amudarya and the zone of perspective planning Maypost-Domalak. Thus, the direct flow of the river waters and migration of fishes from the Amudarya into the Aral Sea will be impossible due to the construction of waterworks facilities in the delta of the Amudarya River. The discharge of water will obviously pass through Mezhdurechensky reservoir and in due time through the system Maypost-Domalak.

This circumstance reduces an opportunity of the fish-pass for barbel and sturgeon to their spawning grounds. For the other Aaral-Amudarya fishes, spawning grounds and ways of spawning migrations, respectively, will be separated in two by the area of water-discharge from Mezhdurechensky reservoir and the system Maypost-Domalak.

However, during stable water supplies and regular functioning of the bed of the River Amudarya, conditions for the spawning of this group of fishes and their natural breeding will be provided to a certain degree. The migration of fishes and their juveniles from the Amudarya will also be possible provided there is a regular water flow in the Amudarya. It is should be taken into consideration that the migration of fish down is a crucial factor in the formation of many commercial fish stocks in the delta of the River Amudarya. Commercial populations of усача and шипа were formed owing to the migration of the offspring down from spawning grounds in the River Amudarya. Support of a small number of barbel and sturgeon under conditions of stable water supplies and the functioning of the River Amudarya will be provided owing to the migration of the juveniles of *Barbus brachicephalus* down the river from spawning grounds between Tahiatash and Tuyamuyun and Acipenser nudiventris from nesting grounds higher than Tuyamuyun waterworks. However, it is reasonable to construct a fish hatchery on Tuyamuyun reservoir in order to establish a stock of spawners in the Amudarya and support their numbers in spawning grounds beyond Tuyamuyun.

To summarize, to maintain spawning migrations and the pass of fish to the Aral Sea upon the restoration in the Aral sea or some of its parts conditions close to natural ones prior the 1960s, it is necessary to:

- Stabilize the water regime in the Amudarya, its regular functioning and a permanent connection of this river with the Aral Sea;
- Set in operation two fish-passes in Tahiatash dyke;
- Consider an important question of construction of fish-passes in the dyke of Tuyamuyun waterworks with the aim of providing a complete breeding of the populations of valuable migratory fishes, Aral barbel and Aral sturgeon;
- To form the stocks of spawners of Aral barbel and Aral sturgeon in the River Amudarya and maintain their numbers, it is reasonable to establish a fish hatchery on Tuyamuyun reservoir. It will be possible to establish a population of these fishes in the Aral Sea owing to the migration of juveniles down the river.

21. Recommendations on Artificial Rearing of Commercial and Endemic Fish Species

Large-scale construction of waterworks facilities in the basin of the River Amudarya and Syrdarya aimed at redirection of water resources for irrigated agriculture and a consequent transformation of the hydrological regime in the rivers and the Aral Sea have caused – and still cause – an extremely adverse effect on the fish population and resources in the basin of the Aral Sea. By early 1980s, a number of aboriginal fish species had vanished from the fauna; the most valuable commercial, anadromous and semi-anadromous fish populations inhabiting the Aral Sea basin had been gone forever. In 1983, the sea fisheries ceased.

Of forty aboriginal fishes inhabiting the plain-land part of the Amudarya, almost all endemics of the Aral Sea basin, except sharpray *Capoetobrama kuschakewitschi* and shemaya *Chalcalburnus chalcoides* are suppressed. Twelve fish species inhabiting the Amudarya river basin were officially included into the Red

Data Book of Uzbekistan (2003). The relict endemics of the Amudarya, such as big and small Amudarya shovelnose sturgeons *Pseudoscaphirhynchus kaufmanni* and *Pseudoscaphirhynchus hermanni*, the endemics of the Aral basin *Aspiolucius esocinus*, as well as the populations of *Barbus brachycephalus brachycephalus* (Kessler, 1872) and *Acipenser nudiventris*, which had made the Aral Sea fisheries famous before, have critically decreased in numbers. Part of them, namely, ship sturgeon *Acipenser nudiventris*, *Pseudoscaphirhynchus kaufmanni* and *P. hermanni*, spined loach *Sabanejevia aurata aralensis,* Aral trout *Salmo trutta aralensis* are included in the IUCN Red Lists (2000).

The death of the Aral Sea and violation of the migratory regime of the Amudarya fishes have resulted in the reduction of the biodiversity of the fish fauna of the Aral-Amudarya basin, vanishing and violation of breeding of many valuable commercial anadromous and semi-anadromous populations of aboriginal fishes, which in turn has adversely affected the quality and amounts of breeding of fish resources in water bodies located in the lower reaches of the Amudarya river. Fish stocks in this zone were largely maintained owing to the populations of several Far-East fishes (silver carp *Hypophtalmichtys molitrix*, grass carp *Ctenopharyngodon idella*, white Amur bream *Parabramis pekinensis*, snakehead *Channa argus* and some others) that settled there in 1960s.

The drought that happened in 2000-2002 has practically caused the drying up of water bodies in the sea zone of the Amudarya and, respectively, the total death of the populations of commercial fishes in this region, undermining resources and bringing about the collapse of fisheries in Karakalpakstan.

Water deficit and irregular water supplies to the delta of the River Amudarya, particularly in low-water seasons in 2000-2001 and the first half of 2002 have resulted in the drying up of most water bodies situated in the region of the Aral Sea. By the time of restored water supply in June 2002, water had been preserved only in 5 to 15% of the area of lakes. This inflicted heavy losses to biological resources, whose reproduction was violated. Fish resources sustained particularly heavy losses, because people were forced to perform total catches. Coupled by large-scale poaching, this brought about the exhaustion of fish stocks and spawners and subsequently collapse of fisheries in Karakalpakstan. Thus, fish catches reached only 200 tons in 2002.

To restore fish resources in the Aral Sea region with subsequent distribution of fishes throughout the rehabilitated ecosystem of the Aral Sea for their fattening, it is reasonable to establish an artificial rearing of valuable commercial aboriginal fishes and artificially form their populations in water bodies of that region.

Of the fishes mentioned before, the artificial rearing of sander *Zander lucioperca*, catfish *Siluris glanis* and asp *Aspius aspius* holds promise. Sander is the most salt-resistant representative of the aboriginal fish fauna. This fish was the last commercial object in the Aral Sea when fisheries had ceased there and levels of salinization reached 20 g/l. The technology of rearing of these fish species in the other regions has already been developed. It will be necessary to adapt this technology (e.g., time and place of catches, conditions of maintenance and obtaining of sexual products taking into consideration climatic peculiarities, etc.) to conditions of southern Aral Sea region. The populations of carp and bream, whose stocks died out during the drought of 2000-2002 need artificial maintenance. It will be reasonable to artificially maintain conditions for fish breeding in lakes by establishing artificial nests for spawning as a measure contributing to the natural breeding of pike perch in water bodies connected to the flow of the River Amudarya (e.g. Reservoir Mezhdurechensky).

Thus, through the artificial rearing of commercial fish species and annual fish stocking of water bodies, the formation of commercial numbers of valuable fish species in water bodies of southern Aral zone, stabilization and increase in numbers of spawning populations of valuable fish species will take place, which will result in the development of independently breeding stocks of valuable fishes.

It is appropriate to develop the artificial rearing of these species, as well as carp and bream on the basis of fish nursery at Village Porlytau of Muinak district, the Republic of Karakalpakstan. This nursery with 150 hectares of growing ponds and output of 500 million larvae and current year fish of 10 metric centners per hectare was formerly part of Muynak Fishing Farm that had 1200 hectares of fattening ponds. It was put into operation in 1979.

The goals Muynak fishery farm was the rearing of current-year carps and phytophagous fishes (silver carp, grass carp) for the stocking of natural lakes of Mezhdurechie and lake farms in the delta of Amu Darya, as well as commercial rearing of fish basically for canning manufacture.

In the span from 1980 to 1995, this fish farm failed to reach the designed capacity; the number of reared larvae was below 35 million, while the number of fish that this fish farm provided Muynak fish-canning combine annually did not reach the designed amounts (500-1200 tons); it only ranged within of 20-462 tons. Part of current year fish were released into Muynak gulf and Mezhdurechie.

However, the functioning of this fish farm was hindered by the extremely adverse conditions, which did not meet the requirements of fish-rearing process. Therefore, this facility (in view of adverse water supplies due to objective reasons) could not reach the designed capacity; by late 1990s, it ceased to operate. Currently, this fish farm is idle; of all its facilities, only the incubatory shop with 150 hectares of growing ponds has remained. The workers of this shop, skilled fish breeders knowing the technologies

of artificial rearing of fish species, still live in Settlement Porlytau in the hope for renewal of fish rearing in this region.
In current conditions of southern Aral Sea region the priority in artificial rearing of food fishes in view of the state of their populations, productive and consumer parameters, is the following:
1. Pike perch (in great demand on the European market in connection due to drops in hake catches)
2. Asp
3. Carp
4. Bream
5. Catfish

Of endemics and endangered species, big and small Amudarya shovelnose sturgeons, Aral barbel and Aral ship sturgeon require artificial maintenance. The biotechnology of the artificial rearing of these fishes, except ship sturgeon, has not been developed, although attempts have been made. One of the main ways of preservation of Red-Data Book species is the artificial reproduction. This method maintains the numbers of many species of осетровых, лососевых and сиговых fishes.
Only owing to artificial rearing it was possible to save белорыбицу from vanishing in the Volga River. Now France, Germany, Italy and Russia have joined their efforts to save атлантического осетра, fish that has almost completely vanished. The fertilized eggs of this most valuable fish were obtained artificially from several spawners in France. Juveniles are being reared now.
Currently, establishment of a specialized expo-research aquarium center of the fauna of fish and invertebrates of the Aral Sea basin on the basis of nature reserve Badai-Tugai is of significant important. The gene pool of big and small Amudarya shovelnose sturgeons, Aral barbel and Aral ship sturgeon could be preserved there and methods of the artificial rearing would be refined for the obtaining of offspring and artificial support of their numbers in natural conditions.
The other promising measure both in research and practical aspects is creation of a low-temperature gene bank of the fauna of the Aral Sea (including fish fauna) jointly by the Institute of Bioecology of Karakalpak Academy of Sciences, the Institute of Zoology of Uzbek Academy of Sciences and nature reserve Badai-Tugai, in which a long-term preservation of sperm, fish eggs and somatic cells could be provided. A similar center is available in Pushchino-on-Oka (Russia) on the basis of the Institute of Biophysics of Russian Academy of Sciences.

Thus, specific proposal includes the following:

1. Rehabilitation of fish nursery (with incubation shop) at Village Porlytau situated in Muinak district, Karakalpakstan;

2. Development of biotechnology of the rearing of commercial fishes in the following priority: pike perch, asp, carp, bream, catfish.

3. By applying artificial rearing of the commercial species and annual stocking of water bodies with fish, formation of the commercial numbers of valuable fish species will take place in the water bodies of southern Aral zone, stabilization and increase in the numbers of spawning populations of valuable fish species will result in the independent breeding of commercial stocks of valuable fish species.

In respect to endemic and red-data-book species, the following is envisaged:

1. Establishment of a specialized expo-research aquarium center of the fauna of fish and invertebrates of the Aral Sea basin on the basis of Badai-Tugai nature reserve, in which the gene pool of big and small Amudarya shovelnose sturgeons, Aral barbel and Aral ship sturgeon could be kept and methods of artificial rearing refined;

2. Artificial rearing of juveniles and artificial support of the numbers of these species in the wild;

3. Creation of a low-temperature gene bank of the fauna of the Aral Sea (including fish fauna) jointly by the Institute of Bioecology of Karakalpak Academy of Sciences, the Institute of Zoology of Uzbek Academy of Sciences and nature reserve Badai-Tugai, in which a long-term preservation of sperm, fish eggs and somatic cells could be provided.

22. Ecological Evaluation of Expected Results

With the existing infrastructure in the Amudarya delta, water supplies allow to maintain Eastern bed within 21 m and 31 m in almost all variants. At this variant, Western bed catastrophically falls to levels ranging between 20 and 26 m. In these same conditions, the expected mineralization in Eastern bed will widely range from 6.5 g/l to 100 g/l, while some extreme values may reach 250 g/l. Western bed shows a stable mineralization growth to 150-270 g/l and only in one variant becomes stabilized at 120 g/l [CR2+3].

This variant is not profitable at all from the ecological view point. The volume of western basin significantly drops and its high mineralization unambiguously leaves no hope to rehabilitate the original ecosystem. Fisheries will render impossible in all variants. As the mineralization continues to grow higher than 200 ppt the water body will lose its importance in terms of artemia catches. Likewise, the catastrophic ecological situation will be unfolding in Eastern basin. Enormous fluctuations of mineralization will prevent any stable biogeocenosis from developing there. Similarly enormous fluctuations in the area of eastern water body will hinder the formation of stable arid and steppe biogeocenoses in part of the Aral Kums. Periodical floods of saline waters will destroy the emerging vegetation and associated fauna. This currently existing variant is the least favorable.

In the variant of water supply suggested in the NATO project (Fig. 9.18), the ecological situation is perhaps similar: sharp fluctuations of volume, area and mineralization of eastern basin will prevent any stable or productive biocenoses from forming there. The water body will represent a trap for biota, in which mass extinctions of organisms will take place as a result of drying, flooding and mineralization fluctuations. This variant will not contribute to the rehabilitation of the original ecosystem of the Aral or even approach it ecological parameters.

From the ecological viewpoint, variant 3 is most promising, in which the maximum flow reaches the Aral bed from the Amudarya delta along the western branches. In this variant, stabilization of water volume and area of western basin takes place and gradual drop in salinity to the level of a brackish water body, which with respective reintroduction measures enables a gradual restoration of the original biota and rehabilitation of fisheries. Considering the fact that the original fish productivity in the Aral Sea reached 5-6 kg/ha, western basin with the area of 5000 sq. km can potentially produce 2500-3000 tons of fish annually. Western basin is a narrow and prolonged water body stretching in meridian direction; therefore, due to a slow convection significant areas of fresh water are formed in the first years in its southern part, which is acceptable for introduction of hydrobionts including commercial fish fauna. Inflow of biogenic elements and organic matter to western basin will contribute to an increase in its overall productivity. A water regulating facility constructed on the canal connecting western and eastern basins could regulate water discharge to eastern basin and therefore control its volume. This, in turn, will enable the development of stable terrestrial biocenoses on the exposed bed of eastern Aral basin.

Another advantage of the realization of variant 3 is an opportunity to develop oil and gas complex. Intensive oil and gas prospecting is under way on the bed of the Aral Sea and production of limited explored deposits has been initiated. The drying and stabilization of Western basin could help to effectively conduct geological prospecting of oil and gas and if successful to begin developing their production.

23. References

1. Aladin, N.V. and Andreev, N.I., 1984. Vliyanie solenosti Aralskogo morya na izmenenie sostava fauni vetvistousikh rakoobraznikh. 20(3):23-28 (in Russian).
2. Aladin, N.V., Filippov, A.A., Plotnikov, I.S., Orlova, M.I. and Williams, W.D., 1998. Changes in the structure and function of biological communities in the Aral Sea, with particular reference to the northern part (Small Aral Sea), 1985-1994: a review. Int. J. Salt Lake Res. 7: 301-343.
3. Aladin, N.V. and Kotov, S.V., 1989. Estestvennoe sostoyanie ecosystemy Aralskogo morya i eye izmenenie pri antropogennom vozdeystvii. Proceed. Zool. Inst. USSR Acad. Sci., 199:4-24 (in Russian).
4. Andreev, N.I., 1989. Zooplankton Aralskogo morya v nachalnyi period ego osoloneniya. Proceed. Zool. Inst. USSR Acad. Sci. 199:26-51 (in Russian).
5. Andreev, N.I., Andreeva, S.I. 2003. Evolutsionnye preobrazovaniya dvustvorchatykh molluskov aralskogo moray v usloviyakh ekologicheskogo krizisa. Omsk. 382 pp.
6. Andreev, N.I., Andreeva, S.I., Filippov, A.A. and Aladin, N.V., 1992. The fauna of the Aral Sea in 1989. 1. The benthos. Int. J. Salt Lake Res. 1:103-110.
7. Andreeva, S.I., 1989. Makrozoobenthos Aralskogo morya v nachalnyi period ego osoloneniya. Proceed. Zool. Inst. USSR Acad. Sci. 199: 52-82 (in Russian).
8. Elmuratov, A.E., 1981. Fitoplankton yuzhnoy chasti Aralskogo morya. Tashkent, Fan (in Russian).
9. Filippov, A.A., 1996. Macrozoobenthos in the inshore zone of the Northern Aral Sea. Int. J. Salt Lake Res. 5:315-327.
10. Joldasova, I.M., Pavlovskaya, L.P., Elbayeva, M.K., Embergenova, M.K., Lyubimova, S.K., Kazakhbaev, S. and Mirabdullayev, I.M., 1999. Kardinalnye izmeneniya v sostave bioty Aralskogo morya. Uzbek. Biol. J. 5:68-70 (in Russian).
11. Kazakhbaev S. Sovremennoe sostoyanie zooplanktona ozera Sudochje. – In: Struktura soobschestv gidrobiontov v nizov'yakh Amudar'i. Tashkent: Fan, 1988. P. 29-37 (in Russian).
12. Karpevich, A.F., 1975. Teoriya i praktika akklimatizatsii vodnikh organizmov. Pischevaya Promyshlennost, Moscow (in Russian).
13. Kiselev, I.A., 1927. Novye dannye o vodoroslyakh Aralskogo Morya. –Depart. Appl. Ichthyol. and Scient. Research. GIOA. 1927. 5 (2):1-64 (in Russian).
14. Mirabdullayev I.V., Getz I. *Halicyclops spinifer* (Kiefer, 1931) (Crustacea, Copepoda) – a new tropical representative of the fauna Central Asia // Proceed. Acad. Sci. Rep. Uzbekistan.. 1996. N4: 43-44 (in Russian).
15. Mirabdullayev, I.M., Joldasova, I.M., Kazakhbaev, S., Lyubimova, S.K., Abdullayeva, L.N. and Turemuratova, G.I., 2001. Sovremennoye sostoyanie ekosistemy Zapadnoy chasti Aralskogo morya. In: I.I.Mirabdullayev (Editor) Problemy sokhraneniya I ratsionalnogo ispolzovaniya biologicheskikh resursov vodoemov Uzbekistana. Chinor ENK, Tashkent, pp. 74-78 (in Russian).
16. Mirabdullayev, I.M., Talskikh, V.N. and Gromiko, K.V., 2001. Ozero Sudochie kak refugiums aralskoy gidrofauny. Proceed. Uzbek Acad. Sci. 5/6:47-50 (in Russian).
17. Mirabdullayev I.M., Jumaniyazova N.I., Kazakhbayev S., Kuzmetov A.R., Niyazov D.S., Joldasova I.M. Brine shrimp *Artemia* (Crustacea, Branchiopoda, Anostraca) in Uzbekistan // TETHYS Aqua Zoological Research. Vol. 1. Almaty: Tethis, 2002. P. 179-180.
18. Nikolsky G.V. Fishes of the Aral Sea // Bulletin of MOIP. N1. 1940. 216 pp. (in Russian).
19. Pichkily, L.O. Fitoplankton Aralskogo morya v usloviyakh antropogennogo vozdeystviya (1957-1980). Kiev, Naukova Dumka. 1981. (in Russian).
20. Yablonskaya E. A. Kormovaya baza rib Aralskogo moray I ee ispolzovanie // Trudy VNIRO. 1960.—43 (1).—C. 150—176.
21. Yablonskaya E. A., Kortunova T. A., Gavrilov G.B. Mnogoletnie izmeneniya bentosa Aralskogo morya // Trudy VNIRO. 1973.—T. 80.—P. 147—158.
22. Zenkevich, L.A., 1963. Biologia morey SSSR. Moscow, Acad. Sci.USSR (in Russian).
23. Zavialov, P.O., Kostyanoy, A.G., Sapozhnikov, F.V., Sheglov, M.A., Khan, V.M., Ni, A.A., Kudishkin, T.V., Pinkhasov, B.I., Ishniyazov, D., Petrov, M.A., Kurbaniyazov, A.K. and Abdullayev, U.R., 2003. Sovremennoe gidrofizicheskoe i gidrobiologicheskoe sostoyanie zapadnoy chasti Aralskogo morya. Oceanologia (Moscow). 43:316-319 (in Russian).

24. Introduction

At present time it is certain that the rehabilitation of the ecosystem and bioproductivity of the Aral Sea by its natural course is impossible. So the development of mesures aimed at stabilization of hydrology and ecology of the waterbody is of primary importance for the region. The main goal of the project INTAS 01-0511 is the forcast of evolution of the Aral Sea under different variants of water menagement in the States of the Aral region. The tasks of the research group CR5 were: the development of mathematical models of different complexity for calculation of hydrological, thermal and salin regimes of the waterbody; the fulfilment of predictiv calculations under different scenarios of Amu Daria water inflow; the estimation of possibility of stabilization of the Aral Sea state under these conditions.
Now the Aral Sea is in the state when under conditons of water scarsity it will be divided into western (more deep) and eastern (shallow and more wide) parts. The research group CR2 has elaborated scenarios of the Aral Sea basin development which were used in our prognostic calculations.
When fulfilling the project numerical models of different dimensions were developed: bulk (zero-dimensional), one-dimensional vertical and three-dimensional ones. Every of them has its own features and can be used for a solving of certain range of tasks. An important part of the work is a detail study of thermodynamic characteristics of high mineralized water, since they essentially affect the hydrophysical processes in water body.
With the use of the bulk and the one-dimensional models calculations for the western part of the Aral Sea were fulfilled. The main tasks of them were to study of long-term dynamics of the sea level, mean temperature and mean salinity under the different scenarios, to estimate possibility of stabilization of level and saline regimes and to investigate the dynamics of vertical stratification. The three-dimensional model was used for calculations of hydrophysical processes in the whole sea as well as in its western part separately. The results of those calculations show more detail the processes of desalination of the sea at the tributary water entry and reveal wind-induced circulation features.

25. Hydrophysical regime of Aral Sea

This section is a brief review of the features of hydrophysical and hydrochemical regimes of the Aral Sea based on the data published before 1990 year. The main source used here is the work [1] which is the last most compete description of these features.
The most attention was paid to the hydrophysical regimes of deep-water regions of the Aral Sea, and first of all to its western part which is the object of our study. The goal of the review is not only the description of sea state in the past but also the revelation of tendencies that were outlined in the annual dynamics of the hydrophysical processes in that time.

25.1 Water Balance and Level Fluctuation

Hydrophysical regime of the Aral Sea is mostly defined by the inflow of two main tributary, Amu-Darya and Syr-Darya. As reported in [1], their total water resources are estimated about 112 km³/yr [1, p. 6].
Since 1961, mostly under anthropogenic factors, the river inflow into the Aral Sea decreased and reached the average value near 2.0 km³/yr in 1981–1986. Underground inflow was relatively small (0.2 km³/yr). Water income due to atmospheric precipitation was about 7 km³/yr, and the evaporation was 46 km³/yr [1, p. 36–38]. From 1780 to 1960 the level fluctuation was between 50 m and 53 m, however because of followed water imbalance from 1960 to 1986 the level dropped by 11.6 m and the waterbody volume decreased by 624 km³ (that corresponds 59% of the average volume in 1960) [1, p. 7, 30]. The annual observation data on the level regime are provided in Table 25.1.

Table 25.1 Annual water balance of the Aral Sea in 1961-1986

Year	River runoff [cm/yr]	Precipitation [cm/yr]	Evaporation [cm/yr]	Level change [cm/yr]
1961	59.3	9.7	103.6	–25.7
1962	52.9	13.0	106.9	–40.0
1963	62.3	17.9	109.4	–23.5
1964	79.8	12.7	100.1	–2.2
1965	46.8	13.4	104.8	–39.8
1966	68.2	10.7	114.7	–40.9
1967	60.8	12.3	94.7	–22.0
1968	59.8	10.0	111.7	–37.5
1969	132.1	16.0	86.6	+50.0
1970	62.9	11.9	102.2	–28.5
1971	39.3	9.7	99.9	–47.3
1972	38.2	9.8	93.9	–52.5
1973	72.5	15.3	96.5	–13.9
1974	13.9	8.2	103.9	–78.2
1975	18.9	7.8	105.7	–83.8
1976	19.5	10.4	91.7	–61.9
1977	13.1	9.2	83.5	–63.0
1978	36.6	11.9	97.3	–47.8
1979	24.7	9.2	98.4	–65.9
1980	16.1	18.8	97.1	–61.5
1981	12.1	23.5	92.9	–56.5
1982	0.0	17.3	78.1	–63.5
1983	0.0	15.4	120.6	–109.0
1984	8.7	7.5	103.7	–89.0
1985	0.0	9.8	85.9	–82.0

Table 25.2 Annual average level, volume and area of Aral Sea. Inflow of water in Aral region in 1962–2002 [2].

Year	Level	Volume	Area	Water inflow (km³/year)		
	(m)	(km³)	(thous. km²)	Syr-Darya	Amu-Darya	Total
1962	52.97	1060	65.9	5.8	27.6	33.4
1963	52.61	1038	64.3	10.6	33.1	43.7
1964	52.49	1030	64.8	15.0	38.3	53.3
1965	52.31	1019	63.1	4.7	25.5	30.2
1966	51.89	993	61.7	9.6	33.1	42.7
1967	51.57	974	60.9	8.7	27.0	35.7
1968	51.24	952	60.1	7.3	28.0	35.3
1969	51.29	955	60.2	17.5	55.5	73.0
1970	51.43	964	60.3	9.8	28.0	37.8
1971	51.06	940	59.7	8.2	15.8	24.0
1972	50.54	909	58.9	7.0	13.2	20.2
1973	50.22	891	58.4	8.9	31.2	40.1
1974	49.85	870	57.9	1.9	6.3	8.2
1975	49.01	822	56.7	0.6	10.6	11.2
1976	48.27	779	55.7	0.6	10.1	11.7
1977	47.63	742	54.6	0.5	9.0	9.5
1978	47.06	713	53.9	0.8	21.3	22.1
1979	46.45	680	52.9	3.2	11.1	14.3
1980	45.75	644	51.7	2.5	8.6	11.1
1981	45.18	616	50.7	7.4	6.3	8.7
1982	44.39	574	49.3	1.7	0.54	2.2
1983	43.55	532	47.7	0.9	2.3	3.2

1984	42.75	499	46.2	0.6	8.0	8.6
1985	41.94	466	44.6	0.7	2.4	3.1
1986	41.10	432	42.8	0.5	0.44	0.95
1987	40.29	401	41.1	1.6	8.2	9.8
1988	39.75	380	39.9	6.9	16.4	23.3
1989	39.08	354	38.4	4.4	1.0	5.4
1990	38.24	323	36.4	3.5	9.0	12..5
1991	37.56	299	43.8	4.0	12.5	16.5
1992	37.20	286	33.9	4.6	28.9	33.5
1993	36.95	278	33.2	7.9	18.8	26.7
1994	36.60	266	32.3	8.9	21.7	30.6
1995	36.11	250	31.3	5.2	5.1	10.3
1996	35.48	230	29.7	5.1	7.5	12.6
1997	34.80	210	28.0	4.6	2 2	6.8
1998	34.24	194	25.5	7.6	23.9	31.5
1999	33.80	181	23.7	5.5	6.4	11.9
2000	33.30	169	22.9	2.9	2.6	5.5
2001	32.16	143	21.2	2.8	0.4	3.2
2002	30.90					

25.2 Salinity Fluctuation

Dynamics of Aral water salinity is caused by the water streams to and from the sea, namely the river run-off, atmospheric precipitations and evaporation. Depending on the water balance, both seasonal and long-term changes in the water body volume and salt storage [3].

Observations performed in years 1956–1985 revealed the regularities in the spatial distribution of salinity and its seasonal dynamics were found as follows [1, p. 72–76].

At the beginning of spring, the salinity distribution in the open sea was almost uniform due to the convective mixing taking place during the winter (see section 2.5). Throughout the season, it is influenced by desalinating river runoff as well as ice melting. In the spring of years 1981–1985 the salinity of surface water was in the range 19.7–20.5 ‰. Further decrease of the river inflow has resulted in disappearance of the zones of low salinity in coastal waters near the mouths of Amu-Darya and Syr-Darya. Low vertical salinity gradients have also become normal for deep-water part of the sea.

In summer, the salinity field is formed by the evaporation and river runoff. Until 1960, the summer vertical distribution remained almost the same as during the spring. However, in the middle 80s the salinity has become growing up with the depth, approximately by 0.2-0.4 ‰ per each 50 m.

In autumn, the salinity distribution became more uniform because of decreasing of river inflow and beginning of convective mixing of water body.

The main feature in the years of anthropogenic influence (1960–1985) was the steady rise of salinity values in all the bulk of water while the seasonal variance of its spatial and vertical distribution remained practically unchanged. Long-term observations have evidenced for the uniform increase of average salinity in time. The salination rate was the highest in the mouths of Syr-Darya, and the lowest in the zone of Amu-Darya influence. In a seasonal aspect, the lowest salination was found to be typical for spring that is due to ice melting as well as to the shift of maximum run-off to earlier months, from summertime to the springtime.

Average salinity had grown up from 1960 to 1985 twice and even more. This fact is explained mainly by reduction in the sea volume, as the salt mass is quite stable in time, so its possible change played a minor role. As for the rate of salinity increase, its absolute value (per year) was 0.8–0.9 ‰ in 1961–1970, then grew up to 3.0–3.5 ‰ in the next decade (1971–1980), and had become about 6 ‰ in 1981–1985 [1, p. 77].

25.3 Thermal and Ice Regime

The thermal regime of the Aral Sea is determined, first of all, by a geographical position, climatic features of region, and geometry of its bottom. The features of a temperature regime of separate parts of the sea are connected also to a character of circulation of waters and influence of a river inflow.

The important role in a temperature mode of the Aral sea up to 1986 year played rather low salinity of water, and therefore temperature of a freezing of water was below than temperature of maximum density.

This factor determined a character of the development of the autumn-winter convection (see section 2.5), that essentially affected vertical distribution and annual dynamics of water temperature [1, p. 43].
Temperature of surface water layer in winter period in central regions of the sea was about 0-1 °C. As a result of intensive convective mixing practically in all water column of the sea to the end of winter homothermy with temperature close to temperature of a surface layer was observed.
The formation of ice on the surface of the sea took place each winter. Up to 1978 year the full cover of water area by ice was observed almost annually; per later years maximum ice cover amounted 45-95 % depending on severity of winter.
In the spring in accordance with a warming of waters the transition from homothermy to vertical temperature stratification of waters and formation thermocline took place. On mouth coastal waters a significant role in forming of thermo- and pycnocline played desalinated water, as a result there was the stable density stratification here which prevents from mixing and promotes rising of vertical gradients of temperature. In remaining regions in the spring temperature of water declined with depth rather uniform. Temperature of waters in near-bottom layers of central region was about 6-7 °C, and this of western basin was 2-3 °C.
In the summer sea water intensively warmed up, and differences in temperature distribution on water area became minimum, the dependence on depth of region of water area disappeared. Surface water temperature changed from 22-23°C in north to 24-25°C in the south. The significant warm-up of surface water layer resulted in increasing of vertical temperature gradients and forming of strongly pronounced thermocline with upper bound on the depth of 10-15 m. The vertical gradients in a layer of saltus on average amounted to 0.7-0.8 °C/m.
The autumn cooling began first of all with shallow regions of northern, eastern and southern coasts of the sea, where temperature of water in October lowered to 10-12 °C. In more deep-water central and western regions, where heat storage was greater than in other parts, the cooling progressed slower.
In the autumn the wind and convective water mixing intensified and the leveling of temperature to depth took place. Homothermy was formed in October in all regions, except the deep-water western region. On vertical cross-sections in a layer of 0-20 m depth isotherms were practically vertical. In western deep-water region on depth more than 20-30 m thermocline with vertical gradients about 0.6-0.8 °C/m was located. Temperature of near-bottom water layer on depth 50-60 m did not exceed 3-4 °C.
The annual dynamics of temperature was observed in the whole water column. The seasonal oscilations of the water temperature gradually damped with depth, and the time when the temperature reached maximum was shifted to autumn and winter. So, the range of seasonal oscillations of temperature of surface water layer could amount to 23-25 °C with the maximum in July – August. On the horizon 60 m the maximum temperature was observed in November. The range of seasonal oscillations of temperature on this depth did not exceed 3 °C. Therefore, the delay in approach of phases of the annual dynamics of temperature was about 10-15 days on each 10 m of depth. The range of daily oscillations of the water temperature did not exceed 2-3 °C as a rule, and fast damped with depth [p. 47–50].
Unlike the internal part of the sea the thermal regime of coastal water was characterized by a more wide range of seasonal and daily oscillations of the water temperature [p. 45].
During the period from 1950-th to 1980-th years there were not sharp changes of a thermal regime of the sea. The most essential changes were observed in transition (spring and autumn) periods and they were related, with a more intensive heating or cooling of the sea water because of significant, more than twice, reduction of volume and heat storage of the sea water.
The analysis of a vertical thermal structure of water of the most deep-water sea regions has allowed coming to a conclusion, that the thermal regime intermediate and near-bottom water layers located below thermocline also has remained practically invariable.
So all water columns of the sea characterized by gradual increasing of a range of annual oscillations of the water temperature due to permanent lowering of temperature of freezing of the sea waters according to growth of salinity, as well as significant shallowing of the sea and decreasing of its heat storage. As a result in winter period practically whole water column cooled up to the temperature of freezing, and in summer the water intensively heated. Thus, the thermal regime of the Aral Sea became more contrast [p. 50].
The surface water temperature in winter period was about 0-1 °C. As a result of convective mixing to the end of winter the homothermy with the temperature close to the surface layer one was observed. The ice-cover took place every winter.
In spring as water heating took place the homothermy was changed by the vertical thermal stratification and the thermocline was formed. The water temperature in the nea-bottom layers of the central basin was about 6-7 °C and in western basin it was about 2-3 °C.
In summer the sea waters heated intensively and the vertical temperature gradient became stronger. The upper border of the thermocline was at the depth of 10-15 m. The surface water temperature changes within 22-23 °C through the area of water.

In autumn the water cooling began and at the same time the convective mixing intensified. The homothermy was settled to the end of October almost in the all regions of the sea. The water temperature of the near-bottom layers at the depth of 50-60 m didn't exceed 3-4 °C.
The seasonal variation of temperature gradually damped with the depth and the time of maximum temperature was shifted to autumn and winter. The range of the variations of near-surface waters was about 23–25 °C with the maximum in July–August and at the depth of 60 m these variations didn't exceed 3 °C.
During the whole observation period from the middle 1950s to the middle 1980s there were no drastic changes in thermal regime of the sea. The most essential changes were traced in periods of transition (spring and autumn) and they were induced by more intensive heating or cooling of sea water due to decreasing of the water heat storage. The analysis of water vertical thermal structure showed that the thermal regime of intermediate and near-bottom waters below thermocline was practically stable.
In the whole the range of annual variations of the water temperature gradually increased due to lowering of ice point with increasing of its salinity as well as to shallowing of the sea and decreasing of its heat storage. So the thermal regime of the Aral Sea became more contrasting [1, cp. 50].

25.4 Density of Water and Hydrostatic Stability

Density and vertical stability of waters are the most important hydrophysical characteristics determining processes of density circulation and convective mixing of water, which in turn cause vertical exchange, cooling near-bottom layers and redistribution hydrological and hydrochemical elements in water column and over water area of the sea. The density of the sea water is determined by its temperature and salinity, therefore field of a density and its vertical structure in the Aral Sea are formed as a result of interaction of temperature and salinity fields and influence of evaporations, circulation of waters, climatic and weather conditions.
In spatial and vertical distributions of density of the Aral water in various periods a number of general regularities were observed. The minimum values of the density, as well as it maximum horizontal gradients in all periods are fixed near the mouth of Amu-Darya. The maximum values of the density marked in gulfs and shallow regions. In a central part of the sea observed of following seasonal dynamics [1, p. 79–82].
In the spring the fast warm-up of the sea waters took place, and due to almost uniform salinity distribution the spatial field of density was determined mainly by the water. The maximum values of the water density in the Large Sea were at this time observed in the northwestern part of the western and central regions, where zone of more cold waters still remained. So, in the Large Sea the density of a surface layer gradually reduced eastward, and also toward mouth coastal waters. In spring the density of sea waters increased with depth rather uniform and reached its maximum value in the near-bottom layer of the western deep-water basin. Therefore with the beginning of intensive spring water heating the stable density stratification on the all water area is observed. The layer of maximum stability coincided with layer of saltus of a density gradually formed at the depth of 5-10 m. To the surface and to the bottom the stability of waters lowed.
In summer the absolute values of the water density almost everywhere decreased by 0.2% in comparison with spring period due to intensive heating. The field of water temperature in this period was rather uniform, and the spatial distribution of the density was formed in main under the effect of the salinity field. As to the vertical density distribution in summer it mainly depends on temperature. Due to intensive heating of the surface water the layer of density saltus was observed at the depth of 10–30 m through the whole water area of the sea.
In the autumn in connection with cooling and further salinization of waters the increase of values of a density on all sea was observed. The vertical distribution of density in this period was mainly determined also by the water temperature, instead of salinity. So, on the greater part of water area of the sea vertical density homogeneity of waters was marked.
During 1956–1985 the significant annual increase of a density and its vertical gradients in whole water column was observed. The significant changes of depth essentially influenced on intensity and terms of heating, evaporation and cooling of the waters, defining seasonal variations of the density field.

25.5 Autumn-winter Convective Mixing

The autumn-winter convection is one of the most important processes forming hydrological structure of the Aral Sea. When the ice point was less than the temperature of maximum density the convective mixing had two stages. First of them started in period of autumn cooling and continued till the mixed

water achieved the temperature of maximum density. Then with the further cooling the density slightly decreased and the stable stratification was settled so the depth of convection penetration did not increase.
When the water temperature achieved ice point the next stage of winter mixing caused by the growing of the surface water density due to salinization while ice forming.
In spring with the beginning of heat accumulation the temperature increased from ice point to the temperature of maximum density. So the conditions for the convection renewing appeared, but the process was far less long than in autumn.
The upper layer about 10 m depth in August was well-mixed due to wind-induced mixing. The autumn-winter convection in the Aral Sea began in the middle of August. To the end of October convective flow reached the bottom almost over the whole water area of the sea except the deepest western part. The depth of the autumn-winter vertical circulation was about 40 m, so the winter convection could reach the bottom of the western part only in sever winters from the middle of November to the middle of January.
With the further increasing of water salinity the autumn-winter convection has to pass in one stage because the ice point will be greater then the temperature of maximum density. So all the water mass will be cooled nearly to the ice point.

26. Modelling of Thermodynamics Properties of Water with High Salinity

Thermodynamic properties of salty water whose values must be known to perform the calculation of heat-and-mass transfer between water body and atmosphere or sediment are as follows:

- density;
- heat capacity;
- evaporation heat;
- relative pressure drop of saturated vapour over salty water;
- freezing point (temperature of ice crystallisation).

External parameters (thermodynamic conditions) that the properties depend on:

- salinity *s*,
- water temperature *T*,
- total pressure *P*.

Thermodynamic salinity *s* is dimensionless and defined as a total sum of weight fractions of all the ionic components per unit weight of the natural water. Also the salinity value can be expressed in a thousandth part "pro mille" (*S*‰).

26.1 Heat Capacity, Freezing Point, Evaporation Heat

26.1.1 Short review of modelling techniques for the thermodynamic functions.

From the chemical point of view, salty water in a sea or a lake represents an aqueous solution of electrolytic salts that dissociated into ions. For the practical purpose only the main components are considered {Na^+, K^+, Mg^{2+}, Ca^{2+}, Cl^-, SO_4^{2-}, HCO_3^-}. There are several approaches to modelling of thermodynamic properties that differs according to a measure of taking into account the chemical nature of ionic components.
In the frame of theory of ideal aqueous electrolyte the ionic dissociation is assumed to be complete as well as the difference in chemical properties of ions is neglected. As a result, the simple linear dependences of the main thermodynamic properties on salinity are usually derived [1]. The equations obtained in this way for heat capacity describe its values quite good the in all the range of existing salinity. Nevertheless, for other thermodynamic properties the error of calculation grows up quadratically with salinity, thus the application of this theory is restricted to $S < 50‰$.
Thermodynamic model by Pitzer is a semi-empirical modification of thermodynamic theory of diluted electrolytes [2]. Empirical parameters of the model are tabulated for all the main ionic components of sea water, thus it can be applied in hydro-chemistry for precise calculation of saturated vapour pressure over salty water of various compositions and freezing point till $S = 260‰$ [3]. Among the problems of using this model, it should mention rather bulky formulae as well as a sharp rise of error when the salinity exceeds the saturation limit [4].
Fitting of empirical parameters of analytical dependences of the properties on temperature and salinity is reasonable if the chemical composition of water body remains stable while valuable fluctuation in total

salinity can occur (this phenomenon takes place in sea water). The data source for the fitting can be obtained from either physical experiment or pre-calculation with more precise models.

26.1.2 Calculation of thermodynamic properties

Heat Capacity

The equation for specific heat capacity of salty water as a function of salinity obtained from the theory of ideal solution is linear:

$C(s, T) = C_w(T)\cdot(1 - s/s_1) + C(s_1, T)\cdot s/s_1$.

The influence of chemical composition on the specific heat capacity (as well as on water density) is rather slight and may be neglected without detriment to the accuracy. International equation of state for sea water (see chapter 4.1.2) is found to be an acceptable method for the calculation of specific heat capacity values at any practical salinity.

Evaporation Heat

The amount of heat required for the evaporation of water from brine, according to the model of ideal solution, is equal to the evaporation heat H_0 from pure water at the same conditions. In reality, the difference between these heats (so called partial enthalpy of water in the seawater, L_1), is less than 0.03% from the value of H_0 at salinity 40‰, but steeply rises with salinity, especially at $T < 25$°C. Nevertheless, even at limiting salinity for all the natural brines the modulus of ratio L_1/H_0 is less than 3%. Thus, for the rough calculations the dependence of heat capacity on salinity can be safely neglected.

The temperature dependence of the evaporation heat is close to linear. As temperature increases from 0° to 40°C, the value of H_0 decreases by 4%.

Humidity at Equilibrium (Relative Pressure of Saturated Vapour)

Model of ideal electrolyte solution being applied to the calculation of equilibrium humidity a_w (the ratio of saturated water vapour pressures over seawater and pure water) gives the Raoul's law in the form:

$$p_w(s, T)/p_w(0, T) = a_w(s, T) = 1/(1 + Rs/(1–s)),$$

where the temperature-independent parameter R depends on the chemical composition. So, for the standard seawater $R = 0.537$ [5], and for Aral water we calculated the value $R = 0.506$. Linearization of Raoul's equation at $s \rightarrow 0$ results in simpler linear dependence:

$$a_w(s, T) = 1 – Rs.$$

The comparison of the equilibrium values calculated according to these formulae with precise Pitzer's model shows that the applicable accuracy of relative humidity values can be obtained over the brines with salinity $S < 50$‰ (*i.e.* $s < 0.05$) and temperature $T < +33$°C. At higher salinity or temperature the relative error can exceed 5% (see Fig. 26.1).

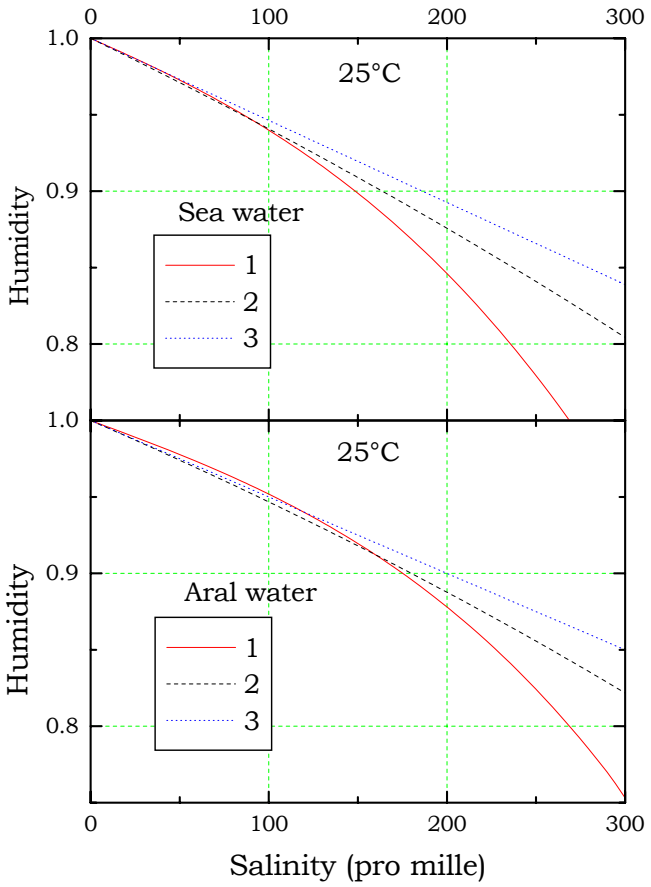

Fig. 26.1 Humidity over salty water at equilibrium. The calculation is made with the models.
1: Pitzer; 2: Raoul; 3: linear.

Freezing point

For water with low salinity, temperature of ice formation is given by Want-Hoff's equation:

$$T = T_0 - \gamma Rs/(1-s),$$

where cryoscopic constant $\gamma = 1.86°C$, freezing point of pure water $T_0 = 0°C$, the parameter R characterizes the chemical composition.

For the calculation of freezing point of seawater at salinity 40‰ and lower, the international empirical equation is widely used (see chapter 27.1.2).

26.2 Equation of State of High Mineralized Water

The dependence of density on temperature and salinity is described by the equation of state. We have compared some formulas by different authors, in particular, that of (a) Knudsen, [6]; (b) Gill, [7]; (c) Chen and Millero, [8]; (d) International equation of state of sea-water, 1980, [6]. It was revealed that in a case of fresh water formulas (b) and (d) are in close agreement, and formula (a) differs from them by ~0.02%. When salinity increases the deviation between those formulas rises and at a salt concentration about 100 g/l formula (a) differs from all others by 20 % whereas the differences between three others are not greater then 2 % (Fig. 26.3). The authors of the formulas in consideration pointed out the range of parameter values under which an accuracy of the formulas was verified. In particular, for the equations (b) and (c) salinity has to be not grater then 1 g/l and temperature has to be positive. But when salinity increases the water friezing-point descends to the values below zero that's why we have to use the equation of state that would be valid under such conditions.

The equation (d) is valid under salinity range from 0 to 42 g/l and temperature range from -2 to 40 ^{0}C. The salinity of Aral Sea water at present time is greater then upper boundary of the interval and as predicted it may achieve values more than 140 g/l. But as far as the dependence of density on salinity has nearly linear character we have chosen the equation (d).

Using formula water friezing-point dependence on salinity given in [6] we have determined that under the Aral Sea water conditions water temperature can go down to -9^{0}C and lower. Furthermore, the character of density dependence on temperature changes when salinity grows. If salt concentration is lower than 21 g/l the temperature of maximum density is higher than friezing-point (Fig. 26.4) therefore the curve of dependence has the inversion point. It leads to stable vertical distribution of density in under the ice period since the water temperature near the ice is close to friezing-point and in the deeper layers it is higher of friezing-point. But under the higher concentrations the dependence becomes monotone and it is close to linear with the maximum in friezing-point. On Fig. 26.4 graphs of dimensionless function at some values of S are shown. In that case the temperature distribution with more high values in deeper layer will be unstable and it will lead to convective processes and full mixing of the whole water column.

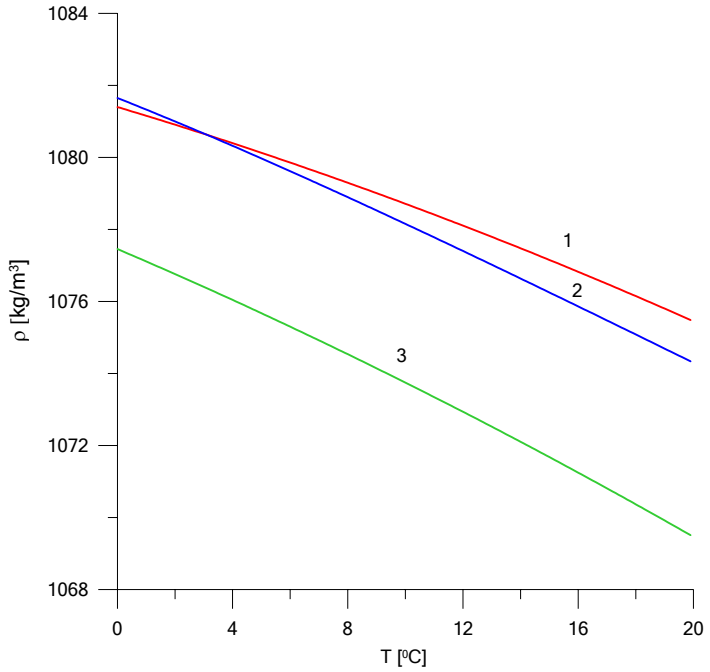

Fig. 26.2 Density dependence on temperature at $S = 100$ g/l.

1 – equation (b); 2 – equation (c); 3 – equation (d)

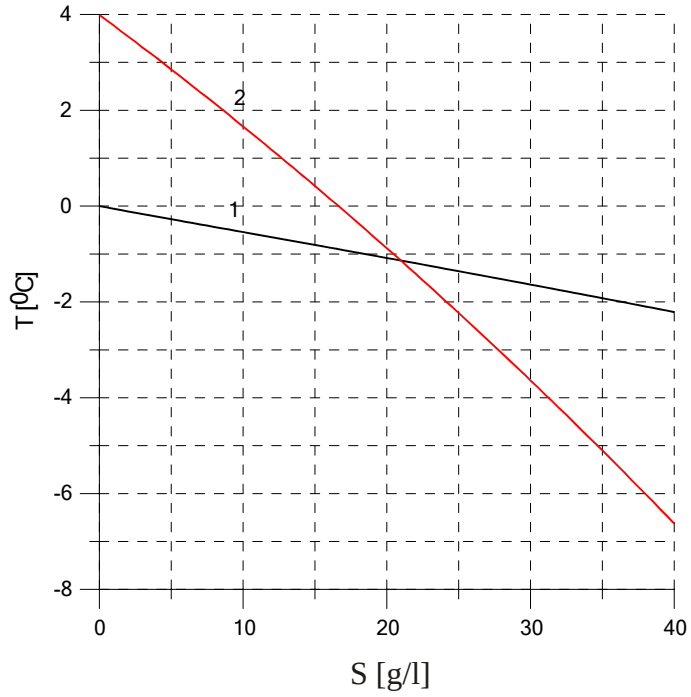

Fig. 26.3 Dependences of water friezing-point (1) and temperature of maximum density (2) of S

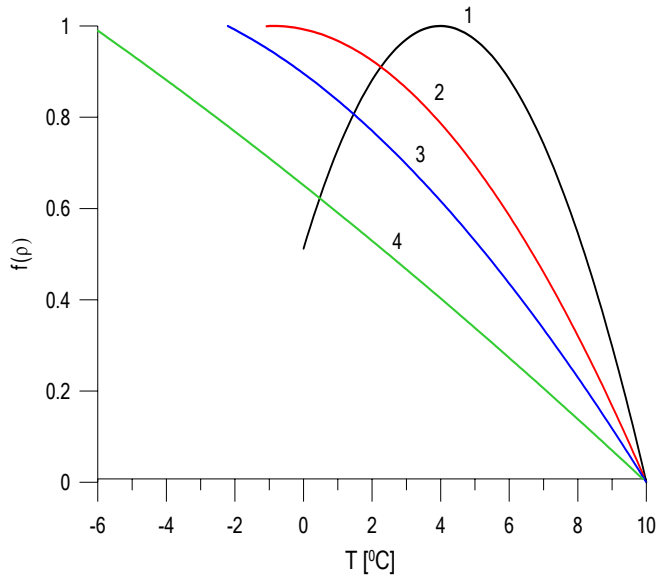

Fig. 26.4 Function $f(S,T)$. 1 – $S=0$; 2 – $S=20$; 3 – $S=40$; 4 – $S=100$ [g/l].

27. Methods of Modelling and Description of the Models in Use

The choice of a method of modelling of hydrodynamic and hydrophysical processes in deep stratified water bodies has great importance for their adequate description and for effective solution of the settled problems. The using of complicated three-dimensional models frequently is not optimal in such cases because those models require large computational resources and information about object suffers of incompleteness and uncertainty. At the same time the most important characteristics of processes under investigation can be revealed applying more simple approximate models. The using of two-dimensional, one-dimensional and bulk (zero-dimensional) models in many cases can be effective enough even under conditions of water bodies of complicated configuration.
In this section two approximate models developed for calculations of hydrophysical processes in the deepest western part of Aral Sea are described: bulk (zero-dimensional) and one-dimensional vertical models. The bulk one allows to describe comparatively simply the dynamics of the main hydrologic processes and to give primary estimation of the speed of water volume decreasing and its mean salinity rising by the use of integral equations of water, salt and temperature balances. The one-dimensional vertical model well-known in limnology allows to describe the vertical distributions of salinity and temperature, and hence the density, i. e. the stratification.
We doesn't abandon the using of three-dimensional model in the cases where it is essential and in section 6 this model finds an application for describing of more complicated hydrodynamics phenomena relating to Coriolis forces effects.

27.1 Bulk Model of Water Level, Temperature and Salinity Change in a Water Body

Calculations of water balance, salt balance and ice-thermal conditions are performed simultaneously, because the corresponding parameters are associated. Water balance determines water body salinity which influences hydrophysical parameters of water and, respectively, water and thermal balance. Model takes into account influence of salinity on freezing temperature, water density, special heat and evaporation intensity. The influence of salinity on freezing temperature is most significant. It strongly shortens freezing period.
The dynamics of ice and snow cover thickness, time of its appearance and disappearance are the essential part of heat balance. Snow-ice cover drastically changes heat flux through water body free surface and directly influences water level, embarrassing evaporation. Also, presence of snow-ice cover significantly influences the nature of currents in a water body, blocking wind effect. Due to increase of salinity and, respectively, decrease of freezing temperature, the role of ice forming processes in the Aral sea thermal balance will decrease, but simulations results have shown that they can not be neglected.
Simulation of ice-thermal conditions is performed basing on Harleman-Rumer method [4, 5], supplemented by accounting of snow cover thickness dynamics and influence of salinity on thermal and water balances.

27.1.1 Water balance

The given model takes into account following components of water balance: river inflow, precipitation and evaporation. Water exchange with groundwater and distributed runoff are not taken into account due to their relative smallness [15]. Thus, the water balance equation is:

$$\frac{dV}{dt} = \sum_{i=1}^{N} Q_i + q_a \Omega,$$

where t – time, h, V – water volume, m^3, N – number of tributaries taken into account (in this work only one tributary is accounted – Amu-Darya river), Q_i – discharge of those tributaries, m^3/h, Ω – surface area of water body, m^2, q_a – water exchange through unit surface area of water body if ice cover is absent or through unit area of water-ice interface if ice cover is present. Water exchange is defined by equation

$$q_a = \begin{cases} q_{pr} - q_{ev} & under \quad \theta_i = 0, \\ -q_f & under \quad \theta_i > 0, \end{cases}$$

where θ_i – ice thickness, m, q_{pr} – intensity of atmospheric precipitation, m/h, q_{ev} – intensity of evaporation, m/h, q_f – intensity of water exchange through water-ice interface, m/h. Formulas for calculation of q_{ev} and q_f are given below under description of heat balance.

Water body volume is understood as the volume of liquid water, i.e. volume of water in ice-snow cover is not accounted. Water level and surface area of water body are calculated as functions of volume by bathymetric curves, and then water level is corrected due to displacement of water by ice and snow:

$$\Omega = \Omega(V), \quad z = z(V) + \theta_i \frac{\rho_i}{\rho_w} + \theta_s \frac{\rho_s}{\rho_w},$$

where z – level of water body free surface, m, θ_s – thickness of snow on ice, m, ρ_w, ρ_i and ρ_s – water, ice and snow density, kg/m^3.

The initial value of water level in water body must be given for calculation of water balance:

$$z\big|_{t=t_0} = z_0.$$

The initial water body volume is also found as a function of water level by the bathimeric curve.

27.1.2 Heat balance

While calculating heat balance the heat incoming with tributary water and the heat flux through unit surface area of water body, if ice cover is absent, or through unit area of water-ice interface, if ice cover is present, are taken into account. The heat exchange with bed is much less intensive than the heat exchange with atmosphere [15], so it can be neglected.

Thus, the heat balance equation is:

$$\frac{d}{dt}(VT_w) = \sum_{i=1}^{N} Q_i T_i + \frac{\Omega \Phi}{c_w \rho_w}.$$

Here T_w – mean water temperature, °C; Φ – heat flux through unit surface area of water body (including inflow / outflow of heat with evaporating, condensing and precipitating water), if ice cover is absent, or through unit area of water-ice interface, if ice cover is present, kcal/(m^2·h); c_w – specific heat of water, kcal/(g·°C); T_i – temperature of water in i-the tributary, °C.

Due to significant increase of the Aral Sea salinity the model takes into account dependence of thermodynamic water parameters (density, specific heat and freezing temperature) on salinity.

Density is defined by the International Equation of State for a sea water under atmospheric pressure [16]:

$$\rho_w = \rho_{w1} + \left(8.24493 \cdot 10^{-1} - 4.0899 \cdot 10^{-3} T_w + 7.6438 \cdot 10^{-5} {T_w}^2 - \right.$$
$$\left. - 8.2467 \cdot 10^{-7} {T_w}^3 + 5.3875 \cdot 10^{-9} {T_w}^4 \right) S -$$
$$- \left(5.72466 \cdot 10^{-3} - 1.0227 \cdot 10^{-4} T_w + 1.6546 \cdot 10^{-6} {T_w}^2 S^{3/2} + \right.$$
$$\left. + 4.8314 \cdot 10^{-4} S^2 \right),$$

where ρ_{w1} – so-called density of the standard oceanic water, accepted as a standard of pure water:

$$\rho_{w1} = 999.842594 + 6.793952 \cdot 10^{-2} T_w - 9.095290 \cdot 10^{-3} {T_w}^2 +$$
$$+ 1.001685 \cdot 10^{-4} {T_w}^3 - 1.120083 \cdot 10^{-6} {T_w}^4 + 6.536332 \cdot 10^{-9} {T_w}^5 .$$

For evaluation of specific heat of the Aral Sea water the formula, given in [17] for sea water, is used under assumption of water pressure is equal to atmospheric pressure:

$$c_w = \left(4.2174 - 3.6608 \cdot 10^{-3} T_w + 1.3129 \cdot 10^{-4} {T_w}^2 - 2.210 \cdot 10^{-6} {T_w}^3 + \right.$$
$$+ 1.508 \cdot 10^{-8} {T_w}^4 +$$
$$\left. + \left(- 6.616 \cdot 10^{-5} + 9.28 \cdot 10^{-6} T_w - 2.39 \cdot 10^{-8} {T_w}^2 \right) S \right) / 4.19.$$

Freezing temperature T_f, ºC, is defined by formula, given in [16] for a sea water, which is simplified under the same assumption:

$$T_f = -0.0575 S + 1.710523 \cdot 10^{-3} S^{3/2} - 2.154996 \cdot 10^{-4} S^2 .$$

The initial water temperature must be given for calculation of heat balance:

$$T_w \big|_{t=t_0} = T_{w0} .$$

If ice cover is absent, heat flux through unit surface area of water body is calculated as the following sum:

$$\Phi = \Phi_{sn} + \Phi_{at} - \Phi_{br} - \Phi_e - \Phi_h - \Phi_{ev} + \Phi_{pr} ,$$

where

- Φ_{sn} – absorbed sun radiation;
- Φ_{at} – absorbed long-wave atmospheric radiation;
- Φ_{br} – long-wave radiation of water surface;
- Φ_e – heat loss while evaporation or heat release while condensation;
- Φ_h – convection conditioned heat flux;
- Φ_{ev} – outflow of heat with evaporating water and inflow of heat with condensing vapor;
- Φ_{pr} – inflow of heat with precipitating water.

Outflow of heat with evaporating water and its inflow with precipitating water and condensing vapor are evaluated assuming the precipitate temperature equal to the air temperature and the evaporating water temperature equal to the water surface temperature (which is assumed equal to the mean water temperature). If the air temperature is lower than the fresh water freezing temperature, than atmospheric precipitate is regarded liquid. Otherwise it is regarded solid, i.e. snow, and respective formula accounts specific melting heat of snow falling to water:

$$\Phi_{pr} = \begin{cases} T_a c_{w0}\, q_{pr} \rho_{w0} & under \quad T_a \geq T_{f0}, \\ \left(\left(T_a - T_{f0} \right) c_i - L_f + T_{f0} c_{w0} \right) q_{pr} \rho_{w0} & under \quad T_a < T_{f0;} \end{cases}$$

$$\Phi_{ev} = \begin{cases} T_w\, c_{w0}\, q_{ev} \rho_{w0} & npu \quad q_{ev} \geq 0 \quad (evaporation), \\ T_a c_{w0}\, q_{ev} \rho_{w0} & npu \quad q_{ev} < 0 \quad (condensation), \end{cases}$$

where T_a – air temperature at 2 m altitude above sea surface, ºC, T_{f0} – freezing temperature for fresh water, ºC; L_f – specific melting heat, cal/g.; c_{w0} and c_i – specific heat of fresh water and ice (i.e. snow), cal/(g·°C); ρ_{w0} **–** fresh water density, kg/m^3. As far as we assume that evaporating, condensing and precipitating water is fresh, values of freezing temperature, specific heat and density in two last formulas are given for fresh water.

Evaporation intensity is evaluated as:

$$q_{ev} = \Phi_e / \left(L_e \rho_{w0} \right),$$

where L_e – specific heat of evaporation, cal/g.

Other components of heat balance are calculated by formulas given in [4]:

$$\Phi_{sn} = \left(1 - \alpha_w\right)\left(1 - 0.65 C^2\right)\Phi_{sc};$$

$$\Phi_{at} = 4.46 \cdot 10^{-13} \left(T_a + 273.15 \right)^6 \left(1 + 0.17\, C^2 \right);$$

$$\Phi_{br} = 4.74 \cdot 10^{-8} \left(T_w + 273.15 \right)^4;$$

$$\Phi_e = f_w \cdot \left(e_w - e_a \right);$$

$$\Phi_h = 0.459 \cdot f_w \cdot \left(T_w - T_a \right).$$

Here Φ_{sc} – sun radiation under clear sky upon the water body surface, kcal/(m^2 h), α_w – albedo, i.e. reflective ability of water, dimensionless, C – cloudiness, dimensionless, $0 < C < 1$; e_w – pressure of saturated water vapor at the water surface temperature, mm mercury, e_a – absolute humidity at 2 m altitude above the sea surface, mm mercury, f_w – so-called wind function.

The values of e_w and f_w are evaluated by the following empiric functions:

$$e_w = \pi \cdot 25.4 \exp\left(17.62 - \frac{5278}{T_w + 273.15} \right),$$

$$f_w = \max\left(4.3 w_a,\ 3.54 w_a + 3.09 \sqrt[3]{\Delta\Theta_v} \right), \quad \Delta\Theta_v = T_{wv} - T_{av},$$

where T_{wv} – virtual temperature of thin vapor layer contacting water surface, ºC, T_{av} – virtual air temperature, ºC, w_a – wind velocity at 2 m altitude above the sea surface, m/s.

In those formulas T_{sv} and T_{av} are given as

$$T_{wv} = \left(T_w + 273.15 \right) / \left(1 - 0.378 e_w / p \right);$$

$$T_{av} = \left(T_a + 273.15 \right) / \left(1 - 0.378 e_a / p \right),$$

where p – atmospheric pressure, mm mercury.

At this stage of work we take into account the dependence of saturated water vapor pressure on salinity π, dimensionless. Formula for this dependence evaluation is obtained according to Raul law [7], basing on results of chemical analysis of the modern Aral Sea water sample given in [8]:

$$\pi = 1 - \frac{1}{1 + 0.5061621 \cdot S / \left(1000 - S \right)},$$

where S – water salinity, g/l.

If ice cover is present, the heat flux through unit area of ice-water interface is evaluated as

$$\Phi = -\Phi_v - \Phi_f ,$$

where

Φ_v – heat exchange between water and ice;

Φ_f – heat outflow with freezing water or heat inflow with melting water.

Φ_v is evaluated by formula from [5]:

$$\Phi_v = k_v \left(T_w - T_f \right);$$

$$\Phi_f = \begin{cases} T_w c_{w0} q_f \rho_{w0} & under \quad q_f \geq 0 \quad (freezing), \\ T_f c_{w0} q_f \rho_{w0} & under \quad q_f < 0 \quad (melting). \end{cases}$$

where k_v – coefficient of heat exchange between water and ice, kcal/(m^2·°C·h). The last formula is true for evaluation of water inflow because of ice melting from below. The inflow of water because of melting of ice-snow cover from above is described similarly, but the freezing temperature T_f is exchanged by the fresh water freezing temperature T_{f0}, because we assume that ice and snow consist of fresh water.

27.1.3 Dynamics of snow-ice cover thickness change

When water temperature falls below freezing point the ice cover appears. Besides ice cover drastically changes heat flux through water body free surface and pattern of currents, it also influences volume of water below and, accordingly, its salinity, because ice consist mainly of fresh water. Thus we must calculate change of ice and snow cover thickness along with water and heat balance. Besides mentioned above, it allows find the time of ice cover disappearance.
The speeds of ice and snow layers thickness changes are described by the following equations:

$$\frac{d\theta_i}{dt} = v_{bi} + v_{pi} - v_{ei} - v_{ti};$$

$$\frac{d\theta_s}{dt} = v_{ps} - v_{es} - v_{ts}.$$

where

v_{bi} – speed of ice growth or melting from below, m/h;

v_{ti} – speed of ice melting from above, m/h;

v_{ts} – speed of snow melting from above, m/h;

v_{pi} – speed of ice thickness growth due to atmospheric precipitation, m/h;

v_{ps} – speed of snow thickness growth due to atmospheric precipitation, m/h;

v_{ei} – speed of ice thickness change due to evaporation and condensation, m/h;

v_{es} – speed of snow thickness change due to evaporation, m/h;

Ice deposition at the Sea coast while the Sea level lowering and its possible emersion are not accounted due to relatively small annual change of the Sea level and, respectively, the Sea surface area.
For calculation of ice and snow cover thicknesses their initial values must be given:

$$\theta_i \big|_{t=t_0} = \theta_{i0};$$

$$\theta_s \big|_{t=t_0} = \theta_{s0}.$$

Reaching of zero thickness by ice cover and falling of water surface temperature below freezing point are accepted as the criterions of snow-ice cover disappearance and appearance respectively.
The intensity of water exchange between water body and snow-ice cover is calculated in the following way:

$$q_f = \frac{\rho_i}{\rho_{w0}}\left(v_{bi} - v_{ti}\right) - \frac{\rho_s}{\rho_{w0}} v_{ts}.$$

The speed of ice growth or melting from below is defined by relations:

$$v_{bi} = \begin{cases} \left(\Phi_\theta - \Phi_v\right)/\left(\rho_i L_f\right) & npu \;\; \Phi_\theta < \Phi_v \;\; (melting), \\ \left(\Phi_\theta - \Phi_v\right)/\left(\rho_i\left(L_f + \left(T_w - T_f\right)c_w\right)\right) & npu \;\; \Phi_\theta \geq \Phi_v \;\; (growth). \end{cases}$$

where Φ_θ – heat flux through snow-ice cover, kcal/(m^2·h).

It is assumed that the temperature of lower ice surface is always equal to the freezing temperature, corresponding to the current salinity of water body, and the temperature of upper surface is never higher than the fresh water freezing temperature.

Vertical distribution of temperature is assumed linear [19] both in ice and snow and continuous through all snow-ice cover, i.e.:

$$\Phi_\theta = \frac{\lambda_i \lambda_s}{\lambda_s \theta_i + \lambda_i \theta_s}\left(T_f - T_s\right),$$

where λ_i and λ_s – heat conductivity of ice and snow, kcal/(m ºC), T_s – temperature of the upper surface of snow-ice cover, ºC. This temperature is conditioned by continuity of heat flux, i.e. the heat flux through snow-ice cover must be equal to the heat flux through its upper surface [19]:

$$\Phi_\theta + \tilde{\Phi} = 0,$$

where $\tilde{\Phi}$ – heat flux through the upper surface of ice-snow cover, depending on temperature of that surface (in distinction with Φ_θ, $\tilde{\Phi}$ is considered positive, if it is directed downwards, like the heat flux through water body free surface).

If this equation gives temperature of the upper surface of snow-ice cover higher than the fresh water freezing temperature, than it is considered equal that temperature [5]. In that case snow is melting from below because of heat incoming from atmosphere and sun. Since the snow is melted away, the ice begins to melt:

$$v_{ts} = \begin{cases} \left(\Phi_\theta + \tilde{\Phi}\right)/\left(\rho_s L_f\right) & under \quad \theta_s > 0, \\ 0 & under \quad \theta_s = 0; \end{cases},$$

$$v_{ti} = \begin{cases} \left(\Phi_\theta + \tilde{\Phi}\right)/\left(\rho_i L_f\right) & under \quad \theta_s = 0, \\ 0 & under \quad \theta_s > 0. \end{cases}$$

Water, produced by melting snow and ice is assumed penetrating down through ice interstices.

The heat flux through the upper surface of snow-ice cover is evaluated similarly to the heat flux though the water body free surface during the ice-free period:

$$\tilde{\Phi} = \Phi_{sn} + \Phi_{at} - \Phi_{br} - \Phi_e - \Phi_h + \Phi_{pr}.$$

Heat inflow with atmospheric precipitates is defined as:

$$\Phi_{pr} = \begin{cases} \left(T_a - T_s\right)c_i \, q_{pr} \rho_{w0} & under \quad T_a \leq T_f, \\ \left(\left(T_a - T_f\right)c_{w0} + L_f + \left(T_f - T_s\right)c_i\right)q_{pr}\rho_{w0} & under \quad T_a > T_f. \end{cases}$$

According to [5], the other terms of the heat flux are evaluated by the same formulas as for the ice-free period, except the water temperature T_w is replaced by the temperature of upper surface of snow-ice cover T_s, and the saturated water vapor pressure at water surface temperaturea e_w is replaced by the vapor pressure at the temperature of snow-ice cover upper surface e_s, which is calculated similarly.

Besides, due to difference of water surface and snow-ice cover surface roughness and because of lower temperature of snow and ice, wind function for snow-ice cover is calculated as [19]:

$$f_s = 4.3 k_e w_a,$$

where k_e – dimensionless coefficient, describing difference of snow-ice cover and water surface roughness.

The speed of ice and snow thickness grow because of atmospheric precipitation is defined as:

$$v_{ps} = \begin{cases} q_{pr}\ \rho_{w0}/\rho_s & under \quad T_a \le T_{f0}, \\ 0 & under \quad T_a > T_{f0}; \end{cases}$$

$$v_{pi} = \begin{cases} 0 & under \quad T_a \le T_{f0}, \\ q_{pr}\ \rho_{w0}/\rho_i & under \quad T_a > T_{f0}, \end{cases}$$

where T_{f0} – fresh water freezing temperature, °C. The speed of snow and ice thickness change because of evaporation and condensation is defined as:

$$v_{es} = \begin{cases} -\Phi_e/(L_s\rho_s) & under \quad \Phi_e > 0 \ \ u \ \ \theta_s > 0, \\ 0 & under \quad \Phi_e \le 0 \ \ или \ \ \theta_s = 0; \end{cases}$$

$$v_{ei} = \begin{cases} 0 & under \quad \Phi_e > 0 \ \ u \ \ \theta_s > 0, \\ -\Phi_e/(L_s\rho_i) & under \quad \Phi_e \le 0 \ \ или \ \ \theta_s = 0, \end{cases}$$

where L_s – special heat of ice sublimation, kcal/g. I.e. under air temperature below the fresh water freezing point atmospheric precipitates are considered solid, i.e. snow, and increase thickness of snow cover, otherwise it is considered liquid and, penetrating through snow, increase ice thickness. If snow cover is present, snow is evaporated, otherwise – ice. If condensation takes place, it always results in increase of ice thickness only, not snow thickness.

27.1.4 Salt balance

According to our estimations (look appendix), when salinity is below 290 g/l the significant settling-out of poorly soluble salts is not anticipated. According to all considered scenarios, salinity is practically never higher than the mentioned value (look part 5.3.1). So the used model of salt balance does not include the term describing settling-out of salt. Also such secondary elements of salt balance as loss of salt due to evaporation and ice growth, inflow of salt with atmospheric precipitates and condensing vapor, inflow and outflow of salt due to water exchange with ground water, income of salt from atmosphere with dust, loss of salt with splashes and so on are not accounted [1]. The only accounted sources of salt are tributaries. Thus, salt balance is described by the following equation:

$$\frac{d(SV)}{dt} = \sum_{i=1}^{N} Q_i S_i \ ,$$

where S – mean water salinity, g/l, S_i – salinity of tributaries, g/l.

The initial salinity must be given for calculation of salt balance:

$$S\big|_{t=t_0} = S_0 \ .$$

27.1.5 Parametrization of model and its numerical realization

The currently used values of parameters of model of ice-thermal conditions and water balance of the Aral Sea are given in Table 27.1.

Table 27.1 Parameters of model of ice-thermal conditions and water balance of the Aral Sea

designation	*dimension*	*description*	*value*
ρ_{w0}	kg/m^3	fresh water density	1000.0
ρ_i	kg/m^3	ice density	917.0
ρ_s	kg/m^3	snow density	270.0
c_{w0}	cal/(g·°C)	specific heat of fresh water	1.0
c_i	cal/(g·°C)	specific heat of ice	0.50668
λ_i	kcal/(m·ºC)	heat conductivity of ice	1.908
λ_s	kcal/(m·ºC)	heat conductivity of snow	0.17868
T_{f0}	ºC	freezing temperature of fresh water	0.0
L_f	kcal/g	specific melting heat	79.7
L_e	kcal/g	specific evaporation heat	585.55
L_s	kcal/g	specific heat of ice sublimation	677.087
k_e	dimensionless	coefficient, describing difference of snow-ice cover and water surface roughness	0.4
α_w	dimensionless	water albedo	0.06

In this work the values of mass and thermal parameters ρ_i, c_i, λ_i, T_{f0}, L_f, L_e, L_s for fresh water at sea level from [23] and [24] were used, the specific heats of ice melting and sublimation were given for 0 ºC, the specific heat of evaporation – for 22 ºC. The other ice parameters were given also for 0 ºC.

As the snow density ρ_s the middle value of density of snow on ice of the Novosibirsk reservoir in 1981-1982 winter, calculated by data from [25], was used. The heat conductivity of snow λ_s was calculated by the Abels formula from [23]: $\lambda_s = 2.451 \cdot 10^{-6} \rho_s{}^2$.

The values of k_e and α_w where the same as in [20].

The albedo of snow-ice cover was calculated by formulas from [20], and the coefficient of heat exchange between water and ice – by formulas from [19]:

$$\alpha_i = \begin{cases} 0.45 & under \quad T_a \le 0, \\ 0.25 + 0.16\, e^{-0.07 T_a} & under \quad T_a > 0; \end{cases}$$

$$k_v = \begin{cases} 597.6 & under \quad \theta_i < 0.03, \\ 23.76 & under \quad \theta_i \ge 0.03. \end{cases}$$

In the case of thin ice the mentioned heat exchange coefficient is artificially increased to imitate destruction of thin ice by currents and wind, because it leads to more intensive melting.

The assignment of initial ice thickness for the moment of water cooling to freezing temperature is described at the discrete level: when water temperature falls below freezing point, ice thickness (ice thickness is considered equal zero if ice cover is absent) is incremented. The value of that increment is calculated to provide heating of water to freezing temperature by the releasing melting heat. Similarly the

necessary corrections are performed at the discrete level to avoid negative values of ice and snow thicknesses.
The numerical solution of the model equations is performed by the Runge-Kutta method of the second order of accuracy.

27.2 One-dimensional Model of Hydrophysical Processes in Water Body

The main equations of the model were obtained by averaging of the three-dimensional hydrodynamic equations over horizontal cross-sections of water body [27-29] carried out in assumption that main hydrophysical parameters change weakly in horizontal direction [29, p. 608-609]. Such approximation may be used in cases when vertical distributions of those parameters is of the most importance.

27.2.1 Main equations of the model

$$\frac{\partial H}{\partial t} = \frac{\int_0^H (q_{in} - q_{out})dz}{\Omega_{surf}} - q_{ev}, \tag{1}$$

$$\frac{\partial \Omega w}{\partial z} = q_{in} - q_{out}, \tag{2}$$

$$\frac{\partial u}{\partial t} - f \cdot v = \frac{1}{\Omega}\frac{\partial}{\partial z}\left(\Omega K \frac{\partial u}{\partial z}\right) - g\left\langle \frac{\partial H}{\partial x} \right\rangle, \tag{3}$$

$$\frac{\partial v}{\partial t} + f \cdot u = \frac{1}{\Omega}\frac{\partial}{\partial z}\left(\Omega K \frac{\partial v}{\partial z}\right) - g\left\langle \frac{\partial H}{\partial y} \right\rangle, \tag{4}$$

$$\frac{\partial T}{\partial t} + w\frac{\partial T}{\partial z} = \frac{1}{\Omega}\frac{\partial}{\partial z}\left(\Omega K_T \frac{\partial T}{\partial z}\right) + \frac{q_{in}(T_{in} - T)}{\Omega}, \tag{5}$$

$$\frac{\partial S}{\partial t} + w\frac{\partial T}{\partial z} = \frac{1}{\Omega}\frac{\partial}{\partial z}\left(\Omega K_s \frac{\partial S}{\partial z}\right) + \frac{q_{in}(S_{in} - S)}{\Omega}. \tag{6}$$

Here $\Omega = \Omega(z)$ is the area of horizontal cross-section of water body; u, v, w are the velocity components in the direction of axes x, y, z correspondingly; f – Coriolis parameter; q_{in}, q_{out} are the specific discharges of inflow and outflow (on unit of depth); q_{ev} is the effective evaporation; H is the water body depth, $\left\langle \frac{\partial H}{\partial x} \right\rangle, \left\langle \frac{\partial H}{\partial y} \right\rangle$ are the mean slopes of free surface in the direction of axes x, y correspondingly (bottom slope considered to be equal to zero); T, S are the temperature and the salinity of water in water body; T_{in}, S_{in} are the temperature and the salinity of inflowing water; $K = \nu + \nu_t$, ν, ν_t are the coefficients of molecular and eddy viscosity; $K_T = \chi + \alpha\nu_t$, χ is the coefficient of molecular thermal conductivity; K_S is coefficient of diffusion (here we suggest $K_S = K$).

27.2.2 Modelling of the turbulent exchange

For the computation of the coefficients of turbulent exchange two models of different complexity were used. First of them is the model based on **formula by Prandtl – Obuhov** frequently used in the tasks of oceanology:

$$K(z) = (0.05h)^2 \sqrt{\left(\frac{\partial u}{\partial z}\right)^2 + \left(\frac{\partial u}{\partial z}\right)^2 - \frac{g}{\rho_0} \cdot \frac{\partial \rho}{\partial z}},$$

where h is the depth of upper mixed layer. It is defined as the depth of first point z^* where the next condition is satisfied:

$$(0.05z_*)^2 \sqrt{\left(\frac{\partial u}{\partial z}\right)^2 + \left(\frac{\partial u}{\partial z}\right)^2 - \frac{g}{\rho_0} \cdot \frac{\partial \rho}{\partial z}} \le K_{\min},$$

where $K_{\min}$ is minimum value of the coefficient of turbulent exchange.
The second one is two-parameter ***e-ε*-model** [27, 30] based on the equations of transfer of kinetic energy of turbulence (*e*) and rate of its dissipation (*ε*).

$$\frac{\partial e}{\partial t} + w\frac{\partial e}{\partial z} = \frac{1}{\Omega}\frac{\partial}{\partial z}\left(\Omega K_e \frac{\partial e}{\partial z}\right) + P - \varepsilon, \tag{7}$$

$$\frac{\partial \varepsilon}{\partial t} + w\frac{\partial \varepsilon}{\partial z} = \frac{1}{\Omega}\frac{\partial}{\partial z}\left(\Omega K_\varepsilon \frac{\partial e}{\partial z}\right) + \frac{\varepsilon}{e}\left(C_1 P - C_2 \varepsilon\right), \tag{8}$$

where $P = \nu_t\left[\left(\frac{\partial u}{\partial z}\right)^2 + \left(\frac{\partial v}{\partial z}\right)^2 + \frac{\alpha_T}{\rho *} g \frac{\partial \rho}{\partial z}\right]$; $K_e = \nu + \alpha_e \nu_t$; $K_\varepsilon = \nu + \alpha_\varepsilon \nu_t$; $\nu_t = C_\mu e^2 / \varepsilon$; ρ is the water density.
Empirical coefficients using here have the next values [28, 31]:

$$\alpha_e = 1; \quad \alpha_\varepsilon = 0.77; \quad C_\mu = 0.09; \quad C_1 = 1.55; \quad C_2 = 1.92$$

The water density is calculated using International equation of state [16] considering its dependence on the water temperature and salinity. The formula is given in section 27.1.2.

27.2.3 Boundary conditions

When using *e*-*ε*-model the boundary conditions for the equations of transfer of impulse, heat and salinity are to be matched with those of turbulence model [28, 30].
On the bottom at $z = 0$:

$$\frac{\partial T}{\partial z} = 0, \ \frac{\partial S}{\partial z} = 0, \ K\frac{\partial \overline{u}}{\partial z} = k_b \,|\overline{u}|\cdot\overline{u}, \ w = 0; \ \frac{\partial e}{\partial z} = 0, \ \varepsilon = C_\varepsilon \frac{e^{3/2}}{l_0}.$$

On the free surface at $z = H$:

$$\rho c_w K_T \frac{\partial T}{\partial z} = \Phi, \ K\frac{\partial \overline{u}}{\partial z} = \frac{\overline{\tau}}{\rho}, \ q_{surf}\cdot S = K_S \left.\frac{\partial S}{\partial z}\right|_{H(t)}, \ \frac{\partial e}{\partial z} = K_\tau \left|\frac{\overline{\tau}}{\rho}\right|^{3/2}, \ \varepsilon = C_\varepsilon \frac{e^{3/2}}{l^0} \tag{9}.$$

Here c_w is the specific heat capacity; Φ is the heat flux through the free surface calculating by the same method that is used in zero-dimensional model (section 27.1.2); $\overline{u} = (u, v)$; $\overline{\tau}$ is the wind stress; $k_b = 0.014$ is friction coefficient; l_0, l^0 are the turbulence scale near the bottom and near the free surface respectively; $C_\varepsilon = 0.314$; $K_\tau = 2.5$.
The mean slopes of free surface are defined by assigning two additional kinematical conditions for horizontal components of velocity:

$$\left.\begin{array}{l} \int_0^H u(t,z)B(z)dz = Q \\ \int_0^H v(t,z)L(z)dz = 0 \end{array}\right\},$$

where $B(z)$ and $L(z)$ are the width and the length of water body respectively; Q is the discharge.

27.2.4 Numerical implementation

As the depth of water body changes with time the calculation area is mapped on the interval [0, 1] using the next change of variables:

$$\tau = t, \quad \sigma = \frac{z}{H(t)}.$$

Then

$$\frac{\partial}{\partial t} = \frac{\partial}{\partial \tau} - \frac{\sigma H'}{H}\frac{\partial}{\partial \sigma}, \quad H' = \frac{dH}{dt}, \quad \frac{\partial}{\partial z} = \frac{1}{H}\frac{\partial}{\partial \sigma},$$

and equations (2)-(8) in the new coordinates assume the form

$$\frac{\partial \Omega w}{\partial \sigma} = H(q_{in} - q_{out}),$$

$$\frac{\partial u}{\partial t} - \frac{H'\sigma}{H}\frac{\partial u}{\partial \sigma} = \frac{1}{\Omega H^2}\frac{\partial}{\partial \sigma}\left(\Omega K \frac{\partial u}{\partial \sigma}\right) - g\left\langle \frac{\partial H}{\partial x}\right\rangle,$$

$$\frac{\partial v}{\partial t} - \frac{H'\sigma}{H}\frac{\partial v}{\partial \sigma} = \frac{1}{\Omega H^2}\frac{\partial}{\partial \sigma}\left(\Omega K \frac{\partial v}{\partial \sigma}\right) - g\left\langle \frac{\partial H}{\partial y}\right\rangle,$$

$$\frac{\partial T}{\partial t} + \frac{(w - H'\sigma)}{H}\frac{\partial T}{\partial \sigma} = \frac{1}{\Omega H^2}\frac{\partial}{\partial \sigma}\left(\Omega K_T \frac{\partial T}{\partial \sigma}\right) + \frac{q_{in}(T_{in} - T)}{\Omega},$$

$$\frac{\partial S}{\partial t} + \frac{(w - H'\sigma)}{H}\frac{\partial S}{\partial \sigma} = \frac{1}{\Omega H^2}\frac{\partial}{\partial \sigma}\left(\Omega K_S \frac{\partial S}{\partial \sigma}\right) + \frac{q_{in}(S_{in} - S)}{\Omega},$$

$$\frac{\partial e}{\partial t} + \frac{(w - H'\sigma)}{H}\frac{\partial e}{\partial \sigma} = \frac{1}{\Omega H^2}\frac{\partial}{\partial \sigma}\left(\Omega K_e \frac{\partial e}{\partial \sigma}\right) + \tilde{P} - \varepsilon,$$

$$\frac{\partial \varepsilon}{\partial t} + \frac{(w - H'\sigma)}{H}\frac{\partial \varepsilon}{\partial \sigma} = \frac{1}{\Omega H^2}\frac{\partial}{\partial \sigma}\left(\Omega K_\varepsilon \frac{\partial \varepsilon}{\partial \sigma}\right) + \frac{\varepsilon}{e}\left(C_1\tilde{P} - C_2\varepsilon\right),$$

where $\tilde{P} = \nu_t\left[\frac{1}{H^2}\left(\frac{\partial u}{\partial \sigma}\right)^2 + \frac{1}{H^2}\left(\frac{\partial v}{\partial \sigma}\right)^2 + \frac{1}{H}\frac{\alpha_T}{\rho *}g\frac{\partial \rho}{\partial \sigma}\right]$

The boundary conditions take the next form:
on the bottom at $z = 0$:

$$\frac{\partial T}{\partial \sigma} = 0,\ \frac{\partial S}{\partial \sigma} = 0,\ K\frac{\partial \overline{u}}{\partial \sigma} = H k_b |\overline{u}|\cdot\overline{u},\ w = 0,\ \frac{\partial e}{\partial \sigma} = 0,\ \varepsilon = C_\varepsilon \frac{e^{3/2}}{l_0};$$

on the free surface at $z = H$:

$$\rho c_w K_T \frac{\partial T}{\partial \sigma} = H\Phi\,,\ q_{surf}\cdot S = K_S H \frac{\partial S}{\partial \sigma}\bigg|_{H(t)}\,,\ K\frac{\partial \bar{u}}{\partial \sigma} = H\frac{\bar{\tau}}{\rho}\,,\frac{\partial e}{\partial \sigma} = H\cdot K_\tau \left|\frac{\bar{\tau}}{\rho}\right|^{3/2}\,,\ \varepsilon = C_\varepsilon \frac{e^{3/2}}{l^0}\,.$$

For difference approximation of the equations the uniform grid on the segment [0, 1] is used. The first order derivatives are approximated by the scheme with directed differences and the second order derivatives are approximated by the central difference scheme. The implicit scheme in time and splitting on physical processes are used. As the equations of *e*-*ε*-model are non-linear the iterative method is used.

27.2.5 Comparison of two turbulence models

The turbulence model effect on the calculation results was studied by the example of 1.5-year scenario described in section 5.1 but without inflow. The differences of the water level, the mean salinity and temperature, the surface temperature were analyzed. Also the dynamics of vertical distributions of temperature and salinity were compared, and the comparison showed that the distributions in two calculations are similar in qualitative respect. The full description of vertical distributions obtained with the use of *e*-*ε*-model is presented in section 28.3. We will point out only that in comparison with the formula by Prandtl – Obuhov *e*-*ε*-model lead to more intensive mixing processes and the thermocline is more strongly marked. The vertical distribution of temperature in autumn-winter period is presented on Fig. 27.1.
The dynamics of vertical distributions of temperature and salinity also were compared. The comparison has shown that those distributions in two calculations are very close in qualitative respect. The full analysis of the vertical profiles obtained using *e*-*ε*-model are given in section 28.3. It is necessary note that *e*-*ε*-model as compared with formula by Prandtl – Obuhov leads to more intensive mixing processes. The temperature distributions in autumn-winter period obtained in two calculations are given on Fig. 27.1. The differences occurred in the calculations using two turbulence models can be explained by the fact that different values of coefficient of turbulent mixing near the water surface entail the different temperature of surface water (as it can be seen from the equations (9)) that effects on evaporation processes and so on salt regime. The typical vertical distributions of the coefficients of turbulent mixing obtained by using *e*-*ε*-model and Prandtl – Obuhov model are shown on Fig. 27.2, Fig. 27.3 respectively. In autumn-winter period the values of the coefficient are by order of magnitude greater in *e*-*ε*-model so the homogeneous state in water body is formed earlier then in case of Prandtl – Obuhov model. In spring-summer period the counter situation is observed: the values of the coefficient in *e*-*ε*-model are by order of magnitude less then in Prandtl – Obuhov model. So it is clear that *e*-*ε*-model quickly responds to disturb of stability of water column by sharp increasing of the coefficient of turbulent mixing that leads to quicker mixing of the water for settling the stable distribution of the density. Therefore the main calculation using one-dimensional model were fulfilled applying *e*-*ε*-model (Section 28.3.2).
The dynamics of mean parameters of the water body and the near-surface water temperature during all calculation period obtained in two calculations using scenario referred above are presented on Fig. 27.4. Numerical estimation of differences of parameters values in two calculations are presented in Table 27.2. The level dropping in the calculation using *e*-*ε*-model over two years amounted 65 cm whereas in calculation with formula by Prandtl – Obuhov it achieved 1 m. Fig. 27.4 shows that the mean temperature as well as the near-surface temperature during the most part of a year are lower when using *e*-*ε*-model due to more intensive mixing processes and drawing in more cold water from lower layers to upper ones. So the evaporation process under those conditions is less intensive and results in less dropping of the level.

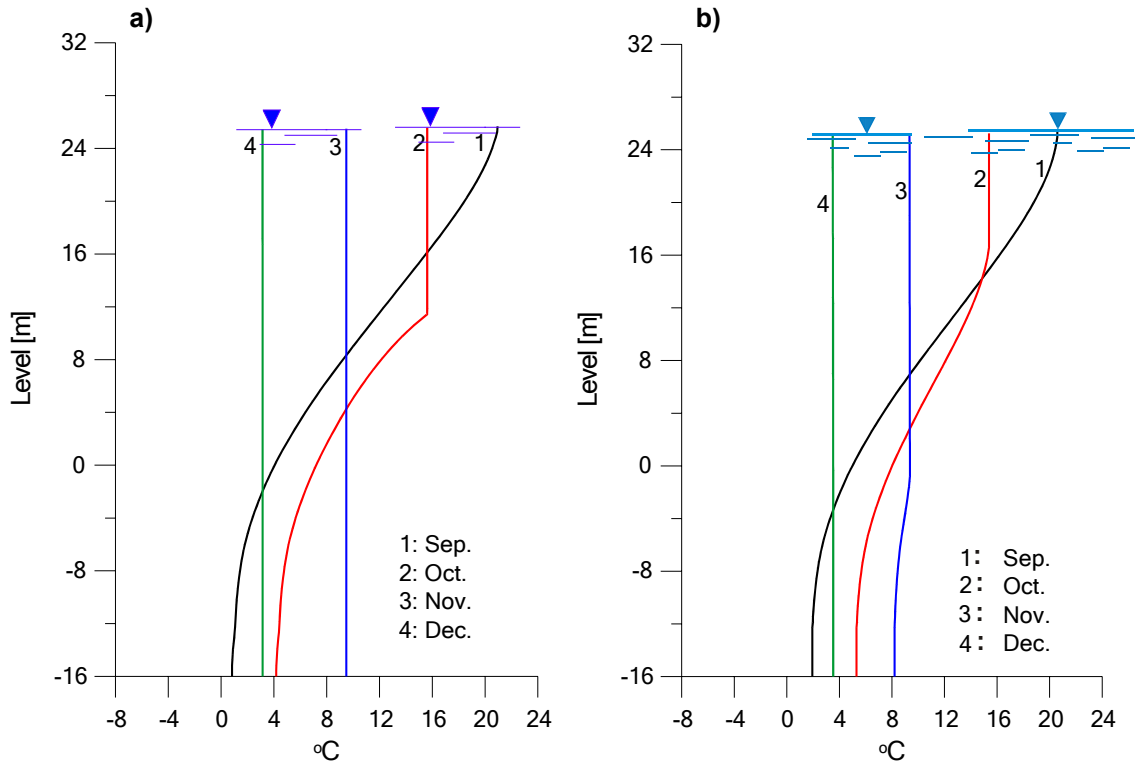

Fig. 27.1 Vertical distributions in autumn-winter period obtained using two turbulence models. (a) – *e*-*ε*-model; (b) – Prandtl – Obuhov model.

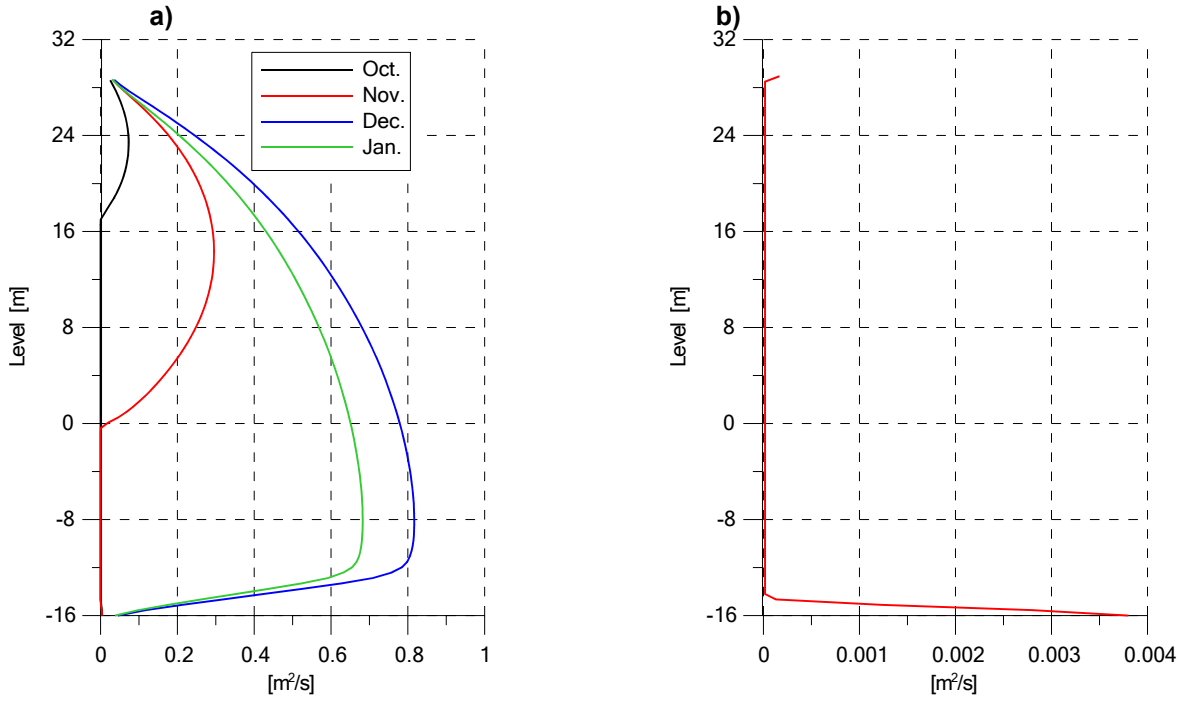

Fig. 27.2 Typical vertical distributions of coefficient of turbulent mixing obtained by *e*-*ε*-model. a) autumn-winter period; b) spring-summer period.

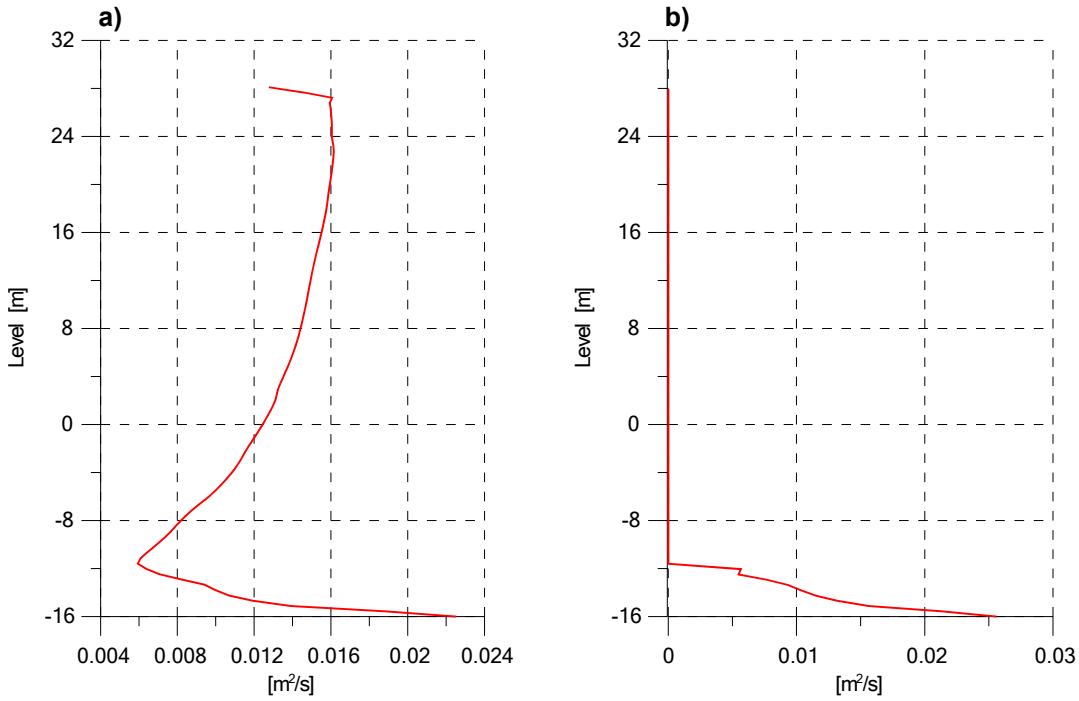

Fig. 27.3 Typical vertical distributions of coefficient of turbulent mixing obtained by Prandtl – Obuhov model. a) autumn-winter period; b) spring-summer period.

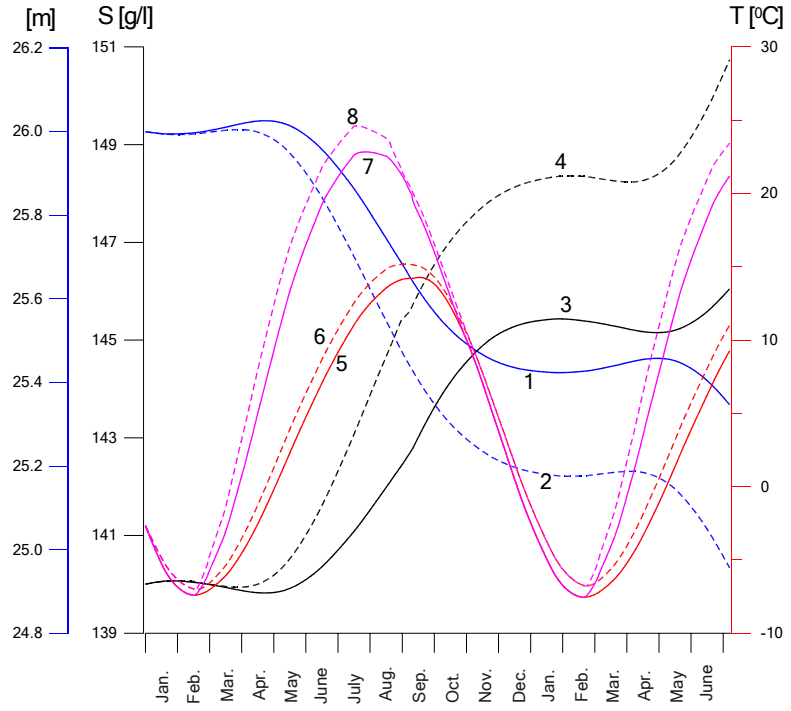

Fig. 27.4 The dynamics of hydrophysical parameters of water-body obtained in experiments with *e*-*ε*-model (solid line) and Prandtl – Obuhov model (dashed line). 1, 2 – the level; 3, 4 – the mean salinity; 5, 6 – the mean temperature; 7, 8 – the near-surface temperature.

Table 27.2 The differences of hydrophysical parameters of water body in calculations applying two turbulence models

	Level	Mean salinity	Mean temperature	Near-surface temperature
Maximum deviation	0.4 m	4.67 g/l	4.75 ^{0}C	3.2 ^{0}C
Relative deviation	~ 1%	~ 3%	~ 12 %	~ 13 %

28. Simulation of Hydrophysical Processes, Water and Salt Balance Calculation for the West Part of the Aral Sea

28.1 Simulation Scenarios

The scenarios of long-term modeling of water level and salinity changes in the west part of the Aral Sera are defined by the scenarios of water supply to that water body. In this work the period of time after separation of east and west parts of the Sea is under consideration, thus we suppose that water exchange between those Sea parts is absent. So, we have 13 simulation scenarios: there are three scenarios of the Amu-Darya runoff (national vision, saving existent tendencies, optimistic scenario) for each of two water management variants providing water supply to the west part of the Sea (w/m variant 1 – delta infrastructure according to NATO SFP 974357 project, w/m variant 2 – so-called hypothetic variant of water supply to the west part of the Sea), and there are minimal and maximal evaluation for each runoff scenario [32]. Additionally the zero inflow scenario, corresponding to existent Amu-Darya delta infrastructure is under consideration. Inflow mineralization for corresponding scenarios is also defined by [32].
As far as inflow temperature date is not given in [32], the Amu-Darya water temperature for 1975, Temirbay river gauge [33], was used (see
Table 28.3).
Mean monthly values of inflow water discharge, temperature and mineralization were used for all simulations. Those values assumed constant during a month, i.e. were given as the step functions.
The brief description of mentioned scenarios and corresponding mean annual water inflow (averaged by all years when it was non-zero) are given in Table 28.1. The scenarios are given in inflow ascending order. The charts of annual inflow according to mentioned 12 scenarios are given at Fig. 28.1 -Fig. 28.6. The "annual inflow" term here stands for total inflow of the Amu-Darya water to the considered water body per a hydrologic year, which starts at October 1 in this case [32].
It is expedient to simulate since east and west Sea parts separation. The level of threshold between the mentioned Sea parts is between 29.25 and 29.5 m Baltic System [34]. While summarizing results of the Big Aral drying given in [4], we can conclude that such water level would be achieved about 2010. At the same time salinity would be about 110 g/l. The initial water level for our simulations must be given on the safe side. I.e. it must be lower than the threshold level to prevent its possible exceeding because of annual oscillations of the Sea water volume. According to inflow scenarios [32] of both water management variants, providing water supply to the west parts of the Sea, this water supply starts at October 1 2010.
So, the initial momentum of simulation – 0 hours October 1 2010, initial water level – 29 m Baltic System and uniformly distributed by depth initial salinity – 110 g/l. It is necessary to note that this initial momentum is to a great extent conditional because the runoff scenarios themselves (and, especially, the date of water supply starting) are conditional and simulation results given in [34] are ambiguous. Similarly the initial salinity is also conditional. But assignment of uniform distribution to the initial salinity is justified, because vertical gradients of salinity in corresponding season are small according to [35] and results of our simulations.
It is assumed that water level in the east part of the Sea also does not exceed the threshold level and water does not spill over from east to west part.
Test simulations by the bulk model for a few years long period with different inflow scenarios had shown that water temperature changed practically periodically under usage of climatic meteorological data. Not depending on its initial value, water temperature at October 1 of the next years was about 18 ºC. So, constant by depth initial value of water temperature 18 ºC and zero initial thicknesses of ice and snow were chosen. Note that the choice of initial water temperature is not the governing factor for heat balance, because in the case of the bulk model water temperature is quickly brought into accordance with meteorological data due to heat exchange with atmosphere (and solar radiation). In the case of the 1D vertical model this process goes slower, but the initial temperature influence on temperature distribution is also erased within one year.
In [32] the scenarios of Amu-Darya water supply to the west part of the Sea since October 1 2010 till October 1 1025 are given. Respectively, all 13 mentioned simulations were undertaken for 15 years long time period.
The climatic (long time averaged) mean monthly meteorological data were used. That data were assigned to the middles of months and then linearly interpolated during period of modeling. Meteorological data for the beginning and the end of the modeling period were also obtained by linear interpolation under assumption of data periodicity.
The values of air temperature and humidity, total cloudiness, wind velocity and atmospheric precipitation were taken as a half-sum of respective data for the weather stations Muynak and Aral Sea [37-40] which

are situated at the opposite south-west and north-east banks of the Aral Sea in the limits of the conditionally-natural period. Such approach was successfully verified at one of the previous stages of this work [41]. As far as atmospheric pressure data for the considered region were absent in [37-40], the averaged data for 1996-2000 for the Muynak weather station from [42] were used. Actually the precise accounting of the atmospheric pressure is not very important here, because it starts to play a significant role in the heat balance only for the artificially heated water body. The clear sky solar radiation was taken as a half-sum of values for 44º and 46º latitude given in [43].
It is necessary to note that the wind speed is measured at the weather-vane altitude which is 11 m for both Muynak and Aral Sea weather stations, while the used models need weather velocity values at 2 m altitude above water. Thus the correction factor was used to convert 11 m velocity to 2 m velocity:

$$w_a = K_w w_{11},$$

where w_a – wind velocity at 2 m altitude, m/s, w_{11} – wind velocity at 11 m altitude, m/s, K_w – correction factor, dimensionless.

$$K_w = \frac{\overline{w}_2}{\overline{w}_{11}},$$

where $\overline{w}_z$ – long-term averaged wind velocity at z m altitude above water.
According to [13], for the Aral Sea $\overline{w}_2 = 4.0$ m/s, $\overline{w}_{1000} = 7.3$ m/s. Based on the logarithmic profile of wind velocity in the atmospheric boundary layer under neutral stratification [45] we can obtain formula for $\overline{w}_{11}$:

$$\overline{w}_{11} = \overline{w}_{1000} - \left(\overline{w}_{1000} - \overline{w}_2\right)\frac{\ln 1000 - \ln 11}{\ln 1000 - \ln 2}.$$

Thus we obtain $K_w \approx 0.82$.
In distinction with the bulk model, the 1D vertical model demands not only module w_a of wind velocity vector, but also its projections on longitudinal w_x and lateral w_y axes of water body, which are used for parametrization of horizontal water velocities. In this work the half-sum of mean monthly climatic values of wind velocity vector components for weather stations Aral Sea and Chimbay [37-40] are used (the respective data for Muynak weather station are absent, but Chimbay station is situated near it). Then the projections of wind velocity vector on longitudinal and later axes of the considered water body are calculated and mentioned correction factor is applied. We assume that the longitudinal axis is deflected 17.4° east from north direction, and lateral axis is perpendicular it. North and east directions are considered positive for wind velocity components.
The used meteorological data are given in Table 28.2.
Besides long-term modeling of water level and salinity changes, the simulation for a year and a half long conditional period was performed for the comparison of bulk and 1D modeling results and for the detailed analysis of hydrophysical processes and annual change of hydrophysical parameters distribution in the west part of the Sea under intensive flood.
For this purpose a graph of water supply must be chosen which is typical for considered scenarios, has a big total runoff and pronounced flood period.
After analysis of various runoff scenarios the following graph was chosen: until April of the first simulation year there was a zero inflow. Then during 12 months discharge and salinity of inflowing water corresponded to 2020-2021 hydrologic year by minimal estimation of optimistic runoff scenario for water management variant 2 (the hypothetic variant of water supply to the west part of the Sea) [32]. Then until the end of simulation period there was a zero inflow again. This graph is given at Fig. 28.7 and
Table 28.3. Total runoff is 14.53 km^3.
The initial water level 26 m was chosen to prevent water level exceeding the level of threshold between parts of the Sea. Uniformly distributed by depth initial salinity 140 g/l was chosen from balance relations to provide about the same total mass of salt as was in initial momentum of long-term simulations described above. Such salinity is approximately equal salinity achieved at the same water level according to modeling results given in [35].
The initial water temperature is chosen in the same way as for long-term simulations: a series of test simulations by both bulk and 1D models for a few years long period with different inflow scenarios had

shown that homothermy is achieved by January 1 and mean water temperature obtained by both models is practically equal -2.5 ºC. So, the inititial momentum of simulation – 0 hours January 1 and constant by depth initial water temperature – -2.5 ºC were chosen.
Note that assignment zero inflow for first months of simulation period allows to achieve natural conditions of water body before beginning flood, and assignment zero inflow for last months – to achieve erasing of intensive flood influence on salinity vertical distribution.
The year and a half long simulation was performed with the same climatic data. As for long-term simulations, mean monthly values of meteorological data, inflow discharge, temperature and salinity were used and were interpolated by time in the same way.
The basic bathymetric information on the west part of the Aral Sea for bulk and 1D simulations, i. e. curves of water body surface area and volume relation to water level, was obtained from [46]. To obtain the additional information, such as water body length at various water levels, the electronic map was used [34]. For that map scaling and water body longitude finding geographical map [47] was implemented. Also by [34] the mention hypsometric curves where extended up to 33 m level (in that case border between parts of the Sea was assumed at the west threshold of the channel connecting those parts).
In all simulations level marks were given with 1 m step. Between those marks water body volume and surface area were linearly interpolated. Below 33 m level mark they were linearly extrapolated.

Table 28.1 Mean annual inflow of Amu-Darya water to the west part of the Aral Sea for various scenarios, in ascending order

Scenario description			№	Inflow, km^3
No inflow			1	0.00
W/m variant 1 *(NATO project infrasctructure)*	national vision	min	2	1.70
		max	3	1.78
	saving exist. tendencies	min	4	2.08
		max	5	2.14
	optimistic scenario	min	6	2.55
		max	7	2.96
W/m variant 2 *(hypothetic variant of water supply to the west part of the sea)*	national vision	min	8	4.50
		max	9	5.00
	saving exist. tendencies	min	10	5.15
		max	11	5.47
	optimistic scenario	min	12	7.46
		max	13	8.94

Table 28.2 Meteorological data (designations are described in part 27.1).

	T_a	q_{pr}	e_a	w_a	p	C	Φ_{sc}	w_x	w_y
	ºC	mm	gPa	m/s	gPa	number	kcal/m^2h	m/s	m/s
jan	-9.7	10.0	2.9	3.7	1017.3	6.1	77.0	-0.07	-0.74
feb	-8.9	10.0	3.0	4.0	1015.9	5.5	117.5	-0.10	-1.14
mar	-1.9	13.0	4.5	4.1	1014.1	5.9	172.5	-0.52	-1.40
apr	9.1	16.0	7.2	4.2	1009.9	5.4	231.0	-0.40	-1.10
may	17.9	10.0	10.8	4.1	1008.2	4.4	270.5	0.12	-1.00
jun	23.5	8.5	14.2	3.9	1003.3	3.5	286.0	0.61	-0.55
jul	26.3	7.5	16.8	3.8	1001.5	3.0	275.0	0.62	-1.13
aug	24.5	6.5	15.3	3.6	1004.6	2.3	241.5	0.10	-1.41
sep	18.3	5.5	11.4	3.5	1008.8	2.7	190.0	0.28	-0.90
oct	9.4	15.0	7.7	3.7	1014.3	4.4	134.0	0.15	-0.42
nov	1.0	12.0	5.4	3.7	1019.8	5.6	88.0	-0.20	-0.49
dec	-5.7	11.0	3.8	3.6	1018.3	6.3	66.0	-0.34	-0.65

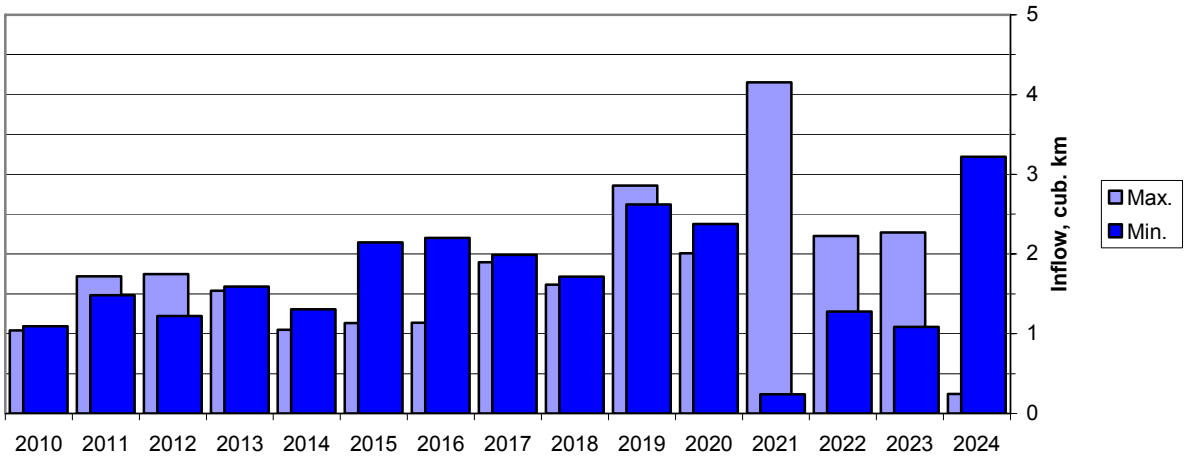

Fig. 28.1 Inflow of Amu-Darya water to the west part of the Aral Sea by hydrologic years according to "national vision" scenario of w/m variant 1.

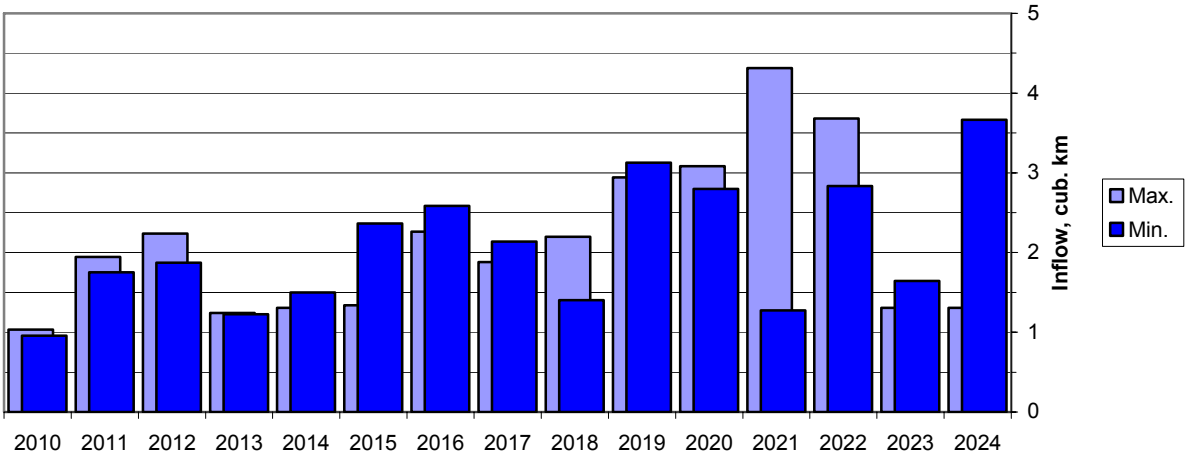

Fig. 28.2 Inflow of Amu-Darya water to the west part of the Aral Sea by hydrologic years according to "saving existent tendencies" scenario of w/m variant 1.

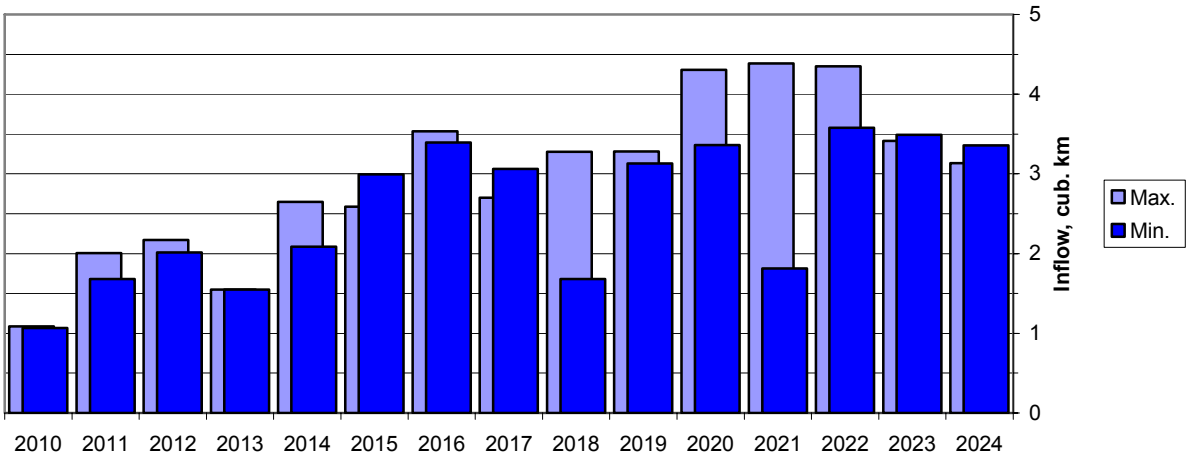

Fig. 28.3 Inflow of Amu-Darya water to the west part of the Aral Sea by hydrologic years according to optimistic scenario of w/m variant 1.

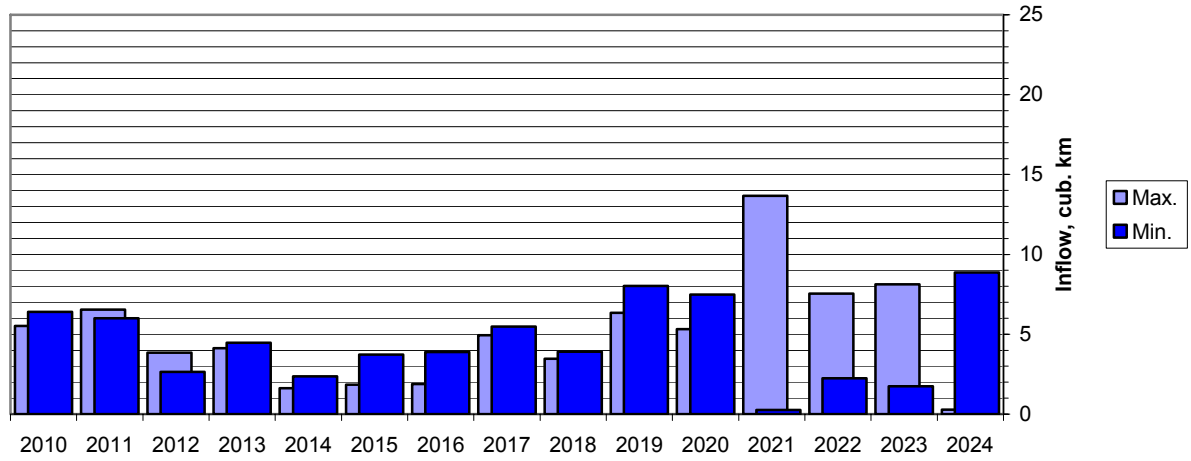

Fig. 28.4 Inflow of Amu-Darya water to the west part of the Aral Sea by hydrologic years according to "national vision" scenario of w/m variant 2.

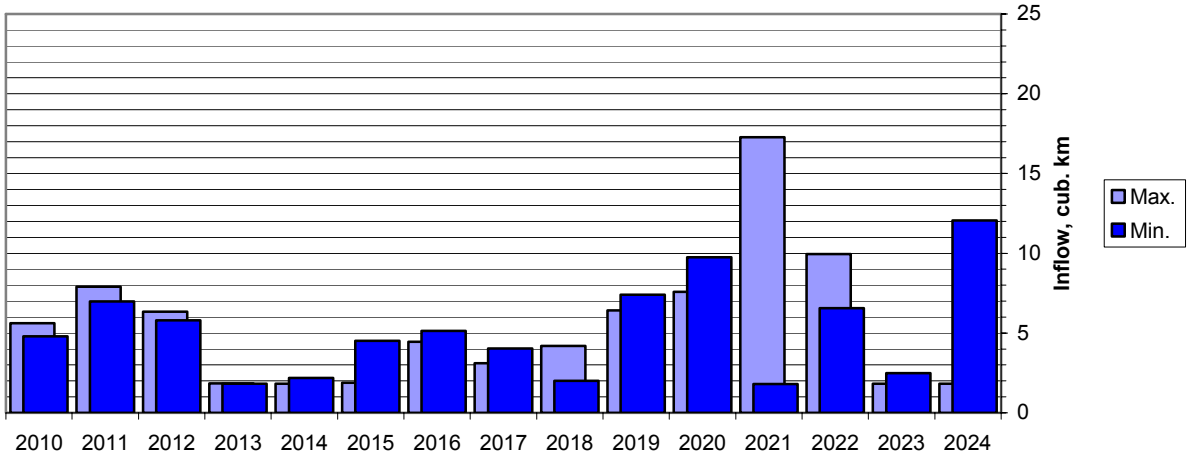

Fig. 28.5 Inflow of Amu-Darya water to the west part of the Aral Sea by hydrologic years according to "saving existent tendencies" scenario of w/m variant 2.

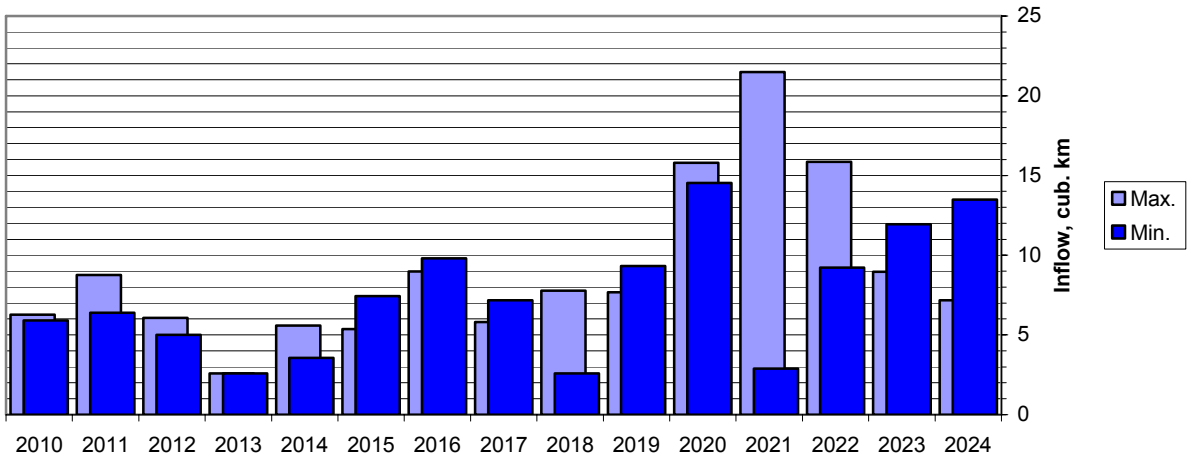

Fig. 28.6 Inflow of Amu-Darya water to the west part of the Aral Sea by hydrologic years according to optimistic scenario of w/m variant 2.

Table 28.3 Parameters of inflow for one and a half year long scenario

		Discharge	Salinity	Temperature
		m^3/s	g/l	°C
Year 1	jan	0.00	0.00	0.0
	feb	0.00	0.00	0.0
	mar	0.00	0.00	3.0
	apr	98.77	1.71	12.0
	may	834.38	1.06	18.3
	jun	1214.04	0.93	22.6
	jul	1163.42	0.94	25.6
	aug	935.33	1.02	21.8
	sep	617.32	1.19	20.5
	oct	173.35	1.58	11.8
	nov	120.76	1.63	5.5
	dec	100.66	1.61	2.2
Year 2	jan	126.64	1.57	0.0
	feb	74.28	1.66	0.0
	mar	40.21	1.83	3.0
	apr	0.00	0.00	12.0
	may	0.00	0.00	18.3
	jun	0.00	0.00	22.6

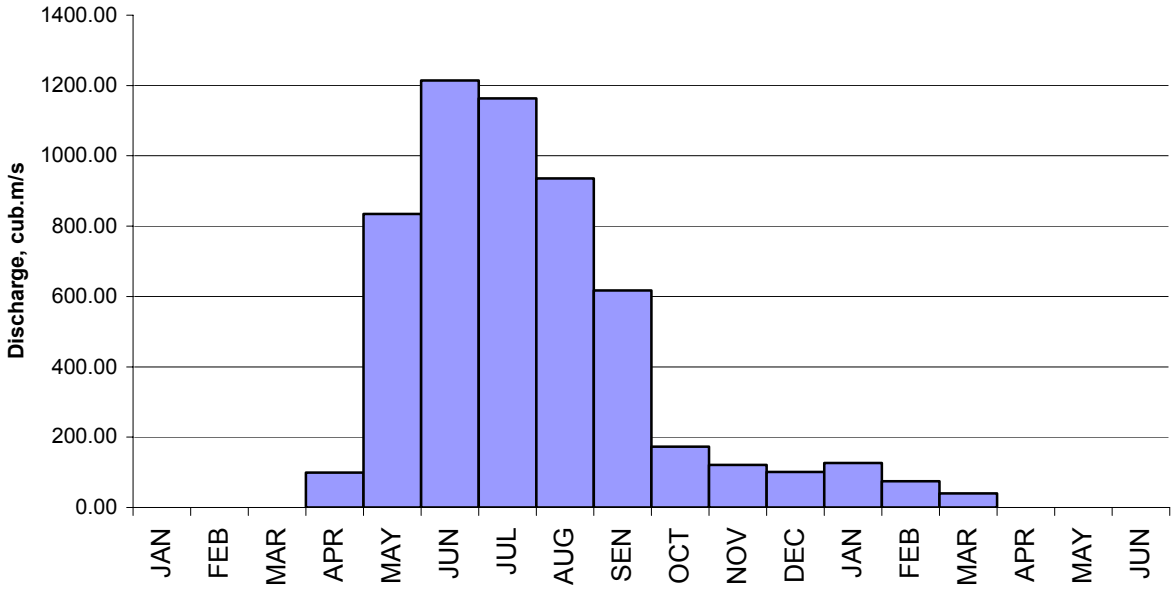

Fig. 28.7 Discharge of inflow for one and a half year long scenario

28.2 Modelling of Hydrophysical Processes at Conventional Water Inflow into Western Part of Aral Sea

The calculation was fulfilled using one-dimensional model in order to describe the annual dynamics of level and the vertical distributions water temperature and salinity. The main questions were how long fresh-water lens exists and by what time the state of full mixing becomes settled. The dynamics of mean temperature, mean salinity and heat flux through free surface also were of interest, and comparison of those parameters obtained by one-dimensional and bulk modes was fulfilled. The 1.5 years scenario (Section 28.1) was used for the calculation.

The vertical distributions of hydrophysical parameters are formed due to processes on the water surface (heat and mass exchange), interaction with the tributary water and mixing processes induced by vertical density stratification. For the analysis of the dynamics of vertical distributions the graphs of the distributions at first days of the months are presented.

28.2.1 Vertical distributions of the salinity

At first four months period (before the water of tributary entry) the slight level rising due to exceeding precipitations over evaporation is observed. From January to the beginning of February the temperature and the salinity are homogeneously distributed in depth and then the temperature of upper layers rises due to heat exchange with atmosphere (Fig. 28.8).
From May to October (Fig. 28.9) the salinity in upper layers constantly dropped because of tributary water entry. The desalinated water penetrates into deep layers because of mixing processes therefore the salinity of near-bottom water also decreases. In the period from May to August with largest the tributary discharges (the flood) the vertical stratification of water body is strongly marked and it is saved until October.
In November-December the discharges are insignificant ant by that time the distribution of the salinity is homogeneous again (Fig. 28.8). It means that the entered desalinated water of the tributary is fully mixed with the sea water.
The distribution remains homogeneous in the beginning of the second computational year (January-March) despite of constant decreasing of salinity in the all depth (Fig. 28.10). The dropping of the concentration near the surface amounts nearly 1 g/l to the beginning of April.

28.2.2 Vertical distributions of temperature

The vertical distributions of temperature are also of interest regarding processes of mixing water of tributary with the sea water. As it was marked in winter (December-February) the full mixing was observed and then (March-April) gradual increase of the near-surface water temperature due to heat exchange began. Besides in April the more warm tributary water entries and it also enlarges the temperature of near-surface layers.
In May-October the strongly marked temperature stratification typical for spring-summer period is observed (Fig. 28.11). In October-November while transfer from summer stratification to winter one the thermocline aroused and then it disappeared in the first decade of November. After that as it was in the first calculation year until the beginning of March the homogeneous temperature distribution remained and from the end of March the warming-up of the near-surface layers began (Fig. 28.12).
In May-June of the second calculation year the temperature distributions were close to those of first year but the near-surface temperature slightly differs because the inflow was absent.
It has to be noticed that the temperature of the near-bottom layer of the sea remained very low and even in the beginning of August it was below zero. Maximum value (near 9.5^0C) is observed in first decade of November before the state of homothermy was settled. After that the temperature constantly went down practically simultaneously in the all depth due to intensive mixing processes.

28.2.3 Density stratification

The density stratification is determined by the vertical distributions of salinity and temperature. At the concentrations assumed in the numerical experiment the salinity has to be the main factor affecting the density. In this calculation salinity in the near-surface layer always was less than in lower layers and in the cases when it was greater the difference was insignificant and because of higher temperature of the upper layer the density stratification was stable or neutrally stable during the whole period.
The vertical distributions of the density in spring-summer periods in the first and second calculation years are shown on Fig. 28.13. The difference between those distributions is explained by the inflow water influence (in the first year).

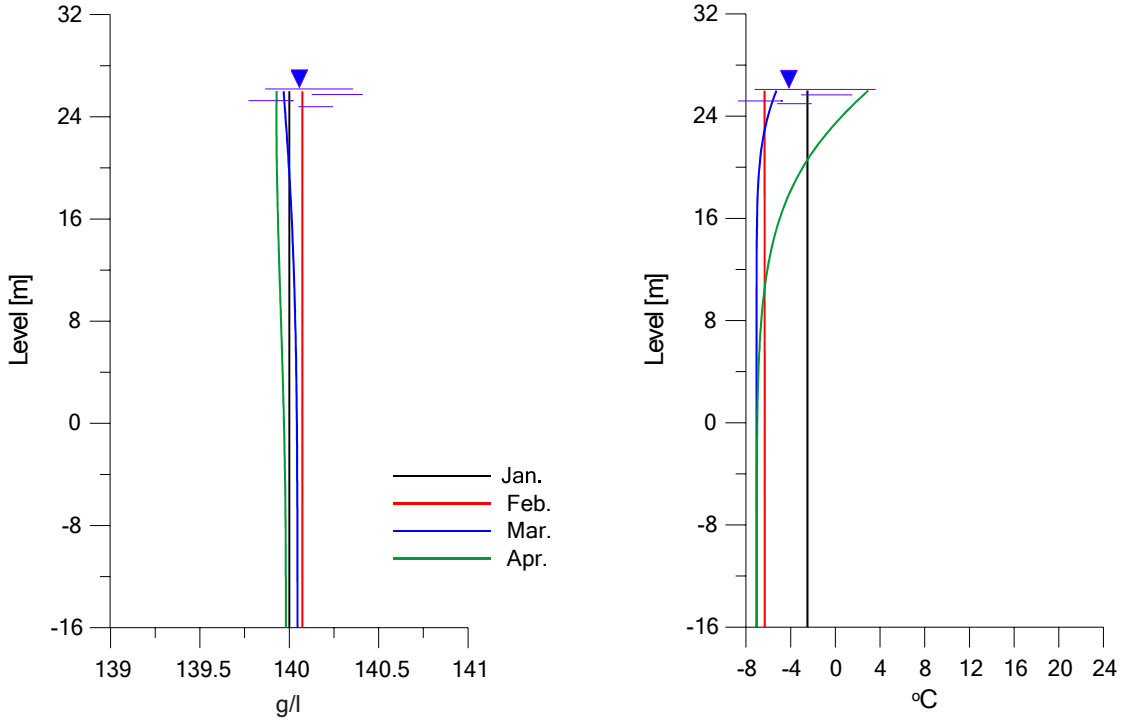

Fig. 28.8 Vertical distributions of salinity and temperature in the initial period before tributary water enter

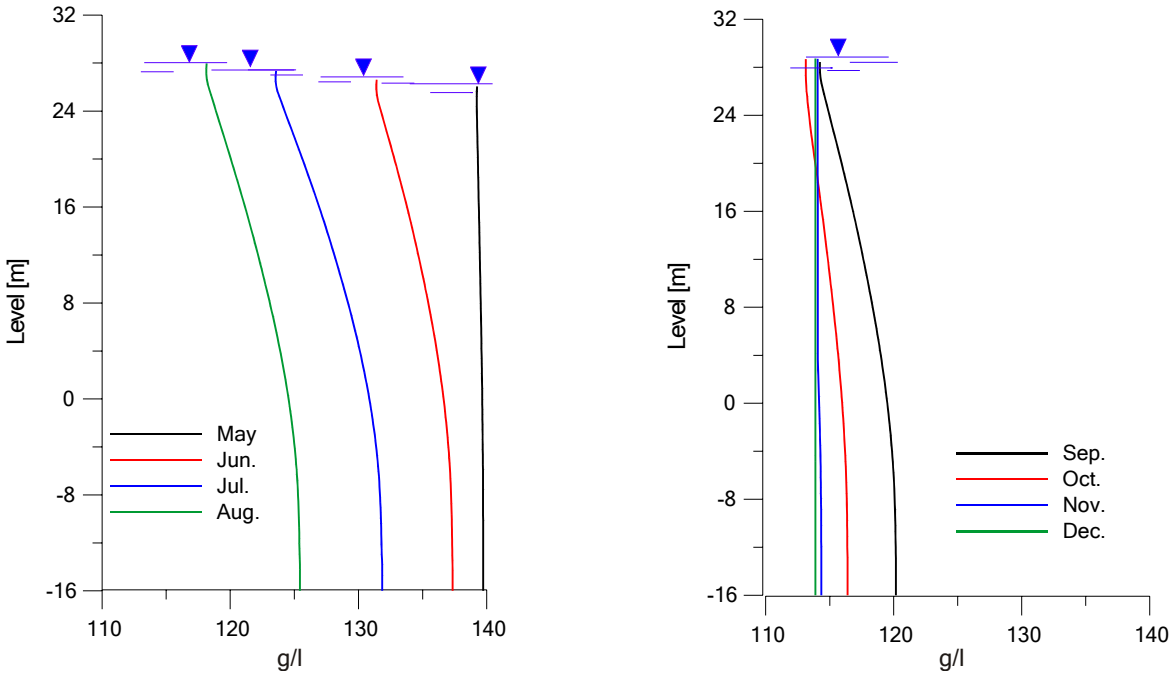

Fig. 28.9 Vertical distributions of salinity in the period of flood and after it

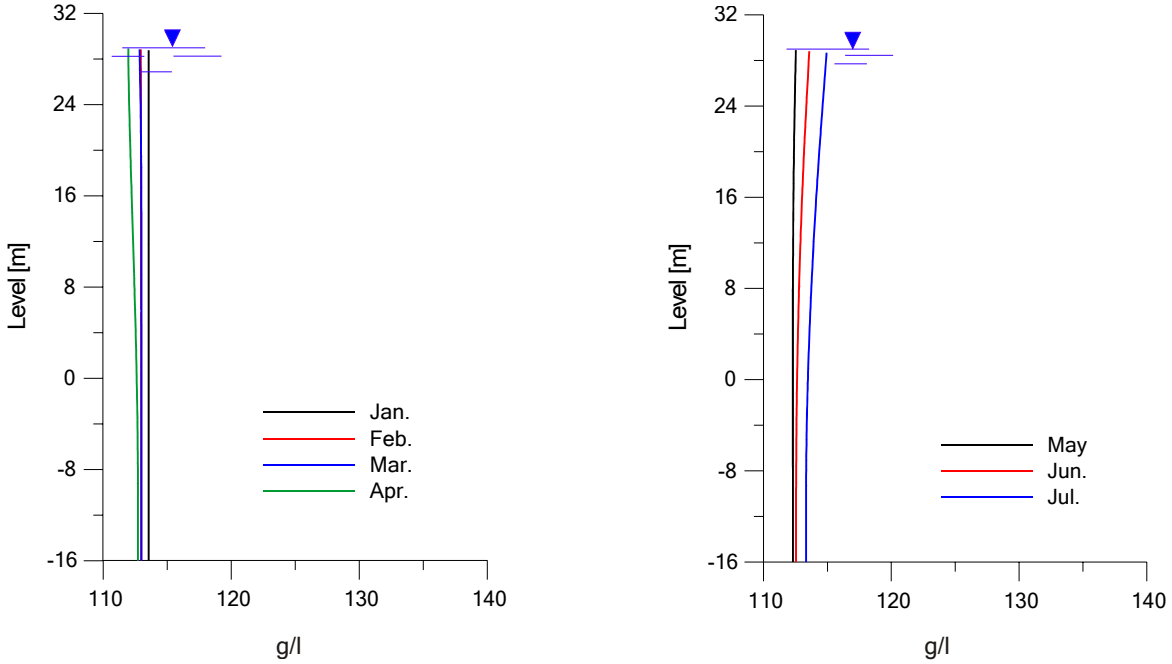

Fig. 28.10 Vertical distributions of salinity in the second computational year

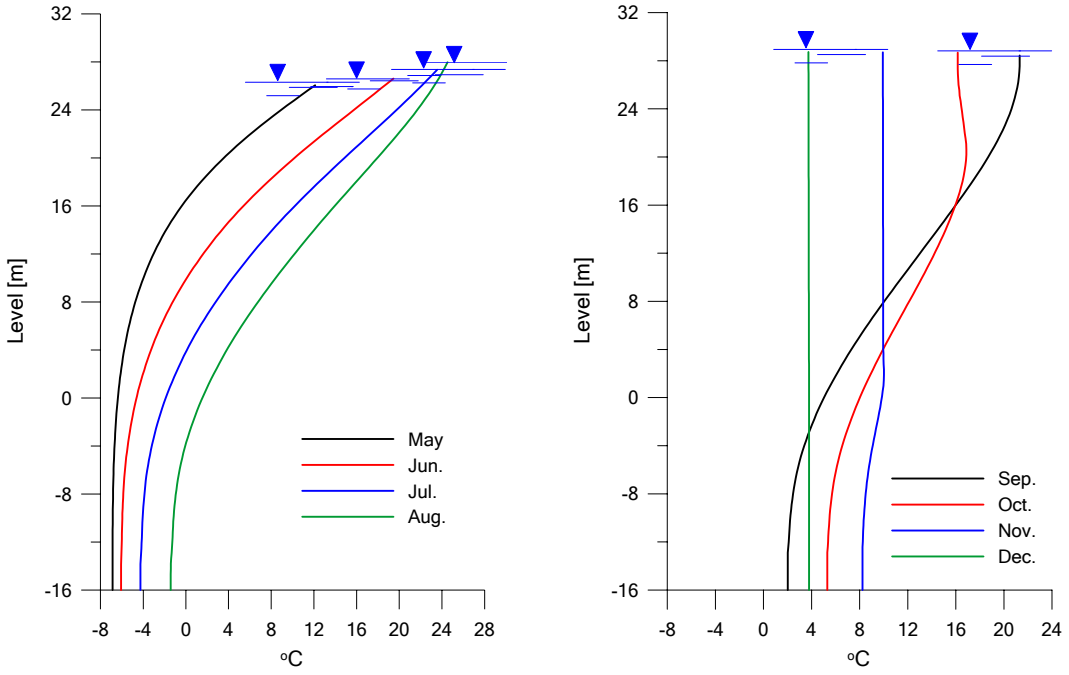

Fig. 28.11 Vertical distributions of temperature in the period of flood and after it

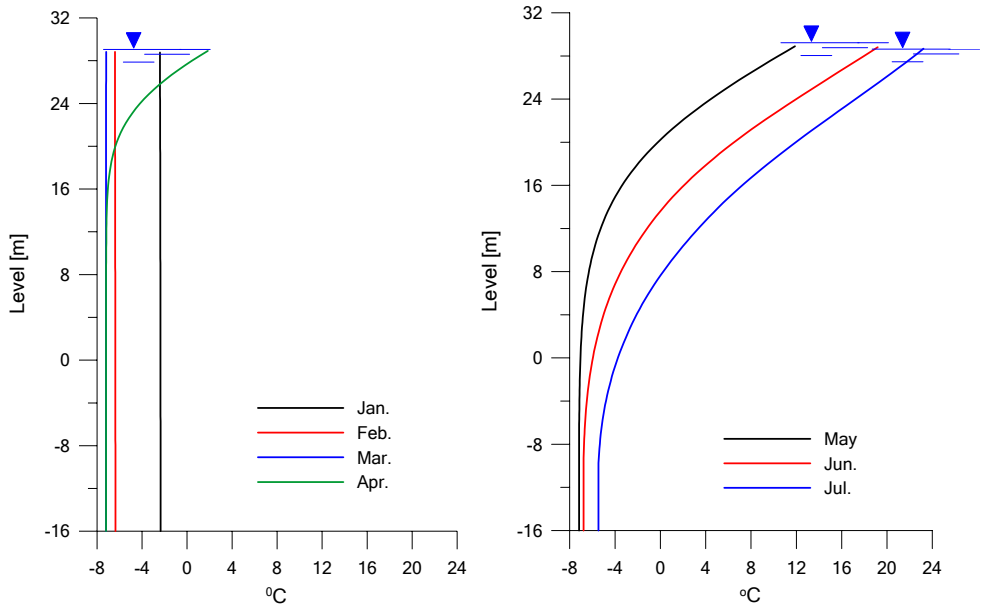

Fig. 28.12 Vertical distributions of temperature in the second computational year

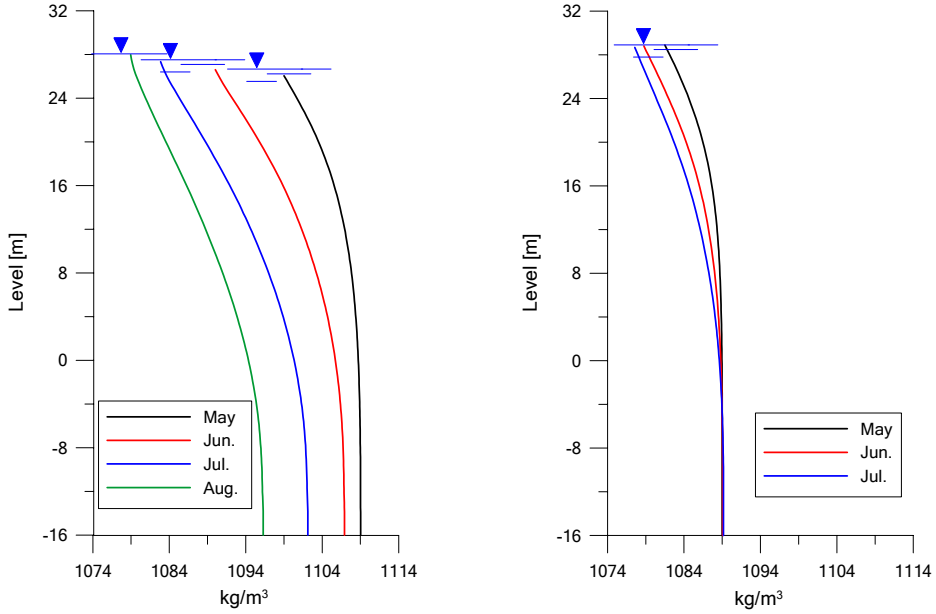

Fig. 28.13 Vertical distributions of density in the period of flood and in the end of calculation period

28.3 Long-term Process of Hydrothermal Regime Fluctuation

28.3.1 Long-term modeling of water level, temperature and salinity of the west part of the Aral Sea by the bulk model

In this part of report the results of long-term modeling of water level and salinity change in the west part of the Aral Sea are described. The simulations where undertaken by the bulk model described in part 27.1 according to 13 simulation scenarios described in part 28.1. As stated above, water temperature and ice-snow cover thickness were also simulated, momentums of ice cover appearance and disappearance were monitored. At Fig. 28.14 and Fig. 28.15 results of water level and salinity simulation under zero inflow are given. In that case water level descends linearly to annual oscillations and by the end of simulation (October 1 2025) its value is 15.77 m Baltic System. At that momentum Salinity is 291.18 g/l.

At Fig. 28.16 and Fig. 28.17 results of water level and salinity simulations for other 12 scenarios, providing non-zero inflow. Those graphs display that in the case of second water management variant water level exceeds the level of threshold between east and west parts of the Sea under any runoff

scenario. It stands for simulations undertaken for the west part of the Sea under the second water management variant not taking into account hydraulic connection with the east part are not correct. So, we will mainly limit ourselves to discussion of results of simulations by the first water management variant. In that case water level by the end of simulations varied between 23.10 m (“national vision” scenario, minimal estimation) to 26.99 m (optimistic scenario, maximal estimation). For those two scenarios respectively maximal and minimal salinity by the end of simulations for the first water management scenario are achieved – 170.34 and 128.76 g/l. Generally, water level values by the end of simulations for the first water management variant are arranged according to total runoff of the corresponding scenarios. At the same time salinity levels are arrenged in the reverse order. It is obvious, because salt settling was not taken into account and salt inflow with inflowing water was insignificant in comparison with total mass of salt in the water body. Minimal and maximal estimations of water level by the end of simulations for "national vision" and "saving existent tendencies" scenarios are close, while both estimations for optimistic scenario differ by more than 1 m at that time. Note that under zero inflow ice does no appear. By all scenarios corresponding to first water management variant ice appears only in the first year for a short period of time and has a little thickness. Under simulations by the second water management variant ice appears almost in all years. As expected, maximal ice thickness and ice coverage duration depend on water salinity. Under simulation by optimistic scenario of the second water management variant with maximal estimation of discharge maximal ice thickness is almost 50 cm, and ice coverage duration – almost 6 months (ice appears in January and disappears in May or even beginning of June). Note that intensive flood not only increases ice cover because of Sea water desalination, but some shorten ice coverage duration because of warm water influx. Maximal annual water temperature in most cases is 25-26 ºC, but for some scenarios of the second water management variant it can decrease below 24 ºC. Minimal temperature is about -7 ºC. For more detailed analysis of first water management variant modeling results the charts of mean annual (for calendar years) simulated values of water level and salinity for all Amu-Darya runoff scenarios (with both minimal and maximal runoff estimation) were built. Mean annual values were calculated only for the part of a year covered by the period of modeling. Those charts are given at Fig. 28.18 - Fig. 28.23. At Fig. 28.24 - Fig. 28.29 charts for the same values averaged over minimal and maximal estimation are given. The latter charts display that by the end of considered 15 years long time period water level under optimistic runoff scenario may be considered as conditionally stabilized at 26.5 m mark. Salinity stabilizes at about 132.5 g/l level. Under "saving existent tendencies" scenario water level is close to stabilization at 24.5-25 m mark, and salinity – at 145-150 g/l level. But in this case it is impossible to talk about stabilization unambiguously. And, finally, under "national vision" scenario water level continue falling, and salinity – respectively increasing, achieving mean annual values about 23.5 m and 165 g/l in the last year of simulation. Mean annual (by calendar years) water level and salinity values under all simulation scenarios are given in Table 28.4 -Table 28.8.

Table 28.4 Mean annual (by calendar years) water level and salinity obtained by long-term modeling without inflow.

	Level	Salinity
	m	g/l
2010	28.86	111.16
2011	28.45	114.60
2012	27.50	122.93
2013	26.57	131.71
2014	25.64	140.90
2015	24.72	150.55
2016	23.80	160.71
2017	22.90	171.36
2018	22.01	182.48
2019	21.13	194.30
2020	20.27	206.90
2021	19.41	220.38
2022	18.57	234.73
2023	17.74	249.96
2024	16.92	266.15
2025	16.27	279.88

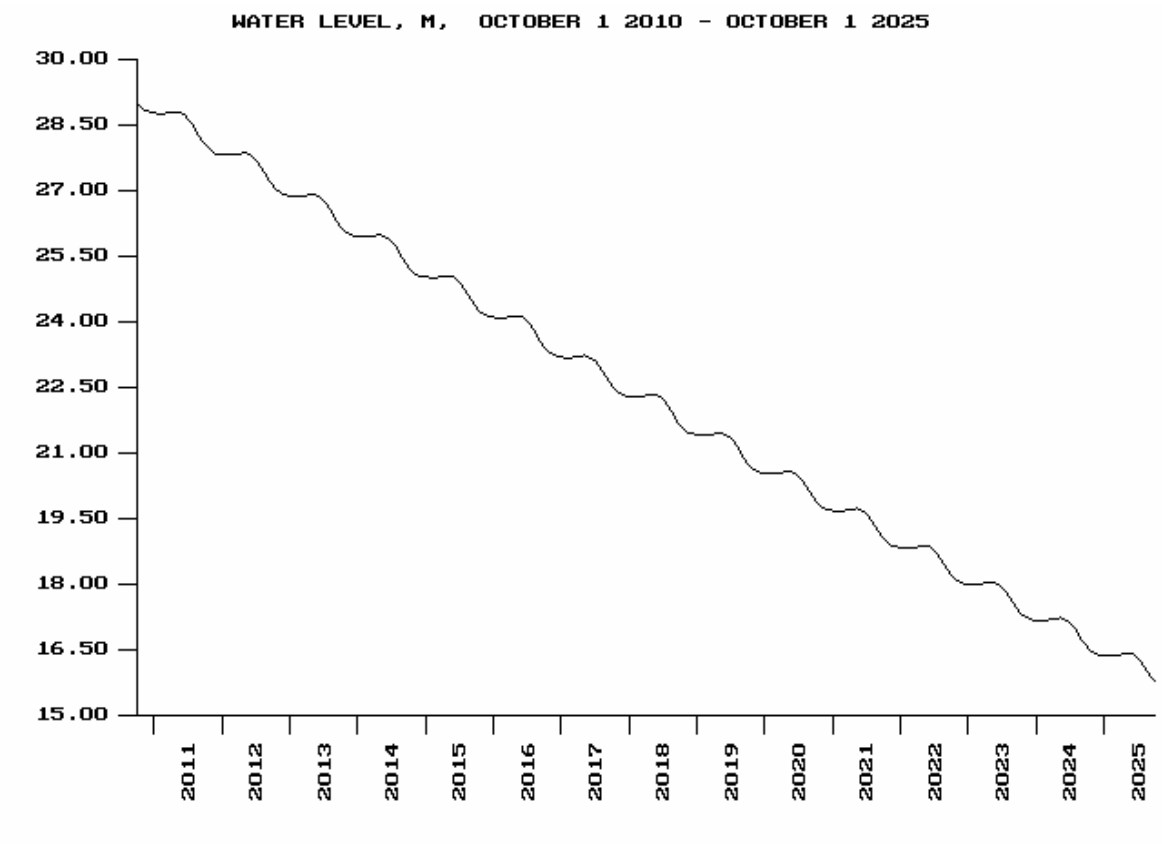

Fig. 28.14 Water level obtained by long-term modeling without inflow.

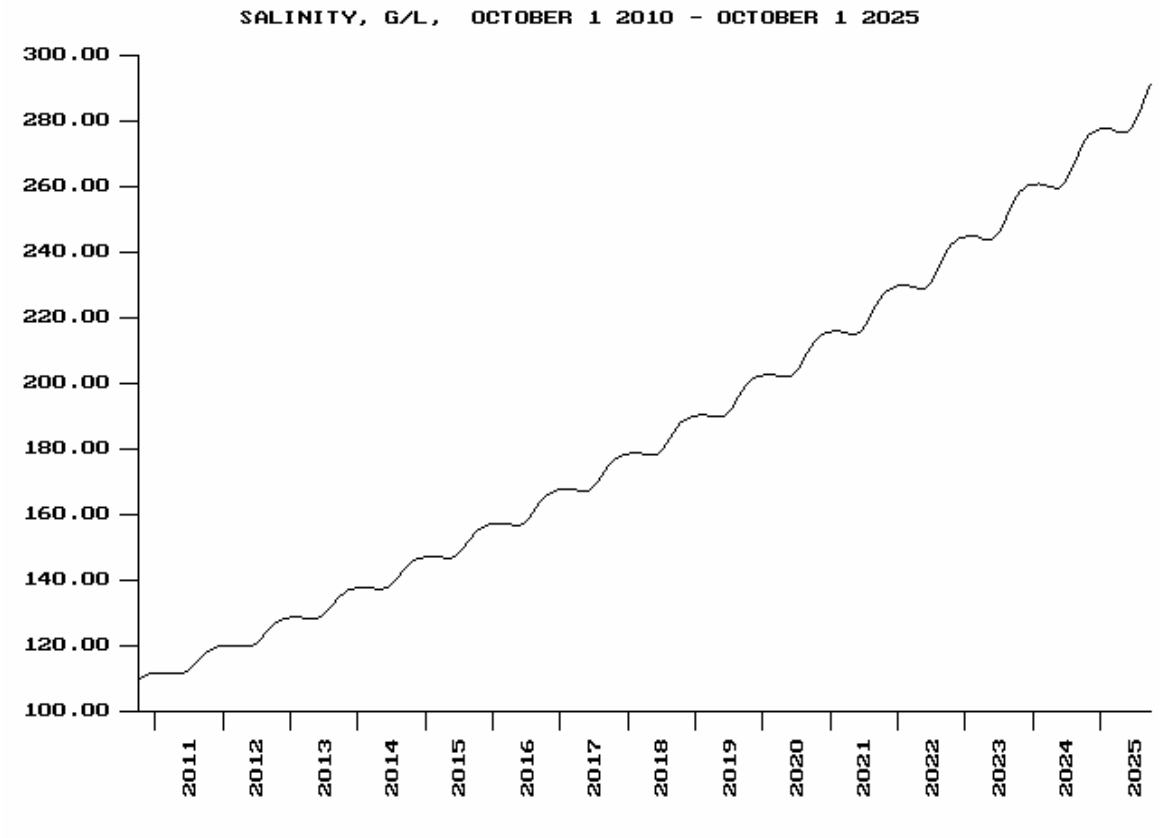

Fig. 28.15 Salinity obtained by long-term modeling without inflow.

Table 28.5 Mean annual (by calendar years) water level obtained by long-term modeling according to water management variant 1, m.

	National vision		Saving existent tendencies		Optimistic scenario	
	min	max	min	max	min	max
2010	28.89	28.89	28.88	28.89	28.89	28.89
2011	28.65	28.65	28.63	28.65	28.65	28.66
2012	28.01	28.07	28.04	28.12	28.06	28.14
2013	27.41	27.60	27.53	27.69	27.61	27.71
2014	27.00	27.14	27.01	27.16	27.14	27.25
2015	26.44	26.49	26.49	26.57	26.73	26.89
2016	26.00	25.78	26.14	26.04	26.50	26.68
2017	25.73	25.36	25.96	25.77	26.50	26.69
2018	25.55	25.02	25.68	25.44	26.46	26.54
2019	25.14	24.65	25.31	25.20	26.18	26.51
2020	24.76	24.48	25.17	25.12	25.97	26.53
2021	24.62	24.43	25.09	25.19	26.00	26.71
2022	24.15	24.55	24.82	25.44	25.86	26.95
2023	23.67	24.72	24.65	25.71	25.82	27.21
2024	23.17	24.51	24.48	25.37	25.88	27.23
2025	23.10	23.90	24.53	24.99	25.97	27.22

Table 28.6 Mean annual (by calendar years) salinity obtained by long-term simulation according to water management variant 1, g/l.

	National vision		Saving existent tendencies		Optimistic scenario	
	min	max	min	max	min	max
2010	110.90	110.91	110.94	110.91	110.90	110.90
2011	112.91	112.96	113.12	112.96	112.93	112.85
2012	118.43	117.94	118.16	117.51	117.99	117.29
2013	123.89	122.13	122.73	121.35	122.10	121.20
2014	127.78	126.41	127.64	126.22	126.42	125.40
2015	133.19	132.65	132.68	131.83	130.41	128.88
2016	137.59	139.66	136.16	137.11	132.61	130.86
2017	140.37	144.05	138.10	139.88	132.75	130.89
2018	142.33	147.66	141.02	143.40	133.19	132.41
2019	146.60	151.79	144.89	145.94	136.03	132.74
2020	150.82	153.59	146.47	146.98	138.27	132.72
2021	152.42	154.38	147.46	146.27	138.06	131.04
2022	157.71	153.05	150.41	143.79	139.57	128.86
2023	163.34	151.38	152.36	141.11	140.07	126.48
2024	169.27	153.76	154.33	144.70	139.55	126.38
2025	170.21	160.72	153.90	148.79	138.68	126.59

Table 28.7 Mean annual (by calendar years) water level obtained by long-term simulation according to water management variant 2, m.

	National vision		Saving existent tendencies		Optimistic scenario	
	min	max	min	max	min	max
2010	29.05	29.00	28.94	28.99	29.02	29.05
2011	29.48	29.31	29.14	29.33	29.38	29.52
2012	29.69	29.71	29.56	30.05	29.74	30.34
2013	29.75	30.04	29.94	30.45	30.08	30.69
2014	30.00	30.10	29.86	30.30	29.98	30.88
2015	29.63	29.55	29.44	29.78	29.76	31.17
2016	29.37	28.90	29.32	29.33	30.01	31.78
2017	29.37	28.65	29.51	29.39	30.93	32.78
2018	29.82	28.80	29.50	29.22	31.85	33.26
2019	29.72	28.70	29.31	29.27	32.21	33.94
2020	29.74	28.97	29.53	29.59	32.71	34.64
2021	30.43	29.50	30.24	30.36	34.15	36.05
2022	30.37	30.66	30.59	32.03	34.94	38.21
2023	29.92	32.20	30.61	33.82	35.31	40.38
2024	29.42	32.97	30.68	33.79	36.06	40.84
2025	29.55	32.57	31.09	33.53	37.10	40.83

Table 28.8 Mean annual (by calendar years) salinity obtained by long-term simulation according to water management variant 2, g/l.

	National vision		Saving existent tendencies		Optimistic scenario	
	min	max	min	max	min	max
2010	109.61	109.98	110.48	110.10	109.84	109.62
2011	106.27	107.54	108.92	107.38	107.03	105.93
2012	104.77	104.60	105.75	101.97	104.37	99.84
2013	104.41	102.19	103.00	99.11	101.93	97.42
2014	102.66	101.89	103.77	100.37	102.80	96.29
2015	105.61	106.21	107.08	104.39	104.56	94.36
2016	107.72	111.43	108.10	107.94	102.80	90.42
2017	107.85	113.56	106.69	107.59	96.28	84.29
2018	104.54	112.38	106.92	109.06	90.28	81.59
2019	105.43	113.34	108.60	108.82	88.06	78.09
2020	105.33	111.21	106.94	106.33	85.14	74.79
2021	100.35	107.12	101.68	100.68	77.50	68.94
2022	100.93	98.54	99.23	89.60	73.67	61.57
2023	104.44	88.37	99.21	79.10	72.17	55.38
2024	108.50	83.88	98.89	79.35	69.22	54.31
2025	107.49	86.37	96.13	80.88	65.54	54.46

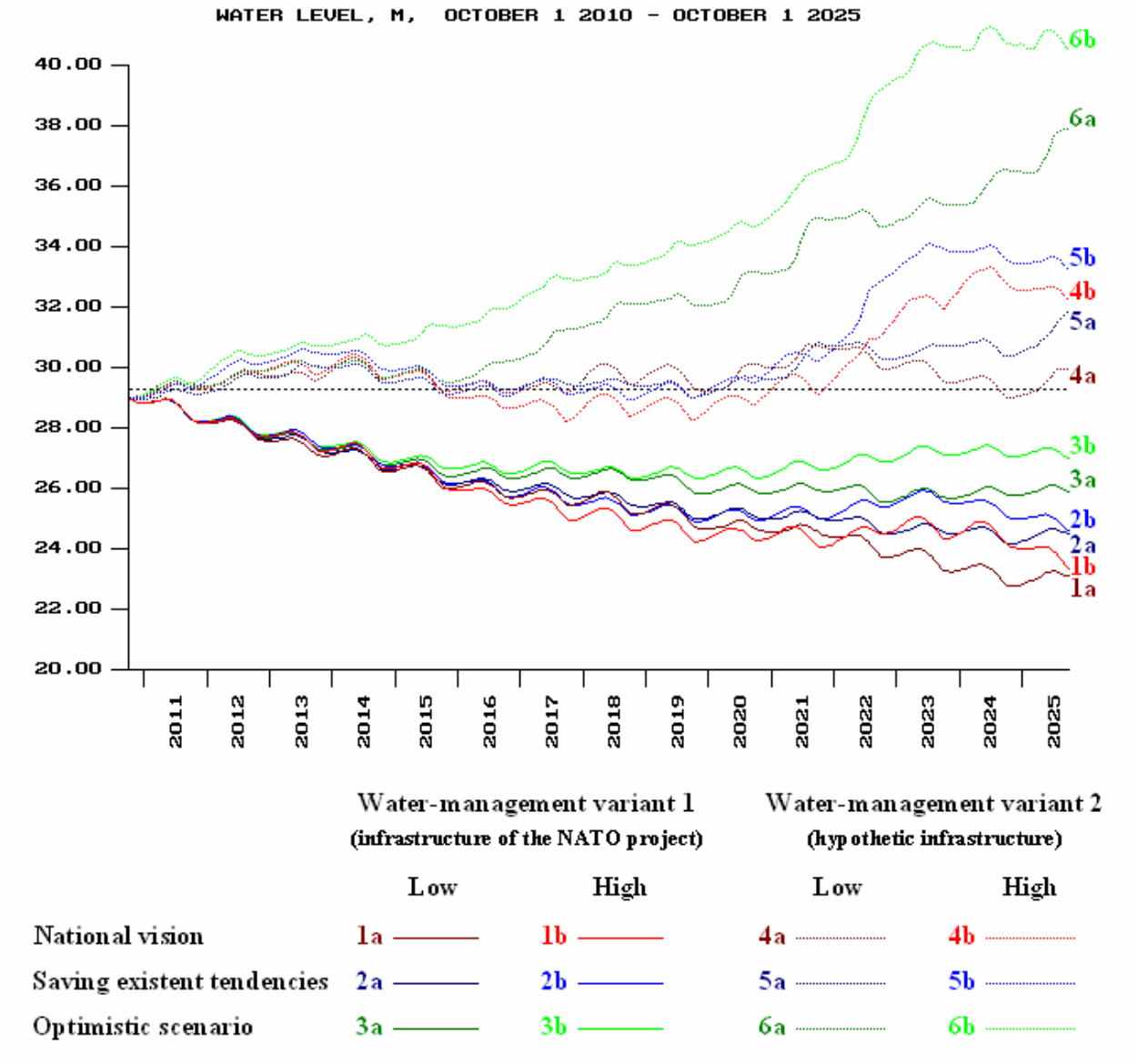

Fig. 28.16 Water level obtained by long-term modeling by various scenarios.

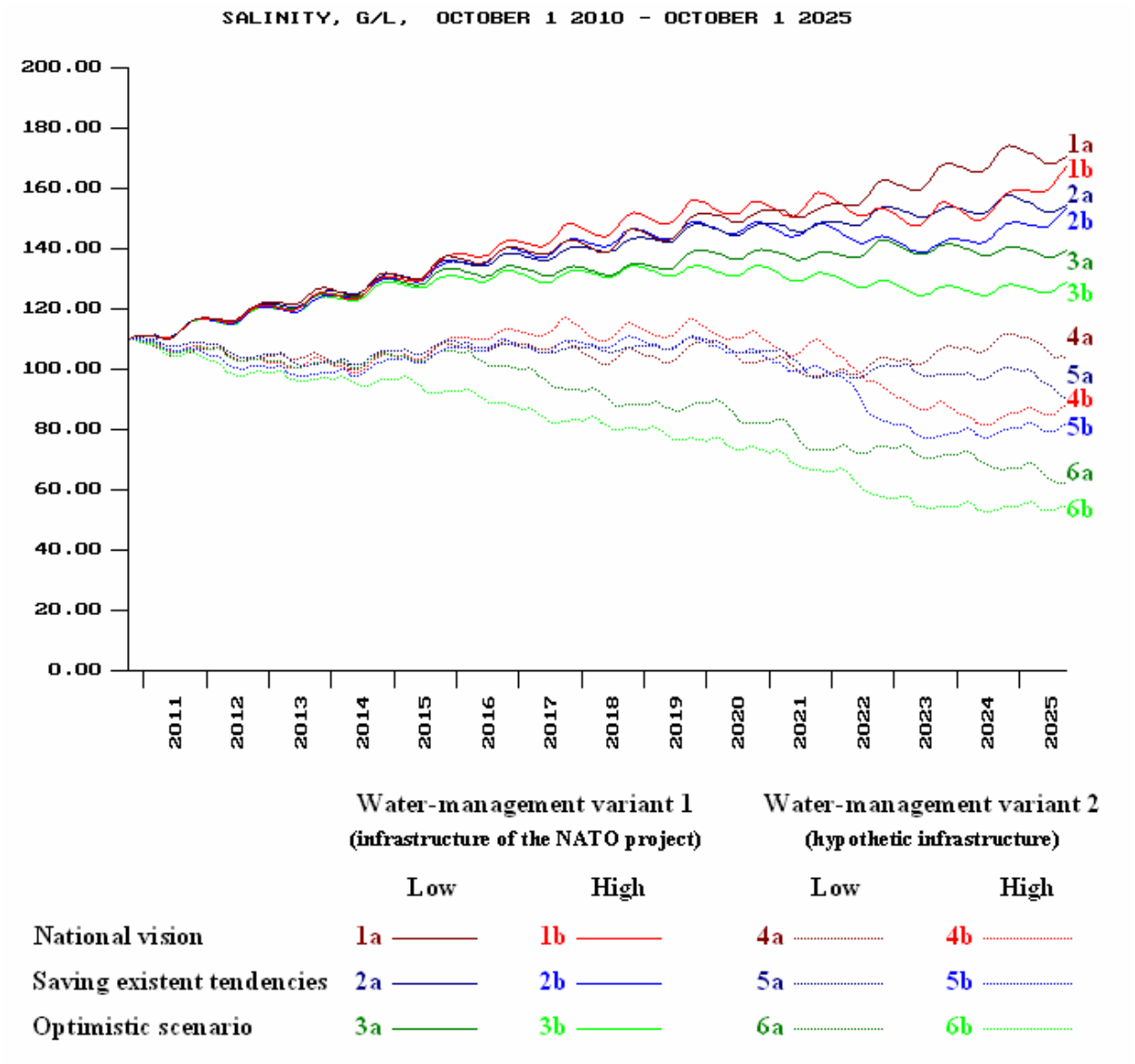

Fig. 28.17 Salinity obtained by long-term modeling by various scenarios.

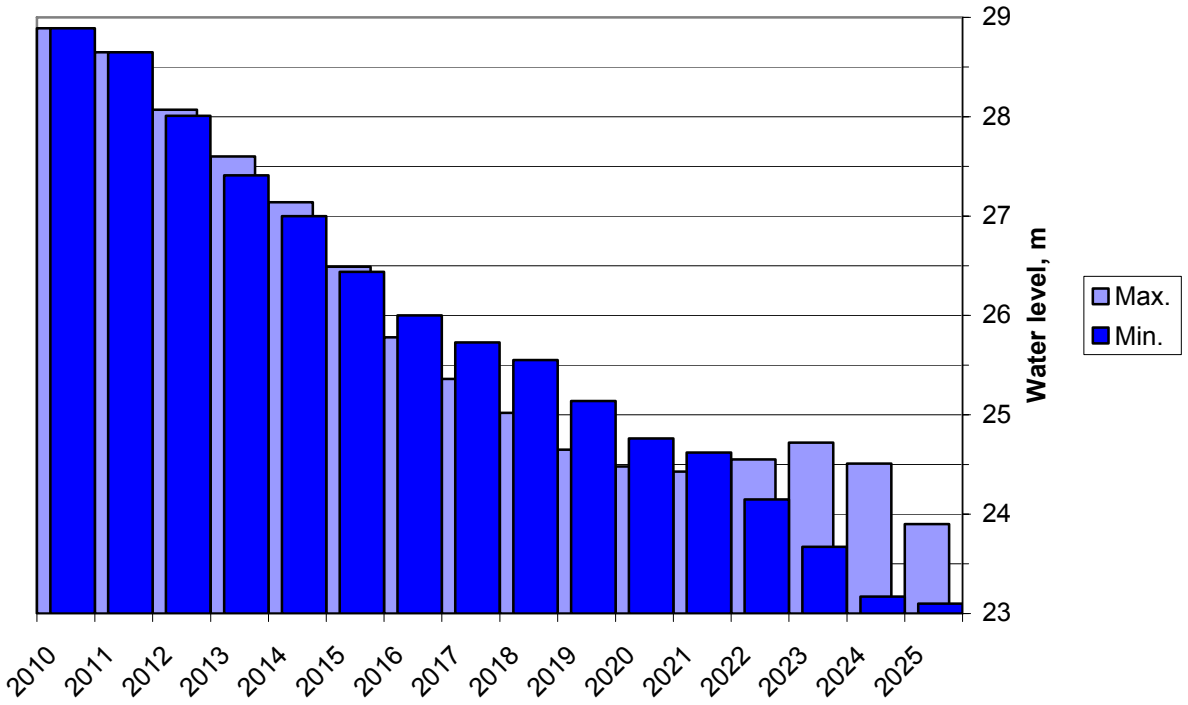

Fig. 28.18 Mean annual (by calendar years) water level obtained by long-term modeling according to "national vision" scenario of w/m variant 1.

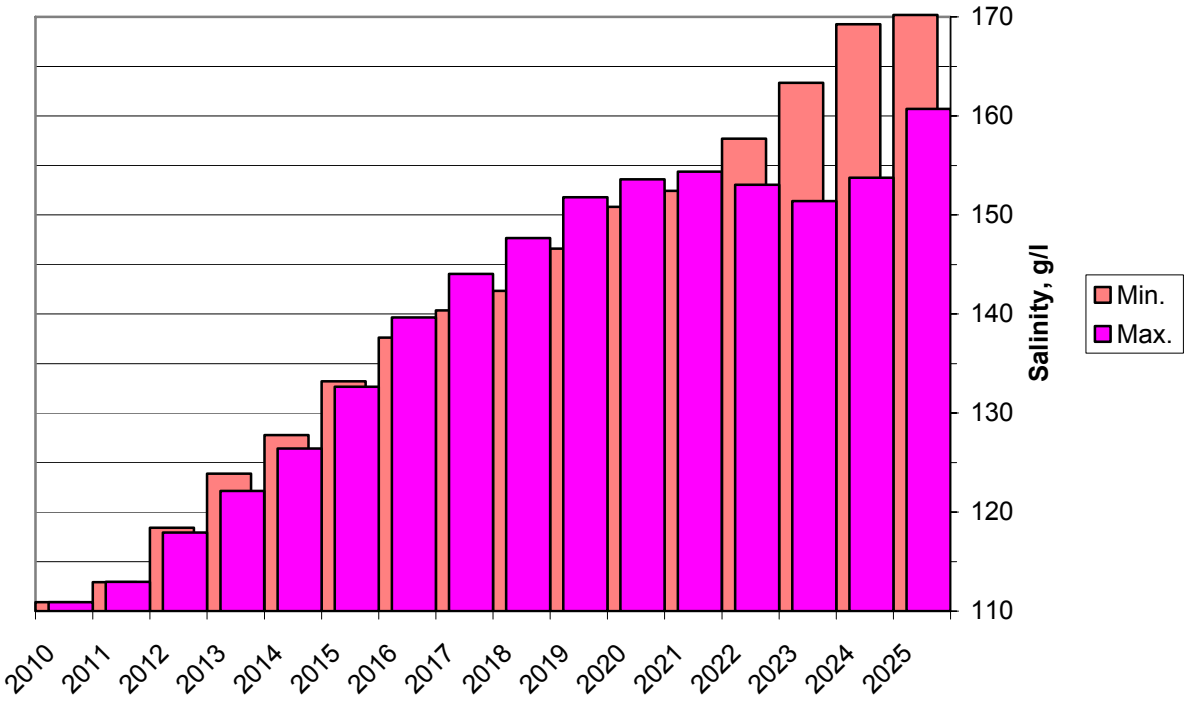

Fig. 28.19 Mean annual (by calendar years) salinity obtained by long-term modeling according to "national vision" scenario of w/m variant 1.

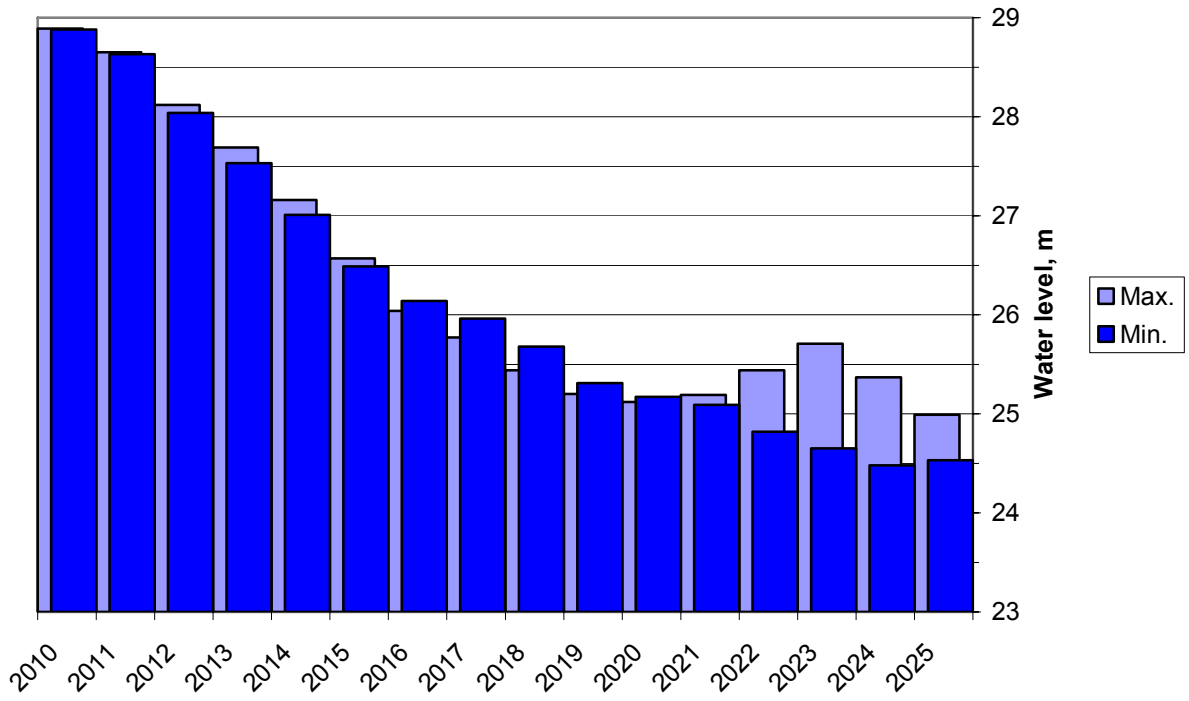

Fig. 28.20 Mean annual (by calendar years) water level obtained by long-term modeling according to "saving existent tendencies" scenario of w/m variant 1.

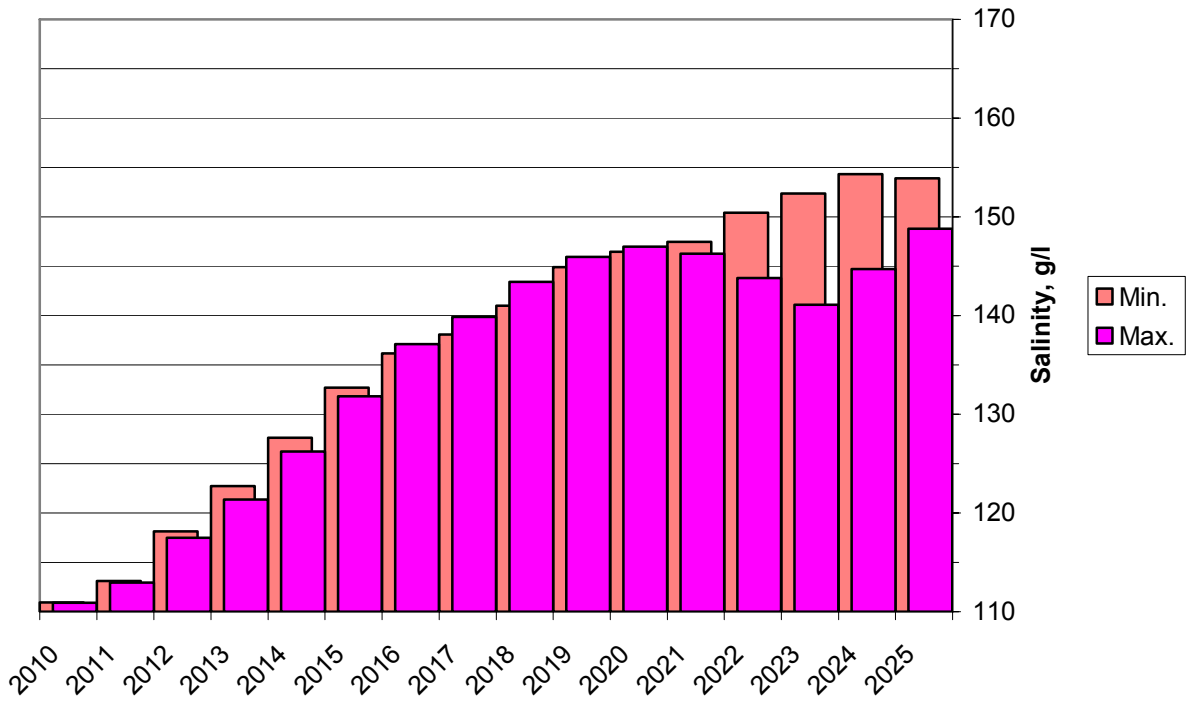

Fig. 28.21 Mean annual (by calendar years) salinity obtained by long-term modeling according to "saving existent tendencies" scenario of w/m variant 1.

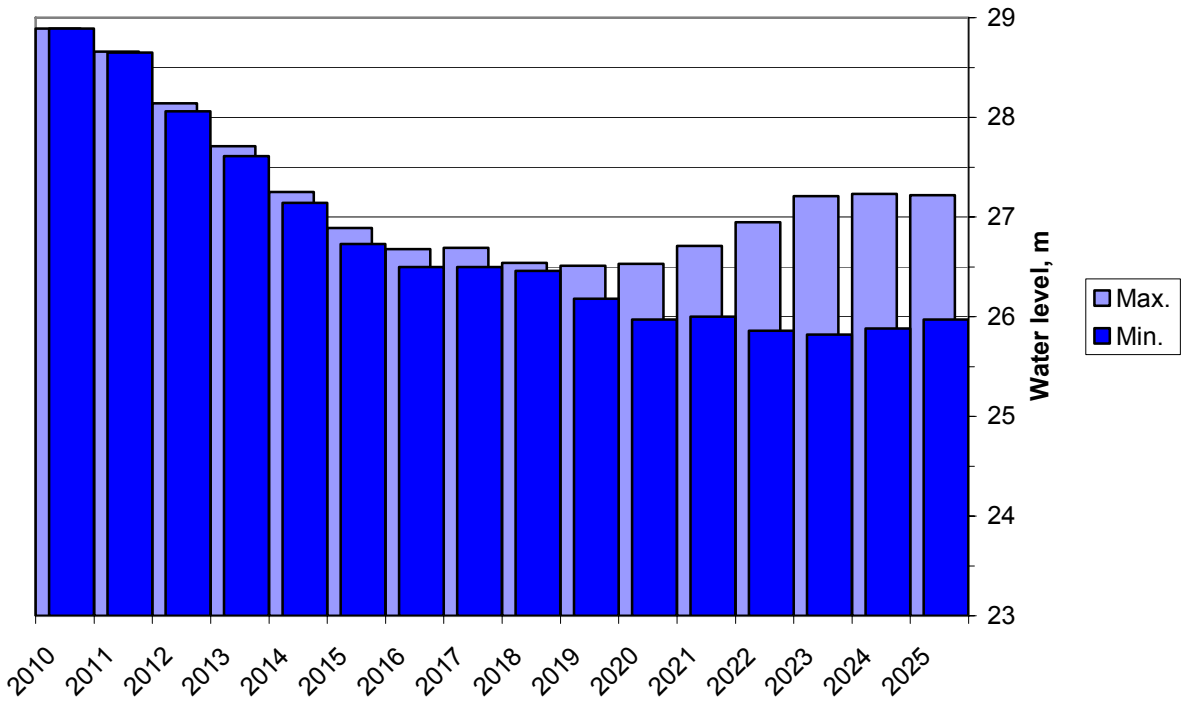

Fig. 28.22 Mean annual (by calendar years) water level obtained by long-term modeling according to optimistic scenario of w/m variant 1.

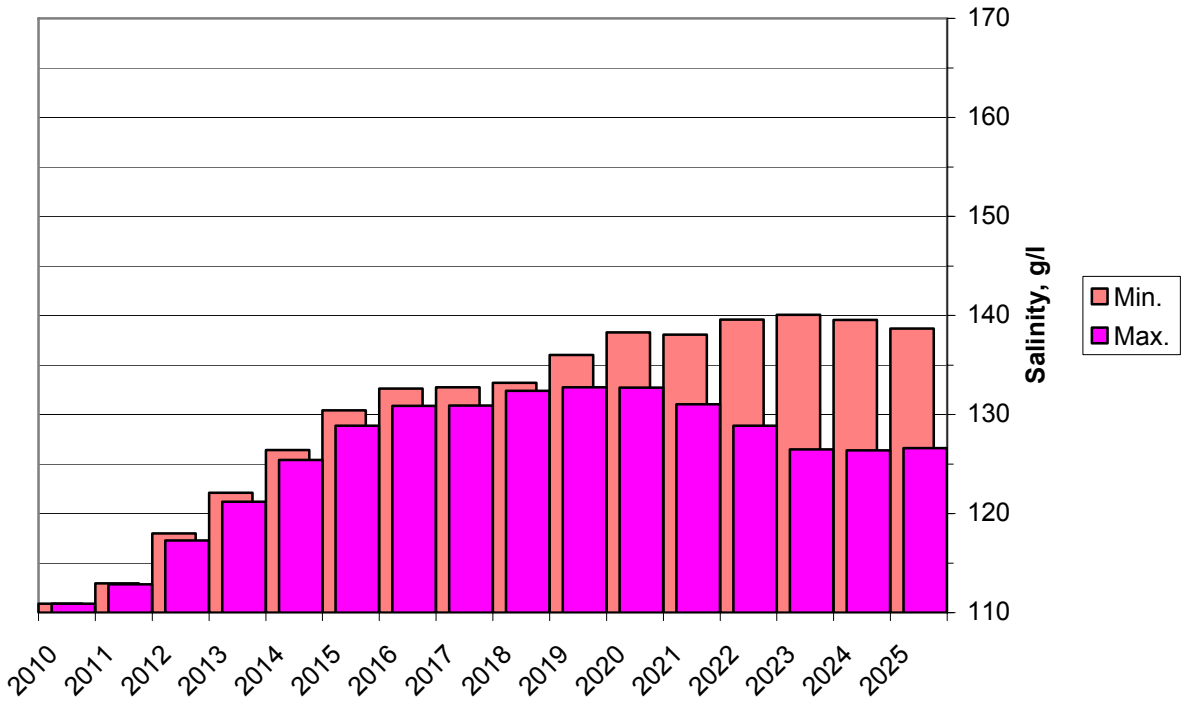

Fig. 28.23 Mean annual (by calendar years) salinity obtained by long-term modeling according to optimistic scenario of w/m variant 1.

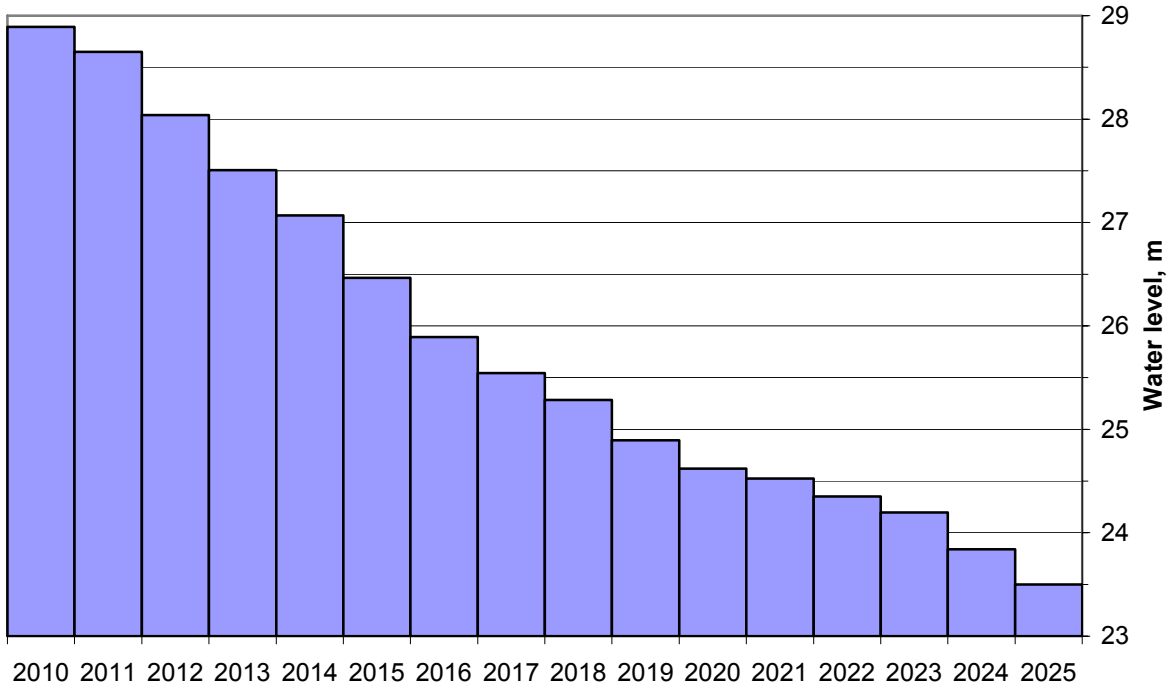

Fig. 28.24 Mean annual (by calendar years) averaged water level obtained by long-term modeling according to "national vision" scenario of w/m variant 1.

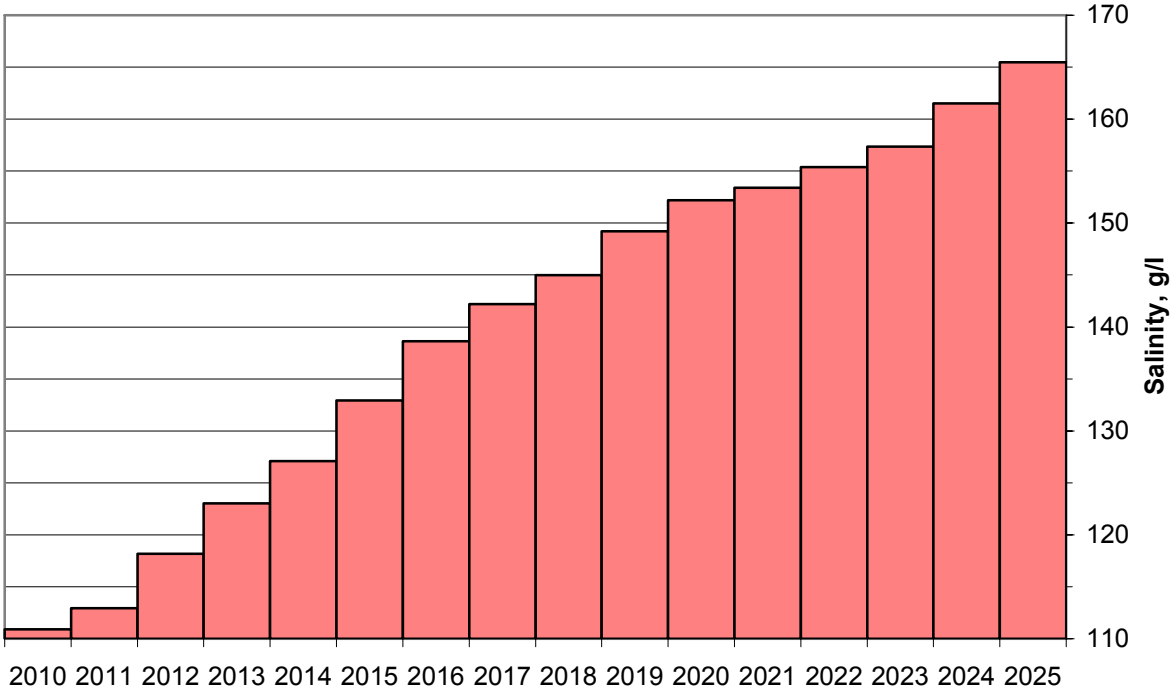

Fig. 28.25 Mean annual (by calendar years) averaged salinity obtained by long-term modeling according to "national vision" scenario of w/m variant 1.

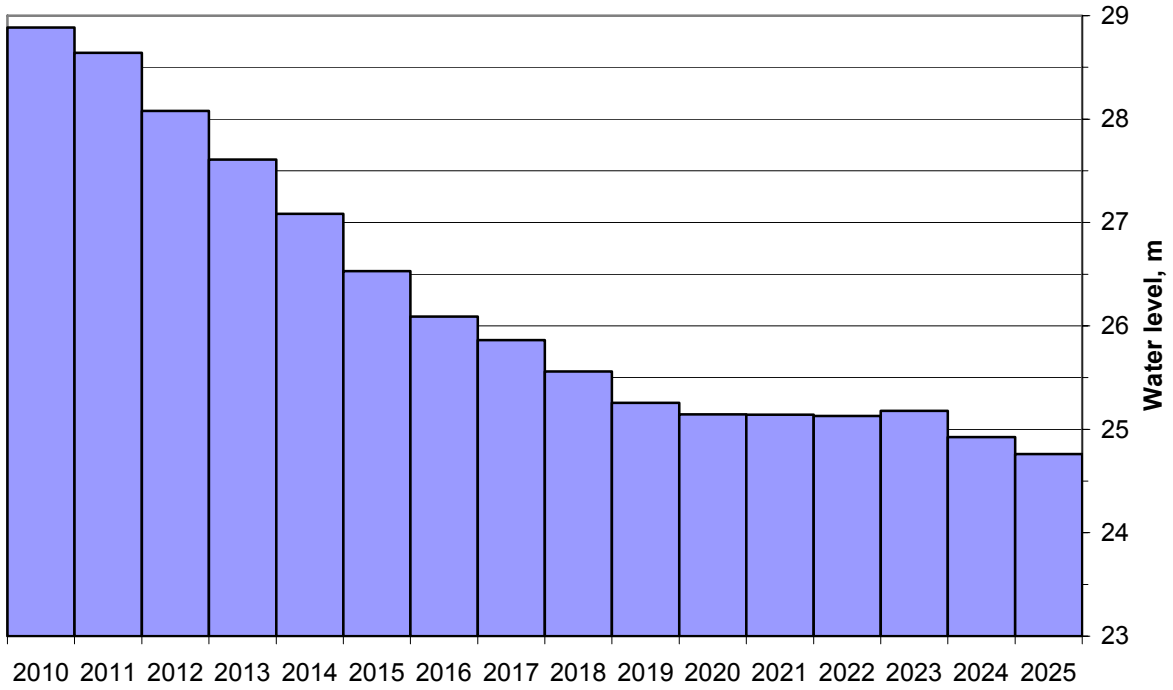

Fig. 28.26 Mean annual (by calendar years) averaged water level obtained by long-term modeling according to "saving existent tendencies" scenario of w/m variant 1.

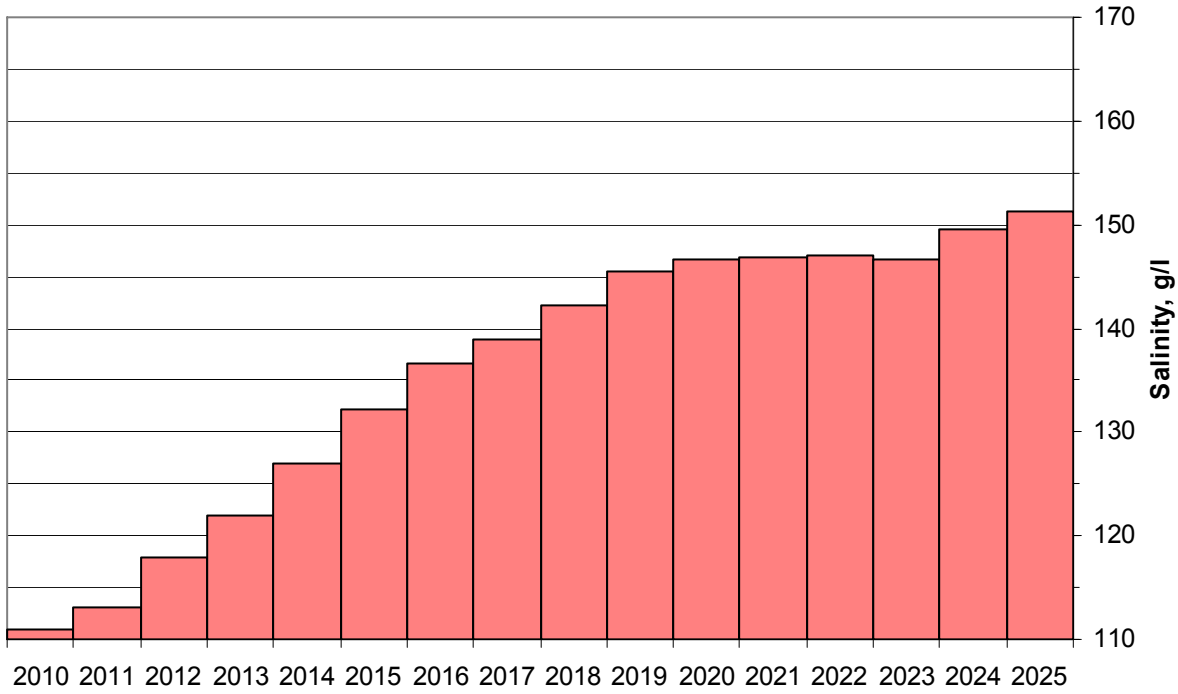

Fig. 28.27 Mean annual (by calendar years) averaged salinity obtained by long-term modeling according to "saving existent tendencies" scenario of w/m variant 1.

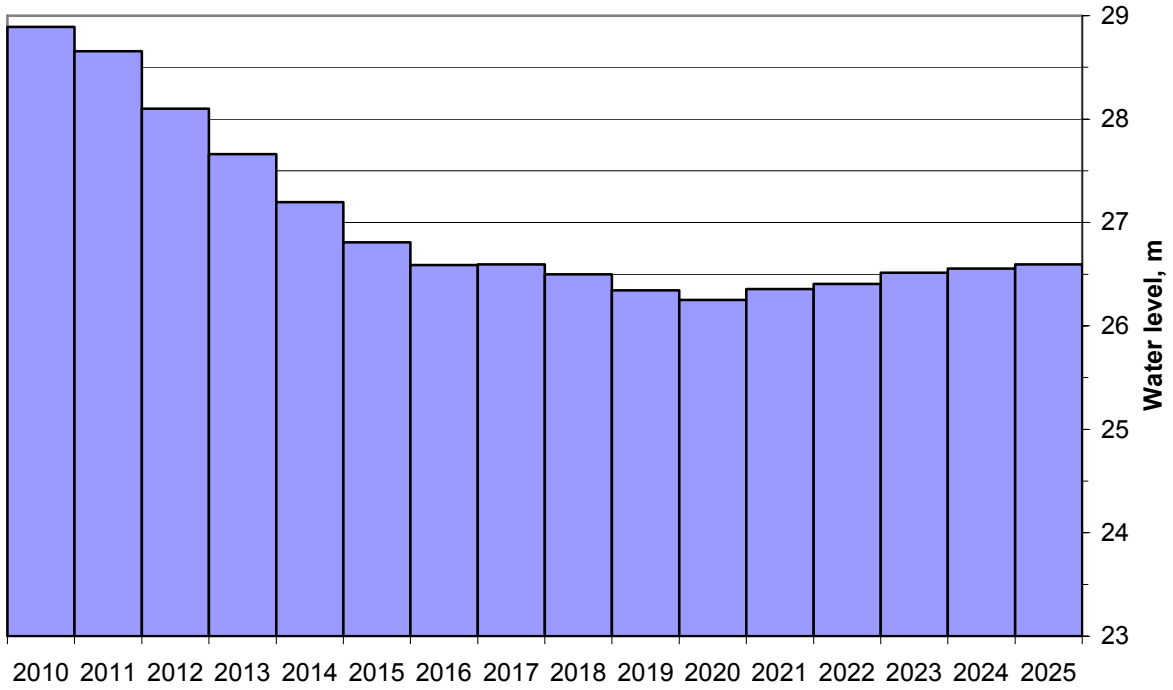

Fig. 28.28 Mean annual (by calendar years) averaged water level obtained by long-term modeling according to optimistic scenario of w/m variant 1.

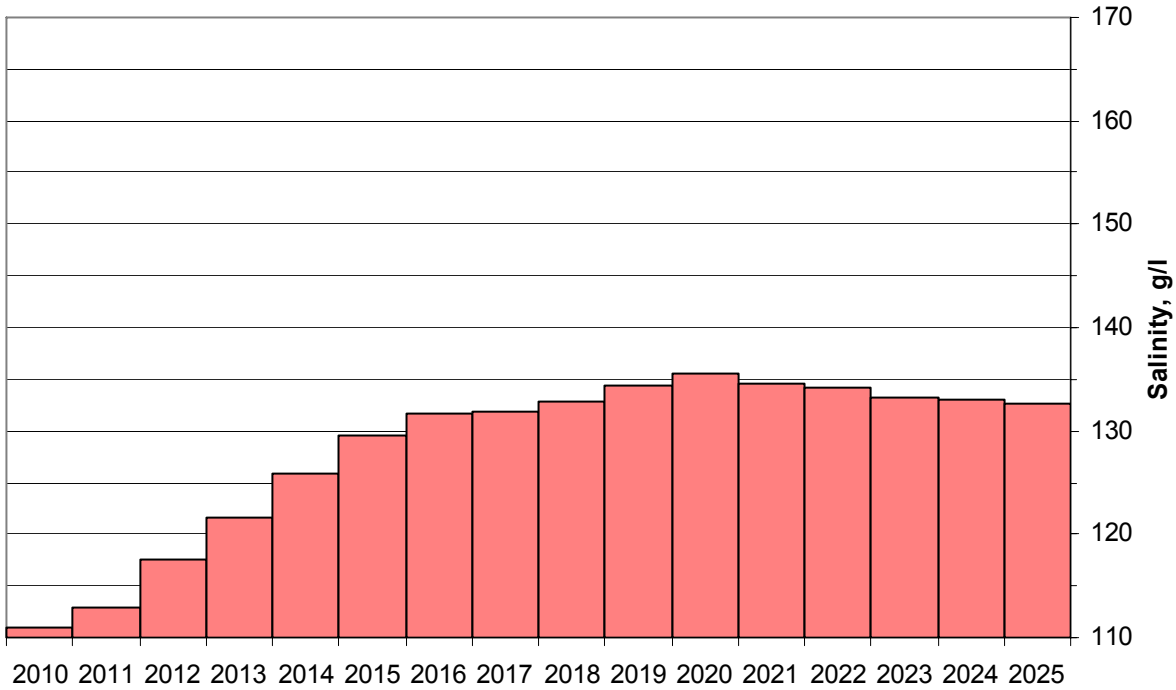

Fig. 28.29 Mean annual (by calendar years) averaged salinity obtained by long-term modeling according to optimistic scenario of w/m variant 1.

28.3.2 Calculation of hydrophysical regime for the 1-st water management variant using 1-D-model

Preliminary calculations of the level dynamics for 1.5-year period without tributary using 1-D and bulk models have shown that level dropping due to evaporation in second of them was faster. Such difference occurs because of discrepancy in a heat fluxes through free surface in two models. In the both models the heat flux is calculated with the same method considering water temperature on the surface of water body (T_{surf}). In zero-dimensional model T_{surf} coincides with the mean temperature, whereas in 1-D model it is really water surface temperature. As a result we have different heat fluxes, different surface temperature and different effective evaporation that lead to differences in level dynamics.
The initial temperature condition was state of homothermy, thereby at first period the dynamics of averaged parameters in two models were very close. But later on the surface temperature almost always excluding periods of full mixing differed from mean temperature. So the heat flux was calculated more precisely in 1-D-model in comparison with bulk model. The dynamics of heat flux through free surface in bulk and one-dimensional models is shown on Fig. 28.30, and the dynamics of effective evaporation is presented on Fig. 28.31. The numerical estimations of the differences between bulk and one-dimensional models in the calculations are given in Table 28.9. The maximum differences were observed in spring–summer period which mainly effects on the level changes.
In accordance with the calculation scenarios meteorological data were the same in all calculations. The data were annually periodic and as they are the main factor effecting heat regime formation in water body the character of mean temperature distribution on long-time period was practically identical in all calculations. Graphs of mean temperature and surface temperature change obtained in scenario "National vision" are presented on Fig. 28.32. The mean and surface temperature in calculations using one-dimensional model were distinctly lower then those in calculations using bulk model.
As it is shown on Fig. 28.31 in the period February–April the amount of precipitation exceeds the amount of evaporated water that leads to level growing even without tributary water.

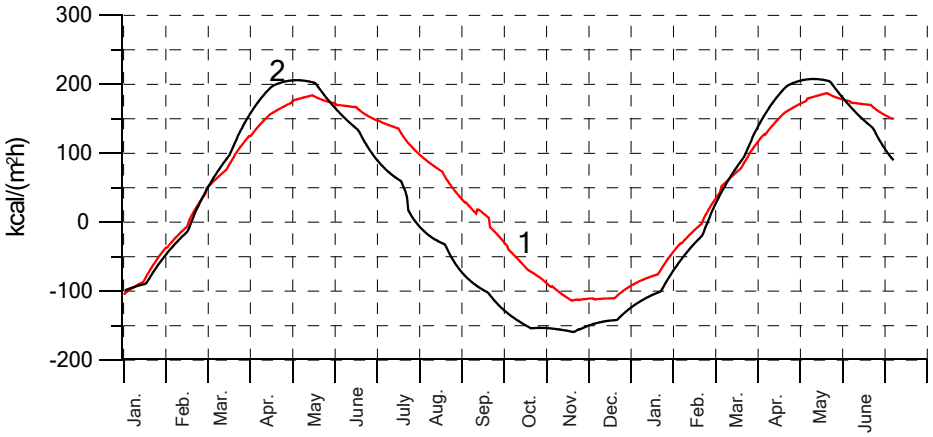

Fig. 28.30 The dynamics of heat flux through free surface in test calculations using scenario without tributary. 1: 1-D-model; 2: 0-D-model

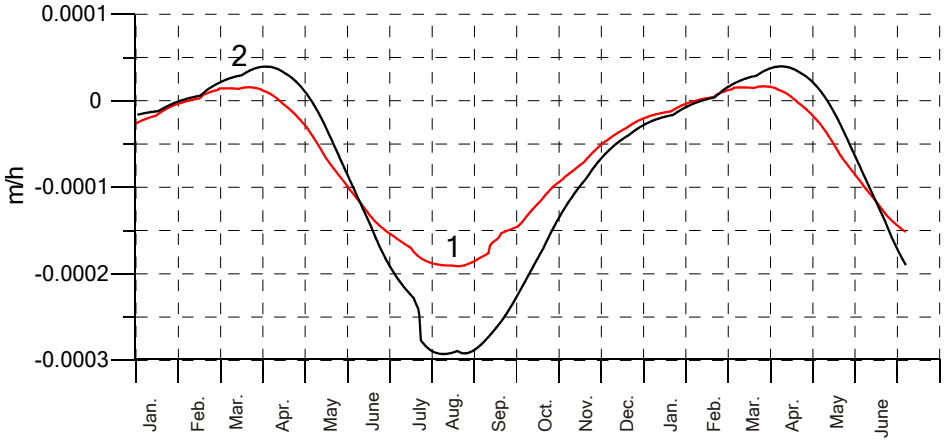

Fig. 28.31 The dynamics of water flux through free surface in test calculations using scenario without tributary. 1: 1-D-model; 2: 0-D-model

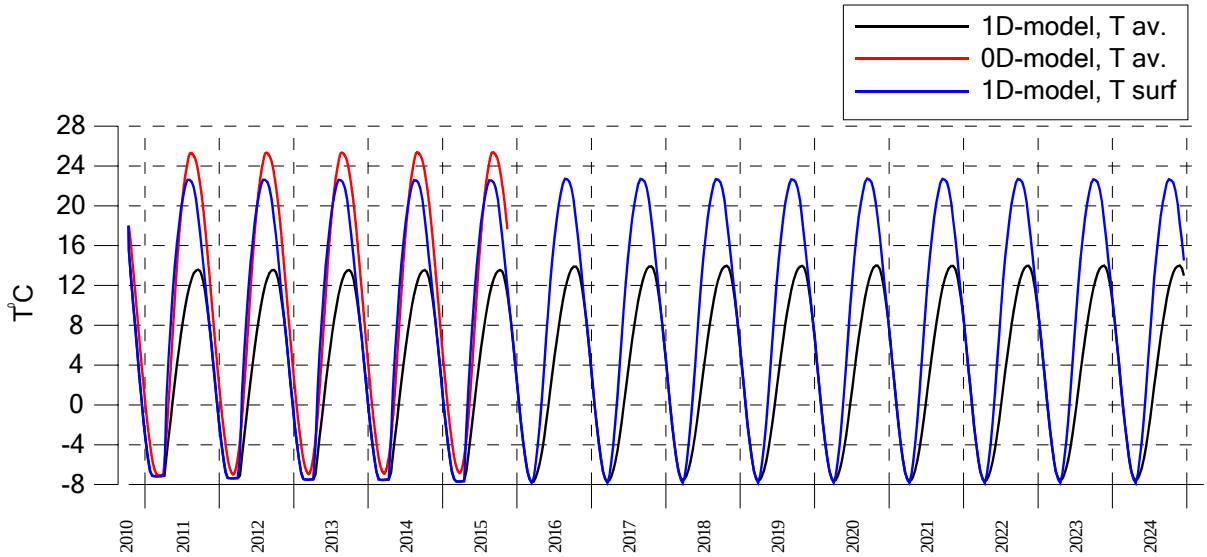

Fig. 28.32 Comparison of long-time water temperature dynamics in calculations using two models

Table 28.9 Differences between bulk and 1-D model

Heat flux	
Mean deviation	24.5 kcal/(m·h)
Maximum deviation	113.6 kcal/(m·h), 31%
Effective evaporation	
Mean deviation	$3.4 \cdot 10^{-5}$ m/h
Maximum deviation	$1.2 \cdot 10^{-4}$ m/h, 37%
Mean water temperature	
Mean deviation	5.9 ^{0}C
Maximum deviation	13.9 ^{0}C, 43%
Surface water temperature	
Mean deviation	1.8 ^{0}C
Maximum deviation	3.8 ^{0}C, 12%

It was found out by analyzing results of calculations using two models for long-time period (15 years) that the difference of calculated levels to the end of period was about 2 m. Hence calculation by 1-D-model for second water management variant would give the level rising above 29.5 m. Therefore, as it was noticed earlier, the calculations for western part of Aral Sea without considering its hydraulic interaction with eastern part would be incorrect, so one-dimensional model was used only for calculations at first water management variant.

The dynamics of level in three scenarios with minimum and maximum flow are shown on Fig. 28.33. At minimum flow in scenario "Saving existent tendencies" a relative stabilization of level near the mark 27.5 m is observed in second part of calculation period. In optimistic scenario also at minimum flow at the end of calculation period the level reaches the same value that at the beginning, so at periodic amount of flow in 15-years cycle the level also becomes relatively stable. In scenario "National vision" at minimum flow the level decreases permanently and the salinity increases.

The differences between levels in scenarios at minimum and maximum flow amount to 1 m at the end of calculation period, and in case of "Saving existent tendencies" scenario the differences just less then in others. In optimistic scenario at maximum flow the level in 2022 year exceeds 29.5 m so the last two years are not considered. In scenario "National vision" at maximum flow a relative stabilization of the level near the mark 27.5 m is observed, and in scenario "Saving existent tendencies" the level fluctuations continue.

The dynamics of mean salinity correspond to the dynamics of level (Fig. 28.34). Minimum value was achieved in optimistic scenario at maximum flow at the end of thirteen calculation year (105 g/l), and maximum value was achieved in sce3nario "National vision" at minimum flow at the end of calculation period (131 g/l).

In February–March ice-cover is observed in most scenarios. In optimistic scenario and in scenario "Saving existent tendencies" ice-cover exists in every year of calculation period. In scenario "National vision" at minimum flow ice-cover is observed only in first ten years, and at minimum flow it forms annually in first five years and in last two years of calculation period. On graphs of the dynamics of mean salinity (Fig. 28.33) short periods of its fast growing caused by ice-forming are observed. Maximum ice thickness was achieved in optimistic scenario at maximum flow (~0.2 m). The dynamics of ice forming at minimum and maximum flow in two scenarios is shown on Fig. 28.35, Fig. 28.36.

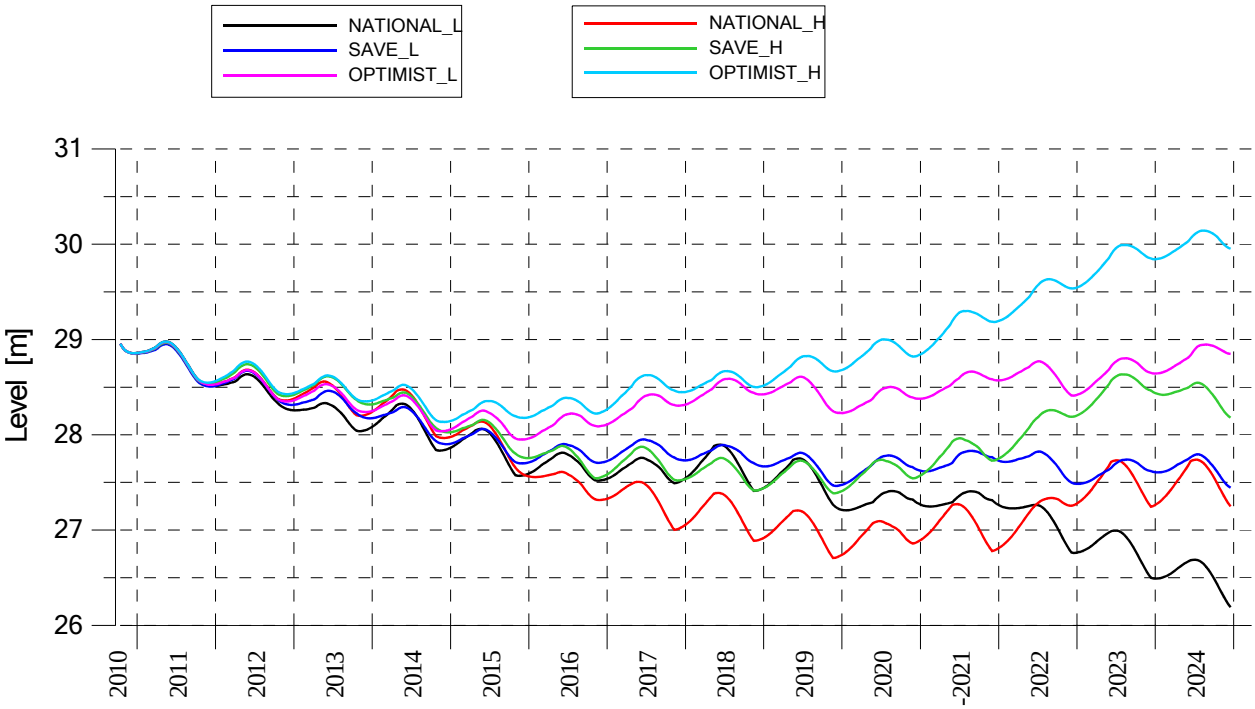

Fig. 28.33 The dynamics of level in first water management variant

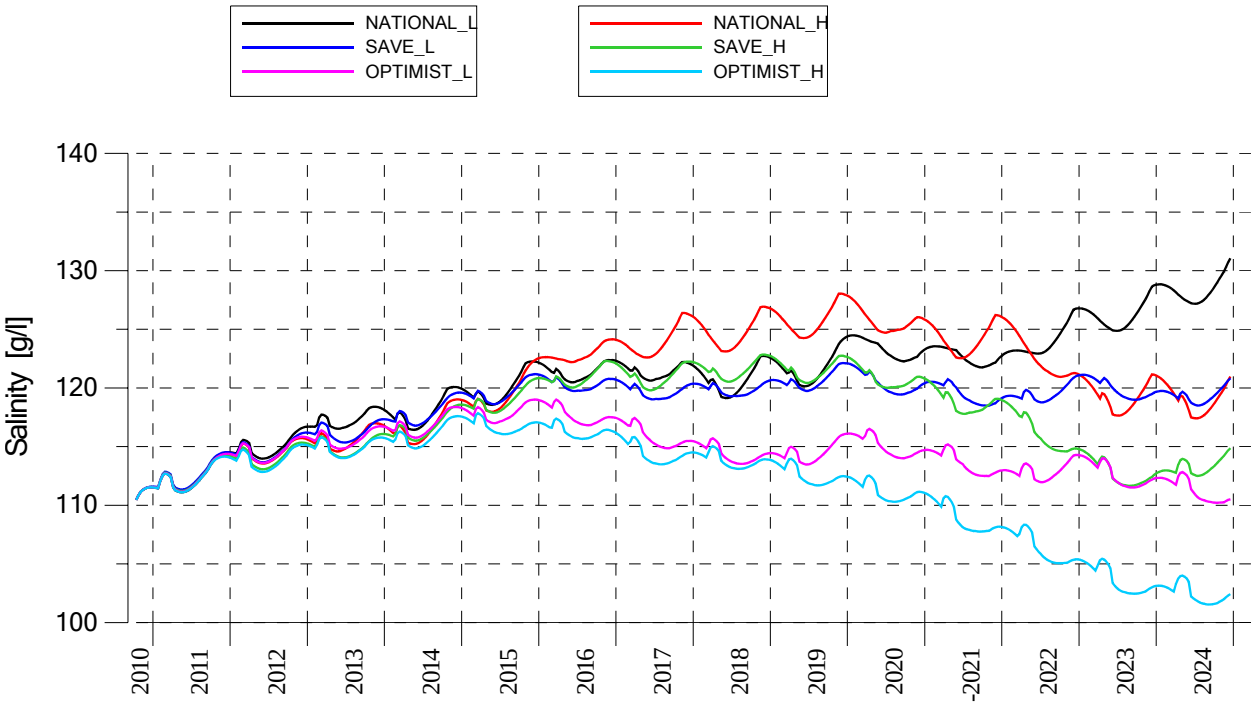

Fig. 28.34 The dynamics of mean salinity in first water management variant

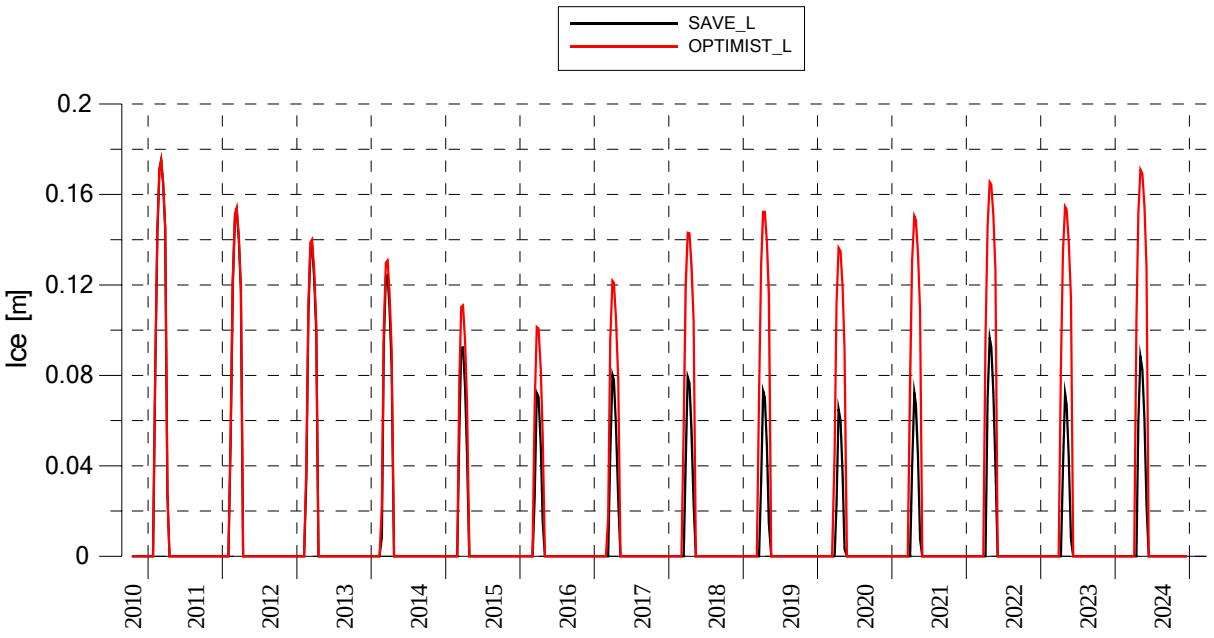

Fig. 28.35 The dynamics of ice-cove at minimum flow

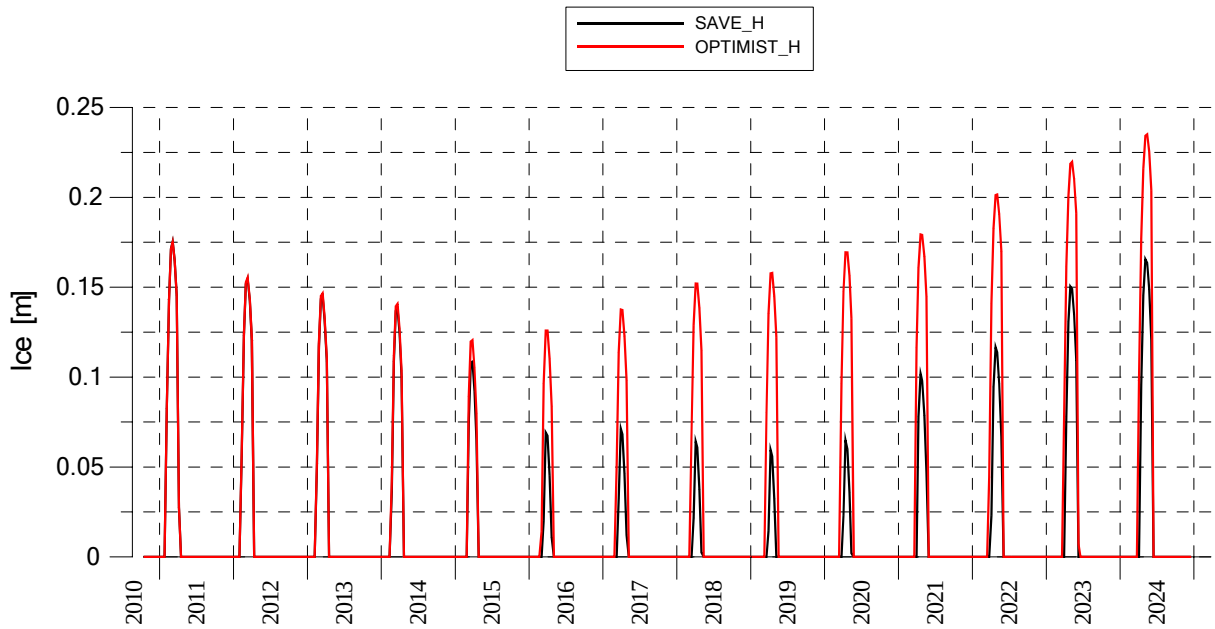

Fig. 28.36 The dynamics of ice-cove at maximum flow

The calculations using one-dimensional model allow estimating how long fresh-water lens formed by tributary water exists. For the analysis the most high-water year from 13-years period and preceding year in optimistic scenario at maximum flow were chosen. 2020 year proved to be the most high-water year. Hydrological year in the analysis lasted from November, 1 to October, 30.

Vertical profiles of salinity at first days of months in 2019/2020 and 2020/2021 hydrological years are presented on Fig. 28.37, Fig. 28.38. Qualitative behavior of vertical distributions was similar in corresponding months of two hydrological years despite of salinity decreasing during all period. Maximum gradient of salinity was observed in April, and in November–February uniform distribution was settled. So desalinated water entirely got mixed over 7 months and fresh-water lens near water surface was washed out over 3 months. In August the transfer to autumn stratification was observed, and in October it is marked strongly.

Vertical distributions of water temperature also are of interest in respect to water body ecology. The dynamics of vertical temperature profiles for the same hydrological years (at first days of the months) are

presented on Fig. 28.39, Fig. 28.40. In period December-April water body stayed in the state of homothermy with temperature changing from +2^{0}C (the beginning of December) to -7^{0}C (the beginning of March). In the beginning of April upper layers of water already began to warm up while lower layers still had the temperature about -7^{0}C.
In the period April-August the temperature of upper layers constantly aroused and in the beginning of August it reached about 24^{0}C. From that time gradual cooling began. More warm water of upper layers penetrated into the near-bottom layers due to mixing processes but there worming processes were much slower. In the beginning of September the near the bottom temperature was below zero yet (near -1^{0}C), and the difference between bottom and surface temperature was nearly 21^{0}C.
In August in the upper layers of water cooling processes began whereas in the near-bottom layers the temperature aroused because of mixing processes. In the beginning of November strongly marked thermocline was observed, but it disappeared in second decade of November, and then the state of homothermy was formed. In that period the near-bottom temperature achieved its maximum (about 7^{0}C). So the range of the near-bottom temperature was about 14°C ([-7, +7] °C), whereas the range of surface temperature changes was equal to 30°C ([-7, +23] °C).
The dynamics of vertical temperature profiles were similar in two hydrological years due to periodic character of meteorological data. Insignificant differences resulted from changes of the water salinity that effected on friezing-point and vaporization temperature and caused the differences of the state of near-surface water layer.

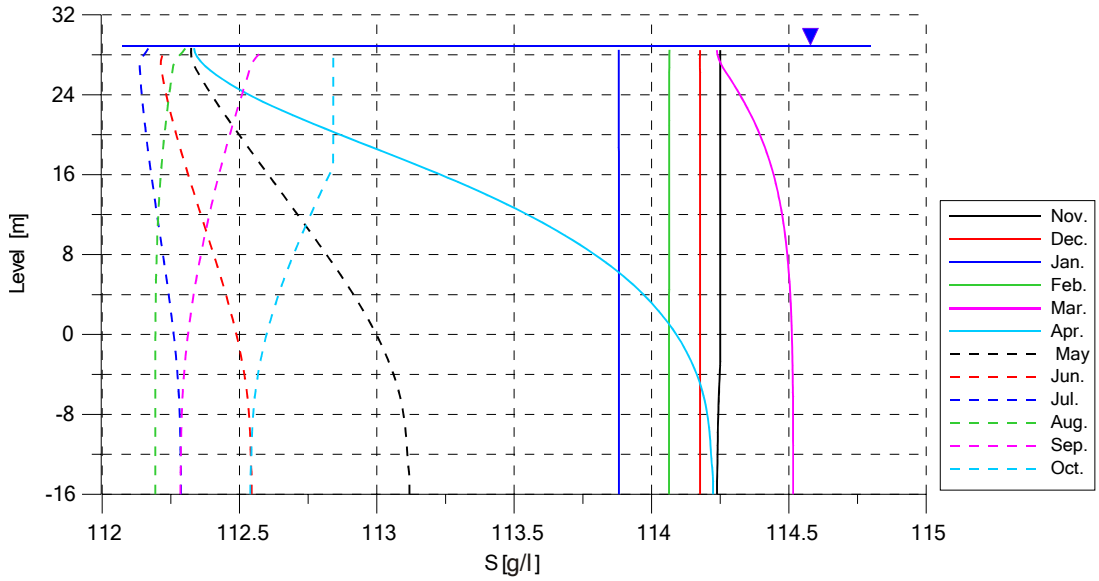

Fig. 28.37 Vertical distributions of salinity in 2019/2020 year

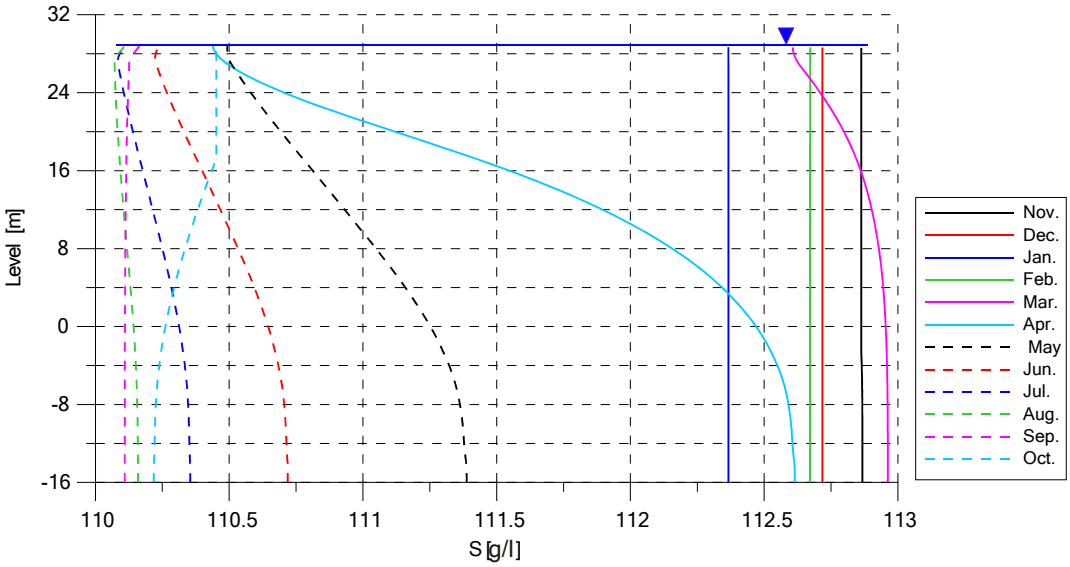

Fig. 28.38 Vertical distributions of salinity in 2020/2021 year

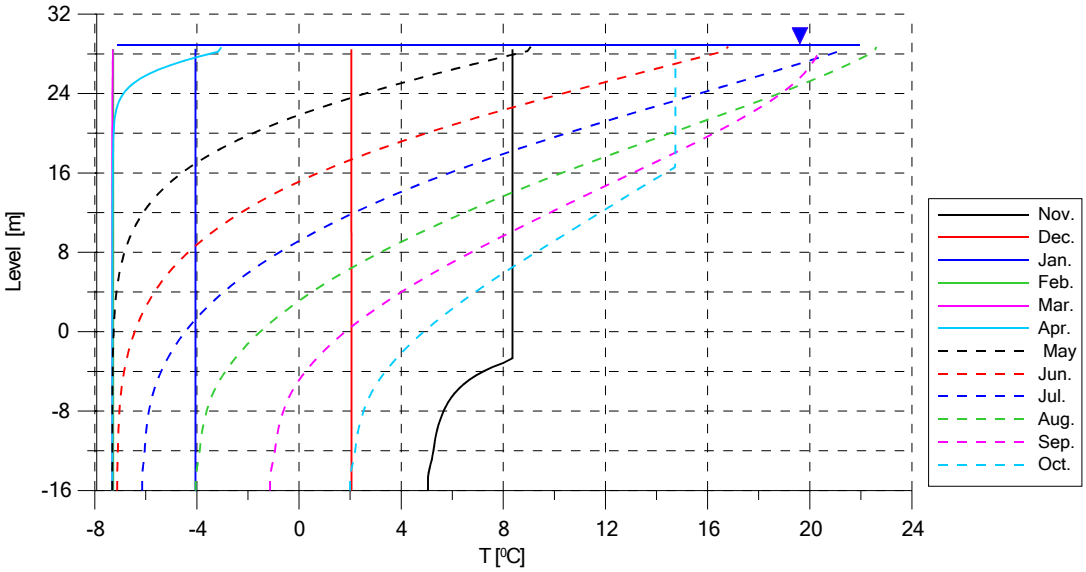

Fig. 28.39 Vertical distributions of temperature in 2019/2020 year

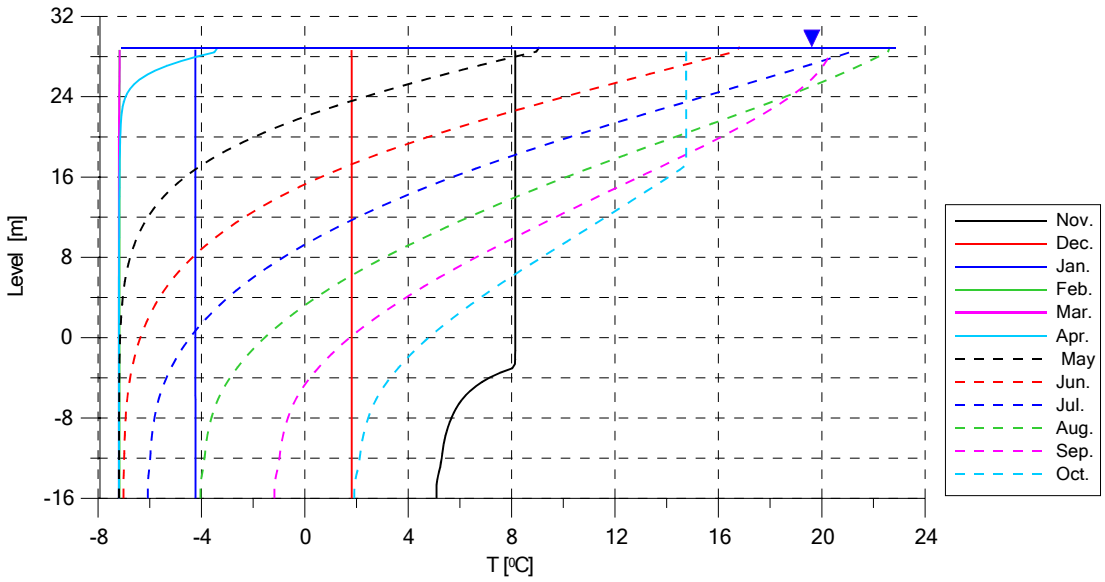

Fig. 28.40 Vertical distributions of temperature in 2020/2021 year

28.3.3 Calculations for the second water management variant with the use of 1-D model considering water overflow from western to eastern part of the sea

The second water management variant is more favourable in respect of stabilization of the level and desalinization of the sea water. Preliminary calculations using bulk model has shown (section 28.3.1) that this variant under the all scenarios of inflow leads to level rising over the mark 29.3 m and then it is necessary to consider water overflow from western to eastern part of the sea. So a calculation of overflow water discharge dependence on level were fulfilled. The calculations were based on hydraulic model of overfall without taking water backing into account. The equations of the model are [48, p. 279]:

$$Q = \omega_{cr}\sqrt{2g(H_0 - h_{cr})}\ , \quad \frac{\omega_{cr}^3}{B_{cr}} = \frac{Q^2}{g}$$

were H_0 is the head above overfall, h_{cr} is the depth at the sill which is equal to critical one, ω_{cr} и B_{cr} are the area of cross-section and the width of flow, Q is the desired discharge of water. Using a map of isobaths [3] we obtained that saddle node of the sill is at the level not higher then 29.336 m. Therefore in further calculations the level of the sill z_0 was equal to 29.5 m BS [3].The cross-section of the overfall was constructed using the map of isobaths [34] (Fig. 28.41). The calculation for 15-years period using bulk model showed that the maximum discharge corresponding to the maximum inflow (1484 m^3/s) is about 1200 m^3/s and corresponds to the value of level 29.866 m BS.
The scenarios of calculations by the one-dimensional model for the second water management variant were the same as for the first one as well as meteorological data and initial conditions (Table 28.10), but the situations with lower initial levels were also considered. In Table 28.11 and Table 28.12 short descriptions of the calculations are presented.

Table 28.10 Initial conditions for the scenarios

Scenario	Flow	Conventional denotation	Mean annual flow, km^3
National vision	min	**A_{min}**	4.50
	max	**A_{max}**	5.00
Saving existent tendencies	min	**B_{min}**	5.15
	max	**B_{max}**	5.47
Optimistic scenario	min	**C_{min}**	7.46
	max	**C_{max}**	8.94

Table 28.11 Initial conditions for scenarios

Level, m	26	27	28	29
Init. salinity (calc.), g/l	137.242	127.596	118.518	110.0
Init. salinity (approx..), g/l	140	130	120	110

Table 28.12 Some results from scenario simulations

Init. level, m	Init. salinity, g/l	Scenario	Final level, m	Final salinity, g/l
29	110	**A_{min}**	28.6	85.3
		A_{max}	28.9	64.1
		B_{min}	29.1	76.7
		B_{max}	29.1	60.1
		C_{min}	29.7	46.9
		C_{max}	29.5	29.7
28	120	**B_{min}**	29.1	80.8
27	130	**B_{min}**	29.1	84.3
26	140	**B_{min}**	29.1	86.8
		A_{min}	28.6	96.5
		C_{min}	29.7	53.2

For an adequate description of the process of sea water desalinization due to inflow of more fresh water and outflow of more salt one it is necessary to take in account that the mean salinity of effluent water is determined by the depth of the layer of water intake. Therefore we have estimated this depth using a model of selective withdrawal [18]. The model is based on the formula for the densimetric Froude number

$$\frac{Q}{S\,h\,N} = Fr, \quad S = \int_{Z_0}^{Z_{SURF}} B(z)\,dz \ ,$$

where

$Fr = \frac{q}{H}\left[\frac{\rho(0)\,H}{g\,(\rho(0) - \rho(Z_{SURF}))}\right]$ is the densimetric Froude number;

$N = \left(g\,\frac{|\rho(Z_{SURF}) - \rho(Z_{SURF} - h)|}{\rho^* h}\right)^{1/2}$ is the Väisälä – Brent frequency;

$B(z)$ is the width of water body; Q is the discharge of overflow; q is the specific discharge per unit of width of withdrawal; h is the depth of selective jet; Z_0, Z_{SURF} are the coordinates of lower edge of withdrawal and the free surface; $\rho^* = \min\{\rho(Z_{SURF}), \rho(Z_{SURF} - h)\}$.

The estimations of the selective jet depth were fulfilled for a case of the most developed density stratification (July) with the level 30 m. The discharge of overflow was equal to 1866.7 m^3/c, the calculated Froude number was about 0.5 and the depth of selective jet was approximately 2.1 m. The analysis of vertical salinity distribution showed that in the layer of such depth the variation of salinity is not grater than 0.02 g/l. Taking into account these estimations it may be considered that the salinity of effluent water is practically equal to that of the surface water. The annual dynamics of mean salinity and surface water salinity at the end of calculation period for the scenario **C_{max}** is presented on Fig. 28.42.

At first we consider the calculations with the initial level 29 m and the salinity 110 g/l. Under these conditions with scenarios **A_{max}, B_{min}, B_{max}, C_{min}, C_{max}** a relative stabilization of the level near the mark 29.5 m was observed at the end of calculation period. With scenario **A_{min}** the level dropping below the mark 29 m was possible. The dynamics of level obtained in these calculations are shown on Fig. 28.43, Fig. 28.44. While comparing these two figures it is easy to see that there are considerable level differences between scenarios with minimum and maximum inflow sometimes amounted to 1 m. The decreasing of the mean salinity due to inflow of fresh and outflow of saline water (Fig. 28.45, Fig. 28.46) was observed in the all scenarios. The most favourable in respect of desalinization of the sea waters was the scenario **C_{max}** (the final salinity was about 29.7 g/l).

An analysis of the dynamics of vertical salinity and temperature distributions in the most high-water year in scenario $\mathbf{C_{max}}$ was fulfilled in order to compare with the distributions obtained in the first water management variant. The distributions were similar but there were quantitative differences between them (see Fig. 28.37, Fig. 28.38 and Fig. 28.46, Fig. 28.47). The desalinization of waters in second water management variant is more intensive because of outflow of saline water to eastern part of the sea that explains the differences. The range of annual variation of the near-bottom water temperature was from -4°C to 6.5°C. The surface water temperature varied in the range from -4°C to +23°C.
The convective processes in the second water management variant were less intensive because the stratification was more stable. The homogeneous distribution was formed only to the last decade of November. In the first variant the mixed layer extended to the level of -3 mBS and in the second variant its lower boundary reached only the level +10 mBS (Fig. 28.39 and Fig. 28.49).
In addition to main six calculations the analysis of the level and the salinity dynamics in the cases when the initial level was lower 29 m was fulfilled. The level dynamics for the scenario $\mathbf{B_{min}}$ with the initial marks 26, 27, 28 и 29 m is shown on Fig. 28.51. In the all cases the level reached the sill mark (in different times) and then the level regimes became stable near the mark 29.5 m. The salinity dynamics is shown on Fig. 28.52.
The calculation using three scenarios with minimum inflow with the initial level 26 m showed that the all cases except scenario $\mathbf{A_{min}}$ led to the level stabilization and the salinity permanently decreased (Fig. 28.53 and Fig. 28.54).

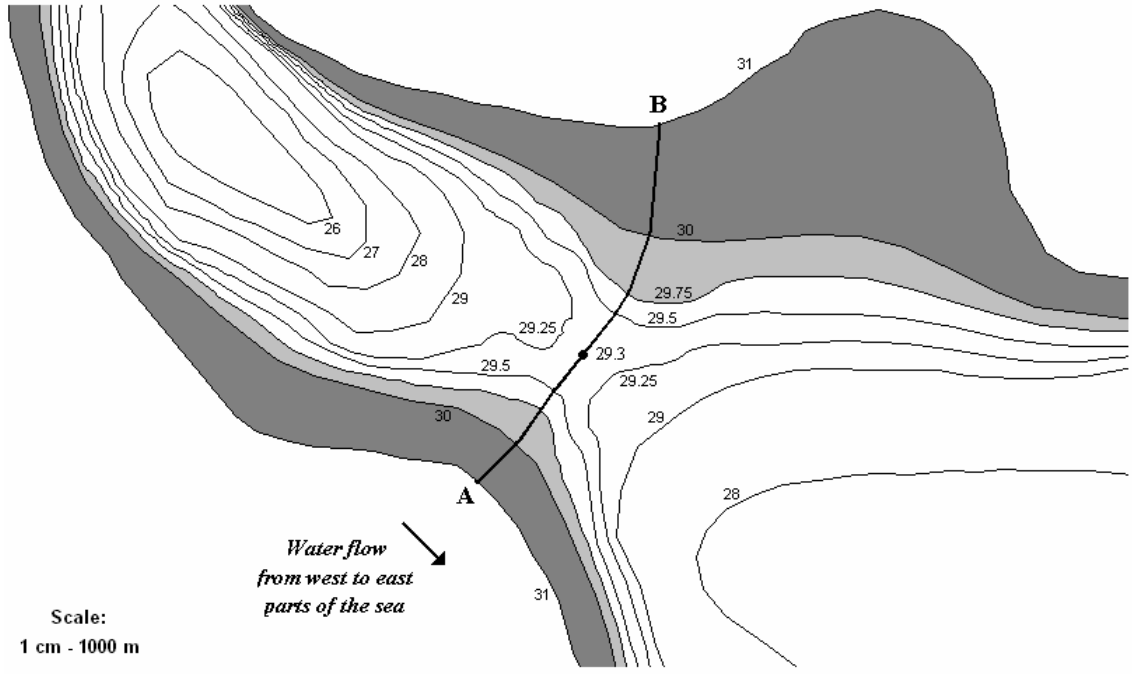

Fig. 28.41 Sill between western and eastern part of the sea

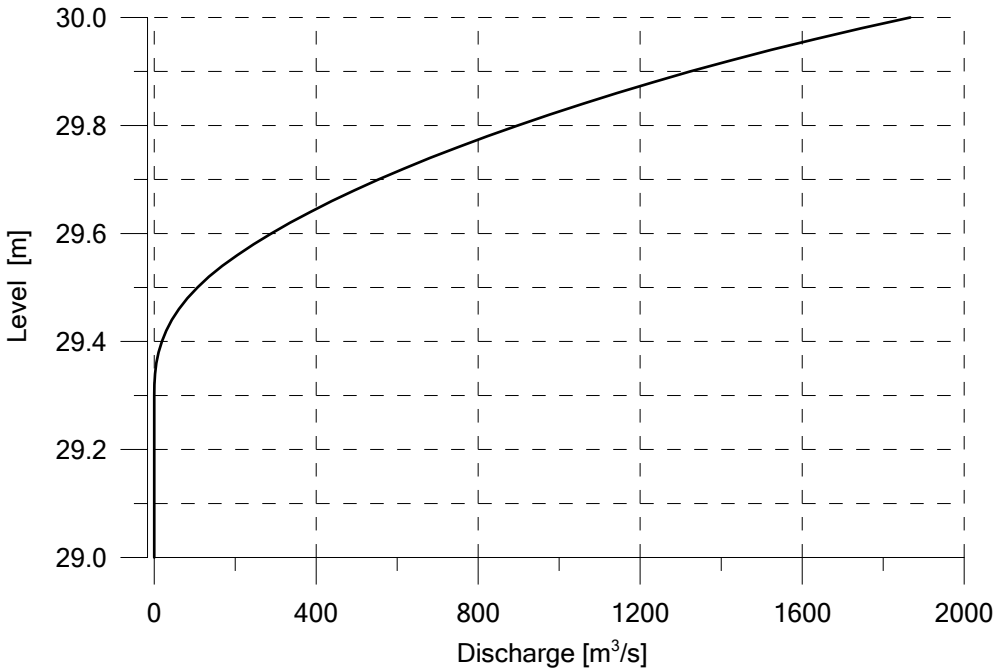

Fig. 28.42 Discharge of overflow dependence on the level

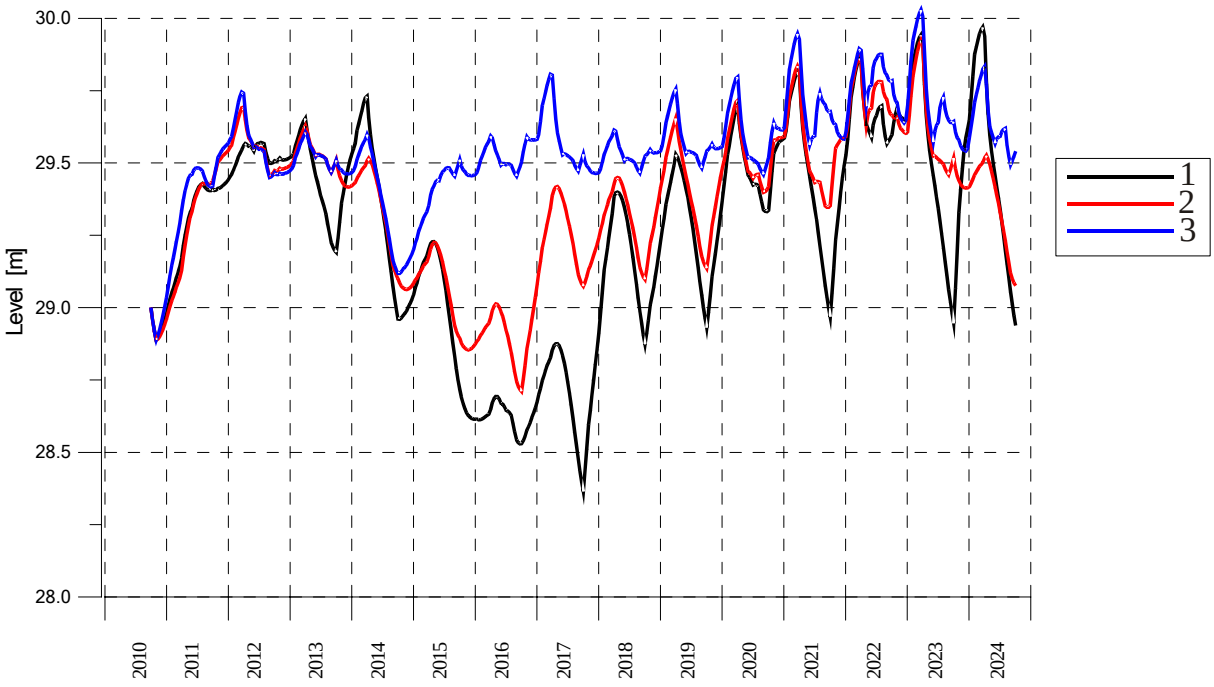

Fig. 28.43 The level dynamics with initial mark 29 m.
Scenarios with maximum inflow. 1 – **A_{max}**; 2 – **B_{max}**; 3 – **C_{max}**

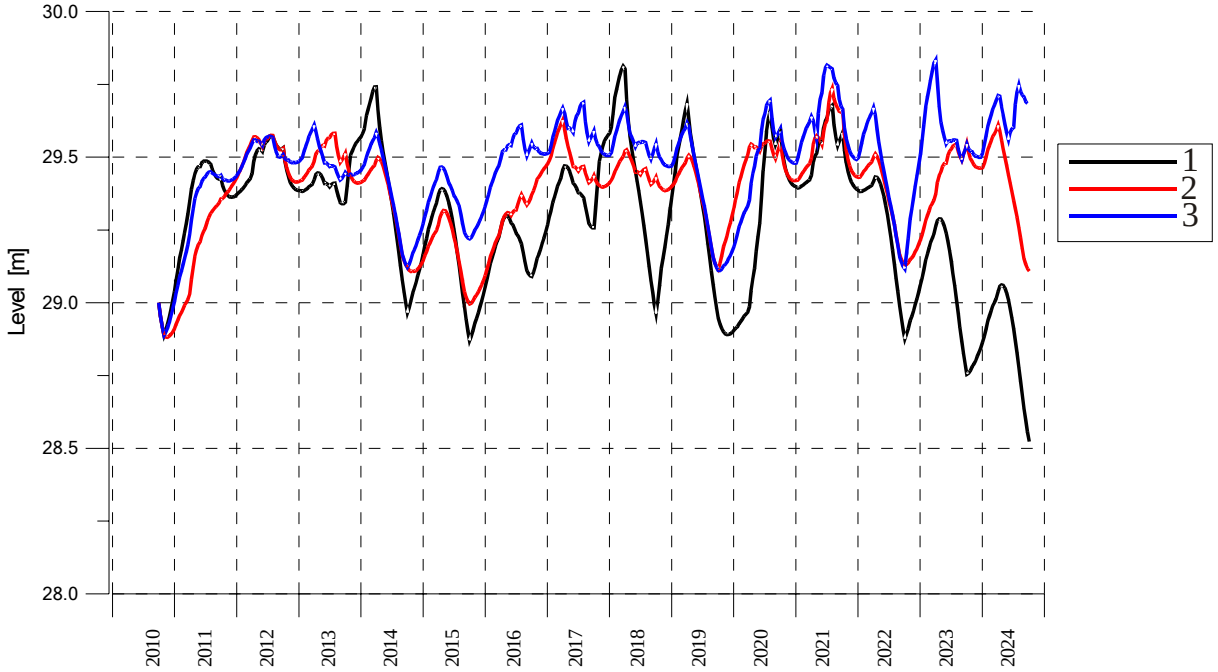

Fig. 28.44 The level dynamics with initial mark 29 m.
Scenarios with minimum inflow. 1 – $\mathbf{A}_{min}$; 2 – $\mathbf{B}_{min}$; 3 – $\mathbf{C}_{min}$

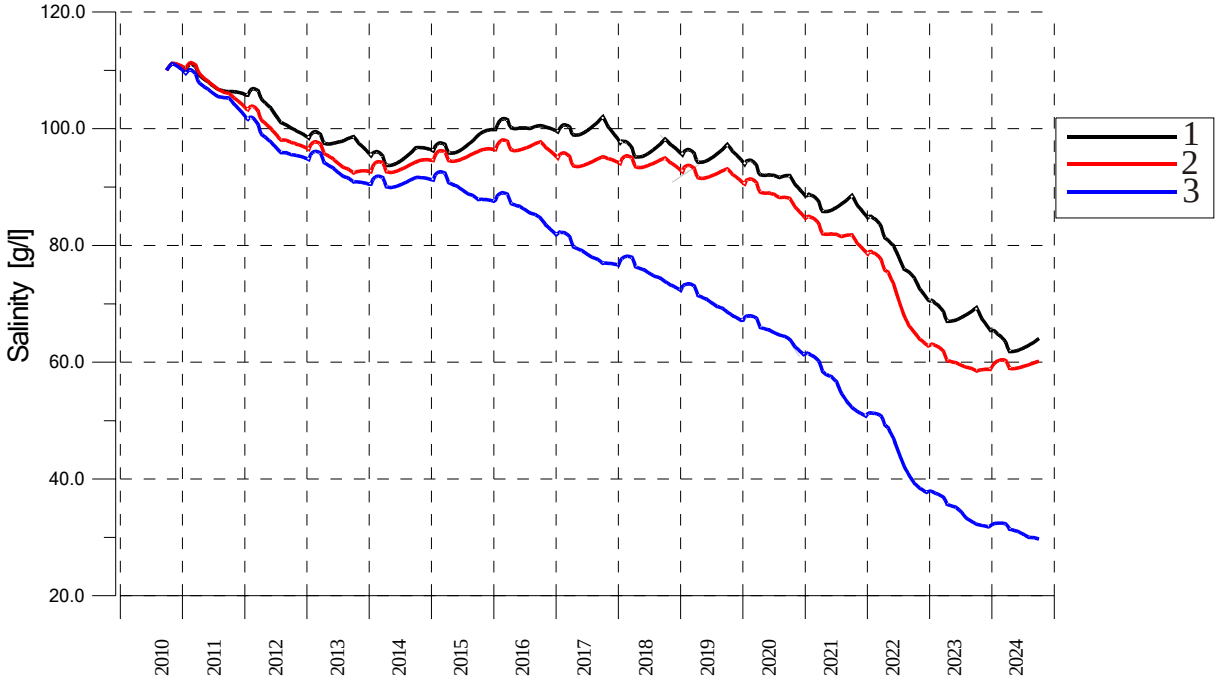

Fig. 28.45 The mean salinity dynamics with initial mark 29 m.
Scenarios with maximum inflow. 1 – $\mathbf{A}_{max}$; 2 – $\mathbf{B}_{max}$; 3 – $\mathbf{C}_{max}$

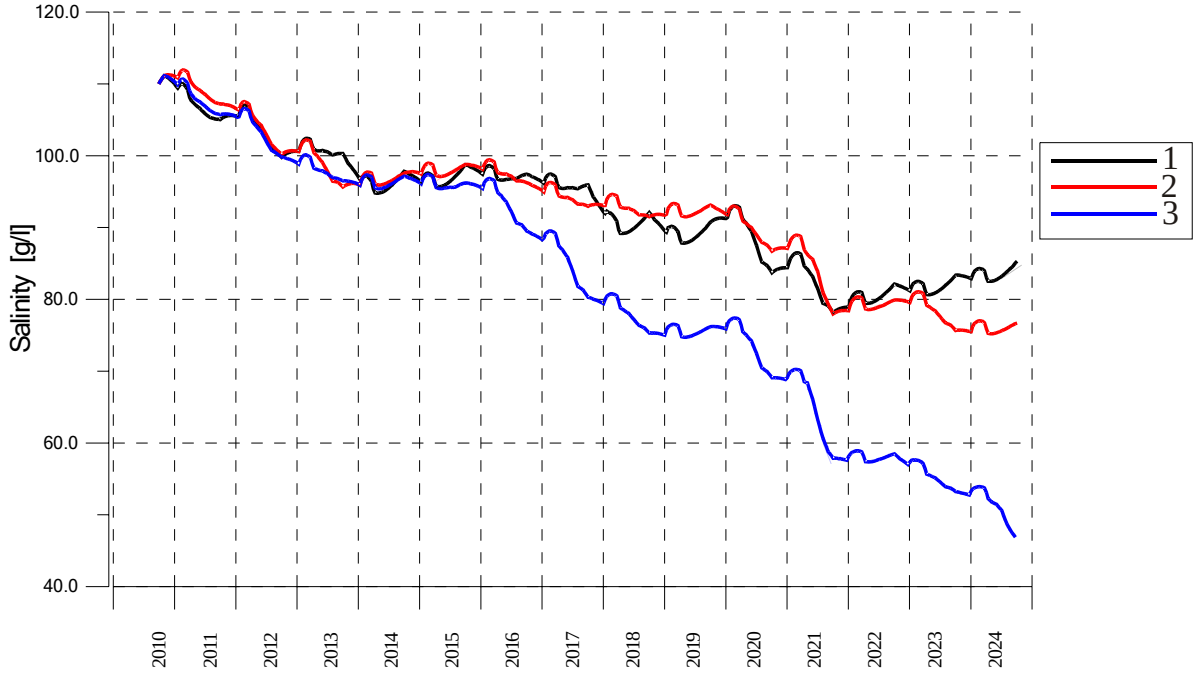

Fig. 28.46 The mean salinity dynamics with initial mark 29 m.
Scenarios with minimum inflow. 1 – $\mathbf{A}_{min}$; 2 – $\mathbf{B}_{min}$; 3 – $\mathbf{C}_{min}$

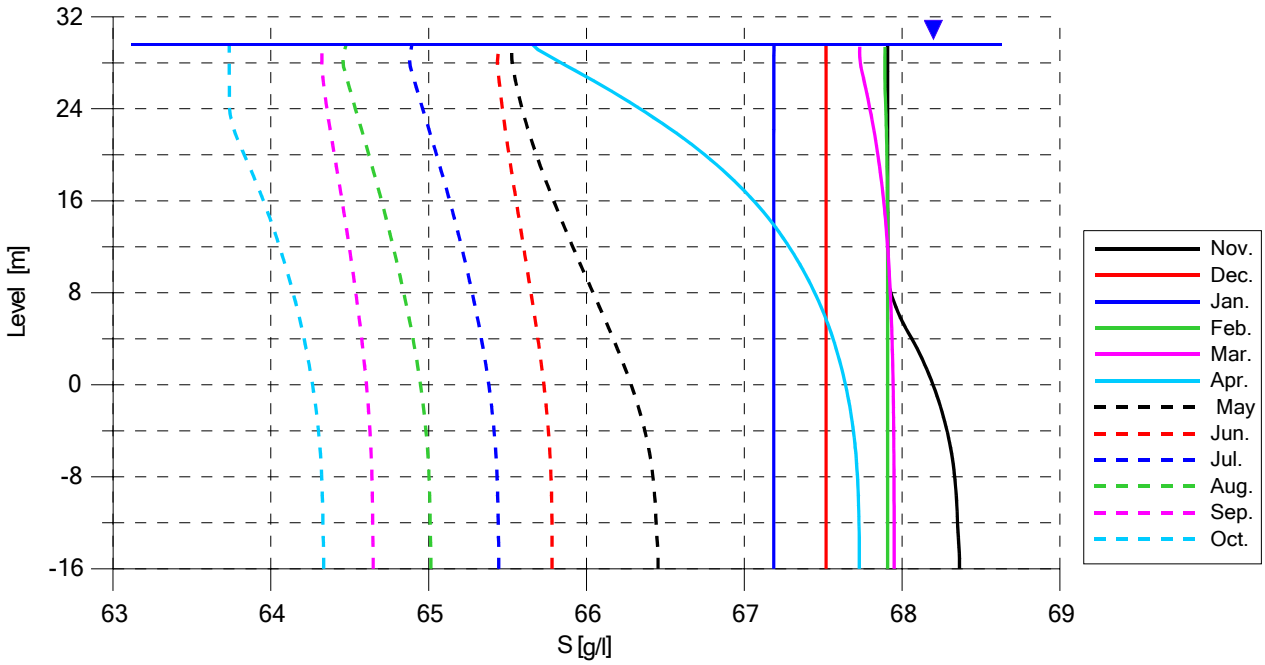

Fig. 28.47 Vertical distributions of salinity in 2019-2020 calculation hydrologic year

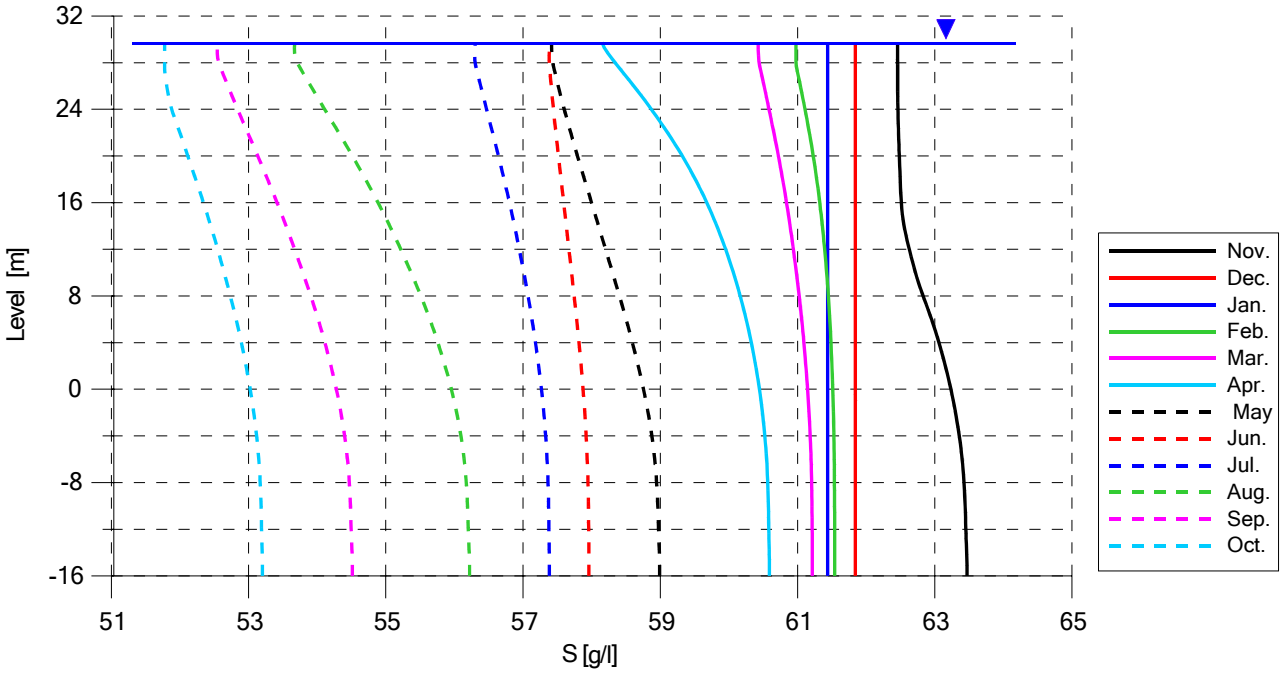

Fig. 28.48 Vertical distributions of salinity in 2020-2021 calculation hydrologic year

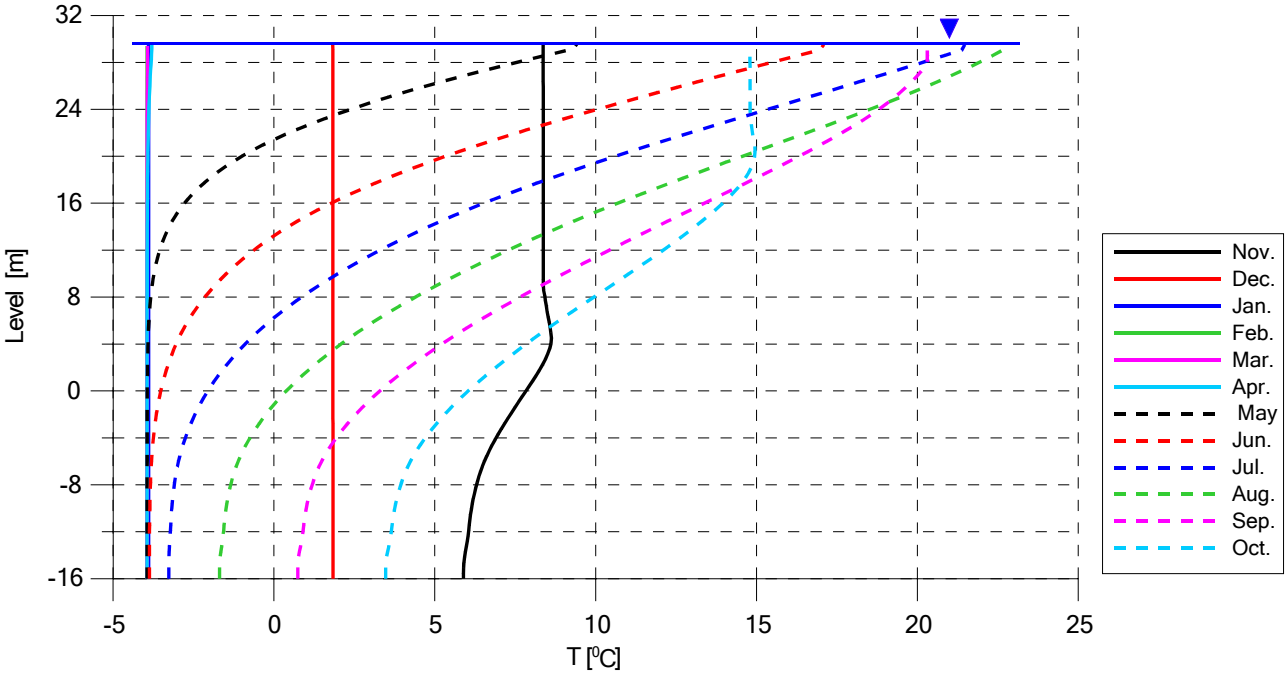

Fig. 28.49 Vertical distributions of temperature in 2019-2020 calculation hydrologic year

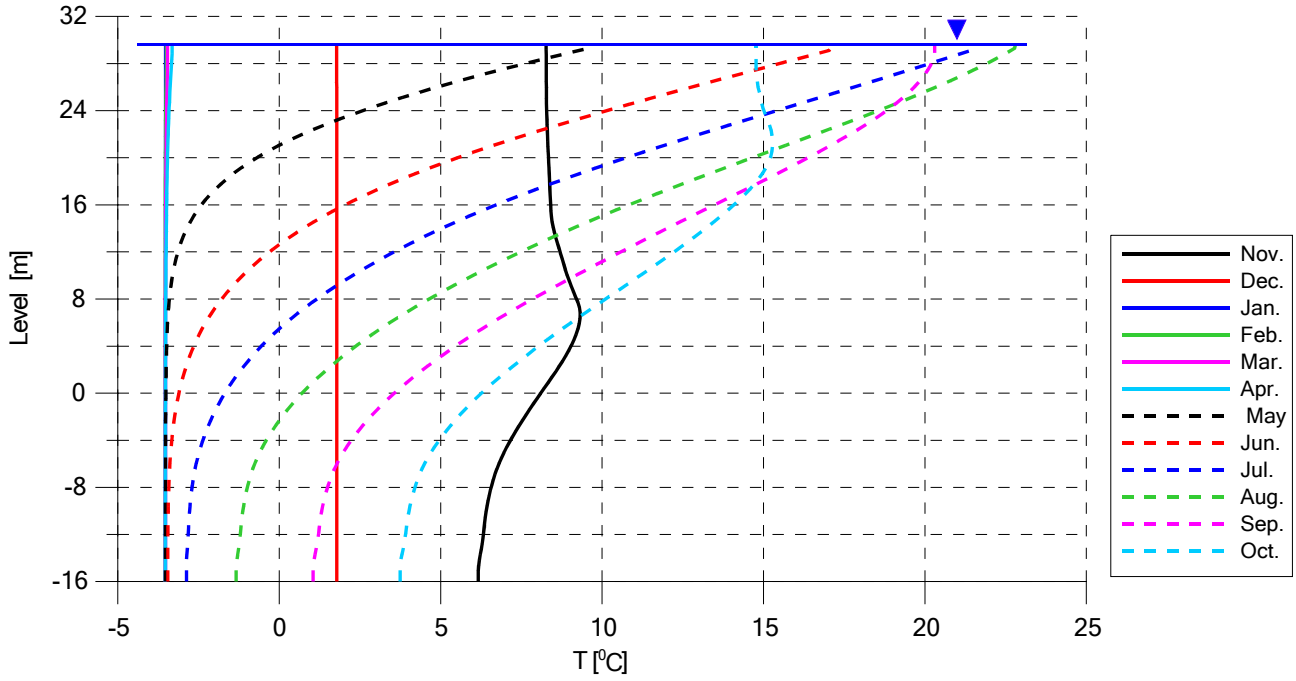

Fig. 28.50 Vertical distributions of temperature in 2020-2021 calculation hydrologic year

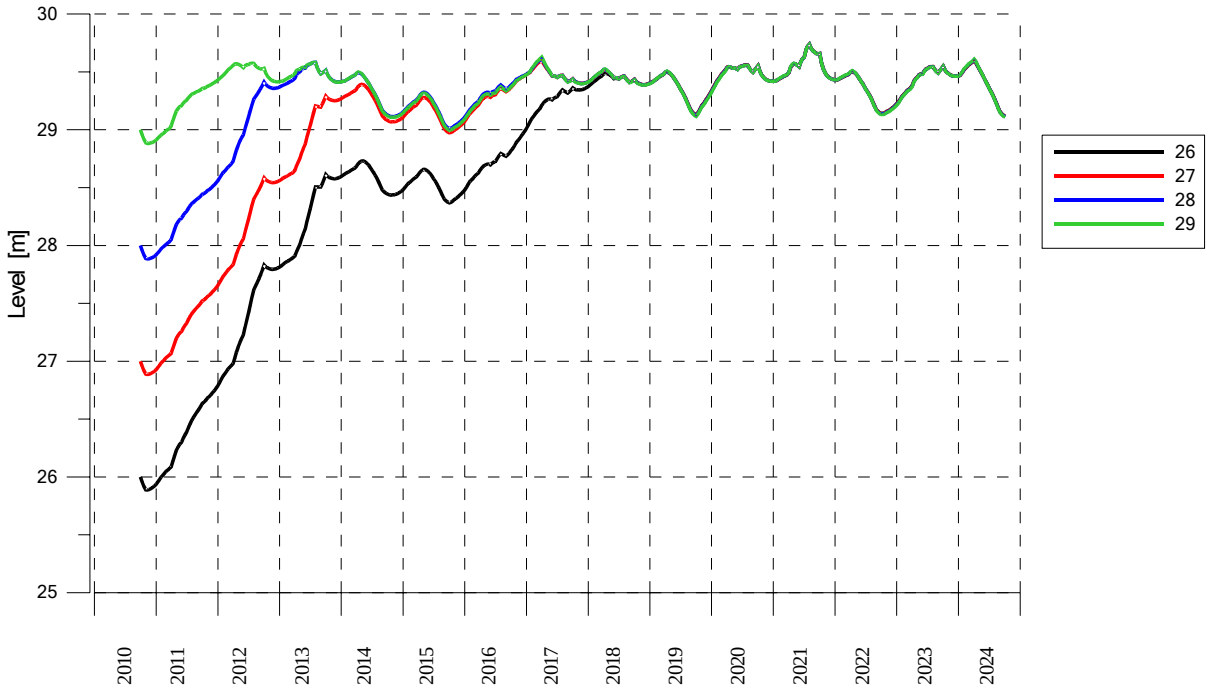

Fig. 28.51 The level dynamics with scenario $\mathbf{B_{min}}$ and initial marks 26, 27, 28 and 29 m.

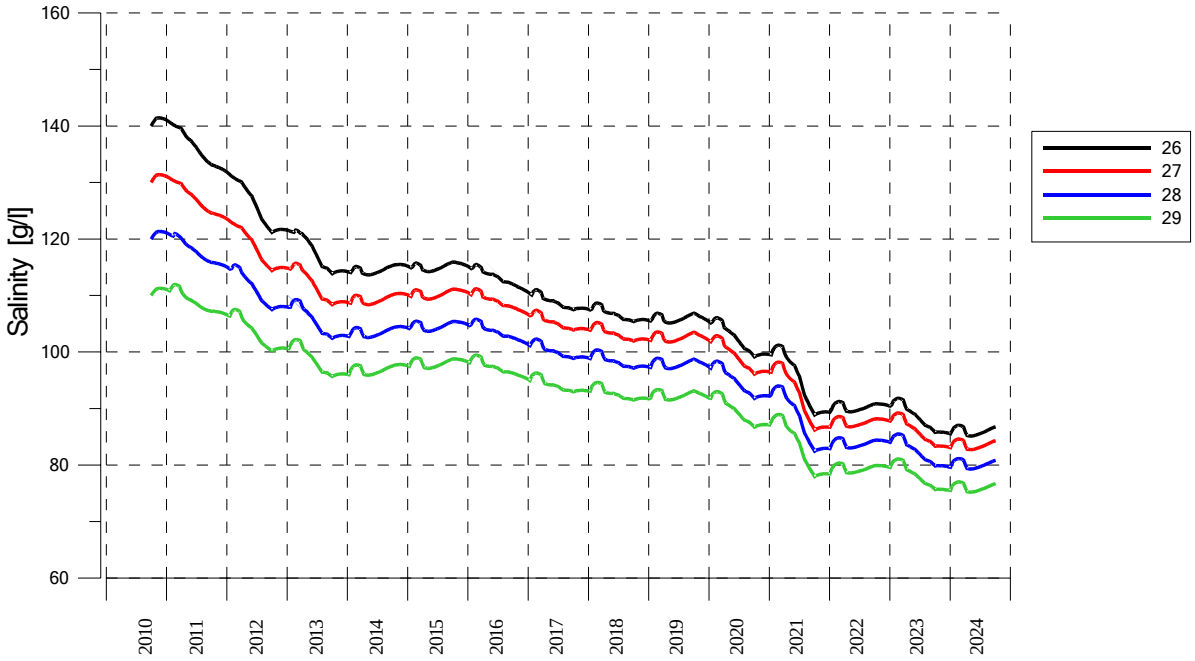

Fig. 28.52 The mean salinity dynamics with scenario $\mathbf{B_{min}}$ and initial marks 26, 27, 28 and 29 m.

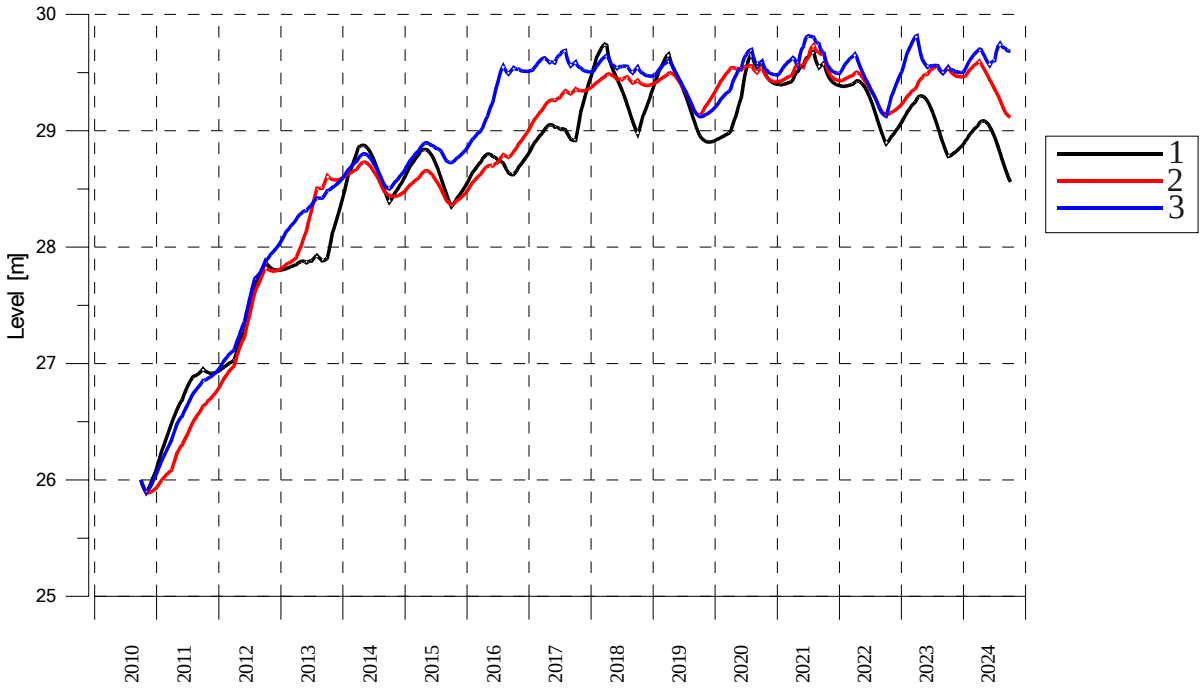

Fig. 28.53 The level dynamics with initial mark 26 m in 3 scenarios.

1 – $\mathbf{A_{min}}$; 2 – $\mathbf{B_{min}}$; 3 – $\mathbf{C_{min}}$

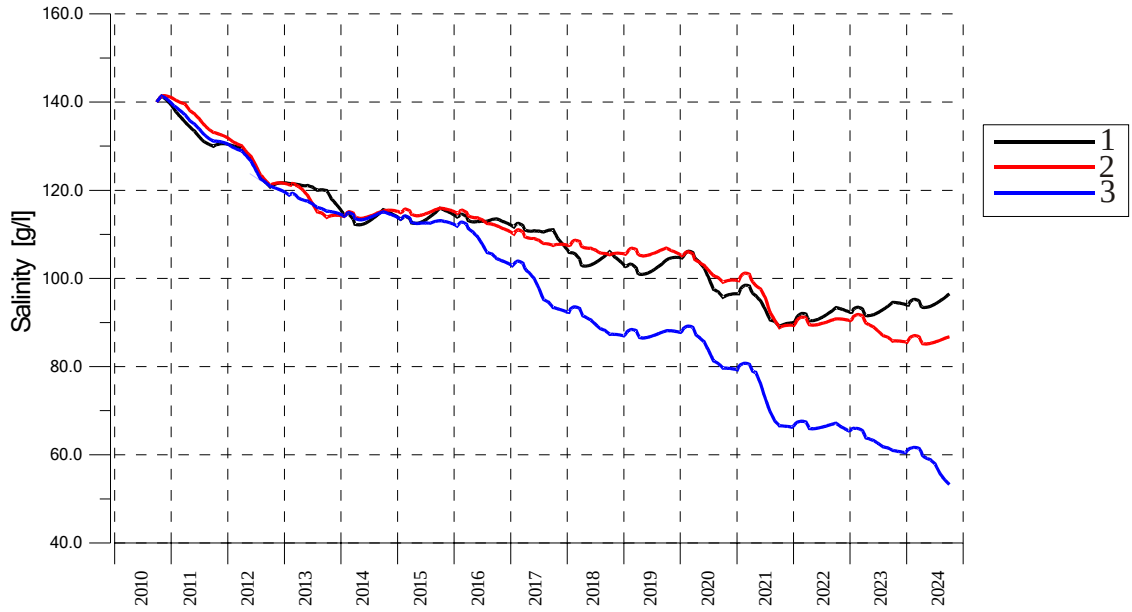

Fig. 28.54 The mean salinity dynamics with initial mark 26 m in 3 scenarios.

1 – $\mathbf{A}_{min}$; 2 – $\mathbf{B}_{min}$; 3 – $\mathbf{C}_{min}$

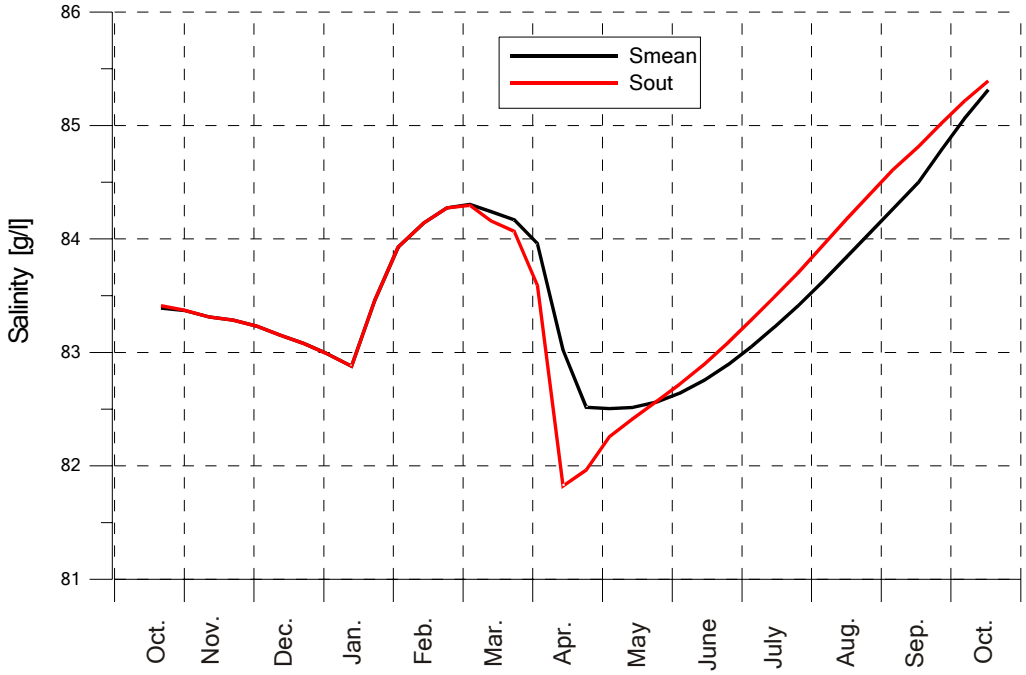

Fig. 28.55 The annual dynamics of mean salinity and salinity of effluent water at the end of calculation period in scenario $\mathbf{A}_{min}$ with initial mark 29 m.

28.4 Analysis of the Results

For the forecasting of behavior of the level of western part of the Aral Sea depending of water inflow regime the date from [34] were used. The two water management variant were considered (section 28.1) with 6 scenarios of inflow (Table 28.10). The bulk model and one-dimensional vertical model (1-D) were used for the calculations.

The bulk model was used for the calculations with initial level mark 29 m for the two water management variants (12 scenarios) and also for the calculations in the case of absence of inflow. The 1-D model was used for the same calculation (except the absence of inflow) and also for some additional scenarios with the second variant with the different initial marks. The 1-D model considered the overflow from western to the eastern part of the sea as well as the possibility of selective withdrawal.

28.4.1 The level dynamics

The calculations using the two models showed that with ***the first water management variant*** the relative stabilization of the level of western part of the sea is to be achieved in scenarios "saving existent tendencies" and optimistic scenario. The scenario "national vision" didn't lead to stabilization almost in all variants of inflow. In the case of absence of inflow the level decreased almost uniformly correct to annual variations and to the end of calculation period it was about 15.77 m.
The values of level at the end of calculation period are presented in Table 28.13. The differences between scenarios wit minimum and maximum inflow obtained by the bulk model are less than those obtained by 1-D model. So the 1-D model gives more adequate description of hydrophysical processes in water body.

The second water management variant is more favourable in respect of the level stabilization. The calculations using 1-D model considering the overflow to the eastern part of the sea showed that with the initial marks from 26 to 29 m the level stabilization near the mark 29.5 m was observed almost in all scenarios (Table 28.13).

Table 28.13 The level values at the end of calculation period, m

Scenario	A_{min}	A_{max}	B_{min}	B_{max}	C_{min}	C_{max}
First water management variant						
0-D model	23.1	23.4	24.5	24.6	25.9	27.0
1-D model	26.2	27.2	27.4	28.5	28.9	30.0
Second water management variant						
1-D model	28.6	28.9	29.1	29.1	29.7	29.5

28.4.2 Salt regime

The change of the sea water salinity is conditioned by two factors: the effective evaporation and the inflow of more fresh water of tributary. The calculations using 0-D model showed that without inflow the mean salinity of the sea waters to the end of 15-years period would be equal to 279.88 g/l.
The inflow of fresh water is the main factor affecting the water salinity. The salinity dynamics corresponds entirely to the level dynamics: when the level increases the salinity decreases.
The mean salinity at the end of calculation period with initial level 29 m are presented in Table 28.14. In the second variant the significant desalinization was observed in all scenarios of inflow, the dynamics of salinity depending on the initial conditions.

Table 28.14 The mean salinity values at the end of calculation period, g/l

Scenario	A_{min}	A_{max}	B_{min}	B_{max}	C_{min}	C_{max}
First water management variant						
0-D model	170.3	167.1	154.2	153.1	139.5	128.8
1-D model	131.0	121.0	120.8	114.0	110.5	102.4
Second water management variant						
1-D model	85.3	64.1	76.7	60.1	46.9	29.7

The calculation have shown that with the inflow of large enough volume of fresh water exceeding the volume of evaporation from the water area a washout of this part of the sea could be provided with the effluent of mineralized water into eastern part of the sea. The question is what time is needed for decreasing of salinity to one or another value. The time of decreasing of the sea water salinity to the level 60 and 30 g/l with the different scenarios of calculations for the second water management variant is given in Table 28.15.

Table 28.15 The time of decreasing of mean salinity to the level 60 and 30 g/l, years

Начальный уровень, м	Начальная соленость, г/л	Сценарий Стока	60 г/л	30 г/л
29	110	$\mathbf{A_{min}}$	–	–
		$\mathbf{A_{max}}$	–	–
		$\mathbf{B_{min}}$	–	–
		$\mathbf{B_{max}}$	12-13	–
		$\mathbf{C_{min}}$	11	–
		$\mathbf{C_{max}}$	10-11	14
28	120	$\mathbf{B_{min}}$	–	–
27	130	$\mathbf{B_{min}}$	–	–
26	140	$\mathbf{A_{min}}$	–	–
		$\mathbf{B_{min}}$	–	–
		$\mathbf{C_{min}}$	13-14	–

According to the data the value 30 g/l was reached at the end of the calculation period only with the initial mark 29 m in scenario $\mathbf{C_{max}}$, and the value 60 g/l was reached only in four scenarios. So the conclusion may be maid that the rate of rehabilitation of the Aral Sea essentially depends on the quickness of taking appropriate measures for water delivery into water body.
The annual dynamics of the vertical distributions of the salinity obtained by 1-D model have shown that in the first water management variant the homogeneous distribution was observed from the beginning of November to the beginning of April, the value of salinity gradually decreasing. In the second water management variant the period of total mixing was shorter a little; it was formed in the middle of November. From the beginning of April and to the end of July there existed the layer of more fresh water in near surface zone. The time of it existence was about 3 months. Then in the first water management variant the distribution with higher values of salinity near the surface was settled due to decreasing of inflow discharges and continuing of evaporation processes. In the second water management variant the surface water salinity is always lower than in more deep layers. The maxim range of salinity vertical changes is about 2 g/l.

28.4.3 Thermal and ice regimes

The main factors effecting on the forming of thermal regime of water body are meteorological data and since the all scenarios used the same data the character of the water temperature behaviour was approximately the same. There were some differences between the values of mean temperature obtained by 0-D and 1-D models. The cause of this is the differences of heat flow through free surface calculated by the two models. The heat flow depends on the water surface temperature and its values were distinctly different in the results of calculations by the two models because in the bulk model the water surface temperature is equal to the mean temperature. The temperature differences for one's turn led to the differences in level and salt regime. The main attention has to be paid to the calculations using 1-D model since it more adequately describes the hydrophysical processes.
The processes of ice cover forming depend on the surface water temperature and salinity. According to this the ice forming dynamics were different in the calculations by two models. Thus the using of 1-D model have shown that in the optimistic scenario and in the scenario "saving existent tendencies" the ice cover was observed every year of calculation period, and in the calculations by 0-D model for the first water management variant the ice cover was observed only in the first year.
The vertical temperature distributions are of much importance for ecological state of water body. On the base of calculations for the first water management variant using 1-D model it was revealed that from November to March (i. e. near 5 months of a year) in the water body the state of homothermy with the temperature from +2°C (in November–the beginning of December) to -7°C (in the end of February–the beginning of March) was observed. In the beginning of April the heating of the upper layers of the water body already began, and the near bottom layers still had the temperature about -7°C. The character of vertical temperature distributions in the second water management variant was similar but the period of homothermy began only in the middle of November and the minimum temperature in that period was about -5°C.
In May–August the heating of the upper water layers continued and at the beginning of August the surface water temperature was about 24°C. The more warm surface water penetrated in near bottom layers due to mixing processes but there the heating processes ran slower. At the beginning of

September the near bottom water had yet the temperature -1°C and the difference with the surface water temperature was about 21°C.
In August the gradual cooling of the near surface water began and the near bottom layer still warmed due to mixing processes. In the beginning of November the strongly marked thermocline was observed but it disappeared to the second decade of November. At that time the near bottom water temperature reached its maximum value (about +7°C). In the first water management variant the range of the near bottom temperature changes was approximately 14°C (from -7°C to +7°C) and that of surface temperature was near 30°C (from -7°C to +23°C). In the second water management variant the minimum temperature is greater a little (-5°C).

28.4.4 Density and hydrostatic stability

Density stratification of the water body depends on the water temperature and salinity and the vertical distribution of salinity in the case of high mineralized Aral Sea may prove to be the decisive factor. In the period of fresh water inflow the density of surface water always was lower then in deeper layers since the tributary is settled at the near surface zone. In the first water management variant in August and September when the discharges f the tributary was low the surface water salinity was sometimes higher than in deeper layers (on the value about 0.1 g/l). But in the same time in the near surface zone the significant positive gradients of the temperature were observed and it prevented the development of hydrostatic instability. So the density stratification of the water column was always stable or neutrally stable (in the periods of total mixing). This character of density stratification was proved by the calculation using 1-D model for the both water management variants as well as in scenario for 1.5-year period.

29. Modeling of Hydrophysical Processes in the Aral Sea with the Use of Three-Dimensional Model

29.1 Three-Dimensional Model of Hydrophysical Processes in the Aral Sea

The Aral Sea circulation model constructed in the Laboratory of the Mathematical Modeling of the Hydrosphere of the Institute of the Computational Mathematics & Mathematical Geophysics, SD RAS, was adopted from the basic circulation model for the investigation in the ocean and in the marginal seas [50, 51].

The general features of such model are as follows:

- A mathematical model is based on the complete “primitive” nonlinear equations of the thermo-hydrodynamics of the ocean
- Temperature and salinity distributions are calculated
- A model provides a possibility to include the calculation of pollutants
- The interaction with the atmosphere is realized via the upper mixed layer with a possibility to include the ice formation
- A model provides a possibility to include the inflows and outflows from the basin
- A model is based on a combination of the finite element and splitting methods
- The triangulated quasi-regular B-grid are used in the models
- There exist two versions of our model which differ by the method of the vertical levels distribution: sigma-coordinate model and z-coordinate model.

The governing equations of the model are as follows:

$$\frac{du}{dt} - (l - mu\cos\theta)v = -\frac{m}{\rho_0}\frac{\partial p}{\partial \lambda} + \frac{\partial}{\partial z}\nu_u\frac{\partial u}{\partial z} + F^{\lambda},$$

$$\frac{dv}{dt} + (l - mu\cos\theta)u = -\frac{n}{\rho_0}\frac{\partial p}{\partial \theta} + \frac{\partial}{\partial z}\nu_u\frac{\partial v}{\partial z} + F^{\theta},$$

$$\frac{\partial p}{\partial z} = g\rho$$

$$m\left[\frac{\partial u}{\partial \lambda}+\frac{\partial}{\partial \theta}\left(v\frac{n}{m}\right)\right]+\frac{\partial w}{\partial z}=0$$

$$\begin{aligned}\frac{dT}{dt} &= \frac{\partial}{\partial z}\nu_T\frac{\partial T}{\partial z} + F^T,\\ \frac{dS}{dt} &= \frac{\partial}{\partial z}\nu_S\frac{\partial S}{\partial z} + F^S,\end{aligned}$$

$$\rho = f(T, S, p)$$

$$t=0:\quad u=u^0,\quad v=v^0,\quad T=T^0,\quad S=S^0$$

$$z=0:\quad \nu_u\frac{\partial u}{\partial z}=-\frac{\tau_\lambda}{\rho_0},\quad \nu_u\frac{\partial v}{\partial z}=-\frac{\tau_\theta}{\rho_0},\quad w=0,\quad \nu_T\frac{\partial T}{\partial z}=\frac{Q_T}{\rho_0 c_p},\quad \nu_S\frac{\partial S}{\partial z}=\frac{Q_S}{\rho_0}$$

$$z=H(\lambda,\theta):\quad \nu_u\frac{\partial u}{\partial N^H}=-C|\vec{V}|u,\quad \nu_u\frac{\partial v}{\partial N^H}=-C|\vec{V}|v,\quad w=mu\frac{\partial H}{\partial \lambda}+nv\frac{\partial H}{\partial \theta},$$
$$\frac{\partial T}{\partial N^H}=0,\quad \frac{\partial S}{\partial N^H}=0$$

$$\Gamma_S:\quad \frac{\partial(\vec{V}\cdot K)}{\partial N}=0,\quad \frac{\partial T}{\partial N}=0,\quad \frac{\partial S}{\partial N}=0,$$

where λ – the longitude,

$\theta=\frac{\pi}{2}-\varphi$, φ – the latitude,

z – is directed downward,

Γ_S – the solid lateral boundary contour,

$H(\lambda,\theta)$ – the bottom topography,

$m=(a\sin\theta)^{-1}$, $n=a^{-1}$ – the spherical coordinates coefficients (a – the Earth's radius),

$l=-2\omega\cos\theta$ – the Coriolis parameter (ω – the Earth's rotation frequency).

$\vec{V}=(u, v)$ – the horizontal velocity vector,

u, v, w – the velocity components along λ, θ, z coordinate axes,

T – the temperature,

S – the salinity,

ρ_0 – the standard density,

ρ – *in situ* density,

p – the pressure,

f – the state function,

g – the acceleration of gravity,

C – the drag coefficient,

τ_λ, τ_θ – the wind stress components,

ν_u – the vertical viscosity coefficient,

ν_T, ν_S – the vertical diffusion coefficients for temperature and salinity,

N, K – the normal and tangential vectors to Γ contour,

N^H – the normal vector to the bottom surface

$$\frac{d}{dt} = \frac{\partial}{\partial t} + mu\frac{\partial}{\partial \lambda} + nv\frac{\partial}{\partial \theta} + w\frac{\partial}{\partial z}$$

$$F^T = \mu_T \Delta T, \quad F^S = \mu_S \Delta S$$

$$\Delta = m^2 \frac{\partial^2}{\partial \lambda^2} + m\frac{\partial}{\partial \theta}\frac{n^2}{m}\frac{\partial}{\partial \theta}$$

$$F^\lambda = \mu_u \left(\Delta u + \frac{2\cos\theta}{a^2 \sin^2\theta}\frac{\partial v}{\partial \lambda} - \frac{\cos 2\theta}{a^2 \sin^2\theta} u \right)$$

$$F^\theta = \mu_u \left(\Delta v - \frac{2\cos\theta}{a^2 \sin^2\theta}\frac{\partial u}{\partial \lambda} - \frac{\cos 2\theta}{a^2 \sin^2\theta} v \right)$$

where μ_u, μ_T, μ_S – are the horizontal viscosity and the diffusion coefficients.

Q_T *and* Q_S are the heat and the salt fluxes respectively.

At the distributed inflow boundaries Γ_I V, T, S and fresh water inflow are prescribed.

The heat exchange through the water body free surface is the main factor that determines the temperature of water in the Aral Sea. It is calculated as sum of the following characteristics:

- Short-wave solar radiation;
- Long-wave atmospheric radiation;
- Water surface radiation;
- Heat loss due to evaporation;
- Conductive heat exchange
- Heat transfer by ice formation and melting.

The following values are required for the heat balance simulation: meteorological data (air temperature, air humidity, wind speed, atmospheric pressure, cloudiness) and the incoming solar radiation (above the clouds).

29.2 Mixed-layer Model

There is a “Richardson number” criterion of the mixed layer treatment, which was used in the 3D Aral Sea model:

The criterion for mixing the layers is the inequality, $Ri \leq Rcr$ where Ri is a Richardson number defined as $Ri = \dfrac{g \partial T / \partial z}{c_p \theta \mid \partial V / \partial z \mid^2}$, and Rcr is its critical value.

29.3 Sea-ice Model

When simulating the heat balance, the possibility of ice formation will be taken into account. In this case, the simulation of ice cover formation, destruction, dynamics of a change of its thickness and heat exchange through ice cover will be performed.

In the dynamics of the sea ice model, it is assumed that the sea ice is treated as a two-dimensional continuum, which is characterized by such a variable as ice thickness h. The equation for this prognostic variable can be presented in the following form:

$$\frac{d}{dt} h = F_h + \Phi_h$$

Here F_h is the diffusion term; Φ_h is the term introducing the forces arising from the air and water stresses and the influence of the internal stresses. This term represents the ice rheology and realizes in elastic-viscous-plastic version.

29.4 INPUT and OUTPUT of the model

The INPUT of the model is as follows:

- At the sea surface:
- The wind-stress calculated by wind at the 2 m height,
- Heat and salt (fresh water) fluxes;
- At the inflow lateral boundaries:
- A fresh water mass flux (a river inflow),
- Temperature and salinity are prescribed.

The initial state (The 1-st of January): Temperature, salinity uniform distribution over the whole basin.

The OUTPUT of the model:

- A 3D velocity field,
- Temperature and salinity fields in the seasonal cycle for 18 months.

29.5 Data Sources

- Meteorological data from CR2 team for the calculation of the heat and salt fluxes
- The Amu-Darya river runoff from CR2 team;
- A monthly state climatic wind for the wind-stress calculation;
- The NCEP/NCAR reanalysis data for the period of the 1-st January, 1998 – the 30-th, June, 1999.

29.6 Designing the Experiments and Analysis of the Results

The Aral Sea domain for the calculation of the 3D currents, thermodynamics as well as spreading of fresh water is constructed on the basis of the bottom topography produced by CR2 team. In the first experiment, the level of 31 m was used as the initial value for the determination of the area of the Aral Sea basin in 1998. In the second numerical experiment with the Western part of the Aral Sea, the level of 26 m is set as the initial value for the determination of the basin area for the Western part. The bottom topography is presented (Fig. 29.1).

An essential difference in the bottom relief of the Western and the Eastern parts of the Aral Sea presents some difficulties in constructing the unique version of the vertical grid. The cross-section across the basin along the latitude is presented in Fig. 29.2 a. Because of this reason, in the initial numerical experiments, the sigma-coordinate model was used for the Eastern part of the Aral basin with a weakly changing depth with a maximal value of 14 m. For the Western part of the Sea where the maximal value of the depth is 44 m, z-coordinate multilevel model was more preferable. A schematic representation of two coordinate systems in the model is shown in Fig. 29.1 b, c.

The numerical model has a horizontal grid with 500*500 m resolution, which corresponds to an array of 335*421 nodes for the whole basin. For the Western part 86*195 nodes were used. For the Western part the non-uniform vertical z-grid is used (34 levels for a maximal depth). In the regions with a minimal depth of 2 m, 5 levels are included. The vertical grid has the following levels:

Z= 0, 0.5, 1, 1.5, 2, 3, 4, 5, 6, 7, 8, 9, 10, 11, 12, 13, 14, 15, 17, 19, 21, 23, 25, 27, 29, 31, 33, 35, 37, 39, 41, 43, 45 m.

29.6.1 First experiment. The whole basin of the Aral Sea, the river inflow into the Eastern part)

At the first stage of the numerical experiment the Aral Sea basin was taken as a whole configuration with a through flow between the Eastern and the Western parts. The Amu-Darya river runoff was directed to the Eastern part.
At the initial stage, the constant values of the temperature (0 C) and salinity (68 g/l) corresponding to the winter season of 1998 were set in the whole basin. The integration of the model was carried out during the period of one and a half year with the wind-stress produced from the NCEP/NCAR wind for the period January 1998 - July 1999. The Amu-Darya runoff was taken from the estimates of the CR2 team report. The ice sea model includes only the thermodynamic part without dynamics, rheology and drift of ice. The time step was one hour. On each time step, the following 3D hydrophysical fields were calculated: velocity, temperature, and salinity.
The results of the numerical experiment allow as obtaining some specific features of the Aral Sea circulation, thermodynamics and fresh water spreading into the Eastern basin.

Circulation
The circulation in the Aral Sea basin is highly varying, and although there are no strongly dominating pictures of the main circulation, it is possible to single out some specific features. First, the circulation is

very sensitive to the wind and is mainly driven by the wind, except a short period of the ice, cover. The Eastern part is shallow and has the fastest feedback to a wind change. A wide area of the Eastern part allows a well-manifested cyclonic (Fig. 29.2, Fig. 29.3) or anticyclonic (Fig. 29.6) circulation to be formed. The transition period between them is characterized by the dipole circulation (Fig. 29.4, Fig. 29.5). The Western basin is narrower and deeper. So, the circulation consists of a larger number of local gyres, but a feedback to the wind change is slower than that of the Eastern one. The circulation variations during the seasons of the integration period may roughly be described in the following way. In the summer of the integration period in the Eastern part, there was a cyclonic circulation. In Fig. 29.2, Fig. 29.3, the integral stream function as well as the velocity field at a depth of 2 m are presented. The velocity value reaches 30 cm/s. The circulation in the Western basin is cyclonic in the South and anticyclonic in the North. There also exist some local circulations caused by the bottom topography and the basin configuration. In autumn, the circulation in the Eastern basin becomes anticyclonic via the dipole circulation, as is presented in Fig. 29.4 - Fig. 29.6. During the winter period, when the ice cover blocks the wind, this circulation is weakening (Fig. 29.7) until the ice cover disappears. In spring, the reconstruction of the circulation leads to the chaotic enough circulation certain periods, becoming sufficiently stable by May (Fig. 29.8, Fig. 29.9).

Thermodynamics
The seasonal variations of the Aral Sea are influenced by the seasonal cycle, but the processes of the seasonal variations in the Western and the Eastern parts are different. In the Eastern part, the processes of heating and cooling on the surface and mixing by wind determine the temperature. This brings about a homogeneous distribution of the temperature in the Eastern part within the range from 27 C to 0 C. In contrast to this, the result of the calculations shows that the thermal conditions of the Western part of the Aral Sea, determined by the seasonal cycle are divided into two main states: the summer stratification and the winter homothermy. The summer distribution has the stratification in the temperature of about 20 degrees, with a strong thermocline, well manifested in Fig. 29.11. The horizontal distribution is characterized by the lower temperature values in the western deep part and higher values in the eastern part (Fig. 29.10). The cooling in the autumn and the winter seasons results in the density convection and in the homothermy. In Fig. 29.12, one can see the convection in the Western part of the basin. The upper layer is completely mixed, whereas a more saline and denser water in the deeper layer prevents the mixing. Nevertheless, finally, the vertical temperature distribution becomes homogenous.

Salinity distribution and fresh water propagation
The salinity conditions during the integration period are defined by the Amu-Darya inflow during May-September, 1998. In this period, the river inflow was extremely high. The pictures present the propagation of the fresh water through the Eastern basin. In Fig. 29.13 the horizontal distribution of the salinity before fresh water inflow are presented. In Fig. 29.14 the horizontal pictures of refreshing are presented. One can see a well-manifested movement of the low saline water from South to North. A pool of the freshened water has a tendency to spread near the surface and mainly along the Eastern coast under the influence of the circulation (Fig. 29.14 – Fig. 29.16). The fresh water reaches a narrow straight between the Eastern and the Western parts of the basins and a certain part of the refreshed water propagates to the Northern part of the Western basin. After the fresh river inflow stops, the horizontal distribution becomes nearly uniform, but the salinity is lower than at the initial moment and reaches about 40g/l. Because of a very vide area of the evaporation from the surface of the Eastern part, after the moment when the high Amu-Darya river inflow stops, the salinity in the basin starts increasing again.

29.6.2 Second experiment (inflow to the Western basin)

At the second stage of the numerical experiments, the Aral Sea basin was taken in a configuration where only the Western part exists. The initial sea level was set as 26 m in Baltic system. The Amu-Darya river runoff was directed to the Western part with the value the inflow estimated by the CR2 team with maximal values in May-September.
At the initial stage, the constant values of temperature (-2.5 C) and salinity (140 g/l) corresponding to the winter season (January) were set in the whole basin. The integration of the model was carried out during the period of 18 months with the wind-stress produced from the climatic wind (see the description of the 0D and the 1D models). The sensitivity experiment for a few months, with the NCEP/NCAR reanalysis wind gives quite analogous picture of temperature, salinity and fresh water spreading. So, the climatic wind was chosen as a control one for the 0D, the 1D and the 3D models. On each step, the velocity field, the temperature and the salinity changes as a result of the river runoff were calculated.
The results of the numerical experiment show some specific features of the Western part of the Aral Sea circulation, thermodynamics and fresh water spreading.

Circulation
The circulation in the Western basin of the Aral Sea, as in the first numerical experiment, is sufficiently varying. Although there are no strongly dominating pictures of the main circulation, it is possible to single out some specific features. First, the circulation is sensitive to the wind and at the surface layers is mainly derived by the wind. However, in the summer season there exists a well-manifested thermohaline circulation. The circulation variations during the seasons of the integration period may roughly be described in the following way. The wind forcing in March allows of some kind of a cyclonic (Fig. 29.17) Ekman circulation to be formed at the surface layers. The northward stream is stronger in the eastern part of the basin, whereas the southward movement in the west is much weaker. The velocity values are weak enough and reach 20 cm/s. This is a consequence of the low values of the climatic winds used. The vertical water overturning in the deep part of the basin realizes the mass conservation law. In the summer season (July) of the integration period, there was no well-manifested cyclonic circulation (Fig. 29.18). In this picture the velocity field at a depth of 1 m is presented. There also exists the intensive enough current near the eastern coast, but at the same time, there arises the northward water movement in the central part of the basin. In the deep layers, there also exist some local circulations caused by the interaction of the thermohaline forcing with the bottom topography and the basin configuration. In autumn, the Ekman drift of water in the Western basin at the surface is directed to the North-East, what is presented in Fig. 29.19. During the winter season, the ice cover period is less than one month because of the high salinity, thus reducing the freezing point to the level -6.5 C and the wind blocking is not very essential. In May of the next year, the surface current is absolutely different from May of the previous year because of the strong changing of wind (Fig. 29.20).

Thermodynamics
The seasonal variations of the Western basin of the Aral Sea are influenced by the seasonal temperature cycle. The result of the calculations shows that the thermal conditions of the Western part, as was shown in the first experiment, are divided into two main states: winter homothermy and summer stratification. In Fig. 29.21, Fig. 29.22, the horizontal as well as the vertical sections temperature distributions in the basin are presented for the periods of March, May, July, October, January and May respectively. Starting from the homogenous temperature conditions in January and coming through the winter cooling in February, in March, the solar radiation begin to heat the upper layers. In May, the temperature gradient has the value about 10 C. The summer temperature distribution (July) has the value at the surface about 23 C and stratification in temperature about 10 degrees, with a strong thermocline, well manifested in Fig. 29.22, VII. The horizontal distribution is characterized by the lower temperature values in the Southern part, where the river inflow is coming, and by the higher values in the Northern part of this basin (Fig. 29.21, VII). The cooling in the winter season results in the density convection, which leads to the homothermy (Fig. 29.22, XIII). In Fig. 29.21, XIII, the distribution of the temperature at a depth 1 m in January is presented. One can see that the cooling is much faster in the shallow zones and slower in the deep, central part of the basin.

Salinity distribution and fresh water propagation
The computations started from the homogenous salinity distribution 140 g/l in January. This distribution is keeping until May, when the intensive river inflow began (Fig. 29.23, III, V). In this scenario the fresh water inflow was done into the Southern part of the Western basin. As one can see from Fig. 29.23, VIII-XIII the fresh water propagates from South to North until the intensive inflow stops. After that, in the winter season because of the density convection, the salinity distribution becomes homogenous with the value about 111 g/l what is less than the initial value of 27 g/l. The vertical fresh water propagation through the latitudinal cross-section is presented in Fig. 29.24, V-X. One can see that the lens of the refreshed water is moving near to the surface and is derived by the intensive current along the eastern coast. In Fig. 29.25 the vertical cross-sections along the longitude from the river inflow until the coast is presented. This picture confirm the previous sentences that the refreshed flow spread in the surface layer to North and after winter convection reaches the homogenous distribution in the vertical. The behavior of the salinity averaged over the basin is presented in the Fig. 29.26. One can see that the stabilization of the averaged salinity reaches near October after intensive fresh water inflow stopped.

29.7 Conclusions

The results of the simulations by the 3D model presented in this chapter can be treated only as the scenarios of the Aral Sea response to the possible water inflow and atmospheric forcing. In these two scenarios, the circulation model of the Aral Sea simulates the main features of the circulation, thermodynamics and salinity distributions in the Aral Sea. On the base of the results we can conclude that:

- The circulation near the surface is very sensitive to the wind and varies with the variation of the wind, especially in the Eastern part. In the Western part in summer season there exist the thermohaline circulation at the deep layers.
- The thermal conditions of the sea is homogeneous in the vertical in the Eastern part of the Aral Sea for each season. In contrast with this, the temperature distribution in the Western basin is characterized by two states: the existence of the strong enough thermocline in summer season and homotermy in the winter season due to the convection.
- The spreading of the fresh water in the Eastern and Western parts has as well the common as the different features. The common features are as follows: the refreshed water distribute from South to North near the surface driving by the main currents. The differences are that after the intensive water inflow stops (October), in the Eastern part the wind mixing leads to the uniform salinity distribution in the vertical very fast. In contrast with this, in the Western part of the Aral Sea the uniform salinity state reaches only during the winter season via thermal convection.

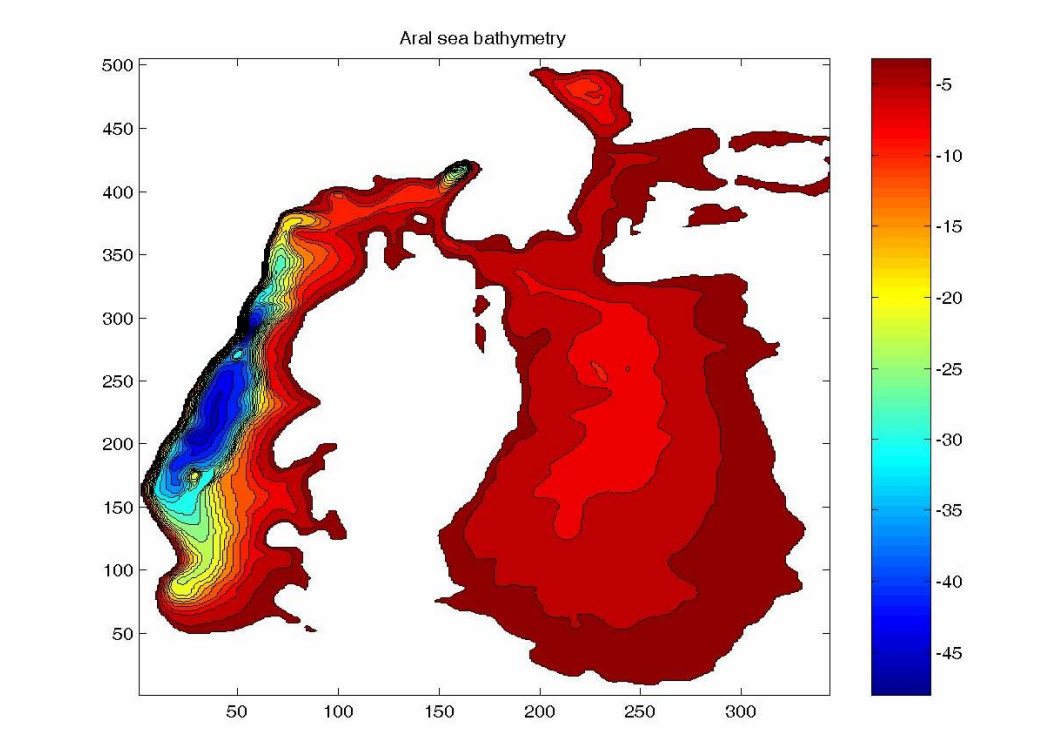

Fig. 29.1 Levels of height (Baltic system) for Aral Sea basin in meters.

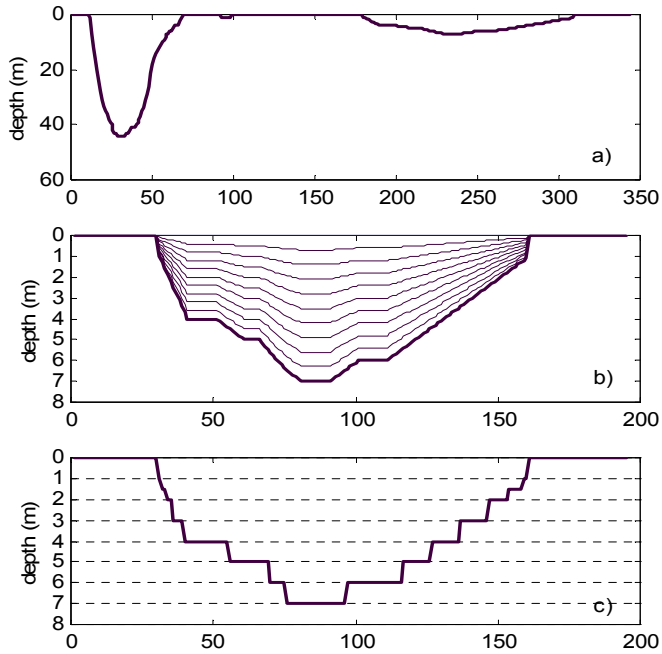

Fig. 29.2 a) Vertical cross-section of Aral Sea alone latitude;
b) Schematic representation of the sigma-coordinate grid;
c) Schematic representation of the z-grid.

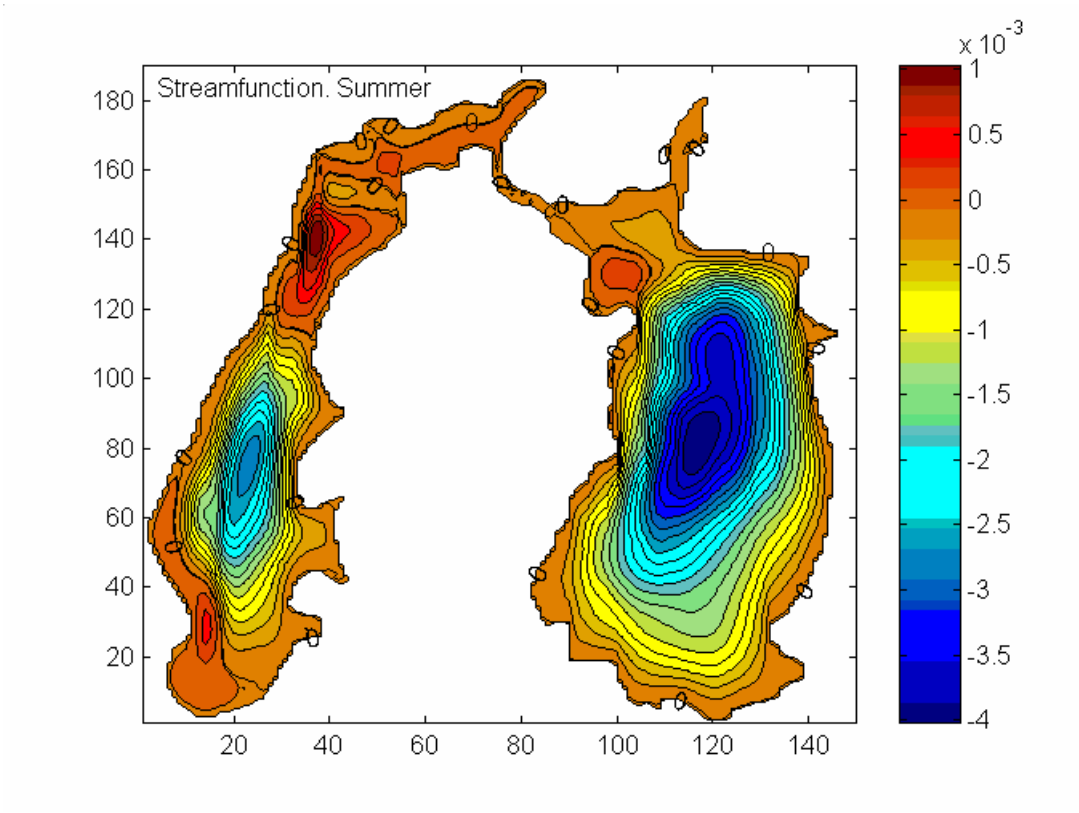

Fig. 29.3 Stream function. June.

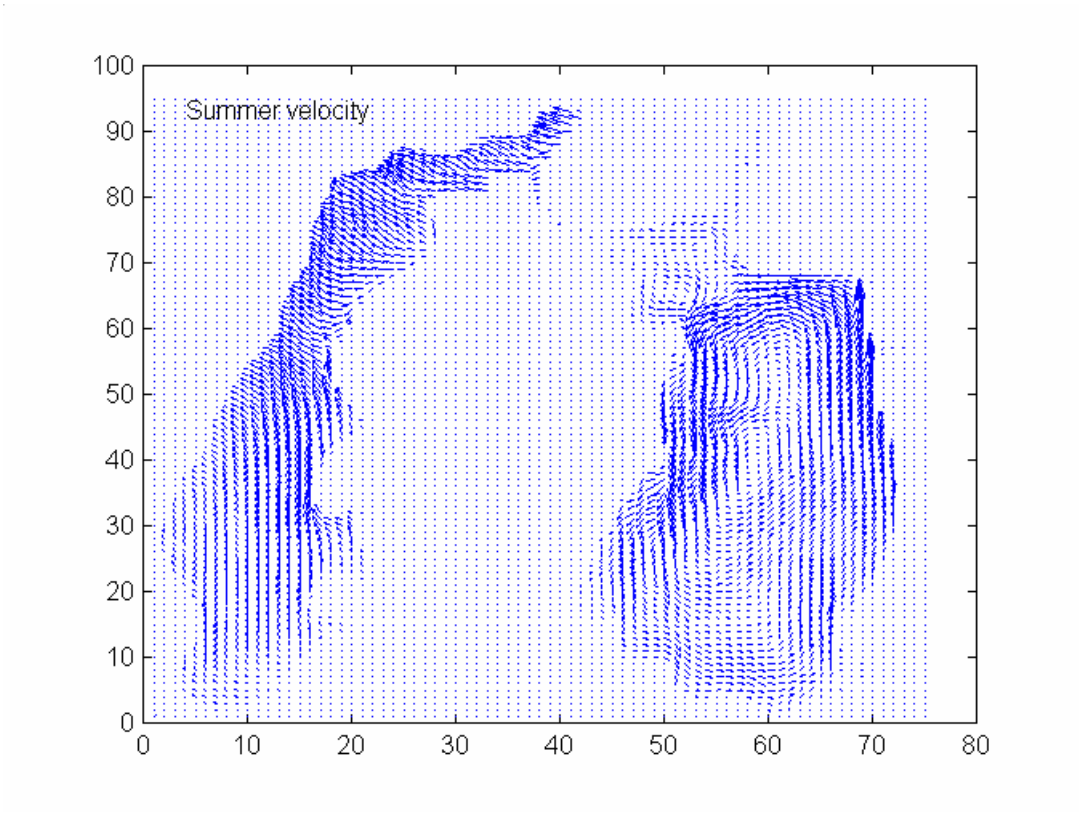

Fig. 29.4 Velocity field at depth 2 m. June.

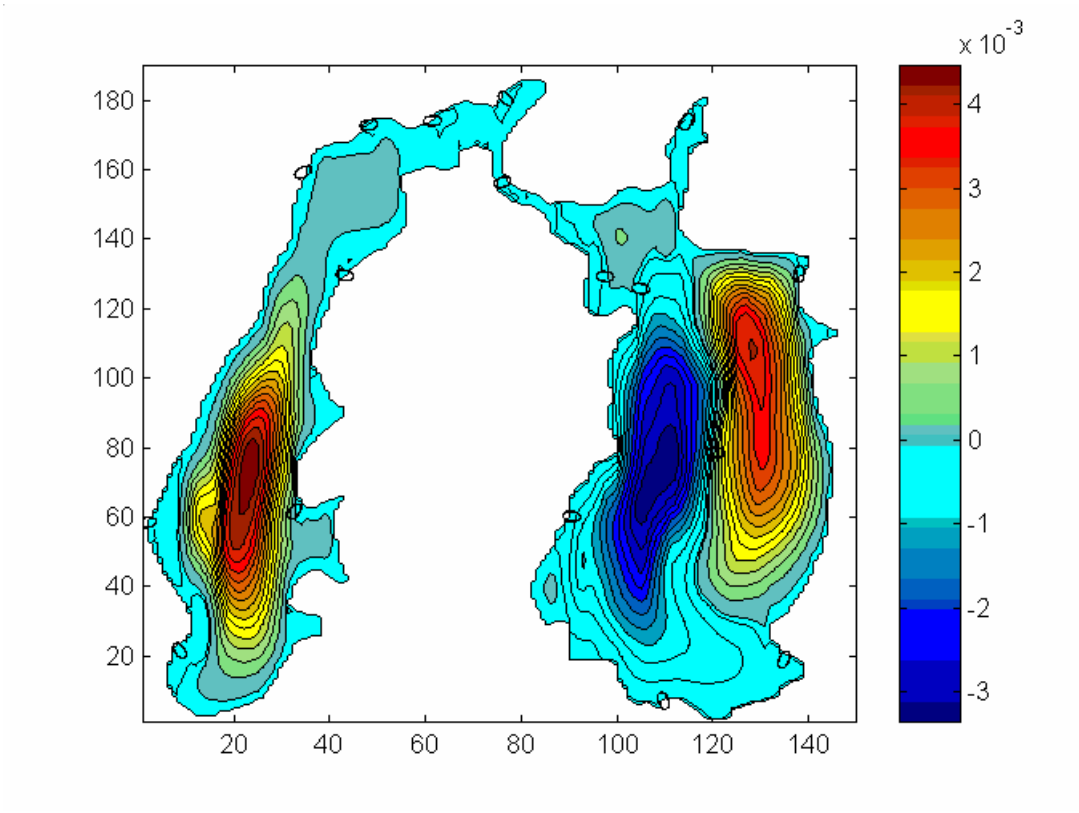

Fig. 29.5 Stream function. December.

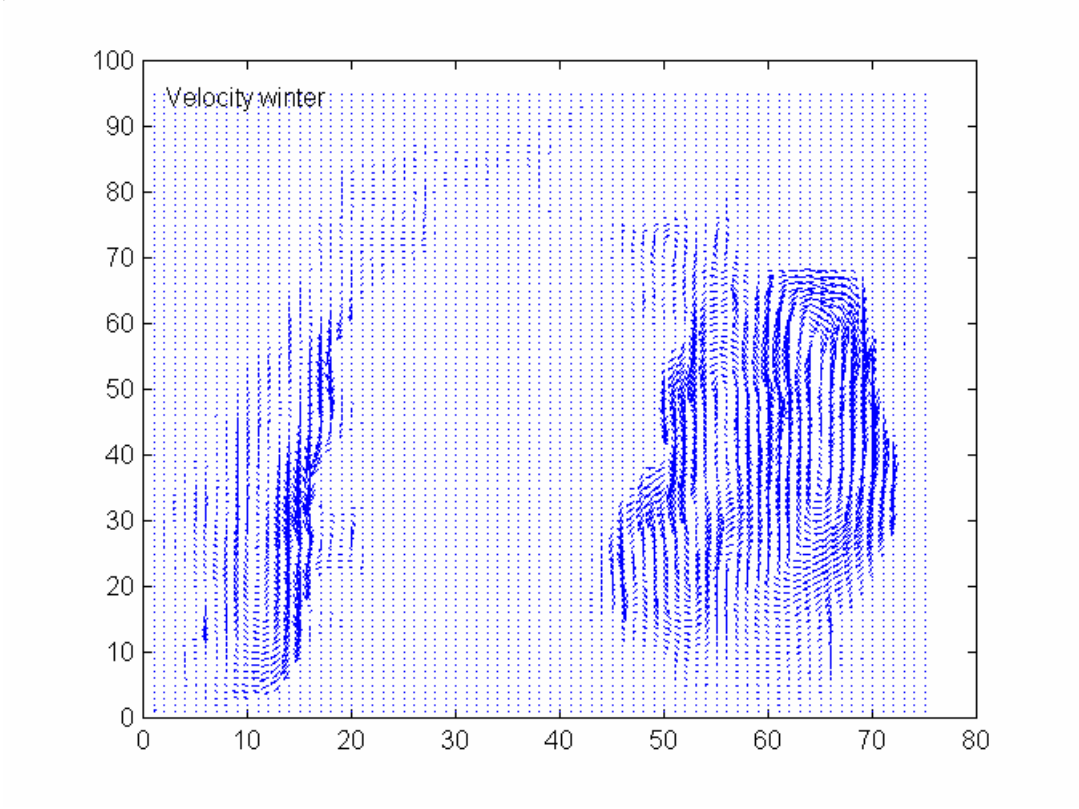

Fig. 29.6 Velocity field at depth 2 m. December.

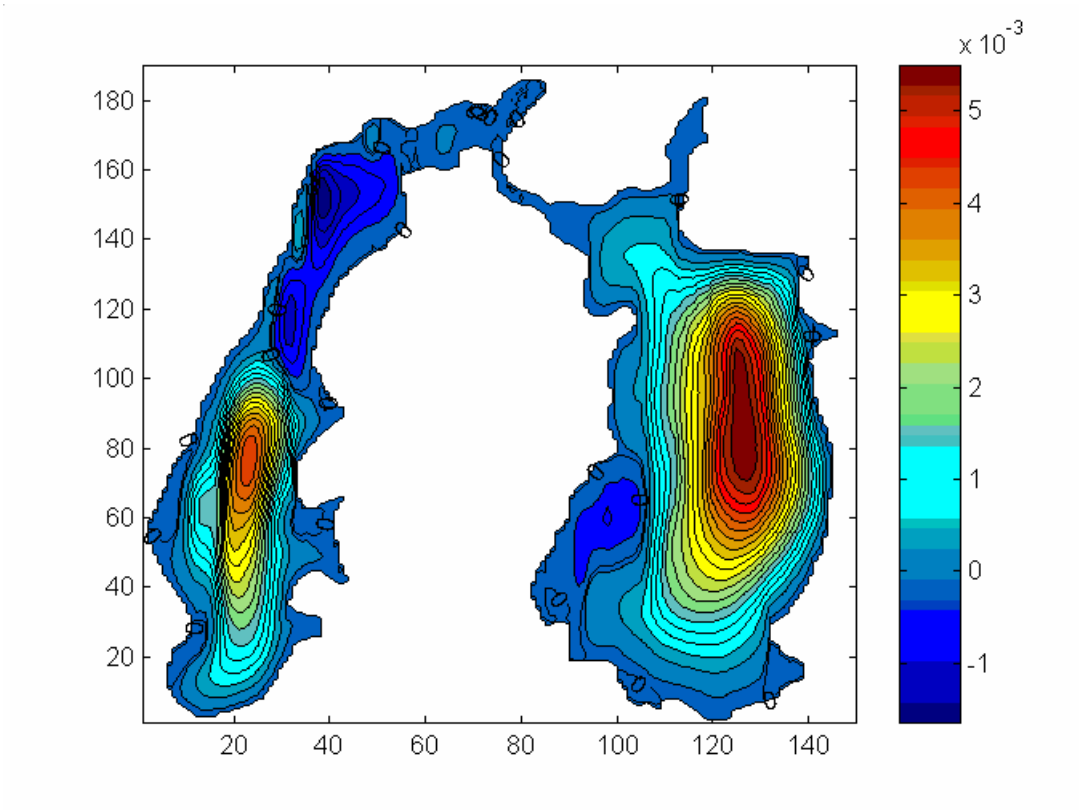

Fig. 29.7 Stream function. January.

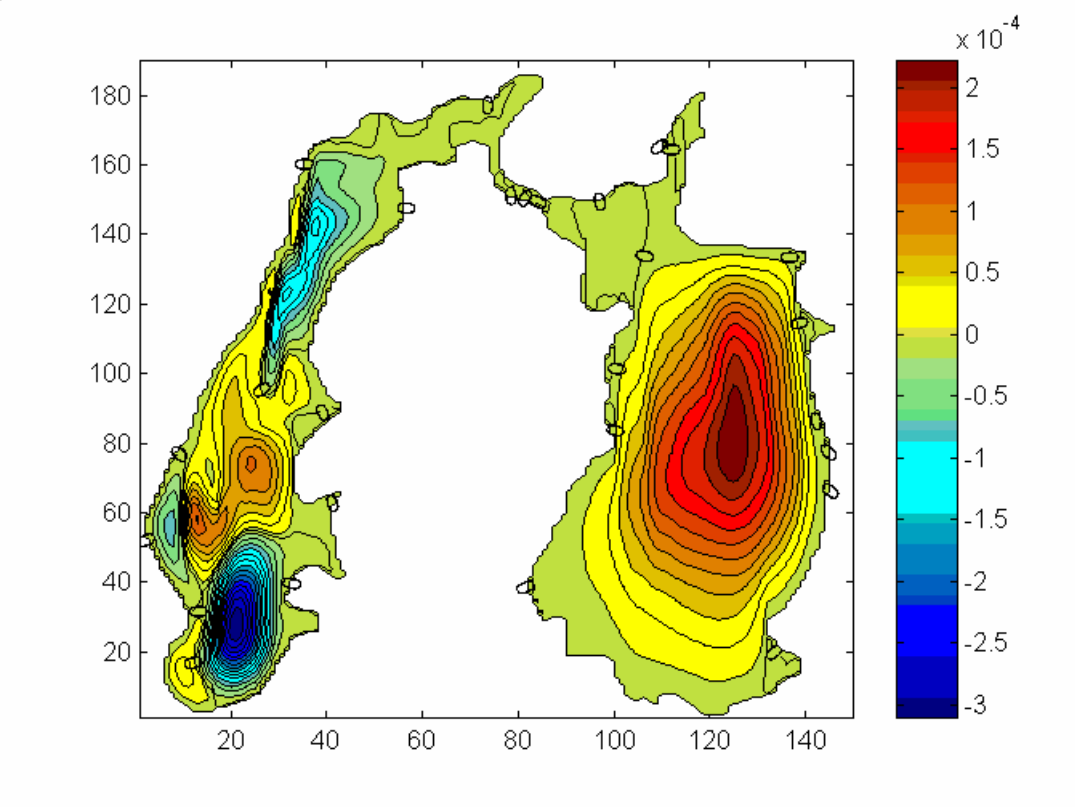

Fig. 29.8 Stream function. February.

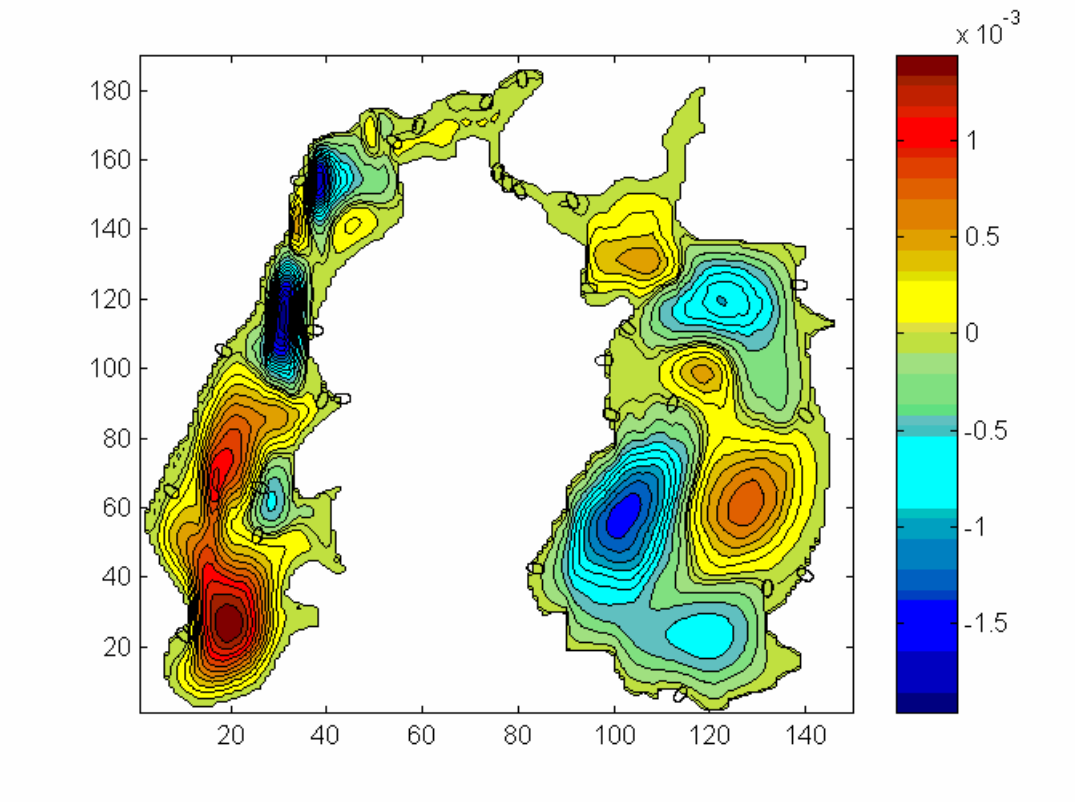

Fig. 29.9 Stream function. March.

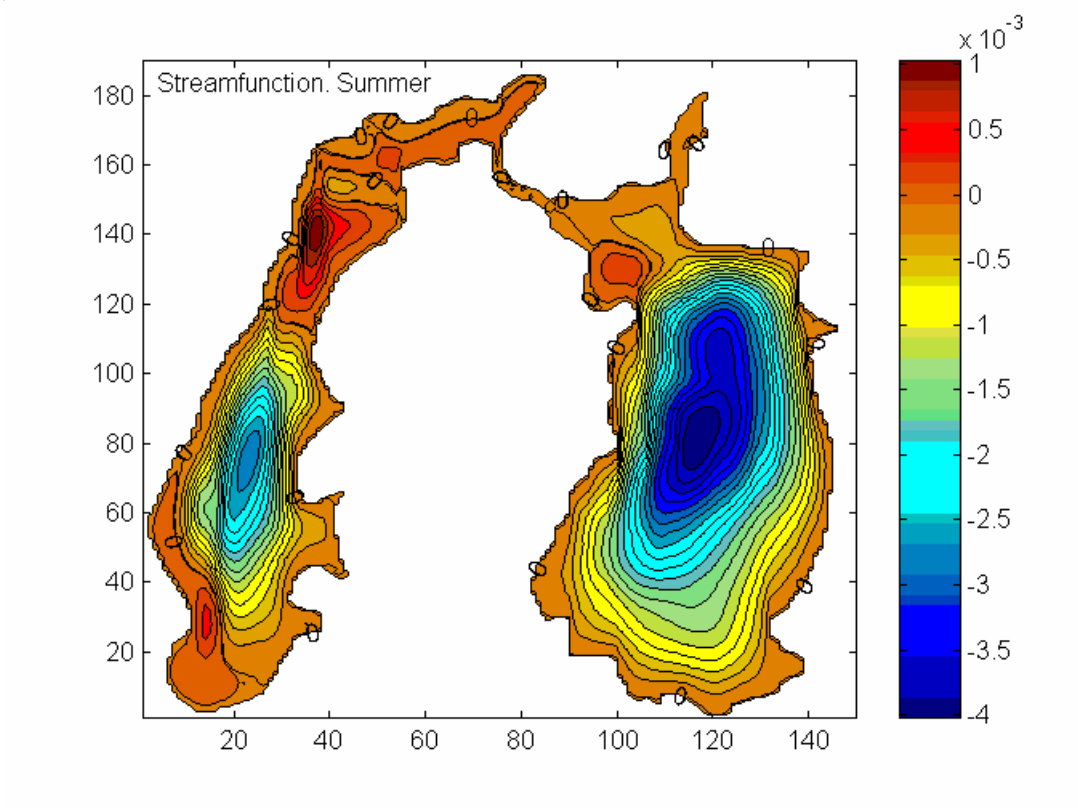

Fig. 29.10 Stream function. May.

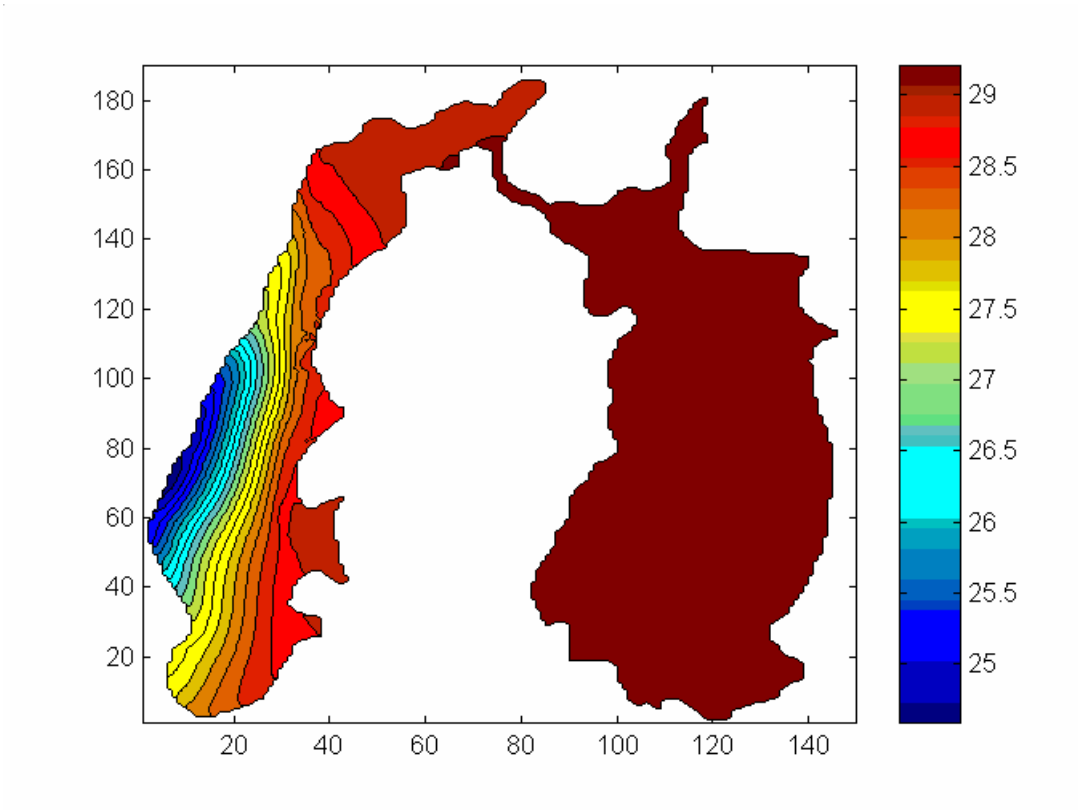

Fig. 29.11 Temperature at depth 2 m. June.

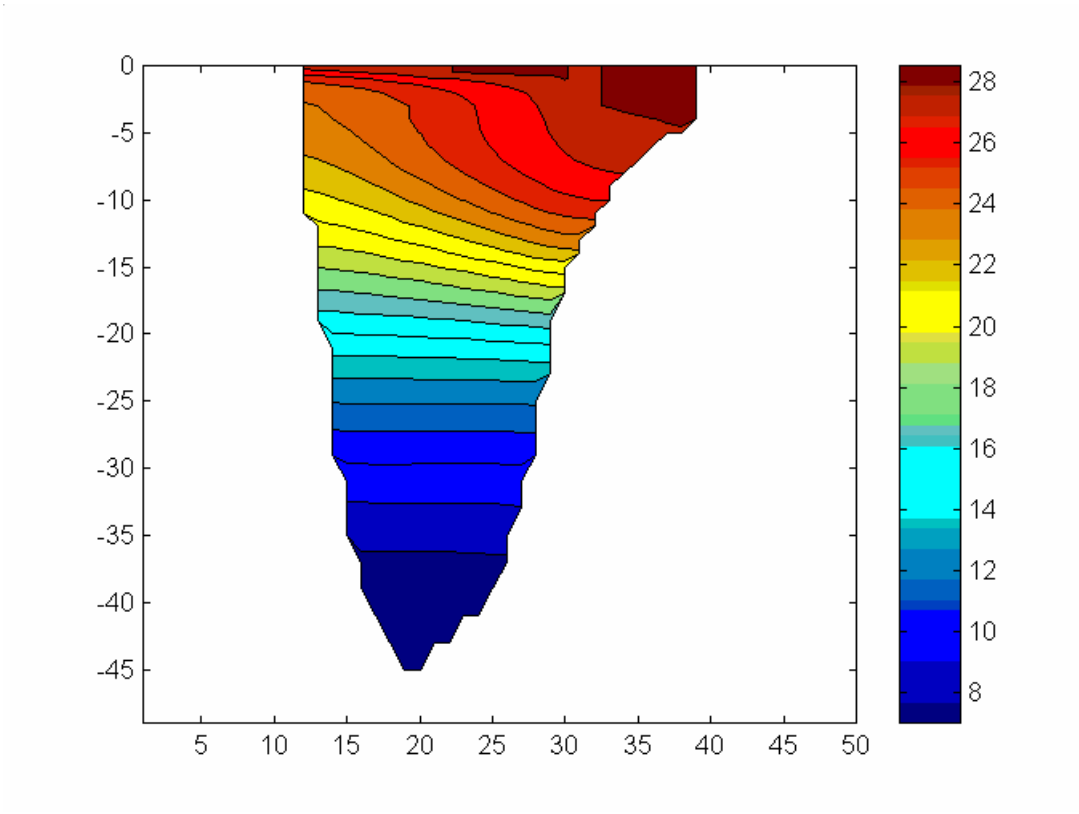

Fig. 29.12 Latitudinal temperature cross-section.
Western basin. Summer.

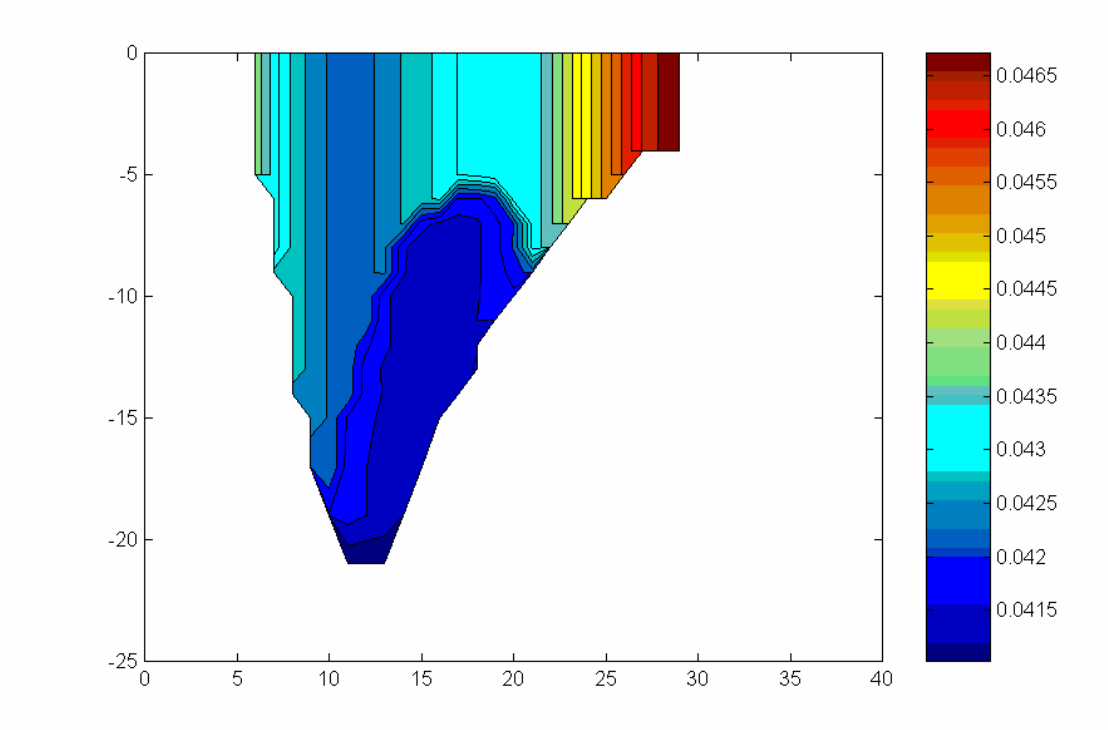

Fig. 29.13 Latitudinal temperature cross-section of the Western basin. Winter.

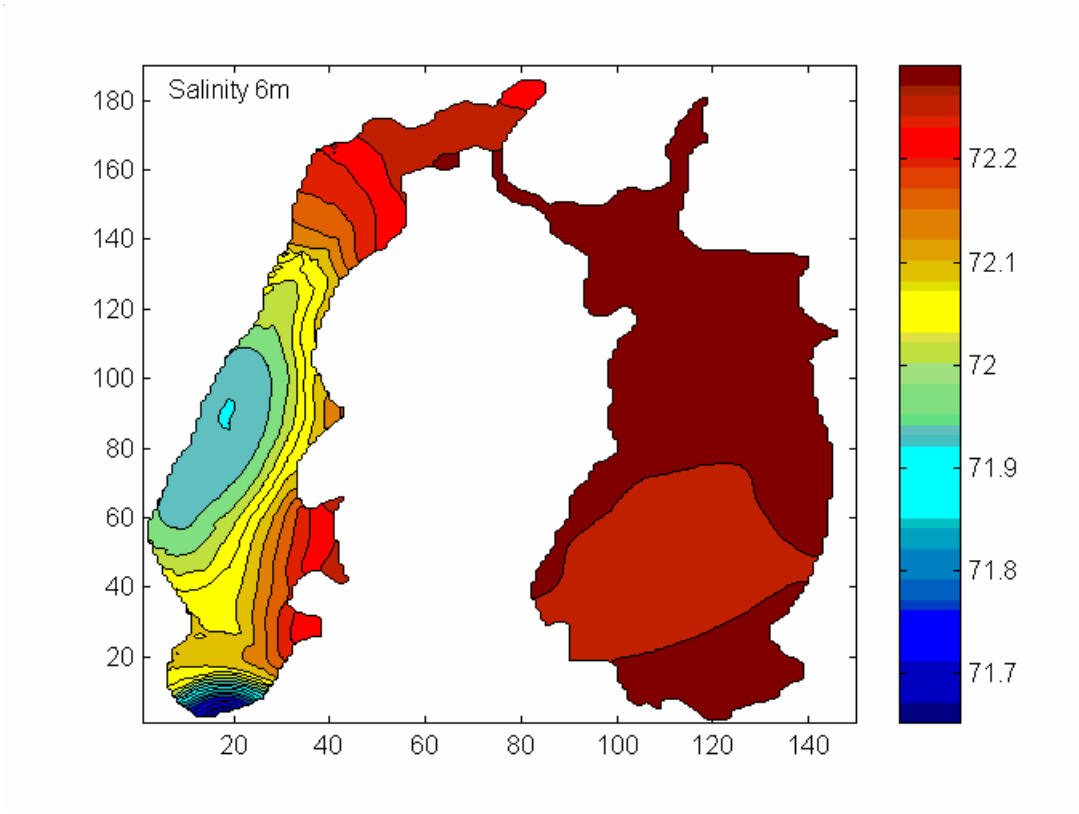

Fig. 29.14 Salinity field at depth 6 m. Summer.

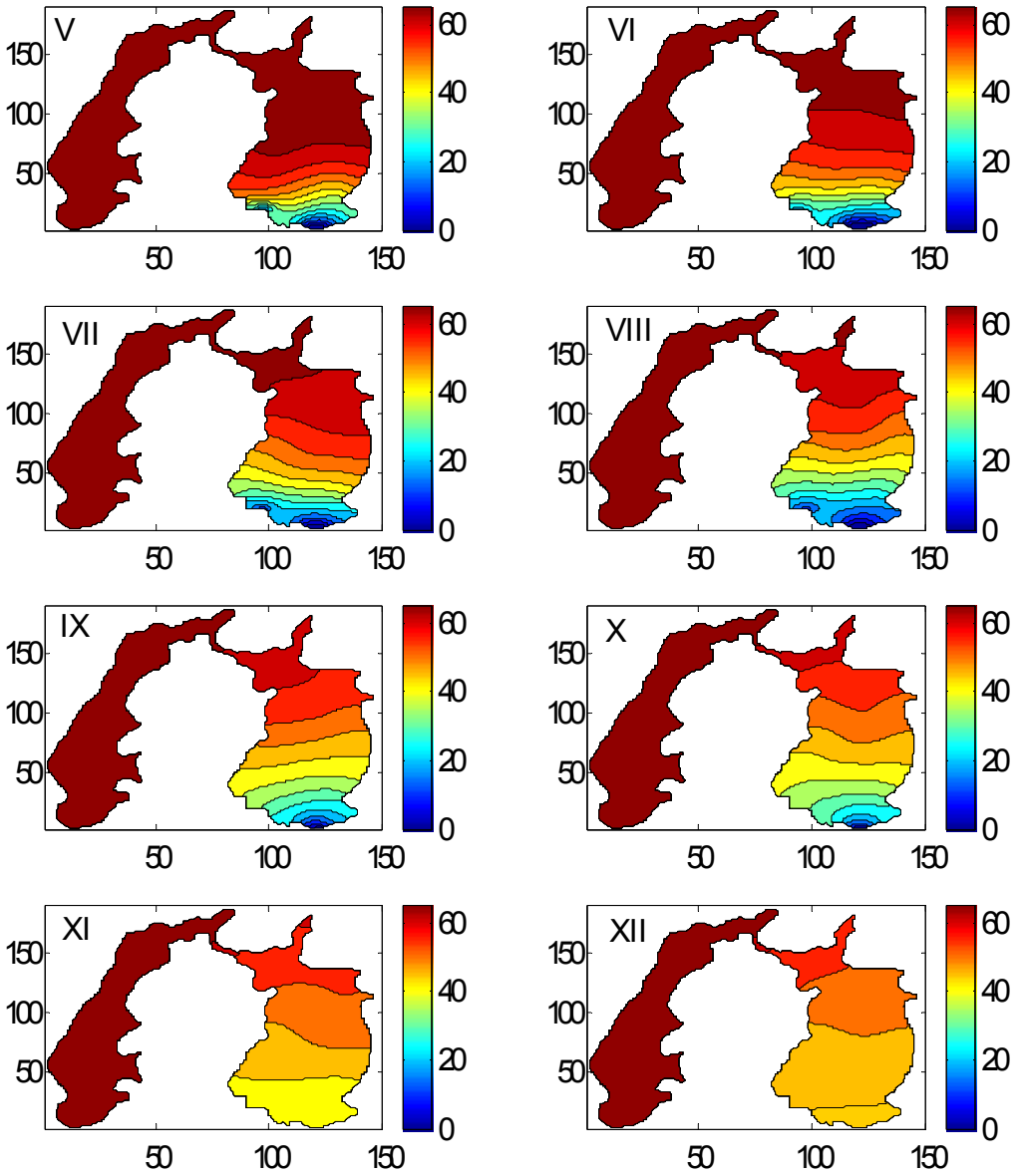

Fig. 29.15 Desalinization of the Aral Sea during the period of V-IX 1998 – high Amu-Darya inflow and X-XII 1998 – low Amu-Darya inflow

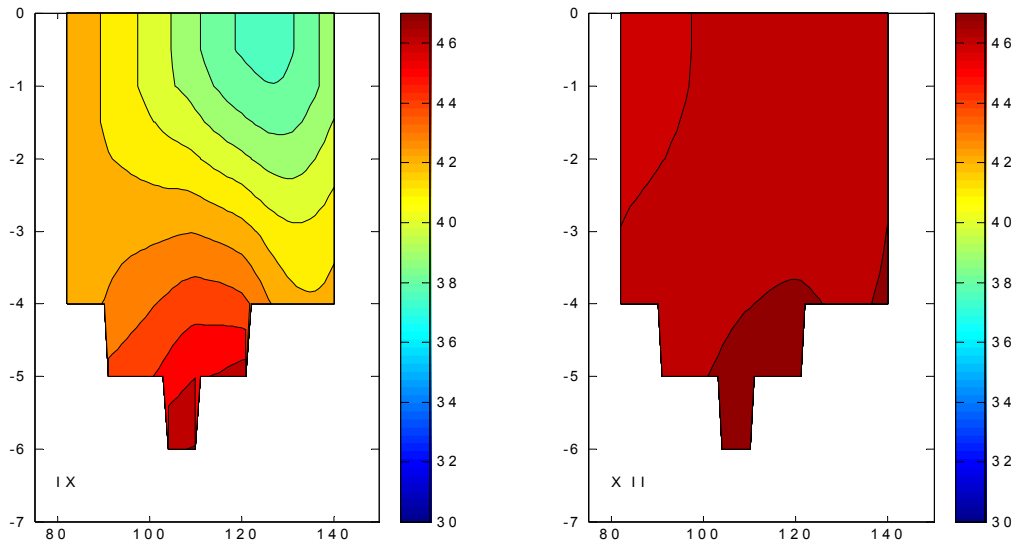

Fig. 29.16 Latitudinal salinity cross-section for June, August, October, December 1998

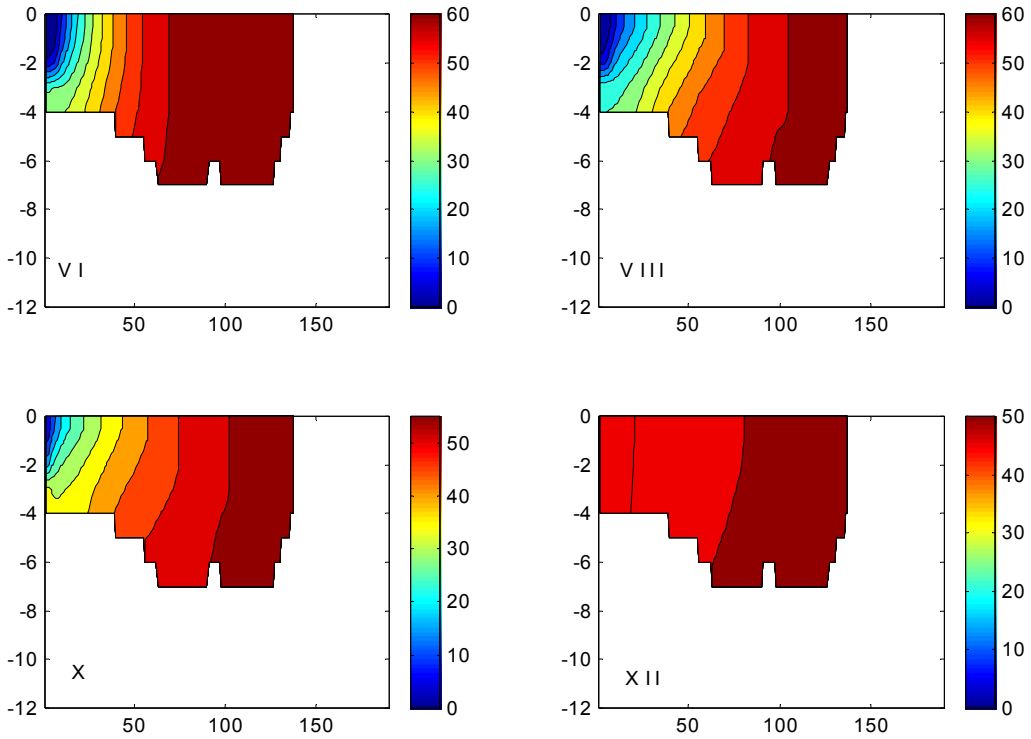

Fig. 29.17 Meridional salinity cross-section for June, August, October, December 1998

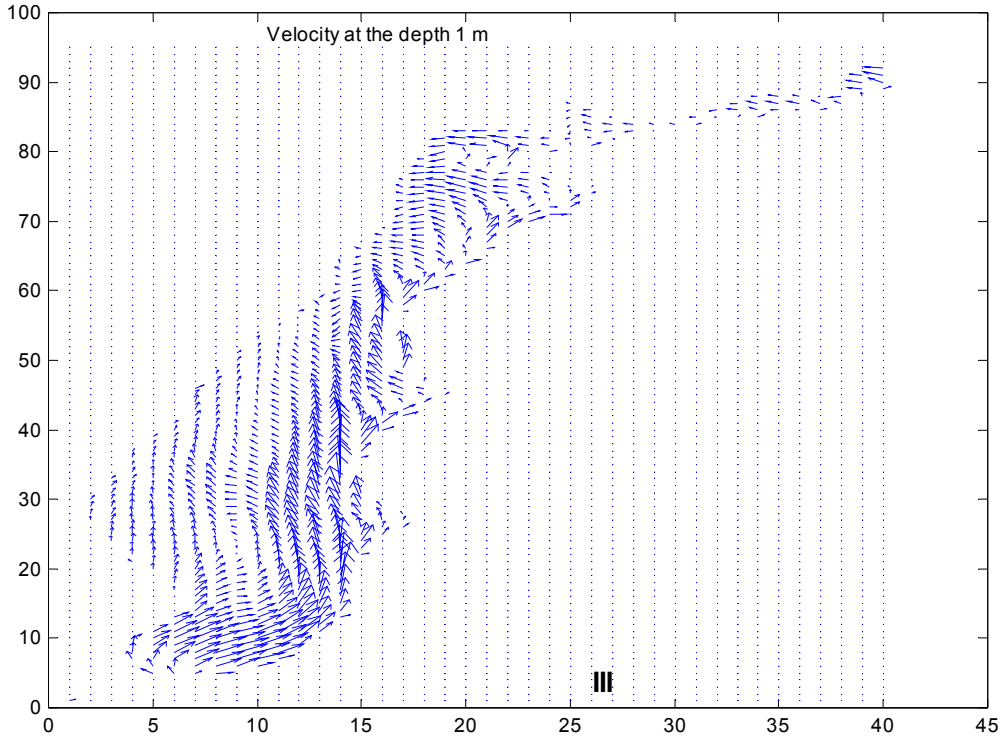

Fig. 29.18 Second experiment. Velocity field at depth 1 m.
March. Maximum velocity 20 cm/s.

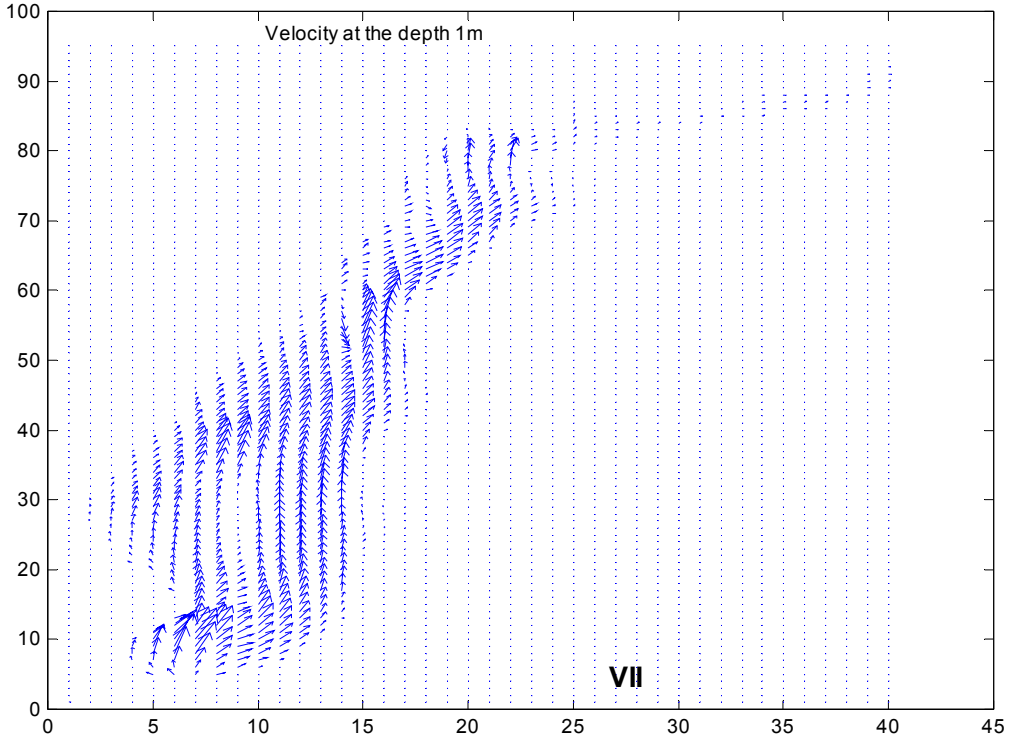

Fig. 29.19 The second experiment. Velocity field at depth 1 m.
July. Maximum velocity 15 cm/s.

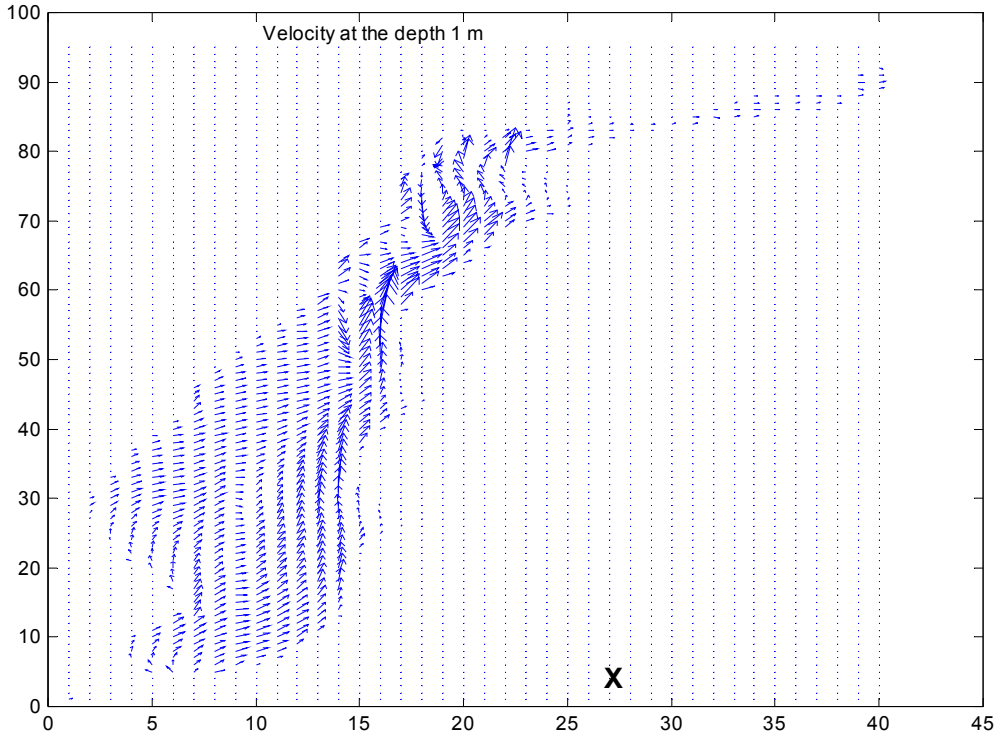

Fig. 29.20 The second experiment. Velocity field at depth 1 m.
October. Maximum velocity 25 cm/s.

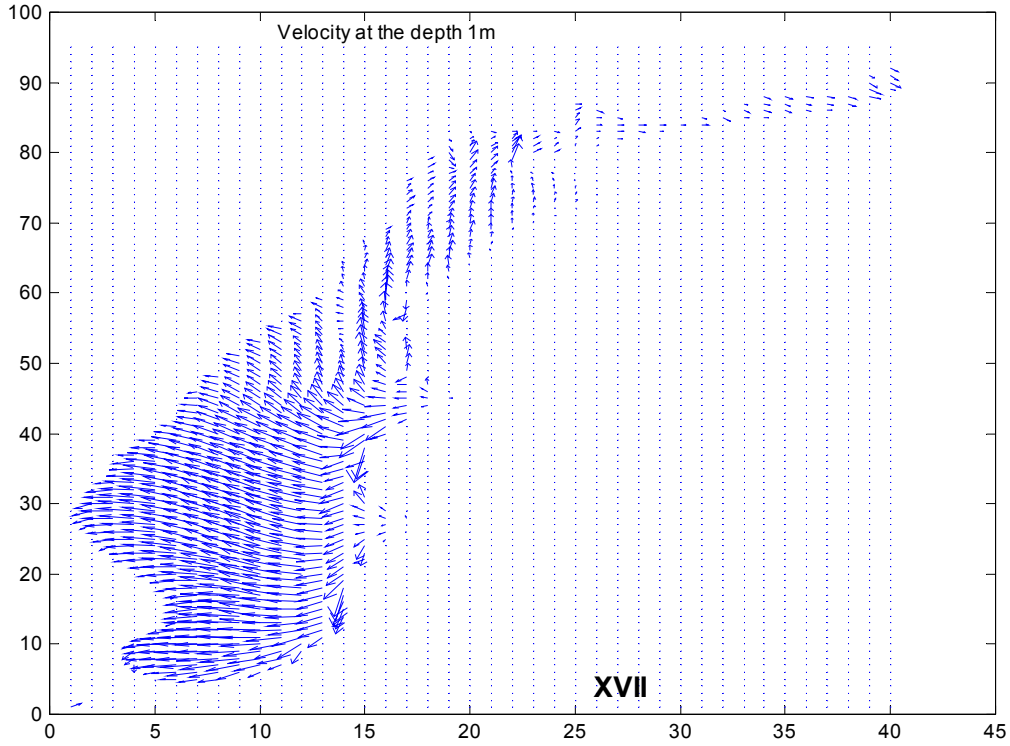

Fig. 29.21 The second experiment. Velocity field at depth 1 m.
May. Maximum velocity 20 cm/s.

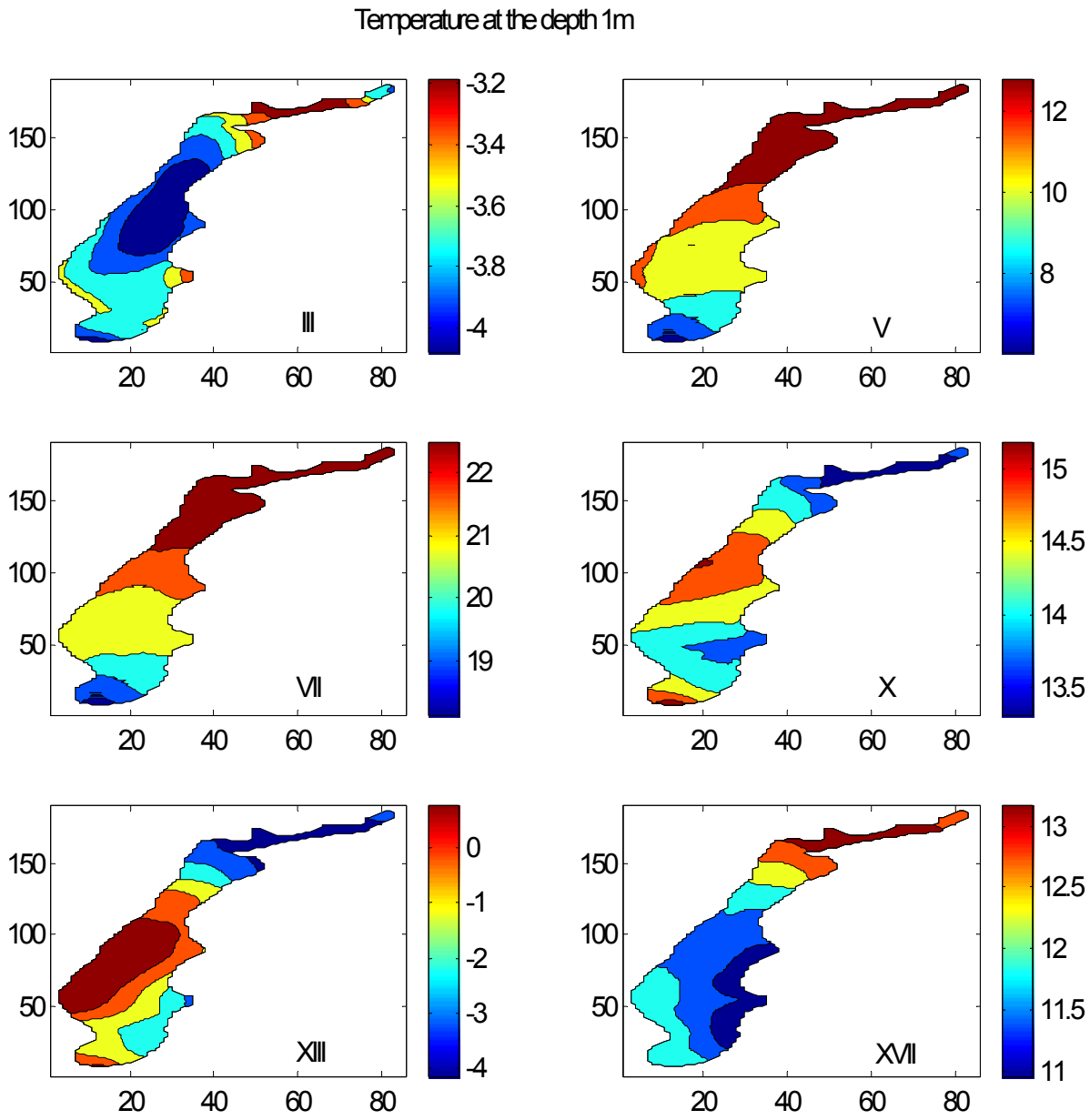

Fig. 29.22 The temperature distribution at the depth 1 m.

March, May, July, October, January, May.

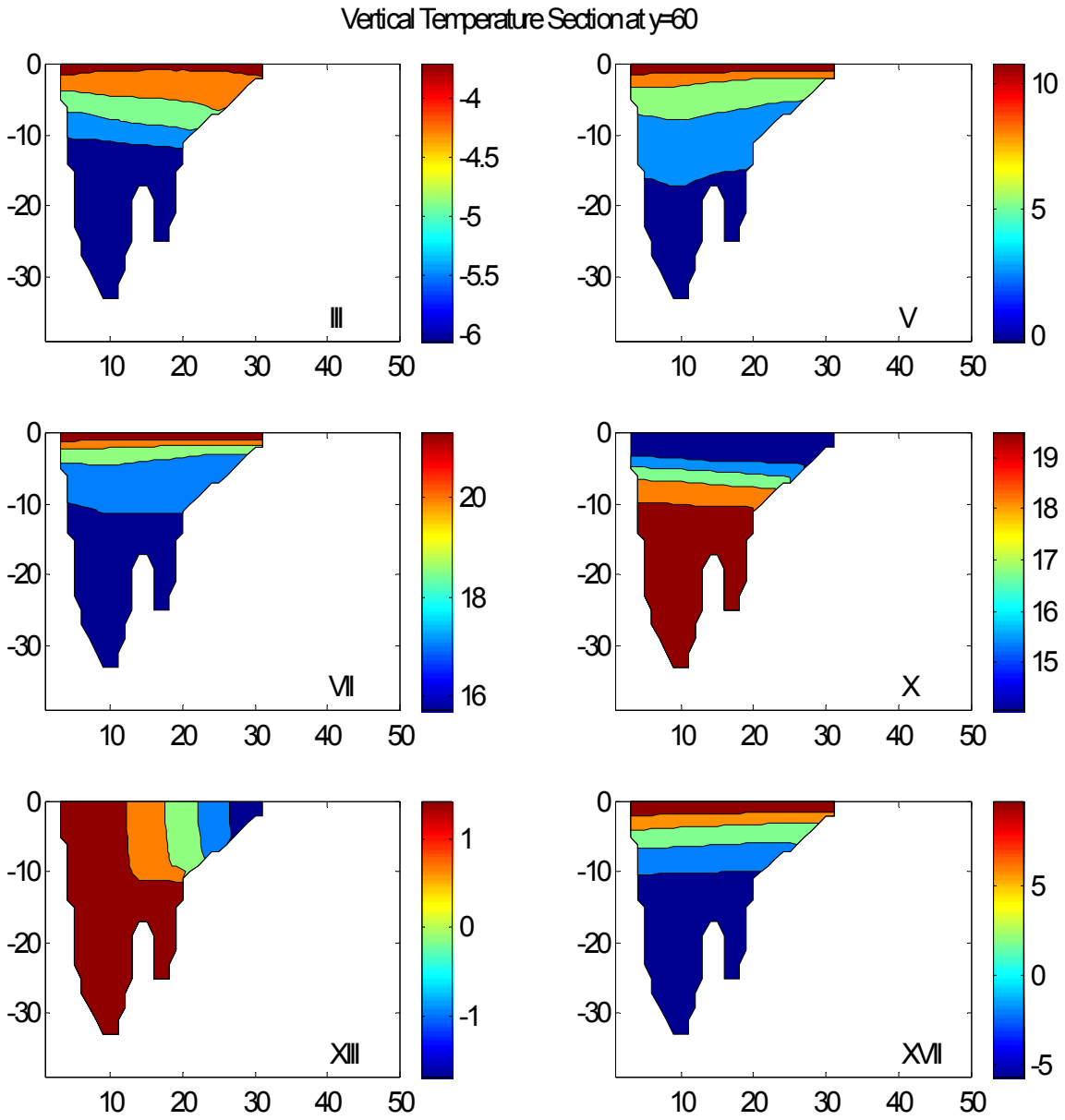

Fig. 29.23 Latitudinal temperature cross-section.
March, May, July, October, January, May.

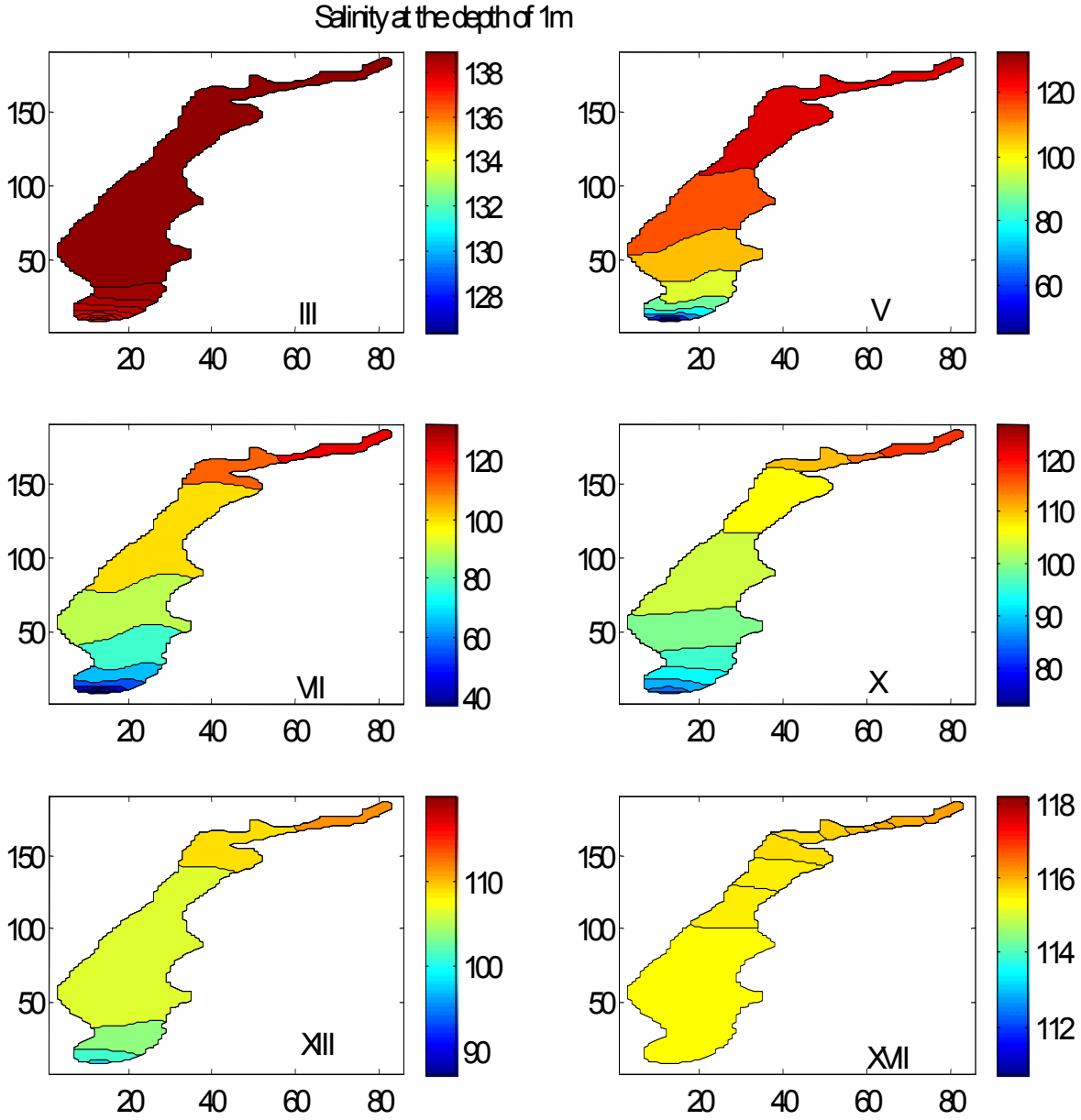

Fig. 29.24 The salinity distribution at the depth 1 m.

March, May, July, October, January, May.

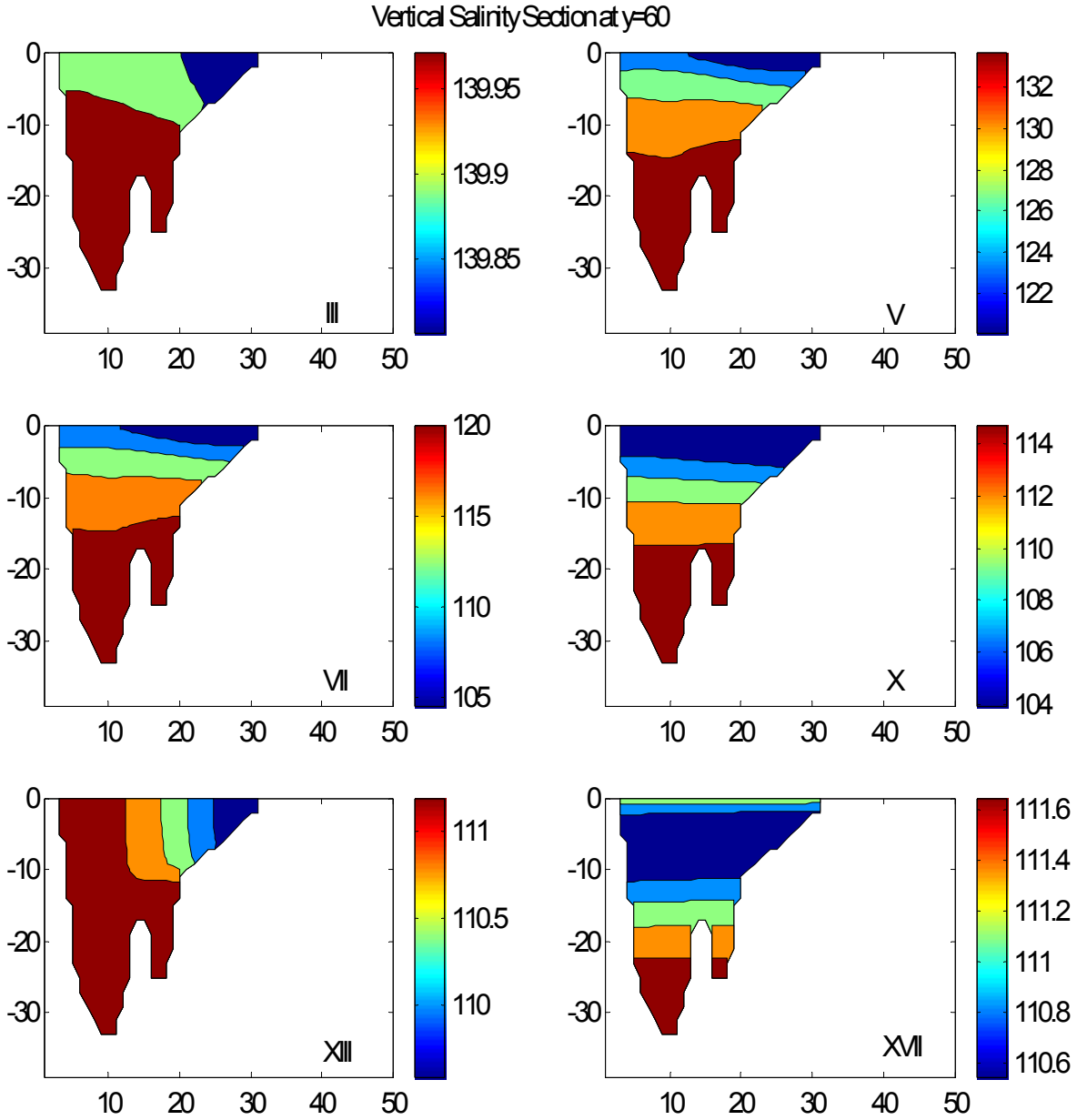

Fig. 29.25 Latitudinal salinity cross-section.

March, May, July, October, January, May.

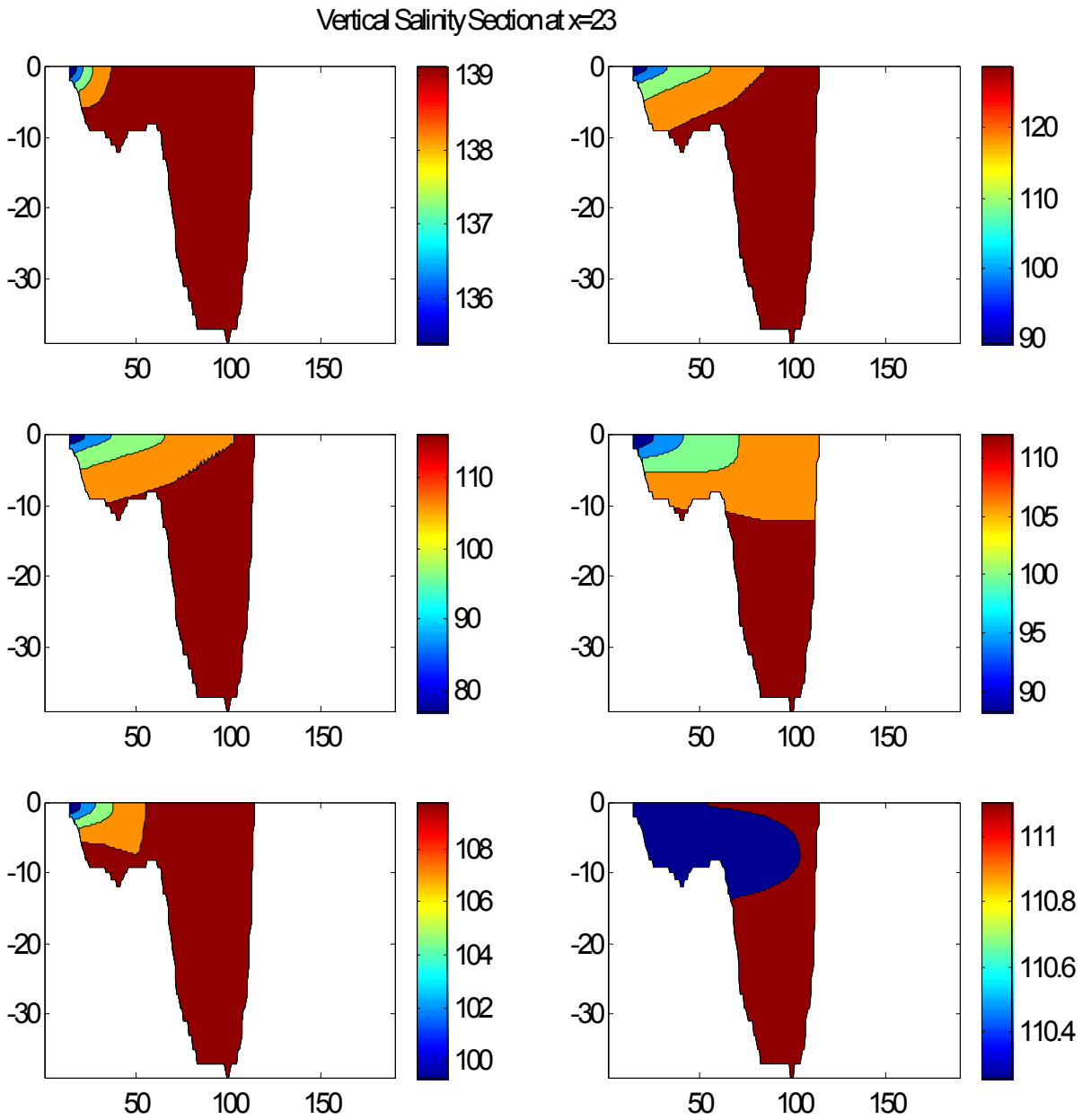

Fig. 29.26 Longitudinal salinity cross-section.

March, May, July, October, January, May.

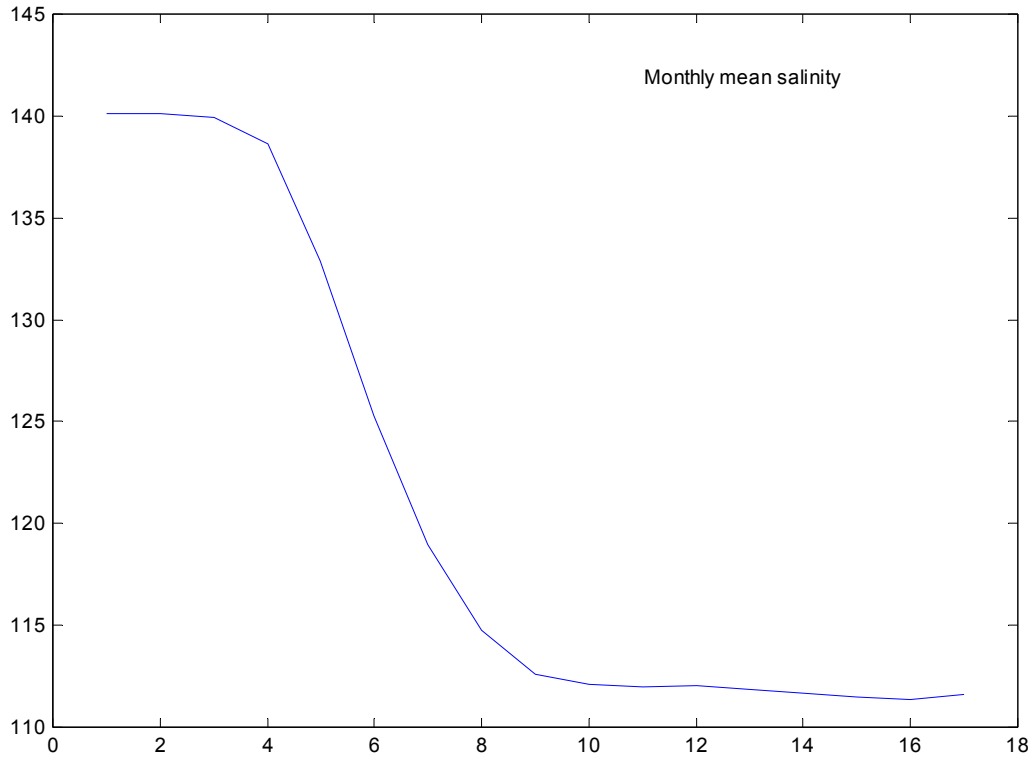

Fig. 29.27 Temporal behavior of the monthly mean salinity averaged by the whole volume.

30. General Conclusion

1. As salinity increases, the ice point of seawater goes down below zero. The anomaly of water density (extreme point on dependence of density on temperature) disappears as the salinity passes the critical value 24.7‰, so that the density of the salt water increases *monotonously* with a decrease of temperature until the freezing.

2. During autumn and winter seasons, the density stratification comes to be unstable. It results to intensive *vertical convective mixing* from surface to bottom. Then water temperature decreases close to the freezing point and ice starts to form. As a result the uniform distribution salinity and temperature is settled; and density stratification disappears. These phenomena have to be taken into account while considering of hydrodynamic, hydrophysical and hydrochemical processes in the sea.

3. The modelling of processes of *the tributary freshwater spread* in western part of the Aral Sea under the conditions of high-water flood and high sea water salinity was fulfilled with the use of the one-dimensional vertical model (section 28.2) as well as three-dimensional one (section 29.6.2).

The calculation has shown that from the very beginning of water entering the intensive mixing between the upper layer of freshwater and the underlying layers of seawater starts and continues due to the vertical turbulent exchange. It results in practically uniform vertical distributions of salinity and temperature that are settled in November and remain undisturbed till March. The maximum temperature gradients appear in the spring period but they slightly affect the water density distribution, and so the density stratification remains stable. The calculations with 1D (chapter 28.2) and 3D (chapter 29.6.2) give the similar picture of the dynamics of vertical distributions of salinity and temperature in the deep-water part of the sea during the 18-month calculation period.

4. The modeling of hydrologic and hydrophysical regime of western part of the Aral Sea with the first water management variant has demonstrated the expected stabilization of water level in the range of 24.5 – 30.0 m BS with relative stabilization of mineralization in the range from 100 to 155 g/l in 15 years

in the case of optimistic scenario and scenario "saving existent tendencies". As for scenario "national vision", even after 15-year term the drop of water level and salinity increase would most likely continue.

Table 30.1 The first water management variant. Annual inflow for 15 years.

Scenario	Variant of inflow	Volume of inflow, km^3/yr
National vision	min	1.70
	max	1.78
Saving existent tendencies	min	2.08
	max	2.14
Optimistic	min	2.55
	max	2.96

Table 30.2 The water level, mean salinity values to the end of calculation period and absolute minimum of water temperature for the period with the 1st water management variant.

Scenario	Variant of inflow	Water level, m	Mineralisation, g/l	T_{min}, °C
National vision	min	26.2	131.0	-7.06
	max	27.2	121.0	-7.06
Saving existent tendencies	min	27.4	120.8	-7.07
	max	28.5	114.0	-7.07
Optimistic	min	28.9	110.5	-7.06
	max	30.0	102.4	-7.06

5. For one of the most high-water years of the calculation period the *annual salt and temperature regime* has been analyzed using optimistic scenario. The features of the vertical salinity and temperature distributions were revealed. The state of nearly uniform salinity distribution is maintained from early November till early April; with mineralization slowly decreasing because of positive water balance during this season (precipitation is greater than evaporation). From early April till early July the desalinization of surface water occurs, but in a month (till early August) this desalinated water is spread to the bottom layers. The maximum variation of water salinity is reached in April; its value at the bottom is about by 2 g/l greater than at the surface.

As for thermal regime of the sea, it has been found that from December till March the state of homothermy take place, with temperature gradually decreasing from +2°C (December) до –7°C (March). During the next month temperature at the bottom remains constant (near –7°C) whereas the upper water layer is continuously warmed till early August when its temperature reaches about +24ºC, with followed cooling down. Because of mixing the bottom water temperature is also warmed till September but only to the value near –1ºC. At the same time in the near-bottom layers the water temperature remains below zero from January till early September when the surface water temperature reaches about 21°C.

In general, the near-bottom temperature varies from –7° to +7°C, while the surface temperature varies from –7° до +23ºC.

6. The calculation for *the second water management variant* has shown that the hydrologic and hydrophysical regime of western part of the sea differs from those of first variant because the water level can exceed the saddle point of the sill between the western and eastern parts of the sea and hence water overflow to the eastern part is possible.

Table 30.3 reviews the main information about scenarios considered, and Table IV presents the initial conditions and the calculated water level, mean salinity, water temperature limits reached in the last year of the period.

The lowest temperature of water is an important factor for living activities of the sea ecosystem. As mineralization increases, the freezing point of salt water becomes lower; therefore, the water temperature could reach very low values. The minimum water temperature is reached in winter under the conditions

of homothermy in the first calculation year. In the last calculation year the minimum temperature in different scenarios varies in the rang from -6 to -2°C. The annual dynamics of the vertical salinity and temperature distributions in the two water management variants were quite alike but there were observed quantitative differences to the end of calculation period. Almost in all cases the ice cover formed every year.

Table 30.5 the term needed for the water salinity dropped to the value 60 and 30 g/l in the second water management variant is presented.

Table 30.3 Scenarios of the second water management variant.

Scenario	Variant of inflow	Volume of inflow, km^3/yr	Notation
National vision	min	4.50	A_{min}
	max	5.00	A_{max}
Saving existent tendencies	min	5.15	B_{min}
	max	5.47	B_{max}
Optimistic	min	7.46	C_{min}
	max	8.94	C_{max}

Table 30.4 Main results of calculation under the 2nd version of water management.

Initial water level, m	Initial mineraliz-ation, g/l	Scenario	Final water level, m	Final mineralization, g/l	Minimum of temperature for the period, °C	Minimum temperature for the last year, °C
29	110	A_{min}	28.6	85.3	-6.96	-5.06
		A_{max}	28.9	64.1	-7.04	-3.78
		B_{min}	29.1	76.7	-7.06	-4.54
		B_{max}	29.1	60.1	-7.02	-3.44
		C_{min}	29.7	46.9	-6.08	-3.04
		C_{max}	29.5	29.7	-6.05	-1.77
28	120	B_{min}	29.1	80.8	-7.83	-4.83
27	130	B_{min}	29.1	84.3	-7.53	-5.06
26	140	A_{min}	28.6	96.5	-6.53	-5.84
		B_{min}	29.1	86.8	-7.09	-5.23
		C_{min}	29.7	53.2	-6.47	-3.53

Table 30.5 Years required to desalinate the sea to the specified level.

Initial water level, m	Initial mineralization, g/l	Scenario and stock	Desalination level of	
			60 g/l	30 g/l
29	110	A_{min}	–	–
		A_{max}	–	–
		B_{min}	–	–
		B_{max}	12-13	–
		C_{min}	11	–
		C_{max}	10-11	14
28	120	B_{min}	–	–
27	130	B_{min}	–	–
26	140	B_{min}	–	–
		A_{min}	–	–
		C_{min}	13-14	–

According to the performed calculation, the inflow of great enough volume of freshwater, (greater than for the water loss due to the effective evaporation) to the western part of the sea allows to wash-out the salts

from it to the eastern part of the sea. The question is what time is needed for the water mineralization could decrease one or another level. When the required level of salinity would reached the volume of inflow could be diminished to the level sufficient for compensation the water loss due to the evaporation.
The calculations have shown that the term needed for desalinization to the environmentally sound level essentially depends on the quickness of realization of measures for Amu-Darya water supply to the western part of the sea. This conclusion is also valid in respect of the annual minimum temperature.
The calculation have shown that flushing out the western part of the sea from the excess of stored salts in order to achieve environmentally sound water salinity are quite possible with the proper water feed from Amu-Darya during 10-15 years.

REFERENCES

1. Hydrometerology and hydrochemistry of seas of USSR. Vol. VII: The Aral Sea. Ed. F.S. Terziev. L.: Gidrometeoisdat,1990. (In Russian)
2. Ashirbekov U.A., Zonn I.S. Aral: the history of disappearing sea. Dushanbe, 2003. (In Russian)
3. Blinov L.K. Hydrochemistry of the Aral Sea. L.: Gidrometeoisdat,1956. (In Russian)
4. Vasiliev V. P. Water electrolytes. M: Himiya, 1988. (in Russian)
5. Pitzer K. S.and Kim J .J.. Thermodynamics of electrolytes, IV. Activity and Osmotic Coefficients for Mixed Electrolytes. *J.Solut.Chem.* (1978), v.7, n.5, p. 5701–5707.
6. Charykova M. V., Charykov N. A.. Thermodynamic modeling of evaporative sedimentation processes. S.-PB: Nauka, 2003. (In Russian)
7. Prokopiev S. I., Aristov Y. I. Concentrated aqueous electrolyte solutions: analytical equations for humidity–concentration dependence.J. Solution Chemistry (2000), Vol.29, No.7, p.633–649
8. Horne R. A. Marine chemistry. The structure of water and the chemistry of hydrosphere. Wiley-Interscience, New-York-London-Toronto, 1969.
9. Mamaev O. I. Thermohaline analysis of World Ocean waters. Leningrad: Gidrometeoizdat, 1987. (In Russian)
10. Gill A. E., (1982), Atmosphere–ocean dynamics, Orlando, F.L.: Academic Press.
11. Chen C.T., Millero F.J. Precise Thermodynamic Properties for Natural Waters Covering Only the Limnological Range. Limnol. Oceanogr. v. 31, No. 3, 1986, 657-662.
12. Bocharov O. B., Vasiliev O. F., and Ovchinnikova T. E. Approximate Equation of State of Water in the Vicinity of the Maximum-Density Temperature. Izv. Akad. Nauk, Fiz. Atmos. Okeana v. 34, No 4, 556-558 (1999).
13. Bocharov O. B., Vasiliev O. F., and Ovchinnikova T. E. Approximate Equation of State of Water in the Vicinity of the Maximum-Density Temperature with Allowance for Mineralization. Izv. Akad. Nauk, Fiz. Atmos. Okeana v. 40, No 3, 423–425 (2004).
14. Pitzer K. S.and Kim J .J.. Thermodynamics of electrolytes, IV. Activity and Osmotic Coefficients for Mixed Electrolytes. *J.Solut.Chem.* (1978), v.7, n.5, p. 5701–5707.
15. Hydrometerology and hydrochemistry of seas of USSR. Vol. VII: The Aral Sea. Ed. F.S. Terziev. L.: Gidrometeoisdat,1990. (In Russian)
16. Mamaev O. I. Thermohaline analisis of Warld Ocean waters. Leningrad: Gidrometeoizdat, 1987. (In Russian)
17. Chen C.T., Millero F.J. Precise Thermodynamic Properties for Natural Waters Covering Only the Limnological Range. Limnol. Oceanogr. v. 31, No. 3, 1986, 657-662.
18. Rayan R. J., Harleman D. R., Stolzenbach F. Surface heat loss from cooling ponds // Water resources research. – 1974. – V. 10, № 5. –P. 930-938.
19. Wake A., Rumer R. R. Modeling ice regime of Lake Eria // J. of the Hydr. Division. – 1979. – Vol. 105, № HY7. –P. 824-844.
20. Aleksandrov I.Ya., Kvon V.I., Filatova T.N., Zhukovskaja O.P. Mathematical modeling of ice conditions of water bodies under big thermal loads // Meteorologija i gidrologija. – 1992. – № 2. – P. 73-81. (in Russian)
21. Kvon D.V., Kvon V.I., Semchukov A.N. Numerical calculation of longitudinal-vertical thermal structure of the Lake Teletskoye in annual cycle. // Vichislitelnie tehnologii. – 2000. – Vol. 5, № 3. – P. 29-45. (in Russian)
22. Durov V.A., Ageev V.P.. Thermodynamic theory of solutes. – Moscow.: URSS, 2003. (in Russian)
23. Report № 3 of group CR3 on INTAS project 2001-0511.
24. Vinokurov S.D., Proskurjakov B.V. Hydrophysics. – Leningrad: Gidrometeoizdat, 1988. (in Russian)
25. Kuhling H. handbook of physics – Moscow: Mir, 1982. (in Russian)
26. State water cadastre. Annual data of the regime and resources of the surface land water. 1982. – Part 2, Vol. I, Issue 10 – Novosibirsk, 1983. (in Russian)
27. Orlob G.T. One-dimensional Models for Simulation of Water Quality in Lakes and Reservoirs. in: Mathematical Modeling of Water Quality: Streams, Lakes, and Reservoirs. IIASA, 1983. p. 227-273.
28. Vasiliev O.F., Zinoviev A.T., Bocharov O.B. Mathematical modelling of hydrothermal processes of deep-water reservoirs. Proc. of the 24-th IAHR Congress, Technical session C. Madrid, 1991. P. 467-476.

29. Vasiliev O. F. Mathematical modelling of hydraulic and hydrologic processes in water bodies and channels. (A review of the works fulfilled in Siberian Branch of the Russian Academy of Sciences). Vodnyje resursy, 1999, v. 25, No 5, p. 600-611. (In Russian)
30. Rodi W. Turbulence Models and their Applications in Hydraulics. – A State of the Art Review. International Association for Hydraulics Research, Delft, 1980.
31. Vasiliev O.F., Dumnov S.V. A Two-Dimensional Model for Salt Water Intrusion in an Estuary. Proc. of the XX IAHR Congress, Moscow, USSR, 1983, v. 2. -P. 10-16.
32. Scenarios of water inflow into the Aral Sea. Appendix to report № 4 of gr. CR2, project INTAS-0511 (REBASOWS).
33. Hydrologic Annual. 1975 g. – Tom V, vyp. 0-2. – Dusanbe: Glav. upr. gidromet. sluzby pri sov. min. SSSR, Upr. gidromet. sluzby Tadj. SSR, 1978. (in Russian)
34. GIS "Aral Sea". (in Russian)
35. Report № 3 of grCR3, project INTAS-0511 (REBASOWS).
36. Hydrometeorology and hydrochemistry of USSR. – Tom VII: Aral Sea. – L.: Gidrometeoizdat, 1990. (in Russian)
37. Scientific and Applied Handbook on Climate of USSR. – Ser. 3, c. 1-6, vyp. 19, book. 1. – L.: Gidrometeoizdat, 1989. (in Russian)
38. Scientific and Applied Handbook on Climate of USSR. – Ser. 3, c. 1-6, vyp. 19, book 2. – Л.: Gidrometeoizdat, 1989. (in Russian)
39. Scientific and Applied Handbook on Climate of USSR. – Ser. 3, c. 1-6, vyp. 18, book 2. – Л.: Gidrometeoizdat, 1989. (in Russian)
40. Scientific and Applied Handbook on Climate of USSR. – Ser. 3, c. 1-6, vyp. 18, book 3. – Л.: Gidrometeoizdat, 1990. (in Russian)
41. Report № 2 of gr. CR5, project INTAS-0511 (REBASOWS).
42. Database on the Aral Sea (Intas Data Base).
43. Instructions to thermal calculation of reservoirs. L.: "Energia", 1969. (in Russian)
44. Braslavskil A.P., Ostroumova L.P. Calculation of water evaporation from surface of theBalhas Lake. Tr. Kaz. NIGMI GOIN, 1989, no. 101. p. 52-78. (in Russian)
45. Byzova N.L. et all. Turbulence in boundary layer of atmosphere. L.: "Gidrometeoizdat", 1989. (in Russian)
46. Report № 3 of gr. CR2 , project INTAS-0511 (REBASOWS).
47. Politic map of USSR scale 1:4000000. (in Russian)
48. Agroskin I.I., Dmitriev G.T., Pikalov F.I. Hydraulics. L.: Gosenergoizdat, 1950. (in Russian)
49. Bocharov O.B., Vasiliev O.F. Semi-empirical model of selective outflow from stratified water body. Wodnye resursy, 1992, № 3. P. 16-21. (in Russian)
50. V.I. Kuzin. Finite Element Method in the modeling of the ocean processes. NCC Publisher, Novosibirsk, P.190.
51. E.N. Golubeva, Yu.A. Ivanov, V.I. Kuzin, G.A. Platov. Numerical modeling of the World Ocean circulation including upper ocean mixed layer // Oceanology. – 1992. – Vol. 32. – No 3. – P. 395-405.
52. V.I.Kuzin, E.N.Golubeva. Modeling of hydrodynamic and hydrophysical processes in the Aral Sea. Proceedings of the Int. Congress «GEO-Siberia», 2005.

APPENDIX III

On a possibility of the precipitation of salts during the Aral water evaporation

Nowadays, because of the evaporation from the Aral Sea exceeding the fresh water income, the concentration of salt in water is increasing. Solubility of ionic compounds is thermodynamically limited, so this water imbalance will eventually result in the saturation of the brine with one of more salts, and then an excess of them will be eliminated from water as a precipitate.

Our results reported here are obtained with the neglect of the precipitation of salts in Aral Sea. Thus, the aim of this chapter is to outline the validity limits of the assumption.

It is known [54] that precipitation of calcium occurs at salinity higher than 20‰. Nevertheless, there are evidences that the solubility of calcium salts in *natural* waters may be sufficiently greater than in distilled water that was used for the experiments in [53]. So, sulphate and carbonate of calcium remain in brine and don't precipitate even if their concentration is 20–50 times higher that their solubility in a chemically pure water.
As our colleagues under the Aral project reported, during the evaporation process the concentrations of ions Ca^{2+} и SO_4^{2-} changes as mentioned in Table below. We calculated the association quotient (the product of thermodynamic activities of ions) *Q* (section 27.4) and found that this value is *permanently increasing* as water is evaporating.

Analysis date	*Mineralization, g/l*	SO_4^{2-}, mg-equiv./l	Ca^{2+}, mg-equiv./l	$Q\times10^2$ $(kmol/m^3)^2$,
30.07.04.	86,1	501,3	74,9	1.05
02.08.04.	142,4	835,2	74,9	1.74
04.08.04.	294,0	1673,8	39,9	2.02
05.08.04.	412,1	2714,6	49,9	3.94

This fact clearly evidences that Aral water even at mineralization 412 g/l (the respective salinity value is near 310‰) remains under-saturated by gypsum (at 30°C, temperature of the experiment); otherwise the quotient *Q* would keep constant and be equal to the solubility product. Thus, the precipitation of gypsum at lower salinity is unlikely.

Also, earlier we evaluated the limiting point of saturation by next soluble salt. So, we have mentioned in section 27.4 that the precipitation of mirabilite or astrakhanite (that depends on temperature) may be observed only at mineralization above 350 g/l (respective salinity is approximately 290‰). As temperature is lower, the saturation limits shift to lower salinity; at 0°C the limiting salinity is expected to be about 250‰.

Therefore, the model, which is ignoring the precipitation of salts, is valid at salinity below 250‰ (or mineralization less than 300 g/l), and the obtained results are adequate.

References

53. Charykova M. V., Charykov N. A.. Thermodynamic modeling of evaporative sedimentation processes. S.-PB: Nauka, 2003. (In Russian)
54. Nikanorov A.N. Hydrochemistry. St. Peterburg, Gidrometeoizdat, 2001. (In Russian)